A COMPARATIVE STUDY OF ARCHAEAN AND PROTEROZOIC FELSIC VOLCANIC ASSOCIATIONS IN SOUTHERN AUSTRALIA

by

CHRIS W. GILES B.Sc.(Hons).

(University of Adelaide)

A thesis submitted in partial fulfilment of the requirements for the degree of

Doctor of Philosophy

UNIVERSITY OF ADELAIDE

October, 1980.

This thesis contains no material which has been accepted for the award of any other degree or diploma in any University and, to the best of my knowledge and belief, contains no copy or paraphrase of material previously published or written by another person, except where due reference is made in the text of the thesis.

October, 1980.

TABLE OF CONTENTS

LIST OF TABLES

LIST OF TABLES Cont'd.

LIST OF TABLES Cont'd.

LIST OF TABLES Cont'd.

LIST OF FIGURES

LIST OF FIGURES Cont'd.

LIST OF FIGURES Cont'd.

LIST OF FIGURES Cont'd.

APPENDIX 2

THESIS SUMMARY

Integrated field, petrographic and geochemical studies of four Precambrian felsic volcanic terrains in Australia have been undertaken with the object of gaining an insight into the processes of magma generation and crustal development in the Precambrian. The areas examined include two Archaean felsic volcanic centres in the Norseman-Wiluna greenstone belt of the Yilgarn Block and portions of two post-orogenic Middle Proterozoic volcano-plutonic terrains in central-southern Australia.

The Archaean felsic volcanic rocks are confined to discrete centres and show no systematic relationship in space or in time with the tholeiitic and komatiitic volcanic members of the greenstone succession. The two suites examined show typical calc-alkaline major element geochemical characteristics, but appear to have evolved along different lines of liquid descent from common parental magmas. On the one hand, extended fractionation of plagioclase and clinopyroxene at shallow depths (<10km) has yielded acid rocks relatively enriched in REE, Zr, Nb and Y, but depleted in Sr. On the other, prolonged fractionation of amphibole at greater depths (20-30km), perhaps near the base of the crust, has resulted in acid differentiates that are relatively depleted in HREE, Zr, Nb and Y, but enriched in Sr. It is postulated that the primary magmas for the calc-alkaline suites were derived by hydrous melting of a LIL element-enriched mantle source over a significant pressure interval (e.g. 10-20kb). Experimental evidence indicates that melting under these conditions will yield a range of primary magmas that differ chiefly in their MgO and SiO_2 contents, and this can account for the variable levels of MgO, Ni and Cr observed in the andesites. Such an origin is also able to explain why many of the low-silica andesites, which may be little removed by differentiation from their quartz-normative mantle-derived parents, are relatively enriched in MgO, Ni and Cr compared with modern andesites. Available data for calc-alkaline volcanic rocks from four other centres in the Yilgarn Block suggests that these conclusions have general applicability.

The two post-orogenic Middle Proterozoic volcano-plutonic terrains, by contrast, lack calc-alkaline andesites and are characteristically bimodal. Both of the provinces studied are comprised of vast subaerial ignimbrite sheets with subordinate intercalated basic flows and voluminous granitoid rocks, and have undergone minimal deformation and metamorphism. The acid intrusive and extrusive rocks are enriched in all LIL elements compared with modern calc-alkaline suites, and geochemical modelling calculations favour an anatectic origin. The moderately low silica contents of the primary magmas (58-65% SiO_2) indicate a relatively basic crustal source, in order to

avoid the necessity of invoking excessive degrees of melting (>60%). This is supported by trace element modelling calculations which show that at degrees of melting in excess of 40%, the enrichment of LIL elements in the melt is insufficient to account for the levels of these elements observed in the acid volcanics. Of the various possibilities tested for the crustal source, a basic granulitic refractory residue is considered most plausible on geochemical grounds. A literature review demonstrates that late-to post-orogenic bimodal igneous activity is widespread in the Proterozoic of other continents. The acid rocks in particular, show comparable geochemical characteristics to the Australian examples, which the present studies indicate could be explained as follows:

1. Relatively high LIL element contents, as the result of a sialic crustal source.
2. Particularly high Zr, Nb, Y, REE, Fe and Ti contents, due to the relatively high temperatures of melting which contributed to the disintegration of minerals normally refractory under low temperature wet melting conditions (e.g. zircon, apatite, sphene, spinel).
3. Relatively low Al_2O_3, CaO and Sr contents, reflecting a high proportion of residual plagioclase probably as the result of the relatively dry conditions of melting.

Although the felsic volcanics of the Archaean and Proterozoic terrains studied have contrasting origins, it is notable that the relatively minor associated basic volcanics have comparable critical geochemical characteristics (e.g. elemental ratios), indicating derivation from similar LIL element-enriched upper mantle sources. It seems likely that mantle diapirism provided the heat for melting of the upper mantle and crust in both the Archaean and the Proterozoic, although the scale of diapirism probably differed. During the Proterozoic, significant amounts of heat for crustal fusion may have also been contributed by basic magmas that were entrapped beneath the relatively thick, bouyant sialic crust existing at that time (c.f. Archaean). The record of felsic volcanism in the Precambrian can thus be explained in terms of an evolving crust, in which the "sialic" component increased in thickness with time through partial melting of basic igneous precursors and also via direct additions from the mantle of acid, calc-alkaline differentiates. Once formed, the sialic crust was reworked at various stages, culminating with the development of the voluminous acid magmas in the post-orogenic, Middle Proterozoic era.

ACKNOWLEDGEMENTS

This thesis has benefited greatly from the wisdom and selflessness of many people, although the writer alone is responsible for any shortcomings.

The writer is indebted to Dr. R.W. Nesbitt who initiated this project and who, with patience and vision, guided the direction of the work in the early stages of the project.

Dr. J.A. Hallberg showed continual interest in the project and his application of basic field and petrographic techniques to the study of fundamental geological problems provided a constant source of inspiration to the writer.

The wisdom and kindness of Dr. S.S. Sun, who demonstrated the method of REE determination by isotope dilution and who willingly shared his deep knowledge in many fields, is gratefully acknowledged. Dr. J.A. Cooper kindly permitted the writer to use the mass spectrometer and his laboratory facilities.

Appreciation is expressed to the South Australian Department of Mines and Energy, particularly Mr. A.H. Blissett, Dr. C.D. Branch and Mr. R. Dalgarno of that Department, all of whom cooperated with the writer in aspects of this study.

Thanks is due to Dr. J. Foden who wrote and demonstrated the usefulness of many of the modelling programs used in this thesis. Considerable assistance, mainly through stimulating discussions and exchange of ideas was provided by colleagues, particularly Mr. G.E. Mortimer, Mr. G.W. Stolz and Mr. G.S. Teale.

Thanks are also due to Mr. J. Stanley for assistance with XRF analytical procedures, Mr. R. Barrett for help with the photographic work and Mrs. J. Howe who typed the manuscript and the numerous tables.

The writer is grateful to the Department of Geology at the University of Adelaide for providing encouragement and material assistance wherever possible, and to the Commonwealth Government for a four year research award.

Finally, sincere acknowledgement is made to my parents who supported me throughout the thesis work, asking nothing in return. My Father acted as a willing and able field assistant and skilful jack of all trades on the many field trips to remote areas. Without this support, successful completion of the thesis would have been considerably more difficult.

"In seeking an answer to a problem, one must first of all ask the right question"

CHAPTER 1

INTRODUCTION

1.1 INTRODUCTION

*Felsic volcanic rocks and their plutonic equivalents constitute an important component of the Precambrian shield areas of Australia. Since these rocks are amenable to detailed petrological study they offer the opportunity of advancing present knowledge of the processes of magma generation and crustal development in the Precambrian.

In spite of their attributes as indicators of prevailing crustal and mantle processes, these rocks have received scant attention in the literature in contrast with their modern counterparts. A combination of factors have probably contributed to the imbalance.

1) Alteration, of variable intensity, is pervasive in Precambrian felsic volcanic rocks owing to their long and often complex history of burial, diagenesis, metamorphism and metasomatism.
2) Commonly recrystallisation, as the result of metamorphism, has obliterated all primary textures making it difficult to positively identify the original rock type and hence its mode of formation.
3) Usually the Precambrian volcanic terrains are deformed with the remainder of the layered sequence, making reconstruction of the original volcanic environment uncertain.
4) Relief in the stable Precambrian shield areas is generally subdued and mountain ranges composed of Precambrian rocks are uncommon. Thus lack of outcrop is a serious problem which inhibits observation, particularly in the third dimension.
5) The tectonic processes which operated during the Precambrian are unknown since unlike modern processes they are not directly observable or measurable.

Although these factors pose formidable obstacles to the study of Precambrian felsic volcanic rocks, much can be learned about them by selecting the study areas for good exposure, minimal metamorphism and deformation and lack of regional alteration.

Using these and other criteria, four areas of Precambrian felsic volcanic rocks have been selected for the purposes of the comparative study undertaken in this thesis work. Two are of Middle Proterozoic age while

---

* In this thesis the term felsic is used for all rocks which contain quartz and/or feldspars as their major component(s).

the other two occur within the Archaean of the Yilgarn Block. An integrated field, petrographic and geochemical approach has been adopted in each case, since it is believed that this offers the most satisfactory method of studying these rocks. The geochemical data has been interpreted with a view to appraising the conditions of formation of the primary magmas and their subsequent crystallisation histories, within the constraints provided by field and petrographic observation.

1.2 AIMS OF THE THESIS

In each of the four studies reported in this thesis the aim was to establish the petrogenesis of the rock suite and to provide a sound basis on which comparisons could be made with other felsic volcanic terrains of similar age. The work was carried out with the intention of investigating a number of general questions.

1) Can general patterns of felsic volcanism be recognised in the Archaean and Proterozoic of Australia?
2) Do the examples studied have analogues in other continents?
3) Are there any secular changes in felsic volcanism between the Archaean and the Proterozoic, both in terms of the origin of the magmas and environment of eruption?
4) What information do the Archaean and Proterozoic felsic volcanic rocks yield concerning the nature of the Precambrian crust and mantle and about the processes that operated to build the Precambrian crust?
5) Do the Archaean and Proterozoic felsic volcanic rocks have any modern analogues?

These questions are evaluated as far as possible within the limitations of the data presented and discussed in this thesis.

1.3 OUTLINE OF THE THESIS

The thesis is divided into three parts, each of which has a common subject. Part 1 is concerned with felsic volcanism in the post-orogenic, Middle Proterozoic period while part 2 deals with felsic volcanic and associated rocks that occur in calc-alkaline centres within Archaean greenstone belts. In both parts, the areas studied in detail form the bulk of the subject matter and in each case reviews are made of the occurrences of these rocks elsewhere in Australia and in other continents.

The first chapter of part 1 (chapter 2) documents the geology, petrography and geochemistry of volcanic and associated rocks in the Lake Everard area which forms part of the vast, post-orogenic 1.5 b.y. Gawler Range volcano-plutonic province of northern Eyre Peninsula, South Australia. Much of this province consists of monotonous and widespread ignimbrite sheets and voluminous comagmatic granites. The Lake Everard area is one of the few regions where a diversity of rock types is exposed and as such it has provided an ideal opportunity to study the earlier volcanic history of this province. The writer's work in this area was associated with a regional mapping program of the South Australian Geological Survey during 1976 and 1977 and subsequently, the writer's detailed mapping has been incorporated on the Gairdner and Childara 1:250,000 geological maps published in 1977.

Analogous 1.1 b.y. volcanics belonging to the Bentley Supergroup in the Blackstone region of Central Australia are the subject of chapter 3. Previous work by the University of Adelaide (Nesbitt, 1966; Blight, 1969; Bowden, 1969) in a portion of this province had resulted in the formulation of possible petrogenetic models which were investigated during the course of the present work.

In chapter 4 the important points arising from the previous two chapters are summarized, and the conclusions drawn are then used as a basis for comparison with published data for other Proterozoic felsic volcanic terrains of similar tectonic setting both in Australia and in other continents.

In part 2, chapters 5 and 6 report the studies of two Archaean felsic volcanic suites in the northern portion of the Norseman-Wiluna greenstone belt in the Yilgarn Block of Western Australia. Much of this work was done in conjunction with a regional geological compilation program currently being undertaken by Dr. Jack Hallberg of the C.S.I.R.O. Division of Mineralogy in Perth.

In chapter 7, the data presented for the two felsic volcanic suites studied in detail (reported in chapters 5 and 6) are combined with additional data for other felsic volcanic rocks in the Yilgarn Block. The general applicability of the findings are then evaluated by comparison with published data for felsic volcanic rocks in other Archaean shield areas.

In the final chapter (chapter 8), which constitutes part 3, the significant points to emerge from the thesis work are drawn together and the implications for Precambrian crustal and mantle evolution are discussed.

The remainder of this chapter is devoted to a number of important subjects including the method of study and the approach adopted in treating the data and dealing with the problem of alteration, so that unnecessary repetition is avoided in subsequent chapters.

1.4 METHOD OF STUDY

It will be evident from the above outline, that the scope of this thesis is quite considerable. A comparative study such as this, like so many before it, runs the risk of being superficial in both the collection and treatment of the data. A conscious effort has been made to avoid these shortcomings in the present case by rigorous adherance to what the writer believes is a sound and proven method of study and data treatment. These aspects will be considered in turn, in the following discussion.

In each of the four areas examined, the same method of study was applied. It involved first of all obtaining a sound understanding of the regional geology and, more particularly, the geology of the area to be sampled. In all areas the detailed geology was unknown and only a broad framework existed and this framework was insufficient, except in the case of the Blackstone region in central Australia, to permit sampling of the range of rock types. Consequently, detailed mapping and division into a number of readily recognisable units was the first step in the study of the four areas. Apart from providing a sound basis for sampling, the mapping yielded valuable information on the nature of the volcanism, the rock relationships and the textural and compositional variation in the volcanic piles.

The majority of the samples collected were sectioned. This permitted selection of not only the freshest samples for analysis but also ensured that the complete textural and compositional range of rock types were analysed. The latter point is often overlooked, but is extremely important since careful selection of the complete petrographic range of samples ensures that any geochemical breaks are not due to sampling bias.

The major elements in the selected samples (excepting Na_2O) were determined using a fully automated X-ray fluorescence spectrometer following the method of Norrish and Hutton (1969). Owing to the oxidized nature of the samples, their FeO and Fe_2O_3 contents bear little relationship to the primary magmatic values, hence only total iron was measured and it is quoted as ferric iron. Na_2O was determined by flame photometer.

TABLE 1.1. Trace element values obtained at the University of Adelaide for international standards.

Standard	AGV-1	AGV-1	BCR-1	BCR-1	BR	BR	DTS-1	DTS-1	G2	G2	GSP-1	GSP-1	W1	W1
	A.U.	R	A.U.	R	A.U.	R	A.U.	R	A.U.	R	A.U.	R	A.U.	R
Zr	227	225	184	190	256	240			308	300	513	500	93	105
Nb	14.5	15	12.5	13.5	115				11.5	13.5	26	29	7.9	9.5
Y	20.2	21.3	39.2	37.1	30	27			9.4	12	25.9	30.4	23	25
Sc	15.0	13.4	31.4	33	24.5		27	3.6	4.2	3.7	6.2	7.1	38	35.1
V	123	125	400	399	269	240	9.9	10.3	36	35.4	53	52.9	271	264
Cr	13.4	12.2	18	17.6	394	420	3992	4000	9	7	13	12.5	139	114
Ni	17.4	18.5	14.2	15.8	258	270	2364	2269	7.3	5.1	16.3	12.5	74	76
Co	19	14.1	39	38	64	50		133	5	5.5	7	6.4	49	47
Rb	67	67	48	46.6	49	45			167	168	250	254	22.5	21
Sr	658	657	334	330	1349	1350			476	479	232	233	191	190
Ba	1188	1208	688	675	1122	1050	1	2.4	1872	1870	1310	1300	159	160

Notes: 1. A.U. refers to value obtained by XRF at University of Adelaide. R refers to the recommended value reported in the literature.

2. The data presented in this table is taken from a compilation by Stanley (1979).

Trace elements, with the exception of complete rare earth elements, were also analysed by X-ray fluorescence using a pressed powder technique (Nesbitt, et al., 1976). Corrections were made for the difference in mass absorption between sample and standard and for inter-element interferences. The trace element values obtained for international standards at the University of Adelaide laboratories are listed in Table 1.1. Sun, et al., (1979) believe that errors for all trace elements, excepting Nb, are within a few percent. In the present case, longer counting times (200 seconds) were used when measuring Nb in order to improve the accuracy.

Rare earth element (REE) contents were determined in particular samples, selected on the basis of their major and trace element geochemistry. The analyses were performed using an isotope dilution method developed by Dr. S.S. Sun at the University of Adelaide. Dr. Sun's method involved chemical separation of the REE on ion-exchange columns (following Arth, written communication, 1973) and measurement, using a technique which suited the operating conditions of the particular mass spectrometer available. The precision for each REE is probably better than 2% (Sun and Nesbitt, 1978).

Particular attention was paid to two aspects of the collection of the geochemical data. Firstly, the contents of a wide range of elements, including those with compatible and incompatible characteristics, were determined in all samples analysed. Secondly, care was taken to ensure that the data obtained was of the highest precision and accuracy. Both factors have great bearing on the confidence that may be placed on the conclusions drawn from the geochemical data.

The complete geochemical data, having been obtained, was then interpreted with a view to arriving at a consistent petrogenetic model. The field and petrographic data were important in providing practical constraints on the various models developed. For example, often simple field observations were able to eliminate complex geochemically-based models, while at other times the field and/or petrographic evidence provided persuasive independent support for a particular model, thus demonstrating the value of an integrated field, petrographic and geochemical study.

1.5 APPROACH TO ALTERATION

An unavoidable aspect of the study of ancient igneous rocks is the effect of alteration. All of the rocks studied were altered to some

degree as the result of their long and often complex history of burial, metamorphism and deformation. Alteration is a serious problem as it casts doubt on the validity and hence usefulness of the geochemistry as a tool in establishing the petrogenesis of rock suites.

The effects of alteration can, however, be minimised by certain approaches which have been adopted in this thesis. The first, and most obvious, is to screen the potential study areas and only work on those that are least altered. This is particularly important in regions such as the Archaean greenstone belts of the Yilgarn Block, where large areas of the volcanic succession may be pervasively carbonated, chloritized or sericitized in contrast to other areas which are little altered. Naturally it is from the latter areas that the most reliable geochemical data may be obtained. The second aspect has been alluded to earlier, viz. of the samples collected only analyse the freshest and least altered, as judged by petrographic observation.

In selecting the freshest samples the following criteria were used:

1) fresh clinopyroxene and/or amphibole phenocrysts;
2) least-sericitized plagioclase phenocrysts,
3) absence of amygdales,
4) least-altered matrix, and
5) minimal amounts of introduced carbonate, chlorite and quartz.

An overriding factor throughout, was the requirement that the complete textural and compositional range be analysed. It was found that good textural preservation was not necessarily synonymous with minimal alteration. Many of the Archaean andesites for example, showed excellent porphyritic textures, yet the phenocrysts of plagioclase and clinopyroxene were often completely sericitized and chloritized, respectively.

Having applied the primary screening and obtained geochemical data for the freshest, least-altered samples, but recognising that these samples are still altered to varying degrees, it is necessary to treat the data in ways that minimise the effects of alteration. This can be achieved in the following manner:

1) By placing most emphasis on the behaviour of the reportedly immobile elements (e.g. Zr, Nb, Y, Ti and REE) rather than the mobile elements (e.g. K, Na, Rb, Sr and Ba; Pearce and Cann, 1973; Smith and Smith, 1976; Winchester and Floyd, 1977).
2) Using as wide a range of elements as possible i.e., both major and minor elements and both compatible and incompatible trace elements, so that a broad data base is established.

3) Only noting variation trends that show minimal scatter, unless the scatter can be shown to be caused by factors other than alteration.
4) By considering patterns of elemental behaviour which are internally consistent (with other elements) and which are consistent with the petrographic and field evidence. This point demonstrates the value of having good field control, which can be used as a cross-check.
5) Comparing the data with that of modern volcanic rock suites, which it is assumed are negligibly altered. This is one reason why, on many of the variation diagrams in this thesis, an average trend compiled from many Cainozoic calc-alkaline suites has been plotted (see section 1.7). If consistent differences are shown by like elements, then the differences are probably real and the data can be treated with confidence. If, on the other hand, the differences (or similarities) are erratic, then the possible effect of alteration may need to be seriously considered.

It is believed that the above approach has produced meaningful geochemical data which can be confidently used to establish the petrogenesis of the Precambrian igneous rock suites studied.

1.6 TREATMENT OF THE GEOCHEMICAL DATA

One of the most convenient ways of examining large amounts of geochemical data involves the use of simple variation diagrams. Because of the compositional range in each of the four rock suites studied, the data for most elements is initially plotted against SiO_2. This has the advantage of "spreading" the data so that meaningful trends become apparent; it also translates the data into a graphical form that is readily interpretable in terms of field names using the generally accepted SiO_2 limits for the divisions of basalt, andesite, dacite and rhyolite. There is, however, an inherent problem with the use of such plots, known as the summation effect (Chayes, 1964). This effect, simply stated, means that as SiO_2 rises, it is an inevitable consequence that the sum of all other elements will decrease in order to maintain constancy in the total; the end result is that trends with no petrogenetic meaning may be produced. This objection does not apply to the trace elements because of their relatively low abundance compared with SiO_2. It could also be argued that the summation effect does not invalidate the use and interpretation of the major element versus SiO_2 plots, because in most cases the percentage decrease in a given major element over a restricted SiO_2 range is considerably greater than the increase in SiO_2 over that

range. Moreover, often the trends evident on the versus SiO_2 plots are verified by other variation diagrams that are independent of the summation effect. Thus although caution is clearly needed when interpreting the major element versus SiO_2 plots, it is believed that their usage is not invalidated by the summation effect. To highlight particular points, not always evident from the versus SiO_2 variation diagrams, other plots are used where appropriate (e.g. AFM, chondrite-normalised REE plots and others).

The various plots are extremely useful in formulating and constraining potential petrogenetic models. However, testing of the possible petrogenetic models is necessary if the study is to be convincing and complete; this can be achieved by quantitative modelling using the geochemical data. Major and trace element modelling was employed in the belief that unless both groups of elements were satisfied, the model could not be regarded as convincing. The major element modelling involved least squares approximation to obtain the best fit in major elements. These calculations required a knowledge of the fractionating or residual mineral compositions. Where possible, these were obtained from electron microprobe determinations of compositions of minerals in the particular samples being modelled. In cases where the mineral compositions could not be determined directly (e.g. mineral in residue or as a result of alteration), estimates were made either from experimental data or from minerals in rocks of similar composition. In all cases the mineral compositions used in the modelling calculations are quoted with the results. All of the cases modelled were tested for a variety of mineral combinations, and the solution quoted is usually the best fit obtainable. The main objection against least squares modelling of the major elements is that the solution is not necessarily unique. However, if the method is used with caution, with a knowledge of the minerals involved either from the petrography or experimental evidence, this ceases to be an objection since it is observed in practice that a unique solution is obtainable in the majority of cases. Wright (1974) considered a least squares solution to be unsatisfactory unless the sum of the squares of the residuals (a measure of the mismatch) is <0.1 In all of the cases considered in this thesis a solution was sought which gave a figure <0.1, although this was not always possible unless one or other of the mobile alkaline elements (i.e. Na or K) was deleted from the modelling calculations.

The trace element modelling used the equation for either surface equilibrium crystal fractionation (Greenland, 1970) or batch partial

melting (using the form of the equation given by Schilling and Winchester, 1967, in which only the residual mineral assemblage at the time of magma segregation is considered), as these seemed most appropriate to the geological processes being tested. A potential error in the trace element modelling calculations is introduced by the uncertainties in the distribution coefficients. Those used in this thesis were taken from Arth (1976), Gill (1978) and Pearce and Norry (1979). The mineral proportions and other parameters (e.g. F) used in the trace element modelling calculations were derived from the major element modelling, thus compounding the possibility for error. The uncertainties in this approach are acknowledged, however in all cases the modelling was applied in a very general way, so that it was only when the discrepancies were too great to be explained by the possible sources of error that a definitive conclusion was drawn. Used in this manner, the major and trace element modelling is a very useful tool, since it can highlight serious difficulties with models which are not always obvious from a qualitative examination of the data. Perhaps the greatest justification for the use of geochemical modelling despite its drawbacks, is that it is a means of gaining the maximum amount of quantitative information out of the geochemistry; it is the writer's opinion that such an approach must lead to petrogenetic models that are more tightly constrained.

1.7 COMPARISONS OF THE GEOCHEMICAL DATA

On many of the variation diagrams a field defined by Cainozoic calc-alkaline volcanic rocks has been plotted to facilitate comparison of the geochemical characteristics of the Precambrian igneous rock suites with modern calc-alkaline volcanic suites. The field of Cainozoic calc-alkaline volcanic rocks was obtained by:

1) Compiling data from the literature for as wide a range of Cainozoic calc-alkaline volcanic rocks as possible, including examples from island arcs, continental margins and intra-continental regions.
2) Plotting the data directly onto SiO_2 variation diagrams.
3) Drawing field boundaries to encompass the plotted data.

The data was taken from a variety of sources which are listed in Table A1.1 (Appendix 1). Volcanics which appeared to be atypical of calc-alkaline suites, such as rocks with shoshonitic or alkaline affinities, were avoided. In all, approximately 120 analyses, many of which are averages, were used to define the fields of the major elements. Unfortunately, the number of trace element analyses available were usually

considerably less, particularly for elements such as Nb, Y, Sc and V, so that the fields in these cases are less well constrained.

Although the Cainozoic calc-alkaline volcanic rocks from the various localities probably have diverse origins in detail, this does not affect the validity of the delineated fields as being representative of such suites. In fact use of a wide data base rather than samples from a single suite, ensures that features of local significance do not bias the Cainozoic calc-alkaline field, thus implying that any consistent geochemical differences between these rocks and those from the Precambrian suites can be taken to be real.

1.8 DEFINITION OF TERMS

Many terms and classification schemes are applied consistently throughout this thesis and it is proposed at this point to briefly examine their usage. In all of the areas studied, three main groups of rocks occurred: extrusive rocks, intrusive rocks and sediments. The terms applicable to each group of rocks naturally differ. The rock names and textural terms used for the igneous rocks were largely taken from the definitions and descriptions given by Joplin (1971).

For the extrusive rocks the names basalt, andesite, dacite and rhyolite were adopted, since they are well known and are readily applicable in the field. In the case of the Gawler Range Volcanics (chapter 2), where a significant number of samples fall near the dacite-rhyolite boundary, the name rhyodacite is also used. Following a consensus of workers, the SiO_2 limits of the fields have been taken as:

basalt-andesite	53%
andesite-dacite	62%
dacite-rhyolite	70%

Where applicable, the rhyodacite field is fitted between 69 and 72% SiO_2. The limits of other fields, such as low-silica dacite and high-silica dacite, are defined when they are used.

The above names are essentially compositional and give no information on the particular origins or textures of the volcanic rocks. Distinction of lavas and pyroclastics requires qualifying terms. Thus "tuff" as used in this thesis always refers to rocks or pyroclastic origin and to this may be added additional qualifers such as crystal, lithic and vitric. For example, a rhyolitic crystal-lithic tuff refers to a pyroclastic rock of rhyolitic composition which contains crystal and lithic components.

The terms used in connection with pyroclastic rocks of ash-flow origin largely follow Smith (1960) and Ross and Smith (1961). Fragmental volcanic rocks, which may originate by a variety of processes, were named according to the guidelines set down by Fisher (1961 and 1966) and Parsons (1971). Some of the terms used in this thesis, are defined below.

1) Ignimbrite, refers to any deposit of ash-flow origin regardless of the degree of welding.
2) Agglomerate, is a volcanic rock containing rounded fragments, and is commonly of pyroclastic origin (incorporating volcanic bombs), or lava-flow origin (rounding due to brecciation and subsequent attrition).
3) Volcanic breccia, contains angular volcanic rock fragments and may form by a variety of methods, including erosion, explosion, flowage and gas-streaming.
4) Blocks correspond in size with cobbles and boulders (i.e. > 64 mm), lapilli with pebbles (2-64 mm), coarse ash with sand (2-1/16 mm) and fine ash with silt and clay (< 1/16 mm).
5) Tuff breccias and lapilli tuffs, are mixed pyroclastic rocks containing block-and lapilli-size lithic fragments respectively, in an ash-size matrix.
6) Vitroclastic, refers to the glassy groundmass textures (e.g. shards, bubbles and pumice) commonly developed in pyroclastic rocks.

The compositional names used for the volcanic rocks (i.e. rhyolite, etc.) are also applied to the associated intrusive rocks if they have similar textures to the volcanics. Thus names such as "porphyritic rhyolite dyke" or "dacite plug" arise. If the intrusive rocks are coarser-grained or their texture differs from the volcanic rocks in other ways, then the appropriate names are used (e.g. granite, diorite, dolerite, gabbro, etc.).

The general term epiclastic is applied to all sedimentary rocks that are composed largely of detritus shed from a volcanic source. The term volcaniclastic, which is commonly used synonymously in the literature, has a wider meaning and in fact includes pyroclastic rocks. The epiclastic rocks of most interest in this thesis are:

1) Greywackes, containing sand-to grit-size volcanic rock fragments and mineral grains derived from the disintegration of volcanic rocks.
2) Lithic wackes, containing an abundance of pebble-, cobble- and boulder-size volcanic rock fragments in a greywacke matrix.
3) Lahars, which are mudflow or mass-flow deposits composed exclusively of volcanic detritus.

PART ONE

FELSIC VOLCANIC AND ASSOCIATED ROCKS OF THE POST-OROGENIC MIDDLE PROTEROZOIC IGNEOUS TERRAINS

Figure 2.1 Regional geology of the Gawler Range volcano-plutonic province.

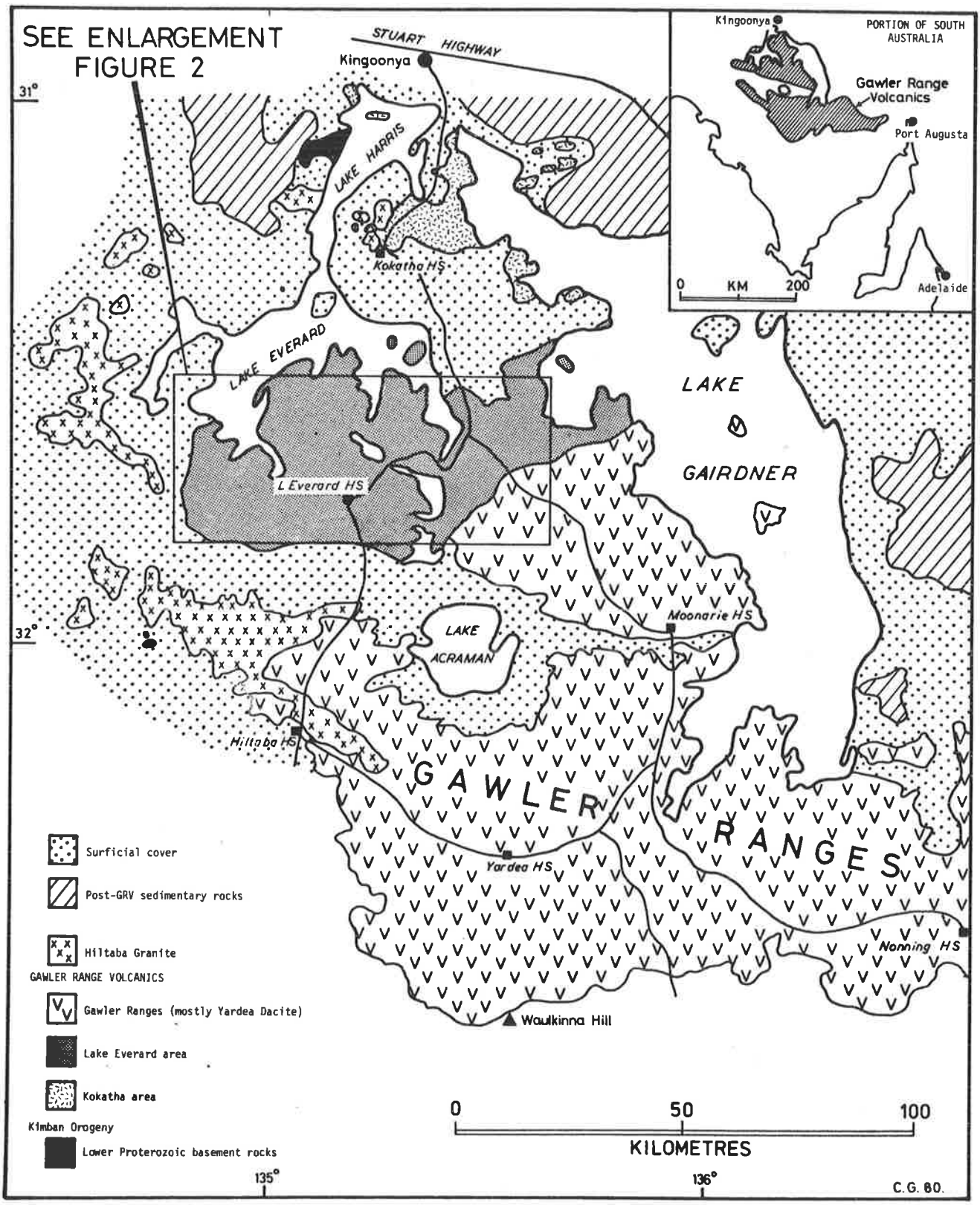

CHAPTER 2

PETROGENESIS OF THE GAWLER RANGE VOLCANICS IN THE LAKE EVERARD AREA

2.1 INTRODUCTION

Rocks comprising the Gawler Range volcano-plutonic province (henceforth, abbreviated to Gawler Range province) cover an area in excess of 25,000 km^2 on northern Eyre Peninsula, South Australia. Principal exposures are found in the Kokatha region, Lake Everard region and Gawler Ranges proper (Fig. 2.1). All volcanic units in the province have been assigned to the Gawler Range Volcanics (GRV), which includes subaerial acid to intermediate ash-flow tuffs and basic lavas (Blissett, 1975). The basalts and andesites are volumetrically minor in comparison with the dacites and rhyolites, occupying less than 1% of the total outcrop area. The widespread Hiltaba Granite, which is believed to genetically related to the acid volcanics, intrudes the volcanic pile in a number of places and forms extensive outcrops to the west of the Gawler Ranges.

The volcanism and plutonism has been dated at roughly 1500 m.y. B.P. and is post-orogenic with respect to the main deformation and metamorphism of the underlying Lower Proterozoic basement, which occurred approximately 1800 m.y. ago (Thomson, 1975). Since their eruption, the GRV have formed part of a stable platform known as the Stuart Shelf, which has remained largely unaffected by subsequent orogenic events manifest in the Adelaide Geosyncline to the east. Consequently, the volcanics are unmetamorphosed and little deformed, except where they are gently warped as the result of the individual or combined effects of: doming by granite intrusions, epeirogenic uplift associated with block faulting, subsidence over evacuated magma chambers or into the roof zones of major granite bodies.

For the purposes of the present study, the Gawler Range province is divided into three subareas that have been defined on combined geographical and geological grounds (Fig. 2.1):

A. The Kokatha area, in which a basal, 400 m thick series of basaltic lava flows overlie deformed, high-grade metamorphic rocks of Lower Proterozoic age. The basalts can be divided into a lower, less evolved suite and an upper differentiated suite characterised by a series of flows with amygdaloidal tops. Thin acid ignimbrites, generally less than 5 m thick, separate some of the basalt flows, which are in turn succeeded

by thick, voluminous dacitic to rhyolitic ash-flow sheets. Within the overlying acid pile, one differentiated basalt unit with a maximum exposed thickness of 20 m, occurs. The volcanic pile is intruded by porphyry dykes and by the laccolithic Hiltaba Granite which forms extensive outcrops in the region.

In a detailed reconstruction of the geological history of the Kokatha area, Branch (1978) cited evidence for an early stratovolcano phase followed by a later caldera phase, similar to that observed in the San Juan ash-flow province of southwestern U.S.A. (Lipman, 1975).

B. The Lake Everard area, where the volcanic pile consists of a series of dacitic to rhyolitic welded ash-flow tuffs with subordinate air-fall tuffs and lava flows (Giles, 1977, see Appendix 2). Andesites and basalts are also present but occupy relatively small outcrop areas. The basalts are confined to one lensoid unit with a total outcrop area of only 2.5 km^2 while the scattered andesites occupy a combined area of 3 km^2 compared with a total outcrop area in excess of 2500 km^2. Numerous dykes and plugs, texturally and compositionally very similar to the acid volcanics, intrude the pile.

C. The Gawler Ranges proper, comprising a vast rhyodacitic to dacitic ash-flow sheet known as the Yardea Dacite (Blissett, 1975). This unit is characterised by remarkably uniform petrographic and geochemical features over most of its 12,000 km^2 outcrop area. It forms a flat-lying blanket cover, and the older sequence of volcanics exposed in the Lake Everard area represents an erosional window in this ash-flow sheet. Where the Yardea Dacite is gently upwarped around the margins of the Gawler Ranges, varied sequences of older ash-flow units are exposed. One such sequence in the vicinity of the Uno arc in the southeast of the Gawler Ranges has been the subject of a petrographic study by Turner (1975), who recognised a series of acid volcanics including crystal tuffs, lithic tuffs and lava flows.

Abundant basic and granitic fragments are found at certain localities within the dacite sheet, possibly representing fragments torn from the vent walls during explosive eruption. In the northern and western portions of the Gawler Ranges, the Yardea Dacite is intruded by large volumes of Hiltaba Granite. The granite extends into sand-dune country up to 300 km beyond the western margin of the Gawler Ranges, where, if the sparse outcrops are a reliable indicator, it assumes batholithic dimensions.

The Lake Everard area was selected for a detailed geochemical study because it contained a variety of fresh igneous rock types and apart from the reconnaissance mapping of Blissett (1975) no work had been done in the region. Because of the large area and scattered outcrops it was necessary to map the region in moderate detail in order to provide a sound basis for sampling. The writer's mapping in the Lake Everard area has been incorporated on the Gairdner and Childara 1:250,000 geological maps (published by the Geological Survey of S.A.), copies of which will be found in Appendix 3. The results of the mapping are considered in the following pages as a preliminary to the detailed discussion of the geochemistry and petrogenesis of the igneous rocks in the Lake Everard area.

2.2 GEOLOGY OF THE LAKE EVERARD AREA

2.2.1 Introduction

The Lake Everard area is a natural geographic region covering approximately 3,000 km^2, bounded by Lake Everard in the north, sand dunes in the west and south, and Lake Gairdner in the east (Fig. 2.1). Sixteen mapping units have been recognised in this area, three having been formally defined by Blissett (1975) and thirteen by the author (Giles, 1977 - see Appendix 3). Of these units, three are composed of intrusive rocks, while the remainder are of volcanic origin and comprise the Glyde Hill Volcanic Complex (Blissett, 1975).

In common with the rest of the Gawler Range province, the volcanic rocks in the Lake Everard area are unmetamorphosed and rarely have dips exceeding 5 degrees. Hence most of the ash-flow tuffs in the region form flat-lying sheets blanketing older volcanic units and because of the low relief much of the earlier volcanic history is obscured. Fortunately, erosion between major ash-flow eruptions and subsequent to volcanism has dissected the succession, enabling an understanding of at least some of the events which have led to the development of the volcanic pile in the Lake Everard area.

In the following discussion, the geological history of the region is examined, based on the mapping and stratigraphy established by the writer (see Figure 2.2 and Giles, 1977 - Appendix 3). The main petrographic features of each of the formally-defined units are summarized in Table 2.1, while in Figure 2.3 photographs illustrating aspects of the field geology are presented.

Figure 2.2 Generalised geological map of the Lake Everard area after Giles (1977).

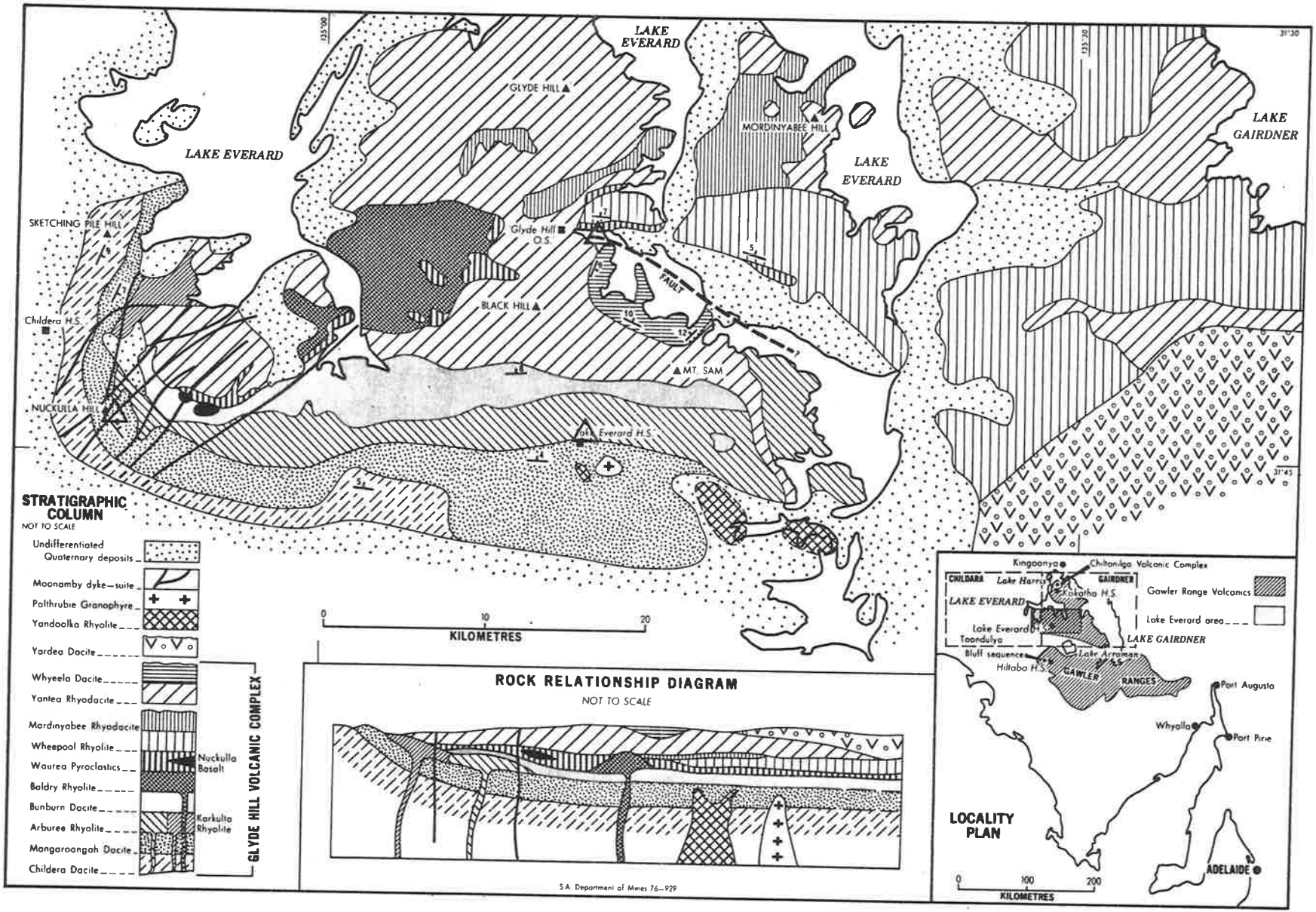

2.2.2 Geological History

The oldest exposed unit in the area is the Childera Dacite, a fine-grained, welded ash-flow tuff characterised by a paucity of phenocrysts. In the west it forms a simple cooling unit, consisting of several welded ash-flow tuff sheets that were probably erupted in rapid succession, ranging from red-brown dacites to dark grey-green low-silica dacites (61-63% SiO_2). As the Lower Proterozoic basement does not crop out in the Lake Everard area, an unknown thickness of unexposed volcanic rocks lie beneath this unit.

Comformably overlying this unit is the compositionally-variable Mangaroongah Dacite, which contains up to 15% phenocrysts. It is of ash-flow origin and forms a composite sheet, consisting of several restricted cooling units that appear to merge into one another. The individual cooling units are welded, grading from rare, dark-green andesites coloured by groundmass chlorite and magnetite to common, red-brown dacites coloured by finely-disseminated hematite. The upper zones of the cooling units are often vesicular and have vapour phase infillings of chlorite, epidote and quartz.

Both of the above units contain abundant basic xenoliths, up to 1 cm in diameter, sometimes as discrete fragments, but more commonly as diffuse clots of chlorite and magnetite. Together the two units delineate an arcuate outcrop pattern, swinging from the west to the south of the mapped area (Fig. 2.2).

Following extrusion of the Mangaroongah Dacite extensive explosive volcanism in the area ceased, and two domes, represented by the Karkulta and Arburee rhyolites, developed. The domes are largely built of rhyolitic lavas, which frequently show zones of contorted flow-banding, with wavelengths up to 10 m in the primary flow folds. Blocks of rhyolite, up to several metres across, within a flow-brecciated rhyolitic matrix are common in the zones of extreme flow folding. They are interpreted to represent the detached parts of flow folds which have been subsequently rotated during movement of the surrounding partially solidified lava.

The Arburee Rhyolite both conformably overlies and intrudes the Mangaroongah Dacite, consistent with its origin as a lava dome. A lower erosional section in the west of the mapped area has revealed the intrusive nature of the feeder. Here, the Arburee Rhyolite is cross-cutting and small dykes and plugs of rhyolite radiate from the margins of the dome into the Mangaroongah Dacite, which shows evidence of contact

TABLE 2.1. A summary of the petrographic features of the rock units in the Lake Everard area.

ROCK UNIT (in stratigraphic order)	ORIGIN	PERCENTAGE OF PHENOCRYSTS IN ROCK	COMPOSITION OF PHENOCRYSTS								COMPOSITION OF GROUNDMASS						COMMENTS
											Qtz. and K-feldspar						
			Quartz	K-feldspar	Plagioclase	Clinopyroxene	Chlorite, after cpx	Orthopyroxene	Biotite	Magnetite	Devitrified mosaics	Granophyric	Microlitic	Microlitic-plagioclase, Qtz. rare	Chlorite alteration	Opaque minerals	
Moonamby dyke suite	Comagmatic intrusive dykes.	25-45	▲	▲	▲		▲			△		●					Range in composition from dacite to rhyolite.
Palthrubie Granophyre	Comagmatic intrusive plug.	-	▲	▲	▲							●					Non-porphyritic, granophyric texture.
Yandoolka Rhyolite	Comagmatic intrusive plug.	50-60	▲	▲	▲		▲			△		●					Phenocryst-rich rock. Contains accessory zircon, apatite and sphene.
Yardea Dacite	Welded ash-flow tuff. Simple cooling unit.	30-40			▲	▲	▲			△		●			●	●	Widespread unit, forming Gawler Ranges proper.
Whyeela Dacite andesitic variant	Welded ash-flow tuff.	8-10		△	▲	▲	△	△		△			●		●	●	Youngest named unit of the Glyde Hill Volcanic Complex in the Lake Everard area.
		6-8			▲	▲	▲	△		▲				●	●	●	
Yantea Rhyodacite	Welded ash-flow tuff. Compound cooling unit.	14-16	△	▲	▲		▲			△		●					Widespread unit in the Lake Everard area. Vitroclastic textures occasionally preserved.
Morbinyabee Rhyodacite	Welded ash-flow tuff.	8-10		△	▲		▲			△	●		●		0		
Wheepool Rhyolite	Welded ash-flow tuff.	15-25	▲	▲	▲						●						Widespread unit in the east of the Lake Everard area.
Nuckulla Basalt	Series of lava flows	-			▲	▲	▲			▲							Pilotaxitic texture, of limited areal extent.
Waurea Pyroclastics	Non-welded lithic tuff of ash flow origin	4-5	▲	▲	△						●						Up to 60% lithic fragments of lapilli and block size in an ash-size matrix.
Baldry Rhyolite	Series of flow-banded lavas and lapilli-tuffs of ash flow origin	6-7	▲	▲	△						●						Up to 40% lithic fragments in pyroclastics. Flows contain abundant spherulites and amygdales.
Bunburn Dacite andesitic variant	Welded ash-flow tuff.	2			▲						●		●			●	Much very fine-grained plagioclase in groundmass.
		4			▲		▲			▲				●	●	●	
Arburee Rhyolite	Series of lava flows forming a linear dome	20-35	▲	▲	▲						●						Commonly shows contorted flow-banding and flow-brecciation.
Karkulta Rhyolite	Series of lava flows forming a localised dome	5-8	▲	△	▲				▲	▲	●						Flow-banding and flow-brecciation common. Epiclastic scree locally developed.
Mangaroongah Dacite andesitic variant	Welded ash-flow tuff.	9-11		△	▲	▲	△	△		△			●		●	●	Contains numerous basic xenoliths with diffuse margins, up to 1 cm across.
		6-7			▲	▲	▲	△		▲				●	●	●	
Childera Dacite	Welded ash-flow tuff.	2-5			▲	▲	▲			▲			●	●	●	●	As for Mangaroongah Dacite.

metamorphism. To the east, strictly conformable relationships are observed between these two units. For example, near Lake Everard Homestead, fragments of Mangaroongah Dacite can be seen within the basal flows of the Aburee Rhyolite. Presumably the fragments have been incorporated as the flows have moved passively over the top. Owing to the viscosity of acid lavas, it is unlikely that the rhyolitic flows comprising the Arburee Rhyolite have moved far from their site of eruption. Therefore the present linear outcrop form of the Arburee Rhyolite may be indicative of eruption from a long fissure.

The Karkulta Rhyolite, although occurring at the same stratigraphic level as the Arburee Rhyolite, can be readily distinguished on petrographic grounds. It is the only unit which contains biotite as a phenocryst component. The biotite occurs in association with plagioclase, often in glomeroporphyritic aggregates, and both minerals are set within a buff-coloured devitrified matrix. Most of the rhyolite was erupted as lava flows and zones of flow-brecciation are common. Immediately to the south of this unit there are localised outcrops of a breccia which contains close-packed, angular, cobble- and pebble-size fragments, exclusively of Karkulta Rhyolite. The absence of a glassy matrix supports the interpretation that this rock originated as a epiclastic gravel or scree, derived by local erosion of the Karkulta Rhyolite dome.

The Bunburn Dacite, a sparsely-porphyritic, welded ash-flow tuff overlies both the Karkulta Rhyolite and Arburee Rhyolite. It forms a variable-thickness simple cooling unit, with a zone of poorly-welded lapilli tuff at the base. In places, a zone of pervasive autobrecciation occurs near the top of the unit and this is attributed to the effects of gas streaming. This unit is particularly high in Al_2O_3, Na_2O and K_2O reflecting an abundance of feldspars in the fine-grained groundmass.

Subsequently, a variety of acid rock types ranging from flow-banded lavas to poorly-welded lapilli tuffs were erupted in a localised area, forming the Baldry Rhyolite. The most common rock type is a welded, lithic-vitric-crystal tuff which has a well-developed eutaxitic texture defined by flattened lithic and pumice fragments. Unlike the voluminous ignimbrite sheets comprising other units, the ash-flow tuffs within this unit appear to be localised and together with the lava flows have built a domal structure. Some of the rocks show contorted flow banding, yet still preserve original vitroclastic textures which are indicative of a pyroclastic origin. They are interpreted to be rheoignimbrites (Schmincke and Swanson, 1967) or ignimbrites that have moved as a mass by laminar flow following deposition, probably due to eruption onto a

slope. Rhyolites with persistent steeply-dipping flow-banding have also been noted and may represent feeders or eroded remnants of small lava domes.

The Waurea Pyroclastics conformably overly the Baldry Rhyolite and consist of poorly-welded lapilli tuffs with localised tuff breccias. The lapilli and blocks are unsorted and are composed of a variety of volcanic rock types, the most common being a flow-banded rhyolite resembling the Baldry Rhyolite. Features such as the lateral extent, uniformity over a wide area and lack of sorting and bedding indicate an ash flow rather than an air fall origin for this unit. Tuff breccias, with blocks up to 1 m across, occur near the centre of the mapped area and are unlikely to have been deposited far from an original vent. The size of the accidental blocks decreases to the west and near the Nuckulla Basalt the unit consists in part of finely-bedded air-fall tuffs presumably distal to the vent.

The Nuckulla Basalt is both overlain and underlain by what are considered to be lateral equivalents of the Waurea Pyroclastics. It is composed of a series of lava flows with amygdaloidal flow-tops and is of restricted areal extent. To what degree the restricted area reflects the limited volume of basalt erupted or blanketing by later ignimbrite sheets is uncertain.

A return to voluminous explosive volcanism followed, with the eruption of the Wheepool Rhyolite, a simple cooling ash-flow unit which crops out extensively in the east of the mapped area. It shows patchy and snowflake devitrification textures typical of the fine-grained groundmass of many of the rhyolitic ash-flow units in the region. In hand specimen, the Wheepool Rhyolite can appear very similar to the Arburee Rhyolite but as the rock relationship diagram shows (Fig. 2.2) the two units are at different stratigraphic levels and therefore cannot be lateral equivalents.

After the eruption of a further rhyodacitic ash-flow unit termed the Mordinyabee Rhyodacite, a significant period of erosion occurred, during which some of the existing units were partially removed and thin epiclastic sediments deposited. The sediments are poorly-sorted and consist of sub-rounded volcanic fragments in a silty, immature matrix, suggesting they were derived by rapid erosion of a local source.

Outpouring of the distinctive, and widespread, Yantea Rhyodacite followed. As a result of the preceding erosional interval, this unit is observed to disconformably overlie a number of older units and in

Figure 2.3. Photographs illustrating aspects of the field geology.

A. ERTS photograph of the northern portion of the Gawler Range volcano-plutonic province. Lakes Gairdner, Acraman and Everard occupy the central, southwestern and western areas, respectively. The prominent jointing in the ignimbritic Yardea Dacite is clearly visible.

B. Outcrop of lapilli-tuff member of Waurea Pyroclastics. The unsorted lapilli, and occasional blocks, are spaced by ash-size material.

C. Tuff-breccia member of Waurea Pyroclastics. Angular blocks up to 50 cm in diameter occur within an ash-and lapilli-size matrix.

D. Lapilli-tuff member of Waurea Pyroclastics. Closely-packed angular lapilli of flow-banded rhyolite are contained within ash-size material.

E. Contact of Mangaroongah Dacite (lower, grey in colour) and Arburee Rhyolite (upper, and porphyritic). As the basal lava flows of the Arburee Rhyolite moved over the Mangaroongah Dacite they evidently engulfed fragments of the latter and themselves became brecciated.

F. Flow-brecciation within Arburee Rhyolite. As the viscous acid lavas moved, flow bands developed and these were contorted in flow folds. Subsequent flowage disrupted the flow folds and produced the randomly-oriented blocks observed.

G. Outcrop of rhyolite dyke, one of many comprising the Moonamby dyke-suite.

H. Porphyritic texture, typical of that in rocks from the Moonamby dyke-suite. Comprised of phenocrysts of coarse-grained K-feldspar (commonly showing evidence of concentric growth), medium- to coarse-grained, euhedral plagioclase and medium-grained, anhedral quartz (dark), set in a microgranophyric quartz-feldspar matrix. F.V. 14 cm.


A


B


C


D


E


F


G

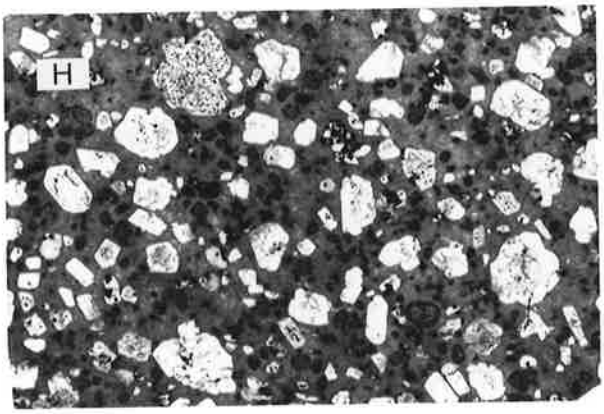
H

places occupies erosional channels in them. The best example of this is seen 10 km to the east of Lake Everard homestead, where a tongue of rhyodacite, superficially resembling a dyke, occupies a palaeovalley cut in the Arburee Rhyolite (Fig. 2.2). One of the rare occurrences of sediment in the volcanic pile occurs between these two units along the margins of the ancient valley. Also, in the far east of the mapped area, another valley-fill occupied by Yantea Rhyodacite has been found, but here the valley has been developed in the Wheepool Rhyolite and associated sediments were not observed.

The Yantea Rhyodacite is a compound cooling unit and is composed of at least four individual welded ash-flow tuff members separated by thin, non-welded tuffs and lapilli tuffs. Typically, the welded tuffs are brick-red in colour and are characterised by microgranophyric intergrowths of quartz and orthoclase in the groundmass, reflecting the relatively slow cooling conditions prevailing within the thick tuff sheets. By contrast, the intervening poorly-welded tuffs and lapilli tuffs are buff-coloured and have well-preserved vitroclastic textures. They are usually less than 10 m thick and merge with the overlying and underlying welded tuffs via zones of vapour phase minerals, flow-brecciation and/or coarse rubble at the base of the tuff sheets.

The Yantea Rhyodacite is conformably overlain by the Whyeela Dacite, which is the youngest member of the Glyde Hill Volcanic Complex. This unit is a welded, ash-flow tuff similar in many respects to the older Mangaroongah Dacite, and it forms an inward-dipping arc, the possible significance of which will be discussed later.

In the east of the mapped area, the voluminous Yardea Dacite ignimbrite sheet disconformably overlies the Wheepool Rhyolite and an erosional remnant of the Yantea Rhyodacite, thus indicating that the Glyde Hill Volcanic Complex was eroded prior to eruption of the Yardea Dacite. In the mapped area, as in the Gawler Ranges to the south, the Yardea Dacite consists of a simple cooling unit at least 150 m thick, with a zone of black dacite at its base (c.f. Blissett and Radke, 1979). The basal, black dacite has suffered less recrystallisation during devitrification than the remainder of the sheet and often shows fragmented phenocrysts and vitroclastic textures attesting to the pyroclastic origin of the Yardea Dacite.

The Hiltaba Granite, although it occurs to the west and south of the Lake Everard area, does not actually intrude the volcanic pile in this region. However, the Palthrubie Granophyre, which forms a circular

plug cutting the volcanic pile near Lake Everard Homestead, may, on the basis of its compatible mineralogy and geochemistry, be a high-level apophysis of the Hiltaba Granite. The other intrusive units mapped appear to have more direct affinities with the acid volcanic rocks, owing to their porphyritic nature. For example, the Moonamby dyke-suite consists of a series of porphyritic dykes that range in composition from dacite to rhyolite, while the Yandoolka Rhyolite contains up to 60% phenocrysts of plagioclase, K-feldspar and quartz and may represent the eroded feeder to an ash flow now removed by erosion.

2.2.3 The source of the volcanic rocks

In volcanic terrains such as the one described here, questions arise as to the location and nature of the edifices from which the magmas have been erupted. Steven and Lipman (1976) in their studies of the San Juan volcanic field of southwestern U.S.A. have been able to relate each major ash-flow sheet to a particular source caldera. Branch (1978) has applied this concept to the Kokatha area, where he has recognised the Chandabooka Caldera, to which he is able to relate many of the acid volcanic units. Blissett (1975) on the other hand, in his regional appraisal failed to find any evidence for cauldron subsidence and interpreted the volcanic pile as a simple layered succession.

The volcanic units in the Lake Everard area are not directly correlatable with those in the Kokatha area and thus it is inferred that they were derived from separate sources. If the analogy with the San Juan ash-flow field is applied, then up to six calderas might be expected, corresponding to the six major ash-flow sheets recognised in the region. However, conclusive evidence for cauldron subsidence structures in the Lake Everard area is lacking. This could be because cauldron subsidence did not in fact occur, as might be the case if eruptions were from linear fissures. Alternatively, cauldron subsidence might have occurred, but owing to faulting, erosion, concealment by later ash flows and lack of outcrop, the evidence for it is not obvious.

There is evidence that at least some units were not erupted from cauldron subsidence structures. For example, the case of the Arburee Rhyolite, which probably developed along a linear fissure, approximately 50 km in length, has been previously cited. The dyke structure referred to by Turner (1975) at the southeastern margin of the Gawler Ranges, provides a further example outside of the Lake Everard area. This structure is roughly 8 km long and is, on average, 0.75 km wide. Drilling

Figure 2.2 Generalised geological map of the Lake Everard area after Giles (1977).

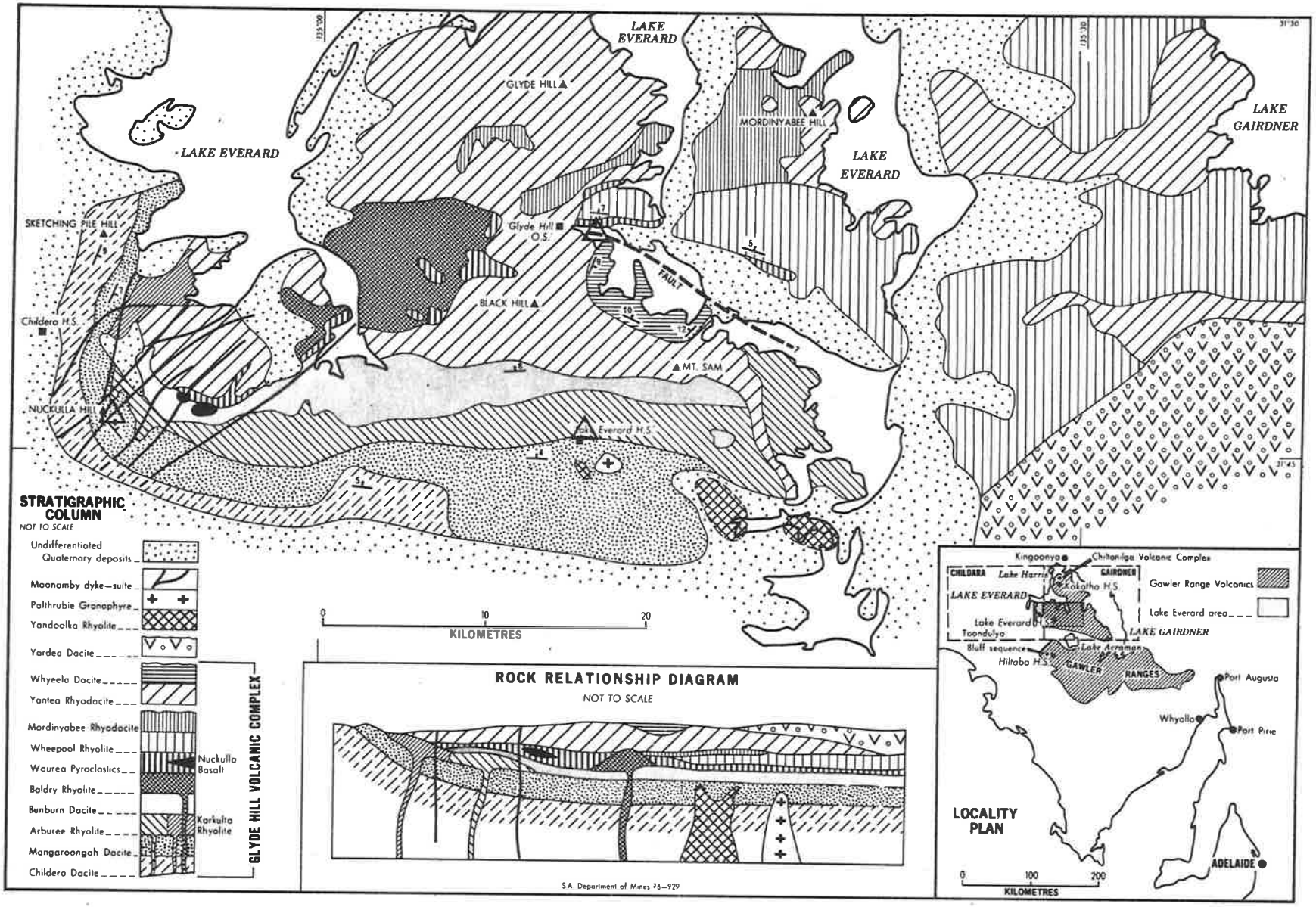

by the South Australian Department of Mines and Energy has conclusively demonstrated the intrusive nature of this body. The dyke, which is petrographically similar to the ignimbrite sheets comprising the Gawler Ranges to the north, could be occupying a fissure from which much of the volcanic material in the vicinity was erupted.

A similar interpretation could be placed on the numerous plug-like bodies (e.g. Yandoolka Rhyolite) that intrude the volcanic pile in the Lake Everard area, viz. they may be occupying the conduits from which the volcanic rocks were erupted. Alternatively, they may simply represent high-level intrusions derived from the same differentiation chambers as the volcanic rocks. Unfortunately erosion has destroyed the critical field relationships, so that distinction between these alternatives cannot be made with certainty in the Lake Everard area.

The only feature in the Lake Everard area which could conceivably be viewed as an expression of central-type subsidence is the semicircular structure defined by the inward-dipping Whyeela Dacite (Fig. 2.2). The Whyeela Dacite conformably overlies the Yantea Rhyodacite around the margins of this structure, often being separated from it by a thin, poorly-welded lapilli tuff, although in the east a narrow rhyolite dyke with diffuse contacts separates the two units for a short distance. Further observations are restricted because the centre of the structure is obscured by a salt lake and the northern portion has been faulted off. There is, however, some indirect evidence that this subsidence feature may have had an influence on volcanism:

1) The coarsest blocks in the Waurea Pyroclastics (up to 1 m across) occur immediately north of the fault and grade finer to the west.
2) The Yantea Rhyodacite is thickest in this vicinity and it is only here that it contains abundant, large granitic xenoliths. The xenoliths are porphyritic and have extremely diffuse margins probably due to partial assimilation.
3) The Whyeela Dacite is confined to this area alone.

Despite these observations, the field characteristics of this feature do not support the interpretation that it represents a cauldron subsidence structure in the strict sense. It is notable that the Childera Dacite and Mangaroongah Dacite also define an arcuate structure, but on a more regional scale. Coincidently, granite crops out to the west and south of the Lake Everard area in proximity to these units, so that their inward dips may be the result of upwarping caused by granite intrusion. This interpretation is consistent with the general observation that

around the margins of the Gawler Ranges, the otherwise flat-lying ignimbrite sheets are upwarped wherever they are in close proximity to granite. Thus the subsidence or downwarping in the centre of the Lake Everard area may be a relative effect only, caused by the tilting or upwarping of the (present) margins of the volcanic pile due to the uprise of diapiric granite plutons. In the absence of other evidence, this hypothesis appears to offer the most plausible explanation for the arcuate outcrop patterns of the volcanic rocks in the Lake Everard area, both on a regional and local scale.

In summary, mapping in the Lake Everard area has permitted recognition of a number of volcanic and intrusive units. This in turn has allowed a simple, although undoubtedly simplistic, reconstruction of the geological history of the region. The stratigraphy established and the understanding of the geology gained, provided a sound basis for the sampling program.

2.3 PETROGRAPHY

Brief thin section descriptions of approximately 120 representative rocks from the Gawler Range province, mostly from the Lake Everard area, are given in Appendix 1 (Table A2.1). This discussion summarizes the conclusions drawn from examination of these thin sections, and for further petrographic details the reader is referred to Appendix 1. Petrographic descriptions of each of the formally-defined units are given in Table 2.1 and in Figures 2.4 and 2.5 photomicrographs are presented for many of the features described below.

In this study the volcanic rocks have been divided into basalt, andesite, dacite, rhyodacite and rhyolite using the SiO_2 limits of 53, 62, 69 and 72% respectively. These categories are defined mainly for convenience of reference, since the petrographic boundaries between andesite, dacite, rhyodacite and rhyolite are in this case all gradational. Nevertheless, the "typical" members of each group have petrographic characteristics quite distinct from the "typical" members of other groups and it is the distinctive petrographic characteristics of each group that are described below.

2.3.1 Basalts

The Nuckulla Basalt is a fine-grained rock with a well-developed pilotaxitic texture defined by oriented, felted plagioclase microlites;

granular clinopyroxene and magnetite comprise the remainder of the rock. The upper parts of the individual lava flows contain scattered, chlorite-filled amygdales. Many of the Kokatha basalts have a similar texture, although hyalopilitic, intersertal and subophitic types are also represented, with the latter textural type sometimes containing chlorite pseudomorphs after olivine.

2.3.2 Andesites

The andesites are invariably porphyritic, containing roughly equal proportions of euhedral plagioclase (andesine), clinopyroxene (augite) and magnetite phenocrysts, set in a matrix of chlorite, plagioclase microlites and devitrified glass. The plagioclase microlites occasionally define a pilotaxitic texture, but more commonly show an intersertal texture indicative of abundant original glass. The glass is now represented by an aphanitic, iron-stained felsic mosaic, containing indeterminate proportions of plagioclase, K-feldspar, chlorite and quartz.

2.3.3 Low-silica dacites (< 65% SiO_2)

With an increasing abundance of quartz and hematite-stained K-feldspar in the matrix, and a decrease in the proportion of clinopyroxene phenocrysts and chlorite in the groundmass, andesite grades into low-silica dacite. The dominant phenocrysts in order of abundance are: plagioclase, clinopyroxene and magnetite. The groundmass usually consists of a devitrified mosaic of quartz and K-feldspar, with lesser amounts of plagioclase, chlorite and magnetite. Commonly, in the less welded examples, vitroclastic textures and amygdales, containing infillings of quartz and chlorite, are observed.

Both the andesites and low-silica dacites contain abundant basic xenoliths consisting of diffuse clots of chlorite and magnetite. They have indistinct margins, indicative of partial assimilation, and unlike the basic xenoliths in the Yardea Dacite they do not preserve any primary textures that are suggestive of a basaltic parentage. Their altered and partially assimilated character may indicate that they represent fragments from near the site of melting.

2.3.4 High-silica dacites and rhyodacites

These dacites are distinguished from the low-silica dacites mainly by the nature and mineralogy of the groundmass. In this case the matrix consists of quartz and K-feldspar with very rare plagioclase, in a variety of intergrowths including microlitic, microgranular and micrographophyric. The coarsest microgranophyric intergrowths are confined to the thick ash-flow sheets (e.g. Yardea Dacite, Yantea Rhyodacite) in which cooling conditions were evidently relatively slow, probably comparable with that existing in intrusive sills. Evidence for an ash-flow origin is seen in the occasional zones of severely-fractured crystals and by the preservation of vitroclastic textures in zones of less intense welding.

The phenocrysts are similar in composition to those in the andesites and low-silica dacites (i.e., andesine plagioclase and augitic clinopyroxene) and occur as isolated euhedral crystals and in glomeroporphyritic aggregates. Generally, the proportion of plagioclase: clinopyroxene is greater in the high-silica dacites than in the andesites, and usually all phenocrysts are more altered.

The Yardea Dacite is by far the most voluminous of the high-silica dacites in the Gawler Range province, and it contains abundant basic and acid xenoliths. The basic xenoliths have sharp boundaries and appear to have been completely solid at the time of incorporation. They are usually plagioclase-rich and have distinctive intersertal to hyalopilitic textures, indicating that they are probably accessory basaltic rock fragments that were torn from the vent walls during eruption. By contrast, the acid xenoliths, including a variety of granites and porphyries, have extremely diffuse margins indicative of partial assimilation. Commonly, coarse feldspar megacrysts have been released from their original granitic host to form isolated xenocrysts in the dacite.

Three important questions are raised by the preceding petrographic observations:

1) The origin of the glomeroporphyritic plagioclase - clinopyroxene aggregates in the high-silica dacites.
2) The reason for the non-equilibrium phenocryst and groundmass assemblages, seen for example in the plagioclase (andesine) and clinopyroxene phenocrysts, which are contained within a matrix of quartz and K-feldspar.
3) The significance and origin of the acid and basic xenoliths.

Figure 2.4. Photomicrographs of selected thin sections.

A. Typical textures in high-silica dacites and rhyodacites. Phenocrysts of complexly-twinned plagioclase and embayed quartz occur in a microlitic to microgranophyric matrix. F.V. 7 mm. B, C and D highlight some details of the plagioclase textures in these rocks.

B. Composite, glomeroporphyritic plagioclase "phenocryst". The individual fine-grained crystals have been moulded to each other along sinuous contacts. F.V. 4 mm.

C. As for B. F.V. 6 mm.

D. Detail of a composite plagioclase "phenocryst", demonstrating that in this case, the diverse cleavage orientations are produced by different crystals. F.V. 2.5 mm.

E. Low-silica dacite, showing tabular, fine- to medium-grained plagioclase phenocrysts in a glomeroporphyritic aggregate, set in an intersertal matrix composed of altered glass and randomly-oriented plagioclase microlites. Amygdales infilled with quartz and chlorite are visible to the right and bottom left. F.V. 4 mm.

F. Glomeroporphyritic aggregate of biotite and partially-sericitized plagioclase, set in a devitrified glassy matrix. From Karkulta Rhyolite. F.V. 4 mm.

G. Typical example of the phenocryst-rich Yandoolka Rhyolite, with phenocrysts of angular quartz (crystal chips), twinned plagioclase and partially-sericitized K-feldspar set in a microgranophyric matrix. F.V. 7 mm.

H. Detail of the matrix of the Yardea Dacite, demonstrating the microgranophyric quartz-K-feldspar intergrowths. The dark patches are sericitized plagioclase and chlorite-magnetite intergrowths. A fine-grained, sericitized plagioclase phenocryst is visible near the centre. F.V. 2.5 mm.

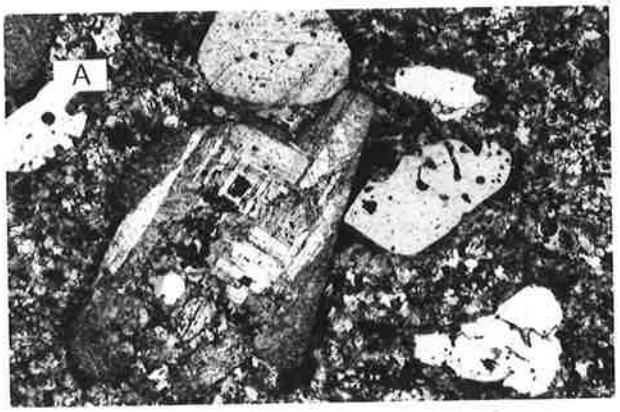
A

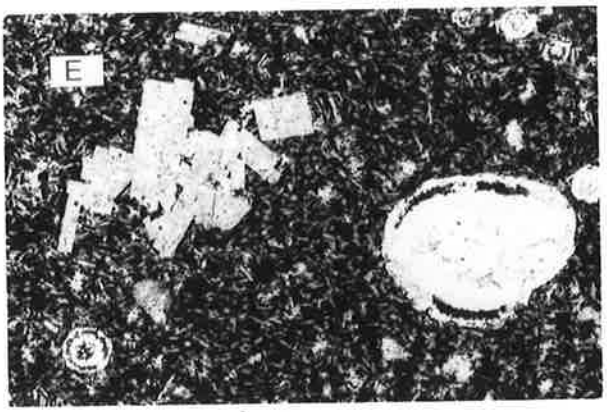
E

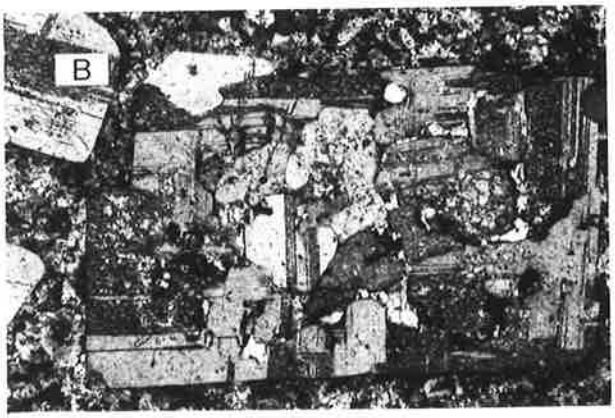
B

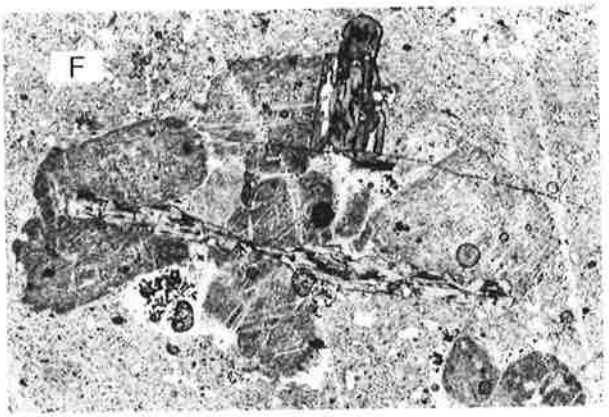
F


C

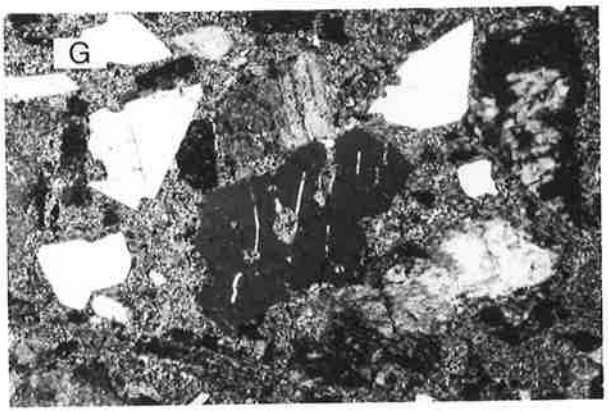
G

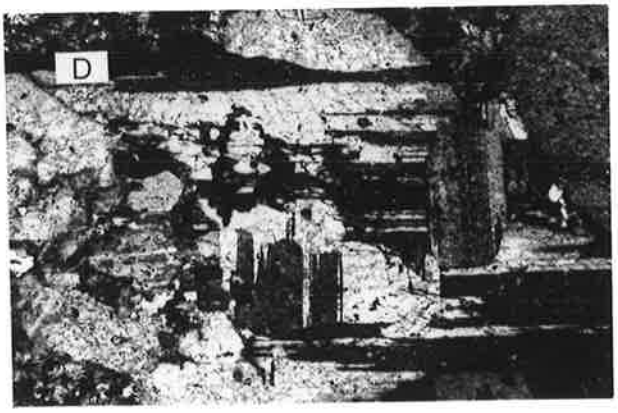
D


H

Similar glomeroporphyritic clinopyroxene - plagioclase aggregates have been recorded by Flood, et al., (1977) in rhyodacitic ignimbrites from the New England region, N.S.W. They considered the aggregates could be either disrupted crystal cumulates or modified restite, and both of these alternatives could apply to the glomeroporphyritic aggregates in the Yardea Dacite. There are several petrographic observations which have bearing on the restite versus crystal cumulate hypothesis and these are summarized below:

1) The isolated plagioclase and clinopyroxene phenocrysts are invariably euhedral. When the phenocrysts occur in glomeroporphyritic aggregates contact is along the crystal faces, hence sharp boundaries are seen between individual phenocrysts in the aggregates. This texture supports synneusis or aggregation of phenocrysts such as might occur in a magma chamber (e.g. Vance, 1969). If the aggregates or individual phenocrysts were restite from a basement source, they might be expected to have anhedral crystal faces and show a granoblastic texture, neither of which are observed (c.f. Flood, et al., 1977).
2) The texture and composition of the Yardea Dacite is extremely uniform over a vast area (> 25,000 km^2). Correspondingly, the compositions of plagioclase (andesine) and clinopyroxene are also extremely uniform. Neither of these observations are indicative of random addition of restite to melt, but rather they are suggestive of controlled conditions of crystal fractionation in a magma chamber.
3) If a granulitic residue remained, orthopyroxene might be predicted as an abundant restite component, however no orthopyroxene has been noted in the Yardea Dacite.
4) Occasionally, rounded "eyes" of clinopyroxene are seen within plagioclase phenocrysts, indicating crystallisation from a melt.

The above observations suggest that the clinopyroxene and plagioclase phenocrysts are not restite from the site of melting, but rather, are accumulative crystals possibly fractionated from an andesitic or low-silica dacitic melt in a crustal magma chamber. Processes of synneusis or gravity settling may have caused aggregation of the crystals. Subsequent engulfment of the crystals by a potassic liquid, yielded by prolonged fractionation, could offer an explanation for the non-equilibrium between crystals and matrix in the high-silica dacites.

The basic and acid xenoliths are interpreted to be fragments either incorporated as the crystal-liquid mush moved towards the surface or

torn from the vent walls during explosive eruption. This view is supported by the non-refractory nature of the acid xenoliths and the igneous textures preserved in both the basic and acid xenoliths. Many of the acid xenoliths for example, are leucocratic quartz-bearing gneisses, granites and porphyries, some of which are similar to rock types exposed in basement outcrops adjacent to the Gawler Ranges. The basic xenoliths commonly show pilotaxitic textures, indicative of a lava-flow origin. These xenoliths, with their sharp margins, contrast markedly with the diffuse, textureless basic xenoliths observed in the andesites and low-silica dacites.

The rhyodacites have similar textures and mineralogy to the high-silica dacites and are distinguished only by their higher proportion of plagioclase phenocrysts relative to clinopyroxene and magnetite. Clinopyroxene in these rocks is invariably altered to green chlorite, which preserves the euhedral outlines of the original phenocrysts.

The plagioclase phenocrysts are superficially extremely complex, and show diverse orientations of combined pericline - albite twinning within the one phenocryst. Closer examination reveals that these phenocrysts consist of numerous smaller phenocrysts in close-packed glomeroporphyritic aggregates. This is not obvious from a cursory inspection because the microphenocrysts are usually moulded to each other along sinuous contacts. Occasionally small grains of magnetite and clinopyroxene occur along the crystal boundaries. The texture, although differing from the loose glomeroporphyritic aggregates characteristic of the Yardea Dacite, does not resemble that of a granular, metamorphic aggregate and therefore is not considered to indicate the presence of restite. It is more likely that this texture has resulted from partial bonding of crystals, perhaps as a consequence of gravity settling and close proximity of crystals in the basal parts of a hot magma chamber.

It follows that the origin of the rhyodacites is probably similar to that proposed earlier for the high-silica dacites. The geochemical differences are attributed mainly to a higher proportion of matrix (quartz + K-feldspar) in the case of the rhyodacites. This in turn was probably dependent upon the conditions of magma separation and availability of crystals in the magma chamber.

2.3.5 Rhyolites

The rhyolites are characterised by K-feldspar and quartz phenocrysts, although plagioclase is still common as a phenocryst component. In the

Figure 2.5.1. Photomicrographs of selected thin sections. All of the samples photographed belong to the Baldry Rhyolite.

A. Zone of flowage, marked by continuous flow bands, within an otherwise shard-rich ash-flow tuff. F.V. 20 mm.

B. Vitroclastic textures indicative of only minor welding and compaction within the ash-flow tuff unit. F.V. 12 mm.

C. "Fiamme" (i.e., glassy, lithic fragments with ragged ends), and quartz phenocrysts set in a flattened, shard-rich matrix. F.V. 15 mm.

D. Vitroclastic groundmass textures in a moderately-welded, crystal-lithic ash-flow tuff. F.V. 10 mm.

E and F. Detail of the flattened, shard-rich matrix in moderately-welded ash-flow tuffs. A measure of the degree of compaction is provided by the draping of the glass shards around the quartz phenocrysts and lithic fragments. Although many shards are quite contorted, some, particularly those in the pressure shadow regions surrounding the rigid phenocrysts and lithic fragments, still preserve delicate shapes. E, F.V. 6 mm; F, F.V. 4 mm.

G. Strongly-welded ash-flow tuff in which the original glassy fragments have been greatly flattened and contorted. Syn-welding flowage has produced semi-continuous flow bands and has obliterated the vitroclastic textures in the groundmass. F.V. 2 mm.

H. Flow-banded rhyolite. The continuity of the flow bands in this sample and its field relationships indicate a lava flow rather than a pyroclastic origin (c.f. G). F.V. 7 mm.

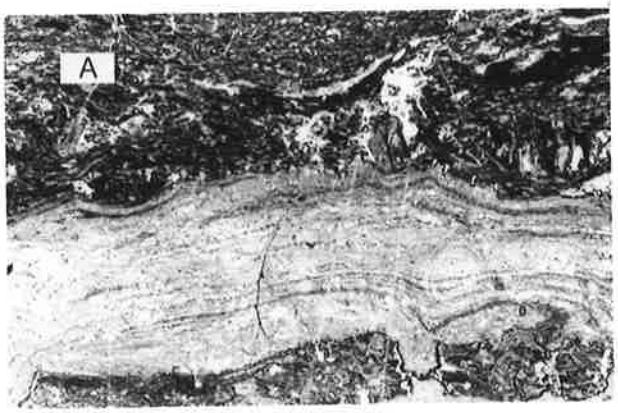
A

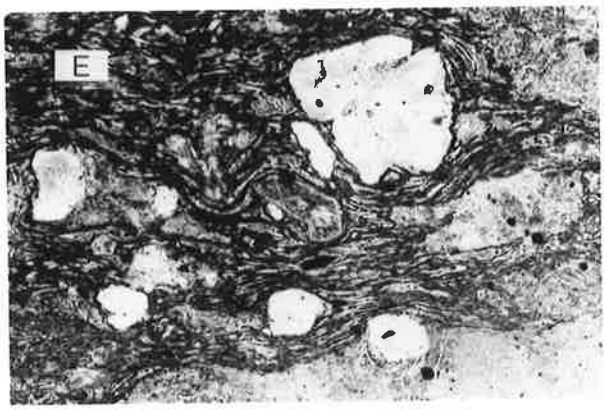
E

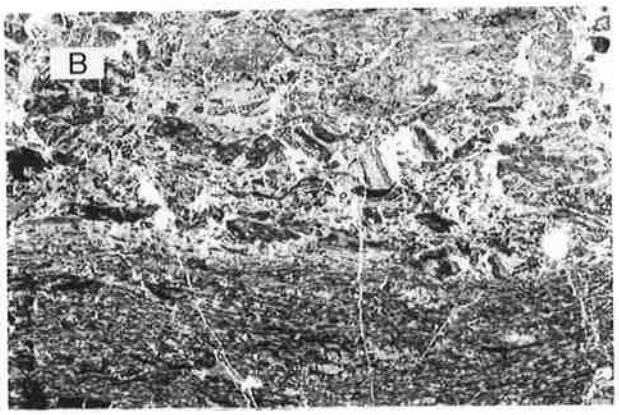
B


F

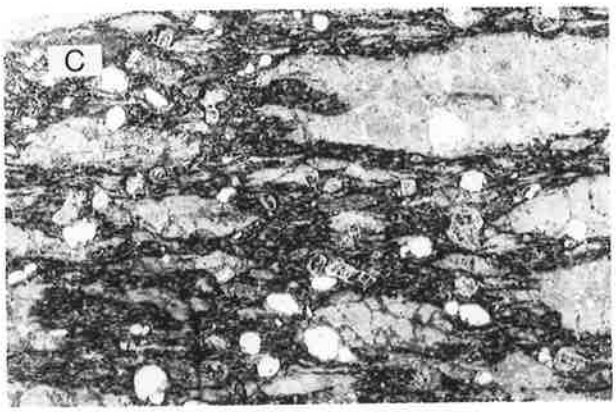
C

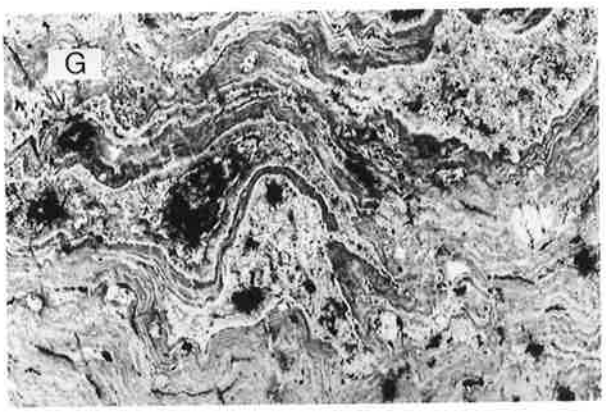
G


D

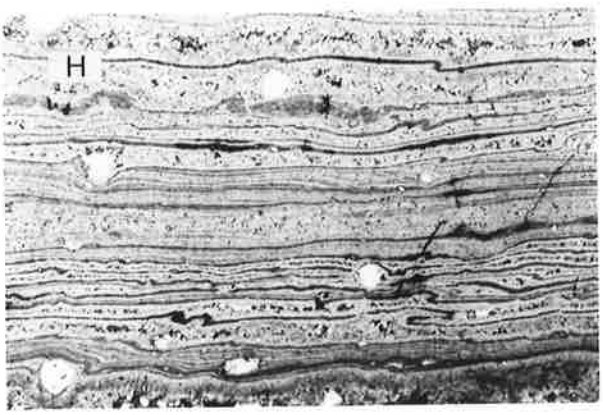
H

Figure 2.5.2. Photomicrographs of selected thin sections. The samples photographed belong to various units.

A. Lithic tuff from the Waurea Pyroclastics. A variety of accessory acid volcanic rock fragments are incorporated in a devitrified felsic matrix. The angularity of the fragments, their poor sorting and the glassy matrix are all indicative of a pyroclastic origin. F.V. 30 mm.

B. Monolithologic autobreccia, probably produced *in situ* by gas streaming. Note the incipient brecciation that has occurred within some individual fragments. F.V. 10 mm.

C. Ragged, glassy fragments within a non-welded ash-flow tuff. F.V. 7 mm.

D. Delicately-shaped glass shards in which bubbles, and Y and X forms have been preserved. From a non-welded ash-flow tuff member of the Waurea Pyroclastics. F.V. 2 mm.

E. Collapsed pumice fragment with included quartz phenocrysts, from a moderately-welded ash-flow tuff. F.V. 3.5 mm.

F. Spherulitic devitrification textures in a glassy rhyolite. F.V. 7 mm.

G. Evolved Kokatha basalt (K33), showing an ophitic intergrowth of plagioclase and chloritized clinopyroxene. The dark patches, rich in opaque minerals, mark the former presence of interstitial glass. F.V. 4 mm.

H. Bedded and graded air-fall tuff. The grading indicates that the younging direction is towards the left. Note the soft-sedimentary diapiric intrusion feature. F.V. 10 mm.

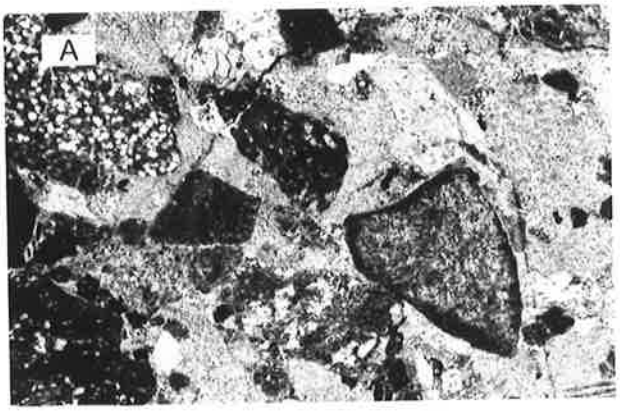
A

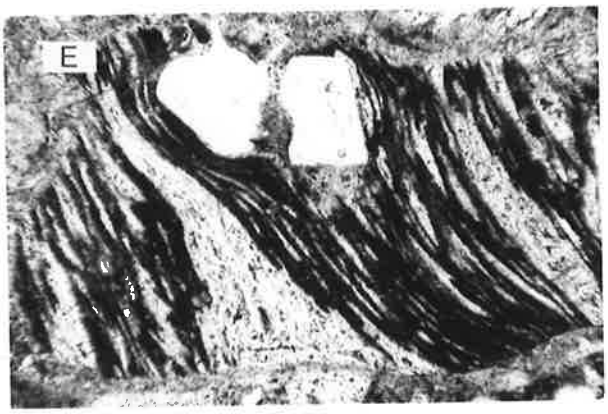
E

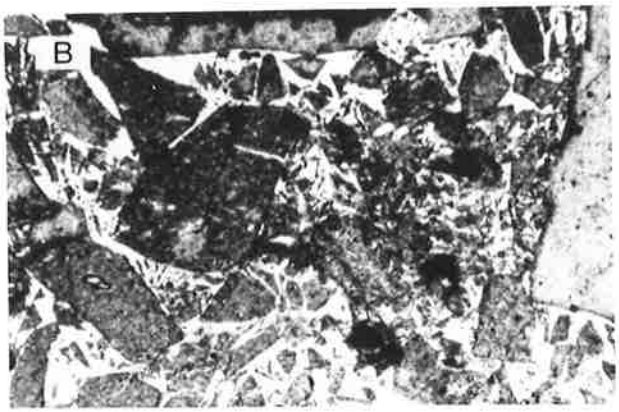
B

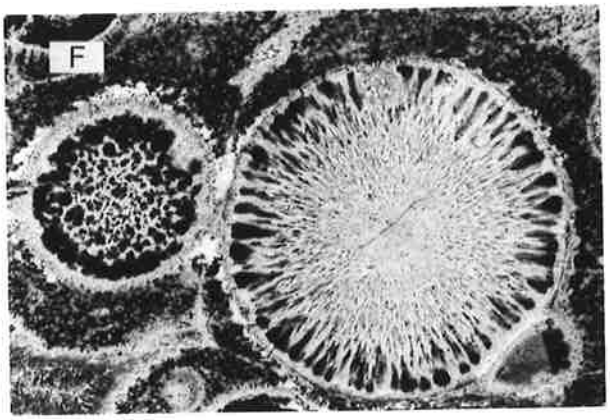
F

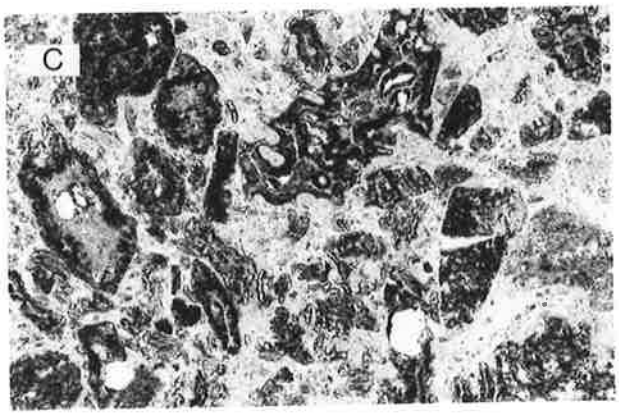
C


G

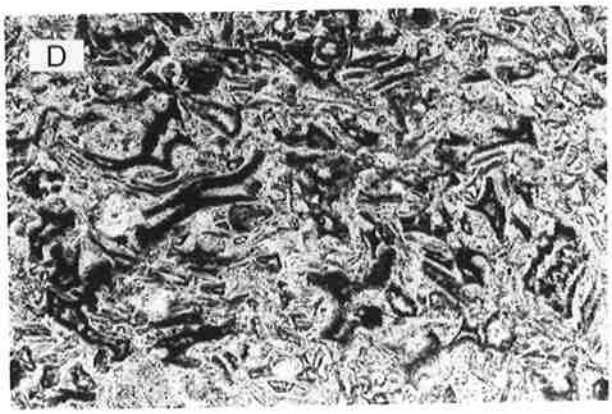
D


H

welded tuffs, the siliceous, originally glassy matrix, has devitrified to produce snowflake and other "patchy polarization" textures. Where the degree of welding is less, excellent vitroclastic textures are visible and a spectrum of rock types ranging from glassy, vitric tuffs through crystal-vitric tuffs to lithic tuffs can be observed. The lithic tuffs contain a vairety of fragments including deformed pumice and accessory volcanic rocks, mostly of lapilli size, set in a tuffacious matrix.

The rhyolites that were erupted as lavas generally show well-developed, pervasive flow-banding and in zones of contorted flow-folding, flow-brecciation is commonly seen. Apart from their association with flow rocks, the flow breccias can be recognised by their monolithologic character and by the absence of vitroclastic textures.

2.3.6 Intrusive rocks

The numerous high-level dykes and plugs intruding the volcanic pile are, with the exception of the Palthrubie Granophyre, porphyritic in nature. They contain abundant phenocrysts of plagioclase, clinopyroxene, K-feldspar and quartz plus rare accessory zircon and apatite, set within a granophyric matrix. Their similar textural features to the high-silica dacites and rhyodacites discussed above, suggest that they have a comparable origin. The high proportion of phenocrysts in the Yandoolka Rhyolite (up to 60%) and the relative abundance of zircon and apatite offers evidence that this unit in particular, has a significant accumulative crystal component.

The even-grained, holocrystalline intrusive rocks such as the medium-grained Palthrubie Granophyre and coarse-grained Hiltaba Granite appear to have crystallised from melts devoid of accumulative phenocrysts. The Hiltaba Granite ranges from a coarse-grained leuco-adamellite to a true granite and contains variable proportions of quartz, plagioclase, microcline and biotite.

2.4 GEOCHEMISTRY

Major element analyses for 79 rocks from the Lake Everard area and trace element contents in 53 of these samples are listed in Table A2.2 (Appendix 1) in order of increasing SiO_2. These analyses are also tabulated in groups, corresponding to the respective formations to which the samples belong (Table A2.3, Appendix 1). Rare earth element (REE)

data for 11 samples, selected to encompass the geochemical variation evident from the major and trace element data, are also listed in Appendix 1 (Table A2.4). All sample locations are indicated on Figure A2.1 (Appendix 3).

Examination of Table A2.2 reveals that the compositional range from basalt to rhyolite is spanned but, that there is an absence of samples within the 52-58% SiO_2 interval. Despite detailed mapping and careful sampling by the writer, no rocks were found in the Lake Everard area which bridged the 52-58% SiO_2 gap. A similar compositional hiatus and lack of intermediate rocks was noted by Branch (1978) in the Kokatha area, and appears to be characteristic of the Gawler Range province. Because of the obvious petrogenetic importance of the andesites, they are, relative to their total outcrop area, disproportionately represented in Table A2.2 It is emphasised that both the andesites and basalts occupy only a fraction (< 1%) of the mapped area (see Fig. 2.2).

In the following discussion variations in the major and trace element contents of the samples collected from the Lake Everard area are systematically examined. To maximize the information obtained, the data is treated in the first instance as if all samples were related by crystal fractionation. In this way the extent of involvement of various minerals can be ascertained and any inconsistencies serve to highlight inadequacies in the simple crystal fractionation model.

2.4.1 Major elements

The Lake Everard rocks show major element trends normally considered to be characteristic of calc-alkaline series, such as decreasing Al_2O_3, $Fe_2O_3{}^t$, MgO, CaO, TiO_2, P_2O_5 and increasing K_2O with rising SiO_2 (Fig. 2.6). This is verified by comparison with the average Cainozoic calc-alkaline trends which are superimposed on the plots in Figure 2.6. There is, however, significant scatter for some major elements and this may be due to alteration, absence of a single line of liquid descent and/or some other primary magmatic control. To permit a closer examination of the data, each major element will be considered individually, with reference to the variation diagrams plotted in Figure 2.6.

A. MgO

MgO decreases with increasing SiO_2, possibly due to fractionation of mafic minerals such as clinopyroxene, amphibole and/or biotite, up

Figure 2.6 Major elements vs. SiO_2 for rocks from the Lake Everard area. The solid lines enclose the field of Cainozoic calc-alkaline volcanics. O undifferentiated units ● Bunburn Dacite ▲ Yardea Dacite ■ Childera Dacite □ Mangaroongah Dacite.

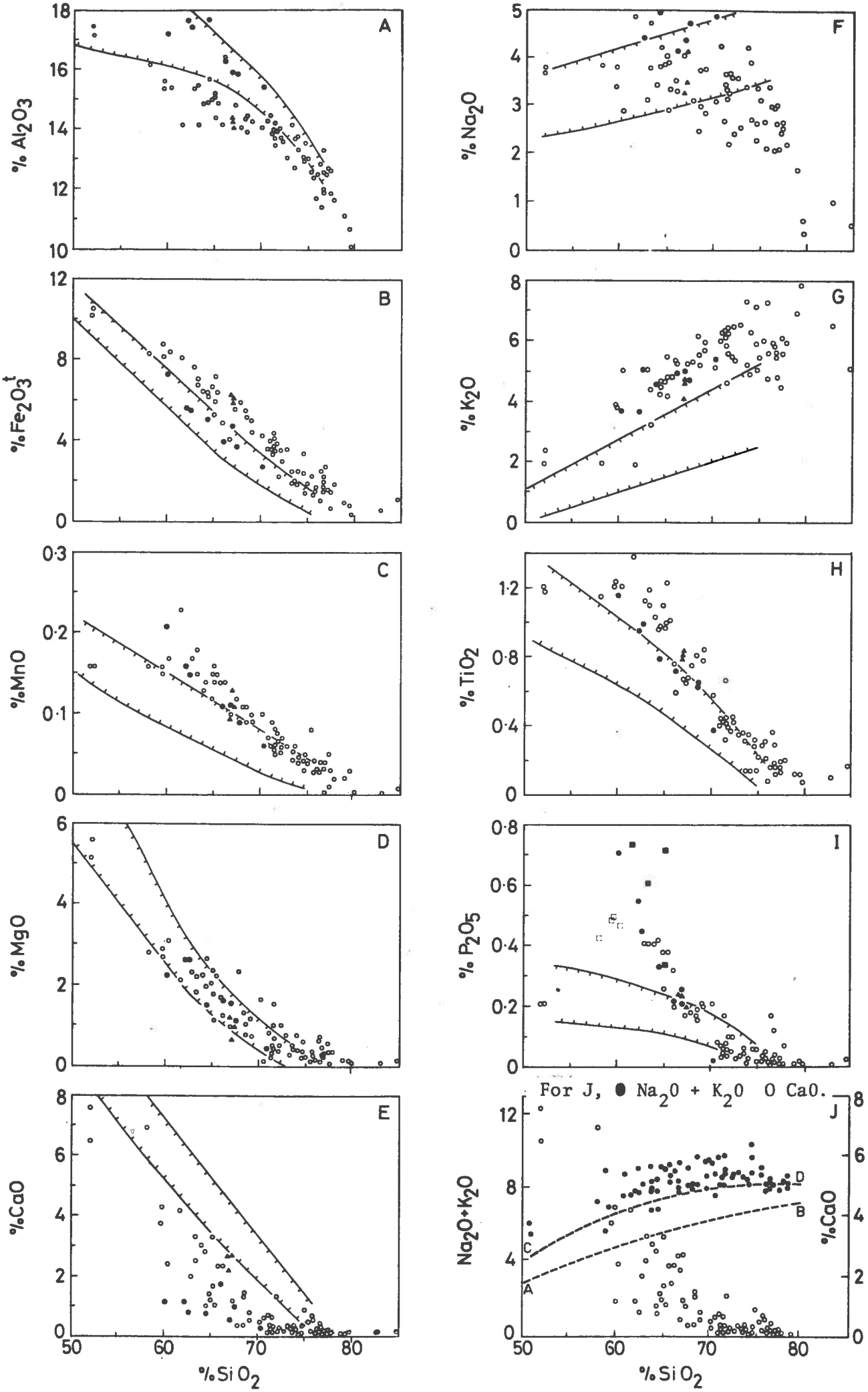

to approximately 68-70% SiO_2, at which point the trend flattens out. The andesites and dacites have comparable MgO contents to the Cainozoic calc-alkaline rocks.

B. $Fe_2O_3^t$ (total iron)

$Fe_2O_3^t$ exhibits a well-defined negative correlation with SiO_2. Several lines of evidence indicate that both magnetite and mafic minerals probably exerted the major control on $Fe_2O_3^t$:

1) Abundant microphenocrysts of magnetite in the andesites and dacites indicates early fractionation of magnetite from liquids of these compositions.
2) At high SiO_2 contents (> 70% SiO_2), the behaviour of MgO (i.e. flattening out of trend) and bulk composition precludes extensive fractionation of mafic minerals. The continued decrease of $Fe_2O_3^t$ with rising SiO_2 must therefore reflect control by a low MgO mineral such as magnetite.
3) Over the 58-70% SiO_2 range, MgO drops 2.5% while $Fe_2O_3^t$ decreases by 4%. If it is assumed on petrographic grounds that clinopyroxene (with $Fe_2O_3^t$/MgO = .89, from microprobe data, Table 2.3) is the dominant mafic mineral fractionating over this interval, then it would be predicted that the 2.5% decrease in MgO should be matched by a corresponding 2.2% decrease in $Fe_2O_3^t$. These calculations show that there is a 1.8% "excess" in $Fe_2O_3^t$ which cannot be accounted for clinopyroxene fractionation alone and therefore fractionation of magnetite appears to be necessary in order to reduce $Fe_2O_3^t$ to the observed level. Fractionation of amphibole or biotite with higher $Fe_2O_3^t$/MgO would reduce the amount of $Fe_2O_3^t$ available for magnetite fractionation, but the petrographic and geochemical evidence presented later, suggests the role of these two minerals has been negligible.

Displaced away from the main trend, but parallel to it, are a number of samples of Bunburn Dacite, all of which have lower $Fe_2O_3^t$ at comparable SiO_2 than the remainder of the samples. The parallelism of the trend indicates $Fe_2O_3^t$ is probably being controlled by the same minerals (e.g. magnetite and clinopyroxene), but evidently the parental magma for the Bunburn Dacite had a lower initial iron content, which is now reflected in its differentiates.

With the exception of the samples of Bunburn Dacite, most rocks have significantly higher iron contents than the Cainozoic calc-alkaline

volcanic rocks, over the 58-70% SiO_2 range. The basalts however, have comparable levels of iron as do the samples of Bunburn Dacite.

C. Al_2O_3

Al_2O_3 decreases from 17% in the basalts to 10-12% in the most fractionated acid rocks. The samples of Bunburn Dacite again define their own separate trend and, like the basalts, have similar Al_2O_3 contents to typical calc-alkaline volcanic rocks. The remainder of the samples from the Lake Everard area contain 1-2% less Al_2O_3 than the samples of Bunburn Dacite at comparable levels of SiO_2 and are therefore relatively depleted in Al_2O_3 compared with the Cainozoic rocks.

D. CaO

Although there is considerable scatter in the data, CaO shows a general decrease with increasing SiO_2 up to approximately 70% SiO_2, beyond which it remains at a uniformly low level. Potentially, clinopyroxene, amphibole and plagioclase fractionation could all contribute to the decrease in CaO. The more basic members of the Bunburn Dacite series have relatively low CaO contents in comparison to other samples and in turn all samples, including the basalts, have lower CaO contents than the Cainozoic volcanic rocks. The above-average level of CaO in the Yardea Dacite is consistent with the petrography, which shows that this unit has a relatively high proportion of andesine plagioclase phenocrysts which may in part be accumulative (see petrography section).

E. K_2O

Despite the scatter, there is a general positive correlation of K_2O and SiO_2, up to approximately 70% SiO_2. In the classification scheme for high-K_2O rocks proposed by Mackenzie and Chappell (1972) most of the intermediate rocks fall in the latite field while all of the acid rocks lie in the toscanite field. The basalts too, are high in K_2O, such that one sample would be classed as a shoshonite.

K_2O in the Yantea Rhyodacite is particularly high (> 6%) and exceeds that in the unaltered granites and rhyolites (5.3-5.6% K_2O). The high K_2O is unlikely to be the result of alteration, since this unit is characterised by uniformly high K_2O contents over a wide area and by abundant K-feldspar in the matrix, which petrographic evidence suggests

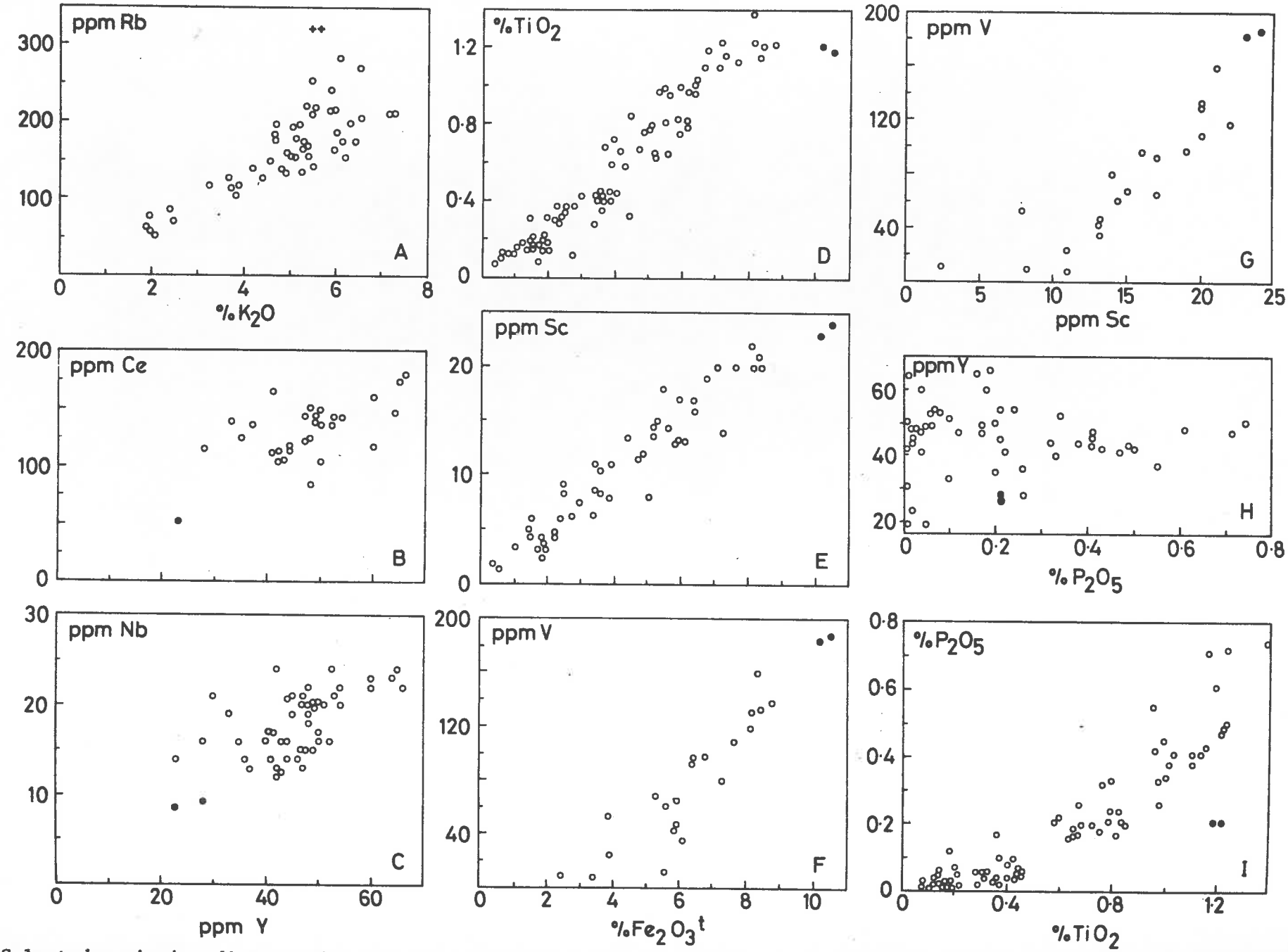

Figure 2.7 Selected variation diagrams for rocks from the Lake Everard area. O units undifferentiated ● Nuckulla Basalt + Hiltaba Granite

has crystallised directly from a melt. Therefore, the geochemistry supports the conclusion previously drawn in the petrography section, viz. the rhyodacites were produced by mixing of a high-K_2O residual liquid with accumulative crystals of plagioclase, clinopyroxene and magnetite.

F. Na_2O

Na_2O shows extreme scatter, almost to the point that little useful information can be gained from the plot. The samples of Bunburn Dacite are particularly high in Na_2O and the levels tend to drop with increasing SiO_2. The remainder of the samples vary about an average Na_2O content of 3.5%, but above 70% SiO_2 a slight decrease is evident, possibly due to control by sodic plagioclase and alkali feldspar.

G. TiO_2

The linear inverse correlation of TiO_2 with SiO_2 over the entire SiO_2 range, suggests TiO_2 is probably being controlled by an oxide mineral such as ilmenite or magnetite. As in the case of $Fe_2O_3{}^t$, samples of Bunburn Dacite form a series parallel to, but displaced slightly towards the low TiO_2 side of the main trend. The similar behaviour of Ti and Fe, verified by their good correlation on the TiO_2 vs $Fe_2O_3{}^t$ plot (Fig. 2.7D), indicates control by the same mineral, which is likely to be magnetite.

It is notable that the basalts have comparable levels of TiO_2 to the andesites, and while the basalts have TiO_2 contents typical of calc-alkaline volcanics, the intermediate to acid rocks have relatively high TiO_2 values, a feature also shared by $Fe_2O_3{}^t$.

H. P_2O_5

P_2O_5 decreases with increasing SiO_2, probably due to apatite fractionation, since modal apatite has been noted in some crystal-rich (accumulative) dykes in the region. The intermediate volcanic rocks are extremely high in P_2O_5 in comparison with the Cainozoic examples, and show a considerable amount of scatter. This scatter is unlikely to be due to alteration however, because the andesitic members of each unit have characteristic levels of P_2O_5. For example, lower P_2O_5 contents are confined to the Mangaroongah Dacite, intermediate contents to the

Figure 2.6 Major elements vs. SiO_2 for rocks from the Lake Everard area. The solid lines enclose the field of Cainozoic calc-alkaline volcanics. O undifferentiated units ● Bunburn Dacite ▲ Yardea Dacite ■ Childera Dacite □ Mangaroongah Dacite.

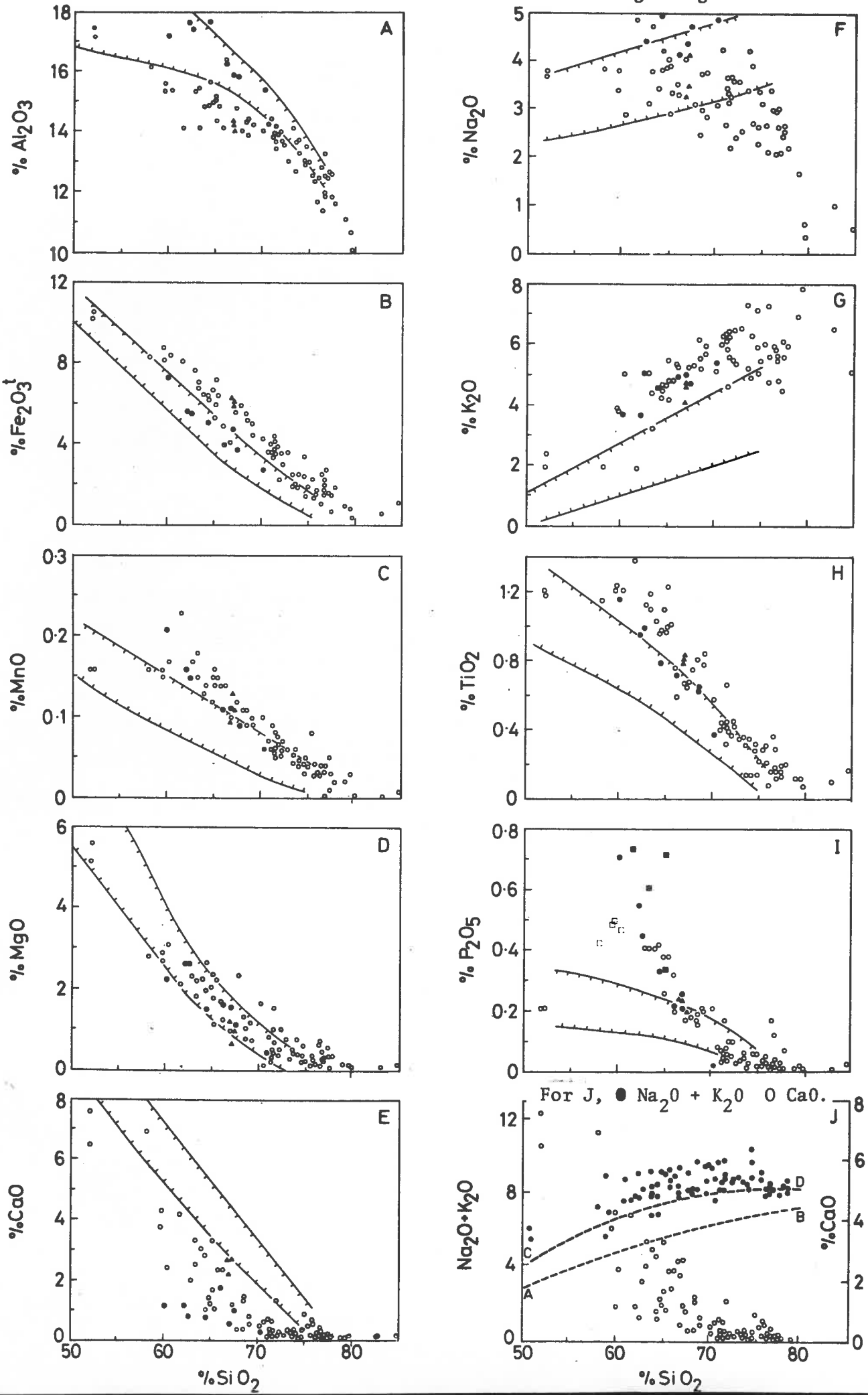

Bunburn Dacite and higher contents of P_2O_5 to the Childera Dacite. The lower P_2O_5 contents of the basic rocks are typical of calc-alkaline basalts.

As might be expected from their relationship with SiO_2, P_2O_5 and TiO_2 correlate well with each other (Fig. 2.7I). High TiO_2 in the andesites is accompanied by high P_2O_5, although the andesitic members of the Childera Dacite do show a relative enrichment of P_2O_5 over TiO_2 compared with the other andesites. Depletion of P_2O_5 and TiO_2 with increasing SiO_2 appears to be typical of calc-alkaline suites and can be attributed to fractionation of apatite and Fe-Ti oxides, which do not necessarily occur as modal minerals (e.g. Mt. Jefferson orogenic calc-alkaline suite, Oregon, Anderson and Gottfried, 1971).

From the above discussion of the major elements, it appears that the Nuckulla Basalt from the Lake Everard area appears to fit the generally recognised category of calc-alkaline basalt (e.g. Jakes and White, 1972; Pearce, 1976; Pearce and Cann, 1973). The intermediate to acid rocks on the other hand, while showing typical calc-alkaline trends, have some atypical characteristics such as, relatively high Fe, Ti, K and P and low Ca and Al contents. Thus, it is pertinent to consider whether the present rock-suite is indeed calc-alkaline in terms of the generally accepted criteria such as the Peacock lime-alkali index, sum of alkalis vs SiO_2 and AFM components. These criteria will be considered in turn, below.

I. Lime-alkalis index (Figure 2.6J)

The relationship between CaO and $Na_2O + K_2O$ was originally used by Peacock (1931) to define the calc-alkali series. Using this relationship Peacock recognised four groups:

rock series	alkali-lime index
alkalic	<51
alkali-calcic	51-56
calc-alkalic	56-61
calcic	>61

based on the alkali-lime index, which is the level of SiO_2 at the point of intersection of the CaO and $Na_2O + K_2O$ vs SiO_2 plots. These elements are plotted in Figure 2.6J, from which it is apparent that the point of intersection is not well defined owing to a paucity of samples with $Na_2O + K_2O < CaO$. If the basalts are considered, it is clear that the

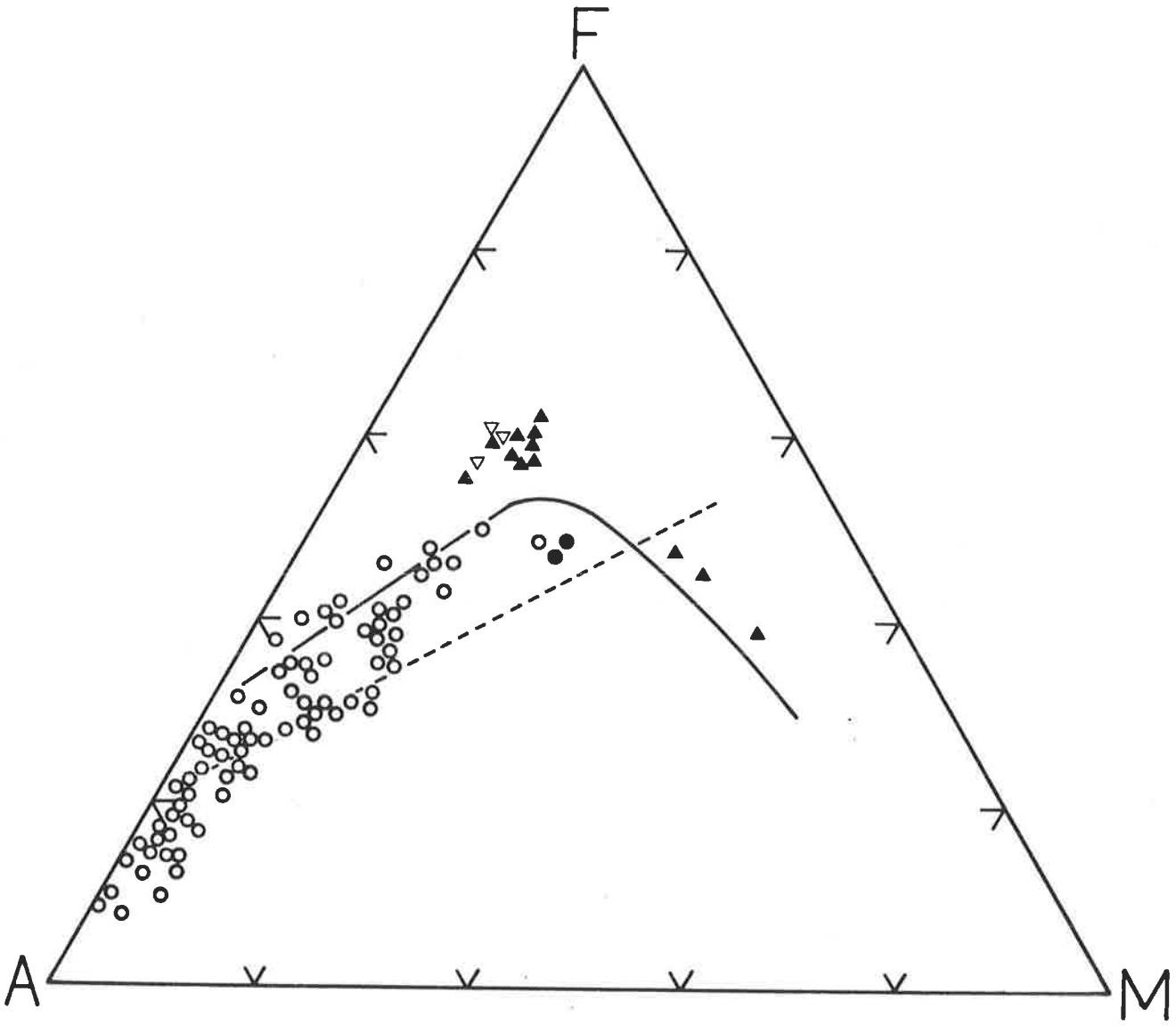

Figure 2.8 AFM plot for rocks from the Gawler Range province.

▲ basalts from the Kokatha area ▽basic xenoliths within Yardea Dacite O undifferentiated units.

The solid line separates the tholeiitic and calc-alkaline fields.

The dashed line is the trend defined by the calc-alkaline Cascades lavas (after Carmichael, 1964).

alkali-lime index must lie between 52-58 corresponding to the alkali-calcic division or the alkalic end of the calc-alkaline series. This is consistent with the relatively low CaO, yet high K_2O (and "normal" Na_2O) of these rocks compared with Cainozoic calc-alkaline volcanic series.

J. Sum of alkalis vs SiO_2 (Figure 2.6J)

The sum of alkalis increases slightly with increasing SiO_2 in the 58-72% SiO_2 range and since Na_2O shows no consistent variation over this interval, the rise must be due to increasing K_2O. Kuno (1969) defined three fields on this plot, corresponding to tholeiitic (low $Na_2O + K_2O$, below line A-B), calc-alkaline (intermediate $Na_2O + K_2O$, between lines A-B and C-D) and alkaline (high $Na_2O + K_2O$, above line C-D). Although in reality there is considerable overlap between the three series, it is clear that upon Kuno's original definition the present rocks are alkaline. Since it has been previously shown that the level of Na_2O is comparable with that in typical calc-alkaline suites, it can be inferred that the alkalic character must be due to the high K_2O in these rocks, a point which has been earlier verified by the K_2O vs SiO_2 plot.

K. AFM (Figure 2.8)

On the AFM plot, the series shows a marked trend towards the alkalis corner, with no obvious enrichment in iron. In addition, the Nuckulla Basalt appears to continue the trend of the acid-intermediate rocks, despite the intervening compositional gap. Compared with the calc-alkaline Cascade lavas the Lake Everard andesites and dacites are displaced towards the iron (F) corner, reflecting their relatively high iron contents. The enrichment in alkalis and corresponding depletion in MgO and Fe_2O_3 in the acid rocks is evident in the extreme trend towards the alkalis corner, suggesting these rocks are highly fractionated.

On the basis of the major elements it is concluded that the Lake Everard rocks, while demonstrating many calc-alkaline characteristics (e.g. no Fe enrichment on AFM plot, consistent trends on variation diagrams), do show some subtle differences arising primarily from their relatively high contents of $Fe_2O_3^t$, TiO_2, P_2O_5 and K_2O and relatively low contents of CaO and Al_2O_3. the trace elements will be examined below to see if they reflect these features and also to determine if they can place constraints on possible petrogenetic models (e.g. crystal fractionation verses partial melting) and on the minerals involved in these processes.

Figure 2.9 Trace elements vs. SiO_2 for rocks from the Lake Everard area. The solid lines enclose the field of Cainozoic calc-alkaline volcanics. Symbols as for Figure 2.6 with the addition of ◆ Yantea Rhyodacite ΔWhyeela Dacite + all intrusive rocks

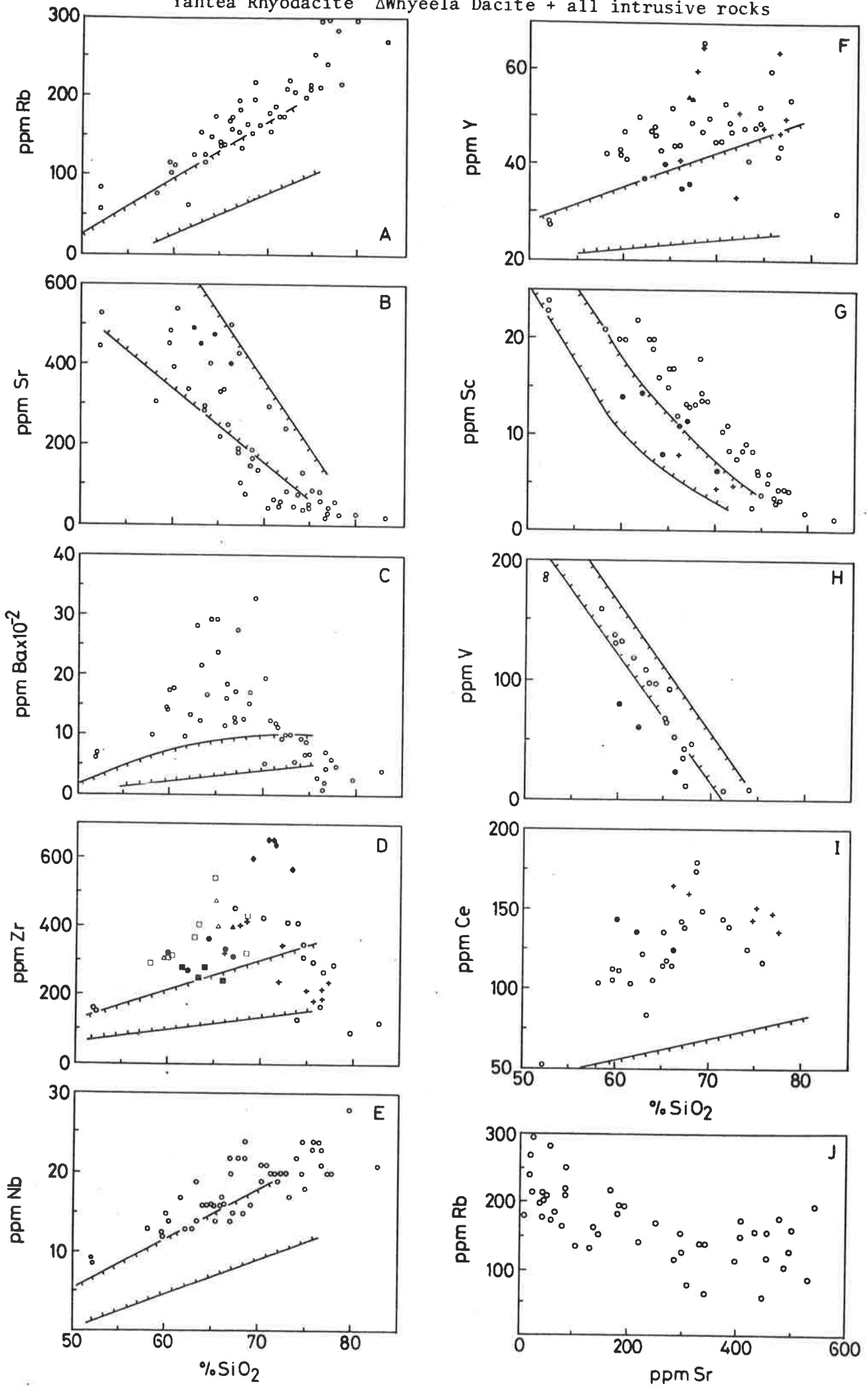

2.4.2 Trace elements (excluding REE)

Various trace elements are plotted against SiO_2 in Figure 2.9 and in the following discussion the behaviour of each trace element will be examined individually.

A. Rb

Rb increases progressively with rising SiO_2, presumably due to residual liquid concentration caused by fractionation of minerals in which it is incompatible. This feature argues against extensive biotite fractionation (Kd Rb biotite/silicate liquid = 2.2-3.2 for acid melts, Arth, 1976). Similarly, the linear Rb vs K_2O relationship (Fig. 2.7A) precludes significant amounts of amphibole removal (D K/Rb = 5.8 for amphibole, Arth, ibid).

Both the Rb vs K_2O and Rb vs SiO_2 plots reveal that some granites are particularly enriched in Rb. This could be due to metasomatism (e.g. addition of Rb in a vapour-rich phase) or extreme fractionation involving K-feldspar and quartz, which has controlled K_2O and SiO_2, but resulted in a residual enrichment in Rb.

B. Sr

Sr shows a significant amount of scatter possibly resulting from alteration (e.g. sericitization of plagioclase) and/or different lines of liquid descent. The latter is probably the cause for at least some of the scatter, since the samples of Bunburn Dacite previously shown to be anomalous with respect to Al_2O_3, CaO, Na_2O, Fe_2O_3 and TiO_2, are also relatively high in Sr.

Sr drops from an average of 450-500 ppm in the andesites and basalts to approximately 50 ppm in the rhyolites. In a fractional crystallisation model, this could be satisfactorily explained by plagioclase-dominated fractionation (Kd Sr plagioclase/acid melt = 3.6, Arth, 1976). For example, assuming: Cl = 50, Co = 450 (Fig. 2.9B), Kd Sr plagioclase/acid melt = 3.6 (Arth, 1976), and F = 0.25 (from the four-fold enrichment in Rb over this interval, assuming Rb is behaving incompatibly), it can be calculated from the Rayleigh fractionation equation that removal of approximately 70% weight fraction of plagioclase would be required in order to produce the observed depletion in Sr. By contrast, it is

doubtful whether variations in the degree of partial melting of the same source could explain such a range in Sr. If, for instance, it is assumed that D solid/liquid = 0.5 for the residue, then the maximum Sr enrichment in the liquid would be two-fold, obtainable only in the unlikely event of a 100% change in the degree of partial melting.

Although these calculations involve many assumptions, it is nevertheless clear that the behaviour of Sr favours a crystal fractionation control rather than a partial melting control. However, it seems probable that some of the scatter observed may be due to differing lines of liquid descent from variable parents (e.g. Bunburn Dacite).

C. Ba

Ba shows an indistinct peak at 64-66% SiO_2, which initially suggests the possibility of residual liquid enrichment in Ba, followed by rapid depletion due to K-feldspar fractionation (Kd Ba K-feldspar/liquid = 6.12, Arth, 1976). This interpretation is not favoured, however, because over a comparable SiO_2 interval (58-66% SiO_2), Rb shows an approximate two-fold increase, whereas Ba shows a three-fold increase. Clearly, if Rb is behaving largely incompatibly as has been previously suggested, the relative enrichment in Ba must be due to other factors. This is supported by the observation that not all samples show the observed enrichment in Ba. Alteration is unlikely to provide an adequate explanation for this behaviour, despite the reported mobility of Ba, because the high-Ba samples do not appear to be more altered than the low-Ba-samples. Moreover, Ba shows predictable behaviour, seen for example in the high SiO_2 rocks (>70% SiO_2) where there is a good inverse correlation of Ba with SiO_2, probably as the result of K-feldspar fractionation (Kd Ba K-feldspar/liquid = 6.12, Arth, 1976). Also, the Rb-rich granites noted earlier are depleted in Ba, consistent with extreme K-feldspar fractionation previously suggested on the basis of the K_2O vs Rb relationship (Fig. 2.7A).

The confinement of abnormally high Ba values to a restricted SiO_2 interval (62-68% SiO_2), could be explained by a process such as mixing in which a relatively high-Ba liquid (e.g. acid melt) is added to a Ba-poor liquid to produce a spread in Ba contents depending on the proportions of mixing. This possibility will be examined in more detail, later.

In comparison with Cainozoic andesites and dacites, the present rocks are considerably higher in Ba (c.f. K_2O and Rb), although the levels of Ba in the "high-K" calc-alkaline series (e.g. Jakes and Smith, 1970;

Mackenzie and Chappell, 1972) do approach those in the less-enriched samples from the Lake Everard area. The rhyolites, which are relatively depleted in Ba, possibly as a result of plagioclase and K-feldspar fractionation, do have comparable contents of Ba to Cainozoic rhyolites.

D. Zr

The Lake Everard rocks show a considerable range in Zr contents. Some rhyolites and granites are relatively depleted in Zr, possibly as a result of zircon fractionation. The Yantea Rhyodacite samples on the other hand, are relatively enriched in Zr and are responsible for the peak on the Zr vs SiO_2 plot at approximately 70% SiO_2. It is possible that a mixing process, similar to that suggested to account for an analogous distribution in Ba, may offer an explanation for the significant variation observed for Zr within the 64-70% SiO_2 interval. For example, it is conceivable that a high-K_2O residual liquid, apart from engulfing crystals of plagioclase, clinopyroxene and magnetite, could have also incorporated cumulate zircon in varying amounts, hence producing the observed range in Zr values. Some evidence for this is seen in certain late-stage, crystal-rich (accumulative) intrusives which contain abundant euhedral zircon (e.g. Yandoolka Rhyolite - up to 60% phenocrysts of plagioclase, K-feldspar, quartz, apatite and including 2-3% zircon).

The level of Zr in the basalts is approximately half that in the andesites and whereas the basalts have Zr contents typical of Cainozoic examples, the andesites, dacites and rhyodacites are markedly enriched.

E. Nb

Nb shows a progressive increase in the Lake Everard rocks, presumably due to formation of the Nb^{4+} complex which prevents entry into the sites of the major fractionating minerals (Taylor, 1965). This behaviour contrasts with that noted in the calc-alkaline Mt. Jefferson suite (Anderson and Gottfried, 1971), which shows a progressive decrease of Nb (and Ti and P) with differentiation due to removal of biotite, sphene and/or ilmenite. The progressive increase of Nb in the present case may indicate that fractionation of these minerals has been negligible. Some samples, notably the acid intrusive rocks, are depelted in Nb and this might be due to late-stage fractionation of apatite or sphene.

The basalts have the lowest Nb contents, but their average value (9 ppm) is significantly higher than that usually quoted for calc-alkaline

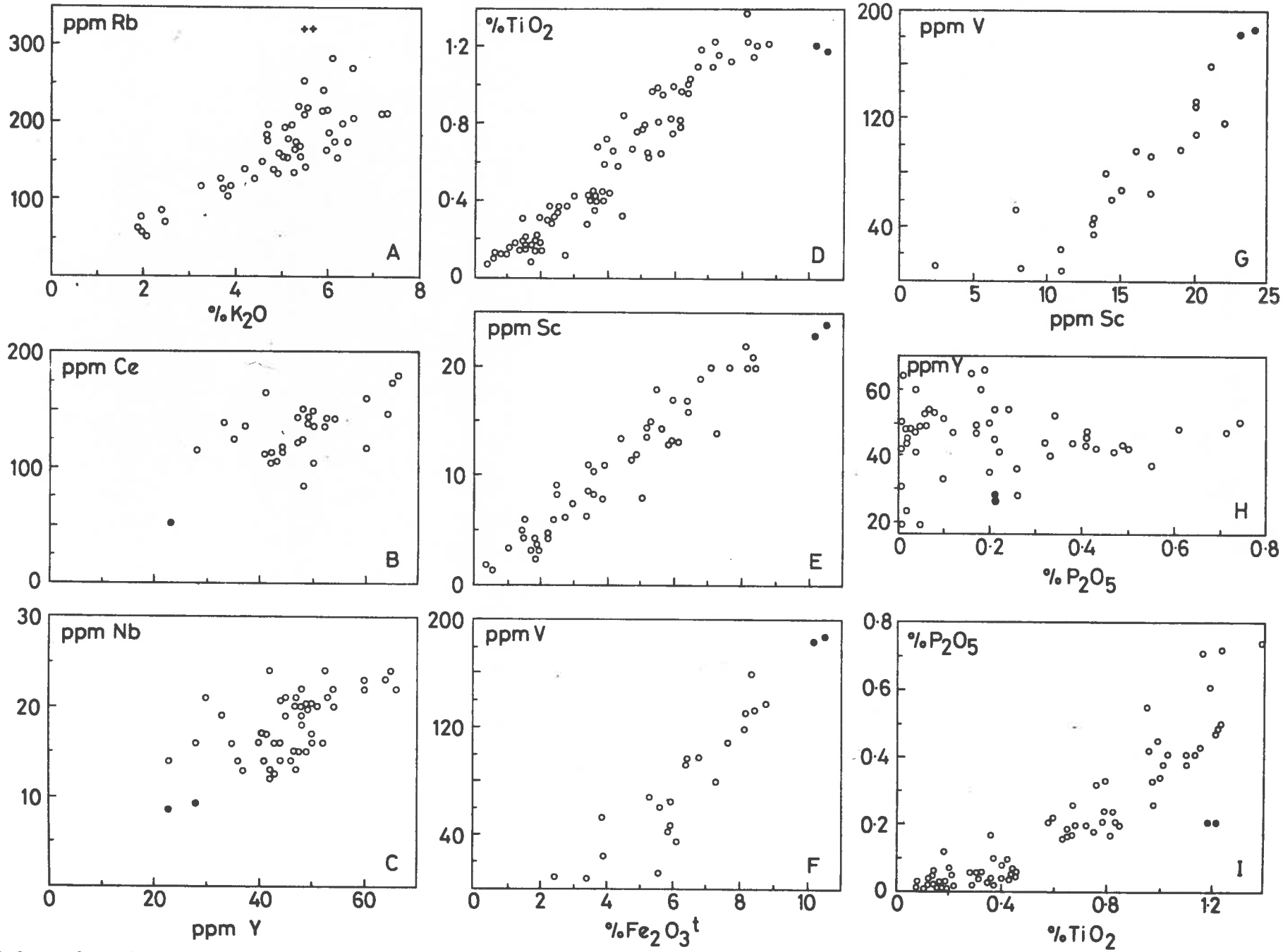

Figure 2.7 Selected variation diagrams for rocks from the Lake Everard area. O units undifferentiated ● Nuckulla Basalt + Hiltaba Granit

basalts (e.g. 2.5 ppm, Pearce and Cann, 1973). What Nb data is available for Cainozoic calc-alkaline suites suggests that the Lake Everard andesites and dacites are enriched by comparison. For example, 4-5 ppm Nb in 57-59% SiO_2 andesites from the Lesser Antilles (Brown, et al., 1977) and 4 ppm Nb in 56% SiO_2 andesites from Bagana volcano, New Guinea (Bultitude, et al., 1978), compared with 12-20 ppm in the Lake Everard andesites and dacites.

F. Y

Y shows a small increase with SiO_2 for the majority of samples, thus precluding extensive amphibole or apatite fractionation (c.f. Lambert and Holland, 1974). Some of the siliceous intrusive rocks are depleted in Y, possibly due to zircon fractionation (Lambert and Holland, ibid.), since they are also relatively depleted in Zr. Other rocks are relatively enriched in Y and this may be due to incorporation of accumulative apatite (e.g. Yardea Dacite and samples of the Moonamby dyke-suite).

It is notable that the samples of Bunburn Dacite are relatively depleted in Y compared with the majority of other samples. Most intermediate and acid rocks from the Lake Everard area have higher Y contents than Cainozoic examples, even including the high-Y calc-alkaline series from Mt. Ararat (Lambert, et al., 1974).

The basalts have significantly lower Y contents than the andesites (28 ppm c.f. 42 ppm), but are slightly enriched compared with average calc-alkaline basalts (28 ppm c.f. 23 ppm).

G. V and Sc

Both V and Sc demonstrate linear, inverse correlations with SiO_2 and could be controlled by amphibole, clinopyroxene, biotite and/or magnetite (Gill, 1978). Extensive amphibole and biotite fractionation have been previously eliminated by other data (e.g. K/Rb and Y for amphibole, Rb for biotite), and in view of the abundant modal phenocrysts of clinopyroxene and magnetite, it is likely that these minerals have exerted the major control on V and Sc. The linear correlation of Sc and V with $Fe_2O_3^t$ (Fig. 2.7E and F) suggests that the effect of magnetite was probably dominant.

The basalts have higher V and Sc contents than the andesites, but the differences are not as marked as those for Zr and Y. At comparable levels of SiO_2, the samples of Bunburn Dacite are significantly lower in V and Sc than the remainder of the samples and this could be related to

the same cause as the analogous behaviour shown by Fe and Ti. Excluding the samples of Bunburn Dacite, the Lake Everard felsic volcanic rocks have comparable levels of V to Cainozoic suites, but are relatively enriched in Sc.

In summary, an examination of the trace element levels in the Nuckulla Basalt reveals that the absolute contents of most trace elements are comparable with the values reported for basalts associated with modern calc-alkaline suites. The intermediate-acid rocks show important differences when compared with Cainozoic calc-alkaline series, such as higher Zr, Nb, Y, Ce, Sc, Rb and Ba contents, particularly for the andesites and dacites. In these rocks, plagioclase, clinopyroxene, magnetite and zircon fractionation appear to have assumed important roles, based on the Sr, V, Sc and Zr data, respectively. The negligible role of amphibole and biotite is deduced from the K/Rb, Rb and Y data. These conclusions are supported by the petrography which demonstrates an abundance of plagioclase, clinopyroxene and magnetite phenocrysts, but a paucity of amphibole and biotite phenocrysts.

Much of the scatter in the trace element data, can be related to one or other of two separate causes:

1) Distinct parental magmas fractionating along parallel trends or in other words, multiple lines of liquid descent (e.g. Bunburn Dacite). This possibility has been previously suggested on the basis of the behaviour of some major elements, particularly $Fe_2O_3{}^t$, TiO_2 and Al_2O_3.
2) Incorporation of accumulative crystals of plagioclase, clinopyroxene, magnetite, zircon and apatite into a highly-fractionated, K_2O-rich residual liquid. This has resulted in a range of trace element contents, particularly in the high-silica dacites and rhyodacites.

Probably the most significant point deducible from the trace element data is that the various units mapped, appear to have distinctive trace element contents suggesting that few, if any, are directly related to each other by crystal fractionation. To explore this possibility further, REE contents were determined in 11 samples selected to encompass the compositional variation evident in rocks from the Lake Everard area. The information yielded by the REE data is examined below:

2.4.3 Rare earth elements (REE)

The rare earth element contents in the eleven samples analysed are listed in Table A2.4 (Appendix 1) and chondrite-normalised plots are given

Figure 2.10 Chondrite-normalised REE plots for selected rocks from the Lake Everard area.

E312 - andesite (59.7% SiO_2)

E747 - dacite (62.9% SiO_2)

E294 - rhyodacite (71.4% SiO_2)

E554, E607, E78 - rhyolites (74.6, 74.0, 75.7% SiO_2 respectively).

The dashed line represents the modelled REE pattern obtained for E554, assuming derivation by fractional crystallisation from E312. The circumpacific average is after Taylor (1969).

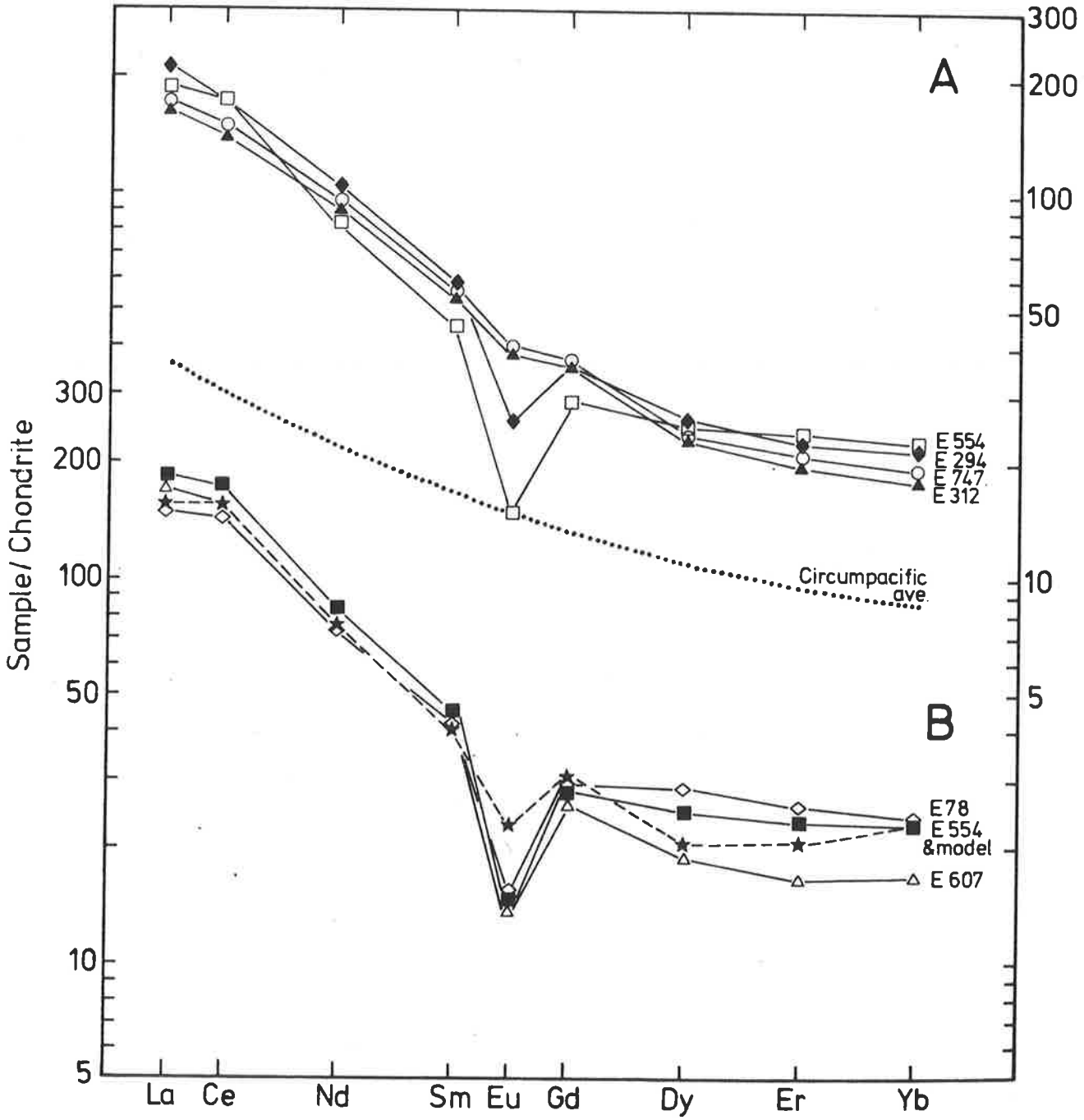

Figure 2.11 Chondrite-normalised REE plots for selected rocks from the Gawler Range province.

K101 - primitive basalt, Kokatha area (51.9% SiO_2, 11.77% MgO).

E231 - Nuckulla Basalt, Lake Everard area (52.1% SiO_2, 5.59% MgO).

E227 - Bunburn Dacite (62.2% SiO_2)

E725 - Yardea Dacite (67.0% SiO_2)

Y734 - Hiltaba Granite (76.6% SiO_2)

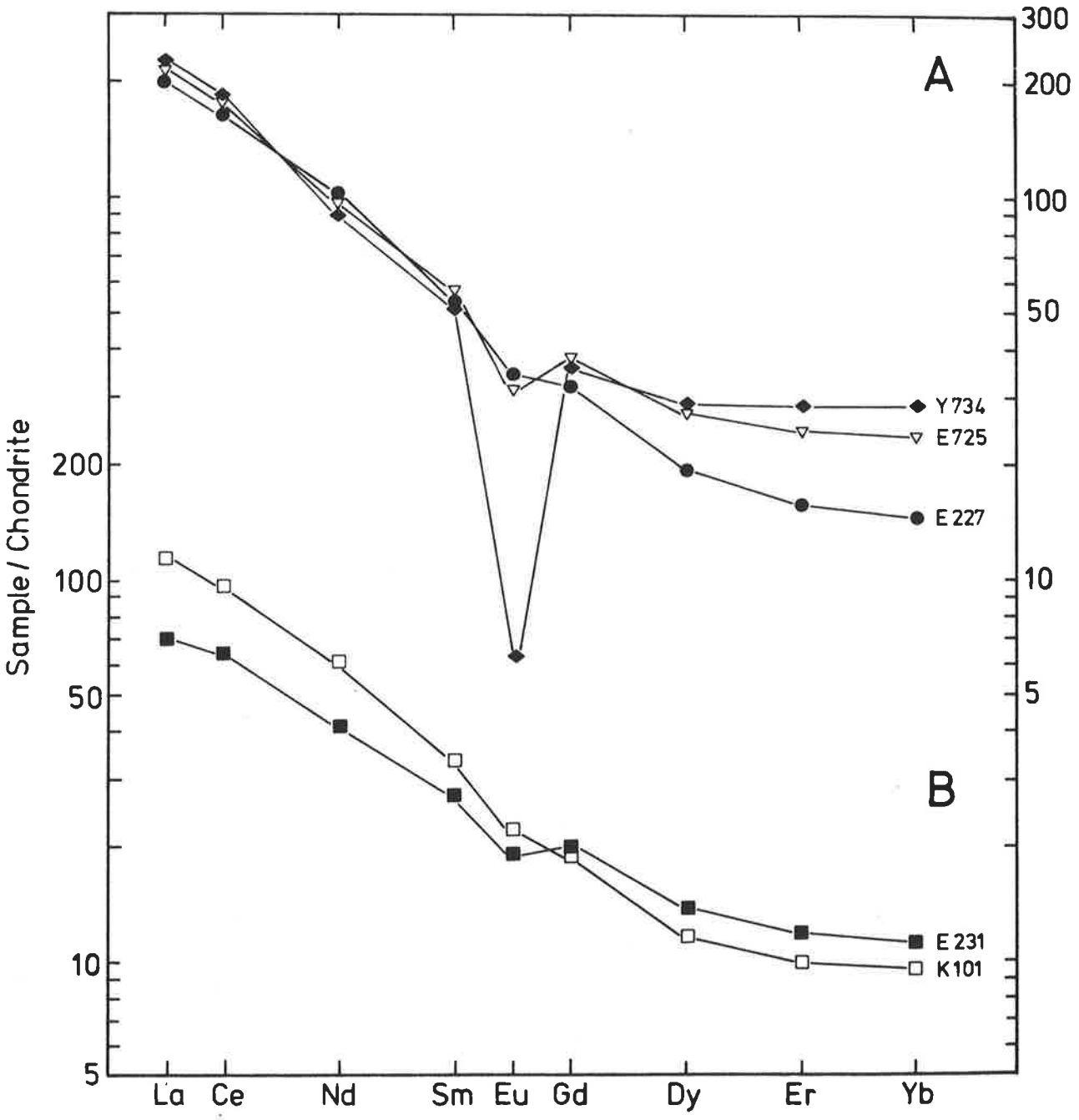

Table 2.3. Results of least squares modelling calculations designed to test possible fractional crystallisation processes in the Lake Everard rocks.

A. Approximation of dacite (E747) in terms of postulated parental andesite (E312) and phenocrysts.

Rock	dacite	dacite	andesite							
Sample No.	747	747	312	Mineral compositions used						
	obs.	est.	parent	cpx.	plag.	apatite	magnetite	Mineral	Wt. fraction	Mineral proportion
SiO_2	63.33	63.33	60.33	50.11	54.57	-	-			
Al_2O_3	15.43	15.43	15.51	2.76	28.95	-	-	cpx.	0.052	0.34
FeO^t	6.89	6.89	7.41	11.57	-	-	74.0	plag.	0.083	0.55
MnO	0.17	0.15	0.15	0.41	-	-	-	apatite	0.0038	0.025
MgO	2.35	2.35	2.72	14.43	-	-	-	magnetite	0.014	0.090
CaO	2.05	-	4.41	19.78	11.16	56.0	-	E747	0.84	
Na_2O	3.13	-	3.84	0.31	5.14	-	-		= E312	
K_2O	5.09	-	3.88	-	0.21	-	-			
TiO_2	1.14	1.12	1.25	0.62	-	-	20.0	ΣR^2	= 0.0006	
P_2O_5	0.41	0.41	0.51	-	-	44.0	-			
Total	100.0	-	100.0							

Notes: 1. A satisfactory match could not be obtained when CaO, Na_2O and K_2O were included in modelling calculations.
2. Clinopyroxene composition from microprobe data for clinopyroxene phenocrysts in 312. (An average of 8 analyses of 4 phenocrysts.)
3. Plagioclase composition is An54.6, after Wright (1974) and is considered realistic on optical grounds.
4. Apatite composition after Wright (1974).
5. Ti content of magnetite adjusted to give a satisfactory match for TiO_2.

B. Approximation of rhyolite (E554) in terms of postulated parental rhyodacite (E294) and phenocrysts.

Rock	rhyolite	rhyolite	rhyodacite							
Sample No.	554	554	294	Mineral compositions used						
	obs.	est.	parent	cpx.	plag.	K-feld.	magnetite	Mineral	Wt. fraction	Mineral proportion
SiO_2	74.59	74.58	71.66	50.11	64.70	63.94	-			
Al_2O_3	13.06	13.09	13.98	2.76	20.72	20.20	-	cpx.	0.003	0.018
FeO^t	2.16	2.16	3.10	11.57	-	-	78	plag.	0.128	0.75
MnO	0.04	0.07	0.06	0.41	-	-	-	K-feld.	0.025	0.146
MgO	0.36	0.55	0.50	14.43	-	-	-	magnetite	0.015	0.088
CaO	0.09	-0.04	0.37	19.78	2.60	0.58	-	E554	0.826	
Na_2O	2.28	-	3.69	0.31	9.32	3.60	-		= E294	
K_2O	7.14	7.12	6.15	-	-	10.86	-			
TiO_2	0.32	0.35	0.44	0.62	-	-	16	ΣR^2	= 0.06	
P_2O_5	0.06	0.06	0.05	-	-	-	-			
Total	100.0	-	100.0							

Notes: 1. Na_2O was excluded from modelling calculations.
2. Clinopyroxene and magnetite compositions as for A.
3. Plagioclase composition is after Deer, Howie and Zussman (1962) for oligoclase in rhyolite. K-feldspar composition is from same source, for perthite in granite.

C. Approximation of rhyolite (E554) in terms of postulated parental andesite (E312) and phenocrysts.

Rock	rhyolite	rhyolite	andesite								
Sample No.	554	554	312	Mineral compositions used							
	obs.	est.	parent	cpx.	opx.	plag.	magnetite	apatite	Mineral	Wt. fraction	Mineral proportion
SiO_2	74.59	74.55	60.33	50.11	53.0	54.57	-	-			
Al_2O_3	13.06	13.11	15.51	2.76	4.7	28.94	-	-	cpx.	0.012	0.023
FeO^t	2.16	2.15	7.41	11.57	14.8	-	78	-	opx.	0.10	0.19
MnO	0.04	-	0.15	0.41	-	-	-	-	plag.	0.28	0.54
MgO	0.36	0.43	2.72	14.43	23.2	-	-	-	magnetite	0.060	0.11
CaO	0.09	0.13	4.41	19.78	3.3	11.16	-	56.0	apatite	0.0114	0.022
Na_2O	2.28	-	3.84	0.31	-	5.14	-	-	E554	0.524	
K_2O	7.14	7.40	3.88	-	-	0.21	-	-		= E312	
TiO_2	0.32	0.37	1.25	0.62	0.9	-	16	-			
P_2O_5	0.06	0.01	0.51	-	-	-	-	44.0	ΣR^2	= 0.083	
Total	100.0	-	100.0								

Notes: 1. MnO and Na_2O were excluded from modelling calculations.
2. Clinopyroxene, plagioclase, magnetite and apatite compositions as for A.
3. Orthopyroxene composition after Green (1969) for experimental runs at 9 kb.

in Figures 2.10 and 2.11. There are a number of important points to note from the plots, in particular:

1) all samples have fractionated REE patterns,
2) the fractionated patterns result from LREE enrichment rather than HREE depletion, in fact no samples have HREE contents that would indicate garnet involvement either as a fractionating or residual mineral.
3) The basalt (231) has the lowest total REE content and La/Yb (9.6) (Fig. 2.11B). The small negative Eu anomally in the basalt REE pattern could be due to alteration of plagioclase or alternatively may reflect some plagioclase fractionation.

The similarity of the REE patterns for four of the samples (Fig. 2.10A) suggests a close relationship, either through crystal fractionation or varying degrees of partial melting of a similar source. The four samples are: an andesite (312), 59.7% SiO_2, La/Yb = 13.9; a dacite (747), 62.9% SiO_2, La/Yb = 13.5; a rhyodacite (294), 71.4% SiO_2, La/Yb = 15.1; and a rhyolite (554), 74.6% SiO_2, La/Yb = 12.1. To test the relationship between the four rocks a combined major element and REE modelling approach was applied. Using a least squares approximation program, major element data and data on mineral compositions, it is possible to estimate the proportions of fractionating minerals necessary to duplicate the geochemistry of the parent and daughter samples. REE modelling, based on the calculated mineral proportions, can then be applied as a test of the internal consistency. In the following, this approach is adopted for pairs of rocks e.g. andesite-dacite, dacite-rhyodacite, rhyodacite-rhyolite and andesite-rhyolite.

A. Andesite-dacite (312-747)

The results of a least squares calculation and the details of the calculation are given in Table 2.3A. The favoured model involves removal of 5% clinopyroxene, 8% plagioclase, 0.4% apatite and 1.4% titanium magnetite. However this model, like other reasonable models tried, does not adequately account for the relative levels of CaO, Na_2O and K_2O in the two rocks; either the two rocks are not related by simple crystal fractionation or alternatively, the CaO, K_2O, Na_2O contents have been modified by alteration. Modelling of the REE using the calculated mineral proportions and Kd's from Arth (1976) reveals a very close match between calculated and observed REE contents, within the limits of the Kd's used (Table 2.4A). It is therefore concluded on the basis of the REE that 312 and 747 are very likely to be related by crystal fractionation, involving clinopyroxene, plagioclase, magnetite and apatite.

TABLE 2.4. Results of trace element modelling calculations designed to investigate possible processes of crystal fractionation in the Lake Everard rocks, using mineral proportions and degree of crystallisation obtained from major element modelling calculations reported in Table 2.3.

	A.				B.			C.		
Rock	E312	E747	E747	E747	E294	E554	E554	E312	E554	E554
	obs.	obs.	calc.1	calc.2	obs.	obs.	calc.	obs.	obs.	calc.
Ce	139	150	150	146.7	176	176	207	139	176	155
Nd	90.8	92.8	93.5	90.5	102.7	84.1	120	90.8	84	74.7
Sm	54.2	55.7	54.8	52.6	58.1	44.9	68.6	54.2	45	41
Eu	37.6	38.7	38.5	31.5	25.2	14.9	21.6	37.6	14.9	23
Gd	35.7	44.1	36.2	34.8	36.2	28.6	42.9	35.7	28.6	29.6
Dy	23	22.5	23.4	22.5	25.4	24.7	30.3	23	24.7	20.5
Er	19.6	20.9	20.5	19.7	22.3	23.1	26.6	19.6	23.1	20.9
Yb	17.7	18.8	19.1	18.5	21.6	22.9	25.8	17.7	22.9	22.4

Distribution coefficients used

	Set 1.				Set 2.			Set 3.		
	cpx.	opx.	plag.	apatite	cpx.	plag.	apatite	cpx.	plag.	K-feldsp.
Ce	0.15	0.024	0.12	34.7	0.33	0.24	18.0	0.50	0.27	0.044
Nd	0.31	0.033	0.081	57.1	0.71	0.17	27.4	1.11	0.21	0.025
Sm	0.50	0.054	0.067	62.8	1.09	0.13	29.3	1.67	0.13	0.018
Eu	0.51	0.054	2.0	30.4	1.04	2.11	20.5	1.56	2.15	1.13
Gd	0.61	0.091	0.063	56.3	1.23	0.090	27.2	1.85	0.097	0.011
Dy	0.68	0.15	0.055	50.7	1.31	0.086	25.6	1.93	0.064	0.006
Er	0.65	0.23	0.063	37.2	1.23	0.084	20.0	1.8	0.055	0.006
Yb	0.62	0.34	0.067	23.9	1.10	0.077	13.1	1.58	0.049	0.012

Notes:
1. E312 → E747 calc.1 used Set 1 Kds., excepting for apatite which were taken from Set 2.
2. E412 → E554 also used Set 1 Kds., which are the average values reported by Arth (1976) for basaltic and andesitic rocks.
3. E312 → E747 calc.2 used Set 2 Kds., which are the values reported by Arth (1976) for dacitic rocks.
4. E294 → E554 used Set 3 Kds., which are the average values reported by Arth (1976) for rhyolitic rocks.
5. Distribution coefficients for magnetite were assumed to be zero.

B. Dacite-rhyodacite (747-294)

A satisfactory model relating the rhyodacite and dacite on the basis of the major elements could not be found by least squares approximation. Again the main problem lay in matching Na_2O, CaO, K_2O, Al_2O_3 and MgO using reasonable mineral compositions. Therefore, despite the similarity in the REE patterns of the two samples, it is concluded from the major elements that they are very unlikely to be related by crystal fractionation.

C. Rhyodacite-rhyolite (294-554)

Least squares modelling of the major elements indicates that the two rocks can be related by fractionation of 12.8% plagioclase, 2.5% K-feldspar, 0.3% clinopyroxene and 1.5% magnetite (Table 2.3B). The REE distribution produced by fractionating the calculated mineral proportions from a 294 parent, does not resemble that in sample 554 (Table 2.4B) and it is therefore concluded that the rhyodacite and rhyolite are unlikely to be related via differentiation.

D. Andesite-rhyolite (312-554)

All of the rhyolites (554, 607 and 78) are marked by large negative Eu anomalies indicative of plagioclase and/or K-feldspar fractionation (Fig. 2.10B). Their HREE and LREE contents are variable, possibly as a result of derivation from differing parental magmas or alternatively, due to late-stage fractionation of accessory minerals such as zircon, apatite or sphene, all of which have extremely high affinities for REE (Dodge and Mays, 1972; Arth, 1976). The latter alternative may be supported by the slight depletion in the MREE in the rhyolites compared with the more basic rocks (Fig. 2.10); this feature could reflect apatite fractionation since this mineral has a preference for MREE (Kd MREE > Kd HREE and LREE for apatite, Arth, 1976).

To test this possibility, one of the rhyolites (554) was modelled by least squares approximation of the major elements from an andesite (312). If was found that fractionation of clinopyroxene, orthopyroxene, plagioclase, Ti-magnetite and importantly, 2.2%, apatite, was necessary in order to obtain a good match in the major elements (Table 2.3C). Modelling of the REE elements using the calculated mineral proportions, F and Kds after Arth (1976), showed that fractionation of such a mineral assemblage did in fact result in a relative depletion of MREE (Table 2.4C). As Figure 2.10B shows, the match in REE for sample 554 is not perfect, nevertheless,

Figure 2.11 Chondrite-normalised REE plots for selected rocks from the Gawler Range province.

K101 - primitive basalt, Kokatha area (51.9% SiO_2, 11.77% MgO).

E231 - Nuckulla Basalt, Lake Everard area (52.1% SiO_2, 5.59% MgO).

E227 - Bunburn Dacite (62.2% SiO_2)

E725 - Yardea Dacite (67.0% SiO_2)

Y734 - Hiltaba Granite (76.6% SiO_2)

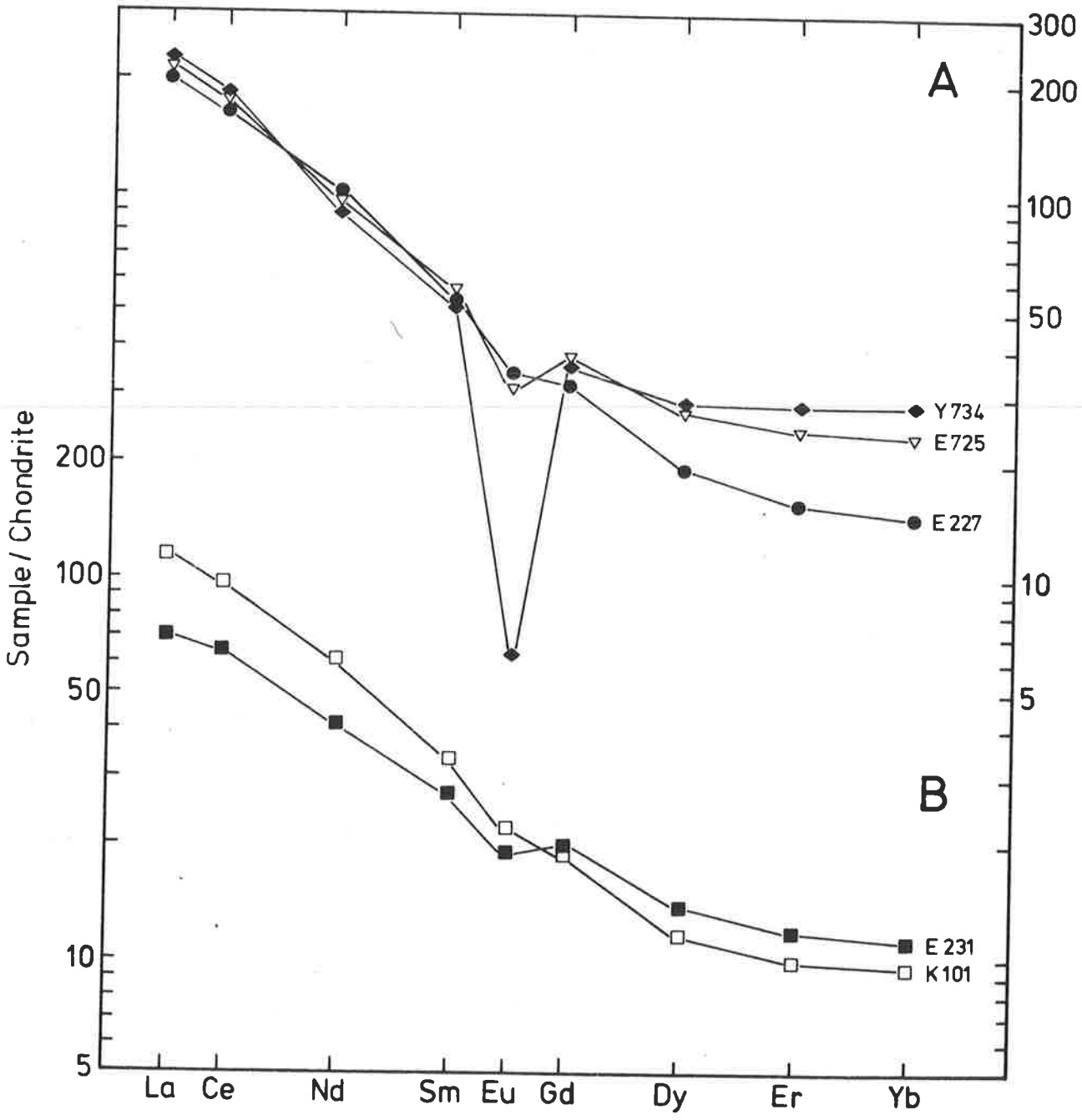

the shape of the calculated and actual REE patterns are sufficiently close to suggest that the rhyolites could be derived by simple crystal fractionation from intermediate parents, with the finer details of the REE patterns being determined by the late-stage accessory minerals. That late-stage accessory minerals have fractionated from the acid magmas is clearly evidenced by the presence of zircon, apatite and sphene in the crystal-rich accumulative rocks (e.g. Yandoolka Rhyolite and some dykes).

Although it has been shown that some of the samples considered above are unlikely to be directly related to each other by crystal fractionation, the similarity of their REE patterns offers persuasive evidence that their ultimate origins must have been similar, differing only in detail. Other samples, however, have REE patterns which clearly set them apart from the four samples examined above:

1) 227 (62.2% SiO_2; Bunburn Dacite; Fig. 2.11A) - this andesitic member of the Bunburn Dacite has an extremely fractionated REE pattern compared with other samples (e.g. 227, La/Yb = 21.1; 312, La/Yb = 13.9 and 747, La/Yb = 13.5), which results from both a relative HREE depletion and LREE enrichment (3.03 ppm Yb c.f. 3.9 ppm Yb for 747 and 64 ppm La c.f. 53 ppm La for 747). To derive this sample from an andesitic parent, such as 312, would necessitate the involvement of amphibole or garnet to explain the HREE depletion, but neither mineral could satisfactorily account for the LREE enrichment. Therefore this unit is considered to have a unique parentage (c.f. 312 and 747) a conclusion which is in accord with the previously noted differences in Na_2O/K_2O, $Fe_2O_3^t$, TiO_2, Al_2O_3, Sr, Y, V and Sc. Possible reasons for the compositional differences will be examined in the discussion on the petrogenesis of the acid magmas.
2) 734 (76.6% SiO_2; Hiltaba Granite) - this sample has the highest total REE content and largest negative Eu anomally of any rock analysed for REE from the province (Fig. 2.11A). The size of the negative Eu anomally (Eu/Eu* = 0.14) implies that the magma from which the Hiltaba Granite crystallised was produced by prolonged crystal fractionation from a more basic parent, probably involving both plagioclase and K-feldspar.

The sample of Yardea Dacite (sample no. 725, 67.0% SiO_2, La/Yb = 13.6) has a very analogous REE pattern to the andesite (312, La/Yb = 13.9) and dacite (747, La/Yb = 13.5). Its slightly higher total REE content suggests that it may be a differentiate from a 312 or 747 type parent (Fig. 2.11A). Least squares modelling, however, showed that the major element geochemistry

could not be duplicated using reasonable mineral compositions (clinopyroxene from microprobe data, plagioclase calculated from optical determinations). Thus, despite the consistent REE, it is concluded that the Yardea Dacite is probably not directly related to a 747 or 312 type parent by simple crystal fractionation. This is in agreement with the petrographic evidence presented earlier which suggested that the Yardea Dacite did not crystallise directly from a liquid, but rather, had a significant accumulative crystal component.

Compared with Cainozoic calc-alkaline volcanic rocks, the Lake Everard andesites, dacites and rhyolites are enriched in all REE and consequently have a much higher ΣREE (c.f. Taylor's average circumpacific andesite, Fig. 2.10A). Similarly, the Nuckulla Basalt has a higher ΣREE than that published for most calc-alkaline basalts (c.f. Taylor, 1969).

The following conclusions can be drawn from the REE data:

1) Plagioclase and clinopyroxene were of major importance as fractionating and/or residual minerals, while amphibole and garnet appear to have assumed negligible roles.
2) Both the basalt (231) and andesite (312) have similar, fractionated REE patterns, although there is a large difference in the absolute contents of the REE.
3) Samples from certain rock units in the Lake Everard area have very similar REE patterns and modelling calculations reveal that some are probably related via simple crystal fractionation. Other samples have distinctive REE patterns indicative of slightly different sources or crystallisation histories. Nevertheless, the REE patterns are sufficiently close to suggest broad analogies in the origin of all samples analysed.
4) The samples of granites and rhyolites analysed have been produced by extreme crystal fractionation and are not primary, unmodified partial melts. The detailed differences in the REE patterns have probably arisen as the result of late-stage fractionation of accessory minerals (e.g. zircon, apatite, sphene).

2.5 PETROGENESIS

2.5.1 General discussion

In this section possible models for the origin of the suite of rocks in the Lake Everard area will be examined in the light of the conclusions drawn from the field, petrographic and geochemical evidence previously

TABLE 2.5. Results of major and trace element modelling calculations designed to test whether the andesites from the Lake Everard area (an average of four samples) could be related to the Nuckulla Basalt by simple crystal fractionation.

A. Least squares approximation of average andesite in terms of Nuckulla Basalt and expected minerals.

Rock	average andesite obs.	average andesite calc.	Nuckulla Basalt parent	Mineral compositions used amph.	plag.	magnetite
SiO_2	60.12	60.12	52.81	42.1	54.44	
Al_2O_3	15.78	15.74	17.51	14.7	28.97	
FeO^t	7.64	7.64	9.43	10.3	0.46	88.0
MnO	0.16		0.16			
MgO	2.90	2.93	5.45	15.5	0.13	
CaO	4.47	4.41	7.22	11.5	10.47	
Na_2O	3.51	3.79	3.80	2.9	5.57	
K_2O	3.73	3.57	3.31	1.0	0.35	
TiO_2	1.22	1.25	1.22	1.5		6.0
P_2O_5	0.47	0.42	0.22			
Total	100.0		100.0			

Mineral	Wt. fraction	Mineral proportion
amph.	0.25	0.53
plag.	0.192	0.405
magnetite	0.031	0.065
andesite	0.53	
	= basalt	
ΣR^2	= 0.11	

Notes:
1. MnO was excluded from modelling calculations owing to an absence of MnO data for amphibole and magnetite.
2. Amphibole composition from writer's electron microprobe data for amphibole phenocrysts in a calc-alkaline basalt (W31, see Table A5.5, Appendix 1).
3. Plagioclase composition is that of labradorite (after Deer, Howie and Zussman, 1962), and is considered to be realistic on optical grounds.
4. Ti content of magnetite adjusted to give a satisfactory match for TiO_2.

B. Calculated trace element abundances, using mineral proportions and degree of crystallisation obtained from major element modelling calculations.

Rock	average andesite obs.	average andesite calc.	Nuckulla Basalt parent	Distribution coefficients used amph.	plag.	mag.	opx.	cpx.
Zr	307	252	159	0.5	0.01	0.10	0.03	0.1
Nb	13	13	9	0.8	0.01	0.4	0.15	0.1
Y	36	37	28	1.0	0.03	0.2	0.2	0.5
Ce	109	89	52	0.20	0.12	0	0.024	0.15
Rb	126	119	71	0.29	0.071	0	0.022	0.015
Sr	462	490	482	0.46	1.8	0	0.017	0.12
Ba	1420	1014	657	0.42	0.23	0	0.013	0.026
Sc	20	<1	24	12.5	0	2	3	3
V	141	<1	186	32	0	30	1.1	1.1
Cr	24	<1	96	30	0	32	13	30
Ni	24	9	105	8	0	8	8	6
Sm	10.4	8.1	5.2	0.52	0.067	0	0.054	0.50
Yb	3.7	3.6	2.3	0.49	0.067	0	0.34	0.62

Note: 1. Distribution coefficients for Zr, Nb and Y after Pearce and Norry (1979); Ce, Rb, Sr, Ba, Sm and Yb after Arth (1976) and Sc, V, Cr and Ni after Gill (1978).

discussed. The two simplest hypotheses are that:

1) The acid and intermediate magmas are related via crystal fractionation to parental basic magmas, implying that all rocks form part of a continuous magmatic series - the "basalt-andesite-dacite-rhyolite" suite.
2) Two separate and unrelated magmatic series exist, represented by the acid-intermediate rocks and basic rocks, respectively. In this model, the basic magmas and acid-intermediate magmas are postulated to have been derived by partial melting of separate, and geochemically distinct, sources.

Both alternatives will be discussed below, beginning with the case of crystal fractionation.

A. Models involving crystal fractionation from a parental basic magma

Such models are confronted with a volume problem, particularly in the Lake Everard area where the exposed volume of basic and intermediate rocks is impossibly low to account for the huge volume of acid rocks. It is possible, however, that the exposures of basic and intermediate rocks do not accurately portray their original magmatic volumes, due to entrapment of the denser magmas within the crust (c.f. Fyfe, 1978). The proposition that the Lake Everard andesites and basalts are related by crystal fractionation can be tested quantitatively using the geochemical data. This is achieved by modelling the major elements using least squares approximation and checking for internal consistency by modelling the trace elements, including the REE. To facilitate the calculations an average basalt and an average andesite from the Lake Everard area have been compiled (Table 2.2). The samples averaged are analogous in most critical respects (e.g. SiO_2, Zr, Nb, Y, Ce, SiO_2 and MgO) and it is anticipated that the average will smooth the more variable components (e.g. Rb, Ba, Sr, Na_2O, CaO and K_2O).

Of the many possibilities tested, the most reasonable fit in major elements was obtained by removal of approximately 25% amphibole, 3% magnetite and 19% plagioclase from the average basalt to yield the average andesite (Table 2.5A). The relatively high proportion of amphibole is predictable from the requirement that SiO_2 increase while MgO, Al_2O_3 and $Fe_2O_3^t$ decrease. Modelling of the trace elements using the calculated F and mineral proportions revealed that the discrepancies in most of the lithophile elements (Zr, Nb, Y, REE, Rb and Sr) were <25% (Table 2.5B). Given the uncertainties introduced by the assumptions of

TABLE 2.2. Geochemical data referred to in text.

	A	B	C	D	E	F	G
SiO_2	59.48	52.10	51.98	53.69	51.91	65.6	54.0
$Al_2O_{3_t}$	15.61	17.29	15.95	14.81	13.65	16.5	19.0
Fe_2O_3	8.40	10.32	9.99	13.57	9.66	3.15	10.0
MnO	0.16	0.16	0.19	0.21	0.18		
MgO	2.87	5.37	8.08	3.53	11.77	0.83	4.1
CaO	4.42	7.10	8.75	6.54	8.55	2.03	9.5
Na_2O	3.47	3.74	2.55	3.23	2.15	4.75	3.4
K_2O	3.69	2.18	1.15	2.20	1.27	5.3	0.6
TiO_2	1.21	1.20	0.84	1.74	0.64	0.64	0.9
P_2O_5	0.47	0.21	0.25	0.40	0.18	0.19	
Total	99.78	99.67	99.73	99.92	99.96		
LOI	2.18	2.53	1.79	0.70	1.51		
Zr	307	159	122	229	102	~500	30
Nb	12.9	9	5.8	9.5	5.3	< 20	4
Y	36	28	24	40	19	~ 40	20
Ce	109	52	56	86	78	143	17
Nd		25	21	45	36	60	
Sc	20	24	31	28	29	7.5	
V	141	186	178	280	180	51	
Cr	24	96	610	8.1	1050	< 2	
Ni	24	105	195	8.4	362	< 15	
Rb	126	71	39	67	45	245	20
Sr	462	482	514	433	510	570	425
Ba	1423	657	780	976	1005	1700	175

A. Average composition of four andesites from the Lake Everard area (average of E532, E312, E524 and E33).

B. Average composition Nuckulla Basalt, Lake Everard area (average of E231 and E459).

C. Average composition of evolved basalt from the Kokatha area (average of K110 and K33).

D. Highly-fractionated basalt from the Kokatha area (K153).

E. Primitive basalt from the Kokatha area (K101).

F. Composition of glass from the Eureka Valley Tuff, California (after Noble, et al., 1976).

G. Calculated composition of the lower crust (after Taylor and McLennan, 1979).

the modelling calculations (e.g. distribution coefficients, least squares approximation of major elements), it is believed that none of the lithophile elements present a major objection to the model. The order of magnitude discrepancy in the compatible elements (V, Sc,Cr and Ni) is not insignificant however, because unless the Kds for these elements differ by an order of magnitude from the published values, the mismatch cannot be reconciled. In the absence of any evidence for this, it is concluded that the differentiation model involving basalts and andesites from the Lake Everard area, is untenable.

At this point it is pertinent to consider the differentiation trends in the Kokatha rocks, where basalts are far more abundant. The basalts from this area show a tholeiitic iron-enrichment trend, presumably produced by olivine + pyroxene + plagioclase fractionation under relatively low PO_2 and PH_2O conditions (Branch, 1978). A typical differentiated basalt from the Kokatha area analysed by the writer (Table 2.2), has relatively high Fe/Mg, TiO_2, P_2O_5, Zr, Nb, Y and LREE and low MgO, Ni and Cr contents. It is clear from a visual comparison of the major elements that to produce the average andesite from such a parent would require magnetite + amphibole ± clinopyroxene fractionation in order to reduce $Fe_2O_3^t$ and MgO and at the same time increase SiO_2 to the required levels. These minerals have Kds solid/liquid >1 for Ni and Cr (Gill, 1978; Leeman, et al., 1978), yet Ni and Cr are significantly higher in the average andesite compared with the basic differentiate, thus precluding a crystal fractionation relationship. Moreover, it is evident that prolonged crystallisation along the tholeiitic trend of the basalts would not yield the major element (nor trace element) contents of the andesites. If water were added, such that amphibole and magnetite became stable and crystallised in large quantities, the relative levels of the compatible trace elements would still present a major objection (particularly Ni, Sc, V and Cr).

B. Models involving partial melting of different sources

The conclusion that the intermediate volcanic rocks are probably not related to the basalts by simple crystal fractionation necessarily implies that the primary magmas in each case originated from separate sources. Basic magmas have an origin in the mantle (Green, 1971), while primary acid magmas are usually considered to be crustal-derived (Wyllie, et al., 1976). The origin of intermediate magmas is controversial (e.g. Mysen and Kushiro, and Nicholls and Ringwood, 1973), but in the present case the geochemistry (particularly the REE) suggests that the intermediate and acid volcanic rocks share a common origin. In the following discussion,

TABLE 2.6. Elemental ratios for basalts from the Gawler Range province.

Ratio	Probable chondritic value	A	B	C	D
$Zr/_{Ce}$	7.4-7.7	1.3	2.2	3.1	2.8
$Zr/_{Y}$	2.5-2.8	5.4	5.1	5.7	8.5
$Ti/_{Zr}$	100-110	38	41	45	24
$Ti/_{Y}$	250-280	202	210	257	202
$Zr/_{Nb}$	16-18	19	21	18	24
$Ti/_{V}$	8.4-10	21	28	39	51
$Ti/_{Sc}$	78-85	132	163	300	363
$TiO_2/_{P_2O_5}$	STP=10	3.6	3.4	5.7	2.6
$Al_2O_3/_{TiO_2}$	20.4	21			
$CaO/_{TiO_2}$	17	13.4			
%MgO		11.77	8.08	5.37	2.87
No. samples		1	2	2	4

A. Primitive Kokatha basalt (K101).

B. Evolved Kokatha basalt (average of K33 and K110)

C. Nuckulla Basalt (average of E231 and E459).

D. Lake Everard andesite (average of E33, E312, E524 and E532).

Notes: 1. Chondritic values after compilations of Nesbitt and Sun (1976), Sun and Nesbitt (1977) and Nesbitt, pers. comm.

2. $TiO_2/_{P_2O_5}$ value of 10 is for Archaean spinifex-textured periodotites which are thought to be derived by high degrees of melting of primitive mantle (Nesbitt and Sun, 1976).

the basic and intermediate-acid rocks will be considered separately, to permit a detailed investigation of their particular origins.

2.5.2 Origin of the basic magma.

A. General discussion

The relatively low Mg number of the Nuckulla Basalt (53) and low Ni and Cr contents preclude equilibration with mantle peridotite (Roeder and Emslie, 1970; Sato, 1970). Consequently, this basalt must have differentiated from a more primitive parent with lower absolute contents of incompatible elements (e.g. Ti, Zr, Nb, Y, LREE, P, K, Rb and Ba). It has been previously noted that the geochemistry of the Nuckulla Basalt in some respects resembles that of calc-alkaline basalts (particularly in the contents of Al_2O_3, TiO_2, P_2O_5, Zr and Y). Basalts with high Al_2O_3 in association with calc-alkaline suites (i.e., high-alumina basalts) are thought to be derived by olivine + clinopyroxene fractionation from an olivine tholeiite parent (Green, et al., 1967). The lower Al_2O_3 and higher Ni and Cr contents of the Nuckulla Basalt compared with high-alumina basalts (Taylor, 1969; Jakes and White, 1972) suggests that olivine and clinopyroxene fractionation may not have been so extreme in this case. It is also possible that small amounts of plagioclase fractionation may have contributed to the lower Al_2O_3 and slight negative Eu anomally in the Nuckulla Basalt, perhaps reflecting lower PTOTAL and/or PH_2O during fractionation (Yoder and Tilley, 1962; Eggler, 1972).

A consideration of the incompatible element ratios for the Nuckulla Basalt reveals that Zr/Nb and Ti/Y are near chondritic whereas Zr/Ti and Zr/Y are significantly greater than chondritic (Table 2.6). This could be due to control of Ti and Y by residual mineral(s) in the mantle and/or fractionating mineral(s) or alternatively it may reflect derivation from a mantle enriched in Zr and Nb relative to Ti and Y. Unfortunately, the limited compositional range of basalts from the Lake Everard area does not permit distinction between these alternatives. To extend the compositional range, analyses of two, more primitive basalts from the Kokatha area are given (Table 2.2). It is notable that both have non-chondritic Zr/Ti and Zr/Y values yet approximately chondritic Zr/Nb, with similar values to those for the Nuckulla Basalt (Table 2.6). In particular, the similarity of these ratios in the primitive Kokatha basalt (K101), indicates that fractionating minerals have not been responsible for the control on Ti and Y. Also, the near chondritic Ti/Y

value suggests that the bulk D (melt/residue) was approximately the same for Ti and Y indicating that little or no garnet was in the residue from which the magma segregated, since this mineral would be expected to retain Y in preference to Ti (assuming the Kd for Y is similar to that for HREE in garnet, e.g. Arth, 1976).

Other notable features of the elemental ratios of the primitive Kokatha basalt (K101) are:

1) V/Ti and Sc/Ti are both significantly less than chondritic, implying control on V and Sc relative to Ti.
2) P_2O_5/TiO_2 is greater than chondritic.
3) Zr/Ce is considerably less than chondritic indicating that Ce is enriched over Zr and Nb. It is notable that Ce and P_2O_5 do not show systematic trends in the more differentiated basalts (measured by P_2O_5/TiO_2 and Zr/Ce in the evolved Kokatha basalt and average Nuckulla Basalt), suggesting that the processes leading to their enrichment were rather more erratic than for Zr and Nb.
4) Al_2O_3/TiO_2 is approximately chondritic indicating that a highly aluminous mineral is not residual in the mantle (e.g. garnet, amphibole or aluminous clinopyroxene), while CaO/TiO_2 is a little less than chondritic suggesting that a calcic mineral may be residual (e.g. clinopyroxene).

Using the expression for batch partial melting in terms of the residual minerals (after Schilling and Winchester, 1967), published distribution coefficients and assumed mantle abundances (after Frey, et al., 1978) it is possible to calculate the proportions of residual clinopyroxene, orthopyroxene and olivine necessary to produce the observed concentrations of the compatible elements, Sc and V, in K101. The favoured residual mineral proportions are: 70% olivine, 20-25% orthopyroxene and 5-10% clinopyroxene at approximately 20-25% partial melting (Table A2.5, Appendix 1). These values could vary slightly because of the uncertainties introduced by the assumptions of the calculations, but it is unlikely that the proportion of clinopyroxene would exceed 10% while the degree of melting is unlikely to be less than 20%.

A crude check on this conclusion can be made by least squares modelling the major elements of the primitive basalt (K101) from a hypothetical mantle composition. The calculations involve the following assumptions:

1) K101 represents the composition of the primary magma;
2) olivine, orthopyroxene and clinopyroxene are the only residual minerals;

TABLE 2.7. Least squares approximation of primitive basalt (K101) in terms of a hypothetical mantle source and possible residual minerals.

Rock	K101 melt	pyrolite obs.	pyrolite est.	Mineral compositions used ol.	opx.	cpx.
SiO_2	52.43	45.2	45.21	41.0	54.4	54.3
Al_2O_3	13.79	3.5	3.43		0.6	1.0
FeO^t	8.78	10.0	10.12	11.1	6.6	4.1
MnO	0.18					
MgO	11.90	37.5	37.47	47.7	33.0	18.5
CaO	8.64	3.1	3.09	0.2	1.6	20.8
Na_2O	2.17					
K_2O	1.28					
TiO_2	0.65	0.17	0.18		0.2	0.3
P_2O_5	0.18					
Total	100.0					

Mineral	Wt. fraction	Mineral proportion
ol.	0.68	.88
opx.	0.050	.065
cpx.	0.037	.048
K101	0.244	
	= pyrolite	

ΣR^2 = 0.0215

Notes:

1. Pyrolite composition is modified from Ringwood (1966). The TiO_2 content of Ringwood's pyrolite has been reduced from 0.7% to 0.17%, while the FeO^t content has been increased from 8.5% to 10% in order to obtain satisfactory matches for these elements. The former modification is consistent with estimates of Archaean pyrolite given by Green (1975) and Sun and Nesbitt (1977), while the latter is consistent with Glikson's (1979) proposal of a more iron-rich Archaean mantle, and the high end of the Archaean pyrolite range (9.7% FeO^t) estimated by Sun and Nesbitt (1977).
2. Addition of variable proportions of olivine to K101 failed to yield a satisfactory match for unmodified pyrolite.
3. Olivine, orthopyroxene and clinopyroxene compositions taken from experimental data of Green (1976) for 1100°C, 10 kb conditions.

3) the mantle source has the composition of a modified pyrolite (after Ringwood, 1966).

The results of the calculations, reported in Table 2.7 show that a melt with the composition of K101 could be derived by 24-25% partial melting of the assumed mantle leaving a residue of 88% olivine, 7% orthopyroxene and 5% clinopyroxene. The important points to note are the relatively high degree of melting (24%) and the presence of residual clinopyroxene, which, considering the assumptions involved, is in remarkably good agreement with the conclusions based on the Sc and V modelling.

The relatively high degree of melting (>20%) implied by the Sc and V, and major element data is notable, as it exceeds the estimate of approximately 15% based on Zr and Nb (using the mantle abundances of Frey, et al., 1978 and assuming complete incompatibility). Ce predicts an even lower degree of melting (approximately 2.5%) and estimates based on K_2O and Rb yield similar values. This, combined with the non-uniform Ce levels in the three basalts (Table 2.2), suggests the possibility that the basic magma may have been derived from a LREE, Zr, Nb (and possibly K, Rb, Ba)-enriched mantle. The consistency of the ratios of the relatively immobile elements (Zr, Nb, Y and Ti) and the near chondritic Zr/Nb and Ti/Y values indicates that crustal contamination is an unlikely cause for the relative elemental enrichments.

Assuming 20% melting with a residue of 70% olivine, 22.5% orthopyroxene and 7.5% clinopyroxene, the hypothetical REE contents of the enriched mantle source (for K101) are: 15 ppm Ce (i.e., 18.5 x chondrite) and 2 ppm Yb (i.e. 9.6 x chondrite). The inferred lower Ce contents in the parental magmas from which the more evolved basalts were derived (Table 2.2), could be taken as evidence that they were generated from a less enriched part of the mantle, thus indicating significant heterogeneity in the source. The alternative possibility, that the parental magmas for the evolved basalts were the products of higher degrees of partial melting of the same mantle source as K101 is not supported by the relative Sc, V, Zr and Nb contents, nor is it consistent with experimental evidence (Green, 1973a).

B. Conditions of magma segregation

Several of the points previously deduced concerning the origin of the primitive Kokatha basalt (K101) can be used to gain some insight into the conditions under which the basic magmas segregated. The points of particular relevance are:

1) the presence of 5-10% clinopyroxene in the residue;
2) the relatively high degree of melting inferred (>20%), and
3) the variable enrichment of LIL elements in the mantle source.

The presence of residual clinopyroxene implies that magma segregation probably did not take place at depths greater than about 60 km (Green, 1972, 1973), assuming water-undersaturated melting. In view of the relatively aluminous nature of K101 compared with typical olivine tholeiites (which contain approximately 12% Al_2O_3) the depth of melting may have been nearer 40 km (Green, 1973). If partial melting under water-saturated rather than water-undersaturated conditions occurred, the depth of magma segregation was still likely to have been less than 60 km, in order to maintain clinopyroxene in the residue (Green, 1973b). Without experimental data for the rocks being considered precise estimates of the pressure and temperature conditions of melting cannot be made, but at the degree of melting proposed (i.e., >20%), it is clear from the experimental constraints cited above, that segregation of the magma from relatively shallow depths and under hydrous conditions, is indicated.

The preceding discussion has been largely concerned with explaining the origin of the primitive Kokatha basalt (K101), since it is the only relatively unfractionated basalt in the province known to the writer. The inference that the Nuckulla Basalt and evolved Kokatha basalt could be derived from a basic parent with the compositional characteristics of K101 is supported by the following evidence:

1) The similarity in major element characteristics e.g. relatively high Al_2O_3 and low $Fe_2O_3^t$ and TiO_2 contents common to all.
2) Major element modelling calculations, which show that both K110 and 231 could be derived by clinopyroxene + olivine fractionation from a K101 type parent.
3) The similar elemental ratios, particularly those little affected by fractionation of olivine and clinopyroxene (Table 2.6).
4) The proximity in the field - the volcanic piles in the Lake Everard and Kokatha areas are approximately contemporaneous and are only 50 km apart.

On the above grounds, it is believed that the conclusions concerning the origin of the primitive Kokatha basalt (K101) can be directly applied to the parental magmas for the Nuckulla Basalt in the Lake Everard area. The only major exception is that the source for the Nuckulla Basalt parent magma was not as enriched in LREE as that for the primitive Kokatha basalt, but this is not inconsistent with the concept of a heterogeneous LIL element-enriched mantle source.

2.5.3 Origin of the acid-intermediate magma

A. General discussion

Green (1976) has shown that intermediate magmas cannot be derived by direct partial melting of the mantle, although some workers would disagree with this conclusion (e.g. Mysen and Kushiro, 1973; Mysen and Boettcher, 1976). If this conclusion is accepted, then the origin of primary intermediate magmas is limited to a two-stage process involving partial melting of basic rocks, either as eclogites or amphibolites, depending on the depth of melting (Green and Ringwood, 1968). However, Stern (1974) has demonstrated that liquids derived from such a source do not resemble calc-alkaline andesites. In most Cainozoic calc-alkaline provinces where subduction has been (or still is) operative, this serious objection can be negated by proposing that the intermediate magmas have differentiated from primary basic magmas that were generated in the mantle wedge overlying the subducted basaltic crust (e.g. Thorpe, et al., 1976; Kay, 1978). Presumably, melting in the mantle is triggered by fluids released from the subducted oceanic crust, perhaps by dehydration reactions (Best, 1975). It is considered that such a model is unlikely to be directly applicable in the present case owing to the lack of any geological evidence for contemporaneous subduction in the region (Glen, et al., 1977). Moreover, the post-orogenic tectonic setting of the province and the development within a large mass of thick, stable continental crust are festures not normally associated with subduction-related magmatism. In particular, the relatively high LIL element contents and high K_2O/Na_2O values in the Lake Everard rocks, strongly suggests a significant sialic crustal contribution.

On experimental grounds, it is feasible that the acid-intermediate magmas could have been derived by direct crustal melting, but as Wyllie, et al., (1976) point out, the temperatures required to generate melts far removed from the eutectic composition (e.g. liquids with the composition of the andesites or low-silica dacites i.e. 58-65% SiO_2) are greatly in excess of temperatures attained during regional metamorphism. For example, to generate an andesitic liquid with 2% dissolved H_2O at 30-50 km depth would require a temperature of 1100^{o}C (Wyllie, et al., 1976). Surface recordings at 1200-1250^{o}C in modern andesitic lava flows (Osborn, 1969) appear to verify the relatively high temperatures involved. Many workers have avoided this problem by invoking variations on the simple partial melting model to explain the origin of acid magmas with non-eutectic compositions. The models proposed include:

1) Those involving a restite component and a near eutectic melt (e.g. White and Chappell, 1977; Wyllie, 1977). In this model it is postulated that sufficient near-eutectic melt is generated to mobilize some (or all) of the residue which then rises and intrudes with the melt. The evidence for this restite is seen in abundant metasedimentary and/or meta-igneous xenoliths, xenocrysts of hornblende, biotite, cordierite, garnet and complexly-zoned and twinned, plagioclase. A number of workers have demonstrated the feasilibity of this process in explaining the origin of granitoids with non-eutectic compositions in eastern Australia (e.g. White and Chappell, 1977; Price and Taylor, 1977).
2) Contamination, in which additions from the wall rocks by reaction and zone refining are invoked to explain rocks with unusually high K_2O, Rb and other LIL element contents, yet with relatively basic major element compositions (e.g. Noble, et al., 1976).
3) Magma mixing, defined by Anderson (1976) as: "that process whereby two or more compositionally distinct magmas are mixed together such that the melts of each are blended into a compositionally uniform single magma (uniform melt + crystals + gas)." Anderson, and more recently, Eichelberger (1978) have argued for the adoption of this model as a general explanation for the origin of circum-pacific andesites.

The applicability of each of these models in explaining the origin of the non-eutectic liquid compositions in the present case, will be investigated below.

B. Models involving a restite component

In a suite of rocks as complex as those from the Lake Everard area, where partial melting of differing sources, crystal fractionation and even contamination and magma mixing may have been operative, it is unlikely that the geochemical data will be able to conclusively verify or dispel this hypothesis. Probably a more rewarding avenue of search would be simple petrographic observation (c.f. White and Chappell, 1977).

If the rocks of low-silica dacite and andesite composition are considered, it is immediately apparent that many of them are remarkably phenocryst poor, particularly those belonging to the Childera Dacite and Bunburn Dacite (2% phenocrysts, Table 2.1). Even the andesitic variants of the Mangaroongah Dacite are relatively phenocryst poor (6-8% phenocrysts, Table 2.1). Moreover, the phenocrysts present (i.e.,

clinopyroxene and plagioclase) appear to have crystallised from melts with the approximate composition of the host rock and have compositions consistent with this. Basic xenoliths, commonly with diffuse margins, are present in two of the units (Childera Dacite and Mangaroongah Dacite) but probably comprise less than 5% by volume. If the generous figure of 15% restite (5% basic xenoliths + 10% crystals, with an average of 50% SiO_2) is assumed in an andesite from the Mangaroongah Dacite, and this is combined with an acid, eutectic melt (75% SiO_2, White and Chappell, 1977), the resulting mixture would have approximately 71% SiO_2, clearly quite different to the 58-62% SiO_2 range observed in andesites from this unit. Thus it is concluded, in the absence of supporting petrographic evidence and from the compositional disparity, that the restite model cannot provide an explanation for the origin of the andesites and low-silica dacites.

One variant on the restite model conveniently examined at this point, is that involving earlier fractionated crystals which have accumulated in a magma chamber to be subsequently disrupted and incorporated into later, more fractionated liquids, as outlined in the petrography section. Although these crystals do not represent material from the site of partial melting, and hence are not restite in the sense originally defined by White and Chappell (1977), they nevertheless have an effect on the geochemistry of the host liquid similar to that produced by restite. Apart from explaining the petrographic observations, this concept is able to account for some of the unusual geochemical features of the acid rocks in the Lake Everard area. Some specific examples are mentioned below:

1) The relatively high Zr contents, characteristic of the Yantea Rhyodacite (Fig. 2.9D) could be explained by proposing that the K_2O-rich residual liquid engulfed significant amounts of accumulative zircon, in addition to plagioclase and clinopyroxene, prior to its final ascent and eruption.
2) The Hiltaba Granite and many of the rhyolites may have crystallised directly from the K_2O-rich residual liquid, hence explaining their highly-fractionated geochemical characteristics.
3) Some dacites with abnormally high Ba contents, may have been produced by the incorporation of plagioclase, clinopyroxene and magnetite phenocrysts into a high-Ba residual liquid that was extracted prior to extensive K-feldspar fractionation.

C. Models involving contamination

Noble, et al. (1976) record the geochemistry of highly potassic, fresh glasses in quartz latites from California an analysis of which is given for comparison in Table 2.2. In general, the Lake Everard dacites have higher iron and titanium, and lower Al_2O_3 contents, but otherwise the geochemical similarity is striking. To explain the high K_2O and other LIL element contents, yet low SiO_2 of the latites, Noble and co-workers suggested that a primary melt, derived by partial melting of LIL element-enriched mantle, is further enriched in LIL elements by zone refining and wall-rock reaction during its ascent. Subsequent crystal fractionation yielded the latites. The net enrichment in LIL elements above the enriched mantle source is approximately 50 times.

Unfortunately, this model is virtually impossible to test quantitatively because of the rather arbitrary assumptions as to the degree of LIL element enrichment in the mantle source and even greater assumptions regarding the contribution of wall-rock reaction. However, there are some serious qualitative objections which can be raised against this model as an explanation for the origin of the Lake Everard rocks:

1) It cannot explain the paucity of intermediate rocks. In this model, since the ultimate source of magma is the mantle and the LIL element enrichment is primarily due to the enriched source source and contamination, it might be expected that a continuum from highly LIL element-enriched basalt through andesite to dacite would occur. Although the basalts in the Gawler Range province are relatively enriched in LIL elements, perhaps through the operation of such a mechanism, it has been previously demonstrated that they could not have given rise to the andesites or dacites by simple crystal fractionation.
2) The process invoked by Noble and co-workers to explain the geochemical properties of the dacitic glasses (65.5% SiO_2) would have had to be far more extreme to explain similar properties in the Lake Everard andesites which have significantly lower contents of SiO_2 (e.g. 58-60% SiO_2).
3) Noble and co-workers place little emphasis on the possibility of a significant LIL element contribution from the crust. This would appear to be overlooking a major source of LIL elements in the case of the Gawler Range volcano-plutonic province, particularly in view of the extent of the province and volume of acid rocks. By increasing the proportion of acid, LIL element contaminant

derived from the crust, the contamination model grades into a magma mixing model similar to that defined by Anderson (1976).

D. Magma mixing models

In this model, the possibility of mixing mantle-derived basic magma with crustal-derived acid magma is presented as a method of generating LIL element-enriched intermediate magma. It is assumed that the high geothermal gradient produced by the basic magmatism and probable mantle diapirism induced partial melting of the lower crust.

Some of the factors which would favour mixing of separate bodies of acid and basic magma are:

1) Both magmas would tend to use the same zones of weakness as channelways during their ascent, hence there would be a high probability of mixing.
2) The silicic magma, being lighter and less dense, would rise above the basic magma tending to entrap it, thus promoting mixing at the contact (Eichelberger, 1978). This could occur either at the base of the crust or within the crust.
3) Once in contact the temperature gradient would ensure much convection and hence mixing (Eichelberger, ibid.)

This model offers the possibility for significant variations in the composition of the products of mixing, making quantitative testing difficult. For example, the basic magma could differentiate to varying degrees prior to mixing and this would greatly affect the levels of MgO, Ni, Cr, $Fe_2O_3^t$, P_2O_5, TiO_2, V and Sc in the resultant mix. There is also the possibility of addition of further batches of basic and acid magma to the mix at any point during its crystallisation history. In addition, varying the proportions of basic and acid magma would produce a range of compositions in the primary mixture. If the mixing model is applicable it should be possible to generate a composition very similar to that of the average andesite (Table 2.2) by mixing the appropriate proportions of basic and acid magma. The main problem is to decide upon appropriate compositions for the parental basic and acid magmas, so that a test can be applied.

Many samples of Hiltaba Granite and some rhyolites approach a eutectic major element composition (c.f. White and Chappell, 1977) despite the fact that their trace element contents show them to be highly fractionated (particularly Rb, Sr and Eu). For the purposes of testing, the major element composition of the hypothetical eutectic acid magma

A.	Average Nuckulla Basalt	Calculated andesite composition	Assumed near-eutetic acid composition	B.	Calculated basalt composition	Average andesite	Assumed near-eutectic acid composition	Average andesite	Average Nuckulla basalt	Minimum melt S-type, after White and Chappell, 1977.
SiO_2	52.10	59.48	74.97		52.11	59.48	74.97	59.48	52.10	75.74
Al_2O_3t	17.30	15.91	13.00		16.85	15.61	13.00	15.61	17.30	12.97
Fe_2O_3	10.32	7.59	1.88		11.51	8.40	1.88	8.40	10.32	1.56
MnO	0.16	0.12	0.04		0.22	0.16	0.04	0.16	0.16	0.03
MgO	5.37	3.70	0.21		4.14	2.87	0.21	2.87	5.37	0.31
CaO	7.11	5.10	0.88		6.11	4.42	0.88	4.42	7.11	1.11
Na_2O	3.74	3.54	3.12		3.64	3.47	3.12	3.47	3.74	3.11
K_2O	2.18	3.24	5.47		2.84	3.69	5.47	3.69	2.18	4.85
TiO_2	1.20	0.88	0.22		1.68	1.21	0.22	1.21	1.20	0.28
P_2O_5	0.22	0.16	0.02		0.68	0.47	0.02	0.47	0.22	0.06
Zr	159	237	400		263	307	400	307	159	
Nb	9	12.2	19		10	13	19	13	9	
Y	28	33	44		32	36	44	36	28	
Ce	52	90	140		94	109	140	109	52	
Sc	24	17	3		28	20	3	20	24	
V	186	127	3		207	141	3	141	186	
Cr	96	67	3		34	24	3	24	96	
Ni	105	72	3		34	24	3	24	105	
Rb	71	106	180		100	126	180	126	71	
Sr	482	359	100		635	462	100	462	482	
Ba	657	929	1500		1386	1423	1500	1423	657	

Table 2.8. Mixing calculations.

A. Results of mixing calculations in which the average Nuckulla Basalt composition is mixed with an assumed near-eutectic acid liquid composition, in the correct proportions to yield the SiO_2 content of the average andesite.

B. Results of calculations in which the assumed near-eutectic acid liquid composition is subtracted from the average andesite in the correct proportions to yield the SiO_2 content of the average Nuckulla Basalt.

was taken from a typical sample of Hiltaba Granite. Selection of appropriate trace element contents presented more of a problem, but it was eventually decided to use the average values from a number of less-fractionated rhyolites. As an initial test, the supposed eutectic melt composition was mixed with the average Nuckulla Basalt in the proportions that gave the SiO_2 content of the average andesite, on an anhydrous basis. Selection of the mixing proportions based in SiO_2 is arbitrary, but theoretically if the model is valid, mixing based on the proportions of any of the other major elements should yield similar results. The results of the calculation are given in Table 2.8A. Comparing the calculated andesite with the average andesite reveals a broad similarity in most major elements. However, in detail, there are a number of significant discrepancies, in particular the calculated andesite has relatively high MgO, CaO, Ni and Cr contents, but is low in TiO_2, P_2O_5, Zr, Ce and Ba compared with the average andesite.

This may demonstrate a failure of the assumptions rather than the model, since it is apparent that if a more differentiated basic melt (higher in TiO_2, P_2O_5, Zr, Ce, Ba, and lower in MgO, CaO, Ni Cr) had been selected, the calculated mix and average andesite would have shown much closer agreement. It is unfortunate that the composition which is known best (i.e., average andesite) is the one being tested. In view of the uncertainty in the basic melt composition and the great variation possible due to differentiation, it was decided to attempt an alternative method of calculation in which the average andesite and eutectic acid melt composition were used to determine the basic melt composition. If the calculated basic melt was of an acceptable composition, this would suggest an internal consistency in the mixing hypothesis. As would be predicted from the previous calculation involving the Nuckulla Basalt, the calculated basic melt has appreciably higher $Fe_2O_3^t$, TiO_2, P_2O_5, K_2O, Zr, Ce and Ba, but lower CaO, MgO, Ni and Cr contents, indicating that it is more differentiated (Table 2.8B). Least squares modelling of the major elements demonstrated that the calculated basic melt could be derived by olivine + clinopyroxene fractionation from a K101 parent. This is the same fractionation trend as that indicated for other basalts from the province (e.g. evolved Kokatha basalts and Nuckulla Basalt) therefore suggesting that the calculated composition is not unrealistic.

Thus is would appear from the calculations that a mixing model could be substantiated on the basis of the geochemistry, although this does not necessarily prove that magma mixing did occur. In fact there are several qualitative arguments which can be raised against this model:

1) If magma mixing occurred, then a continuum from basalt to rhyolite might be expected corresponding with the complete spectrum of mixing proportions possible. In a mixing model no reasonable explanation could be offered for the compositional hiatus in the 52-58% SiO_2 range, unless of course it were proposed, rather fortuitously, that mixing did not occur in the correct proportions to generate magmas of this composition.
2) In view of the evidence for significant differentiation within the acid-intermediate series, it is apparent that mixing can only be applied to the generation of the andesitic and low-silica dacite liquids. This relies on a rather fortuitous set of circumstances, viz. mixing in exactly the right proportions to give these liquids and no others, either more or less basic, and a basic component, differentiated to the required degree to yield the correct elemental contents in the mix.
3) There is a lack of petrographic evidence for mixing. The abundant basic xenoliths in the andesites and low-silica dacites could not be taken as evidence for mixing; rather they suggest quite the reverse, since by their very presence, they indicate that material of basic composition was not miscible in the acid liquids. Moreover, the andesites and low-silica dacites are characteristically porphyritic while the basalts are not, again suggesting that the rocks in question do not represent unmodified magma mixes.
4) It will be shown later (chapter 4) that geochemical features comparable with those in the Lake Everard rocks, characterise many Proterozoic acid volcanics and can be satisfactorily explained in terms of an origin in partial melting of sialic crustal rocks. It would therefore be extremely coincidental if the Lake Everard rocks, having similar geochemical properties, had a markedly different origin.

It is worth noting that the above comments apply not only to the rocks in the Lake Everard area but may be extended to the Gawler Range volcano-plutonic province as a whole.

E. Models involving direct partial melting of crustal sources

In the light of the objections posed against the previous three models, it is pertinent to reconsider the alternative of direct partial melting of the crust as a source for the primary magmas. It is conceivable that the contemporaneous basic magmatism and associated mantle

Table 2.9 . Results of least squares modelling calculations designed to investigate the origin of the primary magmas by processes of crustal fusion.

A. Approximation of average andesite in terms of Taylor and McLennan's (1979) hypothetical lower crustal composition and likely residual minerals.

Rock	crustal source obs.	crustal source est.	average andesite product	Mineral compositions used cpx.	opx.	plag.	magnetite
SiO_2	53.99	53.99	60.12	45.22	49.20	54.57	-
Al_2O_3	18.98	18.99	15.74	4.56	2.30	28.95	-
FeO^t	9.00	9.00	7.64	9.45	26.0	-	82.0
MnO	-	-	0.30	-	-	-	-
MgO	4.12	4.12	2.93	12.08	21.16	-	-
CaO	9.51	9.51	4.41	21.52	0.49	11.16	-
Na_2O	3.53	3.47	3.79	-	0.06	5.14	-
K_2O	0.6	1.83	3.57	-	-	-	-
TiO_2	0.90	0.91	1.25	0.36	0.19	-	11.0
P_2O_5	-	-	0.42	-	-	-	-
Total			100.0				

Mineral	Wt. fraction	Mineral proportion
cpx.	0.139	0.20
opx.	0.071	0.10
plag.	0.45	0.64
magnetite	0.041	0.058
ave.and.	0.328	
	= crustal source	
ΣR^2	= 0.0043	

Notes: 1. K_2O has not been included in the modelling calculations, but a calculated value is given based on the assumption that K is behaving as an incompatible element with Kd=0. It presents a serious discrepancy, the significance of which is discussed in the text.
2. The clinopyroxene and orthopyroxene compositions are taken from electron microprobe data of Collerson (1972) for pyroxenes in a basic granulite which has a similar composition to the assumed crustal source.
3. Plagioclase composition is An54.6, after Wright (1974).
4. The Ti content of magnetite was adjusted to give a satisfactory match for TiO_2.

B. Approximation of average andesite in terms of a hypothetical lower crust with the composition of Hallberg and Williams (1972) average Archaean tholeiite and likely residual minerals.

Rock	crustal source obs.	crustal source est.	average andesite product
SiO_2	52.31	52.31	60.12
Al_2O_3	15.09	15.09	15.74
FeO^t	10.71	10.70	7.64
MnO	-	-	0.30
MgO	6.83	6.84	2.93
CaO	11.01	11.01	4.41
Na_2O	2.75	-	3.79
K_2O	0.18	0.70	3.57
TiO_2	0.98	1.01	1.25
P_2O_5	0.12	-	0.42
Total			100.0

Mineral	Wt. fraction	Mineral proportion
cpx.	0.286	0.37
opx.	0.125	0.16
plag.	0.327	0.42
magnetite	0.036	0.046
ave.and.	0.256	
	= crustal source	
ΣR^2	= 0.0012	

Notes: 1. Mineral compositions used as for A.
2. Na_2O, K_2O and P_2O_5 were excluded from the modelling calculations.
3. The calculated value for K_2O assumes a bulk distribution coefficient for K of 0.

C. Approximation of the average composition of the andesitic members of the Bunburn Dacite in terms of Taylor and McLennan's (1979) hypothetical lower crustal source and likely residual minerals.

Rock	crustal source obs.	crustal source est.	average Bunburn andesite product
SiO_2	53.99	53.99	62.71
Al_2O_3	18.98	19.00	17.87
FeO^t	9.00	8.99	5.94
MnO	-	-	0.18
MgO	4.12	4.13	2.49
CaO	9.51	9.51	1.22
Na_2O	3.53	-	5.60
K_2O	0.6	-	3.79
TiO_2	0.90	0.96	1.08
P_2O_5	-		-
Total			100.0

Mineral	Wt. fraction	Mineral proportion	Mineral proportions for ave.andesite
cpx.	0.20	0.27	0.20
opx.	0.046	0.063	0.10
plag.	0.43	0.60	0.64
magnetite	0.05	0.069	0.058
Bunburn andesite	0.305		
	= crustal source		
ΣR^2	= 0.0033		

Notes: 1. Mineral compositions used as for A.
2. Na_2O, K_2O and P_2O_5 excluded from modelling calculations.
3. Bunburn Dacite average andesite compiled by averaging E227 and E689 (see Table A2.2, Appendix 1.

activity could have increased temperatures sufficiently in the lower crust to permit the formation of non-eutectic intermediate and acid melts. Assuming this to be so, then it is possible to test the feasibility of a partial melting model by a combined major and trace element modelling approach.

From the composition of the average andesite (60% SiO_2), it is evident that a relatively basic crustal source must be invoked in order that the degree of melting is realistic. For the purposes of testing, Taylor and McLennan's (1979) calculated lower crustal composition was used (Table 2.2). Least squares modelling of the major elements of the average andesite from this source established that a good match could be obtained with the expected, granulite facies mineral assemblage (Table 2.9A). The levels of the various trace elements in the source necessary to duplicate the contents in the average andesite were determined using the mineral proportions and F derived from the major element modelling calculations and the most appropriate distribution coefficients. The results, given in Table 2.10A, show that the calculated values of Zr, Ce, Rb and Ba in the source are significantly higher than those predicted for the lower crust by Taylor and McLennan(1979). However, the calculated contents of all trace elements in source, with the exception of Sc, Ni and Cr, are comparable with the levels in the evolved Kokatha basalt (Table 2.10). Thus, if a basic igneous source is proposed, it would be required to have lower contents of Sc, Ni and Cr than most basalts.

As a specific example of a basic igneous crustal source, an average Archaean tholeiite from the Eastern Goldfields Province of the Yilgarn Block of Western Australia was chosen for testing (after Hallberg and Williams, 1972). The reason for selecting an Archaean tholeiite composition was found in the belief that if, as seems likely, an Archaean supracrustal succession lies beneath the Gawler Range province (Thomson and Webb, 1978), then such a composition would, in all probability, provide the most realistic basic source. Moreover, there is a sufficient number of samples and wide enough spread in Hallberg and William's sampling to make their average statistically meaningful. Additional, more recent data for tholeiitic basalts from other parts of the Yilgarn Block indicates that this average has general validity (e.g. Nesbitt and Sun, 1976; Stolz, 1980; writer's own data).

Modelling of the average andesite from the tholeiitic basalt source yielded a good match in major elements, assuming a residue of orthopyroxene + clinopyroxene + plagioclase + magnetite (Table 2.9B).

TABLE 2.10. Trace element modelling results based on the major element calculations reported in Table 2.9 .

	A.					B.		
	1	2	3	4	5	6	7	8
Zr	307	108	30	122	159	307	207	61
Nb	13	4.8	4	5.8	9	13	10	3.2
Y	36	15.4	20	24	28	36	46	20
Ce	109	44	17	55	52	109	24	8.1
Rb	126	46	20	39	71	126	32	9
Sr	462	519	425	514	482	462	123	105
Ba	1420	613	175	780	657	1423		
Sc	20	20		31	24	20	27	40
V	141	242		178	186	141	185	320
Cr	24	155		605	96	24	33	367
Ni	24	48		195	105	24	54	170
Sm	10.4	4.4			5.2	10.4	4.5	1.9
Yb	3.7	1.7			2.3	3.7	4.3	2.1

A. Calculated trace element abundances in source (2), using values in average andesite (1) and the results reported in Table 2.9 A. The calculated values are compared with the values estimated by Taylor and McLennan (1979, (3)) and with the values in the evolved Kokatha basalts (average of K110 and K33, (4)) and average Nuckulla Basalt (5).

B. Calculated trace elements abundances in average andesite (7) compared with observed values (6), using values in Hallberg and William's (1972) average Archaean tholeiite (8) and the results reported in Table 2. 9B.

Notes:
1. Sm and Yb values reported for average andesite (1 and 6) and average Nuckulla Basalt (5) are based on values in samples E312 and E231 respectively, reported in Table A2.2 (Appendix 1).
2. The distribution coefficients used are those reported in Table 2.5B.

Using the calculated F and mineral proportions, and the trace element contents in the average tholeiite, the predicted levels of trace elements in the average andesite were obtained applying the same distribution coefficients as before (Table 2.10B). Comparison with the actual values reveals that the calculated levels of Zr, Ce, Rb and Sr are too low, while Sc, V, Cr and Ni are too high, despite the fact that in the latter case the distribution coefficients used are probably high, rather than low. It therefore appears that a meta-basaltic source composed of Archaean tholeiite when melted would probably yield liquids too high in compatible elements (e.g. Sc, V, Cr and Ni), yet too low in LIL elements (e.g. Zr, Ce, Rb and Ba), although most major elements could be satisfactorily duplicated. It is possible that a refractory granulitic residue, remaining after prior melt extraction events, may provide a more suitable source, since it would be expected to be higher in LIL elements and lower in siderophile elements owing to its sialic crustal derivation. Alternatively, a more calc-alkaline, as opposed to a tholeiitic, basic-intermediate crustal source might be indicated. The various possibilities will be discussed in more detail in Chapter 4.

At this stage, the important conclusion to be drawn is that it would be possible to generate a liquid with the composition of the average andesite (and hence more acid liquids) from a basic, lower crustal source. The mantle activity at this time, clearly evidenced by the contemporaneous basic lavas, may have raised the geothermal gradient sufficiently in the lower crust to permit melting. There are several other indirect lines of evidence which appear to support this model.

1) The ubiquitous basic xenoliths in the andesites and low-silica dacites may represent fragments of the source. This is supported by their diffuse, partially assimilated form and by their confinement to the andesites and low-silica dacites; had these fragments been torn from the conduit walls in the upper crust during eruption, then there is no reason why they should be confined to the more basic members of the acid-intermediate series, which, coincidentally, probably represent little modified melts from the source.
2) No isotopic data is available for rocks specifically from the Lake Everard area, however some data is available for the closely-related and probably contemporaneous association in the Kokatha area to the north. Webb (1978) quotes an initial strontium isotope ratio (Ri) of 0.7056 for a varied suite of volcanic rocks from the Kokatha pile and an Ri of 0.7041 for the intrusive Hiltaba Granite. These Ris are generally lower than those for rocks in the Lower Proterozoic basement succession of Eyre Peninsula (G. Mortimer,

pers. comm.; Webb and Thomson, 1978), thus precluding a high-level crustal source. Also the Ris lie above the mantle growth curve at approximately 1500 m.y. hence eliminating a direct mantle source. However, they are not inconsistent with derivation of the magmas from a Rb-poor, lower crustal source, such as might be expected in the case of a refractory, sialic residue.

3) In this model, where the basic magmas are mantle-derived and the acid magmas crustal-derived, little opportunity is provided for the generation of primary low-silica intermediate magmas (< 58% SiO_2), since experimental evidence suggests that such magmas cannot be direct mantle melts and considerations of composition preclude a crustal origin. Thus the compositional hiatus between the basic and intermediate-acid series can be readily explained.

4) It has previously been noted that samples of Bunburn Dacite show consistent geochemical differences compared with the majority of other samples, viz. higher in Al_2O_3, Na_2O, Sr and LREE and lower in $Fe_2O_3{}^t$, TiO_2, Y and HREE. Major element modelling calculations, using Taylor and McLennan's (1979) lower crustal composition, demonstrate that the higher Al_2O_3 and Na_2O contents could result from lesser proportions of residual plagioclase, while the lower contents of $Fe_2O_3{}^t$ and TiO_2 could result from increased proportions of mafic minerals in the residue compared with the residue calculated for the average andesite (Table 2.9C). The differing proportions of residual minerals, which may be attributable to fluctuations in PH_2O during melting, could conceivably account for the distinctive Sr, Y and REE levels characteristic of the Bunburn Dacite. Thus, in the partial melting model the compositional variability noted for the acid rocks can be satisfactorily explained by changes in the physical parameters during melting (e.g. PH_2O and T), although the effects of minor variations in the source composition are not excluded.

5) Unlike the mixing model, the partial melting model does not rely on a series of fortuitous or coincidental circumstances for its operation. It has the added advantage of being much simpler. By invoking an input of heat from the mantle, the problem of the high temperatures necessary for partial melting is overcome.

For the reasons cited above and because of the general consistency with the major and trace element data, indicated by the modelling calculations, an origin for the magma in partial melting of a basic, lower crustal source is preferred. Probably a range of primary magmas,

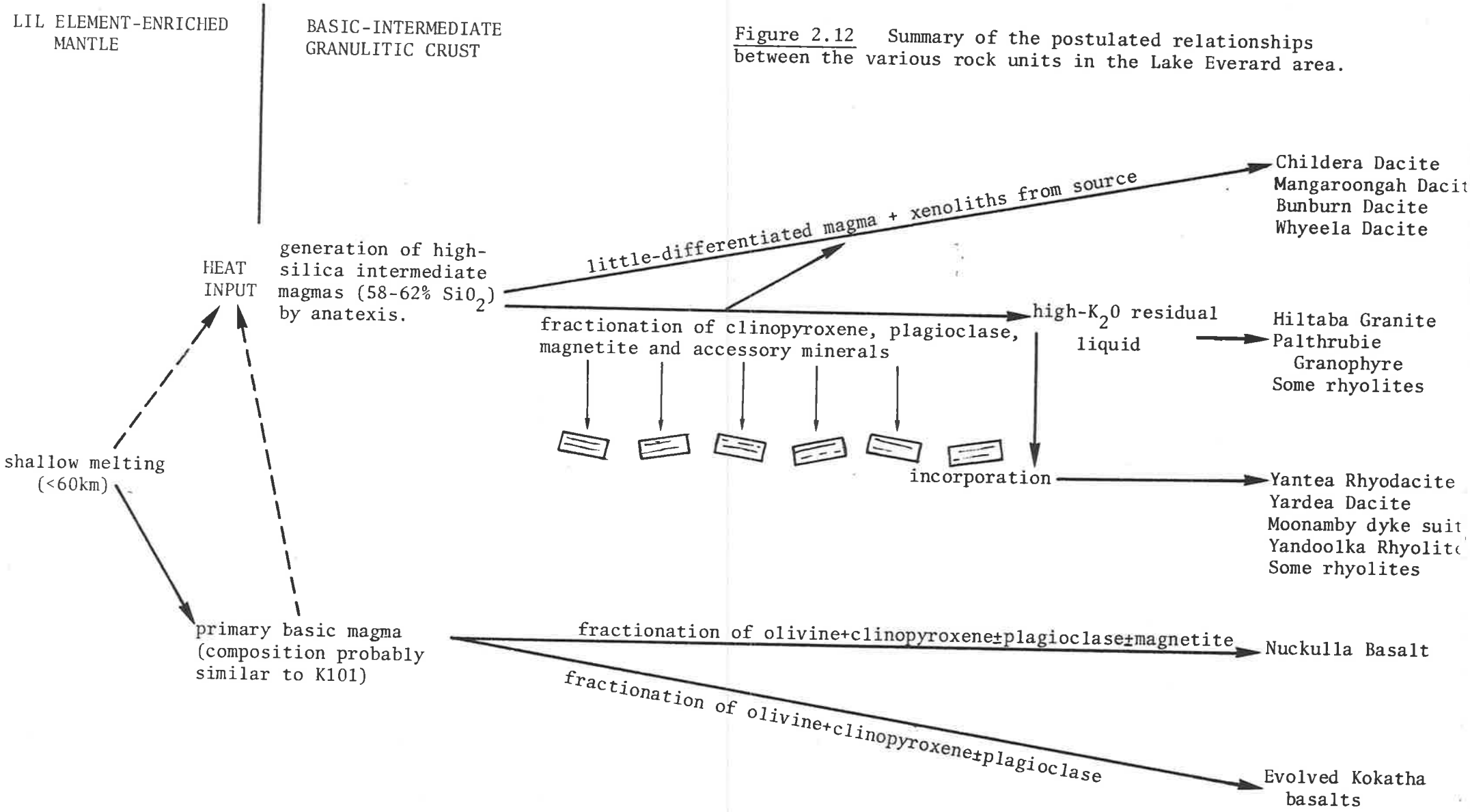

Figure 2.12 Summary of the postulated relationships between the various rock units in the Lake Everard area.

varying in composition from high-silica andesites (approximating the composition of the average andesite) to low-silica dacites (<65% SiO_2) were generated. Subsequent differentiation of the relatively dry magmas is thought to have yielded a variety of acid magmas plus complementary clinopyroxene, plagioclase, magnetite and accessory mineral cumulates. This conclusion is supported by the trace element characteristics of the rhyolites and granites, which are indicative of extreme fractionation. (e.g. high Rb and low Sr and Ba contents and depleted MREE, including Eu), thus demonstrating that they have not originated by melting of more acid rocks at higher crustal levels.

2.6 SUMMARY

The relationships between the various rock types present in the Lake Everard area, as deduced from this study, are summarized diagrammatically in Figure 2.12. A major finding is that the andesites have not been derived from the basalts by crystal fractionation, hence establishing that the basic and felsic rocks had separate origins.

The geochemical characteristics of the basalts are consistent with an origin in relatively shallow, (<60 km) hydrous melting of a LIL element-enriched zone of the mantle. In view of the stable, continental crustal setting, it is considered that the melting was probably caused by a local elevation of the geothermal gradient, possibly above a mantle diapir.

The felsic volcanic and plutonic rocks show the broad outlines of a differentiation series, although each of the mapped units, when examined in detail, are found to possess their own distinctive geochemical and petrographic features. Derivation of the primary magmas by partial melting of a lower crustal, sialic residue of roughly basic composition is favoured. The resultant, non-eutectic melts were relatively enriched in all LIL elements compared with Cainozoic calc-alkaline magmas, reflecting their sialic crustal source. Addition of heat from the mantle either directly, by mantle diapirism, or indirectly, by basic magmatism, is considered to have raised the local geothermal gradient sufficiently to allow melting.

Subsequent differentiation of the primary magmas in upper crustal magma chambers yielded high-K_2O fractionated liquids and crystal cumulates consisting of clinopyroxene, plagioclase, magnetite and accessory minerals such as zircon and apatite. It is postulated that the crystal cumulates were later disrupted and incorporated into the

K_2O-rich liquids to yield the high-silica dacites (e.g. Yardea Dacite), rhyodacites (e.g. Yantea Rhyodacite) and some of the porphyritic rhyolites (e.g. Moonamby dyke-suite, Yandoolka Rhyolite). Many of the highly-fractionated, even-grained intrusive bodies (e.g. Palthrubie Granophyre and Hiltaba Granite) and some rhyolites probably crystallised directly from the high-K_2O residual liquids. This sequence of events can account for the absence of a single line of liquid descent (see Figures 2.6 and 2.9), yet at the same time can explain why trends broadly consistent with crystal fractionation are observed.

It is evident that the model outlined above relies upon an involvement of the mantle and crust. Whereas the mantle has provided some material for the volcanic pile, its chief contribution has been in providing heat for extensive melting of the crust. The processes involved appear to be fundamentally different to those connected with continental accretion through calc-alkaline magmatism. This theme will be expanded in subsequent chapters.

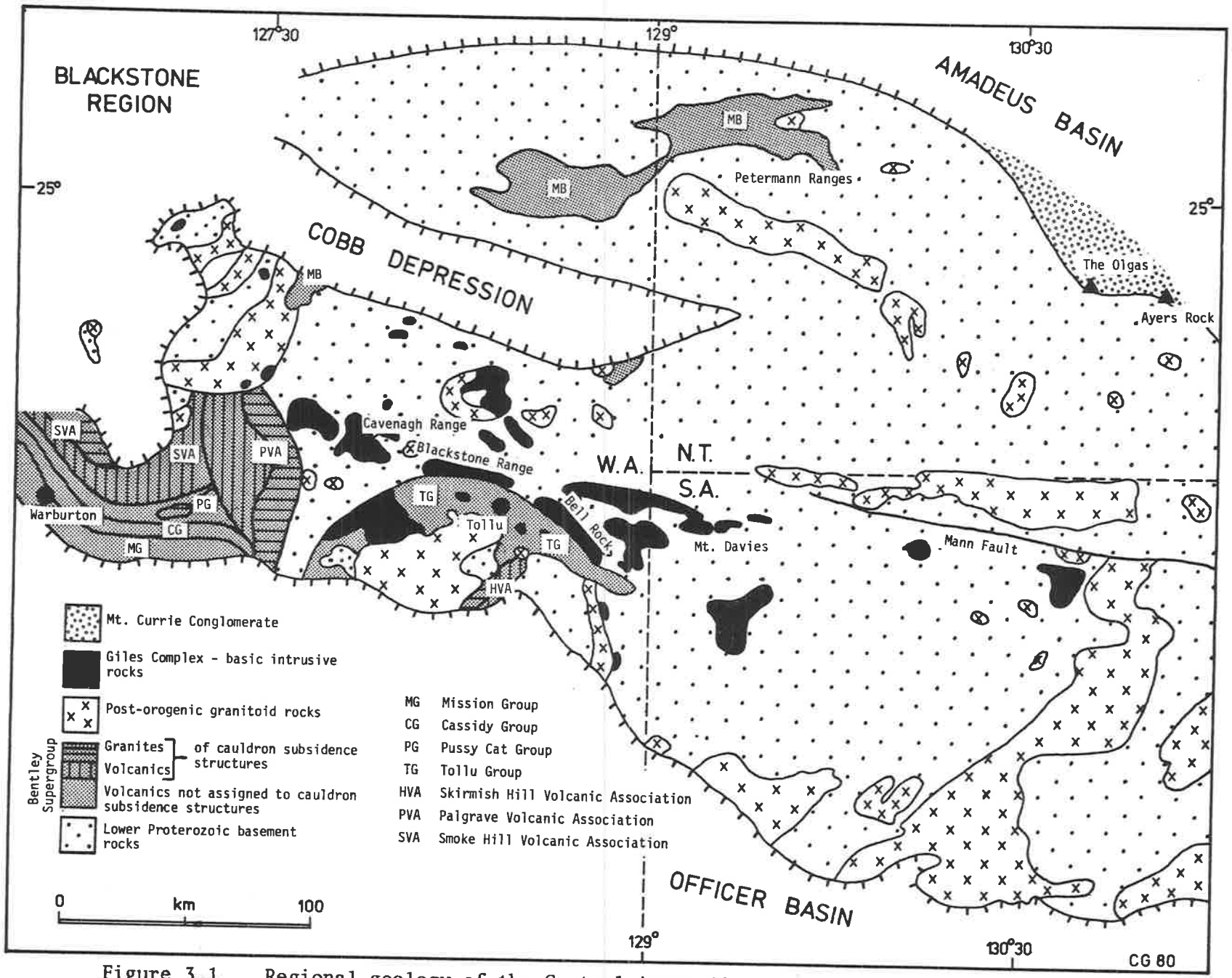

Figure 3.1 Regional geology of the Central Australian volcano-plutonic province.

CHAPTER 3

THE PETROGENESIS OF A PROTEROZOIC BIMODAL VOLCANIC SUITE IN CENTRAL AUSTRALIA

3.1 INTRODUCTION

The volcano-plutonic province examined in this chapter extends from near the join of the S.A., N.T. and W.A. borders, west, 250 km to Warburton in W.A., in an area known as the Blackstone region (Daniels, 1974; see Fig. 3.1). Remnants occur in the Petermann Ranges 150 km to the north, and detritus shed from the province comprises the familiar monoliths of Ayers Rock and the Olgas, some 250 km to the northeast. Thus the province probably covered a far larger area than that indicated by present outcrops (Fig. 3.1).

Past studies have described the volcanic rocks from particular areas (e.g. Nesbitt, 1966; Blight, 1969; Bowden, 1969 - the Tollu area; Daniels, 1974 - the Blackstone region; Forman, 1966 - the Petermann Ranges), and their general time-equivalence has been recognised (Gray, 1971; Thomson, 1975). However, no general name has been applied to the volcanic province and therefore for convenience, the informal name Central Australian volcanics (CAV) has been adopted here to include all volcanic rocks in the Central Australian province.

The area lies entirely within Aboriginal reserves and sampling was done with the permission of the various aboriginal communities, who, in many cases requested that a guide observe the sampling to prevent inadvertant desecration of a sacred site. Because of these restrictions and the logistics in such a remote area, it was not possible to map any areas in detail although many observations were made in areas of critical geological importance. Fortunately 1:250,000 geological maps compiled by the Geological Survey of W.A. and the Bureau of Mineral Resources cover the entire area and these were used to select sample sites. Past studies, including the work of Nesbitt (Nesbitt, 1966; Nesbitt and Talbot, 1966; Nesbitt, *et al.*, 1970) and his students (Blight, 1969; Bowden, 1969), and the comprehensive isotopic studies of Gray (1971) proved useful in interpreting the geological history of the region; the great value of the previous work in the area to the writer's own studies is acknowledged.

The igneous rocks comprising the Central Australian province include basic intrusives (related to Giles Complex, Nesbitt, 1966), basic extrusives, acid intrusives and acid extrusives. Explaining the origin of the various rock types and establishing the relationships between them, poses an important petrological problem. The petrogenetic

hypotheses proposed in the past fall into two main groups:

1) Those relating the acid rocks and basic rocks by differentiation. Specifically, the acid volcanic rocks are interpreted to be the extrusive equivalents of the silicic differentiates of the layered, basic intrusive bodies (e.g. Nesbitt, 1966; Blight, 1969; Bowden, 1969).
2) Those dismissing any genetic relationship between the basic and acid rocks. This hypothesis proposed that the acid magma was derived by crustal fusion while the basic magma had a separate mantle source (e.g. Gray, 1971; Daniels, 1974).

The present study aims to independently re-examine the origin of the igneous rocks in the Central Australian province, in the light of the geochemical data obtained on a range of samples collected by the writer. This will enable an accurate comparison with the Gawler Range province (chapter 2), so that any differences or similarities between the two Proterozoic volcano-plutonic provinces can be established.

3.2 REGIONAL GEOLOGY

The basement to the CAV consists of metamorphic rocks of upper amphibolite to granulite facies, comprising the Musgrave Block (Thomson, 1975). The dominant rock types are granulites of basic to acid composition, amphibolite-facies gneisses and granitic-gneisses, with occasional quartzites and marbles suggesting an original dominantly sedimentary succession. Webb (1973) has dated the granulite facies metamorphism at 1650 ± 170 m.y., which is comparable in age to the Kimban Orogeny which affected Lower Proterozoic sediments in southern Australia (Webb and Thomson, 1977). However, on the basis of detailed work in the Tomkinson Ranges in the western Musgrave Block, Gray (1971, 1979) concluded that the geosynclinal succession accumulated roughly 1600 m.y. ago and was not metamorphosed to granulite facies until much later, at approximately 1250 m.y. B.P. This apparent conflict has little relevance to the present study, since the Central Australian volcanics, which are of chief interest here, rest unconformably on the granulitic basement and quite clearly have not been affected by the intense deformation or the high-grade metamorphism.

The volcanic rocks in the Blackstone Region comprise a major part of the Central Australian province and Daniels (1974, p. 49) has assigned them to the Bentley Supergroup which "includes all sedimentary and volcanic rocks in the Blackstone Region younger than the granulites and related gneisses and schists (Musgrave-Mann Metamorphics, Thomson, 1975) and

older than the Upper Proterozoic glacials." Samples of volcanic rocks from this region have yielded an age of 1060 ± 140 m.y. (Compston and Nesbitt, 1967), which is considered to be their time of eruption, an interpretation that is consistent with their stratigraphic position. This age is in close agreement with the more precise age of 1090 ± 66 m.y. determined by Gray (1971) for volcanic rocks from the Tollu area. The volcanic rocks of the Bentley Supergroup are thought to be equivalent to the Mt. Harris Basalt (Forman, 1966) which crops out in the Petermann Ranges to north (Fig. 3.1) and is separated by the Phanerozoic Cobb Depression. (Horwitz and Daniels, 1967; Thomson, 1975.)

Large sheet-like basic bodies belonging to the Giles Complex (Nesbitt and Talbot, 1966) occur at various stratigraphic levels within the previously described succession (Nesbitt, et al., 1970). Mostly the magmas appear to have crystallised in place and in some cases a distinct mineralogical and compositional layering has developed (Nesbitt, et al., 1970). Among these bodies, three main types can be recognised:

1) Mafic and ultramafic cumulate rocks, that crystallised deep within the crust (see Goode and Moore, 1975). These bodies are found only within the high-grade metamorphic basement terrains.
2) Plagioclase-rich cumulate rocks, including troctolites and anorthosites (e.g. Blackstone Sheet, Nesbitt and Talbot, 1966). These bodies occur almost exclusively as intrusive sheets at the stratigraphic level corresponding with the unconformity between the basement and the Bentley Supergroup.
3) High-level, differentiated gabbros that intrude the Bentley Supergroup (Daniels, 1974).

The time of intrusion of the Giles Complex is not known with certainty. Contemporaneity with the Central Australian volcanics has been advocated on the basis of field relations by Nesbitt (1966) and on isotopic grounds by Nesbitt, et al., (1970). Goode and Moore (1975) on the other hand, suggested that the deep-level bodies intruded significantly earlier, prior to the major erosional event which post-dated the granulite facies metamorphism. A pre-volcanic age of intrusion is also advocated by Gray (1971) on isotopic grounds. The field relationships quite clearly demonstrate that the higher level bodies (2) and 3) above) post-date the Central Australian volcanics on account of their stratigraphic position (e.g. Blackstone Sheet, Daniels, 1974) and cross-cutting relationships (e.g. high-level gabbros in the Tollu area, Blight, 1969 and Bowden, 1969). Thus, if the reasoning of Gray (1971) and Goode and Moore (1975) is correct, a diachronous age of intrusion of the various

levels of the Giles Complex is indicated. Also, if the high-level mafic bodies are approximately contemporaneous with volcanism as Nesbitt, et al., (1970) suggest, then they must have intruded soon after development of the volcanic pile.

Thin shelf sediments overlie, and are intercalated with, the youngest volcanics and are probable lateral equivalents of thick accumulations in the Officer Basin to the south and Amadeus Basin to the north. Sedimentation was terminated by the Petermann Ranges Orogeny (Forman, 1966) roughly 600 m.y. B.P., during which slip along ancient fracture zones produced thrusts and nappe structures (Forman, 1972). The uplift associated with this orogeny resulted in rapid deposition of the Cambrian Mt. Currie Conglomerate in a terrestrial environment either within, or at the margins of, the uplifted block.

The Mt. Currie Conglomerate includes the boulder beds of The Olgas and possibly the 2.5 km section of arkose comprising Ayers Rock. The Olgas are composed of boulders, cobbles and pebbles of volcanic and plutonic rocks which are in the following approximate proportions: basic volcanics 45-50%, acid volcanics 15-20% and acid intrusives 40% (based on the writer's own observations). There are few clasts of high-grade metamorphic rocks whilst porphyritic andesite and basic plutonic rocks are absent. Rapid erosion of an adjacent bimodal volcanic province is therefore indicated. It appears that erosion in this area was sufficient to expose the high-level sub-volcanic granites, but insufficient to strip the volcanic pile down to the Lower Proterozoic basement rocks. Since The Olgas are roughly 180 km from the nearest exposures of volcanic rocks in the Petermann Ranges, the limit of the province is extended east by at least this distance, hence supporting a much wider initial distribution of the CAV.

3.3 GEOLOGY OF THE CENTRAL AUSTRALIAN VOLCANICS

The Bentley Supergroup, which encompasses the major exposed area of the CAV, has been divided into four groups, each consisting of alternating basic and acid volcanic rocks in a simple layered succession (Daniels, 1974). The basic volcanics consist of a series of massive and amygdaloidal basaltic lava flows, while the acid volcanics are mainly dacitic to rhyolitic ash-flow tuffs, forming extensive, gently-dipping sheets. In hand specimen the latter are homogeneous porphyritic rhyolites and dacites, but they probably originated as welded, vitric-crystal tuffs.

Within the Blackstone region Daniels has recognised three cauldron subsidence areas. They are marked by thick accumulations of acid ash-flow

tuffs, mainly crystal-vitric tuffs with lithic tuff intercalations, intruded by high-level granites and granophyres. Blight's (1969) work on Daniel's Skirmish Hill cauldron in the Tollu area failed to reveal any evidence for cauldron subsidence (see Fig. 3.1 for location). However, Blight (1969) did recognise a layered sequence of basalts and rhyolites, resting unconformably on basement gneiss, which he interpreted as part of a major anticline. Similarly, observations by the writer failed to reveal the marginal faults critical to the interpretation of the cauldron subsidence structures, in any of the three areas cited by Daniels. Nevertheless, the association of high-level granites and thick acid volcanic piles noted by Daniels in the west of the Blackstone region, does appear to be valid. It is possible that the spaced acid volcanic piles may have been erupted from discrete centres in which evidence for cauldron subsidence is subtle or non-existent, as proposed by the writer for the Lake Everard area in the Gawler Range province. Owing to alluvial cover in areas where the marginal faults are likely to occur, it is apparent that this problem will only be resolved by detailed mapping of the volcanic units, particularly the lithic tuffs and flow-banded rhyolites, which are ubiquitous in the supposed cauldron subsidence areas.

The Mt. Harris volcanics in the Petermann Ranges to the north are an analogous sequence of interlayered basalts and rhyolites (Forman, 1966; Daniels, 1974). Generally the rocks are weathered, schistose and not well exposed and therefore have not been examined in detail in this study. The volcanics here have been involved in the nappe formation during the Petermann Ranges Orogeny and consequently are much more deformed than equivalents in the Blackstone region, which were folded into broad synclines and anticlines during the same event.

The volcanic clasts in the Mt. Currie Conglomerate at The Olgas are generally fresh and undeformed, and probably represent a good cross-section of the variety of volcanic rock types in the province. Consequently, samples spanning the textural and compositional range were collected from this locality and it is shown later that they are geochemically indistinguishable from volcanic rocks in the Blackstone region.

3.4 PETROGRAPHY

A brief outline of the important petrographic characteristics of the five main igneous rock types in the Central Australian province is given below. All numbers refer to samples, thin section descriptions of which will be found in numerical order in Table A3.1, Appendix 1. Photomicrographs illustrating many of the features descibed below, are given in Figure 3.2.

3.4.1 Composite rocks that have not crystallised directly from a melt

Porphyritic andesites are unknown from the Blackstone region and despite intensive search by the writer no boulders of porphyritic andesite were found at The Olgas. Some rocks analyse as andesites however (e.g. Ol.5, 6, 7 and B55, 59, Table A3.2), and appear to be either mixtures of acid and basic rocks or contaminated basic rocks.

B38, 39, 55, 58, 72 are examples of mixtures: they are lithic tuffs of probable air-fall origin, consisting of fragments of recrystallised acid volcanics and altered basic volcanics. Both fragment types are accessory and were probably torn from the vent walls during eruption. Similar mixed pyroclastics have been described by Bowden (1969) from the Tollu area.

Ol.5, 6, 7 and B59, 10 11 appear to be contaminated rocks. In particular, Ol.6 and B59 are altered basalts in which granular quartz is interstitial to interlocking plagioclase, and needles of green amphibole after clinopyroxene. B10 and B11 are from the contact zone of a small gabbro body and are considered to be contaminated gabbros. They consist of tabular crystals of amphibole (after clinopyroxene) and plagioclase, identical in nature and composition to those in the adjacent massive gabbro, but separated by abundant quartz and K-feldspar presumably engulfed from the acid volcanics. Bowden (1969), however, interpreted these samples as granophyric differentiates of the gabbro, and this point, which has important petrogenetic implications, will be considered in more detail later.

3.4.2 Acid volcanic rocks

The acid volcanic rocks are invariably porphyritic and range from dacites to rhyolites. Porphyritic dacites typically consist of euhedral phenocrysts of partially-sericitized plagioclase and clinopyroxene (now largely altered to amphibole), set in a fine-grained devitrified felsic matrix with abundant magnetite euhedra scattered throughout. The plagioclase phenocrysts are commonly zoned and occur both as isolated crystals and in glomeroporphyritic aggregates. One dacite (B7), consists of phenocrysts set in a chilled, glassy matrix that preserves delicate rod-like shapes, now outlined by fine-grained, dusty magnetite. Since devitrification of the glass and resultant loss of texture did not have time to occur prior to magnetite replacement, it is believed that the magnetite is primary thus implying that the interstitial liquid was very iron rich. This is supported by the clusters of fine magnetite which are scattered through the rock.

Figure 3.2. Photomicrographs of selected thin sections.

A. Skeletal textures, outlined by finely-divided opaques, in a glassy rhyolite (B7). F.V. 4 mm.

B. Perlitic cracking in a glassy rhyolite (B2). The groundmass shows fine vitroclastic textures, indicative of a pyroclastic origin. F.V. 5 mm.

C. Lithic tuff containing accessory acid volcanic rock fragments and large angular glass chips within a vitroclastic, shard-rich matrix. F.V. 7 mm.

D. Crystal tuff, containing an aggregate of poorly-sorted crystals, many of which are fragments of larger crystals, set in a devitrified glassy matrix. A K-feldspar crystal, flanked by smaller crystals of quartz, is visible in the centre. F.V. 8 mm.

E. A "mixed" tuff, comprised of accessory acid and basic (dark) volcanic rock fragments, abundant crystal "chips" of quartz and feldspar, and a chloritic, glassy matrix. F.V. 6.5 mm.

F. Troctolite phase of the Blackstone Range Gabbro, consisting of plagioclase and relatively minor olivine and clinopyroxene. F.V. 7 mm.

G. Dolerite dyke, showing an ophitic intergrowth of plagioclase, clinopyroxene and magnetite. F.V. 5 mm.

H. Ophitic texture, consisting of interlocking plagioclase and chloritized clinopyroxene, typical of that in many basalts from the Central Australian province. F.V. 6 mm.


A

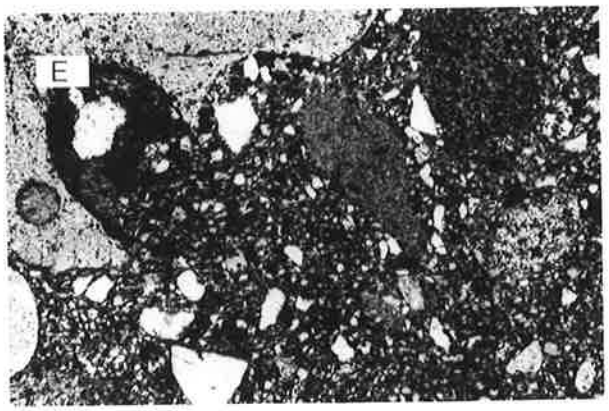
E

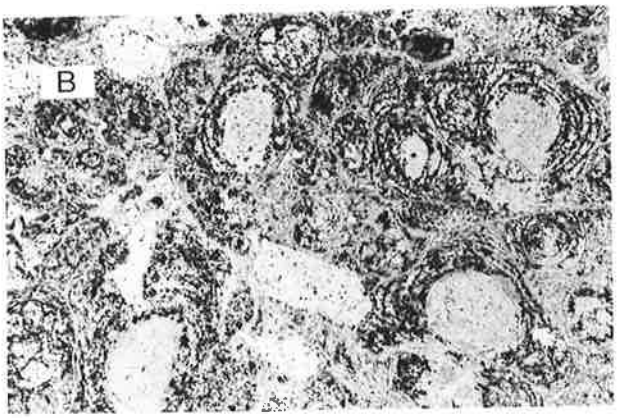
B

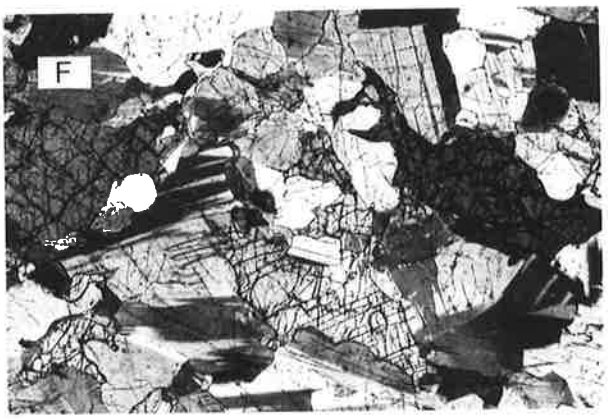
F

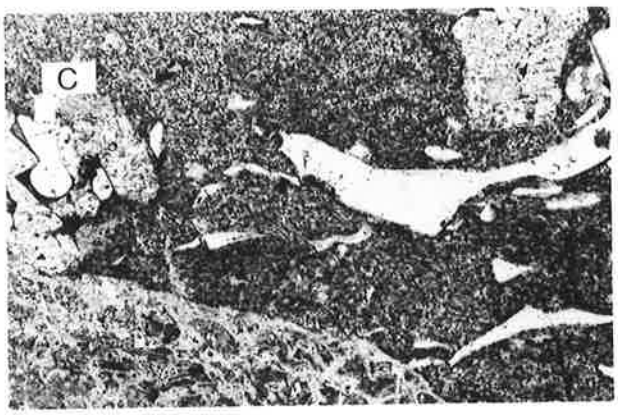
C

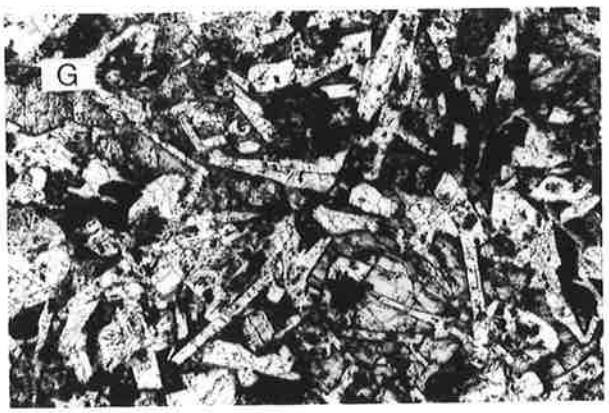
G

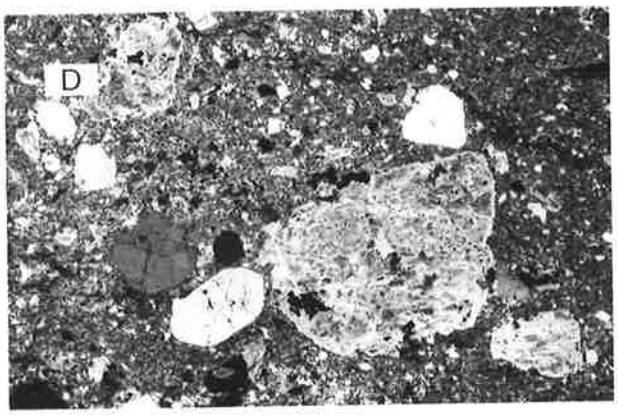
D


H

As the proportion of fine-grained amphibole and magnetite in the matrix drops and quartz phenocrysts become more abundant, dacite grades into rhyolite. The relative proportions of quartz, plagioclase and K-feldspar phenocrysts varies greatly in the rhyolites. Typically, quartz is embayed, while the feldspars occur in glomeroporphyritic aggregates. In general, the groundmass consists of a recrystallised, granular quartz-feldspar aggregate in which primary textures have been obliterated. Where textures are preserved, it is evident that the groundmass was quite glassy, as for example in B2 which shows perlitic cracking. The outlines of glass shards are visible in some samples (e.g. B1), clearly indicating a pyroclastic origin. Usually, however, shards are not visible and evidence of a pyroclastic origin for the majority of the massive rhyolite units is inferred from indirect criteria such as crystal chips, compaction textures (e.g. draping of the matrix around phenocrysts), streaky eutaxitic blebs and primary devitrification textures. Often the field relationships are helpful; for example, the homogeneity and extent of some rhyolites strongly suggests an ash-flow origin, a conclusion supported by the crystal tuffs and lithic tuffs which are commonly intercalated.

3.4.3 Acid intrusive rocks

All of the acid intrusive rocks in the region are leucocratic and are of granitic composition, with tonalites and granodiorites being notably absent. The largest granite bodies are composed of coarse-grained holocrystalline aggregates of quartz, microcline and plagioclase, with scattered patches of biotite and magnetite (B35). The smaller dykes and plugs show variable development of granophyric textures and are rich in quartz and K-feldspar.

3.4.4 Basic volcanic rocks

The least-evolved basalts (B76, O1.4) comprise subophitic intergrowths of clinopyroxene, (now largely altered to amphibole) and plagioclase. Magnetite is scattered throughout as fine to minute euhedra and is variably altered to sphene and leucoxene. No relic olivine or pseudomorphs after olivine were noted.

More differentiated basalts have a higher proportion of plagioclase, magnetite and mesostasis (after glass) and commonly exhibit a marked orientation of plagioclase due to flowage. As previously mentioned, some of the basalts appear to have been contaminated by the addition of silica, evidenced by granular quartz in the matrix, and have SiO_2 contents which place them in the andesite field (e.g. B59, O1.6, O1.7).

3.4.5 Basic intrusive rocks

All of the basic intrusive rocks considered in this study are thought to be related to the Giles Complex (Nesbitt, et al., 1970) and can be divided into two mineralogical and geochemical types, consistent with their intrusion at different stratigraphic levels.

A. The massifs of the Cavenagh Range, Blackstone Range and Bell Rock Range (Fig. 3.1) and various other small bodies in the vicinity appear to be parts of the one lopolithic sheet isolated by erosion (the Blackstone Sheet of Nesbitt and Talbot, 1966, consisting of the Blackstone Range Gabbro of Daniels, 1974). This is supported by the work of Daniels (1974) who has recognised four mineralogical zones which he is able to extend from the Blackstone Range to the 3 km section exposed in the Bell Rock Range. The dominant rock type in all areas is a cumulate troctolite, containing up to 90% plagioclase (An_{65}) with olivine, clinopyroxene and rare, orthopyroxene and red biotite comprising the remainder. Where the proportion of clinopyroxene is higher, it is observed to enclose olivine in a poikilitic intergrowth.

Associated with the Blackstone Range Gabbro is a marginal phase consisting of a granular, recrystallised aggregate of plagioclase, clinopyroxene, greenish-brown amphibole and rare magnetite. Unlike the troctolite, this rock is not cumulate, but may represent a near-contact basalt that has recrystallised in response to heat from the gabbro.

B. In the Tollu area, small plugs and dykes of gabbro, mineralogically and geochemically distinct from the Blackstone Range Gabbro and representing the highest levels of the Giles Complex, intrude the volcanic pile (Blight, 1969; Bowden, 1969). The dominant rock type is an ophitic-textured gabbro containing interlocking sericitized to fresh plagioclase and clinopyroxene (partially altered to amphibole), with scattered euhedra of magnetite. Where the gabbro contacts acid volcanics there is some evidence for contamination, since remnant plagioclase and amphibole crystals are spaced by granular mosaics of quartz and K-feldspar.

3.5 GEOCHEMISTRY

3.5.1 General discussion

An examination of the geochemical data presented in Table A3.2 reveals a paucity of samples with SiO_2 contents in the range 53-66%. It is important to note that all of those samples with SiO_2 contents in this range are hybrid or altered rocks, judging from their petrographic characteristics. For example, B55 and B72 are pyroclastics containing acid and basic rock fragments, while B59, B11, B10 and O1.7 are basic

Figure 3.3 Selected variation diagrams for rocks from the Central Australian province. ● volcanic clasts from The Olgas O undifferentiated samples ◆ averages of volcanic rocks from the Warburton area compiled by Haynes (1972) △ troctolite ■ basic rocks and □ granophyres from the Red Hill layered intrusive, Tasmania (after McDougall, 1962).

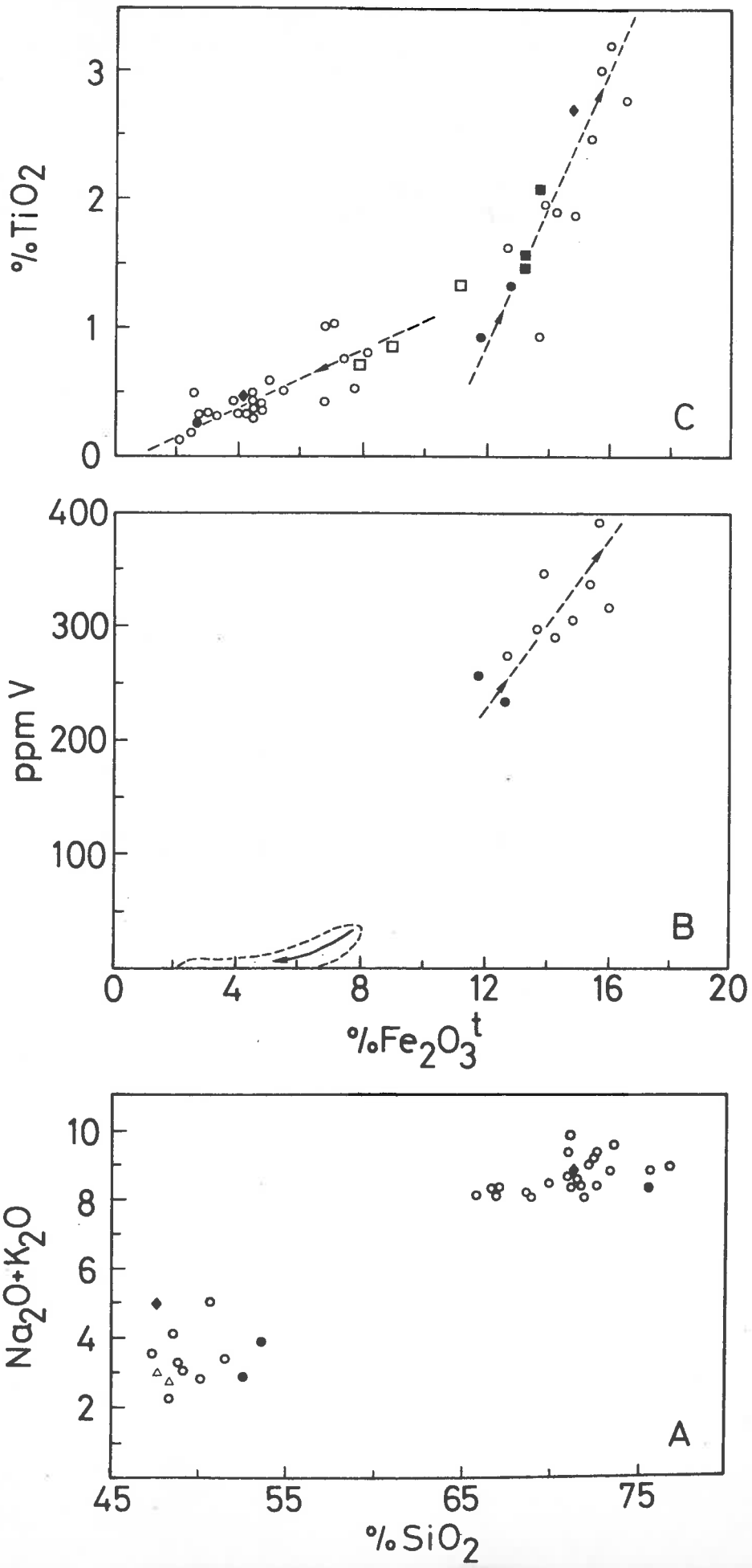

rocks contaminated with silica. Since the compositions of these rocks do not reflect original magmatic compositions they are ignored in the following discussion.

The total alkalis versus SiO_2 plot (Fig. 3.3A) clearly demonstrates the compositional hiatus that exists between the basic and acid rocks. The basic rocks do not show a good trend probably because increasing differentiation, which would be expected to yield higher alkalis by residual enrichment, is not necessarily marked by increasing SiO_2 in rocks of this composition. This arises because the bulk SiO_2 of the crystallising minerals (e.g. clinopyroxene, plagioclase and olivine) is likely to be near that of the melt. The acid rocks show a slight increase in total alkalis with increasing SiO_2 and since Na_2O remains approximately constant over this interval, the increase is due to the contribution of K_2O (average K_2O in dacites is 4.2-4.5% while that in the rhyolites is roughly 5.5%). The significant point to note is the relatively high value for total alkalis which distinguishes these rocks from most Cainozoic dacites and rhyolites, In addition, the uniformity of the values suggests alteration has been minimal.

The hiatus in SiO_2 is also matched by other elements, seen for example on the AFM diagram, where two diverse trends are separated by a large compositional gap (Fig. 3.4). One trend is towards an enrichment in iron and is defined by the basalts, while the other is a trend towards the alkalis corner, defined by the acid volcanics. Similarly, plots of Ti and V vs $Fe_2O_3^t$ (Figs. 3.3B and C) distinguish two trends, one showing an increase in Ti and V with $Fe_2O_3^t$ and defined by the basic rocks, while the other, corresponding to the acid series, shows the reverse trend. Again, there is a marked compositional gap between the basic and acid rocks.

These examples demonstrate that the intermediate rocks, critical in establishing the relationships between the basic and acid series are absent, thus introducing a certain ambiguity in the interpretation. Therefore, in the following discussion, the geochemistry of the basic and acid rocks will be considered separately, to determine whether the fractionation trends in the basic rocks are such, that differentiates with the compositions of the acid volcanic rocks could be produced.

3.5.2 Geochemistry of the basic rocks

Several features of the basic rocks will be apparent from the previous discussion: notably the good correlation of $Fe_2O_3^t$, V and Ti (Figs. 3.3B and C) all of which increase with differentiation,

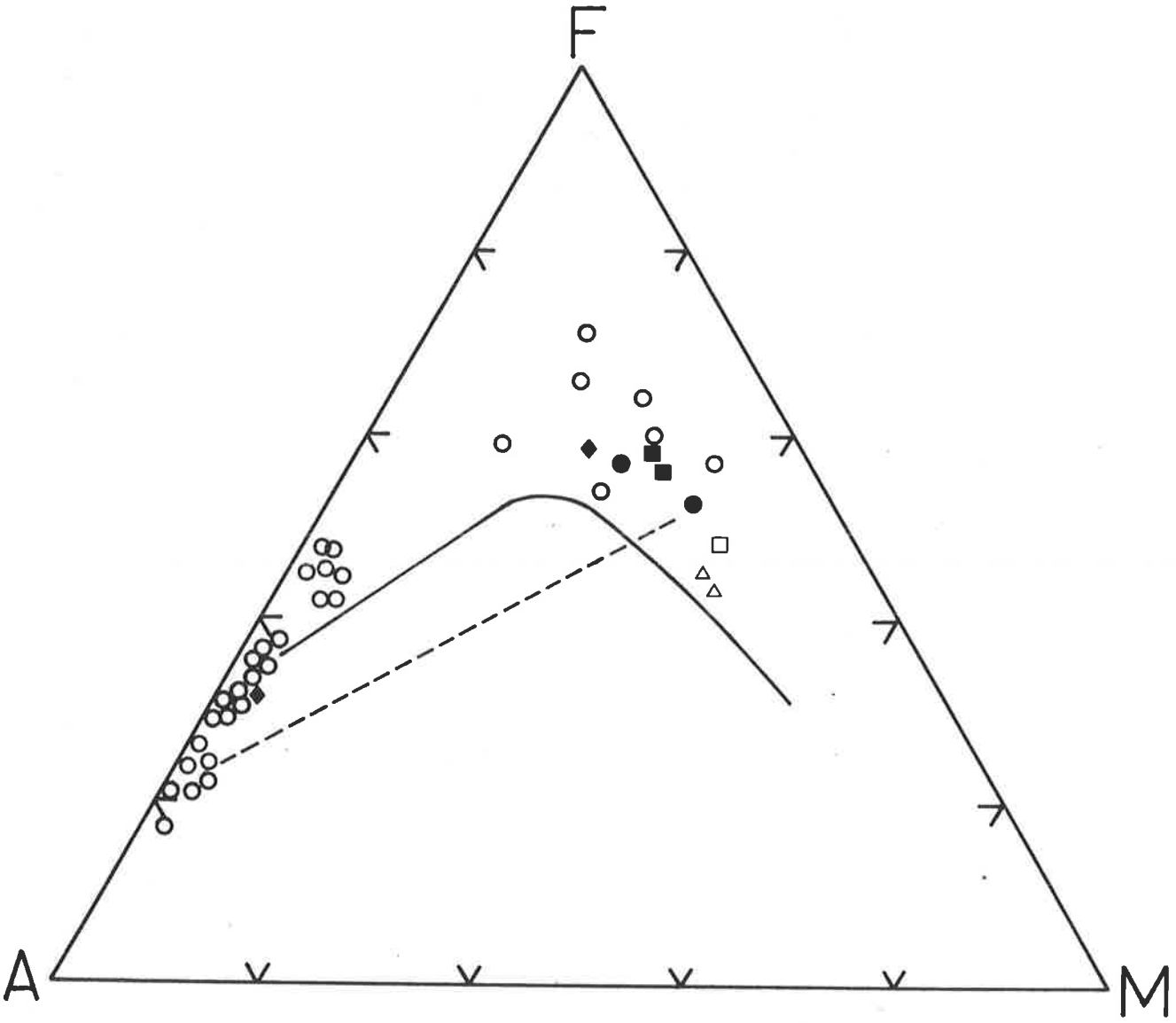

Figure 3.4 AFM plot for rocks from the Central Australian province. Symbols as for Figure 3.3, with the exception of □ which is the marginal chilled phase of the Mt. Davies layered intrusive body (after Nesbitt, et al., 1970) and ■ which are basic dykes related to the Giles Complex.

Figure 3.5 Selected elements vs. $Fe_2O_3^t/MgO$ for basic rocks from the Central Australian province. Symbols as for Figure 3.4.

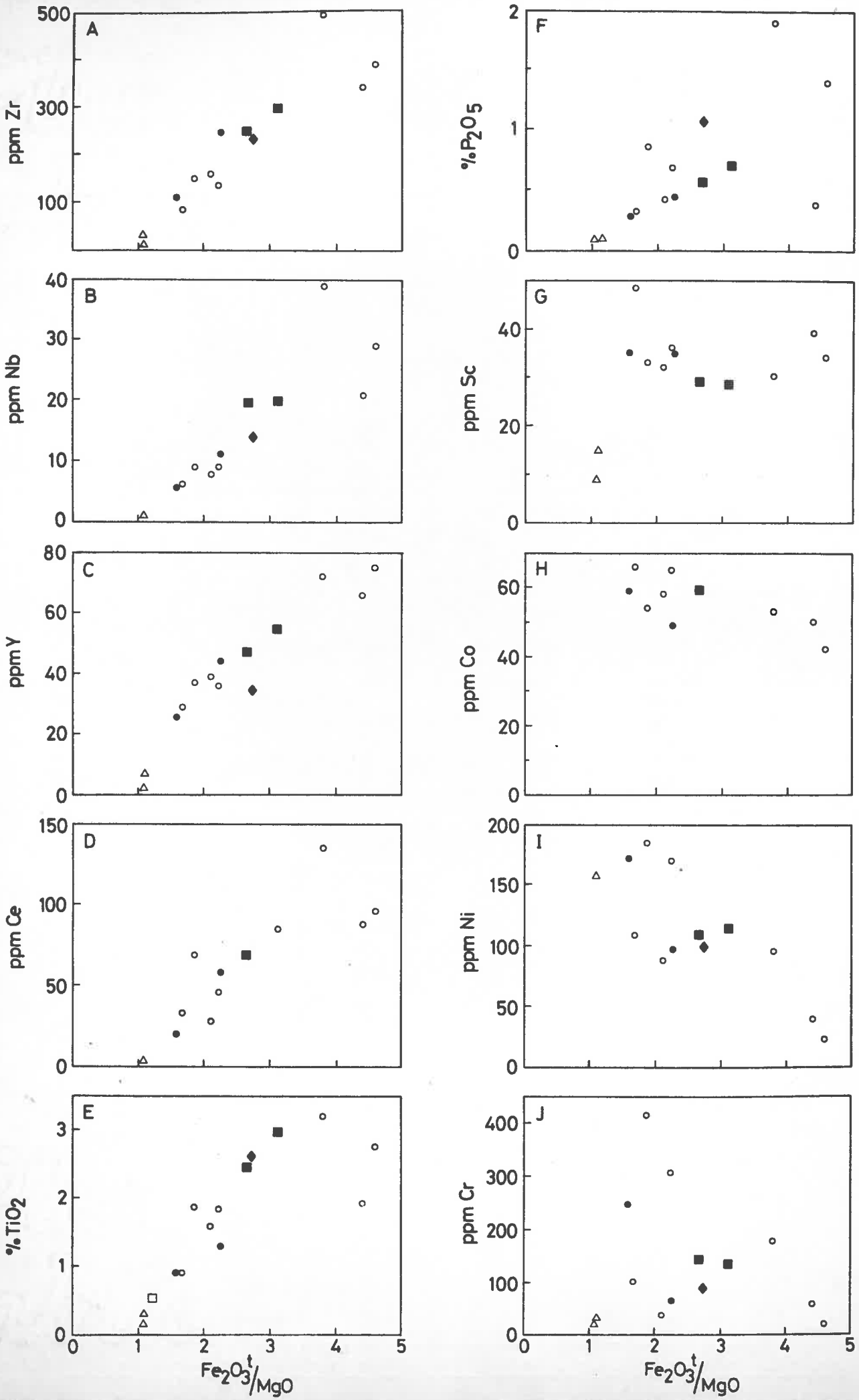

Figure 3.6 Chondrite-normalised Ce-Nd-Nb-Zr-Y-Ti plots for selected basic rocks from the Central Australian province. The dashed lines enclose the field of REE in basalts from the Warburton area (after Haynes, 1972; assumes Y/2 = chondrite-normalised Yb).

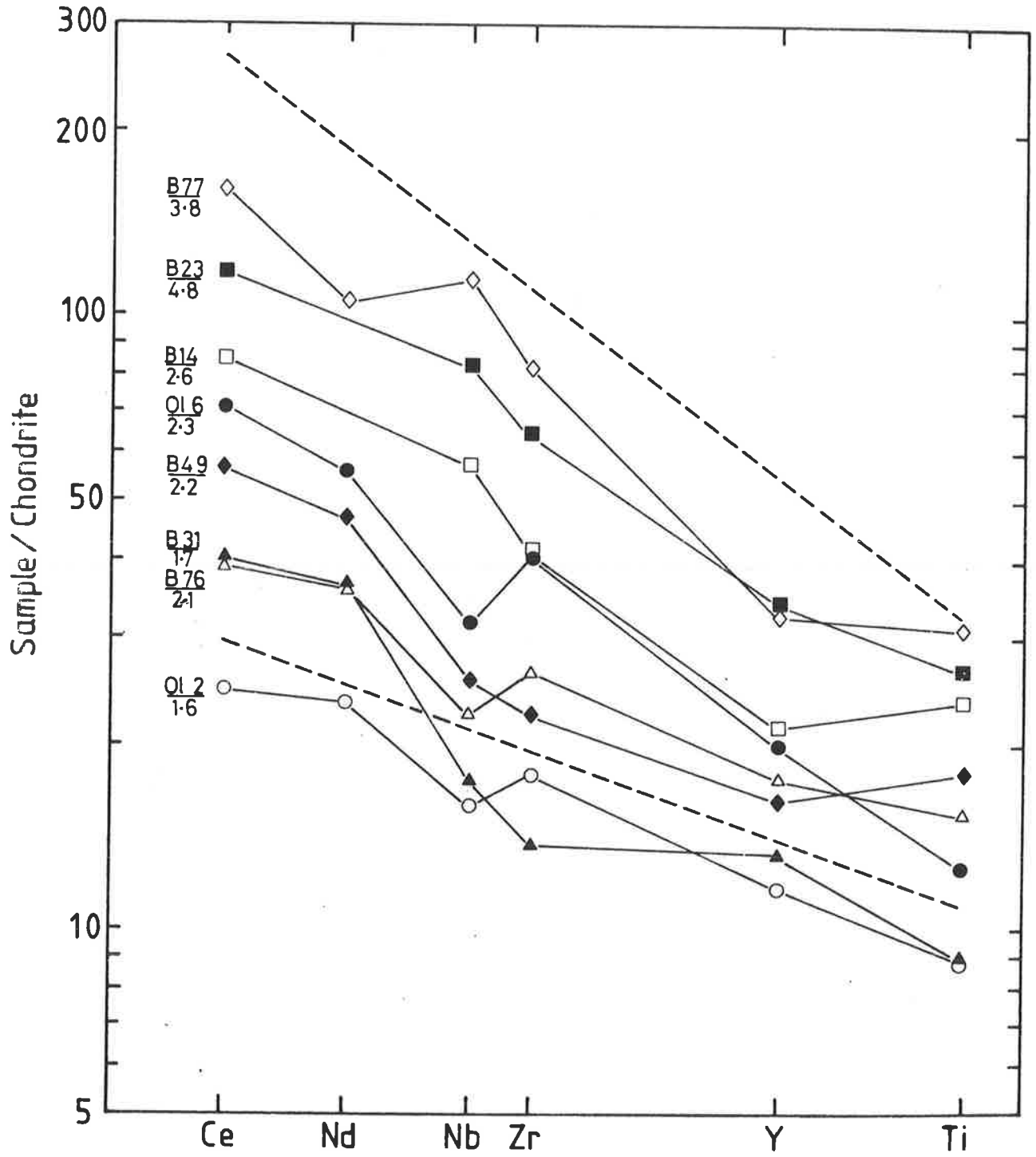

indicating that magnetite has not fractionated up to the degree of differentiation represented by the most evolved samples (e.g. B8, B66, B23, B77). This iron-enrichment trend, typical of continental tholeiites (McDougall, 1962), probably reflects differentiation in crustal magma chambers under relatively low oxygen fugacity conditions (Roeder and Osborn, 1966).

$Fe_2O_3^t/MgO$ can be used as a measure of differentiation, and to examine their behaviour, various elements are plotted against this ratio in Figure 3.5. Zr, Nb, Y, P_2O_5, Ce and TiO_2 all show a linear positive correlation with $Fe_2O_3^t/MgO$ indicating that they are not being controlled by any minerals up to the degree of differentiation recorded by the samples collected. This is consistent with fractionation of olivine, pyroxenes and plagioclase, in which all of these elements are largely incompatible.

The compatible elements, Ni and Cr show a general decrease with differentiation probably due to control by olivine, clinopyroxene and/or orthopyroxene although there is considerable unexplained scatter in the data. Sc on the other hand remains approximately constant, suggesting that it is being moderately controlled by a mineral (e.g. clinopyroxene and/or orthopyroxene, both of which have Kd mineral/liquid ≈3 Gill, 1978) such that the bulk distribution coefficient is near one. Co shows a slight decrease over the same interval which may also be attributable to fractionation of these minerals.

Three additional points are of note on these plots:

1) The basalts from the Blackstone region define trends indicative of a differentiation series. This implies that they have analogous crystallisation histories and can be related to a similar source.
2) The basic intrusive rocks lie on the trends defined by the basalts, suggesting that they are genetically related.
3) The basalt clasts collected from The Olgas also lie on these trends, indicating that they have most probably been eroded from an ancient extension of the Central Australian province.

Complete rare earth element (REE) determinations have not been made for any samples from the province by the writer, but an indication of the REE distribution can be gained by applying the observation of Sun, et al. (1979) that the levels of Zr and Y in basalts can give an indication of the middle rare earth element (MREE) contents and heavy rare earth element (HREE) contents respectively. This is applied in Figure 3.6 where chondrite-normalized Ce, Nd, Zr, Nb, Y and Ti values are plotted for various basic rocks from the province. The absolute

TABLE 3.1. Elemental ratios for basalts from the Central Australian province.

Ratio	Probable chondritic value	B31	B60	B76	01.2	H.B.	N.B.
$Zr/_{Ce}$	7.4-7.7	2.5	2.1	5.3	5.5	4.6	3.1
$Zr/_{Y}$	2.5-2.8	2.8	4	4.1	4.3	6.8	5.7
$Ti/_{Zr}$	100-110	67	77	61	51	69	45
$Ti/_{Y}$	250-280	190	306	248	216	464	257
$Zr/_{Nb}$	16-18	13	16.4	20	19.5	16.4	18
$Ti/_{V}$	8.4-10	18.6	39	41	22	65	39
$Ti/_{Sc}$	78-85	115	344	302	158		300
$TiO_2/_{P_2O_5}$	STP=10	5.8	4.4	7.7	6.5	5.0	5.7
$Ce^n/_{Y^n}$		average value=3.5			$Ce^n/_{Yb^n}$=3.8		5.8
%MgO		8.18	7.67	6.01	7.44	5.42	5.37

H.B. Average basalt from the Warburton area after Haynes (1972).

N.B. Nuckulla Basalt from the Lake Everard area (average of E231 and E459, see Chapter 2).

Note: 1. Same comments apply as for Table 2.6.

values of all of the trace elements clearly increase with $Fe_2O_3^t/MgO$ or differentiation, but Ce^n/Y^n does not vary greatly, maintaining an average value of 3.5. Assuming Y behaves similarly to Yb, Ce^n/Y^n approximates Ce^n/Yb^n and therefore can give an indication of the LREE/HREE. It is notable that the average Ce^n/Y^n (3.5) is comparable to the average Ce^n/Yb^n (3.8) determined by Haynes (1972) in his study of basalts from the Warburton area in the west of the Blackstone region. Moreover, the range of REE in the present samples lies within the range obtained by Haynes (1972) for the Warburton basalts (see Fig. 3.6).

Three important conclusions can be drawn from this data:

1) The constancy of Ce^n/Y^n (and hence Ce^n/Yb^n) with differentiation implies fractionation of minerals which have not preferentially depleted HREE in relation to LREE. This would involve minerals such as olivine, clinopyroxene, orthopyroxene and plagioclase rather than garnet or amphibole.
2) The uniform increase in the absolute contents of all elements (and hence REE) with differentiation suggests that residual liquid concentration due to removal of crystals has been the major process leading to enrichment.
3) The least-evolved basic rocks have fractionated elemental contents (hence REE) and since removal of olivine, orthopyroxene and clinopyroxene will cause negligible change in the slope, either the parental magmas were derived by extremely low degrees of melting (<5%) of a chondritic mantle (e.g. flat 2x chondrites, c.f. Lopez-Escobar, et al., 1977) or by higher degrees of melting of a LREE-enriched mantle.

A consideration of the incompatible element ratios for the least-fractionated basic rocks (B31, B60, B76 and 01.2 Table 3.1) reveals:

1) V/Ti and Sc/Ti are less than chondritic.
2) Zr/Nb and Y/Ti are near chondritic.
3) Zr/Y, Zr/Ti, Ce/Zr and P_2O_5/TiO_2 are greater than chondritic.

Notably, these elemental characteristics are the same as those observed in basalts from the Gawler Range province. The implications of this observation and the other geochemical characteristics of the basalts reported above will be considered later in the discussion on the petrogenesis of these rocks.

3.5.3 Geochemistry of the acid rocks

The acid rocks form a continuum from 66-77% SiO_2 (Table A3.2) and to facilitate an examination of the behaviour of the major and trace elements, all have been plotted against SiO_2 (Figs. 3.7 and 3.8). The

Figure 3.7 Major elements vs. SiO_2 for acid rocks from the Central Australian province. The solid lines enclose the field of Cainozoic calc-alkaline volcanics. O undifferentiated samples ● volcanic clast from The Olgas ■ aplite dyke ▲ granite ◆ average rhyolite from the Warburton area (after Haynes, 1972).

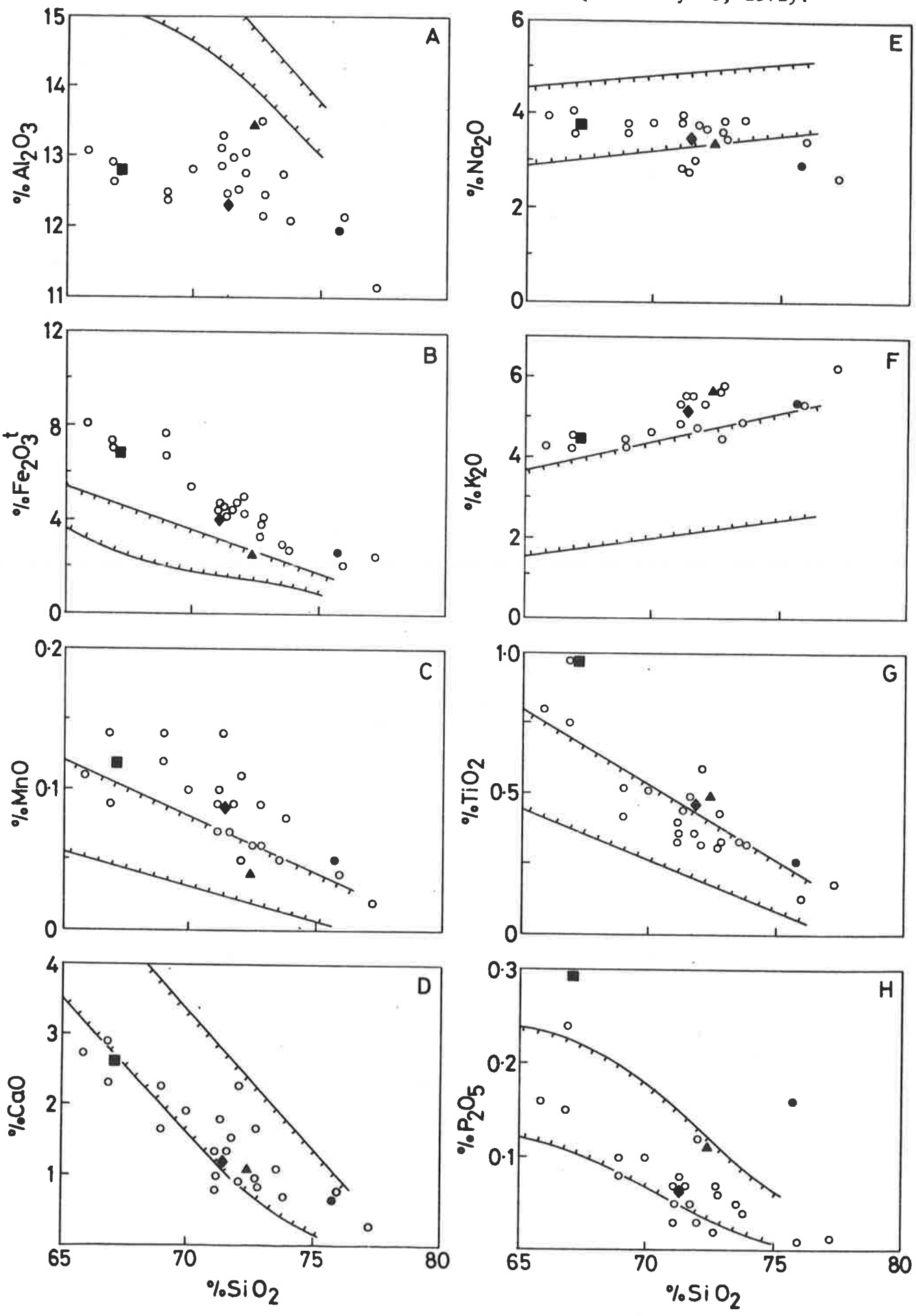

Figure 3.8 Selected trace elements vs. SiO_2 for acid rocks from the Central Australian province. Same comments apply as for Figure 3.7.

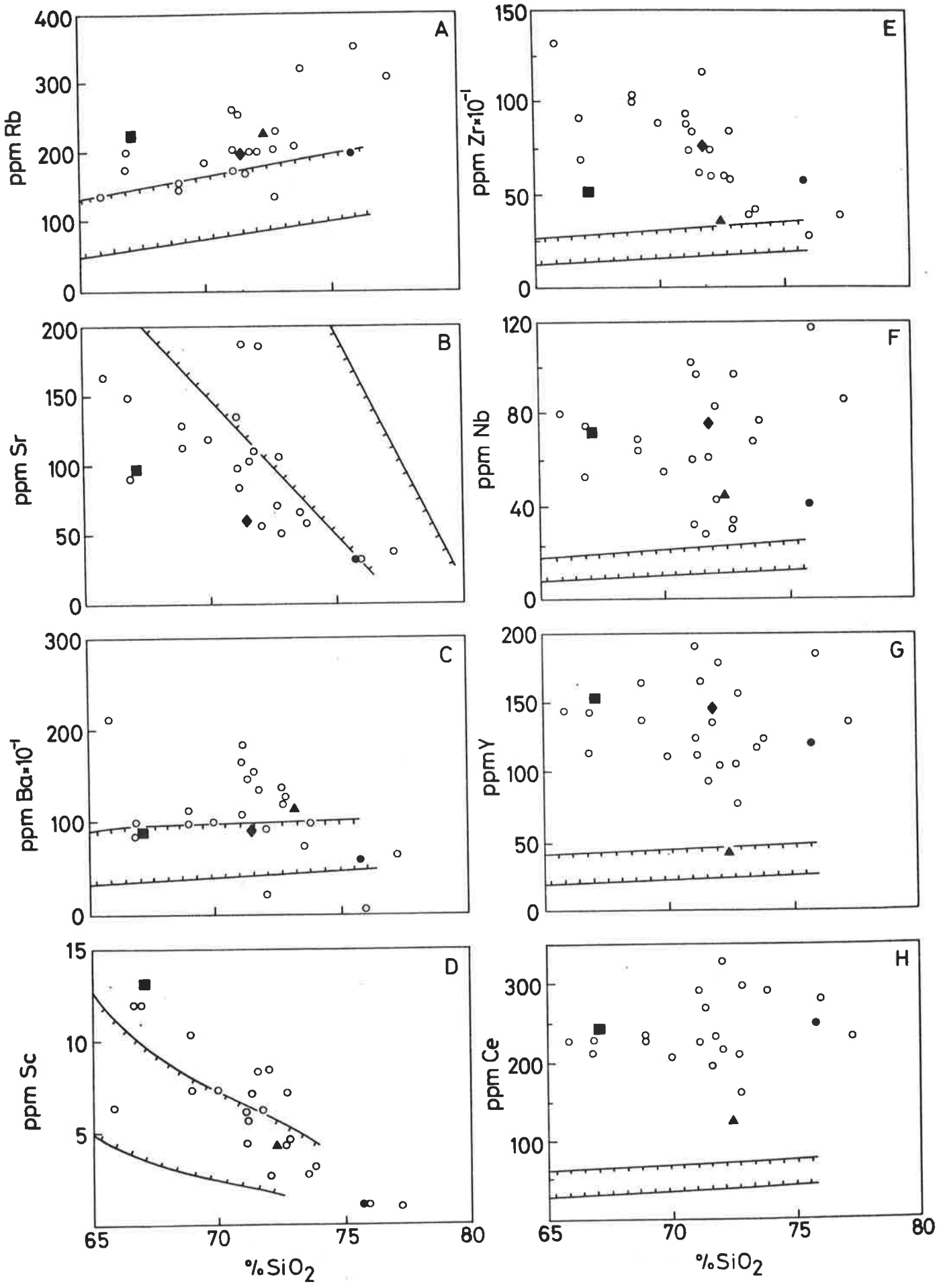

Figure 3.9 Selected variation diagrams for acid rocks from the Central Australian province. Same comments apply as for Figure 3.7.

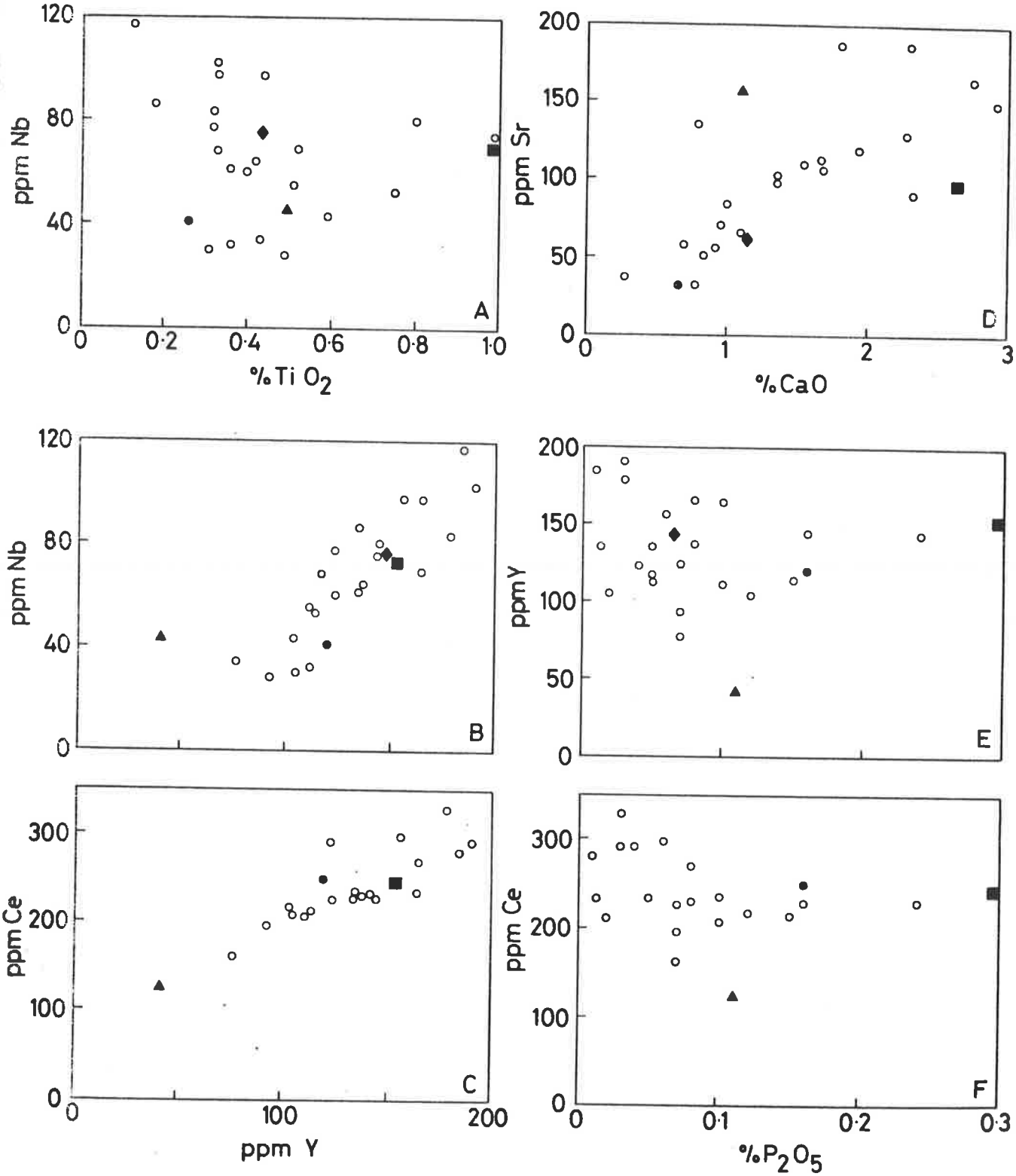

continuity of many of the trends is indicative of a differentiation series. This conclusion is supported by the following observations:

1) The decreasing contents of $Fe_2O_3^t$, TiO_2 and Sc with increasing SiO_2, up to high SiO_2 levels, is consistent with fractionation of magnetite.
2) The inverse correlation of Sr with SiO_2, but positive correlation with CaO (Fig. 3.9D) is suggestive of plagioclase fractionation.
3) The range of Ba contents could be due to the combined effects of residual concentration and variable amounts of K-feldspar fractionation (Kd Ba K-feldspar/liquid = 6.1, Arth, 1976).
4) The general decrease in Zr with increasing SiO_2, which could reflect zircon fractionation.

These features suggest that the rhyolites may have been derived from the dacites by fractionation of plagioclase + magnetite + K-feldspar + zircon, a conclusion not inconsistent with petrographic observation.

The Ce, Nb and Y vs SiO_2 plots (Fig. 3.8) show considerable scatter, and reveal that while some rhyolites are enriched in these elements compared with the dacites, others are relatively depleted. The apparently random variation of Ce, Nb and Y in relation to SiO_2 cannot be readily explained by a simple differentiation model involving a single line of liquid descent. The lack of correlation between Nb and TiO_2 (Fig. 3.9A) shows that Nb is not being controlled by ilmenite or sphene and similarly, the absence of any correlation between Ce and Y, and P_2O_5 suggests that apatite is not removing Ce or Y (Figs. 3.9E and F). Zircon fractionation cannot be controlling Ce, Nb and Y because of the differing behaviour of Zr compared with these elements, in relation to SiO_2 (Fig. 3.8). Thus it appears that Ce, Nb and Y are not being controlled by any fractionating minerals. Nevertheless it is important to note that both Ce and Nb show a linear relationship with Y, suggesting that some common factor is controlling the three elements (Figs. 3.9B and C). The Ce, Nb and Y variations in the dacites may be significant in this regard (see Fig. 3.8), because it is possible that some of the variations in the rhyolites could be inherited from the dacites, particularly as other geochemical data (e.g. Rb, Sr, CaO, Ba, Zr, $Fe_2O_3^t$ and Sc) indicate that they are likely to be related by crystal fractionation. This proposal is supported by the constancy of the Ce/Y and Nb/Y ratios between the dacites and rhyolites which is consistent with the incompatible nature of these elements in the likely fractionating minerals (i.e. plagioclase, K-feldspar and magnetite). Possible reasons for the variability of Ce, Nb and Y in the dacites will be discussed later.

Comparison of the major and trace element abundances in the dacites and rhyolites with those in Cainozoic calc-alkaline volcanic rocks (Figs. 3.7 and 3.8) reveals that the Central Australian acid volcanics differ in a number of respects:

1) they are relatively low in CaO and Al_2O_3;
2) they are relatively high in $Fe_2O_3^t$, TiO_2, K_2O/Na_2O and $Fe_2O_3^t/MgO$ and
3) they are particularly high in Zr, Nb, Y and Ce.

Their high $Fe_2O_3^t/MgO$ and Σ alkalis is reflected on the AFM plot by a displacement towards the A - F side of the triangle relative to the typical calc-alkaline trend (Fig. 3.4). It is also notable that the high K_2O of these rocks, places them in the toscanite field of Mackenzie and Chappell (1972). The relevance of these distinctive geochemical characteristics to the origin of the acid volcanics will be considered in the discussion on the petrogenesis which follows.

3.6 PETROGENESIS

3.6.1 Previous interpretations

Three models have been proposed in the past to explain the origin of the rocks comprising the Central Australian province. It has been postulated that:

1) The basic volcanic and basic plutonic rocks are comagmatic and have given rise to the acid magma by differentiation (Nesbitt, 1966; Blight, 1969; Bowden, 1969).
2) The basic volcanic and basic plutonic rocks are comagmatic and have an origin in partial melting of the mantle. The acid volcanic rocks and granites are comagmatic, but are anatectic and are therefore genetically unrelated to the basic rocks (Gray, 1971; Daniels, 1974, p. 75).
3) The basic volcanic and basic plutonic rocks are unrelated to each other and to the acid rocks (Goode, 1970).

It is the purpose of this section to evaluate which model, if any, is most consistent with the available data. To facilitate this investigation, relevent field, petrographic and geochemical evidence presented earlier, together with the evidence of other workers is summarized below.

3.6.2 Summary of evidence

A. Field evidence

The field relationships of the four main rock types (i.e., acid volcanics, acid intrusives, basic volcanics and basic intrusives) place

constraints on possible petrogenetic models. The field evidence demonstrates that:

1) The acid and basic volcanic rocks were erupted contemporaneously since they alternate in the same volcanic pile. This need not necessarily indicate a common origin, but does indicate that they were formed at the same time.
2) Intermediate volcanic rocks are extremely rare - those that do occur appear to be of hybrid origin, for example, silica-contaminated basalts, and tuffs containing mixed basalt and rhyolite fragments.
3) Thick piles of dominantly acid volcanic rocks and high-level granites are closely associated in the field and are thus interpreted to have a common origin.
4) There is no direct association of basalts with the Giles Complex; for example, the relative amount of basalt in the volcanic pile does not appear to be related to the proximity of large basic intrusives.
5) The Giles Complex intrusives nowhere show the development of voluminous silicic differentiates, a point verified by Nesbitt (1966, p. 276), Gray (1971)and Goode (pers. comm., 1978). This feature is not due to lack of outcrop because in many cases the tops of the layered intrusives are exposed, or nearly so. Where they are exposed a chilled margin is seen indicating that the basic magma was liquid at the time of intrusion.
6) High-level gabbros believed to be related to the Giles Complex intrude the volcanic pile in a number of places and therefore post-date the volcanism (Blight, 1969; Daniels, 1974). The time difference between volcanism and intrusion is critical, because if it is small, the possibility of a genetic relationship still remains.
7) The volume of acid rocks exposed in the province greatly exceeds that of the basic rocks.

Daniels (1974 p. 99) in his regional study, considered that this field evidence favoured an anatectic origin for the acid magma rather than a differentiation origin from a basic parent. Gray (1971) interpreted the evidence similarly. However, opposite conclusions were drawn by Blight (1969) and Bowden (1969) from their detailed work in the Tollu area. They deduced that the acid magma was derived by differentiation of the basic intrusives <u>in situ</u> and was erupted synchronously with basic magma from the same source. Their main evidence came from the discovery of an apparently large granophyre body at the top of an unnamed gabbroic intrusive into the volcanic pile (Fig. 3.10). This granophyre had identical

Figure 3.10 Rock relationships in the Tollu area.

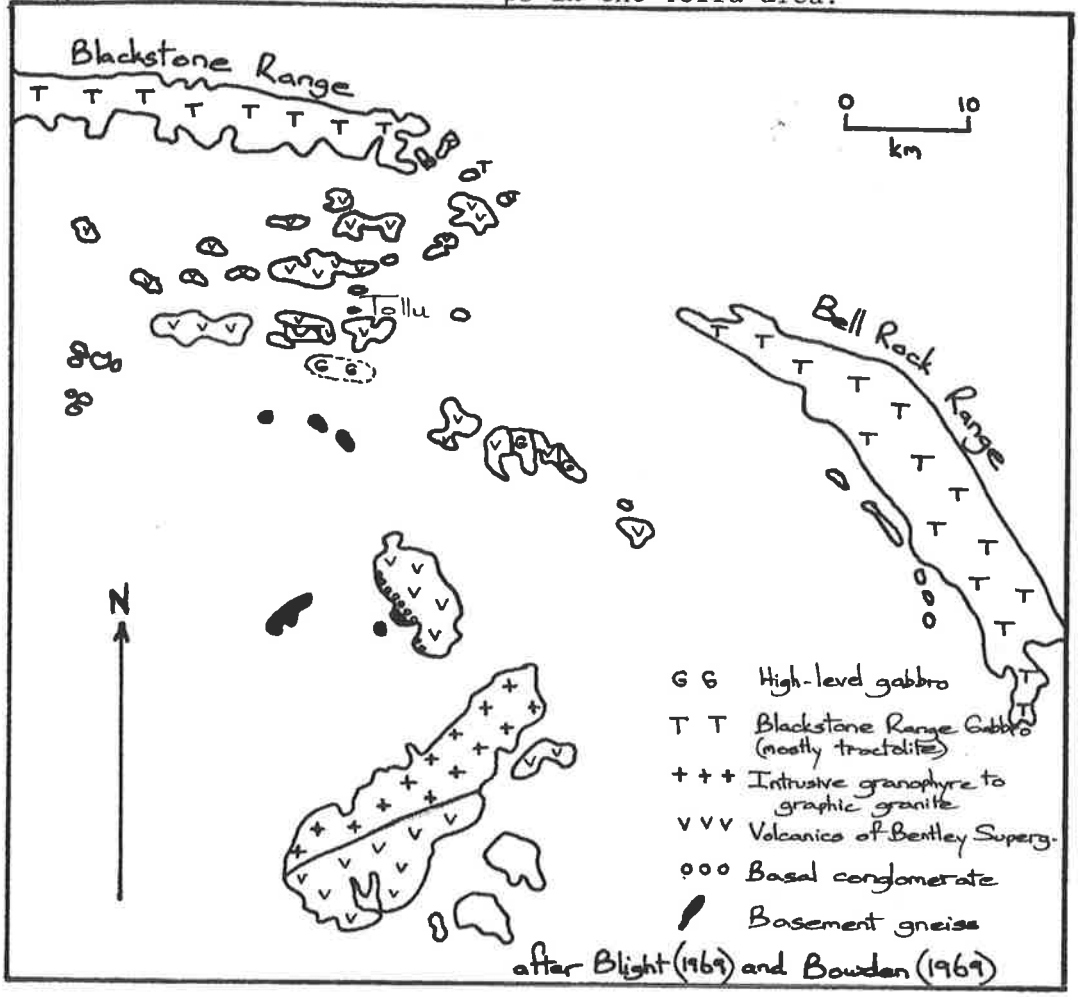

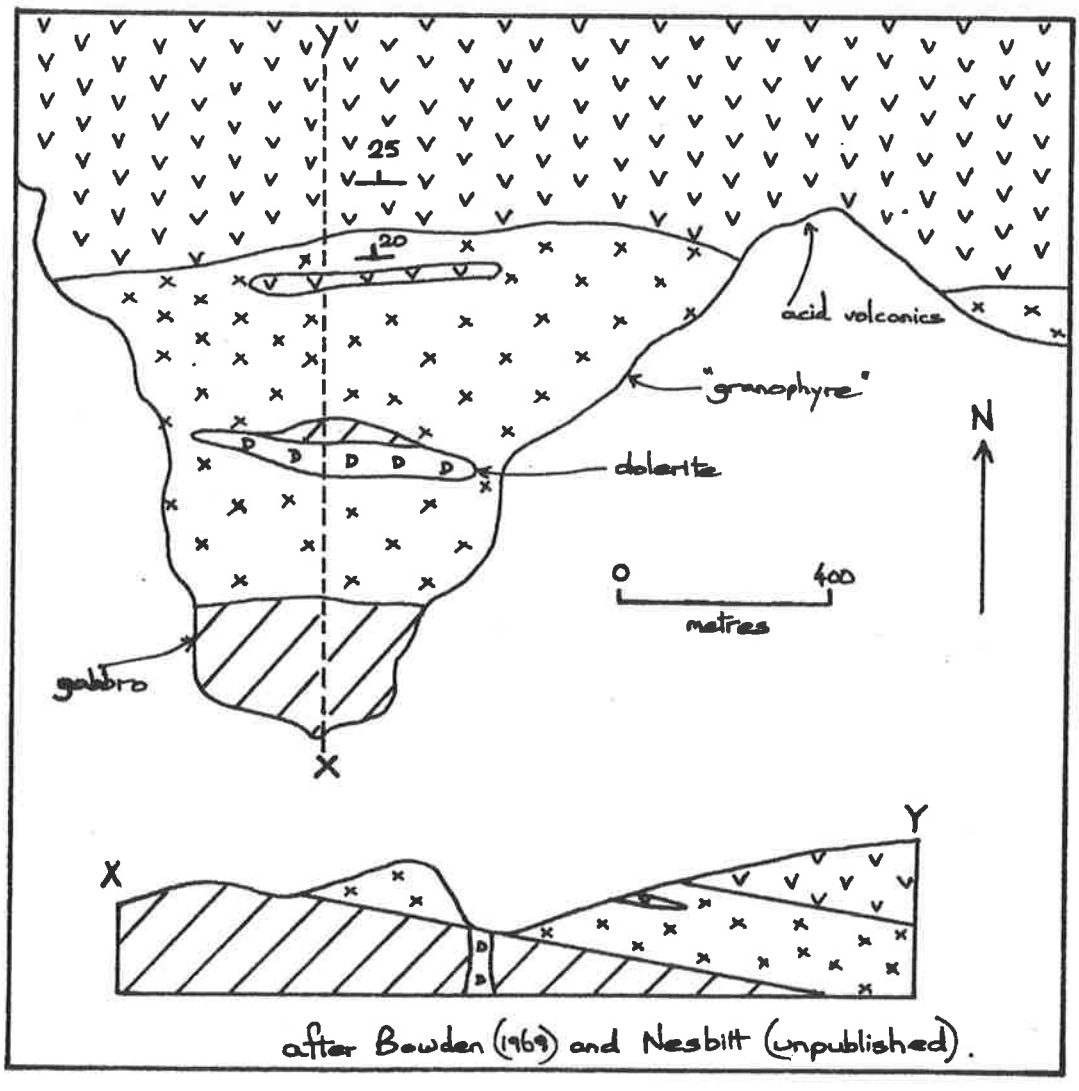

geochemistry to the acid volcanic rocks and was therefore thought by them to be comagmatic.

Nesbitt (1966) had earlier proposed this idea based on the structure of the Tollu area and the stratigraphic position of the Blackstone Range Gabbro. Since the acid and basic volcanic rocks were contained in a basinal structure surrounded by an arc of Blackstone Range Gabbro (Figs. 3.1 and 3.10), he reasoned that the basic magma could have intruded into the upper crust and then been tapped to yield the acid and basic volcanics. The lack of acid differentiates associated with the Giles Complex could be conveniently explained in terms of removal by this method.

The critical field observations by these workers which led to their conclusions were: the stratigraphy and structural relationships of the Blackstone Range Gabbro to the volcanic pile (Nesbitt, 1966) and the presence of a granophyric upper margin to the smaller, unnamed gabbro body which intrudes the volcanic pile (Bowden, 1969).

The former observation is placed in some doubt by the work of Daniels (1974) who records contact metamorphic effects in the acid volcanic rocks adjacent to the Blackstone Range Gabbro and also a chilled margin to this gabbro body. In addition, he notes that the Blackstone Range Gabbro is confined to the stratigraphic level between the Bentley Supergroup and the Lower Proterozoic basement. These points led Daniels (1974) to conclude that the magma intruded as a lopolithic sheet into a major crustal weakness represented by the basement-cover contact. It is therefore inferred that the original form of the intrusive, combined with later folding during the Petermann Ranges Orogeny has led to the apparent "basinal" structure of the Blackstone Range Gabbro and Tollu volcanics rather than the intrusive-extrusive relationship proposed by Nesbitt (1966).

The second observation also has a measure of uncertainty. For example, careful sampling and petrographic examination by the writer suggests that the "granophyre" of Bowden (1969) has two components:

1) A contaminated gabbro (B11, B10), having all the characteristics of a gabbro which has engulfed "granitic" rocks, with resultant silica and potash addition.
2) A contact metamorphosed acid volcanic (B9 (1), B9 (2), B13).

These rocks have pseudo-granophyric textures, similar to those noted by Walraven (1976) in contact metamorphosed sediments adjacent to the Bushveld Complex (Fig. 3.11). No typical igneous granophyres were sampled by the writer from this body, although true granophyres (not

Figure 3.11. View of The Olgas and photomicrographs of rocks from the "granophyre" zone, Tollu area.

A. The rounded domes of The Olgas, which occur some 120 km east of the nearest outcrops of Central Australian volcanics. The Cambrian sediments are composed almost exclusively of detritus shed from the Central Australian province and include large clasts of acid and basic volcanics (e.g. boulders in foreground).

B. This rock is interpreted to be a contaminated gabbro. Evidence for its gabbroic parentage is seen in the abundant, tabular plagioclase laths (now extensively sericitized) and scattered magnetite. The interstitial quartz and K-feldspar is thought to have been introduced during intrusion into the acid volcanic pile. F.V. 4.5 mm.

C. Spherulitic devitrification textures in rhyolite from the "granophyre" zone of Bowden (1969). F.V. 3.5 mm.

D. Pseudo-granophyric textures in rhyolite near the contact with the gabbro. In hand specimen this rock preserves its original (volcanic) porphyritic texture and it is considered that the incipient granophyric textures observed, developed in response to heating from the nearby gabbro body. F.V. 4 mm.


A

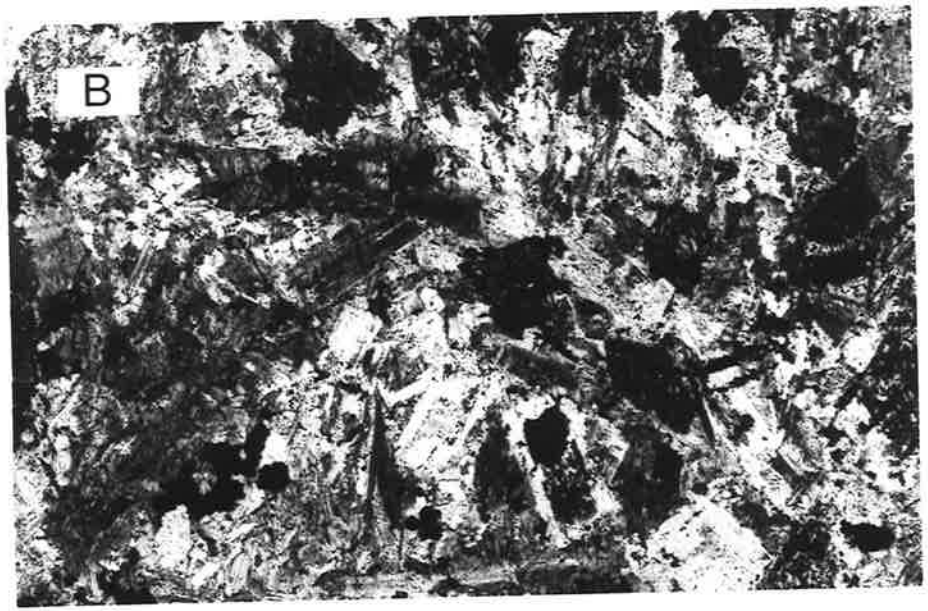
B

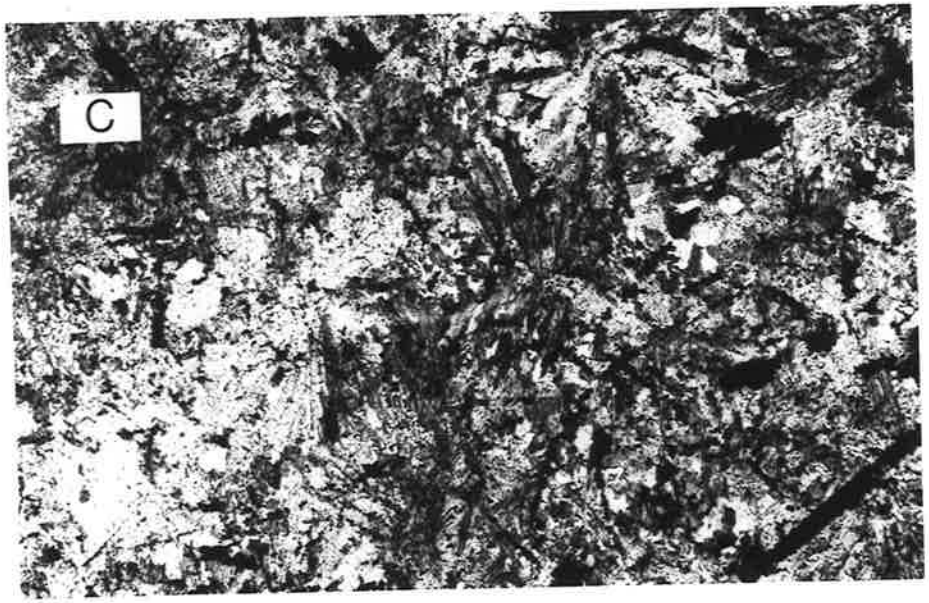
C

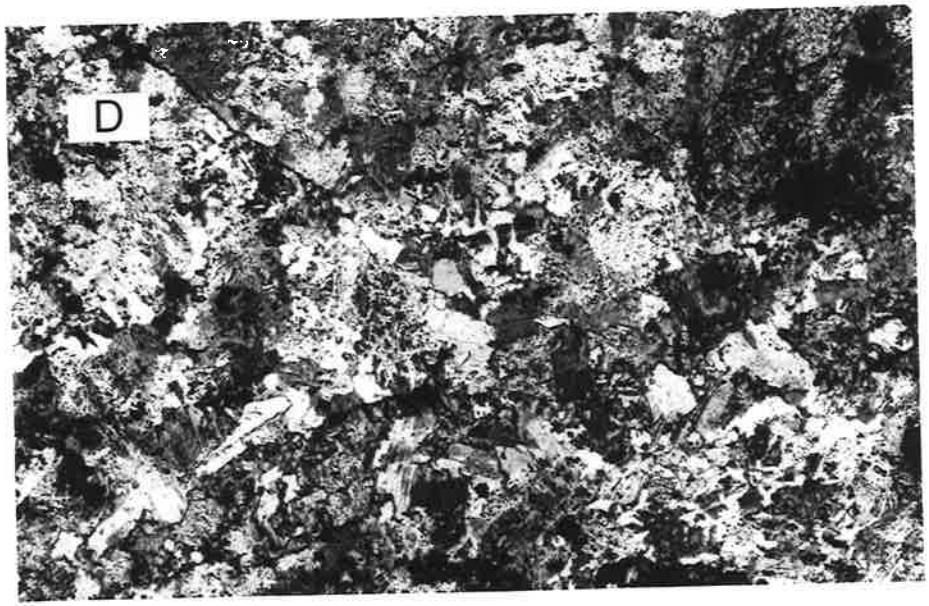
D

associated with gabbros) are common in the province. If part of the granophyre zone is contact metamorphosed acid volcanic rocks as the petrography suggests, then this could explain why the "granophyre" has comparable geochemistry to rocks of the acid volcanic pile (Bowden, 1969). It is also notable that clearly recognisable rafts of porphyritic acid volcanic rocks occur within the supposed granophyre zone quite near the gabbro.

A summary of the contact zone as interpreted by the writer, is given below.

	partially recrystallised acid volcanic rocks	72% SiO_2	
	---------- gradational contact		
two zones noted by writer, thickness varies greatly.	"pseudo-granophyre" rock (mainly recrystallised acid volcanics)	71% SiO_2	granophyre zone of Bowden (1969)
	contaminated gabbro	63-64% SiO_2	
	========== sharp contact		
	gabbro	48% SiO_2	

The completely gradational nature of the "granophyre" - acid volcanic contact at this locality was also recognised by Gray (1971), who like Bowden (1969) considered that it represented a probable volcanic - sub-volcanic relationship; however unlike Bowden, Gray did not relate the granophyre to the gabbro. Gray presented isotopic evidence in support of his view and stated that "no isotopic difference between the (acid) volcanics and granophyres can be detected in either age or initial ratio". Apart from the contrary petrographic evidence presented above, such a volcanic - sub-volcanic relationship is considered improbable because it fails to explain why the granophyre is only found between the gabbro and the acid volcanic pile (assuming the gabbro and granophyre are unrelated as Gray suggests). Also, the isotopic evidence cited by Gray (1971) is equally supportive of the hypothesis that the granophyre represents contact metamorphosed acid volcanic rocks.

In conclusion, it appears that the critical field evidence cited by other workers to favour a differentiation origin for the acid magma, is not conclusive and clearly there is some justification for interpreting the evidence in other ways.

B. Petrographic evidence

The petrographic evidence can be summarized as follows:

1) There are no porphyritic andesites or indeed any intermediate rocks that might suggest a petrographic link between the basic and acid series. The rocks comprising the basic series are usually non-porphyritic and contain plagioclase, altered clinopyroxene, magnetite and altered glass as the chief components. The acid volcanics on the other hand are invariably porphyritic rocks, with phenocrysts of clinopyroxene, plagioclase, K-feldspar and quartz set in an originally glassy matrix.

2) The rocks with intermediate SiO_2 contents have not crystallised from a magma, but are of hybrid origin. They are either silica-contaminated basalts or pyroclastics containing basic and acid rock fragments.

3) As mentioned previously, the granophyre recognised by Bowden (1969) in the Tollu area does not have the textures of a true igneous granophyre (Walraven, 1976). Rather, the textures could be explained by progressive contamination of a gabbro (with SiO_2 and K_2O) and concurrent recrystallisation of the adjacent acid volcanic rocks.

4) There is pronounced recrystallisation and resultant loss of primary textures in the acid volcanic rocks adjacent to the Blackstone Range Gabbro (Fig. 3.1). B29, which is a typical example, consists of an equigranular aggregate of quartz, hornblende, plagioclase and K-feldspar. In hand specimen, the porphyritic textures are preserved, but in thin section all phenocrysts are highly corroded. This texture contrasts with the delicate groundmass textures preserved in samples B1, B2 and B7 (Fig. 3.2), which are from the same volcanic pile only a few kilometres distant. Since the recrystallisation cannot be attributed to a higher degree of deformation in this area, it therefore probably reflects contact metamorphism due to the proximity of the Blackstone Range Gabbro, as previously proposed by Daniels (1974).

5) Two types of basic rocks intrude the volcanic pile in the Tollu area. The first, represented by the Blackstone Range Gabbro is a troctolite, containing up to 90% plagioclase with olivine and clinopyroxene comprising the bulk of the remainder. Although contacts are not seen, its intrusive relationship is inferred from the evidence for contact metamorphism cited above and the field observations of Daniels (1974). The second type of basic intrusive comprises medium- to coarse-grained ophitic-textured gabbros which clearly cross-cut the volcanic pile.

It may be concluded from the petrographic evidence that there are no obvious petrographic links between the acid and basic rocks. In addition,

Figure 3.3 Selected variation diagrams for rocks from the Central Australian province. ● volcanic clasts from The Olgas O undifferentiated samples ◆ averages of volcanic rocks from the Warburton area compiled by Haynes (1972) △ troctolite ■ basic rocks and □ granophyres from the Red Hill layered intrusive, Tasmania (after McDougall, 1962).

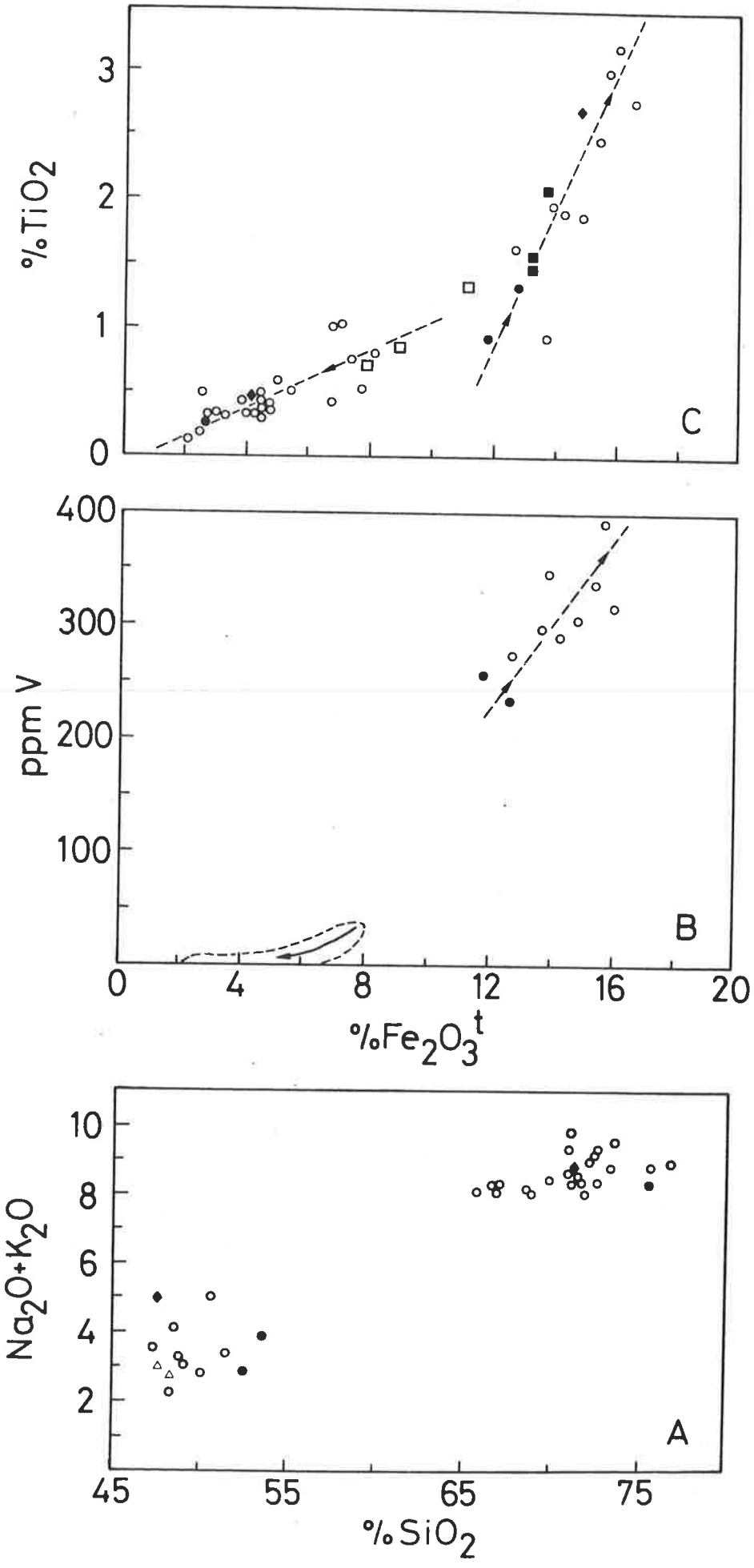

the volcanic pile is intruded by two groups of basic rocks, neither of which show evidence of associated, voluminous silicic differentiates.

C. Geochemical evidence

The geochemistry establishes that there is a break in SiO_2 between 53-66%. There is a similar hiatus in all other elements, particularly $Fe_2O_3^t$, MgO and alkalis (AFM diagram - Fig. 3.4), Zr, Nb, Y and LREE (Table A3.2) and V and Ti (Figs. 3.3B and C).

The acid rocks have extremely high contents of Zr, Nb, Y and LREE and moderately high levels of $Fe_2O_3^t$, TiO_2 and K_2O/Na_2O compared with Cainozoic acid volcanics. They do, however, show typical calc-alkaline trends such as decreasing $Fe_2O_3^t$, MgO, CaO, TiO_2 and P_2O_5 with increasing differentiation.

The variable levels of Ce, Nb and Y in the dacites appear to have been inherited by the rhyolites, via crystal fractionation. The geochemistry of the acid volcanic and acid intrusive rocks overlap, and this, combined with their close association in the field, suggests they are comagmatic.

The basic rocks show an iron-enrichment trend, typical of continental tholeiites. The progressive removal of olivine ± orthopyroxene ± clinopyroxene (± plagioclase) has caused progressive decreases in compatible elements (e.g. Ni and Cr), but enrichment, due to residual concentration, of incompatible elements (e.g. Zr, Nb, Y, LREE, P_2O_5 and TiO_2). All of the basic rocks, whether intrusive or extrusive, are thought to be comagmatic on the basis of their similar geochemistry.

It could be inferred from the hiatus in composition and the diverse crystallisation history of the acid and basic rocks that the two rock groups are genetically unrelated. However this evidence is not compelling because it is possible that the intermediate rocks linking the two series exist as crystal cumulates in the lower crust.

It is notable that some of the differentiated rocks comprising the Red Hill intrusion in Tasmania show similar TiO_2 vs $Fe_2O_3^t$ behaviour to the samples in this study; in particular two opposite, but positively correlated trends are evident (see Fig. 3.3B, data from McDougall, 1962). Further to this, Hamilton (1960) has demonstrated that the granophyric differentiates of many large layered basic intrusives have relatively high total alkali and $Fe_2O_3^t$ contents, but relatively low levels of CaO and Al_2O_3 compared with typical calc-alkaline rocks - characteristics which are in common with the acid volcanic rocks from central Australia (see Table 3.2). Hamilton (1960) cites the Bushveld Complex as a typical

TABLE 3.2. Analyses of rocks from various sources cited in text.

	1	2	3	4	5	6	7	8	9	10
SiO_2	75.4	67.8	75.32	65.21	61.65	66.21	67.0	71.65	72.23	62.64
Al_2O_3	12.2	13.4	13.22	12.53	14.11	11.92	12.3	12.04	12.58	16.77
Fe_2O_3	1.5	1.3	1.57	3.45	2.80	5.95	3.8	1.52	2.05	2.82
FeO	0.8	4.4	0.58	6.83	7.85	4.40	5.1	2.54	1.22	1.49
MnO	0.04	0.07	0.01	0.21	0.15	0.13	0.14	0.12	0.06	0.09
MgO	0.15	1.5	0.15	0.31	0.87	0.58	0.84	0.14	0.03	0.54
CaO	0.60	2.0	0.69	3.72	5.87	3.53	3.6	0.26	0.13	1.47
Na_2O	3.9	3.4	4.26	4.35	2.75	2.75	2.6	6.07	5.98	5.81
K_2O	4.8	3.8	3.86	2.36	2.46	3.08	3.4	4.76	4.54	5.50
TiO_2	0.2	0.7	0.31	0.93	1.20	1.11	0.86	0.29	0.16	0.53
P_2O_5	0.04	0.2	0.03	0.09	0.30	0.34	0.37	0.02	0.01	0.15
Zr								1547	1450	872
Nb								34	220	52
Y								106	164	53
Ce								209	220	212
Ni								<1	4	4.3
Rb								158	337	102
Sr								2	1.3	117
Ba								<10	20	820
No. Samples	7	34	1	1	4	3	9	1	6	3

1. Average of 7 analyses of granophyre and granite associated with Wichita lopolith after compilation of Hamilton (1960).

2. Average of 34 analyses of granophyre associated with Sudbury lopolith, after compilation of Hamilton (1960).

3 and 4. Granophyres associated with Skaergaard intrusion, East Greenland (Wager and Brown, 1968).

5 and 6. Fayalite granophyre and granophyre, respectively, associated with Red Hill intrusion Tasmania (McDougall, 1962).

7. Granophyre associated with Dufek intrusion, Antarctica (Ford, 1970).

8. Comendite, D'Entrecasteaux Islands, Papua New Guinea (Smith *et al.*, 1977).

9 and 10. Comendite and trachyte, respectively, Glass House Mountains, Queensland (Ewart *et al.*, 1976).

example, but more recent work suggests that the salic phase of this body had an anatectic origin. (e.g. Davies, et al., 1970; Lenthall and Hunter, 1977). Ford (1970) advocated a differentiation origin for the granophyre in the Dufek intrusion of Antarctica, but some evidence for contamination led him to conclude that the "analyses of bulk granophyre (Table 3.2) thus may not accurately indicate the true composition of the final Dufek liquid". Consequently, in the absence of detailed isotopic and trace element data for the various granophyres listed in Table 3.2 and hence uncertainties in their origins in some cases, the significance of the geochemical analogies with the acid volcanics of this study remain unclear.

The relatively high Zr, Nb, Y and Ce contents of the acid volcanics might suggest enrichment by extreme crystal fractionation, by analogy with similarly high values in trachytes and comendites, which are generally thought to be differentiates of alkali basalts (e.g. Ewart, et al., 1976; Smith, et al., 1977). Analyses of a comendite from New Zealand (Smith, et al., 1977) and an average comendite from the Glass House Mountains, Queensland (Ewart, et al., 1976) are given in Table 3.2. The Zr, Nb, Y, LREE and Al_2O_3 contents are comparable with the rhyolites from the Central Australian province, but $Fe_2O_3^t$, MgO, CaO, TiO_2, P_2O_5, Sr and Ba are all lower in the comendites indicating more extreme fractionation. It is also notable that the characteristically high K_2O/Na_2O of the Proterozoic rhyolites is not duplicated in the comendites, which by contrast, have $Na_2O > K_2O$. Comparing a Central Australian province dacite with a trachyte (Table 3.2) reveals similarities in Zr, LREE, Rb, Sr, Ba and K_2O, but the trachyte has lower levels of $Fe_2O_3^t$, TiO_2, Nb and Y and significantly higher Na_2O.

The compositional analogies with the comendites and trachytes show that crystal fractionation and resultant residual liquid concentration of incompatible elements is capable of producing relatively high Zr, Nb, Y and LREE contents in acid differentiates of basic parents. However, the higher contents of Sr, Ba, TiO_2, $Fe_2O_3^t$, MgO, CaO and P_2O_5 in the Proterozoic acid volcanics suggests they are not as fractionated as the peralkaline series at comparable SiO_2 and therefore extreme crystal fractionation may not have been the major influence in the present case. Moreover, trachytes and comendites are usually volumetrically insignificant on the scale of an alkali-basalt province (c.f. Ewart, et al., 1976), a feature which is certainly not true of acid volcanics in the Central Australian province.

Qualitative arguments such as those above, fail to be conclusive since they have an inherent subjective element which introduces ambiguity. The proposition that the acid series and basic series are related by crystal

TABLE 3.3. Results of major and trace element modelling calculations designed to test whether the dacites of the Central Australian province (an average of three samples) could be related to the evolved basalts (an average of five samples) by differentiation.

A. Least squares approximation of average dacite in terms of average evolved basalt and expected minerals.

Rock	average dacite obs.	average dacite calc.	average basalt parent	Mineral compositions used amph.	plag.	cpx.	mag.	apatite
SiO_2	67.28	67.27	51.23	42.80	52.07	50.11		
Al_2O_3	13.02	13.02	13.85	14.69	30.63	2.76		
FeO^t	6.86	6.88	14.20	10.29		11.57	75.0	
MnO	0.11		0.20	0.22		0.41		
MgO	0.69	0.69	4.44	15.27		14.43		
CaO	2.69	2.70	8.71	12.53	13.13	19.78		56.0
Na_2O	3.90	3.99	2.78	2.05	3.98	0.31		
K_2O	4.40		1.35	1.31	0.21			
TiO_2	0.87	0.78	2.72	1.49		0.62	19.0	
P_2O_5	0.18	0.17	0.51					44.0
Total	100.0		100.0					

Mineral	Wt. fraction	Mineral proportion
amph.	0.143	0.24
plag.	0.193	0.33
cpx.	0.136	0.23
mag.	0.11	0.19
apatite	0.01	0.017
dacite	0.42	
	= basalt	
ΣR^2	= 0.017	

Notes:
1. MnO and K_2O were excluded from modelling calculations.
2. Amphibole composition from writer's electron microprobe data for amphibole phenocrysts in a calc-alkaline basalt (W31, see Table A5.5 Appendix 1).
3. Plagioclase composition is An_{64} and is after Wright (1974).
4. Clinopyroxene composition is from writer's electron microprobe data for clinopyroxene phenocrysts in an andesite from the Lake Everard area (an average of 8 analyses of 4 phenocrysts).
5. Ti content of magnetite adjusted to give a satisfactory match for TiO_2.
6. Apatite composition after Wright (1974).

B. Calculated trace element abundances, using mineral proportions and degree of crystallisation obtained from major element modelling calculations.

Rock	average dacite obs.	average dacite calc.	average basalt parent	Distribution coefficients used amph.	plag.	cpx.	opx.	mag.	apatite
Zr	959	726	352	0.5	0.01	0.01	0.03	0.10	0
Zr	959	838	352	0	0	0	0	0	0
Nb	69	48	26	0.8	0.01	0.01	0.15	0.4	0
Nb	69	62	26	0	0	0	0	0	0
Y	134	87	63	1.0	0.03	0.5	0.2	0.2	13.1
Ce	213	153	93	0.20	0.12	0.15	0.024	0	18
Ce	213	221	93	0	0	0	0	0	0
Rb	170	81	37	0.29	0.071	0.015	0.022	0	0
Sr	135	391	310	0.46	1.8	0.12	0.017	0	0
Ba	1330	812	400	0.42	0.23	0.026	0.013	0	0
Sc	10	2.3	33	12.5	0	3	3	2	0
V	39	<1	312	32	0	1.1	1.1	30	0
Cr	2	<1	100	30	0	30	13	32	0
Ni	12	3	77	8	0	6	8	8	0
Co	26	1.5	51	13	0	2	6	8	0

Notes:
1. Distribution coefficients for Zr, Nb and Y after Pearce and Norry (1979); Ce, Rb, Sr and Ba after Arth (1976) and Sc, V, Cr and Ni after Gill (1978).
2. Zero distribution coefficients for Zr, Nb and Ce assumed, to enable calculation of the maximum permissable values for these elements within the constraints provided by the major element modelling.

fractionation as originally suggested by Nesbitt (1966) can only be satisfactorily tested with the presently available data by modelling the major elements and checking for consistency using the trace elements. It is evident from Figure 3.3 that, if simple crystal fractionation has been operative, then the rocks most closely related in the two series should be the least-differentiated dacite and the most-differentiated basalt. For the purposes of testing, the parent basic composition was averaged from five of the most fractionated basic rocks analysed (B66, B23, B77, B14 and B8), while the assumed daughter composition was averaged from three of the most basic dacites (B29, B7 and B45). Least squares modelling of the major elements requires relevant mineral composition data, but unfortunately no microprobe data was obtained on minerals in these rocks because either they were too altered (e.g. plagioclase and clinopyroxene) or they were not modal (e.g. amphibole). However, what are considered to be reasonable estimates of the mineral compositions were made, based on the writer's data for minerals in rocks of similar composition from elsewhere (Table 3.3A).

A visual comparison of the assumed parent and daughter compositions (Table 3.3A) suggests that if the rocks are related by differentiation, then fractionation of appreciable amounts of the following minerals will be likely:

1) Ti-magnetite, to reduce $Fe_2O_3^t$ and Ti;
2) mafic minerals (e.g. amphibole and/or clinopyroxene) to reduce MgO;
3) plagioclase, amphibole and/or clinopyroxene to reduce CaO and
4) apatite to reduce P_2O_5.

These predictions are confirmed by the least squares modelling calculations which favour fractionation of : 14.3% amphibole, 19.3% plagioclase, 13.6% clinopyroxene, 11% magnetite and 1% apatite (Table 3.3A).

Modelling of the trace elements using these mineral proportions and distribution coefficients appropriate to the liquid composition reveals large discrepancies, particularly for Sc, Ni, Co, V, Ce, Zr, Nb and Y owing to the marked control of these trace elements by amphibole, clinopyroxene and magnetite (Table 3.3B). In the case of Zr and Nb, even if it is assumed D = 0, the levels of these elements in the average dacite cannot be matched (e.g. 838 ppm Zr calculated c.f. 959 ppm observed and 62 ppm Nb calculated c.f. 69 ppm observed).

Adjustment of the mineral compositions within permittable limits will affect the mineral proportions slightly, but will not alter the basic requirement that removal of large amounts of amphibole and magnetite are necessary to produce the dacitic liquid from the basic parent. While this constraint applies, it would not be possible to match the trace elements

(particularly Sc, Ni, Co and V). Thus, in spite of the assumptions of the calculation method, it is reasonable to conclude that the basic and acid series are probably not related by differentiation. It follows that the compositional hiatus separates two geochemically unrelated rock series, which therefore must have different ultimate origins. This conclusion is consistent with the field and petrographic evidence presented above. It is also supported by the isotopic data of Gray (1971) which shows that there is negligible overlap in the initial strontium isotope ratios of the acid volcanics (plus granophyres and granites) and the basic intrusive rocks belonging to the Giles Complex. This evidence indicates that the acid magma could not have differentiated from a basic parent with the isotopic characteristics of the Giles Complex intrusives. The question of the ultimate sources of the magmas for the two rock series will be examined below.

3.6.3 Origin of the basic magma

Experimental evidence shows that the basic magma must have an ultimate origin in the mantle, although none of the samples analysed have Mg numbers or Ni and Cr contents consistent with equilibration with mantle peridotite (Roeder and Emslie, 1970). This could be attributed to low pressure fractionation of olivine + pyroxene ± plagioclase (c.f. Mertzman, 1977) which in turn has led to the residual concentration of P_2O_5, TiO_2, Zr, Nb, Y and REE and an increase in $Fe_2O_3^t/MgO$ with differentiation (Fig. 3.5). A consideration of the incompatible element ratios has previously demonstrated that Sc and V are depleted relative to the LIL trace elements, suggesting control by either fractionating minerals or residual minerals in the mantle (Table 3.1).

It is notable that the deep-level (cumulate) intrusives of the Giles Complex exposed to the east of the Blackstone region (Nesbitt, et al., 1970; see Fig. 3.1) contain abundant clinopyroxene with pervasive rutile exsolution (Goode and Moore, 1975). Such a pyroxene would control Cr, Sc and V because of the presence of favourable atomic sites for these elements (Taylor, 1965). Nesbitt, et al., (1970) observe that a pronounced iron enrichment in the deep-level intrusives appears to be absent. They state: "the fact that the Mt. Davies and Kalka intrusions end their fractionation trends with only moderate iron enrichment despite the absence of cumulus magnetite, suggests liquid was lost to higher environments" (p. 559). These authors infer that this "lost" liquid is represented by some or all of the basic volcanic rocks discussed in this thesis. It should be noted, however, that the exposed layered intrusives containing significant proportions of

modal clinopyroxene (e.g. Mt. Davies, Kalka and Ewarara), are unlikely to be the direct complementary cumulates of the basalts in the Blackstone region because of the lateral separation (e.g. >80 km, Fig. 3.1). Therefore if the crystal fractionation hypothesis is correct, cumulate bodies comparable with those described by Goode and Moore (1975) must lie beneath the entire Blackstone region. This requirement is in disagreement with the predictions of Nesbitt, et al.,(1970) that the depth of emplacement of the basic cumulates became progressively shallower in the west. Thus, it appears unlikely that the basic extrusive and deep-level basic intrusive rocks in the province have a liquid-cumulate relationship, although it is probable that the ultimate sources of the magmas were the same and that they were generated during the same general event.

The other alternative, involving control by residual clinopyroxene in the mantle, is consistent with the published distribution coefficients for Sc and V in clinopyroxene in equilibrium with primitive basic melts (Kd clinopyroxene/liquid for Sc and V > Kd orthopyroxene, olivine/liquid for Sc and V; Frey, et al., 1978). If the degree of melting was relatively high (> 20% by analogy with basalts from the Gawler Range province), then this necessarily implies derivation from a hydrous LREE-enriched mantle source at depths < 50-60 km in order to maintain sufficient clinopyroxene in the residue (Green, 1972, 1973) and to explain the fractionated REE patterns in the basalts (Fig. 3.6). If, on the other hand, the degree of melting was relatively low (< 5%), the basic magma may have been generated in deeper zones of the mantle which were not enriched in LIL elements. This alternative is unlikely, however, because experimental work shows that the melts produced under these conditions will be of undersaturated alkaline affinities (Green, 1972) in contrast to the obviously tholeiitic parentage of the basic rocks from the Central Australian province.

In conclusion, it is suggested that the similarity of the elemental ratios to those in the Gawler Range basalts (Table 3.1), indicates an analogous origin for the primary basic magma, viz. shallow melting of a hydrous LREE-enriched mantle source. This proposal cannot be conclusively established with the available geochemical data, but it is supported by the comparable tectonic setting, viz. post-orogenic magmatism and eruption of the volcanics onto a stable continental crust. Subsequent low-pressure fractionation of olivine, pyroxene and plagioclase has probably produced the range in compositions observed.

TABLE 3.4. Estimates of crustal composition from various sources.

	1	2	3	4	5	6	7	8	9	10
SiO_2	63.3	60.6	60.5	62.2	60.01	66.0	58.0	54.0	52.71	51.39
Al_2O_3	16.4	15.4	16.2	17.3	15.95	16.0	18.0	19.0	19.05	16.67
Fe_2O_3	7.08	7.2	6.2	0.3	8.10				1.83	12.47
FeO				5.9		(t)4.5	(t)7.5	(t)9.0	7.03	
MnO	0.10	0.2		0.1	0.12				0.18	0.19
MgO	2.7	3.9	3.9	2.4	3.05	2.3	3.5	4.1	6.38	5.03
CaO	4.6	5.7	6.0	5.2	4.82	3.5	7.5	9.5	7.71	8.40
Na_2O	3.6	2.8	3.5	3.3	3.64	3.8	3.5	3.4	3.80	3.14
K_2O	1.4	2.6	2.1	2.3	2.73	3.3	1.5	0.6	0.55	1.23
TiO_2	0.6	0.9	0.9	1.1	1.13	0.6	0.8	0.9	0.77	1.32
P_2O_5	0.1	0.2							0.03	
Zr		310			296	240	100	30		114
Nb						25	11	4		
Y						27	22	20		
Ce			55			80	38	17		
Sc						10	30			
V						60	175			
Cr			50		74	35	55			116
Ni						15	20			
Rb		70	70-100		56	110	50	20	15	22
Sr		340	300-500		630	350	400	425	578	451
Ba		1090	600-1000		1503	700	350	175		793
No. Samples	2	23			25					17

1. Average composition of five massive granulites from the Musgrave Block (Gray, 1977).
2. Average composition of Musgrave Block granulites (Lambert and Heier, 1968).
3. Average siliceous granulite compiled by Condie (1978)
4. Synthetic starting composition used by Green (1969) in his experiments.
5. Average composition of intermediate granulites (55-65% SiO_2) from the Precambrian Brazilian basement (Sighinolfe, 1971).
6, 7 and 8. Average compositions of upper, bulk and lower continental crust, estimated by Taylor and McLennan (1979).
9. Mafic granulite from the Musgrave Block (Collerson, 1972).
10. Average composition of basic granulites (<55% SiO_2) from the Precambrian Brazilian basement (Sighinolfe, 1971).

3.6.4 Origin of the acid magma

A. Models other than direct partial melting of the crust

It has previously been shown that the acid magma is unlikely to have differentiated from a basic parent with the composition of the basalts exposed in the Central Australian province, but this does not exclude the possibility of differentiation from a modified basic parent. For example, Barker, et al., (1975), in explaining the origin of the Pikes Peak Batholith, suggested a model in which alkali-olivine basalt reacted with a granulite crust to produce a syenitic magma, which in turn reacted with higher levels of the crust to produce potash-rich granites. Kranck (1969) on the other hand, to explain the association of rapakivi granite - anorthosite and anorthosite - mangerite in the North Atlantic Shield, proposed mixing of an olivine basalt melt and anatectic granitic liquid to produce an intermediate liquid with high K_2O (e.g. basic mangerite or quartz-monzonorite). Subsequent plagioclase and clinopyroxene fractionation in the crust yielded the rapakivi granites. The advantage of such models is, that by magma mixing an intermediate magma is formed, hence later clinopyroxene + plagioclase fractionation (with a bulk SiO_2 less than the mix) is able to move the differentiates to higher silica contents (i.e. granitic composition).

There are two important objections to the application of a model of this type in the present case:

1) In view of the small amount of fractionation that is necessary to produce a dacite (with 66% SiO_2) from an intermediate magma (e.g. mangerite with 56-60% SiO_2), it is considered that the associated residual liquid concentration of incompatible elements would be insufficient to account for the extremely high levels of Zr, Nb, Y and Ce in the Central Australian dacites.
2) There is no evidence for intermediate composition mixtures (e.g. mangerites or monzonorites) in the Central Australian province. Since the Musgrave Block reveals a good cross section of the crust and numerous deep-level intrusive bodies are exposed (Nesbitt, et al., 1970), it might be expected that any intermediate rocks would also be exposed, by analogy with the North Atlantic Shield (Kranck, 1969; Bridgwater and Windley, 1973). Their total absence can be taken as evidence against a model involving an intermediate "mixed", magma stage.

TABLE 3.5. Results of least squares modelling calculations designed to investigate possible crustal sources for the primary acid magmas.

A. Least squares approximation of average dacite in terms of Lambert and Heier's (1968) average Musgrave Range granulite composition and likely residual minerals.

Rock	average granulite obs.	average granulite calc.9kb	average granulite calc.13.5 kb	average dacite product	Mineral compositions used: opx. 9kb	opx. 13.5kb	cpx. 9kb	cpx. 13.5kb	plag.	mag.
SiO_2	60.6	60.57	60.57	67.28	53.0	53.0	51.3	51.1	54.6	
Al_2O_3	15.4	15.33	15.31	13.02	4.7	6.1	5.2	9.6	29.0	
FeO^t	6.5	6.56	6.51	6.86	14.8	11.2	14.4	10.8		74
MnO				0.11						
MgO	3.9	3.96	3.96	0.69	23.2	27.0	14.9	17.2		
CaO	5.7	5.71	5.73	2.69	3.3	2.6	12.3	10.7	11.2	
Na_2O	2.8	3.50	3.50	3.90			0.7	0.8	5.1	
K_2O	2.6	2.43	2.56	4.40					0.21	
TiO_2	0.9	0.69	0.85	0.87	0.9	0.8	1.2	1.2		20
P_2O_5				0.18						
Total				100.0						

Mineral	9 kb Wt. fraction	9 kb Mineral proportion	13.5 kb Wt. fraction	13.5 kb Mineral proportion
opx.	0.095	0.218	0.03	0.073
cpx.	0.092	0.211	0.159	0.39
plag.	0.249	0.57	0.213	0.52
mag.	0.0004	0.0009	0.0062	0.015
dacite	0.554		0.582	
	= source		= source	
ΣR^2	= 0.58		= 0.50	

Notes: 1. Orthopyroxene and clinopyroxene compositions taken from Green's (1969) experimental data at pressures of 9 and 13.5 kb.

2. Plagioclase composition is An_{54} after Wright (1974), and is considered to be realistic on the basis of Green's (1969) experiments.

3. Magnetite was set at the composition indicated and no attempt was made to match the TiO_2 contents.

B. Least squares approximation of average dacite in terms of Condie's (1978) average siliceous granulite and likely residual minerals.

Rock	granulite obs.	granulite calc.9kb	granulite calc.13.5kb	dacite product
SiO_2	60.5	60.49	60.49	67.28
Al_2O_3	16.2	16.19	16.18	13.02
FeO^t	6.2	6.25	6.21	6.86
MnO				0.11
MgO	3.1	3.10	3.11	0.69
CaO	6.0	6.00	6.01	2.69
Na_2O	3.5	3.68	3.67	3.90
K_2O	2.1	2.43	2.50	4.40
TiO_2	0.9	0.72	0.85	0.87
P_2O_5				0.18
Total				100.0

Mineral	9 kb Wt. fraction	9 kb Mineral proportion	13.5 kb Wt. fraction	13.5 kb Mineral proportion
opx.	0.058	0.13	0.0052	0.012
cpx.	0.093	0.21	0.15	0.36
plag.	0.285	0.65	0.255	0.61
mag.	0.004	0.0091	0.008	0.019
dacite	0.552		0.574	
	= source		= source	
ΣR^2	= 0.17		= 0.19	

Note: 1. Mineral compositions used are those reported in Table 3.5A and the same comments apply.

C. Least squares approximation of average dacite in terms of Taylor and McLennan's (1979) calculated lower crustal composition and likely residual minerals.

Rock	lower crust obs.	lower crust calc.	average dacite product	Mineral compositions used: cpx.	opx.	plag.	mag.
SiO_2	54.0	53.99	67.28	45.22	49.20	54.6	
Al_2O_3	19.0	18.98	13.02	4.56	2.30	29.0	
FeO^t	9.0	9.0	6.86	9.45	26.0		79
MnO			0.11	0.22	0.51		
MgO	4.1	4.12	0.69	12.08	21.16		
CaO	9.5	9.51	2.69	21.52	0.49	11.2	
Na_2O	3.4	3.53	3.90		0.06	5.1	
K_2O	0.6		4.40			0.21	
TiO_2	0.9	0.90	0.87	0.36	0.19		15
P_2O_5			0.18				
Total			100.0				

Mineral	Wt. fraction	Mineral proportion
cpx.	0.136	0.164
opx.	0.111	0.134
plag.	0.538	0.651
mag.	0.044	0.053
dacite	0.194	
	= source	
ΣR^2	= 0.033	

Notes: 1. Clinopyroxene and orthopyroxene compositions after Collerson (1972), for these minerals in a basic granulite which has similar major element geochemistry to Taylor and McLennan's (1979) calculated lower crustal composition.

2. Plagioclase composition is An54 after Wright (1974).

3. The Ti content of magnetite was adjusted to give a satisfactory match for TiO_2.

B. Models involving direct partial melting of the crust

The possibility of an origin by direct partial melting of the crust, as favoured for the acid-intermediate series in the Lake Everard area (chapter 2), remains to be examined. In considering this alternative, it is important to ascertain the composition of the crustal source. If the crust becomes increasingly basic with depth as some workers contend (e.g. Lambert and Heier, 1968; Taylor and McLennan, 1979), then the question of the composition of the source is closely allied to the level of the crust being melted. Of the various estimates of the crustal composition given in Table 3.4 probably the analysis of the average Musgrave Range granulite (after Lambert and Heier, 1968) is the most realistic estimate of the composition of the upper-middle zones of the crust in this region, although Gray (1977) argues for a more acid (granodioritic) composition. Its suitability as a source can be tested by least squares modelling of the average dacite composition, provided compositions of the residual minerals are known. Fortunately Green (1969) has carried out experimental work on crystallisation relationships, using a starting composition very similar to the average Musgrave Range granulite, at likely crustal pressures (i.e. 9kb and 13.5kb; for starting composition, see Table 3.4). If the mineral compositions quoted by Green (1969) are used in the least squares calculation it is found that the degree of melting is between 55-58% (Table 3.5A). Choice of the particular mineral compositions used (i.e. 9kb or 13.5kb assemblage) has little effect on the degree of melting, although it does alter the residual mineral proportions slightly. The "fit" obtained is not particularly good ($\Sigma R^2 > .1$), but this mainly arises because of the mismatch in Na_2O. In this connection it is significant that the average Musgrave Range granulite used in the calculations is very similar in composition to the average siliceous granulite quoted by Condie (1978) excepting for Na_2O which is higher in Condie's average (3.5% Na_2O c.f. 2.8% Na_2O, Table 3.4). Modelling using Condie's average yields a much better fit, but the degree of melting remains almost unchanged (Table 3.5B).

Probably the most important point deducible from these calculations is the excessive degree of melting required (i.e. 55-58%). Apart from the physical problems involved in attaining this level of melting, the model cannot reproduce the observed levels of most trace elements in the average dacite without assuming excessive abundances in the source. For example, comparison of the calculated source abundances (columns A and B in Table 3.6) with the crustal averages given in Table 3.4 reveals that the required contents of Zr, Nb, Y, Ce and Ba are roughly a factor of two higher than

TABLE 3.6. Trace element modelling results, based on the major element calculations reported in Table 3.5.

	average dacite	A.	B.	C.	average evolved basalt
Zr	959	546	543	209	352
Nb	69	40	40	17	26
Y	134	84	83	40	63
Ce	213	128	128	59	93
Rb	170	98	98	40	37
Sr	135	138	147	156	310
Sr*	135	104	108	85	310
Ba	1330	820	827	424	400
Sc	10	11	10	10	33
V	39	30	33	68	312
Cr	2	9.3	8.5	13	100
Ni	12	23	19	27	77
Co	26	35	29	40	51

A. Calculated trace element abundances in Lambert and Heier's (1968) average Musgrave Block granulite, using values in average dacite and the results reported in Table 3.5A.

B. Calculated trace element abundances in Condie's (1978) average siliceous granulite, using values in average dacite and the results reported in Table 3.5B.

C. Calculated trace element abundances in Taylor and McLennan's (1979) hypothetical lower crustal source, using values in average dacite and the results reported in Table 3.5C.

Note: 1. Distribution coefficients used are those reported in Table 3.3B, excepting for Sr* which used Kd plagioclase/liquid = 0.8.

the typical values in crustal rocks of similar major element composition. Moreover, the necessary contents of the compatible elements Co, Ni and V are also probably excessively high considering the acidity of the crustal source tested. It is therefore unlikely that the dacitic magma was generated from a granulitic crustal source of the type presently exposed in the Musgrave Block. This conclusion is supported by the work of Gray (1971, 1977) which demonstrated that the granulites of the Musgrave Block have not suffered large-scale melting. His evidence included: rarity of migmatites and other evidence for in situ melting, preservation of sedimentary layering in the granulite sequences and the geochemical analogies with typical supracrustal rocks, thus implying that the granulites do not represent refractory residues left after extensive crustal fusion.

This conclusion does not necessarily exclude the possibility of generation from a more basic, lower crustal source and to test this alternative the lower crustal composition quoted by Taylor and McLennan (1979) was used as the source in a least squares modelling calculation (for composition, see Table 3.4). Since experimentally-determined residual mineral compositions were not available, the compositions used in the modelling calculations were taken from minerals in basic granulites from the Musgrave Block (Collerson, 1972); the particular basic granulite chosen had similar major element geochemistry to the estimated lower crust of Taylor and McLennan (1979; see analysis 9, Table 3.4). The calculations reveal that approximately 19% partial melting of this lower crustal source is needed to produce a magma with the composition of the average dacite (Table 3.5C). The relatively low proportions of clinopyroxene and orthopyroxene in the residue indicate that reasonable variations in their compositions (particularly FeO/MgO) are unlikely to greatly affect the result.

Using the mineral proportions and F derived from least squares modelling of the major elements, it was found that the calculated source contents of Zr, Nb, Y, Ce, Ba and Rb were of the same order as the contents in the differentiated basalts from the province, while the calculated V, Sc, Cr, Ni and Co contents were significantly less (column C in Table 3.6). This demonstrates that a basic granulitic source, with the minor element contents of the differentiated basalts from the Central Australian province, would be capable of accounting for the levels of LIL elements in the average dacite. However, the V, Sc, Cr, Ni and Co contents, which are relatively high in the basalts compared with the calculated source, may indicate that such a meta-basaltic source is not strictly applicable. Rather, a refractory sialic residue of basic-intermediate composition,

remaining after prior melt extraction events, may be a more appropriate source since it would be expected to have lower V, Sc, Cr, Ni and Co contents, yet at the same time have relatively high levels of LIL elements. This aspect will be considered in more detail in chapter 4.

An origin in partial melting of a basic lower crustal source, apart from requiring a more realistic degree of melting (<20%) and showing a general internal consistency with the trace elements, is also compatible with available isotopic evidence. For example, the isotopic data of Gray (1971) shows that the acid volcanics from the Tollu area have initial strontium isotopic ratios (Ri) of 0.708, which fall at the low end of the range for the Musgrave Block granulites (Ri = 0.708 -0.713). Gray notes that: "there is no simple explanation for this in terms of the anatectic hypothesis", since it would be expected that if these granulites provided the source, the resultant melt should inherit a similar range in Ri. Homogenisation between acid and basic granulite layers leading to a relative decrease in the acid granulite Ri is suggested as a possible explanation by Gray. However in the present model, where a basic granulite crustal source is proposed, the relatively low Ri of the acid volcanics is readily explainable - if indeed the basic granulites have significantly lower Ri's than the acid granulites as Gray suggests.

The model outlined above allows little possibility for the generation of primary, low-silica intermediate magmas. It has been pointed out that the constraints imposed by experimental evidence and crustal composition are inhibitive to the production of intermediate magmas from even a basic crustal source, while the fractionation trends shown by the basalts indicate that they are unlikely to yield voluminous intermediate differentiates. This illustrates perhaps the greatest attribute of this model in that it conveniently accounts for the paucity of intermediate rocks and hence the bimodal character of the Central Australian province.

3.7 SUMMARY

Petrographic and field evidence thought to favour a common origin for the contemporaneous acid and basic rocks comprising the Central Australian volcano-plutonic province is re-interpreted here, and it is concluded that the previous evidence for a comagmatic origin is not compelling. The geochemical evidence confirms this conclusion and demonstrates the existence of two genetically-unrelated rock series.

The geochemical data suggests that the high-level gabbros intruding the bimodal volcanic pile are related to the basic lavas: both show a

characteristic iron enrichment typical of tholeiites fractionating under low PH_2O and PO_2 in crustal magma chambers. All basic rocks analysed are fractionated to varying degrees, since none have Ni and Cr contents or Mg numbers consistent with equilibration with mantle peridotite. The elemental ratios (particularly > chondritic Zr/Ti, Zr/Y, Ce/Zr and P_2O_5/TiO_2) and the fractionated REE patterns of the basalts indicate derivation of the primary magmas from a LIL element-enriched mantle source. It is suggested, by analogy with the basalts from the Gawler Range province, that the less than chondritic values for Sc/Ti and V/Ti reflect the presence of residual clinopyroxene. This, in turn, implies that the primary magmas segregated from relatively shallow levels (possibly < 50-60 km).

The majority of the acid rocks show characteristics consistent with a differentiation series from dacite to rhyolite and consequently it is thought that variations in the Nb, Y and LREE contents of the rhyolites can be related to similar variations in the parental dacites. However, the possibility that some of the rhyolites may represent direct partial melts cannot be excluded. The major element geochemistry of the dacites (with lowest SiO_2 contents) is consistent with derivation by 19% partial melting of the lower crust, assuming it has the composition of a basic granulite. The relatively low proportion of residual magnetite (perhaps due to the relatively low PH_2O and/or PO_2 during melting) can account for the high $Fe_2O_3{}^t$ and TiO_2 contents of the dacites, while conversely, the high proportion of residual plagioclase is able to explain the characteristically low CaO, Al_2O_3 and Sr contents. It is possible that the relatively high temperatures during melting may have contributed to the instability of normally refractory minerals (e.g. zircon, apatite and sphene), leading to the release of Zr, Nb, Y and REE into the melt, - hence explaining the abnormally high contents of these elements in the acid volcanics. Some of the variability of these elements in the dacites may be attributable to differing degrees of melting or alternatively to variations in concentrations of refractory minerals in the source.

In view of the post-orogenic timing of the igneous activity, it is extremely unlikely that partial melting of a refractory granulitic crust could have occurred without the addition of heat either directly or indirectly from the mantle (c.f. Fyfe, 1978). Involvement of the mantle at this time is independently evidenced by the abundant, contemporaneous basic magmatism.

Finally, it is concluded that the model outlined above, offers the most plausible explanation for the characteristic, bimodal volcanic-plutonic

association in the Central Australian province. The implications of the findings of this study and that reported previously for the Gawler Range province, will be examined in the review chapter which follows.

CHAPTER 4

A REVIEW OF PROTEROZOIC POST-OROGENIC IGNEOUS ACTIVITY

4.1 INTRODUCTION

To date Proterozoic felsic volcanic and plutonic rocks have received scant reviews in the literature in comparison with their Archaean and Phanerozoic counterparts. Consequently general models for the evolution of Proterozoic felsic igneous terrains on a global scale have not been developed; indeed, it is not known with certainty whether such terrains do, in fact, conform to any generalised conceptual models of formation. In this chapter a review will be made of the literature for data concerning Proterozoic post-orogenic felsic volcano-plutonic provinces both in Australia and other continents, paying particular attention to the geochemistry of the rocks and the models invoked to explain their origin. It is anticipated that if any general modes of formation exist, they will emerge.

Before attempting such a review, it is first of all necessary to have a sound basis for comparison and testing. This is provided by the two Proterozoic volcano-plutonic provinces examined in detail in this thesis (see chapters 2 and 3). The initial approach in this chapter is therefore directed towards the development of a model capable of satisfactorily explaining the origins of the igneous rocks comprising the Gawler Range and Central Australian provinces. Having developed this model and considered its limitations and implications, a review will be made of other Proterozoic volcano-plutonic provinces in an effort to determine the generality of the model.

4.2 DEVELOPMENT OF THE MODEL

From the previous discussions in chapters 2 and 3 it will be evident that the Gawler Range and Central Australian volcano-plutonic provinces have many features in common. Some of the more important characteristics shared by the two provinces are summarized below:

1) They are post the main tectonothermal event affecting the basement on which they unconformably rest.
2) In both provinces there is a distinctive bimodal character imparted by the abundance of basic and acid rocks relative to intermediate rocks. The field evidence clearly demonstrates that the basic and acid rocks are related in space and in time, but the geochemical evidence indicates that they are not genetically related.
3) The primary basic magma in each case has fractionated along typical continental tholeiite trends leading to progressive enrichment in all

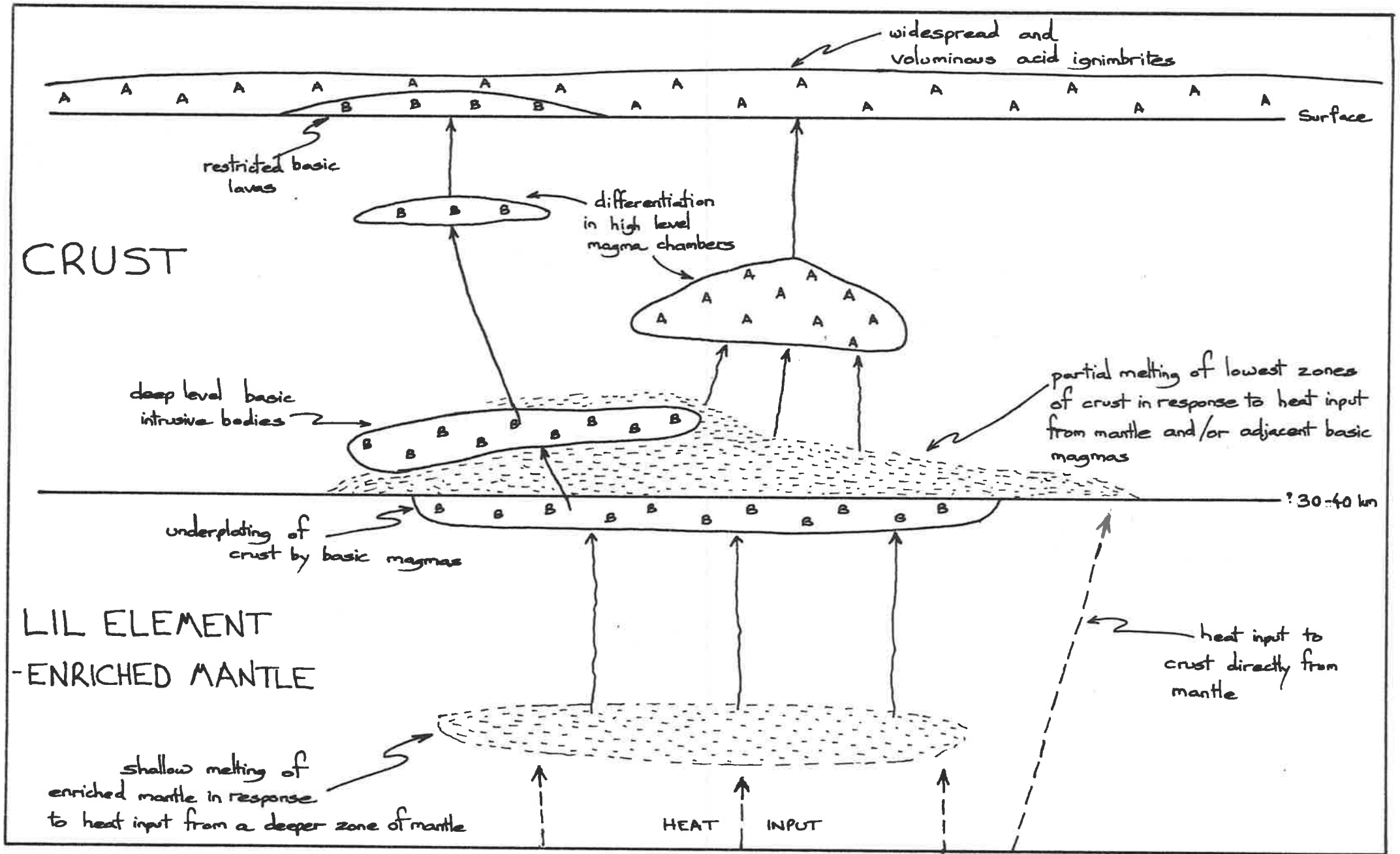

Figure 4.1 A general model for the evolution of post-orogenic Proterozoic volcano-plutonic terrains.

incompatible elements (e.g. Zr, Nb, Y, REE, P_2O_5 and TiO_2) and $Fe_2O_3{}^t/MgO$, but control on compatible elements (e.g. Cr and Ni). Similar fractionation trends in other basic magmatic series have been attributed to prolonged crystallisation in shallow crustal magma chambers under low PO_2 and PH_2O (Roeder and Osborn, 1966). The primary basic magma in the case of the Gawler Range province is considered to have been derived by shallow, hydrous melting of a LIL element-enriched mantle source. In the case of the Central Australian province a similar origin is inferred on the basis of the geochemistry and elemental ratios of the basalts which are comparable with those in the Gawler Range province.

4) The acid rocks (including intrusives and extrusives) from both provinces have distinctive geochemical characteristics when compared with Cainozoic calc-alkaline suites. In particular K_2O/Na_2O, $Fe_2O_3{}^t/MgO$, K_2O, $Fe_2O_3{}^t$, TiO_2, Zr, Nb, Y, Rb, Ba and REE are relatively high in the Proterozoic rocks by comparison, while CaO, Al_2O_3 and Sr are significantly lower. It has been previously argued that these characteristics indicate an origin by partial melting of a basic granulitic, lower crustal source. Thus the addition of heat, either directly or indirectly from the mantle would appear to be necessary in order to raise the geothermal gradient sufficiently to cause melting of the basic crust and generation of the primary, non-eutectic acid and/or high-silica intermediate magmas. The contemporaneous basic magmatism in both provinces could be taken as evidence for mantle involvement.

The above observations can be summarized in the form of a simple model which is diagramatically represented in Fig. 4.1. The model can be viewed in terms of its primary or essential features and its secondary or non-essential features. The essential features of the model are:

1) A shallow mantle source for the basic magma.
2) A source of heat for melting of the lower crust, which may be directly from the mantle diapir and/or from the voluminous basic magma variously underplating and intruding into the crust.
3) A basic, lower crustal source for the acid magma.

The secondary or variable aspects of the model include:

1) The degree of differentiation of the primary basic and acid magmas in upper crustal magma chambers prior to final eruption and/or intrusion.
2) The amount of contamination or mixing of acid magma with basic magma during ascent. In an environment where acid and basic magmas are being generated simultaneously, the possibility of mixing, either in the lower crustal zone of generation, or in the high-level magma chambers

cannot be excluded, particularly as both magma types are likely to be using similar channelways.

4.3 DISCUSSION OF THE MODEL

4.3.1 General comments

Having presented a model which can satisfactorily explain the origin of the igneous rocks in both the Gawler Range and Central Australian provinces, it is now desirable to examine the model in more detail, considering specifically its strengths and weaknesses, and its broader implications. This is attempted in the following discussion, in addition to investigating some of the aspects of the generation of non-eutectic acid magmas not pursued in detail in the previous two chapters.

The following general points can be cited in favour of the model:

1) It offers little opportunity for the generation of primary, low-silica intermediate magmas (<58% SiO_2), since experimental evidence shows that such magmas are unlikely to represent direct partial melts from the mantle, and compositional constraints would appear to preclude a crustal source. Moreover, two-stage processes involving subduction (c.f. Green and Ringwood, 1968) are not supported, either by the tectonic setting or the associated rock record. Therefore, the paucity of andesites in both provinces is readily explainable.
2) The objection on experimental grounds regarding the high temperatures necessary for the production of non-eutectic acid melts is negated by invoking heat input from the mantle.
3) Being geochemically based, the model is able to offer a satisfactory explanation for the geochemistry of both the basic and acid rocks. The relatively high LIL element contents in the Proterozoic acid rocks compared with rocks of equivalent composition in the Cainozoic calc-alkaline suites is believed to be a direct result of the sialic crustal source. The relatively high $Fe_2O_3^t$ and TiO_2 contents, high $Fe_2O_3^t/MgO$ ratio and low Al_2O_3, CaO and Sr contents are thought to be a direct result of the residual mineral assemblage; in particular, the low proportion of magnetite:pyroxenes and high proportion of plagioclase, respectively.
4) The model is consistent with experimental evidence. Green (1973, 1976), has shown that shallow (<60 km), wet melting of a pyrolite mantle will produce basic liquids with the major element characteristics of the primitive basalt from the Gawler Range province. Furthermore, the experimental work of Brown and Bowden (1973) supports the proposal that high-K_2O acid liquids can be produced from a dry, refractory

crustal source, while Green (1969) has demonstrated that the residual mineralogy is likely to be dominated by plagioclase and pyroxenes.

5) The available isotopic evidence is consistent with a basic granulitic, lower crustal source, since the relatively low initial strontium isotopic ratios in the acid rocks would appear to necessitate a source with low Rb/Sr over a long term.

Like all models, however, objections can be raised against it and perhaps the most important of these concerns the validity of the assumption that lower crust of basic composition does exist. Green and Lambert (1965) have shown that seismic velocity measurements are better explained by an intermediate composition lower crust rather than a denser, basic granulitic lower crust. Others (e.g. Tarney and Windley, 1977) have advocated an intermediate composition lower crust on the basis of averaging presently exposed high-grade metamorphic terrains, but as Heier (1973) points out, this describes "at best the top layer and the geological arguments for this to continue to the mantle are not given or are not convincing". In any case it is doubtful whether the concept of an intermediate composition crust could be rigorously applied since to deny the existence of any large areas of basic granulite in the lower crust would be to deny the possibility that Archaean greenstone sequences may lie beneath many of the Proterozoic terrains - an argument to which few would hold. That basic granulites do exist in the lower crust is clearly indicated by the xenoliths of such rocks commonly found in kimberlites, alkaline basalts and other rocks (e.g. Padovani and Carter, 1977; Rogers, 1977). Furthermore, crustal melting or reworking has been a recurring phenomenon throughout the earth's history and a natural consequence of such processes is the formation of refractory residues dominated by intermediate and basic mineral assemblages (Lambert and Heier, 1968; Tarney and Windley, 1977).

4.3.2 The nature of the basic crustal source

The above discussion has raised a point not conclusively resolved by previous discussions in chapters 2 and 3, concerning the precise nature of the basic crustal source. There appear to be three possibilities which require detailed consideration:

1) a tholeiitic basic igneous source (e.g. meta-Archaean tholeiite);
2) a source of calc-alkaline basaltic-andesite composition (e.g. Taylor and McLennan's (1979) calculated lower crust);
3) a refractory residue source, produced by prior removal of acid melts.

On regional geological grounds the first alternative might appear most reasonable if it is accepted that Archaean crust underlies much of southern Australia (Webb and Thomson, 1977). The crude geochemical modelling applied in chapter 2, however, suggested that such a source would be too high in Cr, Ni, V and Sc and at the same time too low in LIL elements for it to satisfactorily account for the trace element contents of the least evolved acid and high-silica intermediate volcanics. A calc-alkaline basic-intermediate source might alleviate this discrepancy to some extent, since it would be expected to be lower in Cr, Ni, V and Sc but higher in LIL elements than the tholeiitic basic source. However, tangible field evidence for such a source appears to be lacking in the Precambrian rock record in Australia, at least in the interval between the Middle Proterozoic and the oldest exposed Archaean rocks. Interestingly, Nance and Taylor (1977) noted that Archaean sediments from near Kalgoorlie had REE contents very comparable with calc-alkaline andesites, but in the absence of any evidence for a voluminous calc-alkaline source in the adjacent Archaean terrain, they suggested that a combined basic and acid provenance might be indicated. Such a mixed provenance is unlikely to provide a satisfactory magma source because the acid component would melt first imparting its geochemical fingerprint to the melt, leaving the basic component as a residue.

The remaining alternative of a sialic, refractory residue source would be expected to be lower in Cr, Ni, V and Sc than the other basic sources but it may be questioned whether this source, in view of the prior melt extraction events it has suffered, could yield the necessary levels of LIL elements. In the case of some LIL elements, such as Zr, Nb, Y and REE, this may not constitute a serious objection since these elements are contained in minerals normally thought to be refractory under relatively low temperature, wet melting conditions (e.g. zircon, apatite, sphene and monazite). In this connection, Sighinolfi (1971) has noted that Zr, Nb and Y rise with increasing basicity of granulites to the point that the levels of these elements in intermediate granulites exceed those in typical upper crustal igneous and sedimentary rocks. This is supported by the geochemistry of high-grade granulites in Norway (Green, et al., 1972), which are observed to have similar REE contents to typical upper crustal rocks (based on a composite of forty North American shales). Also, Tarney and Windley (1977) note that Precambrian granulites, which they consider to be representative of the lower crust, have comparable or slightly higher contents of Zr and REE than upper crustal gneisses.

It is possible that the high temperatures of melting, necessary for the generation of the non-eutectic acid magmas, may have led to the break-

down of the normally refractory minerals such as zircon, apatite and sphene, thus releasing Zr, Nb, Y and REE into the melt and hence explaining the relatively high contents of these elements in the Proterozoic acid volcanics. Some evidence for this is seen in the corroded zircon, apatite, sphene and monazite grains commonly found in granulites. An additional factor may have been the relatively dry melting conditions, since Shaw (1978) has demonstrated that the presence of a fluid phase can greatly affect the concentration of trace elements in a silicate melt. For example, at 30% partial melting, Ce is 20 X enriched in a silicate melt which has no associated fluid over a melt which has a large excess of fluid. This arises because the bulk distribution coefficient of Ce fluid/solid is greater than that of Ce silicate melt/solid. Whether this reasoning is applicable in the present case is debatable because the amount (if any) of fluid phase associated with an anatectic silicate melt in equilibrium with the souce is uncertain. If the amount of fluid is significant then it is evident that dry magmas, produced by melting of granulites, would be expected to have the highest primary REE contents (and by analogy Zr, Nb and Y), of any anatectic magmas. Partial melting under relatively low PH_2O and PO_2 conditions may have also contributed to the instability of the oxide minerals, particularly magnetite (e.g. Roeder and Osborn, 1966; Nesbitt and Hamilton, 1970; Eggler and Burnham, 1973). Breakdown of magnetite will release Fe and Ti into the melt and may therefore account for the relatively high contents of these elements in the acid rocks. Unfortunately, similar evidence concerning the stability of other refractory minerals (e.g. zircon and apatite) under these conditions is not available.

While the above reasoning may account for the levels of LIL elements normally held in refractory minerals (i.e. Zr, Nb, Y and REE), it does not satisfactorily explain the contents of LIL elements which occur in the low-melting point fraction (e.g. Rb, Ba, K, Th and U). In a refractory residue of the type proposed above, it would be expected that Rb, Ba and K would be severely depleted (c.f. Lambert and Heier, 1968), yet this is not consistent with the relative enrichment of these elements in the acid rocks. One solution would be to propose that prior melt extraction events did not remove all of the low-melting point fraction, but left some entrapped in the pore spaces between the residual minerals. Subsequent anatexis would have mobilized the low-melting component and mixed it with the high-temperature melt to yield a hybrid melt with relatively high K, Rb and Ba contents. An alternative possibility is that the mantle provided these elements in an aqueous fluid. Such a component, apart from providing K, Rb and Ba, would add water to the lower crust thus lowering the solidus and thereby promoting melting. In the absence of detailed isotopic data,

distinction between these two alternatives is very difficult since neither proposal can be tested quantitatively using the geochemical data. The available Sr isotopic data for the acid rocks from both provinces (all Ri < 0.708) could be interpreted as favouring either hypothesis, e.g. contribution from a relatively radiogenic mantle or alternatively, addition of a radiogenic low-temperature interstitial melt to a high temperature, relatively non-radiogenic melt. It is worth noting that the alternative of addition of an aqueous fluid from the mantle is not entirely consistent with the relatively "dry" residual mineral assemblage in the crust nor is it compatible with the presumed "dry" nature of the primary acid-intermediate magmas. Moreover, if the mantle did provide such a component, it is puzzling why the contemporaneous basalts are not extremely enriched in K, Rb and Ba and why they did not, in the presence of excess water, fractionate along calc-alkaline trends.

On the basis of the available evidence it is concluded that the alternative of a 'sialic, refractory residue of roughly basic composition is the most likely source for the non-eutectic, acid to high-silica intermediate magmas in the Central Australian and Gawler Range provinces. Thus in the generalised model outlined earlier, the nature of the basic lower crustal source can be more tightly constrained. The wider applicability of this concept within the framework of the generalised model can be tested by reviewing the literature for other Proterozoic acid igneous rocks. The search for comparable volcano-plutonic provinces is directed first of all to the Australian Proterozoic.

4.4 COMPARISON WITH PROTEROZOIC VOLCANO-PLUTONIC PROVINCES IN AUSTRALIA

4.4.1 General discussion

Australia, with its vast exposure of Proterozoic shield and associated record of volcanism and plutonism, provides an unparalleled opportunity to study and document the characteristics of Proterozoic volcano-plutonic provinces. The Tectonic Map of Australia and New Guinea (GSA, 1971) subdivides the major Proterozoic rock provinces in Australia into:

1) Orogenic provinces and metamorphic complexes, characterised by highly-deformed meta-sedimentary and/or meta-igneous rocks.
2) Transitional domains, which involve "late to post-orogenic developments associated with cratonisation; transitional in time, place and style between orogenic and cratonic tectonism".
3) Platform covers, which consist mainly of thin, but widespread sequences of shallow water continental shelf type sediments resting unconformably on rocks belonging to the previous two divisions.

Figure 4.2 Location of the post-orogenic Proterozoic volcanic terrains referred to in the text.

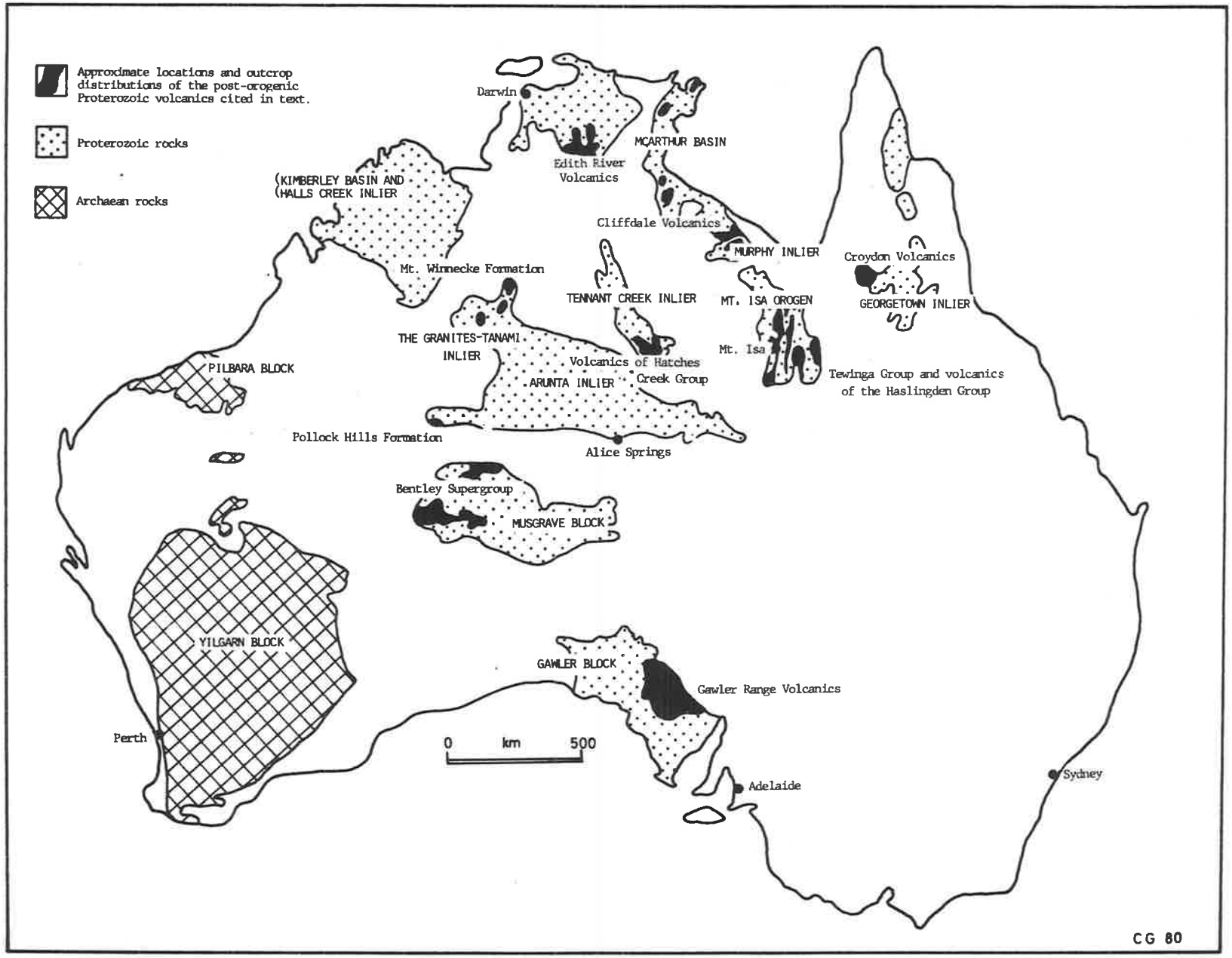

TABLE 4.1. General information concerning the post-orogenic Proterozoic volcano-plutonic provinces cited in text.

PROVINCE (identified by most important volcanic unit)	TECTONIC PROVINCE (after Tectonic Map of Aust., 1971)	ACID VOLCANIC UNITS	BASIC VOLCANIC UNITS	ACID INTRUSIVE UNITS	BASIC INTRUSIVE UNITS
BENTLEY SUPERGROUP	Musgrave Block	Various units within Bentley Supergroup (1060 ± 140 m.y.)	Various units within Bentley Supergroup	Unnamed granites, granophyres and porphyries	Various phases of the Giles Complex
CROYDON VOLCANICS	Georgetown Inlier	All units belong to Croydon Volcanics (1429 ± 75 m.y.)	Not present	Esmeralda Granite (~ 1411 m.y.)	Not present
GAWLER RANGE VOLCANICS	Gawler Block	Various units within Gawler Range Volcanics (~ 1500 m.y.)	Various units within Gawler Range Volcanics	Hiltaba Granite and associated granophyres and porphyries	Not present
POLLOCK HILLS FORMATION	Arunta Block	All units assigned to Pollock Hills Formation (1526 ± 25 m.y.)	Not present	Mt. Webb Granite	Not present
HATCHES CREEK GROUP	Davenport Geosyncline	Various units within the dominantly sedimentary Hatches Creek Group	Various units within the Hatches Creek Group	Unnamed granites, granophyres and quartz-feldspar porphyries	Unnamed dolerites and gabbros
TEWINGA GROUP	Northwest Queensland Province	All units assigned to Argylla Formation (1777 ± 3 m.y.) Tewinga Group	All units assigned to Magna Lynn Metabasalt	Ewen Granite Wonga Granite	Not present
KATHERINE RIVER GROUP	Pine Creek Geosyncline	All units assigned to Edith River Volcanics (1750 m.y.) Katherine River Group	Units occur within Edith River Volcanics and Kombolgie Formation	Various granites including the Cullen Granite and Grace Creek Complex	Unnamed dolerites
CLIFFDALE VOLCANICS	Murphy Tectonic Ridge and adjacent McArthur Basin	All units assigned to Cliffdale Volcanics (1770 ± 20 m.y.)	Seigal Volcanics	Norris Granite (1773 ± 24 m.y.)	Unnamed dolerites and gabbroic dykes
MOUNT WINNECKE FORMATION	Granites-Tanami Block	All units assigned to Mt. Winnecke Formation (1808 ± 15 m.y.)	Not present	Winnecke Granophyre (1802 ± 15 m.y.)	Not present

TABLE 4.2. Petrographic information concerning the post-orogenic Proterozoic volcano-plutonic provinces.

PROVINCE (identified by most important volcanic unit)	ACID VOLCANIC ROCKS	BASIC VOLCANIC ROCKS	ACID INTRUSIVE ROCKS	BASIC INTRUSIVE ROCKS
BENTLEY SUPERGROUP	Dominantly subaerial dacitic to rhyolitic welded tuffs. Occasional lithic tuffs.	Ophitic, subophitic, pilotaxitic and hyalopilitic textures in basalts. Amygdaloidal zones common.	Leucocratic, holocrystalline. coarse-grained granites ranging to granophyres and quartz porphyry dykes.	Include cumulate troctolite and ultramafic bodies and ophitic-textured gabbros and dolerites.
CROYDON VOLCANICS	Dominantly subaerial, rhyodacitic to rhyolitic welded tuffs.	Not present	Esmeralda Granite is a medium- to coarse-grained biotite adamellite to biotite granite.	Not present
GAWLER RANGE VOLCANICS	Dominantly subaerial, andesitic (rare) to rhyolitic welded tuffs. Lesser lavas, air-fall tuffs and non-welded lithic tuffs.	As for Bentley Supergroup	As for Bentley Supergroup	Not present
HATCHES CREEK GROUP	Porphyritic dacites and rhyolites forming extensive ignimbrite sheets.	Basalts characterised by interlocking plagioclase microlites and uralitized clinopyroxene. Some amygdaloidal zones.	Coarse-grained holocrystalline granite to adamellite. Also granophyre grading to quartz-feldspar porphyry.	Mainly ophitic-textured dolerite and gabbro.
TEWINGA GROUP	Range from porphyritic dacites to rhyolites. Probably include both lavas and ash-flow tuffs.	Consist of fine-grained aggregates of sodic plagioclase, amphibole and epidote. Amygdaloidal flow tops common.	Coarse-grained granites. Dykes and sills of porphyritic microgranite.	Not present
KATHERINE RIVER GROUP	Dominantly subaerial dacitic to rhyolitic welded tuffs. Some units may be of lava-flow origin.	Generally altered basalts, showing ophitic, porphyritic and pilotaxitic textures. Amygdaloidal zones common.	As for Bentley Supergroup	Mainly ophitic-textured dolerites
CLIFFDALE VOLCANICS	As for Gawler Range Volcanics	As for Katherine River Group	As for Bentley Supergroup. A 3 km diameter andesitic intrusive body is also present.	Medium-grained subophitic and intersertal dolerites and gabbros. Generally little altered.
POLLOCK HILLS AND MT. WINNECKE FORMATION	Subaqueous acid lavas associated with water-lain tuffaceous sediments.	Not present	Include adamellites, granites, granophyres and acid porphyries.	Not present

TABLE 4.3. Setting of the post-orogenic Proterozoic volcano-plutonic provinces.

PROVINCE (identified by most important volcanic unit)	AGE OF IGNEOUS ACTIVITY	NATURE OF BASEMENT	AGE OF BASEMENT OROGENIC EVENT	NATURE OF COVER	AGE OF COVER DEFORMATION	DEFORMATION OF VOLCANICS	METAMORPHISM OF VOLCANICS
BENTLEY SUPERGROUP	1000-1100 m.y.	Granulite-upper amphibolite facies metasediments - Musgrave-Mann Metamorphics	~ 1650 ± 170 m.y. (Webb, in Thomson, 1975) or ~1250 m.y. (Gray, 1971)	Adelaidean shelf sediments marginal to Officer Basin (south) and Amadeus Basin (north)	~ 600 m.y. in Petermann Ranges Orogeny	Broad folding in east, tilting only in the west	Negligible, excepting near intrusive bodies
CROYDON VOLCANICS	1400-1450 m.y.	Multiply-deformed and metamorphosed (to granulite facies) metasediments.	1500-1600 m.y.	Paleozoic sediments and volcanics of the Tasman Geosyncline	No major episode affecting volcanic rocks	Gently warped	Negligible
GAWLER RANGE VOLCANICS	~ 1500 m.y.	Granulite-upper amphibolite facies metasediments-Lincoln Complex	~ 1800-1600 m.y. (Kimban Orogeny)	Flat-lying to gently dipping Adelaidean shelf sediments marginal to Adelaide Geosyncline	No major episode affecting volcanic rocks	Mostly flat-lying to gently tilted	Negligible
POLLOCK HILLS FORMATION	~ 1500 m.y.	High-grade metasediments of the Arunta Complex	~ 1800 m.y.(?)	Adelaidean shelf sediments	Various periods	Broad upright folds.	Negligible
HATCHES CREEK GROUP	? 1700-1800 m.y.	Low grade thermally metamorphosed shales, silts, sandstones and tuffs of Warramunga Geosyncline	~ 1810 m.y.	The basic and acid volcanics are interlayered with arenaceous shelf sediments of the Davenport "Geosyncline"	Uncertain	Broad concentric folds forming basins and domes	Negligible
TEWINGA GROUP	1700 m.y.	Variably-deformed and meatmorphosed igneous rocks including Leichhardt Metamorphics and Kalkadoon Granite	~ 1860 m.y.	Arenaceous shelf sediments and extensive basic volcanics (e.g. Eastern Ck. Volcanics) ~ 1450 m.y.	Continued deformation and metamorphism up to ~ 1450 m.y.	Volcanic and plutonic rocks affected by mild fault-controlled deformation up to 1450 m.y.	Rarely exceeds greenschist facies
KATHERINE RIVER GROUP	1750 m.y.	Variably-deformed and metamorphosed igneous & sedimentary rocks, up to amphibolite grade	pre-1750 m.y.	Carpentarian shelf sediments, mainly arenaceous, but some carbonates, gradational with volcanics	No major episode affecting volcanic rocks	Some warping, probably fault-controlled	Negligible
CLIFFDALE VOLCANICS	1770 m.y.	Schists and migmatites comprising the Murphy-Metamorphics and foliated granitoid rocks of the Nicholson Granite Complex	pre-1850 m.y.	Carpentarian, arenaceous shelf sediments of the Tawallah Group, deposited in the McArthur Basin	No major episode affecting volcanic rocks	Minor warping	Negligible
MOUNT WINNECKE FORMATION	~ 1800 m.y.	Low-grade metasediments and metavolcanics of the Granites-Tanami Complex	~1960 m.y.	Carpentarian, arenaceous shelf sediments of the Birrindudu Group	Various periods	Broad folds	Negligible

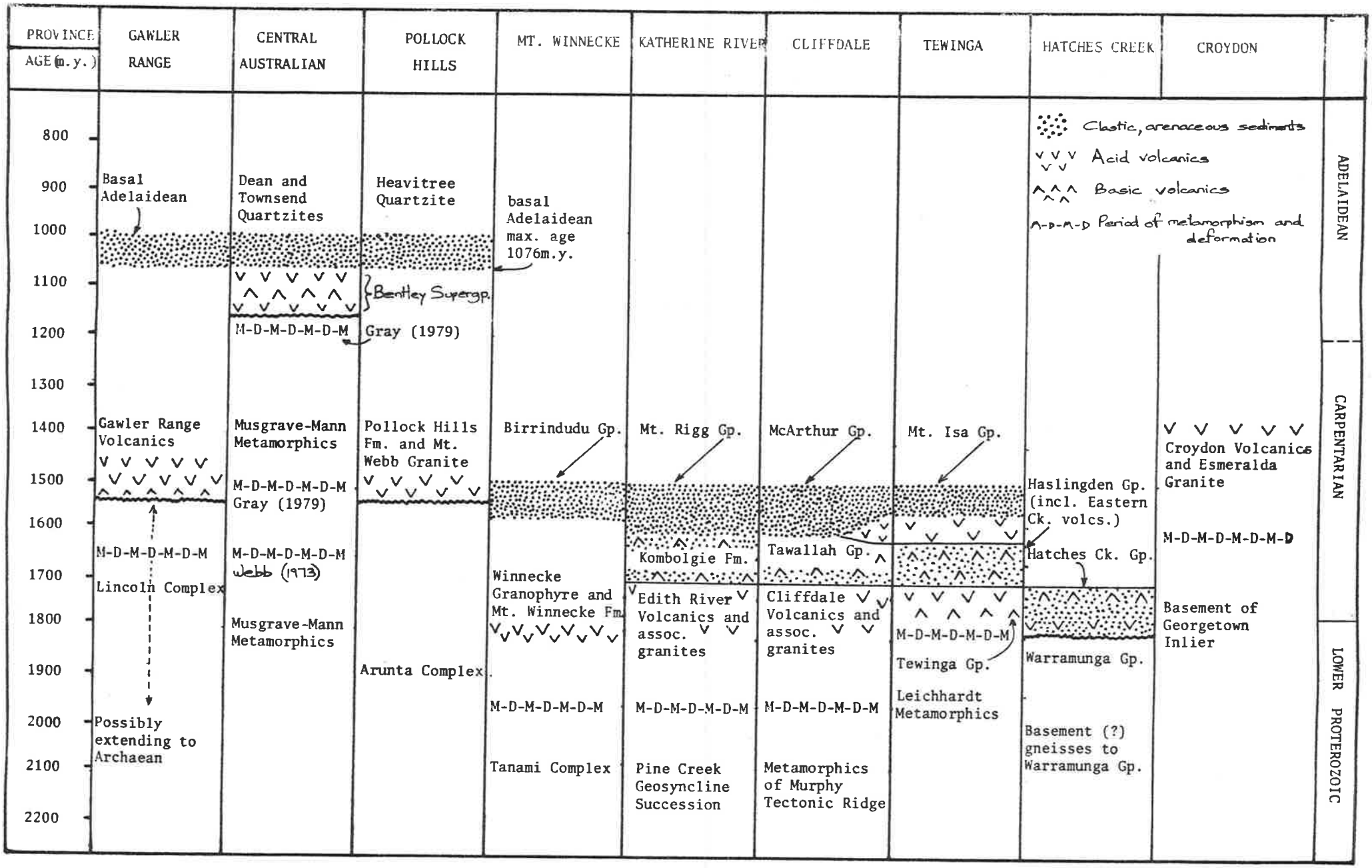

TABLE 4.4. Stratigraphic relations of the post-orogenic Proterozoic volcano-plutonic terrains.

It is notable that a number of volcano-plutonic provinces, including the Gawler Range province and Central Australian province, are placed within the intermediate transitional domains on the Tectonic Map. Such domains are characterised by: "downwarps, cauldron subsidences and rifts; molasse-like sediments; abundant volcanic and plutonic rocks; moderate deformation and rare metamorphism of fill". The important conclusion to be drawn is that post-orogenic plutonism and volcanism formed a significant and integral part of the evolution of the Proterozoic crust in Australia.

The Proterozoic volcanic units assigned to this period on the Tectonic Map (other than Gawler Range Volcanics and Central Australian volcanics) are:

1) Cliffdale Volcanics of the Westmoreland region, northern Australia.
2) Edith River Volcanics of the Katherine River - South Alligator River region of the Northern Territory.
3) Volcanics belonging to the Hatches Creek Group in the Tennant Creek region.

Information available since the publication of the Tectonic Map suggests that the following volcanics may also fit this category:

4) Croydon Volcanics of the Georgetown Inlier, northeast Queensland (Sheraton and Labonne, 1978).
5) Pollock Hills Formation of the Arunta Block, west of Alice Springs (Black, 1977).
6) Units comprising the Tewinga Group, northwestern Queensland (Derrick, et al., 1976; Wilson, 1978).

The locations of these volcanics, their stratigraphic relationships and further general information are given in Figure 4.2 and Tables 4.1, 4.2, 4.3 and 4.4, respectively. To permit a closer examination of the field relations and the geochemistry of the volcanics, they, and the provinces of which they form a significant part, will be considered individually below.

4.4.2 Details of individual provinces

A. Cliffdale Volcanics

The Cliffdale Volcanics, dated at 1770±20m.y., rest unconformably on the meta-sedimentary and meta-igneous succession of the Murphy Tectonic Ridge (Mitchell, 1976). These volcanics are of particular significance as they define the base of the Carpentarian in northern Australia (Plumb and Derrick, 1975). They are mostly composed of undeformed and regionally unmetamorphosed ignimbrite sheets, grading from rare andesites through

TABLE 4.5. Analyses of selected rocks from the Australian post-orogenic Proterozoic volcano-plutonic provinces.

	CLIFFDALE PROVINCE					KATHERINE R. PROVINCE		CROYDON PROVINCE		POLLOCK HILLS PROVINCE		MT. WINNECKE PROVINCE		ARGYLLA FORMATION	
	1	2	3	4	5	6	7	8	9	10	11	12	13	14	15
SiO_2	61.17	62.05	65.24	70.02	75.21	69.08	69.22	73.93	73.10	70.24	74.43	72.60	75.4	66.14	71.90
Al_2O_3	13.34	15.99	16.68	13.88	12.43	14.33	14.25	12.71	13.52	13.06	13.06	13.25	12.88	13.73	12.28
Fe_2O_3 t	6.24	7.04	4.68	4.56	2.14	5.10	5.69	3.72	3.21	5.38	2.66	3.90	2.12	6.85	5.04
MnO	0.08	0.10	0.06	0.06	0.04	0.07	0.11	0.07	0.05	0.08	0.04	0.08	0.04	0.03	0.02
MgO	5.75	2.09	1.19	0.39	0.32	1.17	0.65	0.27	0.29	0.74	0.36	0.49	0.22	1.01	0.54
CaO	5.19	5.19	3.00	1.86	0.66	0.82	1.98	1.03	1.41	2.60	1.76	1.15	0.87	2.15	1.25
Na_2O	2.11	2.67	3.13	3.54	2.64	2.70	3.00	2.08	2.66	2.63	2.71	2.49	2.71	3.64	3.07
K_2O	4.64	3.58	4.78	4.72	5.59	6.88	5.25	5.27	5.10	4.33	5.29	5.25	5.73	4.57	5.21
TiO_2	0.59	0.80	0.51	0.46	0.14	0.59	0.57	0.37	0.31	0.83	0.21	0.41	0.26	0.70	0.47
P_2O_5	0.32	0.20	0.12	0.09		0.16	0.15	0.15	0.14	0.19	0.06	0.15	0.10	0.18	0.12
Total	99.05	99.23	99.37	99.31	99.10	100.90	100.86	99.58	99.79	99.80	100.58	99.60	100.2	99.00	99.90
LOI	2.62	1.96	0.84	1.16	0.80	2.32	1.79	1.52	1.42	1.20	0.64	1.14	0.58	1.20	0.66
Zr	220	220	380	320	170	352	334	294	236					512	539
Nb	15	10	10	10	25	17	17							26	29
Y	20	30	25	30	65	47	50	85	59					74	77
Ce	100	110	100	140	100			131	103					110	116
Sc						11	12								
V						33	30							32	25
Cr						12	15	~4	~4					62	71
Ni	120	5	0			8.5	9	~3	~3					5	2
Rb	220	130	185	210	310	216	208	277	291					133	
Sr	340	310	340	220	50	66	140	65	78					67	
Ba	1400	1050	1150	1400	1700	1132	1148	951	585					845	
No. samples.	1	1	1	1	1	1	1	21	30	5	5	6	7	6	30

dacites to rhyolites; lesser proportions of flow-banded rhyolites and acid tuffs have also been recorded (Mitchell, 1976).

The available geochemical data for the Cliffdale Volcanics (after Mitchell, 1976) includes several analyses of andesites, two of which are given in Table 4.5. Like the high-silica andesites from the Gawler Range province, the Cliffdale andesites have relatively high LIL element contents (i.e. K, Rb, Ba, Ce, Zr, Nb and Y) in comparison with Cainozoic calc-alkaline andesites. This in turn suggests a significant sialic crustal contribution and hence an origin possibly similar to that proposed for the primary acid-intermediate magma in the case of the Gawler Range province, viz. partial melting of a basic granulitic, lower crustal source. The variation diagrams (Figs. 4.3 and 4.4) reveal that the Cliffdale andesites are lower in $Fe_2O_3^t$, TiO_2, P_2O_5, Zr and Y and higher in Al_2O_3 and CaO than the Gawler Range andesites, based on the rather limited data available. If a crustal origin is valid, then these features may reflect upon the composition of the source (e.g. higher in Al_2O_3 and CaO, but lower in $Fe_2O_3^t$ and TiO_2 than the magma source for Gawler Range Volcanics), or alternatively, upon the conditions of melting and hence the residual mineralogy (e.g. less residual plagioclase in the case of the Cliffdale Volcanics).

It is notable that the dacites and rhyolites form a continuum with the andesites on all variation diagrams; they also appear to "inherit" the geochemical characteristics of the andesites e.g. lower $Fe_2O_3^t$, TiO_2, MgO, P_2O_5, Zr, Nb and Y and higher Al_2O_3 and CaO compared with the Gawler Range Volcanics (see Figs. 4.3 and 4.4). Both observations suggest that the majority of the dacites and rhyolites are related to the andesites either by differentiation or by partial melting of a similar source.

Although basic volcanics do not occur within the Cliffdale Volcanic unit, the province as a whole is bimodal if the overlying, basic Seigal Volcanics are included. The voluminous Seigal Volcanics are separated from the Cliffdale Volcanics by a major clastic unit known as the Westmoreland Conglomerate, which on a geological time scale was probably very rapidly deposited. It is also noted that the Cliffdale Volcanics are intruded by the comagmatic Norris Granite (dated at 1773 ± 24 m.y.).

It is evident that the volcano-plutonic province encompassing the Cliffdale Volcanics is closely analogous to the Gawler Range volcano-plutonic province in a number of important respects and hence it is inferred that the igneous rocks in both provinces are likely to have had comparable origins.

Figure 4.3 Major elements vs. SiO_2 for acid rocks from Australian post-orogenic Proterozoic volcano-plutonic terrains. The fine stipple represents the field of Cainozoic calc-alkaline volcanics. Solid, dashed and dotted lines enclose fields of Gawler Range Volcanics, Cliffdale Volcanics and Central Australian volcanics, respectively. ▲ Tewinga Group (Argylla Formation) Δ Edith River Volcanics ● Pollock Hills Formation O Mt. Webb Granite ■ Croydon Volcanics □ Esmeralda Granite ◆ Mt. Winnecke Formation ◇ Mt. Winnecke Granophyre.

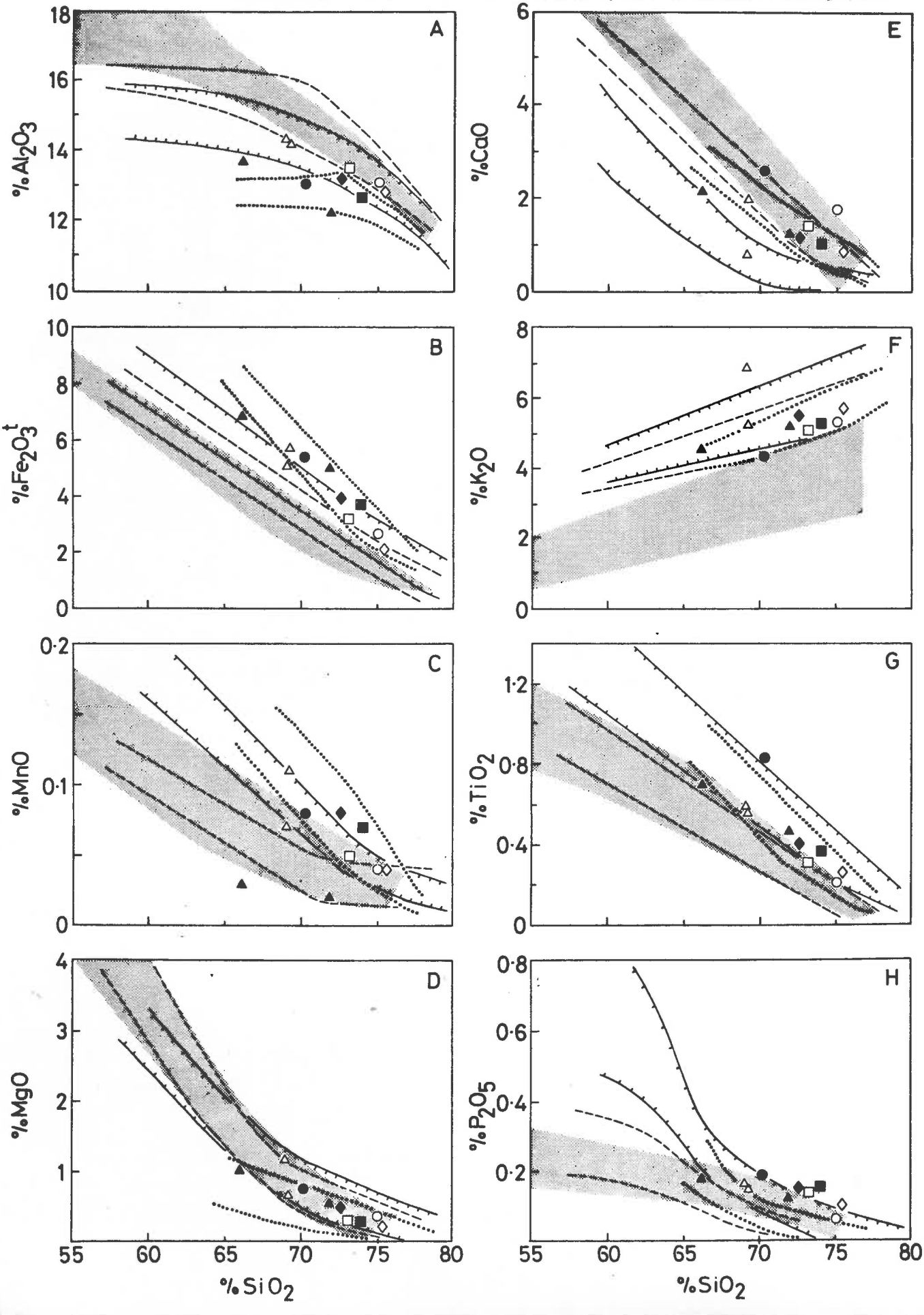

B. Edith River Volcanics

The Edith River Volcanics form the basal unit of the Katherine River Group which rests unconformably on the meta-sedimentary succession of the Pine Creek Geosyncline (Walpole, et al., 1968). The similar age (approx. 1750 m.y.) and stratigraphic position of the Edith River Volcanics and Cliffdale Volcanics suggests they may be lateral equivalents (Plumb and Derrick, 1975; also see Table 4.4). Like the Cliffdale Volcanics, the Edith River Volcanics have not been regionally metamorphosed and deformation is restricted to gentle warping.

The volcanic succession is dominated by laterally-extensive, subaerial ignimbrite sheets, mostly of dacitic to rhyodacitic composition with lesser volumes of intercalated basic lavas and terrestrial, clastic sediments (Stewart, 1965). The Edith River Volcanics are overlain by the Kombolgie Formation comprising a thick sequence of coarse-grained (often conglomeratic), arenaceous clastic sediments with occasional intercalated units of basic lavas and acid ignimbrites. The Malone Creek Granite (approx. 1750 m.y., Plumb and Derrick, 1975) may be comagmetic, but published field evidence suggests it is significantly older (e.g. Stewart, 1965; Walpole, et al., 1968).

In hand specimen, the porphyritic acid volcanics greatly resemble samples of the Gawler Range Volcanics and Central Australian volcanics but unfortunately no reliable published geochemical data is available to check if the analogy extends to the geochemistry. Preliminary investigations on some samples collected by the writer does suggest that there is a marked geochemical analogy (Table 4.5). In particular, the data for two samples plotted on Figures 4.3 and 4.4 suggests that the Edith River Volcanics have absolute contents of most elements comparable with the Gawler Range Volcanics, viz. relatively high $Fe_2O_3^t$, TiO_2, K_2O, Zr, Nb, Y, Rb and Ba, and low CaO, Al_2O_3 and Sr compared with Cainozoic acid volcanics.

The Edith River Volcanics and associated units and granites form a post-orogenic, bimodal association comparable with the Gawler Range and Central Australian provinces. On these grounds, and on the basis of the analogy in the limited geochemical data available, it is suspected that the primary magmas formed in a similar way.

C. Volcanics of the Hatches Creek Group

Little information is available concerning this province and to date no geochemical data on the igneous rocks have been published. The chief source of information is Smith, et al., (1961) who have recognised the following igneous rock types in the province:

Figure 4.4 Selected trace elements vs. SiO_2 and Na_2O vs. K_2O for acid rocks from the Australian post-orogenic Proterozoic volcano-plutonic terrains. Similar comments apply as for Figure 4.3. Sources of data cited in text. The Ce, Zr and Y contents in the Central Australian volcanics lie above the dotted line, while Nb plots above the diagram.

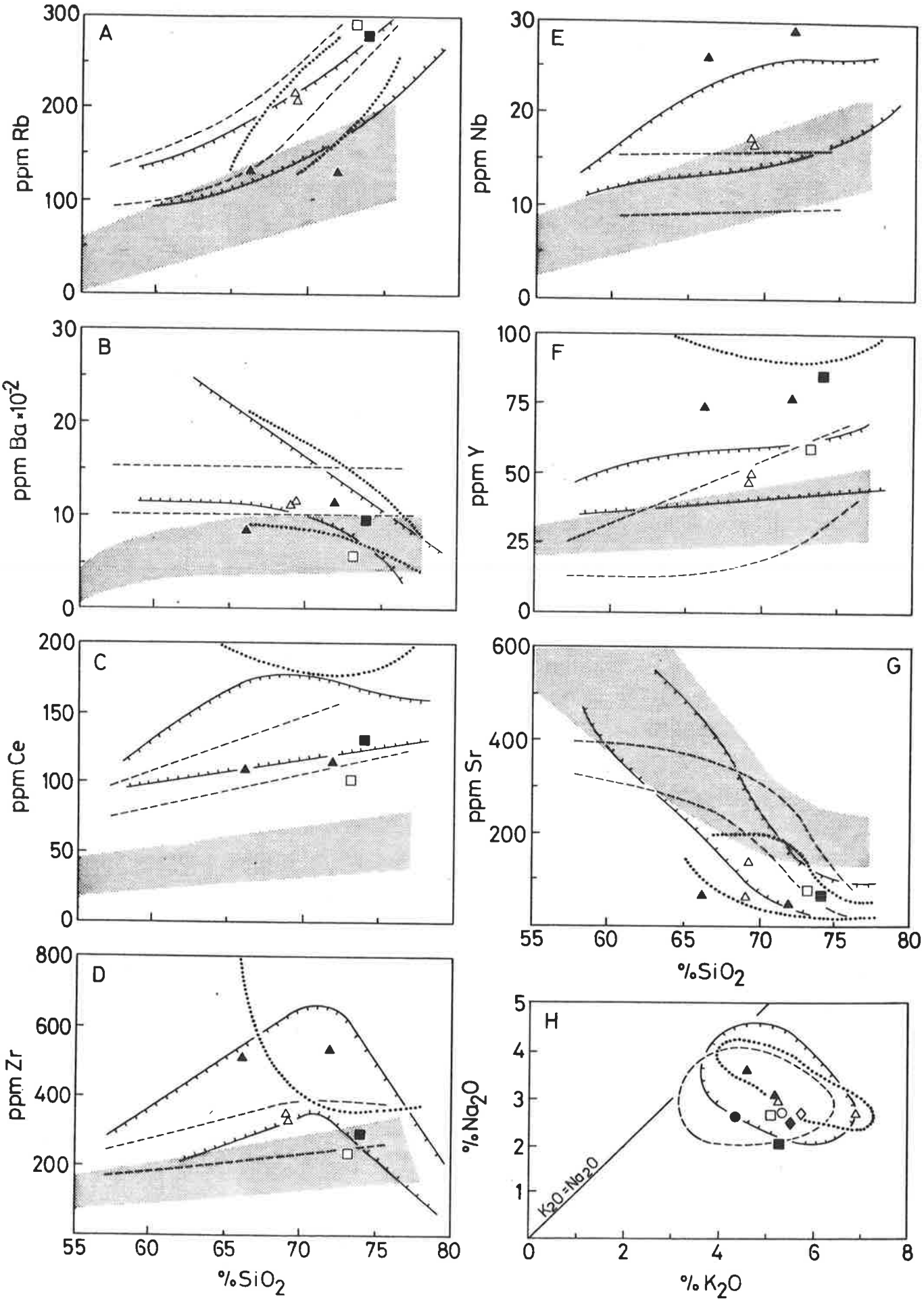

1) Porphyritic dacites and rhyolites; although no interpretation is given as to the origin of the acid extrusives (i.e., pyroclastic vs lava), their lateral extent as recorded by Smith, et al. (1961) may indicate an ash-flow origin.
2) Probable basic lavas, consisting of interlocking plagioclase and uralitized clinopyroxene and containing frequent amygdaloidal zones.
3) Ophitic-textured dolerites and gabbros.
4) Acid intrusives, ranging from coarse-grained granite and adamellite to quartz-feldspar porphyry.

The acid and basic volcanics are intercalated with arenaceous shelf sediments (mainly quartz sandstones) of the Davenport "Geosyncline" and are collectively known as the Hatches Creek Group. The mildly-deformed Hatches Creek Group rests unconformably on the low-grade, but strongly-folded metasediments of the Warrumunga Geosyncline. The precise age of the magmatism is uncertain, but it may be within the 1700-1800 m.y. time range (Black, 1978) suggesting a broad time equivalence with the Edith River and Cliffdale Volcanics. It is evident that this province is extremely analogous to the other provinces examined with respect to the distribution of rock types and tectonic setting. However, the absence of geochemical data permits no conclusions to be drawn, regarding the mode of origin of the primary magmas.

D. Croydon Volcanics

The flat-lying Croydon Volcanics rest unconformably on the highly-deformed and metamorphosed basement of the Georgetown Inlier in northeast Queensland. They have been dated at approximately 1400 m.y. and are intruded by the comagmatic Esmeralda Granite of similar age (Sheraton and Labonne, 1978). The Croydon Volcanics consist of rhyolitic to rhyodacitic welded tuffs that are mostly confined to a cauldron subsidence structure; they contain phenocrysts of quartz, K-feldspar and plagioclase set within a devitrified, glassy matrix. The Esmeralda Granite, the majority of which is a grey biotite adamellite to biotite granite, forms a batholith covering an area in excess of 650 km^2.

The geochemistry of the Croydon Volcanics (and Esmeralda Granite) is very comparable with that of the other Proterozoic acid volcanics examined, in particular: relatively high $Fe_2O_3{}^t/MgO$, K_2O/Na_2O, $Fe_2O_3{}^t$, TiO_2, MgO, K_2O, Zr, Y, Ce, Rb, Ba and Th and low CaO, Al_2O_3 and Sr contents compared with Cainozoic acid volcanics (see Table 4.5 and Figs. 4.3 and 4.4). The work of Sheraton and Labonne (1978) is of particular interest in this regard since they have noted that the Croydon Volcanics are characterised by higher

$Fe_2O_3^t/MgO$, $Fe_2O_3^t$, K_2O, Rb, Ce, Zr and Y and lower Sr contents than adjacent Paleozoic acid volcanics from the same tectonic province (i.e., Georgetown Inlier). From this they concluded that "the most probable source materials for the Esmeralda-Croydon magma are sialic crustal rocks, fairly rich in K and with high Fe/Mg ratios", an origin not unlike that proposed in the general model (Fig. 4.1).

E. Volcanics of the Pollock Hills Formation

A detailed description of the Pollock Hills Formation, which crops out in a very localised area some 600 km west of Alice Springs, is given by Page, et al., (1976) and it is from this source that the following information has been summarized. The Pollock Hills Formation consists of acid lavas overlain by tuffaceous and non-tuffaceous sandstone, with minor intercalated lapilli-tuff and agglomerate. The base of the formation is not exposed, but it is inferred to rest unconformably on the Lower Proterozoic metamorphic rocks of the Arunta Block. Intruding the sequence is the high-level, medium to coarse-grained Mt. Webb granite; it has an age of approximately 1500 m.y. which is statistically indistinguishable from that of the lavas. The major element geochemistry of both the lavas comprising the Pollock Hills Formation and the Mt. Webb Granite share many characteristics in common with the other Proterozoic acid igneous rocks plotted on Figure 4.3, in particular, relatively high $Fe_2O_3^t/MgO$ and K_2O/Na_2O. The analogy is not complete however, since like the Croydon Volcanics, the acid volcanics of the Pollock Hills Formation are not obviously associated with any basic rocks and therefore apparently do not form part of a bimodal volcano-plutonic suite.

Similar comments apply to the older (~ 1800 m.y.) acid volcanics comprising the Mt. Winnecke Formation and associated Winnecke Granophyre in the Granites-Tanami region (Page, et al., 1976), data for which is also plotted on Figure 4.3.

F. Volcanics comprising the Tewinga Group

Two of the three units comprising the Tewinga Group are of particular interest to this discussion, viz. the Magna Lynn Metabasalt consisting of fine-grained meta-basalt flows, and the Argylla Formation composed largely of rhyolitic to dacitic acid volcanics of probable ash flow origin (Derrick, et al., 1976). The deformation history in this area is far more complex than in any of the five areas described previously and on the Tectonic Map of Australia and New Guinea (GSA, 1971), the Tewinga Group has been included within the Mt. Isa orogenic domain. However, Wilson

TABLE 4.6. Geochemical data for the Magna Lynn Metabasalt and other basalts.

	1	2	3
SiO_2	50.80	50.04	52.10
$Al_2O_{3_t}$	14.75	13.95	17.30
Fe_2O_3	12.32	14.95	10.32
MnO	0.27	0.21	0.16
MgO	5.49	6.11	5.37
CaO	11.46	8.19	7.11
Na_2O	2.31	3.00	3.74
K_2O	0.36	1.08	2.18
TiO_2	1.86	2.13	1.20
P_2O_5	0.35	0.35	0.22
Total	100.00	100.00	99.70
LOI	1.42	2.77	2.53
Zr	188	239	159
Nb	14		9.0
Y	40	49	28
Ce	47		52
Sc		38	24
V	296	277	186
Cr	215	90	96
Ni	75	79	105
Rb	9	25	71
Sr	246	185	482
Ba	78	253	657

Ratio	Probable chondritic value	1	2	3	4
Zr/Ce	7.4-7.7	4		3.1	5.3
Zr/Y	2.5-2.8	4.7	4.9	5.7	4.1
Ti/Zr	100-110	59	53	45	61
Ti/Y	250-280	279	261	257	248
Zr/Nb	16-18	13		18	20
Ti/V	8.4-10	38	46	39	41
Ti/Sc	78-85		336	300	302
TiO_2/P_2O_5	STP=10	5.3	6.1	5.7	7.7

1. Magna Lynn Metabasalt, average of 3 samples (after Wilson, 1978).
2. Eastern Creek volcanics, Mt. Isa region; average of 20 samples (after Glikson, *et al.*, 1977).
3. Nuckulla Basalt, Lake Everard area; average of 2 samples
4. Basalt (B76) from Warburton area, Blackstone region.

(1978) notes that "the volcanic rocks in this formation (i.e., Argylla Formation) show little evidence of metamorphism" and further, "deformation is restricted to shear zones". Plumb (1979) considers that the two units represent transitional tectonic volcanism and this conclusion is supported by the isotopic data of Page (1978) which suggests that the underlying Leichhardt Metamorphics represent a significantly older basement.

Wilson (1978) observed that the rocks of the province have "a bimodal distribution that lacks true andesite (56-62% SiO_2)" and he quotes average analyses of basalts, dacites and rhyolites from the province in his paper. Plotting his data for the acid volcanics on the variation diagrams (Figs. 4.3 and 4.4), demonstrates marked geochemical analogies with the Central Australian volcanics, thus suggesting a comparable origin. Also, the elemental ratios of the average Magna Lynn Metabasalt are comparable with those in the basalts from the Gawler Range and Central Australian provinces (see Table 4.6). This is unlikely to be fortuitous because the overlying Eastern Creek Volcanics in the Mt. Isa region also have similar elemental ratios (Table 4.6, data after Glikson, et al., 1977). Hence, an origin in shallow melting of a LIL element-enriched zone of the mantle may be indicated, analogous to that proposed for the primary basic magmas of the Gawler Range province.

From the brief descriptions of the six Proterozoic volcano-plutonic provinces given above, it is evident that they have many characteristics in common with the Gawler Range and Central Australian volcano-plutonic provinces, in addition to their generally recognised post-orogenic setting. The similarity in the geochemistry of the rocks from the various provinces in particular, suggests that the primary magmas in all cases may have had comparable origins explainable in terms of the general model outlined earlier (Fig. 4.1). This indicates that the Gawler Range and Central Australian volcano-plutonic provinces are not alone in the Proterozoic rock record; rather they are two examples of what appears to be a general pattern of Proterozoic volcanism and plutonism in Australia. With these conclusions in mind attention will now be focussed on examples from other continents, in an effort to determine whether they too share similar characteristics.

4.5 COMPARISON WITH PROTEROZOIC VOLCANO-PLUTONIC PROVINCES IN OTHER CONTINENTS

4.5.1 General Comparison

A useful introduction to the literature is provided by Bridgwater and Windley (1973) who review the work of numerous authors on rocks of roughly

Middle Proterozoic age in the North Atlantic Shield. They draw the following conclusions in their paper:

1) A similar geological history can be recognised in a belt of rocks 1000 - 2000 m.y. old, extending from the Urals to western North America.
2) There is an early period (1800 - 2000 m.y.) of low pressure, high temperature metamorphism and deformation;
3) this is followed by post-orogenic igneous activity and emphasis is given to the bimodal nature of the magmatism. Notably, this does not often express itself as basalt-rhyolite volcanism (c.f. Australia), but more commonly by an association of gabbros, norites and anorthosites of ultimate mantle origin and crustal-derived granites (often rapakivi type). This association is termed the anorthosite-rapakivi granite suite by Bridgwater and Windley and is a characteristic association through this region. It may reflect generally deeper levels of erosion of the Proterozoic terrains in the North Atlantic Shield compared with the Australian Shield.

Other workers have documented this association from particular areas; for example Emslie (1978) describes anorthosite-adamellite complexes (1400 - 1500 m.y.) in the Labrador region of Canada and notes that igneous activity of similar age and type extends in a belt across central U.S.A., Most of the information on this "mid-continental belt" as it is known, has come from drilling since much of it is covered by younger sediments. The major, post-orogenic Proterozoic volcano-plutonic provinces recognised in the mid-continental belt developed during: the St. Francois igneous activity (at approx. 1500 m.y., Bickford and Mose, 1975); Spavinaw igneous activity (at approx. 1200 m.y., Muehlberger, et al., 1967) and Panhandle igneous activity (at approx. 1150 m.y., Muehlberger, et al., 1967). All are characterised by extensive ignimbritic acid volcanics and associated granites, with a total area in excess of 100,000 km^2 (Muehlberger, et al., 1967). In many cases basic rocks are also present; for example, basic volcanics are associated with the igneous activity in eastern New Mexico and in the Panhandle volcanic terrain in Texas, while basic intrusives occur in the St. Francois terrain. (Muehlberger, et al., 1967; Bickford and Mose, 1975). The bimodal nature of the magmatism in the mid-continental belt has been emphasised by Emslie (1978), who also noted that the igneous activity followed a major period of orogenesis in the Lower Proterozoic and was in turn succeeded by Upper Proterozoic sedimentation. There is a close correspondence between this sequence of events and the three-fold division previously noted for the Australian Proterozoic. Moreover, Bridgwater and Windley (1973) indicate that a similar tectonic setting

characterised post-orogenic magmatism throughout the North Atlantic Shield. As in Australia many of the Proterozoic volcano-plutonic provinces are little deformed, reflecting the extreme stability of the Shield areas following cratonisation in the Lower Proterozoic (e.g. flat-lying rhyolitic ignimbrite sheets in the St. Francois Mountains, Missouri - Bickford and Mose, 1975; also in the Panhandle volcanic terrain, Muehlberger, et al., 1967).

In the Baltic Shield the rapakivi granite - anorthosite association and related, rhyolite-basalt association are both represented, although the volcanics are far less extensive than in North America (Hjelmqvist, 1956). Vorma (1975) has interpreted a general sequence of events as follows:

rise of rapakivi granite magma plus associated ignimbrite eruptions
formation of deep fractures, extrusion of basic magma
erosion of up to 10 km of basement
cratonisation
} Subjotnian (1700 m.y.)

Svecokarelidic orogenic rocks (1900 m.y.)

The bimodal Subjotnian volcanic are widespread, and include the Dala Volcanics of western Sweden (Lundqvist, 1968), volcanics on the Island of Hogland (Wahl, 1947) and volcanics occurring as roof pendants in the Wiborg rapakivi massif, southeastern Finland (Vorma, 1975).

Well documented examples of post-orogenic Proterozoic volcano-plutonic provinces outside of the North Atlantic Shield, are rare in the literature. The Bushveld Complex of South Africa is a notable exception: it consists of mafic-ultramafic intrusives, acid intrusives and copious acid extrusives. The complex developed after a major Lower Proterozoic orogenic episode and has suffered little post-crystallisation deformation (Lenthall and Hunter, 1977).

The Guayana Shield of northern South America provides a further example: Gaudette, et al., (1978) describe the 1550 m.y. Parguaza rapakivi granite which they consider "represents one of the larger apparently anorogenic intrusive rocks of the world". Rocks of similar age and type also occur under the Amazon Basic in Brazil (Kovach, et al., 1976). This has led Gaudette, et al., (1978) to conclude that the igneous activity associated with the generation of the Parguaza rapakivi granite represents "a major episode in the (tectonic) development of this part of northern South America". Significantly this igneous activity occurred post- the major 1800 - 2100 m.y. trans-Amazonian orogenic cycle.

The examples cited in this brief review indicate that Proterozoic volcano-plutonic provinces comparable in tectonic setting and type to those found in Australia, are widespread in other parts of the world. This poses the rather speculative question of whether the post-orogenic Proterozoic volcano-plutonic provinces were generated in response to a common, global process in the same manner for example, that Cainozoic circumpacific calc-alkaline suites are generally thought to be related to plate-consuming processes. To examine this question further, the available geochemical data for these rocks and the interpretations placed on this data by other workers will be considered below.

4.5.2 Geochemical comparison

Unfortunately few detailed geochemical studies of Proterozoic volcano-plutonic provinces in other continents have been published, but what is available is of particular interest. Condie (1978), for example, has presented data on 1400 - 1800 m.y. granitic plutons from New Mexico, which form part of the vast mid-continental, Proterozoic volcano-plutonic province of North America referred to earlier. Analyses of granites from this region are very similar to analyses of Proterozoic acid volcanics from Australia (Table 4.7). Condie noted that these rocks possess relatively high $Fe_2O_3^t/MgO$ values and low contents of CaO and Sr; the data given in Table 4.7 shows that they are also relatively enriched in K_2O, Rb, Ba, Ce, Zr, $Fe_2O_3^t$ and TiO_2. Trace element modelling by Condie revealed that the acid magma could be derived by 20-30% partial melting of a siliceous granulite, or alternatively, by fractionation from a dacitic parent derived in turn by 50% partial melting of siliceous granulite. Condie favoured a model in which mantle plumes ..."in addition to giving rise directly to basaltic magmas, cause widespread regional heating and partial melting of the lower crust (silicic granulite), producing large volumes of granitic magma" (p. 147).

In another example from North America, Anderson and Cullers (1978) have shown that the Proterozoic, Wolf River Batholith of northern Wisconsin is marked by relatively high total REE, Rb, K_2O, $K_2O + Na_2O$ and $Fe_2O_3^t$ and by relatively low CaO, MgO, Al_2O_3 and Eu. They considered that the acid magma (with 75% SiO_2) was derived by partial melting of tonalitic-granodioritic crust at a depth of 25-36 km. These authors further demonstrated that low Ca, Al and Mg and high Fe/Mg and total alkalis (particularly K_2O) characterise the entire anorogenic, acid igneous suite of the mid-continental belt. The data presented by other workers from various parts of the mid-continental belt supports this

TABLE 4.7. Compositions of selected, late-to post-orogenic Middle Proterozoic acid igneous rocks from other continents.

1,2,3. Selection of 1.4 - 1.8 b.y. granitoid plutons, New Mexico (after Condie, 1978).

4. Lower silica phase of the Wolf River Batholith (after Anderson and Cullers, 1978).

5. Proterozoic rhyolite, south-central Wisconsin (after Smith, 1978).

6,7,8. Representative 1.5 b.y. acid volcanics from the St. Francois Mountains, Missouri after Kisvarsanyi (1971).

9. Analysis of a rapakivi granite from the Laitila granite suite, Finland (after Vorma, 1976).

10,11. Subjotnian (~1.7 b.y.) acid volcanic roof pendants in rapakivi granite, Finland (analyses given in Table 2, Vorma, 1975).

12. Average of 15 samples from the Parguaza rapakivi granite, Venezuela (after Gaudette, *et al.*, 1978).

13. Average composition of felsite (acid volcanic) from the Salic Phase of the Bushveld Complex, Potgietersrus tin-field (after Lenthall and Hunter, 1977).

14. Average composition of stratiform granite from the same locality and source as 13.

15. Average composition of Bobbejaankop granite (tin bearing) from the same locality and source at 13.

TABLE 4.7. Compositions of selected, late-to post-orogenic Middle Proterozoic acid igneous rocks from other continents.

	1	2	3	4	5	6	7	8	9	10	11	12	13	14	15
SiO_2	67.4	70.2	73.9	67.29	73.73	63.15	68.38	72.23	71.48	68.50	70.33	69.2	71.93	75.47	75.28
Al_2O_3	14.8	15.3	12.3	14.19	12.09	14.81	13.94	13.21	13.42	13.37	12.64	14.7	12.00	12.10	12.49
Fe_2O_3 t	5.0	3.21	3.49	4.36	3.32	7.13	5.69	2.95	4.24	5.73	6.56	4.2	6.97	3.27	2.40
MnO				0.08	0.11	0.33	0.10	0.06	0.05	0.08	0.05	0.08	0.13	0.05	0.03
MgO	0.91	0.48	0.10	0.57	0.04	1.20	0.63	0.22	0.20	0.52	0.43	0.4	0.27	0.22	0.17
CaO	2.34	1.41	1.12	1.93	0.36	1.99	1.70	0.88	1.40	0.93	1.32	2.0	1.01	0.75	1.19
Na_2O	3.46	3.06	2.89	3.16	3.50	4.15	2.73	3.19	2.47	2.18	2.18	3.3	2.65	2.97	2.88
K_2O	4.68	5.27	5.30	5.82	6.03	5.33	5.12	5.55	5.62	6.90	5.56	5.1	4.32	4.91	4.85
TiO_2	0.79	0.55	0.40	0.70	0.29	0.71	0.77	0.34	0.47	0.56	0.83	0.6	0.38	0.20	0.07
P_2O_5					0.0	0.20	0.21	0.06	0.06	0.11	0.17	0.2	-	0.02	0.02
LOI					0.37	0.88	0.68	0.82	1.25	0.60	0.45				
Total				98.1	99.84	99.88	99.95	99.51	100.66	99.48	100.52	99.48	99.66	99.96	99.38
Zr	424	453	573		550				266	~650			395	433	328
Nb													18	24	83
Y				~90	85								56	97	146
Ce	222	300	234	257	(La) 120				227				100	139	150
Sc					3								9.6	3	3
V					5										
Cr	14		1		27										
Ni					10										
Rb	231	190	276	188	152				393				176	225	408
Sr	200	386	34	170	11				71				70	40	7
Ba	1040	1790	300	1256	390				644				1100	890	260

contention, e.g. south-central Wisconsin (Smith, 1978) and St. Francois Mountains, Missouri (Kisvarsanyi, 1972; see Table 4.7).

Emslie (1978) in his general review of post-orogenic Proterozoic magmatism in North America adds further evidence in support of these conclusions; in particular he noted that the acid magmas "as the relatively low-temperature melt fraction in a dry, reducing environment, (i.e. granulitic lower crust) are strongly enriched in iron relative to magnesium, in alkalis and especially K, and relatively poor in calcium" and further, "Zr is typically high and this may indicate that zircon, normally a refractory mineral, becomes unstable in the presence of an alkali-rich melt...". Both observations are of relevance to the present discussion, but the explanations offered are untested to the writer's knowledge.

Vorma (1976) has also recorded relatively high Zr contents in Proterozoic rapakivi granites comprising the Laitila massif, Finland. He considered the explanation lay in anatexis under dry, intermediate to high pressure granulite facies metamorphic conditions, at temperatures 100 - 200°C higher than that for wet melting. In another study, Vorma (1975) described roof pendants of bimodal Subjotnian volcanics (1650-1700 m.y.) in the Wiborg rapakivi massif, Finland. The basic volcanics appear to be fractionated continental tholeiites from their relatively high $Fe_2O_3^t/MgO$ value and high TiO_2 and P_2O_5 contents. Vorma noted that the acid volcanics had analogous geochemical characteristics to the rapakivi granites, which he stated were: relatively high levels of $Fe_2O_3^t$, TiO_2, K_2O, Rb, Ba and Zr, lowish Al_2O_3, CaO and Sr contents and relatively high $Fe_2O_3^t/MgO$ (Table 4.7). Gaudette, et al., (1978) have drawn attention to the analogies in the geochemistry of the Finnish rapakivi granites and the Parguaza rapakivi granite of Venezuela, noting that the latter also has affinities with the high-Ca granites of Turekian and Wedepohl (1961) and some iron-rich granophyres. The acid magma for the Parguaza batholith was interpreted by Gaudette and co-workers to be the product of partial melting of a charnockitic or trondhjemitic crustal source.

Similar geochemical characteristics typify the acid intrusive and extrusive phases of the Bushveld Complex, and as the data of Lenthall and Hunter (1977) shows, the Y, Nb and LREE contents are also relatively high, approaching the values found in acid volcanics from the Central Australian province (Table 4.7). In the past it has been postulated that the acid phase of the Bushveld Complex differentiated from the basic phase (e.g. Hamilton, 1960), but more recent data favours a crustal origin (e.g. isotopic data of Davies, et al., 1970), as summarized by Lenthall and Hunter (1977): "basaltic magma (now forming the Mafic Phase of the Bushveld

Complex) was injected into a sialic crust largely composed of tonalitic gneisses, interlayered with plagioclase - amphibolites and various potassic granites ... and ... the basaltic magma reacted with, and partially melted this (granulitic) sialic crust".

These examples demonstrate that post-orogenic acid igneous rocks of Proterozoic age from widely scattered localities, have analogous geochemistry to the Australian examples. A model involving the mantle and/or basic magmatism as a source of heat for high-temperature, dry melting of a granulitic lower crust is favoured by a consensus of workers. This model will be recognised as the "primary" or "essential" part of the generalised model developed earlier, to explain the origin of the two Proterozoic volcano-plutonic provinces studied in this thesis (Fig. 4.1). Thus it may be concluded that post-orogenic igneous activity formed an integral and important part of the development of the Proterozoic crust in all continents and moreover, the generation of the magmas can, with the available evidence, be satisfactorily explained in terms of the one general model probably akin to that schematically illustrated in Figure 4.1. These conclusions have several important implications, some of which will be investigated below.

4.6 DISCUSSION

4.6.1 Relationship of post-orogenic and orogenic events in the Proterozoic

One of the significant points to emerge from the above review is the general agreement among workers concerning the importance of heat input from the mantle in the generation of the post-orogenic Proterozoic volcano-plutonic suites. This view is aptly summarized by Bridgwater and Windley (1973): "the most satisfactory explanation for the general thermal activity and specific magmatic events in the area (North Atlantic Shield) is that it marks the location of a major rise of mantle material (for example, the top of a convection cell) which remained active during the period 1000 - 2000 m.y. ago".

The general concept of high mantle heat flow and associated crustal reworking has been invoked to explain another characteristic of the Proterozoic: the ensialic mobile belts. Kroner (1977) for example, concluded that the Proterozoic mobile belts in Africa were not the result of lateral continental accretion, but rather represented zones of disruption within a large continental plate, probably induced by mantle diapirism. Muehlberger, et al. (1967) also emphasised crustal reworking as opposed to lateral accretion for the Proterozoic mid-continent terrain of North America, while Wynne-Edwards and Hasan (1970) extended these same basic

conclusions to include the entire North Atlantic Shield. The Musgrave-Fraser belt of high-grade metamorphic rocks is an example of an ensialic mobile belt in Australia which can be attributed "to high heat flow in narrow zones of lithosphere reactivation, rather than to continental collision" (Rutland, 1973, p. 1013). Rutland also noted that the bimodal volcanic association of this belt (the Central Australian volcanics of chapter 3) was more akin to an intracontinental suite rather than a continental margin suite (c.f. Cainozoic), a conclusion in accord with the writer's, based on the geochemical study of the province reported in this thesis (see chapter 3). These observations suggest that the processes leading to the formation of the Middle Proterozoic post-orogenic magmas cannot be viewed in isolation from the Lower Proterozoic orogenic events. This raises the important question: does the generalised model of magma generation outlined previously (Fig. 4.1) apply exclusively to the post-orogenic era, or has it more general applicability to non post-orogenic (i.e., orogenic) situations in the Lower Proterozoic? If the model is applicable to the Lower Proterozoic terrains, the question arises as to why there is an apparent concentration or peak in igneous activity in the largely stable late-to post-orogenic period.

4.6.2 Timing of magma generation

If Lower Proterozoic orogenesis is related to high mantle heat flow then the possibility exists that the basic and acid magmas were generated during the Lower Proterozoic and stored until the post-orogenic era, when they were variously intruded and extruded. Such a mechanism has been proposed by Vorma (1976) for the acid magmas which gave rise to the Laitila rapakivi granite massif in Finland. Why the magmas were released in the post-orogenic period is a matter for conjecture. It may have been that they were effectively entrapped at the base of the crust during the compressional orogenic event and it was not until the upper crust cooled sufficiently after orogenesis that tensional brittle fracturing facilitated tapping. Certainly such a mechanism would explain why Lower Proterozoic orogenesis was commonly followed by widespread igneous activity.

This hypothesis must, however, be considered in the light of two additional factors:

1) the significant time lag sometimes existing between the peak of orogenesis and the post-orogenic igneous activity, and
2) the depth of erosion of the Lower Proterozoic basement prior to post-orogenic volcanism in many cases. An example is provided by the Central Australian volcanics, which are observed to rest unconformably on a granulitic basement (chapter 3).

TABLE 4.8. Summary of possible models of Middle Proterozoic post-orogenic bimodal magmatism.

MODEL	FOR	AGAINST	IMPORTANT ASSUMPTIONS
1. Generation of acid magmas during the Lower Proterozoic tectono-thermal event and "storing" until eruption in the Middle Proterozoic.	1) Magma generation occurs during period of highest heat flow in upper crust. 2) Accounts for the post-orogenic timing of volcanism and plutonism.	1) In some provinces a significant period of time and interval of erosion occurred between orogenesis and post-orogenic volcanism. 2) Would expect much more volcanism and plutonism during Lower Proterozoic, continuous with that in Middle Proterozoic.	1) Maximum heat input into the crust from the mantle occurred during the Lower Proterozoic. 2) Negligible magma generation occurred in the Middle Proterozoic owing to the reduced heat flow.
2. Continued, but waning mantle heat input from Lower to Middle Proterozoic, with generation of bulk of acid magmas in the Middle Proterozoic due to pressure relief and lowering of solidus.	1) Accounts for the post-orogenic timing of volcanism and plutonism. 2) Explains why volcanic and plutonic activity peaked in the post-orogenic (pressure relief) era.	1) The major assumptions involved. 2) Assumes temperature-pressure conditions in Lower Proterozoic were such that minimal anatexis occurred.	1) Pressure relief occurs in the post-orogenic Middle Proterozoic era. 2) The drop in pressure lowers solidus sufficiently to promote extensive crustal fusion.
3. Generation of acid magmas in response to an interval of high mantle heat input that was confined to the Middle Proterozoic	1) Feasible mechanism if considered in isolation from other events.	1) Doesn't account for the post-orogenic timing of igneous activity. 2) What explains the high heat flow evident during the Lower Proterozoic tectonothermal events? 3) Why should such heat input events peak in the Middle Proterozoic?	1) A period of high mantle heat input occurred in the Middle Proterozoic quite independent of similar(?) events in the Lower Proterozoic. 2) The heat input was sufficient to promote extensive crustal fusion.
4. Melting due to the lowered solidus caused by rapid uplift in response to isostatic adjustments following Lower Proterozoic orogenesis.	1) Can account for the post-orogenic timing of igneous activity.	1) Doubtful if pressure relief alone, without heat input, could produce the extensive crustal fusion required. 2) Does not explain the presence of basic magmas. 3) Rapid uplift does not always precede post-orogenic igneous activity.	1) Rapid uplift always precedes post-orogenic igneous activity. 2) Uplift and associated lowering of the solidus would alone be sufficient to cause melting.
5. Generation of the acid magmas during burial metamorphism.	1) A feasible mechanism postulated on numerous occasions, particularly for Phanerozoic granitoid plutons.	1) Does not explain the presence of basic magmas. 2) The heat of melting is unlikely to be sufficient to generate the high temperature, non-eutectic post-orogenic acid magmas. 3) Would expect igneous activity to be syn- rather than post-orogenic.	1) Deep burial occurred. 2) Temperatures attained would be sufficient to promote melting.

These observations suggest that generation of the magma during the orogenic period and storing, may not be a satisfactory mechanism in all cases.

If heat input from the mantle continued unabated in the post-orogenic era the question arises as to why the orogenic event ceased. On the other hand, if the heat input declined in the post-orogenic period, the further question is raised as to why the acid magmas should develop under the lower temperatures of the post-orogenic era compared with the higher temperatures of the orogenic era. One possible explanation may be provided by the relaxation of deformation pressures during the post-orogenic period, since a lowering of the confining pressure will decrease the temperature of melting of the crustal rocks and so promote anatexis. This possibility has been suggested by Gray (1971) who considered that generation of the acid magmas for the Central Australian volcanics may have been promoted by pressure relief associated with rapid uplift following orogenesis. Owing to the relatively high temperatures necessary for the fusion of refractory granulitic crust (e.g. in the case of the Central Australian volcanics - see chapter 3), it seems unlikely that melting could occur as the result of pressure relief alone, as suggested by Gray, without some form of additional heat input. It is possible that sudden release of pressure, whether by uplift or transition from compressional to tensional strain, may have been the trigger which promoted extensive fusion of the lower crust in the presence of heat supplied by the mantle. The possibility also exists that relatively high temperatures were maintained in the lower crust, long after orogenesis had ceased in the upper crust, by repeated additions of underplating basic magmas (c.f. Fyfe, 1978).

Alternative hypotheses can be advanced but for various reasons they are considered unsatisfactory. For example it could be suggested that mantle diapirism occurred in the Middle Proterozoic, quite independent of events in the orogenic Lower Proterozoic period. However, since mantle diapirism is essentially a "chance" happening, this hypothesis does not explain why the magmatism invariably followed orogenesis. Alternatively, it could be proposed that the acid magmatism was unrelated to mantle diapirism, but rather was the result of crustal thickening and burial metamorphism connected with the orogenic event. Such an origin would not account for the contemporaneous basic magmatism, nor is it likely that the regional metamorphic gradient associated with burial, would have been sufficient to cause melting of the refractory lower crust.

The various possibilities discussed above are summarized in Table 4.8. All are speculative to some extent, however it is evident that choice of the most likely alternative must be governed by :

1) The conclusion that the igneous activity in the Middle Proterozoic cannot be divorced from the orogenic events in the Lower Proterozoic.
2) The necessity of mantle heat input to provide the temperatures required for anatexis of the granulitic lower crust.
3) The common bimodal association indicating involvement of the mantle and crust.
4) The evidence against extended periods of magma storing in some cases.

Of the alternatives listed, the second model involving pressure release and continued, but reduced heat input from the mantle is considered most probable, although the possibility that a combination of processes operated over a considerable time span cannot be excluded. In view of the sub-continental setting it seems likely that the high heat flow was caused by upwelling of mantle material, probably in the form of a diapir.

4.6.3 Siting of Proterozoic post-orogenic igneous provinces in relation to ancient continental margins

If the concept of intra-continental mantle diapirism as a driving force for the post-orogenic magmatism is applicable, then it follows that continental margins would not necessarily have been more or less favoured as sites of magma generation, since there appears to be little evidence that pre-existing crustal features exert any influence on the location and development of mantle diapirs. Thus it follows that the post-orogenic Proterozoic volcanic rocks do not necessarily indicate the sites of ancient continental margins. This situation contrasts markedly with the case of modern calc-alkaline suites which are typically developed at active continental margins and are thus diagnostic of this environment.

These conclusions are supported by the observation that the post-orogenic provinces have a rather irregular age distribution when viewed on the scale of a continent. This point led Muehlberger and his co-workers (1967) to propose that the Proterozoic post-orogenic igneous activity in North America resulted from many episodes of crustal reworking rather than from a continuous accretionary process. Similar conclusions can be drawn for the Australian case if the available isotopic data for the provinces is examined in relation to their spatial distribution. For example, apart from the lack of any well-defined trends in age, the approximate contemporaneity of igneous activity in the vast area encompassed by the Edith River Volcanics, Cliffdale Volcanics, Argylla Formation and volcanics of the Hatches Creek Group, argues against continuous continental accretion in the Proterozoic (see Table 4.4 and Figure 4.2).

Figure 4.2 Location of the post-orogenic Proterozoic volcanic terrains referred to in the text.

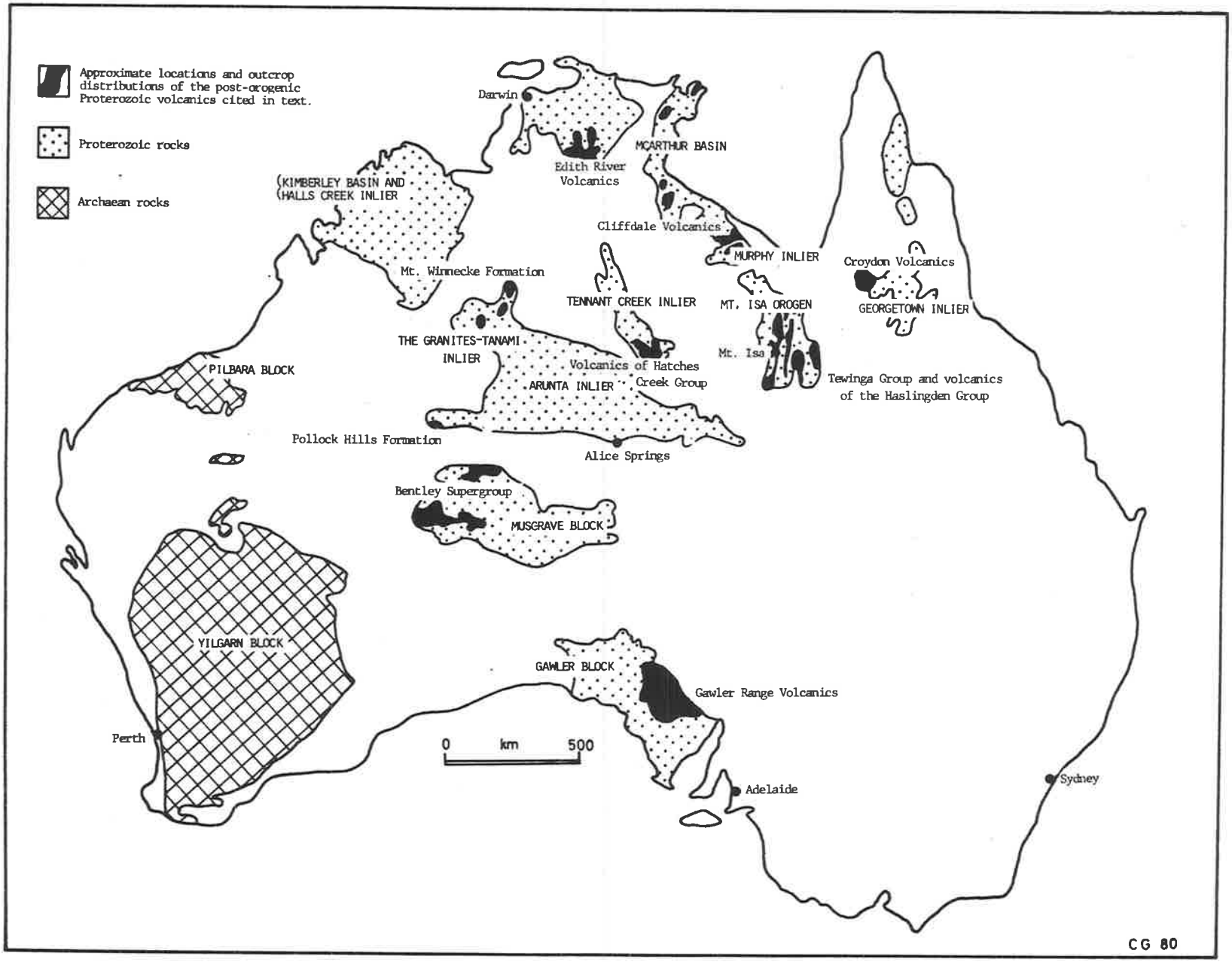

In southern Australia, the igneous activity associated with the development of the 1500 m.y. post-orogenic Gawler Range Volcanics also encompassed a large area, with no obvious systematic progression in age in any direction (Giles and Teale, 1979 - see Appendix 3). Similar conclusions apply to the 1100 m.y. Central Australian province. There is no evidence for a northward progression in ages from the Gawler Range province to the Central Australian province and in any case, if such a progression were postulated it would be difficult to reconcile with the approximately 1500 m.y. age determined for acid volcanics comprising the Pollock Hills Formation further to the north (Page, et al., 1977; see Fig. 4.2, for relative positions).

4.7 SUMMARY

It has been found that the two Proterozoic volcano-plutonic provinces examined in detail in this thesis have many features in common with other post-orogenic Proterozoic igneous provinces, both in northern Australia and elsewhere in the world. The similarity in the geochemistry of the acid intrusive and extrusive rocks from the various provinces is marked, and it is significant that many workers have proposed models of origin that are analogous to the generalised petrogenetic model developed for the Gawler Range and Central Australian provinces (Fig. 4.1). The model involves an interaction of the mantle and crust, with the mantle yielding basic magmas and either directly or indirectly providing heat for melting of the crust, from which the acid magmas were generated.

The details of the model, developed in this thesis for the Gawler Range and Central Australian provinces, are believed to offer a plausible explanation for the distinctive geochemical characteristics of the acid rocks comprising the Proterozoic post-orogenic suites. Aspects of particular importance are:

1) The "sialic" crustal source (albeit a refractory residue), being initially moderately enriched in LIL elements (c.f. basaltic sources) can account for the relatively high LIL element contents in the acid rocks.
2) The relatively high temperatures of melting may cause the disintegration of normally refractory minerals, including:
   a) zircon, apatite, sphene and monazite, releasing Zr, Nb, Y and REE into the melt;
   b) magnetite and ilmenite, releasing Fe, Ti Sc, V and Nb into the melt.
3) The relatively dry conditions of melting (and hence low PH_2O and PO_2)

may have further contributed to the instability of magnetite and ilmenite.

4) The residual mineral assemblage of plagioclase, pyroxenes and magnetite is consistent with experimental evidence and can explain some of the major and trace element features such as:
   a) Relatively low Al_2O_3, CaO and Sr - due to a relatively high proportion of plagioclase in the residue. It is notable that the stability of plagioclase will be favoured by the dry conditions of melting.
   b) Relatively high $Fe_2O_3^t$, TiO_2 and $Fe_2O_3^t/MgO$ - due to a high proportion of pyroxenes relative to magnetite (or ilmenite) in the residue.
5) The bimodal distribution of rock types, due to the paucity of andesites, results from the two separate magma sources proposed, viz. mantle and crust. On experimental grounds neither of these sources are likely to yield primary low-silica intermediate magmas by direct partial melting.
6) The lower crustal source of basic-intermediate composition eliminates the need to invoke excessive degrees of melting (> 50%) in order to explain the major element geochemistry of the non-eutectic acid to high-silica intermediate magmas. Also, the lower degree of melting implied by such a source is more readily reconcilable with the relatively high LIL trace element contents observed in the acid rocks.

It is evident from this review that post-orogenic igneous activity played an integral and important role in the development of the Proterozoic crust. Moreover, it appears that the origin of the igneous rocks comprising the post-orogenic provinces can be explained in terms of the one, generalised model. The applicability of this model to Proterozoic volcano-plutonic provinces that are not post-orogenic and the reason why post-orogenic igneous activity occurs at all, are matters for conjecture at this stage. However, these questions will be examined in the final chapter of this thesis when the present conclusions will be combined with the conclusions drawn from a study of Archaean felsic volcanic rocks.

PART TWO

FELSIC VOLCANIC AND ASSOCIATED ROCKS OF THE ARCHAEAN CALC-ALKALINE VOLCANIC CENTRES

CHAPTER 5

THE PETROGENESIS OF THE ARCHAEAN WELCOME WELL VOLCANIC COMPLEX

5.1 INTRODUCTION

The Welcome Well volcanic complex consists of a sequence of dominantly intermediate volcanic rocks and associated epiclastic sediments which crop out within an area of 160 km^2 roughly 35 km east of Leonora (Fig. 5.1). The complex lies within the central portion of the main Norseman-Wiluna greenstone belt in the Eastern Goldfields Province of the Archaean Yilgarn Block of Western Australia (Gee, 1976). This area was chosen for study because of the minimal alteration and the relatively good outcrop compared with many other intermediate-acid volcanic centres in the Eastern Goldfields Province.

During the course of compiling the LAVERTON 1:250,000 geological map, Gower (1974) recognised a "felsic volcanic complex" apparently centred on Welcome Well, where "the unit consists of agglomerate and breccia containing boulders over 1m in diameter". Subsequent observations by Hallberg (pers. comm., 1977) revealed that the complex was mainly composed of intermediate volcanics and that the "agglomerates and breccias" noted by Gower (1974) were in fact lithic wackes of sedimentary origin. Hallberg further noted that the main centre of volcanism lay approximately 7 km to the north of Welcome Well. The writer mapped the centre and immediate environs in detail in June 1977 and succeeded in establishing a workable stratigraphy in the area. This was greatly facilitated by the relatively good outcrop and the excellent textural preservation which characterises the volcanic complex.

5.2 REGIONAL GEOLOGY

5.2.1 Setting

Gower (1974) subdivided the Norseman-Wiluna greenstone belt sequence on the Laverton 1:250,000 Sheet area into five structural sectors, each separated by tectonic lineaments. The Welcome Well complex lies within the Murrin sector which is characterised by: large ultramafic and mafic intrusives bodies, explosive felsic volcanism, lack of mature sediments and true banded-iron formations, complex fold and fracture patterns, and high-level granitic intrusions (after Gower, 1974).

Unfortunately reconstruction of the stratigraphy across the entire Norseman-Wiluna greenstone belt at this locality is hindered by the structural discontinuities which prevent simple lithological correlation, although within individual sectors stratigraphic columns can be constructed

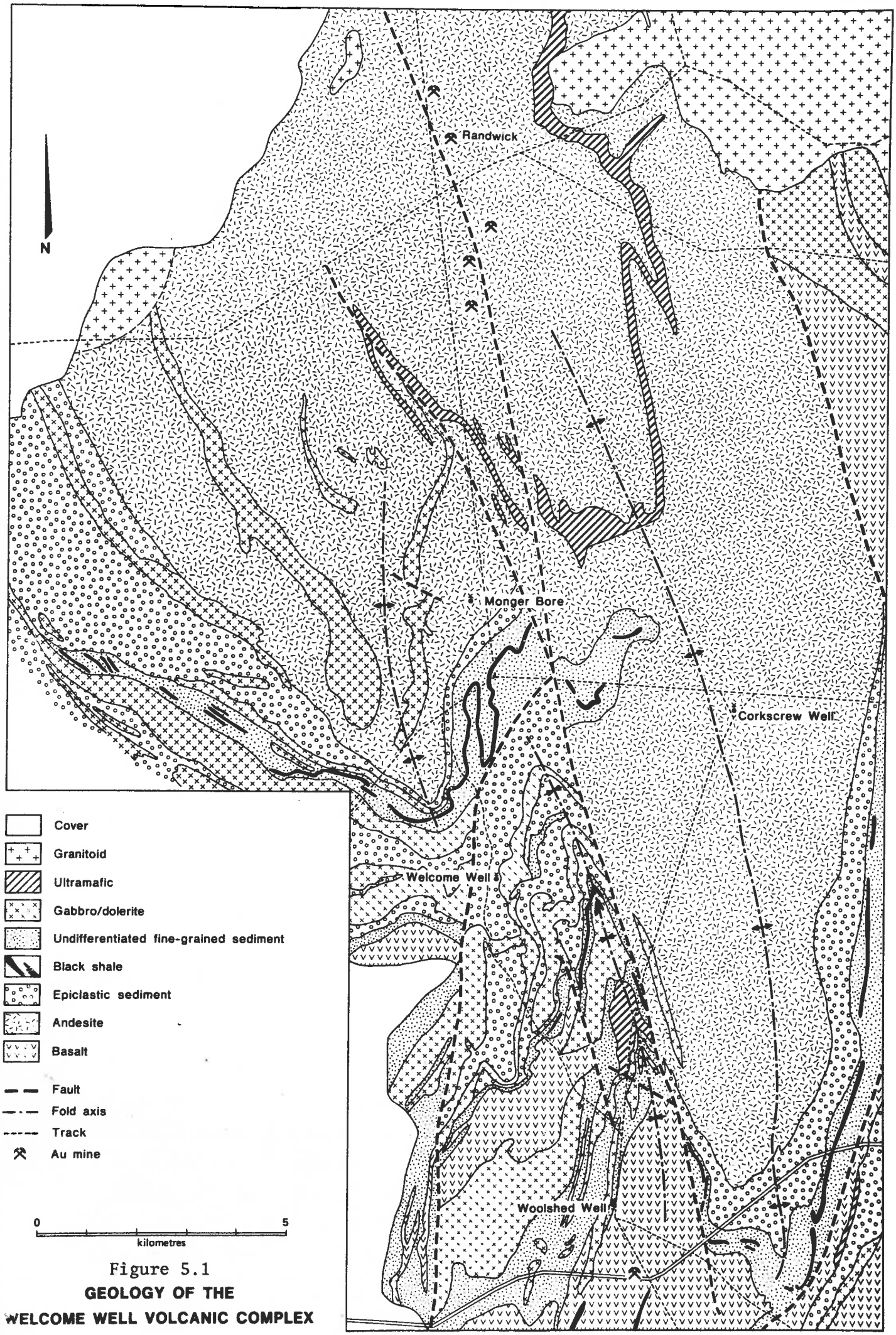

Figure 5.1

GEOLOGY OF THE

WELCOME WELL VOLCANIC COMPLEX

with reasonable certainty. On the basis of detailed mapping in the Leonora-Laverton area, Hallberg (1980) has recognized two greenstone rock associations. The first is a probable older sequence characteristically containing ultramafic lavas, mafic sediments, true banded-iron formations, nickel deposits and stratigraphically-controlled gold mineralisation, typical of the lower succession in the Kalgoorlie region. The second association shows none of these features, but is characterised by highly-differentiated tholeiites (of both intrusive and extrusive origin) and felsic volcanics with associated epiclastic sediments, and is interpreted to overlie the older sequence, although in the field the two associations are separated by major faults (e.g. Celia lineament). Hallberg (1980) considers that the volcanics comprising the Welcome Well complex lie near the base of the second association, which on the Laverton 1:250,000 sheet area, is not exposed.

5.2.2 Stratigraphy

Mapping by Hallberg (1980) and the writer has outlined the detailed stratigraphy in the vicinity of the Welcome Well complex. The mapped sequence is exposed in a series of major anticlines and synclines separated by strike faults (Fig. 5.1). In the core of the major anticline to the north of Welcome Well, volcanics and sediments comprising the Welcome Well complex are well exposed; they represent the lowest stratigraphic level exposed to the west of the Celia lineament (or the lowest exposed level of Hallberg's second greenstone association). The "centre" is dominated by porphyritic lavas with some interlayered sediments interpreted to be lahars, and very rare pyroclastics. Further details of the rock relationships and the rock types exposed in the centre will be discussed later.

The volcanics are overlain by a thick sequence of lithic wackes composed entirely of detrital material shed from the intermediate volcanic pile. The clasts range from boulder through cobble to pebble size and are set in a sandy matrix composed of rock fragments and plagioclase grains cemented by secondary carbonate, quartz and chlorite. The succeeding unit comprises fine-grained black shales and silts, which, because of its susceptibility to deformation, or incompetance, is commonly sheared to form quartz-sericite schists. In places the black shales are silicified, as the result of near-surface weathering, to form massively-outcropping rocks resembling ferruginous cherts and/or banded-iron formations. The prominent outcrop of these silicified zones makes them very useful markers which aid in tracing the structure of the area (Fig. 5.1).

The upper zones of the black shales are interlayered with tholeiitic basalts which in turn grade upward into a monotonous thick sequence with occasional zones of pillows, extreme flow-brecciation and steam-fracturing, and interbeds of fine silty sediments, all indicative subaqueous eruption. It is notable that the tholeiitic basalts are overlain by high-magnesium spinifex-textured basalts to the south and the sequence is capped by a layered tholeiitic sill at Mt. Kilkenny (Hallberg, 1980).

The sequence of intermediate volcanics and associated sediments is intruded by a variety of compositionally-distinct rock types, including:
A. Gabbros and dolerites, which typically form sill-like bodies wedging the volcanic pile apart and adding greatly to the apparent stratigraphic thickness (Fig. 5.1). They are interpreted to be the subvolcanic feeders to the overlying thick, tholeiitic basalt pile. This is supported by an occurrence of a distinctive variant of the gabbro, known locally as "cat-rock" which contains large (up to 6 cm) corroded and altered megacrysts of bytownite in an ophitic gabbroic matrix. Similar megacrysts, though rarely as large, occur in the overlying basalts thus indicating a common source and hence a volcanic-subvolcanic relationship.

B. Ultramafics, which have intruded as sills and more rarely, as small dykes. The major occurrence is a sill in the north of the area mapped, which like the basic sills described above, has been folded with the remainder of the sequence (Fig. 5.1). The outcrop of this body for the most part is marked by rubbly laterite and jasperoidal silicified zones, typical of the surface expression of many ultramafic rocks in the Eastern Goldfields Province. 3.4 km to the north of Monger Bore, the intrusive contact relationships with the intermediate volcanics are well exposed and at this locality fresh outcrops of the ultramafic reveal that it is a cumulate peridotite (e.g. W24). The small dykes are usually less magnesium-rich and are clearly cross-cutting (e.g. W7).

C. Dacite porphyries, which typically form large homogeneous bodies with rather subdued outcrop. They cover extensive areas in the vicinity of Christmas Well (20 km west northwest of Welcome Well) and Aermotor Well (30 km east of Welcome Well). Their geochemistry and petrography is very similar to dacite lavas of the Welcome Well complex, suggesting that they represent comagmatic subvolcanic intrusives.

D. Megacrystic adamellite, which forms a large homogeneous pluton truncating the volcanics in the north of the area mapped; it is typical of many of the granitoid bodies in the Eastern Goldfields Province. The adamellite is clearly intrusive into the volcano-sedimentary pile, since it is bounded by a wide zone of hornfelsed country rocks which are invaded

by numerous linear dykes of microgranite, quartz porphyry and aplite. Within the margins of the adamellite large rafts of contact metamorphosed country rocks are commonly found.

5.2.3 Structure

The structural history of the region mapped appears to be relatively simple, with evidence for only one major deformation, which is responsible for the macroscopic folding. The macroscopic folds do not refold a pre-existing schistosity, thus excluding an earlier period of deformation, nor is there any crenulation of the existing schistosity which would indicate post-folding deformation. In general, the axial plane schistosity associated with the macroscopic folding is only obvious in the fold hinges where it is best developed in the easily-sheared, fine sediments. There is, however, a very strong schistosity developed in the country rocks adjacent to the adamellite and this is believed to have been produced by re-orientation of minerals during recrystallisation in the stress field created by the intrusive body. This conclusion is supported by the marked orientation of the long axes of the xenoliths and perthite megacrysts in the adamellite, parallel with the schistosity in the country rocks, indicating that the principal stress during intrusion and cooling of the adamellite body was indeed coincident with that which produced the parallel schistosity in the adjacent country rocks.

Lithologic and structural continuity between the adjacent south-plunging folds has been disrupted by prominent faults which are roughly parallel with the regional strike. The strike faulting prevents tracing of individual units from one fold to the next, but as the geologic map shows (Fig. 5.1), it is possible to broadly correlate the stratigraphy indicating that the throw on the faults was not great.

5.2.4 Metamorphism

The regional grade of metamorphism lies in the greenschist facies (Gower, 1974) and this has resulted in excellent textural, and in many cases mineralogical preservation. Because of the low metamorphic grade, distinction between metamorphic effects and primary deuteric alteration is often difficult. It is probable that the pervasive development of chlorite in the volcanics and epiclastic sediments is a direct result of low-grade metamorphism. This may not be the case for pumpellyite however, which is extensively developed in the frothy, glassy flow-tops of the lavas. In some of the lithic wackes and flow-top agglomerates, volcanic fragments containing no pumpellyite are adjacent to those containing large

amounts of the mineral; these features indicate that the pumpellyite developed during deuteric alteration of the volcanics prior to metamorphism. It is likely that much of the visible alteration of the minerals (e.g. clinopyroxene → chlorite, plagioclase → sericite, Ti-magnetite → sphene + leucoxene) and introduction of secondary carbonate and quartz also took place at this time.

Higher grades of metamorphism, with complete obliteration of primary textures, are locally developed adjacent to the adamellite pluton in the north of the mapped area. Here, contact metamorphism has converted all mafic and intermediate rocks to a hornfels consisting of a completely recrystallised aggregate of plagioclase and amphibole. The hornfels forms a band up to 3/4 km wide flanking the margin of the pluton, clearly indicating that the adamellite has supplied the heat responsible for the metamorphic recrystallisation.

5.3 DETAILED GEOLOGY OF THE VOLCANIC CENTRE

While the above has been concerned with the regional aspects of the geology, this discussion will concentrate on the details of the evolution of the volcano-sedimentary sequence as far as can be determined from the exposures in the Welcome Well complex. Attention will be focussed on the rocks cropping out in the core of the anticline to the north of Welcome Well in what is regarded as the true volcanic "centre". Photographs illustrating some of the aspects of the field geology are given in Figures 5.2 and 5.3.

The actual centre is largely composed of andesitic volcanics of lava-flow origin, with subordinate occurrences of thin basalt and dacite flows. The majority of the volcanics are porphyritic and range from sparsely- to highly-porphyritic types, the latter containing >50% phenocrysts. Zones packed with chlorite, carbonate and/or quartz-filled amygdales are common and are interpreted to represent the tops of individual lava flows. They often grade into zones characterised by extreme brecciation produced as a result of flowage while the lava was in a partially solidified state. The flow-top breccias range from true breccias packed with angular fragments with cuspate margins, to agglomerates containing rounded fragments. In both cases the fragments are usually mono-lithologic and are contained within a highly-contorted, glassy matrix little different in composition to the fragments themselves. Possibly the angularity of the fragments was determined to some extent by the state of solidification of the lava at the time of fragmentation. For example if the lava was largely fluid, rounded shapes would result as the

fragments were rotated during flowage, but if the lava had largely solidified (at least near the top) subsequent flowage would have produced brittle fracture and angular fragments. This is supported by the petrography which shows that in thin section many of the agglomerates are often not obviously fragmental because the fragments tend to merge with the matrix, whereas the fragment boundaries in the breccias are always clearly defined. Few lavas show visible flow banding, but those that do, reveal an extreme contortion of the flow layers to the point that fracturing and dislocation has occurred.

In places there is good evidence for *in situ* fracturing probably produced by steam or vapour streaming in the upper zones of the lava flows. This type of fragmentation is sometimes superimposed on the flow brecciation and results in extremely angular, cuspate and "close-packed" breccia textures. It is therefore a late-stage effect probably developed in the lava after flowage had ceased.

Interlayered with the lava flows in places are poorly-sorted lithic wackes. These rocks superficially resemble pyroclastic breccias, but the groundmass textures are characterised by close-packed granular aggregates, clearly indicating a sedimentary origin. The lack of sorting, abundance of boulder-size volcanic clasts and clastic textures suggests that the lithic wackes may represent mud-flow deposits or lahars. The lithic wackes are intimately associated with the volcanics, intertwining and in places engulfing large volcanic rafts, and often it is difficult to determine whether the lava flows have engulfed the lahars or vice-versa, owing to the lensoid character of the individual members. Similar features have been observed on the slopes of Mt. Rainier, where a complete gradation from autobrecciated lava to hydrovolcanic breccia and laharic breccia has been recorded (Fiske, *et al.*, 1963). Explanations offered in the case of Mt. Rainier include: shattering of thin lava streams by steam explosions and subsequent mixing with mud and water as the brecciated mass moves down the slope of the volcano, or alternatively, true mud flows, perhaps triggered by water saturation, earthquakes or explosive eruption, which have engulfed rafts and blocks of lava. It is probable that similar processes may have operated to produce the analogous volcano-sedimentary deposits observed in the Welcome Well complex.

Immediately to the south of the Welcome Well centre, in the northern part of the Welcome Well synclinal structure there is a thick sequence of coarse lithic wackes. The absence of interlayered lava flows in this sequence indicates that deposition occurred away from the immediate vent zone, while the abundance of boulder-size clasts and lack of sorting

Figure 5.4 Diagrammatic reconstruction of the geological environment during formation of the Welcome Well complex.

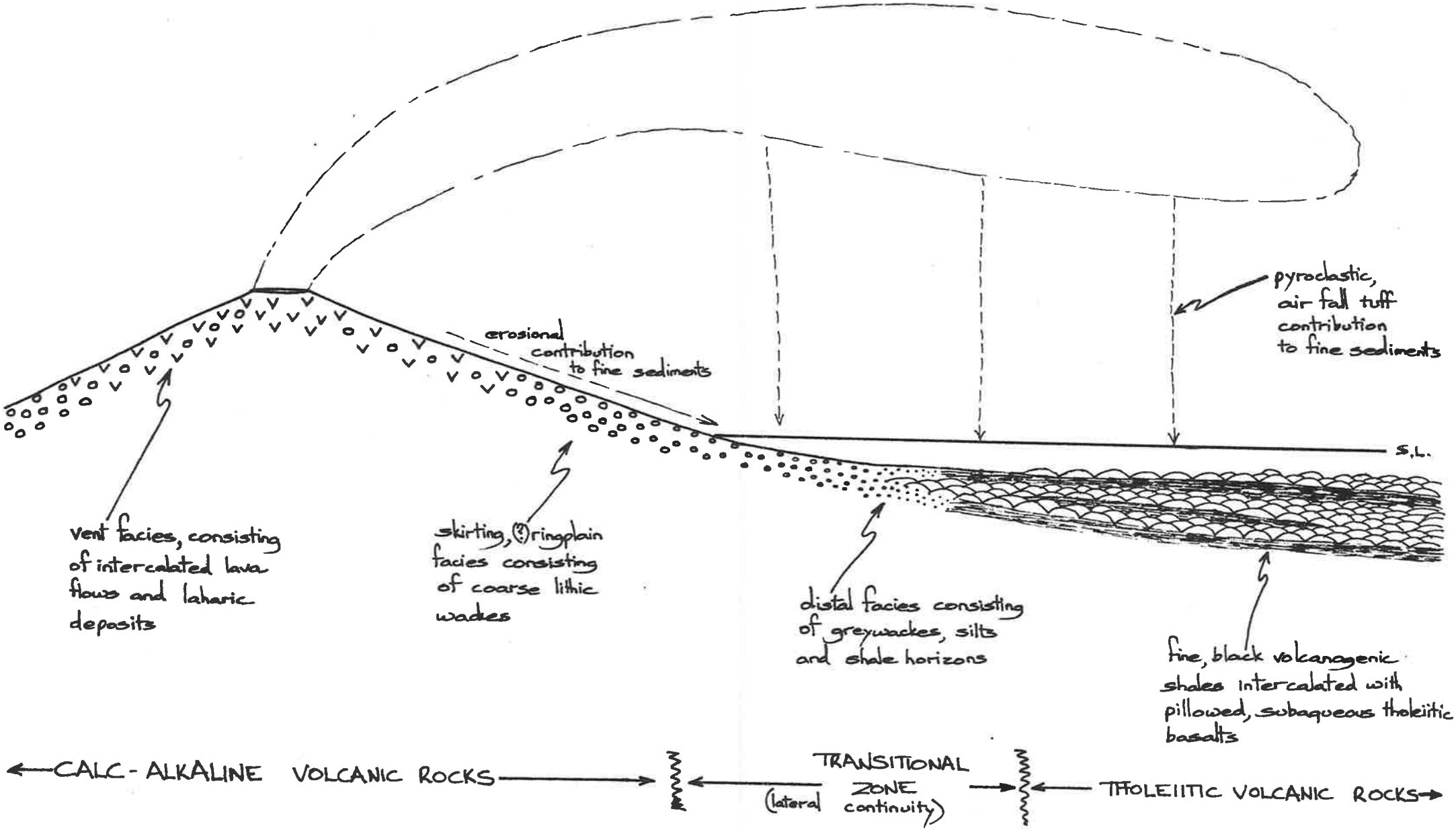

indicates a high energy environment possibly on the lower slopes of the volcano. This suggests that the coarse lithic wackes in the vicinity of Welcome Well are probably mud-flow deposits or lahars which originally spread out as a ring-plain skirting the lower slopes or base of the volcano. The rapid decrease in the proportion and size of the volcanic clasts evident in greywackes to the south of Welcome Well indicates an abrupt change in energy, possibly corresponding with the change in slope at the base of the volcano. A good exposure of greywackes is found 2.2 km to the south of Welcome Well, where the sediments consist of bedded (sometimes graded) grits and sands composed of clastic plagioclase phenocrysts and volcanic rock fragments. Occasional cobbles and pebbles of volcanic clasts are found in the greywackes and these are invariably well-rounded in contrast to the subangular to subrounded clasts found in the lithic wackes to the north. Several features of the greywackes such as good sorting, graded bedding and cross-bedding indicate that they have been deposited in response to regular current activity rather than by large-scale slumping (c.f. lithic wackes). Thus, it is likely that the greywackes represent alluvial fan deposits that originally spread out from the base of the volcano, as a result of active stream erosion of the volcanic-laharic pile. Further away from the centre the greywackes become noticeably finer and the pebble- and cobble-size fragments are absent. The association of the fine, distal greywackes with pillowed basalts and marine black shales, clearly indicates deposition under subaqueous conditions.

It is evident from the above discussion that the vertical stratigraphic sequence outlined previously (see also Fig. 5.1) is also recognisable in a lateral sense. The impression gained from the field relationships is therefore one of a subaerial intermediate volcanic centre surrounded by a skirt or ring-plain of volcanic detritus, which, distal to the centre merged with black shales and basalts in a subaqueous environment. A diagrammatic reconstruction of the probable environment based on the above interpretation is given in Figure 5.4

The actual size of the volcanic centre in the present case is difficult to ascertain because of structural and erosional modification, however it probably covered an area less than 300-400 km^2, which is small in comparison with modern stratovolcanoes (Macdonald, 1972). Other acid to intermediate centres or their root zones crop out sporadically in the northern part of the Norseman-Wiluna greenstone belt, at approximately the same stratigraphic level as the Welcome Well complex (Hallberg, 1980).

Figures 5.2 and 5.3 (combined). Photographs illustrating aspects of the field geology.

A. Autobrecciation, probably caused by gas-streaming, within an andesitic flow.

B. Flow-top zone of an andesitic lava flow. The massive, amygdaloidal upper part of the flow (right) merges into a monolithologic flow breccia at the top. The cuspate, recurved shapes of many of the fragments indicate that they were plastic at the time of disruption.

C. Flow breccia within an andesitic lava flow. The angular, amygdaloidal blocks of andesite, which were probably incorporated in a solidified state, are contained within a plagioclase-rich andesitic host.

D. An epiclastic lithic wacke, composed of poorly-sorted, angular blocks of andesite set in a gritty matrix. These units, which are intercalated with andesitic flows within the centre, are interpreted to have been deposited from lahars.

E. Detail of an epiclastic lithic wacke. Note the angularity of the fragments, the poor sorting and the gritty nature of the matrix. Rocks such as these form thick deposits flanking the Welcome Well centre and are thought to be the remnant of an ancient ringplain. F.V. 1 m.

F. Bedded, epiclastic grits and coarse sands of fluvial origin, several kilometres distant from the centre. The infrequent cobble- and pebble-size volcanic clasts are invariably well rounded, indicating significant transport.

G. Cross-bedding in the above epiclastic grits, indicative of a moderately high energy fluvial environment, probably corresponding with the outwash at the flanks of a volcano.

H. Thinly-bedded tuff unit within andesitic flows of the centre. F.V. 40 cm.


A


E


B

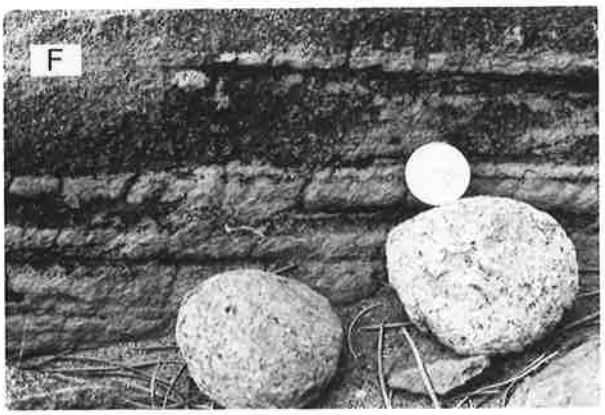
F


C


G


D


H

This suggests that the Welcome Well centre may have formed but one of a series of approximately contemporaneous, spaced volcanoes. However, the configuration of the Archaean volcanoes was unlikely to have resembled a modern island arc since the individual centres are discrete and are separated from each other by zones devoid of any acid to intermediate volcanics. A closer analogy could perhaps be drawn with the isolated Tertiary igneous centres of eastern Australia which are commonly thought to have formed over 'hot-spots' (c.f. Wellman and McDougall, 1974).

It is concluded that the rock types and the rock relationships recognisable in the Welcome Well complex are very comparable with those found in modern stratovolcanoes. Thus, it is considered that the Welcome Well complex evolved as a volcano and was subsequently eroded, in much the same way as modern examples (e.g. Bagana, Bultitude, et al., 1978; Mt. Rainier, Fiske, et al., 1963; numerous examples described by Macdonald, 1972).

5.4 PETROGRAPHY

A great variety of rock types are represented in the Welcome Well complex and the petrographic characteristics of the more important of these will be examined below. Brief petrographic descriptions of a representative selection of samples from the area, some of which are referred to in the following text are given in Table A5.1, Appendix 1. Photomicrographs illustrating many of the textural features described below will be found in Figures 5.5 and 5.6.

5.4.1 Volcanic and related intrusive rocks comprising the Welcome Well complex

The rocks comprising the complex show a complete mineralogical gradation from basalt to rhyolite. The basalts are porphyritic to micro-porphyritic in contrast to the tholeiitic basalts adjacent to the Welcome Well complex, which are rarely porphyritic. Most of the basalts are pyroxene porphyries containing abundant fine-to medium-grained phenocrysts of clinopyroxene and very rare plagioclase, commonly in glomeroporphyritic aggregates, set in a pilotaxitic matrix of flow-oriented plagioclase microlites, clinopyroxene, chlorite (after glass) ± epidote (e.g. W111, W115, W121). W2 is exceptional in this regard as it contains abundant euhedral phenocrysts of sericitized plagioclase and rarer chloritized clinopyroxene, plus skeletal crystals of both, in a feathery uralitized matrix after basic glass. W3 was the only basalt sectioned which appeared to contain original olivine, now pseudomorphed

Figure 5.5. Photomicrographs of selected thin sections.

A. "Cat-rock", composed of coarse-grained bytownite phenocrysts set in an ophitic gabbroic matrix.

B. Fresh peridotite from the folded sill in the north of the mapped area (W24). This sample shows anhedral olivine enclosed by clinopyroxene in a poikilitic intergrowth. F.V. 7 mm.

C. Granular, anhedral olivine and skeletal clinopyroxene set in a glassy matrix. Sample collected from an ultramafic dyke (W7) that intrudes the Welcome Well complex. F.V. 5.5 mm.

D. A basalt, comprised of phenocrysts of tabular plagioclase and chloritized clinopyroxene within a feathery-textured, uralitized glassy matrix through which are scattered plagioclase microlites. This basalt (W2) has marked geochemical affinities with the andesites. F.V. 3.7 mm.

E and F. Porphyritic andesites, containing phenocrysts of sericitized, tabular plagioclase and zoned, euhedral clinopyroxene. Numerous oriented plagioclase microlites set in chloritic glass, define a hyalopilitic texture in the matrix. E, F.V. 7 mm; F, F.V. 5 mm.

G. Detail of a zoned, euhedral clinopyroxene phenocryst within porphyritic andesite. F.V. 4 mm.

H. Phenocryst-rich, porphyritic andesite, containing close-packed phenocrysts of fine-grained, flow-oriented plagioclase and subhedral, chloritized clinopyroxene. F.V. 6 mm.


A

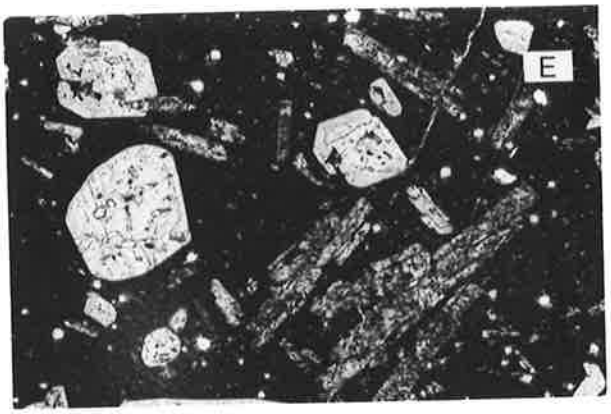
E

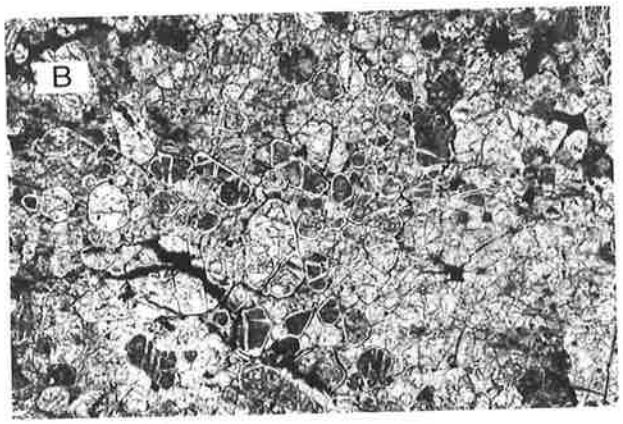
B


F

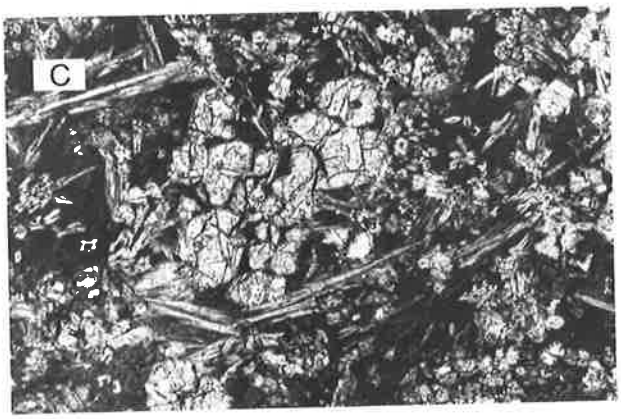
C

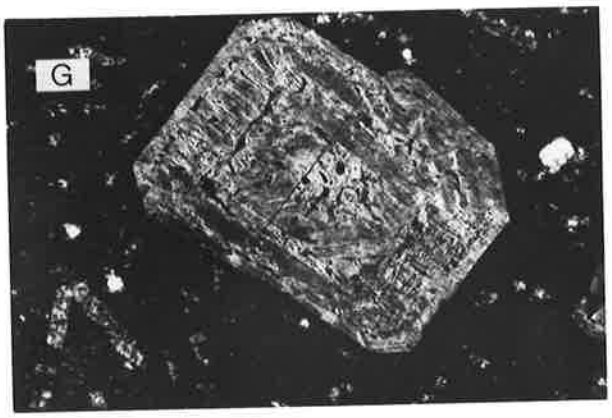
G


D

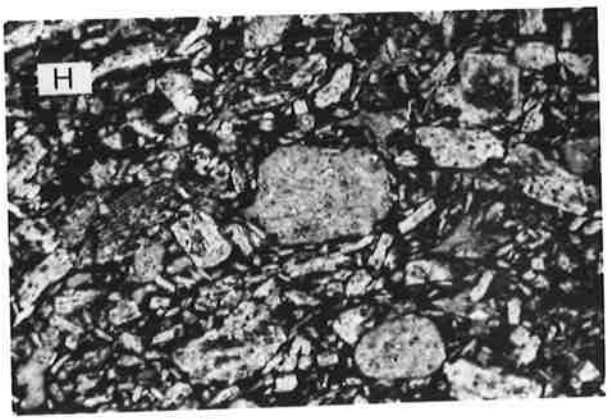
H

by chlorite. Some of the rocks of basaltic composition (e.g. W31, W131) are hornblende-clinopyroxene porphyries; they contain zoned, euhedral phenocrysts of primary brown hornblende and clinopyroxene usually in glomeroporphyritic aggregates in a finely-crystalline matrix of plagioclase, brown hornblende, sphene and epidote.

The basalts grade into andesites with decreasing proportions of clinopyroxene phenocrysts relative to plagioclase phenocrysts and a reduction in the abundance of mafic minerals in the matrix. Like the basalts, the andesites are usually porphyritic and typically contain zoned, euhedral phenocrysts of plagioclase and clinopyroxene in a pilotaxitic matrix defined by flow-oriented plagioclase microlites. Electron microprobe results show that the clinopyroxene phenocrysts are sub-aluminous augites (Table A5.5, Appendix 1); many are partially resorbed indicative of non-equilibrium conditions during ascent and cooling. Hornblende and magnetite are less common phenocryst components, while orthopyroxene is absent. The proportion and size of phenocrysts in the andesites varies greatly: those with a high proportion of phenocrysts (> 40%) often show trachytic textures defined by the flow-oriented, tabular plagioclase crystals (e.g. W4, W125, W118), while the finer-grained more sparsely porphyritic variants typically contain glomeroporphyritic aggregates of plagioclase, clinopyroxene and/or amphibole. A lava-flow rather than a pyroclastic origin for the majority of the andesites (and basalts) is evidenced by the strong flow alignment of both plagioclase phenocrysts and microlites in the matrix, and by the paucity of vitroclastic textures.

Amygdales filled with quartz, chlorite and/or carbonate occur in the massive andesites, but assume far more importance in the flow-top zones. These zones are characteristically glassy and often show cuspate, deformed glassy fragments which have been clearly stretched and contorted by flowage while still in a plastic state. As previously noted, mono-lithologic agglomerates and breccias, produced as a result of flowage while the lava was in various states of solidification, are ubiquitous in these zones. The rounded, agglomeratic fragments are often difficult to distinguish from the matrix. The flow-top zones are usually altered to assemblages dominated by quartz, chlorite, epidote, pumpellyite, sericite and carbonate, probably as a direct result of the abundant fluids entrapped within the flow-top zones. Similar alteration, though less severe, is pervasive in the massive andesite and basalt lava flows where plagioclase is often extensively sericitized, clinopyroxene is chloritized and magnetite has been converted to sphene and leucoxene and the matrix contains scattered chlorite, epidote, sericite and carbonate. Rarely,

Figure 5.6. Photomicrographs of selected thin sections.

A. Porphyritic dacite (W94), containing abundant plagioclase phenocrysts in a microcrystalline felsic matrix. F.V. 7 mm.

B. Porphyritic rhyolite (W148), containing phenocrysts of zoned, sericitized plagioclase and anhedral, embayed quartz within a devitrified matrix. F.V. 7 mm.

C. Contorted flowage features preserved in a flow-top agglomerate. The fragments comprising the agglomerate have cuspate margins and often feldspar phenocrysts project from the fragments into the matrix. Both features indicate disruption prior to complete solidification in this part of the flow. F.V. 8.5 mm.

D and E. Contorted flowage textures in the glassy portion of a flow-top agglomerate. The grey areas with angular, cuspate margins represent patches of glass, now replaced by chlorite. Evidently these areas took much of the strain as the adjacent agglomeratic fragments moved with the flow. D, F.V. 4 mm; E, F.V. 6.5 mm.

F. Amygdales infilled with carbonate and chlorite, in the upper zone of an andesitic flow. F.V. 8 mm.

G. The matrix of an epiclastic lithic wacke, in which numerous intermediate volcanic rock fragments and plagioclase grains form a close-packed aggregate, now cemented by carbonate and chlorite. F.V. 7 mm.

H. Details of the matrix of an epiclastic lithic wacke. The grains are rimmed by quartz and the interstitial cementing material consists of carbonate and chlorite. Although the grains are well sorted, they are extremely angular, and thus have been transported little distance from their source. F.V. 3 mm.

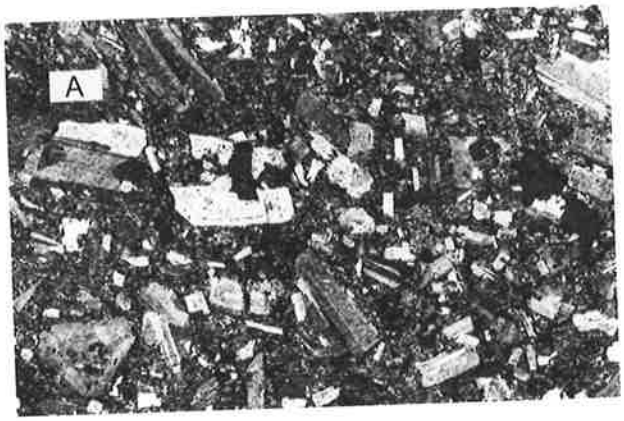
A

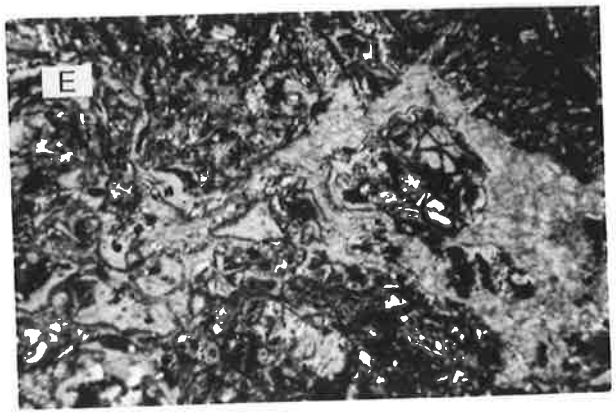
E


B

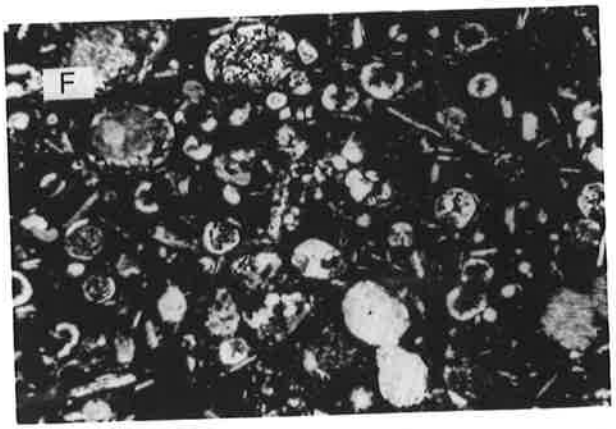
F

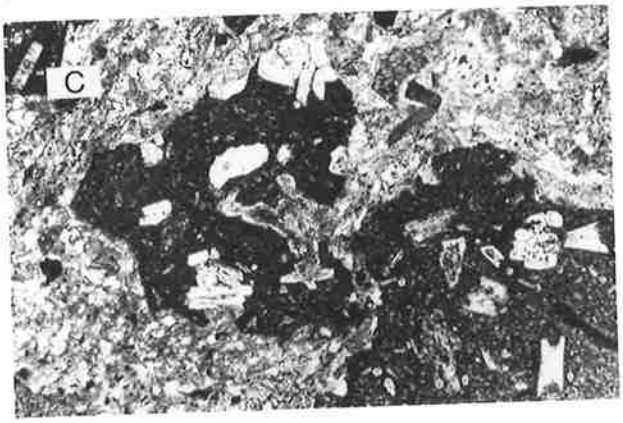
C

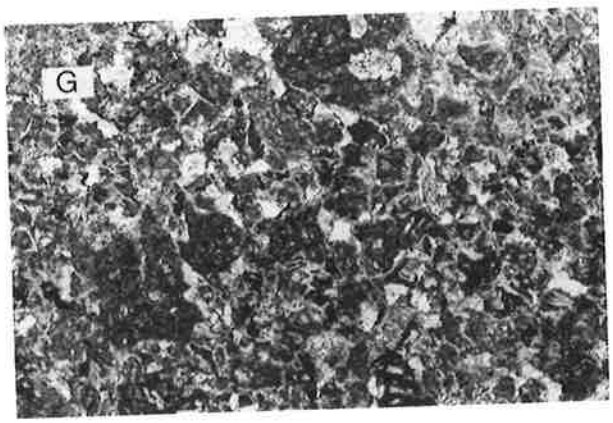
G


D

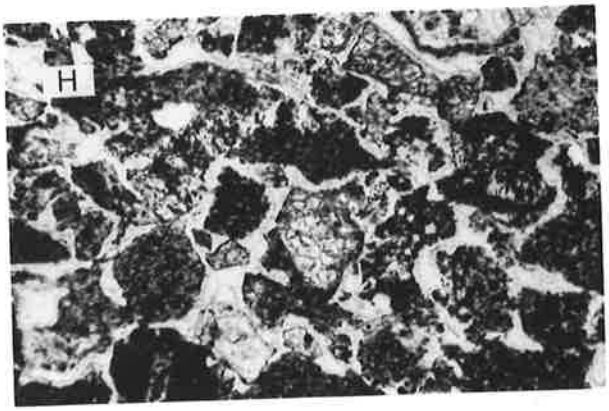
H

however, are textures completely destroyed. This suggests that alteration is on the scale of individual minerals and has not caused migration of elements over large distances. Nevertheless, the samples chosen for analysis were those showing minimal alteration.

The dacites are characterised by abundant euhedral, zoned plagioclase phenocrysts and rarer amphibole and/or clinopyroxene phenocrysts in a felsic matrix; most are either lavas (e.g. W8, W17, W29, W74) or homogeneous subvolcanic intrusives (e.g. W144, W145). Plagioclase is also the dominant phenocryst component in the volumetrically minor rhyolites, where it occurs with embayed, anhedral quartz and rare K-feldspar in a siliceous, sericitized felsic matrix. Ghosted shard outlines in one of the rhyolites (W147) are indicative of a pyroclastic origin, but the other rhyolites are probably intrusives or were erupted as lavas (W146, W148).

5.4.2 Epiclastic sediments

The matrix textures of the epiclastic sediments, whether coarse lithic wackes or even-grained greywackes are distinctive, consisting of a variety of clastic volcanic rock fragments and plagioclase grains in a close-packed aggregate cemented by quartz, chlorite and carbonate. Secondary quartz often forms a rim to the grains, but never occurs as a clastic component thus indicating erosion of the local intermediate volcanic pile. This is supported not only by the textural immaturity of the sediments, but also by the variety of lithic fragments which span the compositional range exposed in the Welcome Well volcanic pile. Furthermore, the volcanic clasts, particularly those of boulder, cobble and pebble size, become noticeable less angular with increasing distance from the vent zone, consistent with increasing distances of transport and abrasion.

5.4.3 Intrusive rocks, unrelated to the intermediate volcanism

A. Ultramafics

Fresh outcrops of the ultramafic sill in the north of the mapped area reveal that it is a peridotite, consisting of cumulus anhedral crystals of olivine poikilitically-enclosed within clinopyroxene. The small cross-cutting dykes are typically composed of anhedral olivine phenocrysts and skeletal clinopyroxene within a dark, feathery, originally glassy matrix.

B. Gabbros and dolerites

The gabbros consist of medium-to coarse-grained cumulate crystals of uralitized clinopyroxene in an intercumulus, plagioclase-rich matrix (e.g. W50). Subophitic to ophitic intergrowths of uralitized clinopyroxene

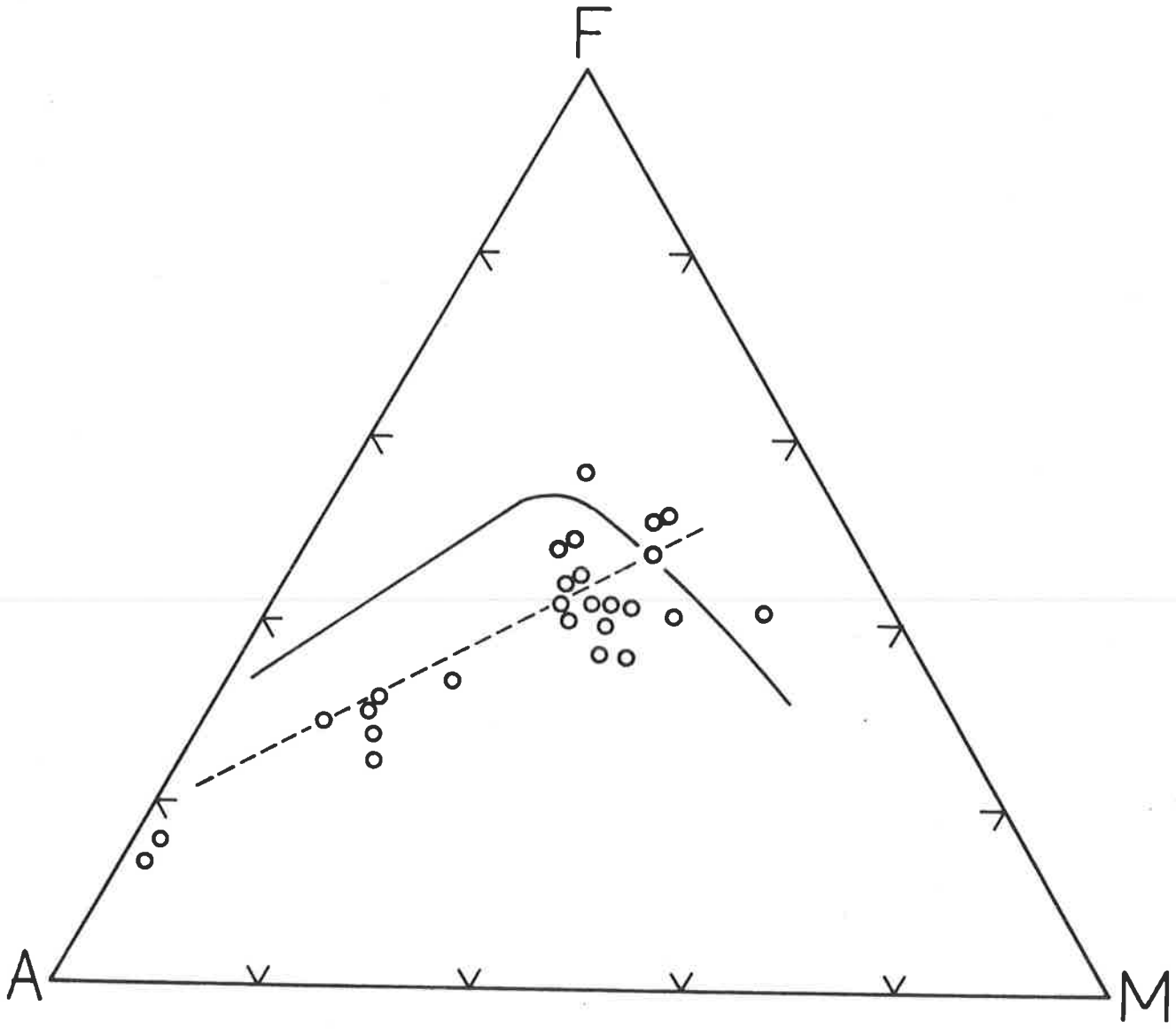

Figure 5.7 AFM plot for rocks from the Welcome Well complex. The solid line separates the tholeiitic and calc-alkaline fields. The dashed line is the trend defined by the calc-alkaline Cascades lavas (after Carmichael, 1964).

and plagioclase characterise the fine-grained dolerites.

C. Porphyritic adamellite

The adamellite pluton is characterised by megacrysts of perthite and less commonly microcline, within a holocrystalline matrix composed of roughly equal proportions of quartz, K-feldspar and zoned plagioclase (e.g. W43). Amphibole, biotite and magnetite also occur, but generally comprise less than 5% of the rock. Porphyritic acid dykes, consisting of phenocrysts of anhedral quartz, euhedral plagioclase and K-feldspar in a siliceous, felsic matrix, occur near the margins of the adamellite body.

5.5 GEOCHEMISTRY

Major and trace element data for a representative suite of the least-altered samples from the Welcome Well complex are listed according to increasing SiO_2 in Table A5.2 (Appendix 1). In Table A5.3 the same data is presented, but the samples with analogous geochemical characteristics have been grouped.

A division of the volcanic rocks into basalt, andesite, dacite and rhyolite using the SiO_2 limits of 53%, 62% and 70% has been adopted for convenience of reference. The additional qualifier low-silica andesite has been used to refer to andesites with < 57% SiO_2. It should be noted that andesites are by far the most voluminous volcanic rock type and that relative to their respective outcrop areas the dacites and basalts are disproportionately represented in Table A5.1.

In the following discussion the geochemical data is interpreted in the first instance as if the samples are related by crystal fractionation to facilitate discussion and to highlight any deficiencies in the simple crystal fractionation model. The alternative of partial melting control on the geochemical behaviour will be developed as the discussion proceeds. The major and trace element results will be considered separately beginning with the case of the major elements.

5.5.1 Major elements

The major element characteristics of the volcanics comprising the Welcome Well complex are typically calc-alkaline. This is demonstrated by:

1) The AFM plot (Fig. 5.7), where the samples define a trend coincident with that of the calc-alkaline Cascades lavas (Carmichael, 1964).

Figure 5.8 Major element variation diagrams for rocks from the Welcome Well complex. The solid lines enclose the field of Cainozoic calc-alkaline volcanics.

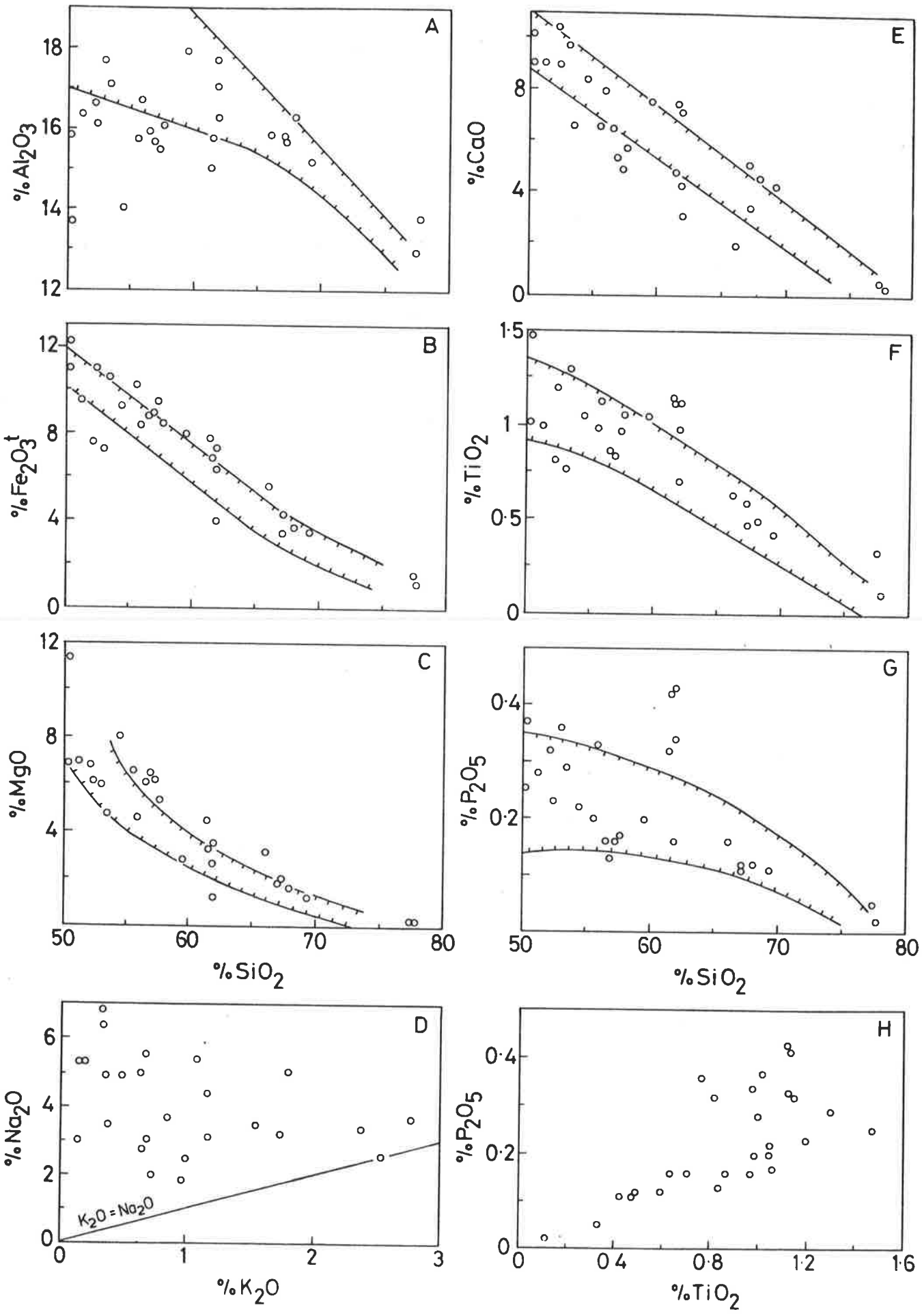

2) The inverse correlations of Al_2O_3, $Fe_2O_3^t$, MgO, CaO, TiO_2 and P_2O_5 with SiO_2 (Fig. 5.8). In each case the majority of the samples lie within or close to the field of Cainozoic calc-alkaline volcanics, indicating that the absolute contents of the major elements at any given SiO_2 are analogous.

It is notable that between 50-60% SiO_2 there is considerable spread in Al_2O_3, TiO_2 and P_2O_5 which cannot be ascribed to a simple differentiation series. Moreover, some high-silica andesites (> 57% SiO_2) are particularly enriched in P_2O_5 and TiO_2 and lie above the general trend. The scatter in the P_2O_5 vs TiO_2 relationship for rocks with low silica contents indicates that the relative enrichments (or depletions) of these two elements are related to different causes (Fig. 5.8H).

Additional features of significance, observable on the variation diagrams and the possible interpretations that may be placed on them are listed below:

1) The relatively tight inverse correlation of $Fe_2O_3^t$ and SiO_2 is suggestive of a differentiation control on Fe. Comparable behaviour of TiO_2, Sc and V, particularly at higher SiO_2, is very likely related to a similar cause (Figs. 5.8F, 5.9E and 5.9F, respectively). This interpretation is supported by the excellent positive correlation of TiO_2, Sc and V with $Fe_2O_3^t$, which provides persuasive evidence that the same mineral(s) are controlling the four elements (Figs. 5.10A, B and C). The chief control on Ti in the calc-alkaline series is likely to be titanium-rich magnetite (Anderson and Gottfried, 1971; Ewart, 1976), since mafic minerals such as clinopyroxene and amphibole usually contain comparable or lower contents of TiO_2 than the melt. Over its interval of crystallisation, Ti-magnetite will also exert the major control on Fe, Sc and V (Kds_c V magnetite/liquid >> Kd Sc, V amphibole, clinopyroxene/liquid, Gill, 1978). Therefore it is probable that the good correlation of Sc, V, TiO_2 and $Fe_2O_3^t$ in rocks with > 55% SiO_2 is due to fractionation of Ti-magnetite. The role of Ti-magnetite fractionation is likely to be particularly important at high silica levels (> 65% SiO_2), where the effects of fractionation of mafic minerals will be considerably reduced. At lower silica levels (between 50-55% SiO_2) complications may be introduced by variable amounts of fractionation of mafic minerals and primary magmatic variations and this may explain in part the poorer correlation of TiO_2, Sc and V with SiO_2 within this silica range.

Figure 5.9 Trace elements vs. SiO_2 for rocks from the Welcome Well complex. The solid lines enclose the field of Cainozoic calc-alkaline volcanics.

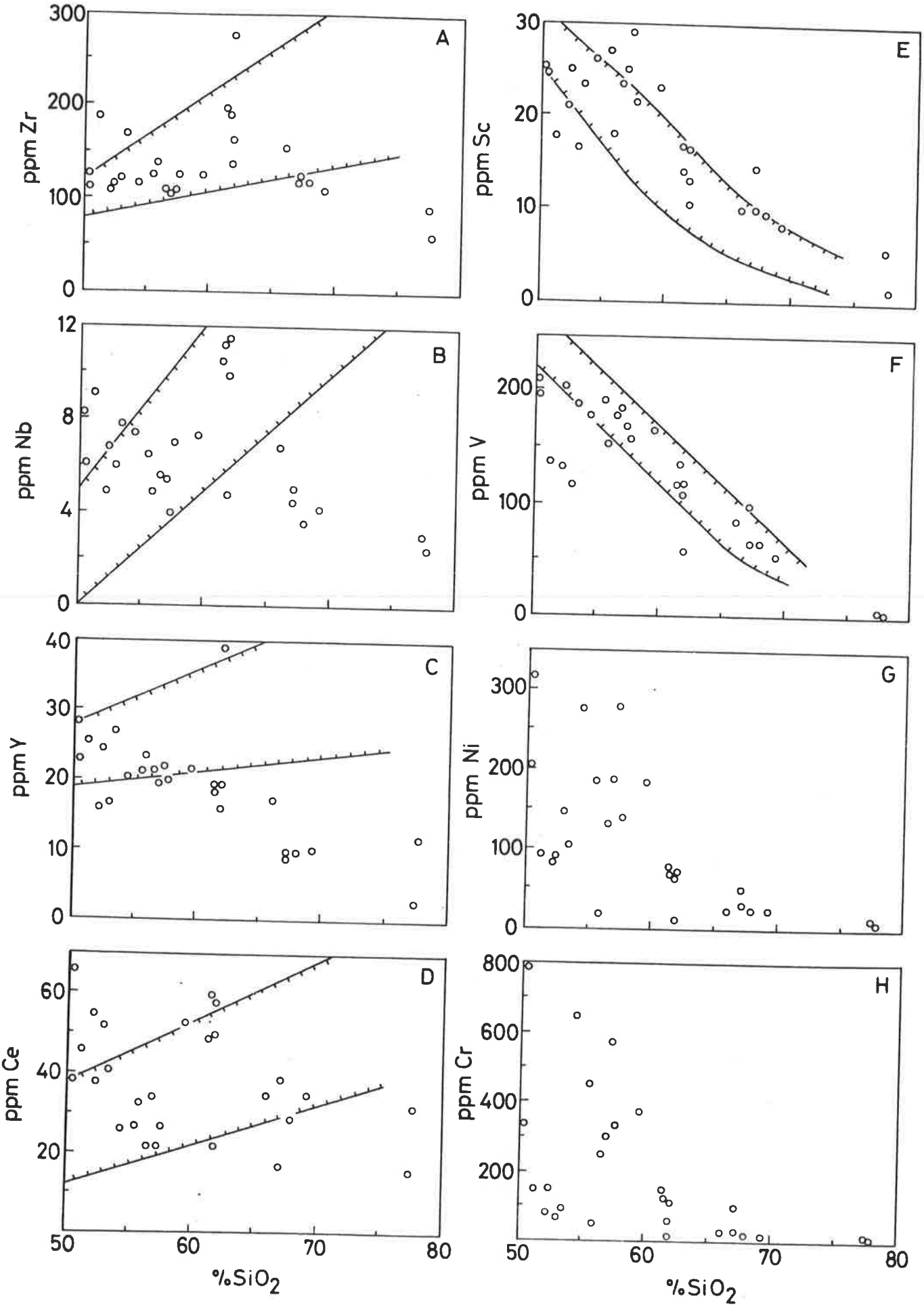

2) Compared with Cainozoic calc-alkaline andesites, some low-silica andesites from the Welcome Well complex are relatively enriched in MgO (Fig. 5.8C). It is notable that MgO does not vary systematically within the 50-57% SiO_2 range, indicating that the samples have not differentiated from a single parent. The subsequent decrease in MgO at higher silica levels however, is consistent with fractionation of mafic minerals.
3) The Al_2O_3 vs SiO_2 plot (Fig. 5.8A), although showing considerable scatter, suggests that plagioclase fractionation may have assumed more importance at higher silica levels (> 60%).
4) Despite the mobility of Na_2O and K_2O during alteration, K_2O is consistently less than Na_2O (Fig. 5.8D), suggesting this characteristic is a primary magmatic feature.

From the above examination of the major elements it is concluded that, in general, the volcanics comprising the Welcome Well complex show typical calc-alkaline trends and similar elemental abundances to modern suites. However, the behaviour of MgO, TiO_2 and P_2O_5 in the basalts and low-silica andesites reveals that not all volcanics can be related to a single parent; rather, derivation from differing parents along parallel lines of liquid descent may be indicated.

5.5.2 Trace elements

A. Ni, Cr

Ni and Cr show a general decrease with rising SiO_2 and significantly, the basalts and andesites are markedly enriched in these elements compared with Cainozoic examples (Fig. 5.9G and H). Collectively, the basalts and andesites show a considerable range in Ni and Cr, presumably reflecting variable amounts of olivine and clinopyroxene fractionation. However, the rocks cannot be related via simple differentiation since sympathetic variations are not shown by MgO (Fig. 5.10E and F). For example, within the 6-7% MgO interval, the range of Ni and Cr contents is too great to be explained by fractionation of olivine and clinopyroxene from a single parent. The linear correlation of Ni and Cr (Fig. 5.10G) suggests that a common factor, other than alteration, has affected the behaviour of both elements. The most plausible explanation is considered to be that offered previously to account for the behaviour of certain of the major elements, viz. differentiation along similar lines of liquid descent from variable parental magmas. How the variations in the parental magmas arose and why the Archaean andesites are relatively enriched in Ni and Cr will be discussed later.

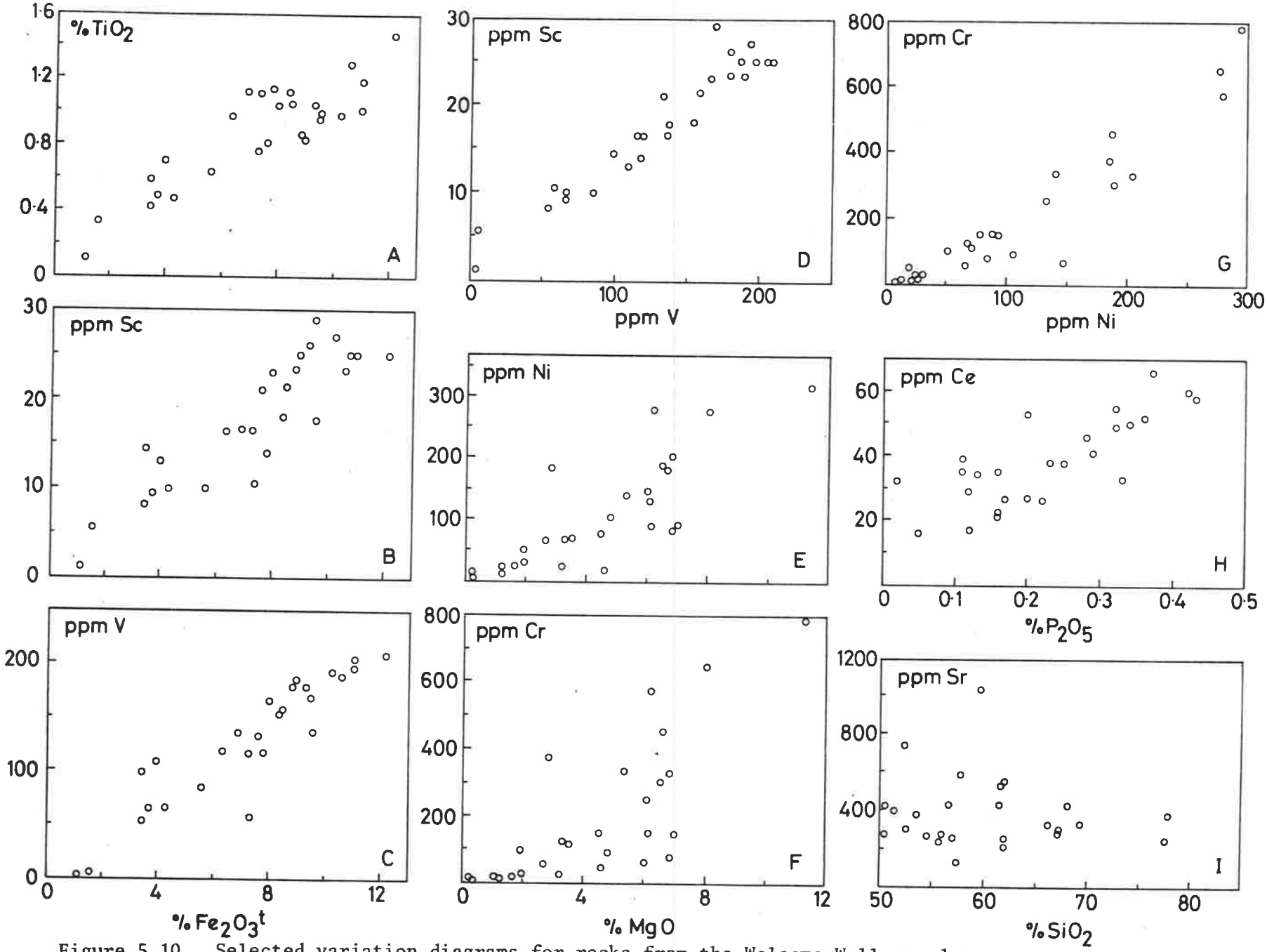

Figure 5.10 Selected variation diagrams for rocks from the Welcome Well complex.

B. Zr, Nb, Y

Zr and Nb show a small, but significant, decrease with rising SiO_2 indicating that they are not behaving incompatibly but rather are being controlled by a mineral or minerals (Fig. 5.9A and B). In both cases a group of samples (W59B, W95, W96, W65) are markedly enriched in Zr and Nb and lie off the general trends. Notable, these samples fall within the general field of Cainozoic calc-alkaline volcanics whereas by comparison the remainder of the samples with similar or greater SiO_2 contents, are relatively depleted in Zr and Nb.

The inverse correlation of Y with SiO_2 (Fig. 5.9C) is of particular note as it parallels the "low-yttrium" trend noted for some lavas from Mt. Ararat and attributed to control by amphibole (Lambert, et al., 1974). If the Kd mineral/liquid for Y is assumed to approximate that of the HREE, then this interpretation is probably applicable in the present case since amphibole is the only modal mineral in the Welcome Well volcanics likely to effect significant control on Y.

While the uniform trend of decreasing Y with increasing SiO_2 could be taken as evidence for a simple, amphibole-dominated differentiation series, the anomalous Zr and Nb data points indicate a more complex history. To explain the samples with relatively enriched Zr and Nb contents it is necessary to invoke either an enriched parental magma or alternatively, diverse trends of crystallisation from a common parent (c.f. Lambert, et al., 1974). The latter alternative is difficult to reconcile with the Y data which indicates that the anomalous samples (excepting W96) have had a similar crystallisation history, at least with respect to amphibole. This question will be examined in greater depth following consideration of additional data.

C. REE (and P_2O_5)

The plot of Ce vs SiO_2 shows considerable scatter, but if the relatively enriched samples are ignored (ie., W59B, W96, W95, W65) an inverse correlation of Ce with SiO_2 is discernable (Fig. 5.9D). Significantly, the samples that are relatively enriched in LREE are the same samples that were previously noted to be enriched in Zr, Nb and P_2O_5. The correlation of high P_2O_5 with high Ce (Fig. 5.10H) verifies this observation and suggests that a common factor is controlling the enrichment of both P_2O_5 and the LREE. It is pointed out that the correlation of P_2O_5 and Ce does not define a differentiation trend, but rather can be viewed as separating the samples into a relatively P_2O_5 and LREE "enriched" group and "normal" group, with both groups showing

Figure 5.11 Chondrite-normalised REE plots for rocks from the Welcome Well complex. W3 - primitive basalt (50.29% SiO_2, 11.37% MgO). W2 - basalt (50.03% SiO_2, 6.82% MgO). W131 - basalt (53.01% SiO_2 5.99% MgO). W5 - andesite (56.9% SiO_2, 6.51% MgO). W14 - andesite (55.87% SiO_2, 4.60% MgO). W95 - andesite (61.90% SiO_2, 3.53% MgO). W17 - dacite (67.12% SiO_2, 1.92% MgO). W146 - rhyolite (77.38% SiO_2, 0.22% MgO).

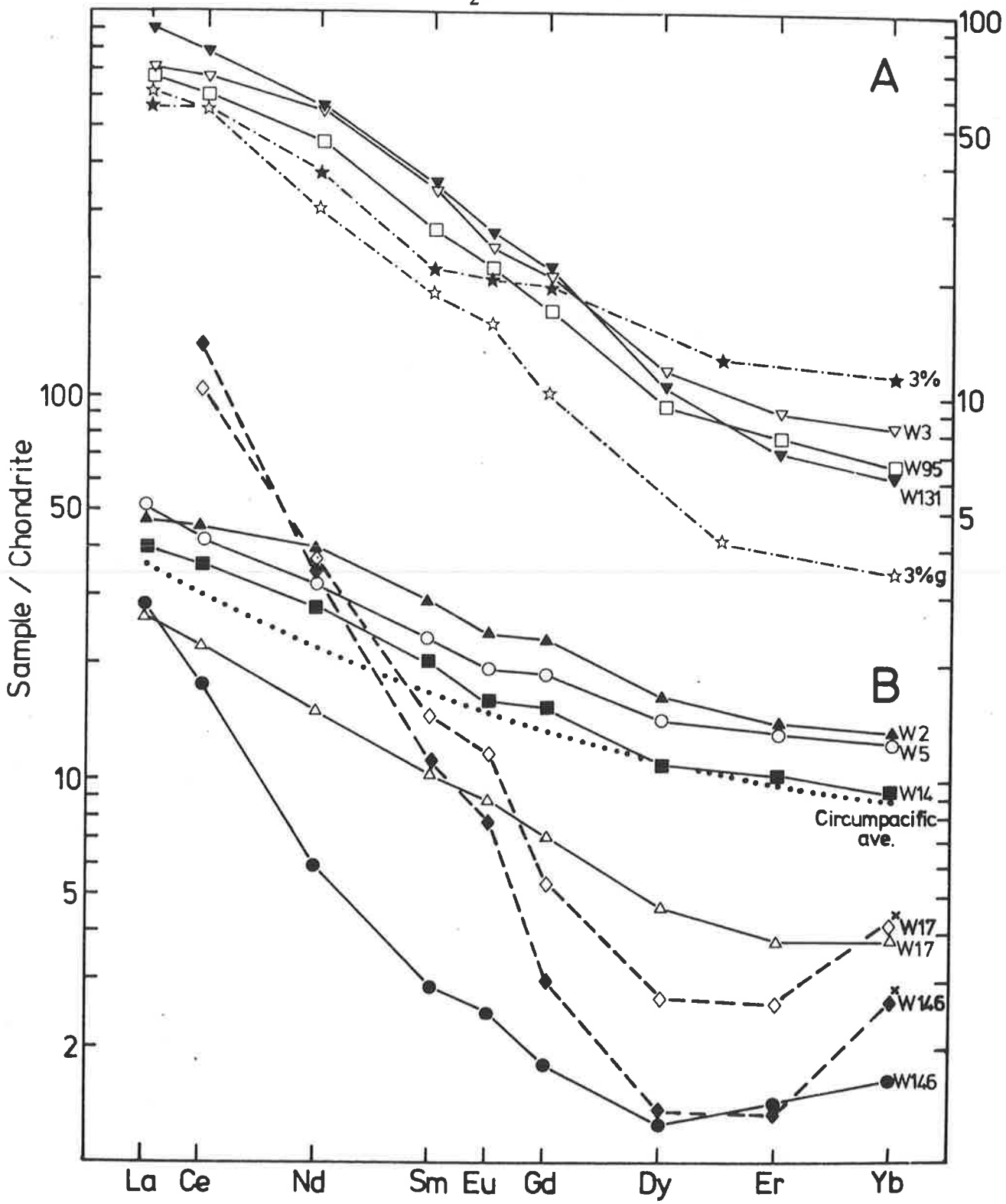

The dash-dot lines are modelled REE patterns assuming 3% partial melting of a flat 2X chondrite garnet-peridotite (3%g - open stars) and non-garnet bearing peridotite (3% - solid stars), followed by 20% fractional crystallisation of olivine (80%) and clinopyroxene (20%) - after Lopez-Escobar, et al., (1977).

The dashed lines are the modelled REE patterns for W17 and W146, assuming derivation by fractional crystallisation from W2. The dotted, circumpacific average REE pattern is after Taylor (1969).

overlap in major elements (see Table A5.3 and Fig. 5.8).

To investigate the question of variable LREE enrichment further, complete REE determinations (by mass spectrometer) were made for eight samples selected to encompass the compositional range, including the P_2O_5 and Ce "enriched" and "normal" examples (data given in Table A5.4, Appendix 1). Predictably, the REE patterns for the basalts and andesites fall into two major groups (Fig. 5.11). One group consists of samples with moderately fractionated patterns (Fig. 5.11B) with La/Yb ranging from 5.5 to 6.2, which is similar to the average circumpacific andesite compiled by Taylor (1969). The other group consists of samples with more fractionated patterns (La/Yb 13-22) resulting from both a HREE depletion and a LREE enrichment relative to the samples from the former group. Garnet is the only mineral in equilibrium with basic magma which could have any significant effect on the slope of the REE patterns, however its removal will only deplete the HREE and effect little change on the LREE. Since garnet fractionation cannot satisfactorily account for the differences between the two patterns it is believed that the distinctive REE characteristics of the two groups of rocks have probably been inherited from the source.

Least squares modelling of the major elements for the samples within the relatively fractionated REE group, reveals that if W131 and W95 were related to W3 and W95 to W131 by crystal fractionation, then amphibole, clinopyroxene, plagioclase and magnetite were likely to have been the major minerals involved (Table 5.1). Since published REE distribution coefficients for all of these minerals in equilibrium with a basic-intermediate melt are < 1 (Arth, 1976), it follows that progressive increases in the absolute contents of all REE should be observed if W3, W131 and W95 are related by crystal fractionation. However, this is contrary to the observed relationship, where HREE are lower in W131 compared with W3 and all REE are lower in W95 (Fig. 5.11A). In view of this, it seems reasonable to conclude that the three samples were derived from separate parental magmas, each with its own distinctive, but fractionated, REE distribution.

Similar conclusions can be drawn from a detailed examination of the group of samples showing less-fractionated REE patterns. For example, fractionation of minerals in the proportions suggested by least squares modelling of the major elements (Table 5.1) could not yield the lower REE content of W5 or W14 compared with W2, again because the published distribution coefficients for the minerals in equilibrium with basic and intermediate melts are all < 1.

TABLE 5.1. Summary of least squares modelling calculations designed to investigate possible paths of crystal fractionation in rocks from the Welcome Well complex.

PARENT				MINERALS									DAUGHTER					
				olivine	clinopyroxene		amphibole		plag.	mag.	apatite							
W3	W2	W131	W95	W3	W3	W95	W22	W31	I12	An54			W5	W14	W95	W17	W146	ΣR^2
*				7.2	1.4			40.6			2.3	0.5			48.3			0.016
	*						15.6		13.5	28.7	6.2	0.46	36.0					0.014
	*						7.3		23.6	18.6	4.8	0.22		45.7				0.004
	*						6.5		35.6	28	6.5	0.51				23.3		0.019
	*						8.2		36.5	33.8	6.8	0.55					14.5	0.0059
		*				1.9		26.5		21.3	1.0	0.43			47.3			0.05
		*				3.4		31.8		26	2.1	0.55				36		0.002
		*				5.2		33.8		33.6	2.6	0.79					23	0.0009
			*			1.7			12.6	11.1	2.2	0.57				74		0.0001
			*			5.8			16.8	28.8	3.1	0.72					46	0.000

Notes:

1. Olivine composition for W3 calculated using the program of Duke and Naldrett (1978).
2. Clinopyroxene and amphibole compositions taken from electron microprobe analyses of phenocrysts in the Archaean calc-alkaline rocks (see Table A 5.5, Appendix 1). The particular compositions chosen were considered most appropriate to the fractionation schemes tested.
3. The plagioclase and apatite compositions are after Wright (1974).
4. The Ti contents of magnetite were adjusted in each case to give the best match for TiO_2. The compositions used ranged from 94% FeO^t and 0% TiO_2 to 80% FeO^t and 14% TiO_2.
5. All weight fractions expressed as percentages.

This reasoning may not necessarily be applicable to the case of W17 (dacite) or W146 (rhyolite) however, since published distribution coefficients for amphibole in equilibrium with acid melts, do exceed one (Arth and Barker, 1976). To test this possibility, the REE contents of W17 and W146 were modelled assuming W2 to be the parent and using the mineral proportions and degree of crystallisation, F, obtained from least squares modelling of the major elements (Table 5.2). The calculated REE patterns show an enrichment in Yb relative to Er and show no negative Eu anomally, both of which are features characterising the REE patterns of W17 and W146 (Fig. 5.11B). However, the calculated LREE contents are much too high, suggesting that either W2 is not a suitable parent (too high in LREE) or Kd amphibole/liquid for LREE is > 1. Assuming the parent to be W2 would require Kd Ce amphibole/liquid to be > 5, which, judging from published distribution coefficients appears to be unrealistically high. It is notable that the Ce contents in the other dacites and rhyolites from the Welcome Well complex (determined subsequently by XRF), are a factor of two higher than in W17 and W146 and thus the discrepancy between the calculated and observed Ce contents may not be significant in these cases. It is also notable that fractionation of the calculated mineral assemblages can account for the levels of Zr, Nb and Sr in W17 and W146, assuming the distribution coefficients for Zr and Nb lie between the values reported for intermediate and acid melts by Pearce and Norry (1979), and that the distribution coefficients for dacitic liquids are applicable to Sr (Arth, 1976).

The important point deducible from these calculations, despite the uncertainties in distribution coefficients and the contents in the source, is that fractionation of the mineral assemblage predicted by the major elements can account for the general characteristics of the REE distribution in the dacites and rhyolites, particularly the HREE (and Y) depletion and absence of a negative Eu anomaly. It can also account for the observed levels of Zr, Nb and Sr in the acid volcanics.

In summary, the complete REE data verifies the separation of the andesites and basalts, indicated by the Ce and P_2O_5 data, into two groups with one showing a relative LREE and P_2O_5 enrichment and HREE and Y depletion compared with the other. Fractionation of the mineral assemblages predicted by the major elements cannot duplicate the levels of REE in samples within each of the groups or between the groups. This suggests fractionation from a range of parental magmas which in turn may have inherited their variability from heterogeneities in the source. The acid rocks possess significantly lower HREE and Y contents and comparable to slightly lower

TABLE 5.2. Results of major and trace element modelling calculations designed to investigate possible crystal fractionation relationships between W2 and W17, W146.

A. Least squares approximation of W17 in terms of W2 and expected minerals.

Rock	W17 obs.	W17 calc.	W2 parent	Mineral compositions used amph.	cpx.	plag.	mag.	apatite
SiO_2	67.12	67.12	50.55	45.66	51.64	54.57		
Al_2O_3	15.78	15.78	15.94	11.10	2.91	28.95		
FeO^t	3.11	3.09	11.03	12.00	9.45		84	
MnO	0.06		0.17					
MgO	1.92	1.91	6.89	15.23	15.85			
CaO	5.08	5.09	10.13	11.86	20.16	11.16		56
Na_2O	5.57		2.53	1.97		5.14		
K_2O	0.68		1.01	0.40		0.21		
TiO_2	0.59	0.72	1.48	1.76	0.60		10	
P_2O_5	0.12	0.11	0.25					44
Total	100.0		100.0					

Mineral	Wt. fraction	Mineral proportion
amph.	0.356	0.46
cpx.	0.065	0.084
plag.	0.28	0.36
mag.	0.065	0.084
apatite	0.0051	0.0066
W17	0.23	
=	W2	
ΣR^2	= 0.018	

Notes:
1. Na_2O, K_2O and MnO were excluded from modelling calculations.
2. Amphibole and clinopyroxene compositions from electron microprobe data for phenocrysts in Archaean calc-alkaline volcanics (in samples W22 and I12 respectively, Table A5.5, Appendix 1).
3. Plagioclase (An_{54}) and apatite compositions after Wright (1974).
4. Ti content of magnetite adjusted to give a satisfactory match for TiO_2.

B. Least squares approximation of W146 in terms of W2 and expected minerals.

Rock	W146 obs.	W146 calc.	W2 parent
SiO_2	77.38	77.38	50.55
Al_2O_3	12.95	12.95	15.94
FeO^t	1.39	1.40	11.03
MnO	0.03		0.17
MgO	0.22	0.22	6.89
CaO	0.50	0.49	10.13
Na_2O	6.84		2.53
K_2O	0.33		1.01
TiO_2	0.33	0.25	1.48
P_2O_5	0.05	0.06	0.25
Total	100.0		100.0

Mineral	Wt. fraction	Mineral proportion
amph.	0.37	0.43
cpx.	0.082	0.096
plag.	0.34	0.39
mag.	0.068	0.08
apatite	0.0055	0.0064
W146	0.145	
=	W2	
ΣR^2	= 0.006	

Notes:
1. Na_2O, K_2O and MnO excluded from modelling calculations.
2. Mineral compositions as reported in Table 5.2A excepting for magnetite which has the composition 83% FeO^t and 11% TiO_2.

C. Calculated trace element abundances using mineral proportions and degree of crystallisation obtained from major element modelling calculations.

Rock	A. W2 obs.	W17 obs.	W17 calc.1	W17 calc.2	B. W146 obs.	W146 calc.	Distribution coefficients used amph.	cpx.	plag.	mag.	apatite
Ce	42.9	22.2	103.4	71.5	17.6	89	0.9(0.34)	0.33(0.21)	0.24(0.28)	0	18.0
Nd	40	15	77.3	16.9	5.94	15.2	2.8(0.56)	0.71(0.43)	0.17(0.20)	0	27.4
Sm	29.2	10.3	42.3	5.3	2.88	3.93	3.99(0.93)	1.09(0.74)	0.13(0.17)	0	29.3
Eu	23.9	8.9	24.9	2.4	2.53	1.26	3.44(1.1)	1.04(0.75)	2.11(0.73)	0	20.5
Gd	23	7.2	29.2	1.57	1.8	0.94	5.48(1.1)	1.23(0.87)	0.09(0.21)	0	27.2
Dy	16.5	4.6	22.6	0.7	1.27	0.38	6.2(1.0)	1.31(1.0)	0.086(0.19)	0	25.6
Er	14.1	3.78	19.9	0.76	1.46	0.43	5.94(1.0)	1.23(1.1)	0.084(0.24)	0	20.0
Yb	13.1	3.86	19.4	1.56	1.67	1.07	4.89(0.98)	1.1(1.0)	0.077(0.30)	0	13.1
Sr	262	294		313	251	308	0.46	0.12	1.8	0	0
Zr i	125	121		194	91	245	1.4	0.25	0.03	0.2	0
Zr a	125	121		29	91	24	4	0.6	0.1	0.8	0.1
Nb i	7.2	4.5		10.9	3.1	13.6	1.3	0.3	0.025	1	0
Nb a	7.2	4.5		1.4	3.1	1.0	4	0.8	0.06	2.5	0.1
Y i	28	9.4		14	2.9	13	2.5	1.5	0.06	0.5	20
Y a	28	9.4		0.66	2.9	0.28	6.	4	0.1	2	40

Notes:
1. REE distribution coefficients for W17 calc.1 are in brackets and are the high values reported by Arth (1976) for basaltic and andesitic rocks.
2. The REE and Sr calculations for W146 and W17 calc.2 utilize the values for dacitic rocks reported by Arth (1976).
3. The Zr, Nb and Y distribution coefficients are after Pearce and Norry (1979). The subscripts i and a refer to calculations which utilize values quoted by these authors for intermediate and acid rocks, respectively.
4. All of the REE abundances quoted are chondrite normalised.

Ce contents than the intermediate and basic rocks. Modelling calculations suggest that fractionation of amphibole-bearing mineral assemblages from intermediate or basic parents could account for the HREE and Y contents in the acid rocks, although distribution coefficients higher than those published in the literature would be required to accomodate the observed levels of Ce.

5.6 ORIGIN OF THE PRIMARY MAGMA

5.6.1 General discussion

Several important points emerge from the data presented above:

1) There is a close association of all volcanic rock types in the field; all are confined to the one volcanic pile and were presumably erupted from the same general vent zone.
2) There is a petrographic and geochemical gradation from basalt through andesite to dacite.
3) The rocks display marked calc-alkaline patterns of elemental behaviour.
4) A detailed evaluation of the geochemical data suggests a complex origin for the primary magma as well as a complicated crystallisation history.

Models proposed to account for the origin of Archaean acid-intermediate magmas are diverse, but fall into three main groups:

1) Partial melting of an amphibolitic (basic) lower crust. This model has been suggested by Taylor and Hallberg (1977) to explain the origin of andesites from the Marda Complex. Condie and Harrison (1976) proposed a similar model to account for the origin of the intermediate and acid volcanics in the Midlands greenstone belt of Rhodesia, although they considered the melting occurred under eclogite rather than amphibolite facies conditions. Similarly, Glikson (1976) in his general review of Archaean magmatism, favoured a mafic crustal source for the Archaean intermediate magmas.
2) Partial melting of the mantle and subsequent crystal fractionation to produce the spectrum of compositions observed. This model has been proposed by Hawkesworth and O'Nions (1977) from their study of Rhodesian calc-alkaline volcanics: they considered the primary mantle-derived magma was modified by garnet ± amphibole fractionation to yield a series of volcanics with calc-alkaline affinities.
3) A combination of 1) and 2) with the added possibility of involvement of the tonalitic upper crust in the generation of the acid magma (c.f. Glikson, 1976; Condie, 1976).

TABLE 5.3. Results of least squares modelling calculations for W14, W23, W95 and W17 in terms of likely residual minerals and a hypothetical crustal source with the composition of Hallberg and William's (1972) average Eastern Goldfields Archaean tholeiite.

Rock	W14 product	crustal source obs.	crustal source calc.	W23 product	crustal source calc.	W95 product	crustal source calc.	W17 product	crustal source calc.
SiO_2	56.57	52.31	52.31	57.96	52.28	62.13	52.31	67.12	52.31
$Al_{2}O_{3}$	16.91	15.09	15.09	16.16	15.16	16.31	15.09	15.78	25.09
FeO^t	7.62	10.71	10.71	7.64	10.71	5.72	10.70	3.11	10.71
MnO	0.15			0.13		0.10		0.06	
MgO	4.66	6.83	6.83	5.34	6.97	3.54	6.82	1.92	6.83
CaO	8.00	11.01	10.99	5.72	10.95	7.10	11.02	5.08	11.01
Na_2O	3.76	2.75		3.43		3.08		5.57	
K_2O	0.86	0.18		2.38		0.69		0.68	
TiO_2	1.13	0.98	0.86	1.06	1.02	0.97	1.12	0.59	1.02
P_2O_5	0.33	0.12		0.17		0.34		0.12	
Total	100.0	100.0		100.0		100.0		100.0	

Component	Wt. fraction	Mineral proportion		Wt. fraction	Mineral proportion		Wt. fraction	Mineral proportion		Wt. fraction	Mineral proportion
W14	0.065		W23	0.48		W95	0.45		W17	0.346	
amph.	0.041	0.11					0.13	0.23		0.17	0.255
cpx.	0.19	0.47		0.25	0.47		0.19	0.34		0.20	0.31
plag.	0.122	0.30		0.22	0.42		0.176	0.32		0.22	0.33
mag.	0.046	0.12		0.061	0.114		0.06	0.114		0.074	0.112
	= source			= source			= source			= source	
ΣR^2	0.014			0.0315			0.019			0.0017	

	Mineral compositions used amph.	cpx.	plag.	mag.
SiO_2	42.1	51.92	52.07	
$Al_{2}O_{3}$	14.7	2.45	30.63	
FeO^t	10.3	6.82		88
MgO	15.5	17.67		
CaO	11.5	21.13	13.13	
Na_2O	2.9		3.98	
K_2O	1.0		0.21	
TiO_2	1.5	0.60		6

Notes:
1. Na_2O, K_2O, MnO and P_2O_5 excluded from modelling calculations.
2. Amphibole and clinopyroxene compositions taken from electron microprobe data for phenocrysts in basaltic rocks from the Welcome Well complex (W31 and W3 respectively, see Table A5.5, Appendix 1).
3. Plagioclase is $An_{64.6}$ after Wright (1974).
4. Magnetite composition for W14 model is 94% FeO^t and 0% TiO_2.

If the basic crustal source is assumed to approximate the composition of an average Archaean tholeiite (e.g. after Hallberg and Williams, 1972; see Tables 5.3 and 5.4), then it is evident that compositional limitations would preclude derivation of the Welcome Well basalts and low-silica andesites from the crust, since most of these rocks have MgO, Ni and Cr contents comparable with the average tholeiite. This does not necessarily exclude a crustal origin for the more acid rocks however (e.g. high-silica andesites, dacites and rhyolites), and to test this possibility a combined major and trace element modelling approach was adopted.

It was assumed for the purposes of modelling that the basic source had the composition of Hallberg and William's (1972) average Archaean tholeiite with a flat 10 X chondrite REE pattern (c.f. Condie, 1976; Sun and Nesbitt, 1978; Stolz, 1980). Least squares modelling of the major elements of W23 (high-MgO, low-silica andesite), W14 (fractionated, low-silica andesite), W95 (high-silica andesite) and W17 (dacite) in terms of this source and likely residual minerals, yielded satisfactory solutions which indicated varying proportions of residual clinopyroxene, amphibole, plagioclase and magnetite (Table 5.3). Other mineral combinations involving plagioclase and amphibole with or without garnet and/or orthopyroxene, failed to give acceptable solutions.

Trace element modelling computations using the calculated mineral proportions and degrees of melting, and appropriate distribution coefficients failed to duplicate the observed trace element levels in any of the four samples examined (Table 5.4). For example in the case of W14, W23 and W95 the calculated contents of Ce, Zr, V, Cr and Sr fall short of the actual values by significant amounts. Similar comments apply to W17, excepting for Ce which shows a close match; however it is evident that the markedly higher Ce contents in the other dacites (W29, W145 and W144) could not be matched. The calculated Ni content in W23 and W95 also falls short of the observed value. This does not apply in the case of W14 and W17 presumably due to their more fractionated nature. A further important observation is that the calculated HREE and Y contents in all samples exceeds the actual values. This disparity could be eliminated by invoking small amounts of garnet in the residue, but residual garnet would further add to the mismatch in V and Cr and would not alleviate the relatively low calculated contents of Ce and Zr.

In all cases the discrepancies are so great as to preclude an explanation in terms of the uncertainties in the modelling calculations. Moreover, with few exceptions, the discrepancies are consistent over the

TABLE 5.4. Calculated trace element abundances in W14, W23, W95 and W17 assuming a basic crustal source and using mineral proportions and degree of melting obtained from major element modelling calculations reported in Table 5.3

	crustal source	W14 obs.	W14 calc.	W23 obs.	W23 calc.	W95 obs.	W95 calc.	W17 obs.	W17 calc.
Zr	61	138	94	125	119	160	113	121	133
Nb	3.2	5.3	4.7	7	6	9	5.4	4.5	6
Y	20	24	26.5	20	32	16	29	9.4	32
Ce	8	29	12	27	15	49	15	18	18
Sm	1.9	3.8	2.6			5.11	3.1	9.0	3.5
Yb	2.1	2.02	2.8			1.35	3.3	2.0	3.7
Sr	105	278	122	586	116	552	124	294	126
Sc	40	18	22	21	30	16	14.7	14	12.6
V	320	154	89	158	127	119	49	99	40
Cr	367	51	41	336	39	119	31	101	27
Ni	170	19.6	67	140	70	70	53	51	47

Notes:
1. Distribution coefficients used are those reported in Table 3.3B.
2. Zr, Ni, Cr, V and Sr values in assumed basic source are after Hallberg and Williams (1972) average Eastern Goldfields Archaean tholeiite. The remainder of the values are best estimates based on the data of Nesbitt and Sun (1976), Purvis (1978), Stolz (1980) and unpublished data of the writer.

compositional range tested, and thus it appears that a basic crustal source, with the composition of an average Archaean tholeiite, is improbable for the andesitic and dacitic magmas. It will be noted that rhyolitic compositions (e.g. W146) were not modelled from this source mainly because of uncertainties in the residual mineral compositions and the errors these uncertainties introduce, owing to the relatively high proportion of residue. On qualitative grounds such a source is thought unlikely however, since Helz (1976) has shown experimentally that low-degree melts from analogous basic sources have $K_2O > Na_2O$, contrary to that consistently observed in the rhyolites from the Welcome Well complex. In addition, the probable relatively high proportion of residual plagioclase would be expected to yield a negative Eu anomaly and severe Sr depletion in the equilibrated acid magma - neither of which characterise the rhyolites analysed.

The possibility of a more basic crustal source (e.g. ultramafic - high Mg basalt composition) cannot be excluded, but in this case although the degree of melting would be significantly lower, the discrepancies in Ce, Zr, V and Sr would not be removed owing to the lower contents of these elements in this source compared with a tholeiitic source (Sun and Nesbitt, 1978; Glikson, 1979a; Stolz, 1980). To explain the short-fall in LIL elements (e.g. Ce and Zr) it could be proposed that they were contributed from tonalitic rocks which may have also been involved in anatexis. However, the following points argue against this possibility:

1) The tonalitic contribution would not account for the discrepancies in V, Sc, Y, HREE, Ni and Cr, even if it were able to explain the LREE and Zr contents of the andesites and dacites.
2) Experimental evidence shows that melts derived from a tonalitic source have higher K_2O/Na_2O than the source (often $K_2O/Na_2O > 1$, Brown and Bowden, 1973). The extremely low K_2O/Na_2O of the andesites and dacites (less than that in typical tonalites) therefore argues against any addition of melt from a tonalitic source. This evidence also indicates that the rhyolites (e.g. W146) with their extremely low K_2O/Na_2O values are unlikely to be direct melts from a tonalitic source.
3) Melts derived from a tonalitic source would be expected to show a negative Eu anomaly because of the abundant residual plagioclase (Brown and Bowden, 1973). Significantly, neither the dacites nor rhyolites are depleted in Eu, further suggesting any tonalitic contribution must have been negligible.

TABLE 5.5. Least squares approximation of primitive basalt (W3) in terms of a hypothetical mantle source and possible residual minerals

Rock	W3 melt	pyrolite obs.	pyrolite est.	Mineral compositions used ol.	opx.	cpx.
SiO_2	51.00	45.2	45.22	41.0	54.4	54.3
Al_2O_3	13.88	3.5	3.29		0.6	1.0
FeO^t	10.03	10.0	10.30	11.1	6.6	4.1
MnO	0.18					
MgO	11.53	37.5	37.41	47.7	33.0	18.5
CaO	9.11	3.10	3.08	0.2	1.6	20.8
Na_2O	1.89					
K_2O	0.98					
TiO_2	1.02	0.17	0.26		0.2	0.3
P_2O_5	0.38					
Total	100.0					

Mineral	Wt. fraction	Mineral proportion
ol.	0.655	0.844
opx.	0.087	0.112
cpx.	0.0338	0.044
W3	0.231	
	= pyrolite	
ΣR^2	= 0.1515	

Notes:

1. Pyrolite composition is modified from Ringwood (1966). The TiO_2 content of Ringwood's pyrolite has been reduced from 0.7% to 0.17%, while the FeO^t content has been increased from 8.5% to 10.0% in order to obtain satisfactory matches for these elements. The former modification is consistent with estimates of Archaean pyrolite given by Green (1975) and Sun and Nesbitt (1977), while the latter is consistent with Glikson's (1979) proposal of a more iron-rich Archaean mantle and the high end of the Archaean pyrolite range (9.7% FeO^t) estimated by Sun and Nesbitt (1977).
2. Addition of variable proportions of olivine to W3 failed to yield a satisfactory match for unmodified pyrolite.
3. Olivine, orthopyroxene and clinopyroxene compositions taken from experimental data of Green (1976) for 1100°C, 10 kb conditions.

The important point resulting from the modelling calculations and the above discussion is that the geochemistry of the acid and intermediate volcanics is incompatible with an origin by simple batch partial melting of typical crustal source rocks. This fact, combined with experimental evidence, which indicates that low-MgO acid and intermediate magmas are unlikely to be derived by direct partial melting of the mantle (Green, 1976; Wyllie, et al., 1976), leads to the inescapable conclusion that the acid and intermediate rocks must have been derived by crystal fractionation from more basic parents, which in turn implies an ultimate mantle origin. The petrographic and geochemical continuity of the basic, intermediate and acid rocks, in combination with their close association in the field, provides persuasive independent support for this proposal.

5.6.2 Conditions of magma segregation

Of the rocks analysed from the Welcome Well complex, W3 is the most primitive, judging from its Mg number (70) and Ni and Cr contents (317 ppm Ni and 800 ppm Cr). Least squares approximation of the major elements of this sample in terms of a hypothetical mantle composition (modified pyrolite, after Ringwood, 1966) and possible residual minerals (compositions after Green, 1973) shows that a good match can be obtained assuming 20-25% partial melting leaving a residue of olivine, orthopyroxene and clinopyroxene (Table 5.5). This result is in agreement with trace element modelling which demonstrates that in order to duplicate the absolute contents of V (197 ppm) and Sc (28 ppm) in the primitive basalt, approximately 20-25% melting of the mantle leaving a residue of 70% olivine, 20-25% orthopyroxene and 5-10% clinopyroxene is necessary (mantle abundances of Sc and V and Kds after compilation of Frey et al., 1978; calculations reported in Table A2.5, Appendix 1).

Significantly, at the relatively high degrees of melting indicated (ie., 20-25%), clinopyroxene is stable only under relatively hydrous conditions and at low pressures (< 20 kb, Green, 1973, 1976). The important implication of this is that the primitive basalt was probably generated by relatively high degrees of melting of hydrous mantle at shallow depths.

It has been previously noted that, as a group, the more evolved basalts and low-silica andesites show a limited range in MgO (6-8%) over a wide SiO_2 interval (50-57%) and that within this MgO interval Ni and Cr vary greatly (Ni, 80-300 ppm and Cr, 100-600; see Figs. 5.8C, 5.10E and F). Neither feature can be reconciled with a simple differentiation series in which the evolved basalts and andesites have fractionated from

TABLE 5.6. Experimentally-determined melt compositions compared with calc-alkaline volcanic rocks from the Welcome Well complex.

	A	W3	W14	B	W4	W123	W49	C
SiO_2	49.8	50.29	55.87	55.5	54.42	55.55	57.30	53.8
$Al_2O_{3_t}$	12.0	13.69	16.70	12.3	14.03	15.73	15.46	9.7
Fe_2O_3	10.4	10.99	8.37	8.0	9.29	10.22	9.47	10.44
MnO	0.2	0.18	0.15	0.10	0.16	0.16	0.15	0.2
MgO	12.6	11.37	4.60	9.3	8.02	6.58	6.19	14.1
CaO	10.4	8.98	7.90	10.4	8.32	6.50	4.84	8.6
Na_2O	2.0	1.86	3.71	2.0	3.15	3.50	4.44	1.7
K_2O	0.5	0.97	0.85	0.5	1.18	0.38	1.17	0.4
TiO_2	2.6	1.01	1.12	2.5	1.04	0.98	0.96	2.0
P_2O_5		0.37	0.33		0.22	0.20	0.16	
Total		99.71	99.60		99.83	99.80	100.14	
LOI		3.70	1.81		2.22	3.80	4.27	
Zr		111	138		116	125	108	
Nb		6.1	5.3		7.4	6.5	4	
Y		23	24		21	21	22	
Ce		55	29		27	27	22	
Nd		34	17		24	21	21	
Sc		28	18		26	27	29	
V		197	154		179	193	169	
Cr		799	51		650	455	575	
Ni		317	20		276	186	279	
Rb		24	18		25	13	22	
Sr		421	278		266	235	128	
Ba		270	251		256	80	271	

A. Preferred equilibrium liquid composition produced by water-saturated melting of pyrolite at 1100°C, 20 kb (27% partial melting).

B. As for A. at conditions of 1100°C, 10 kb.

C. As for A. at conditions of 1200°C, 10 kb (35% partial melting).

Note: Compositions of A, B and C taken from experimental work of Green (1973, 1976).

parental magmas of similar type. Alteration or preferential partitioning of Ni into sulphide phases are also considered to be unlikely explanations for this behaviour, owing to the moderately good positive correlation of Ni and Cr which indicates that some common factor, other than differentiation, is controlling the behaviour of both elements simultaneously (Fig. 5.10G).

A possible explanation is provided by the experimental work of Green (1973, 1976), which demonstrates that under conditions of hydrous melting in the upper mantle, a variety of primary basic magmas, differing chiefly in their SiO_2 and MgO contents, can be produced in response to varying pressures. At 20 kb, basic magmas comparable in composition to the primitive basalt are produced (compare analysis A with W3, Table 5.6), while at 10 kb the primary basic magmas are significantly higher in SiO_2 (55-56% SiO_2) and lower in MgO (approximately 9% - see analysis B, Table 5.6, after Green, 1976). Thus, it is possible that the primary magmas which gave rise to the low-silica, high-MgO andesites (e.g. W4, W123 and W49, Table 5.6) were initially relatively high in SiO_2 and low in MgO, comparable with melts produced at 1100°C, 10 kb (analysis B, Table 5.6). Consequently, many of these andesites may be little removed from their parental magmas, hence explaining why they are relatively enriched in MgO, Ni and Cr for their particular SiO_2 contents. On the other hand, the more fractionated andesites with lower Ni and Cr contents (e.g. W14, Table 5.6), may have been derived by extended differentiation from a lower SiO_2 and higher MgO parent more like the primitive basalt (W3, Table 5.6). It therefore appears that the variability of MgO, Ni and Cr observed in the low-silica andesites and basalts can be satisfactorily explained in terms of differentiation from a range of primary magmas that have been produced as a result of partial melting of the uppermost mantle over a pressure interval of roughly 10-20 kb.

5.6.3 Nature of the mantle source

The basic and intermediate rocks comprising the Welcome Well complex show two important REE characteristics which must be explained in any petrogenetic models, viz. relatively fractionated REE patterns and two groups of REE patterns.

Some andesites from the Andean volcanic chain have very similar REE patterns to the most-fractionated group (Fig. 5.11A) and Lopez-Escobar *et al.*, (1977) have satisfactorily modelled the patterns by assuming 3% partial melting of a flat 2x chondrite garnet-peridotite mantle source followed by 20% fractionation of olivine (80%) and clinopyroxene (20%). Similarly these authors have modelled the REE of a high-alumina basalt,

Figure 5.11 Chondrite-normalised REE plots for rocks from the Welcome Well complex. W3 - primitive basalt (50.29% SiO_2, 11.37% MgO). W2 - basalt (50.03% SiO_2, 6.82% MgO). W131 - basalt (53.01% SiO_2, 5.99% MgO). W5 - andesite (56.9% SiO_2, 6.51% MgO). W14 - andesite (55.87% SiO_2, 4.60% MgO). W95 - andesite (61.90% SiO_2, 3.53% MgO). W17 - dacite (67.12% SiO_2, 1.92% MgO). W146 - rhyolite (77.38% SiO_2, 0.22% MgO).

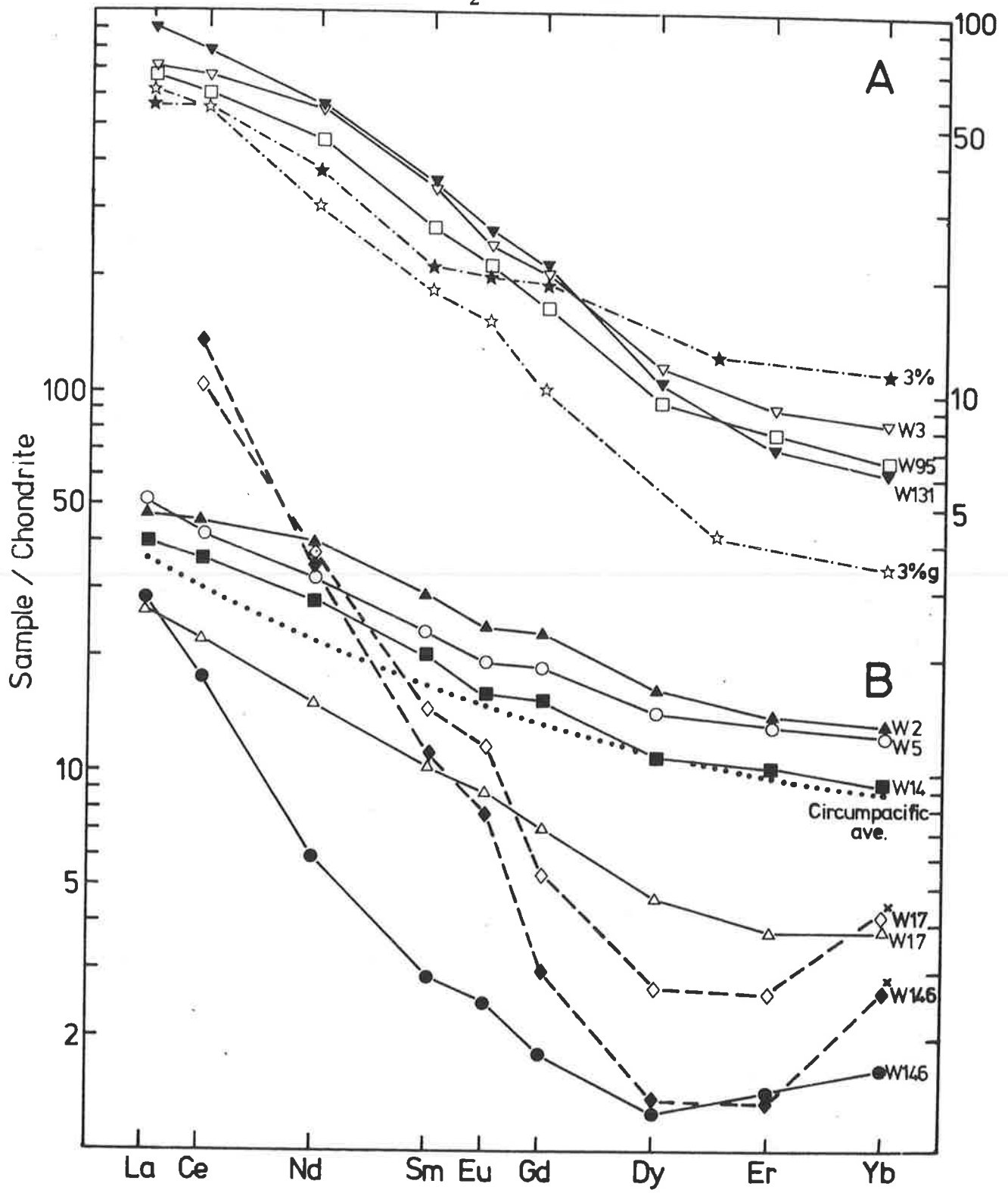

The dash-dot lines are modelled REE patterns assuming 3% partial melting of a flat 2X chondrite garnet-peridotite (3%g - open stars) and non-garnet bearing peridotite (3% - solid stars), followed by 20% fractional crystallisation of olivine (80%) and clinopyroxene (20%) - after Lopez-Escobar, et al., (1977).

The dashed lines are the modelled REE patterns for W17 and W146, assuming derivation by fractional crystallisation from W2. The dotted, circumpacific average REE pattern is after Taylor (1969).

which has a comparable REE pattern to the less-fractionated group (Fig. 5.11B), by assuming it was derived by 3% partial melting of a flat 2x chondrite peridotite source (non-garnet bearing), followed by 20% fractionation of olivine (80%) and clinopyroxene (20%). Although the REE can be satisfactorily explained in this manner, experimental evidence suggests that melts produced under these conditions (ie. 3% partial melting) are undersaturated olivine melilitites or olivine nephelinites (Green, 1971) and do not resemble the presumed parental magmas for the Welcome Well complex. Moreover, the relatively low degrees of melting are inconsistent with the previously cited calculations based on the major element and Sc and V contents of the primitive basalt (W3), which indicated degrees of melting in excees of 20%.

The constraint imposed on the degree of melting by the LREE, can be negated if it is proposed that the mantle source was relatively enriched in LREE, in contrast with the flat REE distribution assumed by Lopez-Escobar, et al. (1977). This proposal is supported by the greater than chondritic values for Ce/Zr in the basalts and low-silica andesites (Table 5.7). The greater than chondritic values for Zr/Ti, Zr/Y and P_2O_5/TiO_2 also suggest a relative enrichment of Zr, Nb and P, in addition to LREE, in comparison with a primitive, chondritic mantle (Table 5.7). Presumably the mantle source in this case was variably-enriched in P and LREE in order to account for the variable Ce/Zr and P_2O_5/TiO_2 values and the variable LREE contents in the basalts and andesites (Table 5.7 and Fig. 5.11, respectively).

A LIL element-enriched mantle source does not explain the difference in HREE between the two groups of samples however, and it is possible that garnet involvement as invoked by Lopez Escobar, et al. (1977), may have some merit in explaining these differences. Apart from controlling HREE, garnet would also be expected to control Sc, V and Y (Kd Sc garnet/liquid $\simeq$ 4; Kd V garnet/liquid $\simeq$ 8; Kd Y garnet/liquid $\simeq$ Kd Yb garnet/liquid $\simeq$ 4; Gill, 1978), but there are no significant differences in the values of the elemental ratios involving these elements between the two groups of samples (e.g. Ti/V, Ti/Sc, Ti/Y and Zr/Y for W3 compared with W125 or W123, Table 5.7), suggesting that garnet control has been negligible. Furthermore, experimental data for shallow, hydrous melting of the mantle demonstrates that garnet is not stable in the residue under these conditions. Thus, two independent lines of evidence do not favour garnet at the site of partial melting as being responsible for the observed depletion in HREE in the group of samples with more fractionated REE patterns.

TABLE 5.7. Elemental ratios for the most basic rocks from the Welcome Well complex.

Ratio	Probable chondritic value	W24	W7	W150	W3	W2	W111	W131	W4	W123	W125	W5	W23
$Zr/_{Ce}$	7.4-7.7	1.9	6.2	10	1.7	3.3	3.0	2.3	4.4	4.6	5.0	6.0	4.6
$Zr/_{Y}$	2.5-2.8	4.2	4.2	2.65	4.8	4.5	4.7	7.2	5.6	5.9	5.1	5.4	6.3
$Ti/_{Zr}$	100-110	138	57	100	55	70	62	38	54	47	47	47	50
$Ti/_{Y}$	250-280	581	238	265	263	315	291	271	304	276	241	255	315
$Zr/_{Nb}$	16-18	7.4	16	19	18	19	17	20	16	19	19	19	18
$Ti/_{V}$	8.4-10	20	18	23	31	42	35	39	35	30	29	27	40
$Ti/_{Sc}$	78-85	142	106	171	242	353	286	276	239	217	231	199	294
TiO_2/P_2O_5	STP=10	10	8.5	9.8	2.7	5.9	5.2	2.1	4.7	4.9	5.4	6.4	6.2
$\%SiO_2$		40.78	50.25	47.98	50.29	50.03	52.39	53.01	54.42	55.55	56.51	56.90	57.63
%MgO		34.95	17.26	5.74	11.37	6.82	6.13	5.99	8.02	6.58	6.07	6.51	5.31

Notes: 1. W24 and W7 are ultrabasic dykes, intrusive into the calc-alkaline volcanic pile. W150 is a tholeiitic basalt overlying the calc-alkaline volcanics. The remainder of the samples are volcanics from the Welcome Well complex.

2. Source of chondritic values given in Table 2.6.

It is possible that the HREE (and LREE, P, Zr and Nb) characteristics of the mantle source may have been superimposed prior to, or during, the magma segregation event by the introduction of a component from a deeper zone of the mantle in which garnet was stable. The signature of residual garnet would thus be imprinted on the REE distribution, and it is probable that a spectrum of HREE depletion would be produced depending on the extent of incipient melting and hence amount of residual garnet. A similar hypothesis has been advanced to explain the supposed zonation of the modern low velocity zone (Green and Liebermann, 1976) and the generation of suites of basalts showing variable LREE and HREE enrichments (Frey, et al., 1978).

It is concluded that the geochemical properties of the basaltic and low-silica andesitic members of the Welcome Well complex are most consistent with an origin involving fractionation from primary magmas derived by shallow, hydrous melting of a LIL element-enriched mantle source. Models which propose a crustal source for the high-silica andesites, dacites and rhyolites fail when tested quantitatively, but a hypothesis involving crystal fractionation from parental, basic magmas can be substantiated with the available data. The genetic relationship between the basic, intermediate and acid members of the Welcome Well complex implied by the crystal fractionation link is strongly supported by the close field association of all rock types and by the petrographic gradations observed between them.

5.7 CRYSTALLISATION HISTORY

In view of the direct and indirect evidence previously cited for the importance of differentiation in producing the calc-alkaline Welcome Well volcanic series, it is relevant to investigate the crystallisation history of the magmas. At the outset it is important to ascertain the minerals which have been involved. On petrographic grounds it would be expected that clinopyroxene, amphibole, plagioclase and magnetite would have exerted a major influence on the crystallisation and this conclusion is supported by the geochemistry of the samples discussed previously.

For example, evidence of amphibole involvement is provided by the major element modelling calculations, all of which necessitate significant amount of amphibole fractionation in order to obtain a satisfactory solution (Table 5.1). Also, the control on Y (Fig. 5.9C) and HREE (Fig. 5.11) can only be satisfactorily explained by removal of amphibole.

Fractionation of Ti-magnetite is indicated by the control on Fe, Ti, Sc and V, particularly at high SiO_2 levels where the effect of fractionation

of mafic minerals is likely to be negligible. This is consistent with experimental evidence which shows that magnetite crystallises later than most silicate minerals under oxygen fugacities normally thought to exist in calc-alkaline magmas (e.g. Eggler, 1972; Eggler and Burnham, 1973).

Involvement of clinopyroxene and plagioclase is inferred not only from modelling calculations but also from their relative abundance as phenocrysts. It is notable that although these two minerals are far more abundant in the mode than amphibole, their proportions of fractionation, as indicated by the major element modelling calculations, are invariably less than for amphibole. Thus, it appears that the role of amphibole in producing the fractionation trends is camouflaged to some extent by the present mineral assemblages in the andesites. Additional evidence for the involvement of amphibole, clinopyroxene, Ti-magnetite and plagioclase is provided by the Zr, Nb and Sr modelling calculations for W17 and W146 (Table 5.2C), which show that this mineral assemblage can account for the observed controls on these elements (Fig. 5.9A and B and Fig. 5.10I, respectively).

The previous observations can be summarized in the form of a hypothetical crystallisation path in P-T space (Fig. 5.12). As the magma moved upwards from its site of generation in the upper mantle (assumed to be 10-20 kb at 1100°C), the confining pressure, and to a lesser extent the temperature of the melt, would drop until eventually the olivine stability field was intersected and olivine began to crystallise. Assuming the melt was hydrous and the pressure not excessive (< 10kb), clinopyroxene would begin to crystallise at temperatures a little lower than for olivine (Yoder and Tilley, 1962; Holloway and Burnham, 1972; Foden, 1979). Fractionation of this mineral combination would result in a moderately rapid decrease in MgO, Ni and Cr, but because the bulk SiO_2 of the cumulate would be little different to that of the melt (ie., near 50%), negligible SiO_2 enrichment would occur in the remaining liquid. Moreover, as Foden (1979) has pointed out, the melt will move to undersaturated ne-normative compositions since residual alkali enrichment is occurring in the melt concurrent with olivine and clinopyroxene removal. If the melt is relatively hydrous such that the plagioclase solidus is at significantly lower temperatures than that of clinopyroxene, then Al_2O_3 enrichment will also occur. Only two rocks from the Welcome Well complex are ne-normative (W31, 3.9% ne and W131, 1.5% ne) and notably they possess relatively high Al_2O_3 contents. These characteristics, combined with their relatively low Ni and Cr contents, suggest that they may be the products of extended olivine and clinopyroxene fractionation. However, the quartz and/or hypersthene normative character

Figure 5.12 Stability fields of major crystallising phases for water-saturated and water-undersaturated conditions.

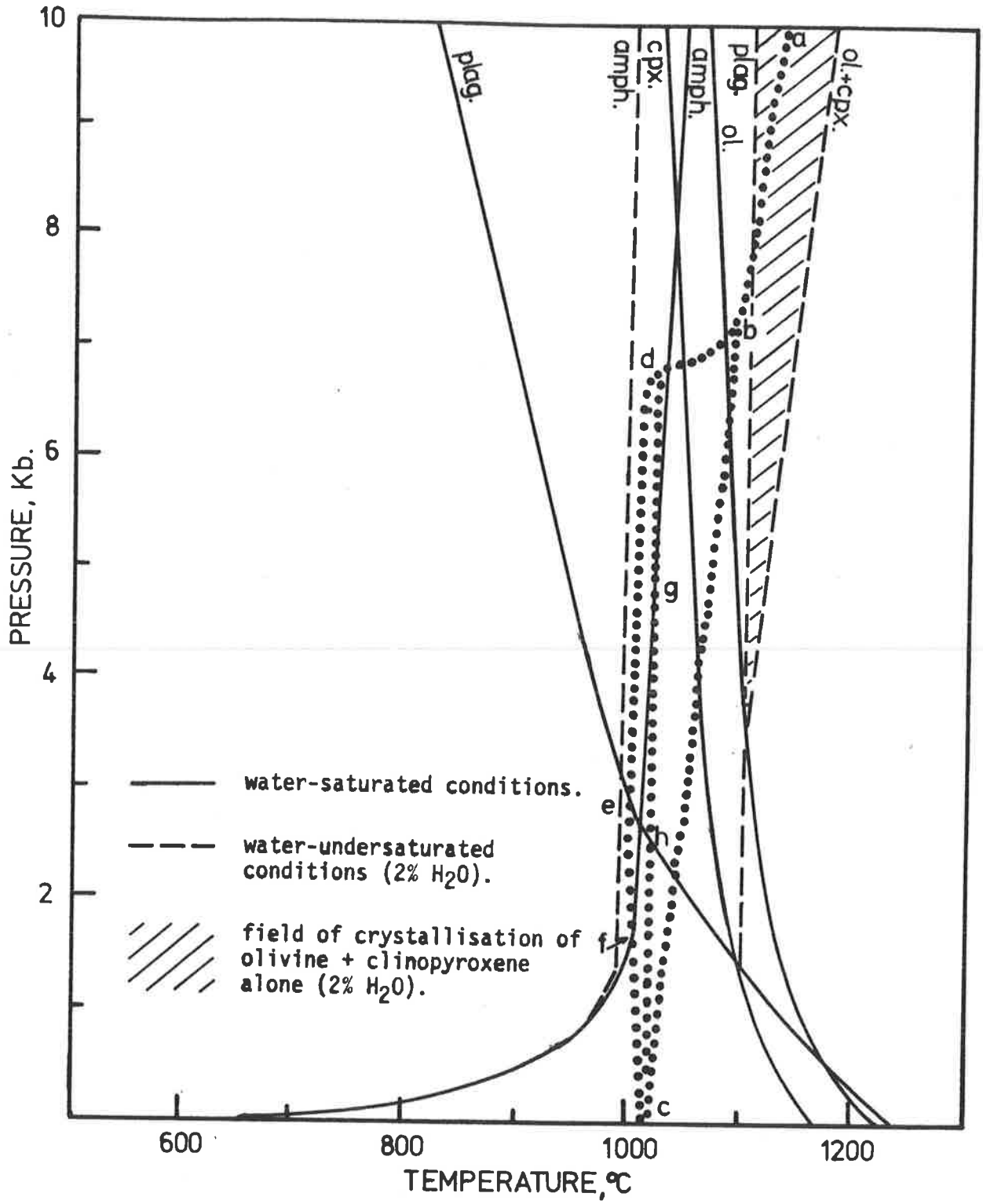

Notes:
1. Stability fields for water-saturated conditions after Yoder and Tilley's (1962) data for high-Al basalt composition.
2. Stability fields of amphibole and plagioclase for 2% H_2O after Eggler's (1971) data for Paricutin andesite and supported by Foden's (1979) data for Rindjani high-Al basalt.
3. Stability field of olivine + clinopyroxene for 2% H_2O after Foden's (1979) data for Rindjani high-Al basalt.
4. Indicated positions of stability fields will vary for the particular rock-compositions being considered.

of the remainder of the samples and the paucity of high Al_2O_3 rocks (e.g. high-alumina basalts) indicates that, in general, the trend towards ne-normative compositions produced by olivine and clinopyroxene fractionation was replaced quite early by a trend towards silica-oversaturation. A number of studies have demonstrated that amphibole fractionation is capable of effecting this change (Cawthorn, et al., 1973; Foden, 1979).

Optimum conditions for amphibole fractionation appear to be produced by PH_2O < PTOTAL with PTOTAL in the range 5-10 kb (Holloway, 1973). Under these conditions amphibole will begin crystallising at slightly lower temperatures than clinopyroxene. The amount of clinopyroxene and olivine fractionation prior to the onset of amphibole crystallisation will be governed by the extent of the divergence from the optimum conditions. This factor is also affected by the water content of the magma since the liquidus temperature is reduced as the weight percentage of water is increased and thus the field of olivine + clinopyroxene fractionation is effectively diminished (Eggler and Burnham, 1973; Foden, 1979). Once the amphibole stability field is entered, olivine and clinopyroxene are in reaction relationship with the liquid and will no longer crystallise (Cawthorn and O'Hara, 1976).

A consequence of fractionation under relatively hydrous conditions is that the plagioclase stability field is suppressed relative to that of amphibole (Figure 5.12). The relative positions of the amphibole and plagioclase stability fields leads to a number of possible paths of crystallisation (assuming water-saturated conditions).

A. If isobaric conditions prevail initially, an extended interval in which amphibole is the only mineral to crystallise, will result (between band d, Fig. 5.12). These conditions may occur if the magma is hindered in its ascent to near the base of the Archaean crust (ie., 7-10 kb or 20-30 km, c.f. Foden, 1979). Subsequent rapid ascent along either of the paths indicated and eventual eruption would allow little opportunity for re-equilibration to lower pressure mineral assemblages.

B. If the magma rises slowly along path d-e-f-c (Fig. 5.12) initial amphibole fractionation will be replaced by amphibole + plagioclase fractionation between e and f and clinopyroxene + plagioclase fractionation after f. The extent to which each of these assemblages fractionates, will be controlled by the resident time within the respective stability fields and hence the opportunity for re-equilibration.

C. Slow ascent of the magma along path d-g-h-c will result in extensive clinopyroxene + plagioclase fractionation between h and c after earlier intervals of amphibole fractionation (between d and g) and clinopyroxene fractionation (between g and h).

The possible lines of liquid descent outlined above demonstrate that the crystallisation history could be extremely complex in detail. Added complexities could be produced by rapid fluctuations in PH_2O as the result of periodic venting of the magma chambers to the surface. Some evidence for the latter may be provided by the zoning observed in the amphibole, clinopyroxene and plagioclase phenocrysts. However, the geochemical data can be interpreted as favouring a prolonged period of amphibole and/or amphibole + plagioclase fractionation followed by plagioclase + clinopyroxene + magnetite fractionation. Thus it appears that a hypothetical path of crystallisation approximating b-d-e-f-c may be closest to the real path in this case. Certainly, crystallisation under relatively dry conditions in which amphibole appears very late, if at all, is not supported by the available evidence.

A crystallisation path resembling b-d-e-f-c can offer possible explanations for two characteristic features of the Welcome Well complex calc-alkaline volcanics.

A. The abundance of clinopyroxene and plagioclase phenocrysts relative to amphibole phenocrysts in the andesites, is probably due to late-stage fractionation at relatively low pressures (e.g. between e and f). Under these conditions any amphibole crystals remaining in the liquid would be expected to breakdown, further enhancing the deficiency in this mineral (Yoder and Tilley, 1962; Cawthorn and O'Hara, 1976).

B. The small compositional gap between the dacites and andesites may result in part from re-equilibration of highly plagioclase-normative liquids, produced by extended amphibole fractionation, at low pressures. The ensueing extensive plagioclase fractionation would rapidly move the residual liquid to higher SiO_2 and the relatively small volume of liquids recording the transition may not be preserved.

In both cases it is necessary to invoke an earlier period of amphibole fractionation at high PTOTAL and a later period of clinopyroxene and plagioclase fractionation, forced in response to re-equilibration of the residual liquid at relatively low pressures. This implies that magma ascent from the site of segregation was interrupted at different levels to allow time for equilibration and fractionation of the mineral assemblages appropriate to the particular conditions. One of the halts

during ascent may have been at or near the base of the crust to permit fractionation of amphibole or amphibole + plagioclase at the optimum conditions of PTOTAL = 7-10 kb, PH_2O < PTOTAL and T > 1000°C (Foden, 1979). Presumably these minerals remained in the lower crust forming basic, crystal cumulates. From this level the residual liquid moved upwards possibly to a near-surface magma chamber where re-equilibration and fractionation of clinopyroxene and plagioclase occurred. It was probably from this level that the magma for the volcanic eruptions was tapped.

5.8 SUMMARY

The greenstone succession in the vicinity of the Welcome Well complex can be assigned to a well-defined stratigraphy. Andesitic flows and intercalated laharic deposits occur at the base of the succession and form the true volcanic centre. They give way to thick deposits of volcaniclastic lithic wackes which grade both laterally and vertically into greywackes. Fine shales, some distance from the vent zone, are intercalated with pillowed tholeiitic basalts. The succession can be satisfactorily interpreted as the eroded remnant of a stratovolcano in which the subaerial, composite near vent facies is flanked by probable ring-plain deposits which merge with subaqueous fluvial sediments distal to the vent.

A complete petrographic gradation exists from porphyritic basalts through porphyritic andesites to porphyritic dacites; clinopyroxene and plagioclase are the dominant phenocrysts while amphibole and magnetite assume lesser importance. The majority of the volcanic rocks were extruded as flows and agglomeratic and brecciated flow-top zones are readily recognisable.

The rocks show general calc-alkaline patterns of major and trace element behaviour consistent with fractionation of variable amounts of olivine, clinopyroxene, amphibole, plagioclase and Ti-magnetite from primitive parents. Among these minerals, amphibole appears to have assumed a major role in producing the geochemical characteristics of the high-silica andesites, dacites and rhyolites, evidenced by the behaviour of Y, MREE and HREE. A crystal fractionation relationship for the majority of samples is confirmed by modelling calculations which show that the trace element abundances in the andesites and dacites cannot be satisfactorily explained by partial melting of a basic crustal source approximating the composition of an average Archaean tholeiite.

The geochemical features of the basalts and low-silica andesites indicate that they differentiated from primitive basic parents which had

a range of major element contents (particularly MgO and SiO_2) and LIL element contents. The most plausible origin for the primary magmas involves shallow, hydrous melting of a LIL element-enriched mantle source over a significant pressure range (e.g. 10-20 kb). Some of the andesites with relatively high MgO, Ni and Cr contents may have differentiated from low-pressure primary magmas (with relatively high SiO_2 and low MgO), while other more evolved andesites may have been derived by extended differentiation from higher MgO and lower SiO_2 parents, generated at higher pressures.

Figure 6.1A Geology of the Spring Well complex, Spring Well area.

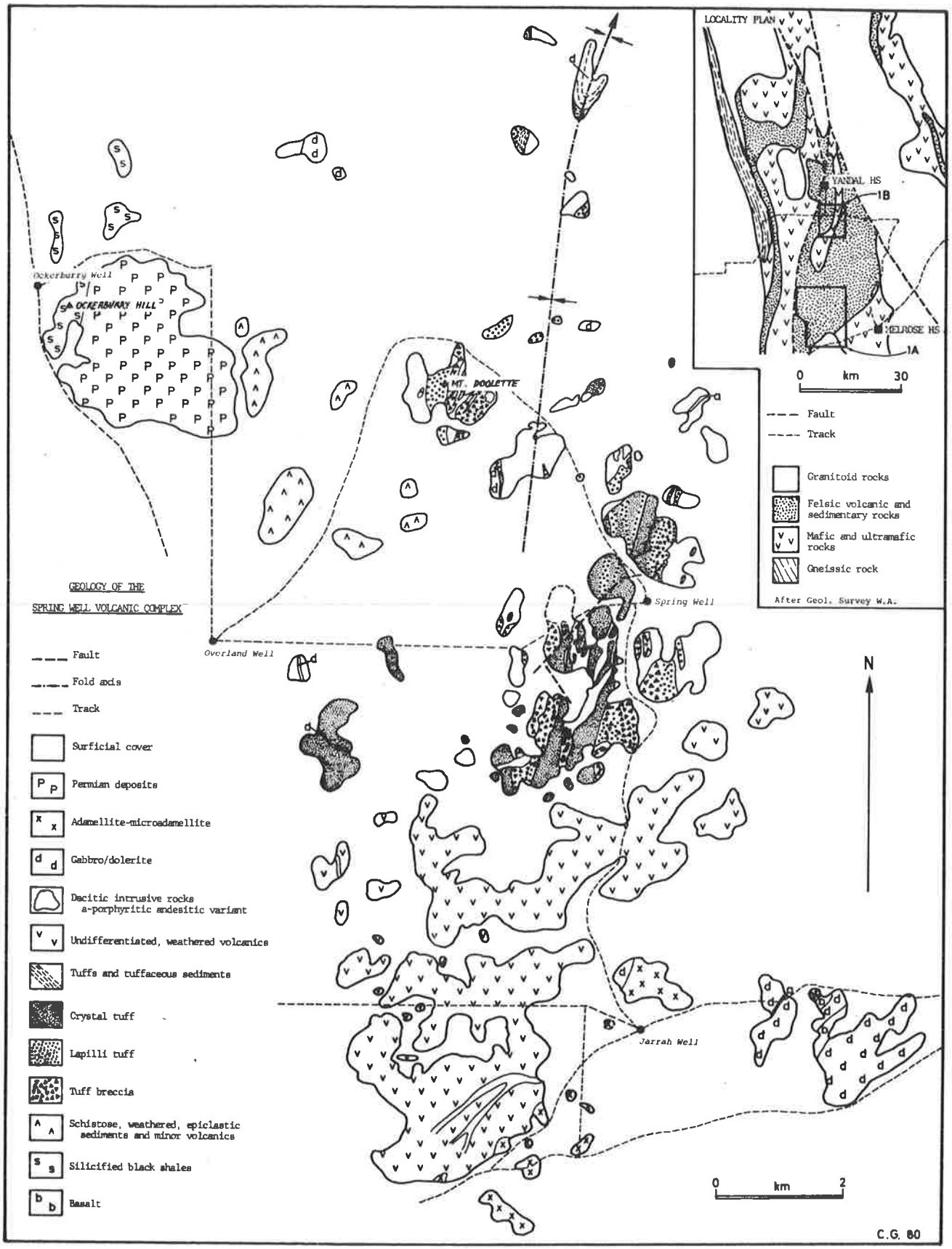

CHAPTER 6

THE PETROGENESIS OF THE ARCHAEAN SPRING WELL VOLCANIC COMPLEX

6.1 INTRODUCTION

The Spring Well complex lies 320 km north of Kalgoorlie in the northern portion of the Archaean Eastern Goldfields Province of W.A.. It is probably one of the freshest and best-exposed acid volcanic centres in the entire Yilgarn Block and in this respect is comparable with the Marda complex (Hallberg, et al., 1976a).

The centre was first documented by Bunting and Williams (1976) who assigned the acid volcanics to the Spring Well complex after Spring Well which lay within the complex. Bunting and Williams (1976) considered the Spring Well complex was "a major felsic volcanic centre comprising a thick pile of coarse fragmental rocks with associated tuffs, lavas and intrusive rocks" and further, "the coarser fragmentals contain angular blocks up to 50 cm across of quartz and feldspar-phyric lava and crystal tuff." They noted that the Spring Well complex was calc-alkaline in character and showed marked analogies with the Welcome Well complex (see chapter 5) and the Marda complex (Hallberg, et al., 1976a). These authors concluded that "the good exposure and lack of secondary alteration in the Spring Well area makes this a highly suitable area for further work on the genesis of Archaean felsic volcanic complexes". Acting on this suggestion and the recommendation of Mr. J. Bunting, the writer mapped the area in detail in May 1977, confirming the general conclusions of Bunting and Williams (1976). The results of a detailed study of this area are presented in the remainder of this chapter.

6.2 REGIONAL GEOLOGY

The Spring Well complex lies with the Yandal greenstone belt, one of several branching segments of the main Norseman-Wiluna greenstone belt in this area (Fig. 6.1A). Each of the segments are separated by acid plutonic rocks and have distinctive characteristics. The Yandal belt is characterised by a lack of ultramafic rocks and clastic sediments, but an abundance of basic (tholeiitic) volcanics and intrusives, and acid volcanics. It is bounded to the east by a major fault and granite, and to the west by gneisses of uncertain relationship (Bunting and Williams, 1976). With the Yandal greenstone belt it is possible to recognise a lower, dominantly basic volcanic and dolerite sequence and an upper, acid volcanic sequence which includes the Spring Well complex. Bunting and Williams interpret the rocks in the Yandal greenstone belt as forming a

Figure 6.1B Geology of the Spring Well complex, Yandal area.

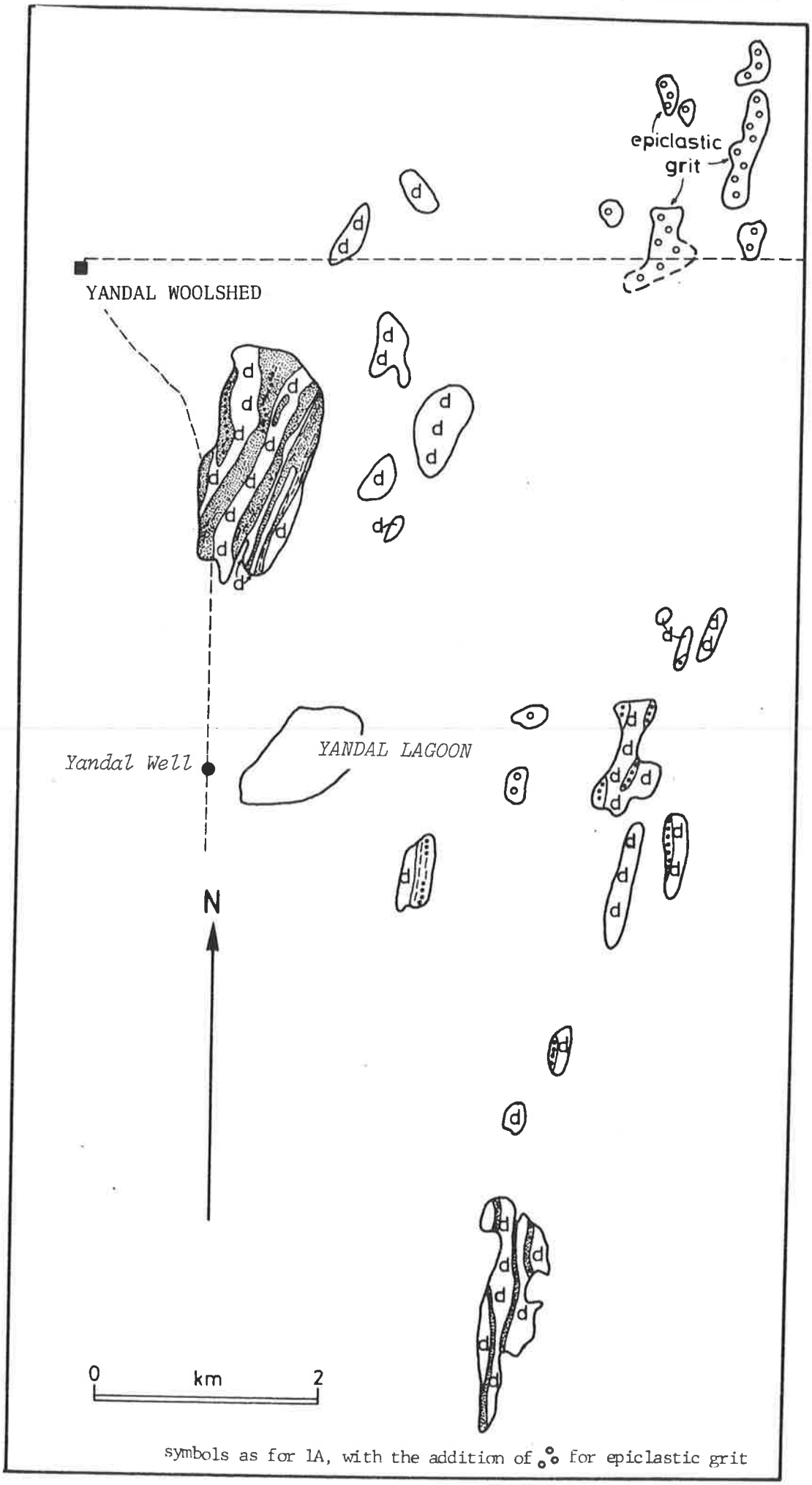

symbols as for 1A, with the addition of ∘∘ for epiclastic grit

simple west-facing succession with basalts and dolerites grading up through acid volcanics to fine shales and cherts at the top, the latter occurring in the vicinity of Ockerburry Hill (Fig. 6.1A). A major fault to the west of Ockerburry Hill is thought to repeat the sequence in the west.

The writer's mapping in the area favours an alternative interpretation in which the acid volcanics (ie. Spring Well complex) are contained within a tight, north-plunging syncline at the top of the greenstone succession (Fig. 6.1). Several independent lines of evidence support this view:

1) In the north of the mapped area a small, layered tholeiitic sill has been folded into a tight syncline which plunges to the north at approximately 15^{o} (Fig. 6.1A). The mineralogical variation in the basic sill, ranging from a pyroxenite at the base containing poikilitic plagioclase, to an ophitic dolerite at the top, supports this structural interpretation.
2) Sedimentary structures in finely-laminated waterlain tuffs and air-fall tuffs in low outcrops 2 km to the southwest of the folded sill give a definite east facing, while repetitive grading in acid pyroclastics near Spring Well yields a west facing (this aspect will be discussed in more detail later).
3) Coincident with the southerly projection of the axial plane of the syncline in the folded sill, is a zone of moderately well developed schistosity. Elsewhere within the rocks of the centre, the schistosity is very weakly developed, if at all.
4) The sequence of coarse pyroclastics at Mt. Doolette greatly resembles that exposed to the north and south of Spring Well (Fig. 6.1A) perhaps suggesting a folded repetition, although this evidence is admittedly tenuous when the complexity of the volcanic history is considered.

The important observation that the acid volcanics are contained within the core of a syncline, implies that the Spring Well complex must be bounded by older rocks to the east and west, assuming that no major faults exist. This is in accord with the acid volcanics overlying the easterly basalt-dolerite sequence as proposed by Bunting and Williams (1976) but conflicts with their interpretation in which the black shales at Ockerburry Hill form the top of the volcanic pile. Clearly, on structural grounds, and in the absence of any evidence for major faulting between Mt. Doolette and Ockerburry Hill, the black shales must underlie the acid volcanics and are therefore thought to be unrelated to the volcanism. In this connection it may be significant that all rocks exposed between Mt. Doolette and

Ockerburry Hill are extremely schistose perhaps indicating that they may have been deformed prior to eruption of the acid volcanics. Alternatively, the high proportion of fine sedimentary component may have rendered these rocks more susceptible to deformation than the relatively incompetent acid volcanics, so that they have developed a more pronounced schistosity. Distinction between these two alternatives is difficult owing to the extremely poor outcrop in the critical area between Mt. Doolette and Ockerburry Hill and the deep weathering suffered by those rocks that do outcrop.

Another important implication arising from the fact that the acid volcanics are folded into a tight syncline is that the thickness of the acid volcanic sequence is likely to be considerably less than the 5-6 km estimated by Bunting and Williams (1976). In the writer's opinion the total thickness of the acid pile including intrusives is probably between $1\frac{1}{2}$ to 2 km.

The volcanics are truncated to the south by a small tongue of granite which probably extends from the large mass bounding the eastern margin of the Yandal greenstone belt. Beyond the granite is an area of poor outcrop, but percussion drilling has shown that it is underlain by andesite (Hallberg, pers. comm.). The andesite in turn links with a series of acid volcanics and porphyries further to the south which are possibly at a similar stratigraphic level to the Welcome Well complex east of Leonora (see chapter 5). In the north, the acid volcanics rapidly decrease in abundance as they are replaced to a large extent by epiclastic sediments and basic extrusive and intrusive rocks.

6.3 DETAILS OF THE VOLCANIC HISTORY

Aspects of the detailed geology of the Spring Well complex will be described below and photographs illustrating many of the features mentioned are given in Figure 6.2. The rocks in the Spring Well complex are divisible into two broad groups:

1) acid volcanics including crystal tuffs and lithic tuffs, and
2) acid and intermediate intrusives including non-porphyritic microdiorites and porphyritic andesites, dacites and rhyolites.

The geological map of the Spring Well complex shows that intrusive rocks comprise a significant part of the sequence (Fig. 6.1). They originally invaded as sills, wedging the volcanic pile apart and adding greatly to the apparent stratigraphic thickness. Locally, small plugs and sinuous dykes are observed. Contact metamorphic effects on the acid

volcanics and chilling of the intrusives near contacts is negligible, suggesting the sills and dykes may have represented subvolcanic feeders to flows now removed by erosion.

The acid volcanics are mainly of pyroclastic origin and show a considerable textural range including: coarse tuff breccias, lapilli tuffs, crystal tuffs and fine bedded tuffs. The coarsest pyroclastics are found in the outcrops in the vicinity of Spring Well while the finest are found near Yandal Lagoon (Fig. 6.1). It is therefore inferred that the volcanics near Spring Well are closest to the ancient vent and constitute the "centre" of volcanism in the Spring Well complex.

A particularly instructive succession is preserved on the hill immediately to the north of Spring Well (Fig. 6.1A). At the base of the sequence are coarse, unsorted tuff breccias which contain angular, accessory volcanic rock fragments in a glassy, moderately-welded matrix. The blocks are generally less than 20 cm in diameter, although a few scattered blocks are up to 1.5 m long, indicating that the tuff breccias must have been deposited in close proximity to a vent. The tuff breccias grade up into lapilli tuffs which contain increasing proportions of crystal tuff fragments and crystals in the matrix, eventually merging into a brecciated crystal tuff with abundant compressed pumice fragments. This in turn merges with a homogeneous crystal tuff which is capped by finely-bedded air-fall tuff, yielding a total thickness for the sequence of approximately 100 m. Similar successions, although not so well developed, are recognisable along strike to the south and also on Mt. Doolette. To explain the gradational nature of the sequence and the extremely lensoid character of the individual units, it seems probable that deposition occurred via a "lag-fall" mechanism analogous to that described by Wright and Walker (1977). Lag-fall deposits form by collapse of a vertical eruptive column in which the order of deposition in controlled by the gravity stratification in the column. Consequently, the coarsest (and heaviest) lithic fragments are deposited first (i.e., at the base) with the crystals later and the fine ash last, at the top of the deposit. Provided deposition is moderately rapid, sufficient heat may be retained to cause welding. It is possible that much of the pyroclastic sequence accumulated in this manner although some deposition may have been directly from small nuēe ardente eruptions.

Massive quartz-plagioclase porphyries outcrop prominently to the west and south of Spring Well; the homogeneity of these rocks and lack of diagnostic textures, often makes it difficult to determine whether they are intrusive or extrusive. In what may be considered to be a type area

Figure 6.3 Detailed geology of the vent zone, Spring Well complex.

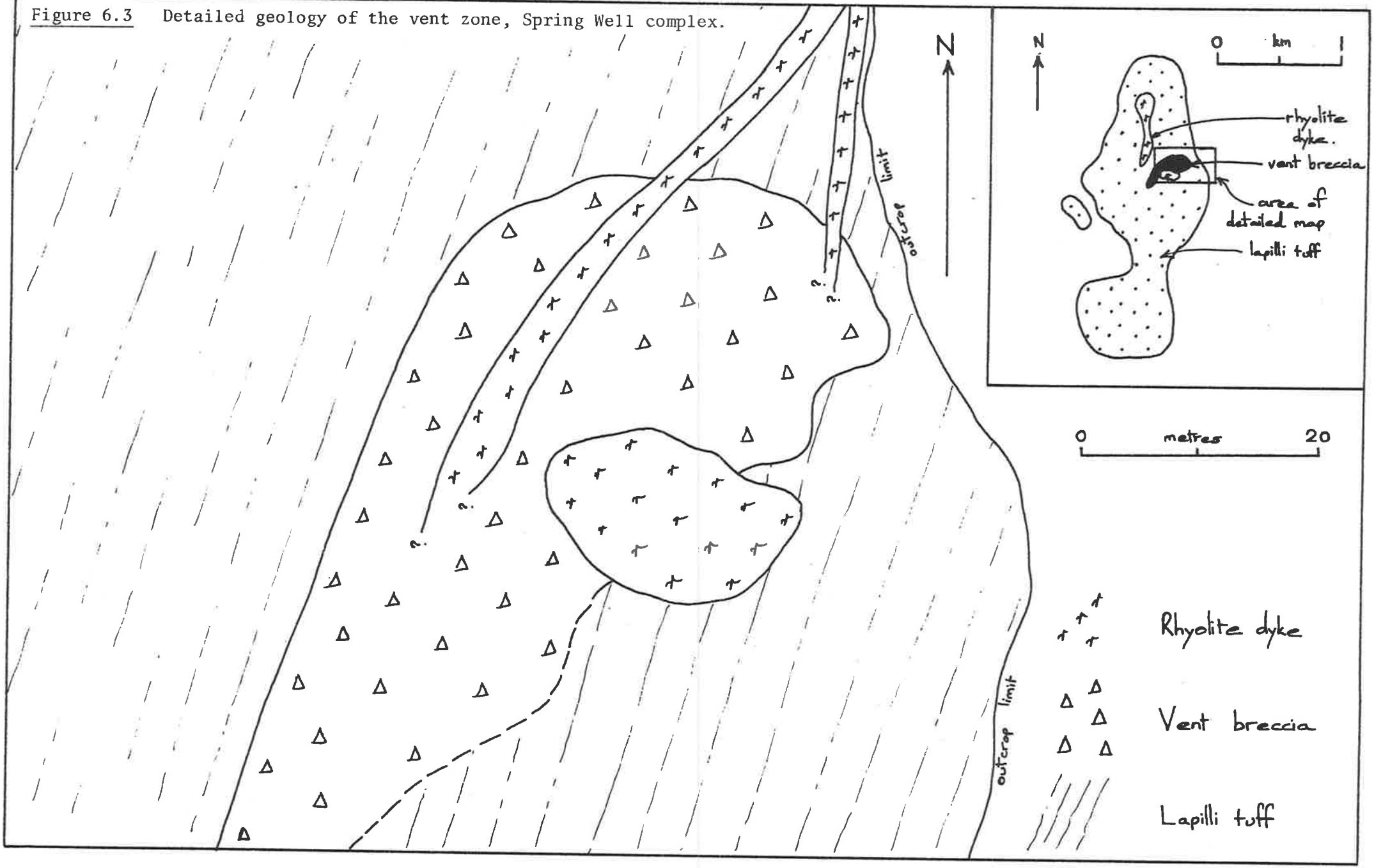

of the porphyry 500 m west of Spring Well, clear flow-banding is visible. The flow-banding is generally very regular and continuous, but at this locality it has been contorted into flow folds. The contortion has continued to the point that rupturing of the flow folds has occurred resulting in a flow breccia, which is very reminiscent of the flow breccias commonly seen in rhyolitic lava flows. However, along strike to the south, the porphyry shows vitroclastic textures in thin section and clear shard outlines are visible on some weathered surfaces of outcrop. Thus the outcrop to the west of Spring Well, showing the flow-folding could represent a rheoignimbrite (Schmincke and Swanson, 1967) or an ignimbrite that has flowed while in a plastic state subsequent to deposition. It is therefore concluded that while a lava flow origin cannot be excluded in all cases, the bulk of the extrusive porphyries are probably crystal tuffs of pyroclastic derivation.

What is considered to be true vent breccia has been recognised at only one locality, 2.2 km north-northwest of Spring Well. The actual breccia covers an elliptical area of approximately 1500 m^2 and consists of a jumbled, unsorted and unstratified aggregate of angular, accidental blocks. Most blocks are composed of rhyolite and there is little interstitial matrix of lapilli- or ash-size. The breccia clearly truncates a layered sequence of lapilli tuffs which are striking roughly north-south and part of the contact zone has itself been invaded by rhyolitic dykes and plugs (Fig. 6.3). Adjacent to the breccia are small areas of bleached, sericitized and silicified lapilli tuff quite unlike any other rocks seen in the Spring Well complex. The localised alteration could readily be explained by fluids emanating from the breccia pipe. In the writer's opinion the field evidence cited above strongly supports the interpretation that this feature does represent a breccia pipe which has been exposed as a result of fortuitous erosion in this area. This being the base, the breccia pipe described above gives a unique and valuable insight into the nature of the feeders which may have erupted much of the volcanic pile mapped in this area.

Although the intrusives lacing the volcanic pile have been referred to earlier, one body in particular, deserves special mention. It is a small rhyolitic plug exposed on the east of the Mt. Doolette outcrop. This body shows spectacular flowage textures including: vertical flow-banding, flow-brecciation and a type of rodding. These textures clearly indicate that the rhyolite intruded as a viscous, sticky mass and it is conceivable that it may have been the root zone of a lava dome.

Figure 6.2. Selected photographs and photomicrographs of rocks from the Spring Well complex.

A. Prominent flow banding and flow folds in an ash-flow tuff that has moved subsequent to deposition. An ash-flow origin is supported by vitroclastic textures visible in thin section and on some weathered surfaces.

B. Continued flowage has resulted in disruption of the flow folds to produce a flow breccia with diverse orientations of flow-banding.

C. Lapilli-tuff, consisting of angular, accessory acid volcanic rock fragments set in a glassy, ash-size matrix.

D. Block of accessory rhyolite within a lapilli-tuff similar to that illustrated in C. The rocks in both C and D are interpreted to represent near-vent lag-fall deposits, that have retained sufficient heat to partially weld.

E. Porphyritic crystal tuff (lower) intercalated with fine-grained water-lain tuff (upper) in the distal regions of the Spring Well complex (Yandal area).

F. Crystal-vitric tuff, consisting of angular crystal chips of plagioclase and quartz (and some complete phenocrysts), set in a shard-rich, glassy matrix. F.V. 6 mm.

G. Welded ash-flow tuff, composed of plagioclase phenocrysts and glassy lithic fragments, set in a matrix of moderately compressed glass shards. F.V. 6 mm.

H. Welded, crystal-vitric ash-flow tuff. Many of the crystals are chips or fragments of larger phenocrysts. The glass shards are draped around the phenocrysts, indicating significant compaction during welding. F.V. 6 mm.

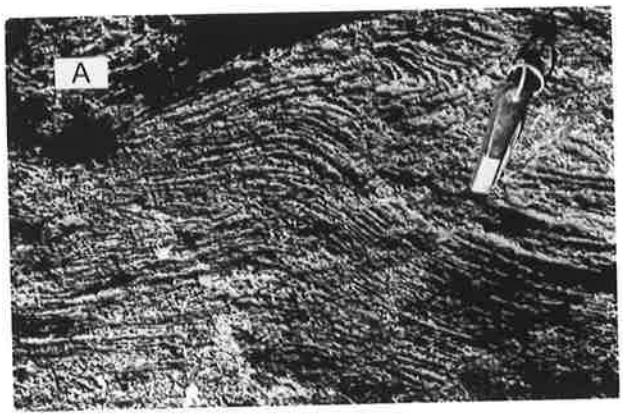
A


E


B

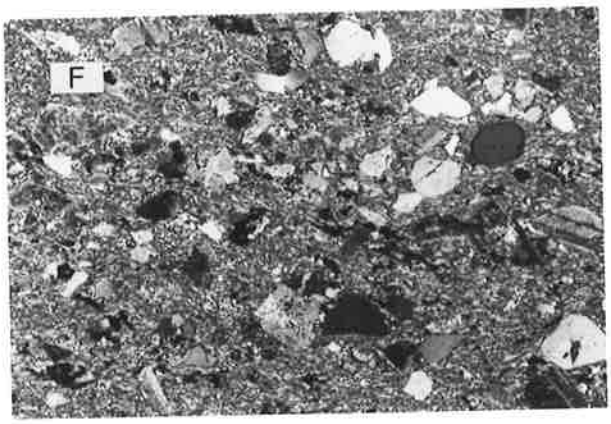
F


C


G


D


H

The discussion hitherto has concentrated on the well-exposed rocks proximal to the eruptive centre. To the north, outcrop becomes sparse, but what outcrops there are clearly indicate a fining of the pyroclastics. For example, in the outcrops near Yandal Lagoon (Fig. 6.1B) tuff breccias are absent and the sequence consists of crystal tuffs, crystal-lithic tuffs and vitric tuffs interbedded with fine sediments. The sediments and probably some of the tuffs were deposited under water in an environment which was distal to the eruptive centre. This interpretation assumes that the rocks in the Yandal area are at the same stratigraphic level as those near Spring Well. If, however, the north-plunging syncline can be projected into the Yandal area with no structural dislocation, and this is not entirely certain due to lack of outcrop, then the Yandal succession, apart from demonstrating a lateral fining, may also indicate a vertical fining attributable to waning volcanism as originally suggested by Bunting and Williams (1976).

Also outcropping in the Yandal area are some curious rocks which in the field superficially resemble intrusive quartz-feldspar porphyry. Thin sections of rocks from these outcrops however, reveals that they are in fact immature epiclastic sediments of arkosic composition. Again, if the synclinal structure is projected into the Yandal area, these deposits would be the youngest in the succession in this region and may represent coarse material shed from the volcanic centre during emergence. It is likely that these arkoses may correlate with some feldspathic sediments noted by Bunting and Williams (1976) further to the north near the eastern margin of the Yandal belt and which were thought by them to have probably been derived "from erosion of penecontemporaneous felsic volcanic rocks".

In summary, the Spring Well complex, which is exposed in a tight synclinal structure, represents a well-preserved example of an Archaean acid volcanic centre. The volcanic pile near Spring Well formed proximal to the ancient vent(s) while the sequence in the Yandal area was clearly deposited distal to the vent. Textural preservation is excellent and as a result it is possible to recognise welded lithic, crystal and vitric tuffs, flow breccias and even vent breccias, suggesting that the volcanic processes operating then were probably little different to those observable today.

6.4 PETROGRAPHY

Within the Spring Well complex it is convenient to make a broad distinction between the extrusive and intrusive rocks. Sometimes the

division is not obvious even after careful petrographic examination, however in the following discussion attention will be focussed on the typical members of each group. Brief petrographic descriptions of a representative collection of samples, including those analysed, are given in Table A6.1, Appendix 1. Photomicrographs illustrating some of the petrographic features described below, are presented in Figures 6.4 and 6.5.

6.4.1 Extrusive rocks

Among the acid volcanics it is possible to recognise two extremes: crystal tuffs containing up to 40% by volume of crystals, and lithic tuffs with up to 50% by volume of lithic fragments. These represent the end-members of a continuous series which includes abundant crystal-lithic tuffs intermediate between these two extremes. In places, for example near Spring Well, a complete gradation is recognisable in what are interpreted to be possible lag-fall deposits (see discussion earlier).

The crystal tuffs range from porphyritic dacites to porphyritic rhyolites. They usually contain anhedral, embayed phenocrysts of quartz and euhedral plagioclase in a felsic matrix which shows variable recrystallisation. The dacites are characterised by a higher proportion of plagioclase phenocrysts relative to quartz phenocrysts than the rhyolites and sometimes contain rare amphibole or clinopyroxene phenocrysts. Despite careful search no extrusive andesites were found.

Where the field relationships are not diagnostic, the pyroclastic character of many of the porphyries is inferred from indirect criteria such as abundant crystal "chips" and relic vitroclastic textures. It is likely that some of the porphyries that superficially resemble crystal tuffs are of lava flow rather than pyroclastic origin. In thin section the flow rocks are characterised by pseudo-pilotaxitic textures, consisting of numerous oriented plagioclase microlites scattered between the phenocrysts although it is notable that some intrusive porphyries show similar textures.

The lithic tuffs contain scattered crystal chips and abundant angular, accessory rock fragments that have been torn from the pre-existing acid volcanic pile. The volcanic fragments are of block, lapilli and ash-size and include porphyritic, non-porphyritic and vesicular rhyolites and dacites and numerous types of ignimbrites with glassy textures; exotic fragments are exceedingly rare. Some of the fragments possess a lighter-coloured rim, possibly as a result of reaction due to incorporation in a

Figures 6.4 and 6.5 (combined). Photomicrographs of selected thin sections.

A. Subophitic to intersertal texture in a microdiorite dyke. The tabular plagioclase laths are intergrown with chloritized clinopyroxene and pools of interstitial material (after glass). F.V. 7 mm.

B. Porphyritic andesite (dyke), consisting of phenocrysts of euhedral, zoned clinopyroxene and tabular, sericitized plagioclase in a microcrystalline matrix. F.V. 5 mm.

C. Detail of a euhedral, embayed and zoned clinopyroxene phenocryst in a porphyritic andesite dyke. F.V. 3 mm.

D. Tabular plagioclase lath in a pilotaxitic matrix composed of flow-oriented plagioclase microlites. Sample is from a dacite that is interpreted to be of lava-flow origin. F.V. 4 mm.

E. Porphyritic dacite, consisting of phenocrysts of twinned plagioclase and rarer anhedral quartz in a microcrystalline felsic matrix. F.V. 6.5 mm.

F. Glomeroporphyritic aggregate of plagioclase phenocrysts in a dacite. F.V. 6.5 mm.

G. Rhyolitic ash-flow tuff showing a variety of forms of quartz, ranging from a large fractured and partially-embayed phenocryst (centre) to complete, anhedral phenocrysts and small crystal chips, fragmented from larger phenocrysts. F.V. 7 mm.

H. An embayed quartz phenocryst in a rhyolitic ash-flow tuff. F.V. 4 mm.


A

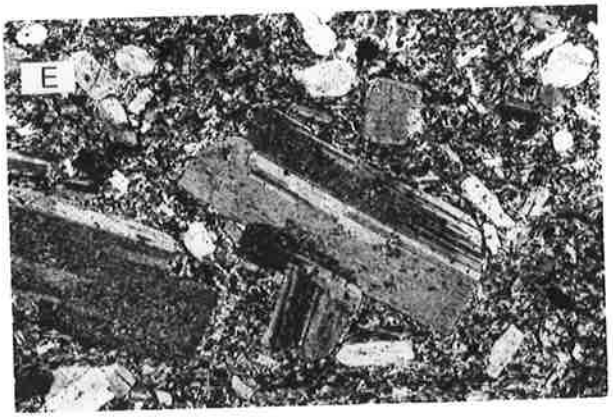
E

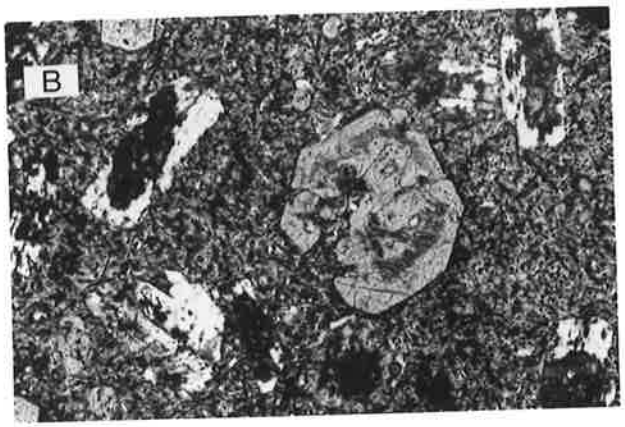
B

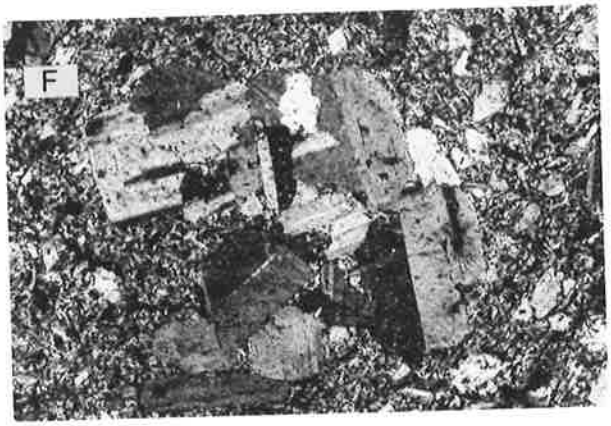
F


C

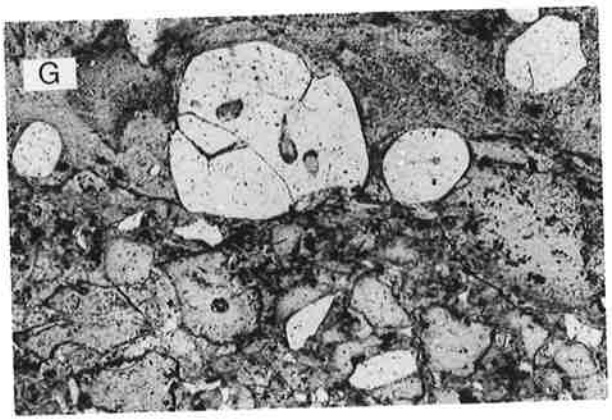
G

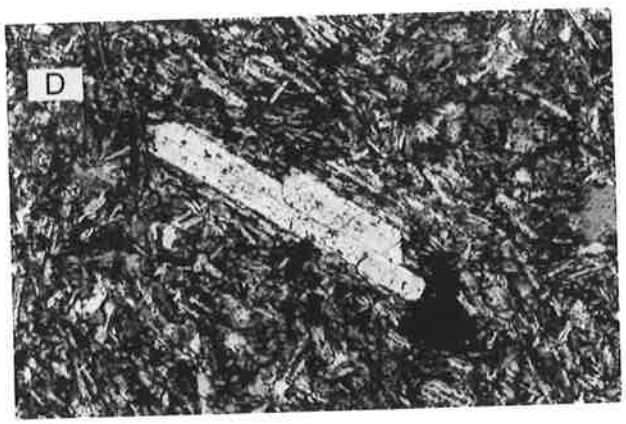
D

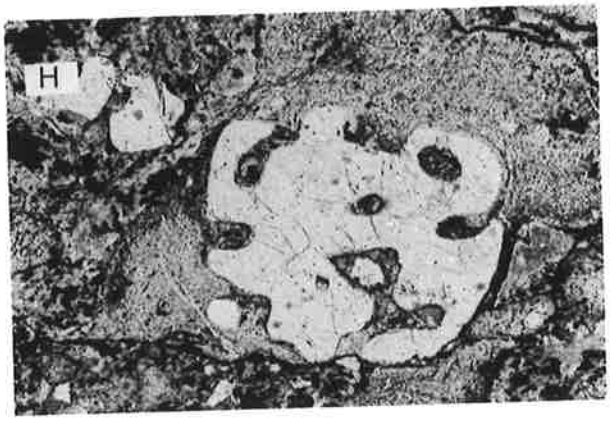
H

cold state (also observed by Bunting and Williams, 1976). The fragments are invariably contained within a glassy matrix in which vitroclastic textures are commonly well preserved, clearly attesting to a pyroclastic origin. Dark glassy patches, almost certainly after compressed pumice, are also evident in some of the tuffs.

Fine, bedded tuffs and vitric tuffs are found in the more distal regions of the volcanic pile and are usually intercalated with fine, waterlain sediments. Unfortunately, most of these rocks are homogeneous microgranular felsic mosaics containing no diagnostic textures so it can only be inferred from their field relationships that they were most probably deposited under water.

6.4.2 Intrusive rocks

The intrusive rocks show a wider compositional range than the volcanics (from andesite to rhyolite) in addition to great variations in form and texture. Sills and dykes of medium-grained microdiorite to microgranodiorite are most abundant; they consist of even-grained aggregates of plagioclase, clinopyroxene and magnetite with interstitial feldspar and quartz. Occasionally, they merge into, or are cut by porphyritic andesites and dacites which contain phenocrysts of clinopyroxene, plagioclase and magnetite within a fine, microcrystalline felsic matrix. One particular intrusive porphyritic andesite was observed to contain zoned phenocrysts of plagioclase and clinopyroxene in a microcrystalline matrix composed of plagioclase microlites, acicular amphibole and quartz, and nobably, it greatly resembled porphyritic andesite lavas from the Welcome Well complex. For convenience of reference all of the intermediate intrusive rocks will be referred to as andesites in the following discussion. The porphyritic dacites and rhyolites contain phenocrysts of embayed quartz and euhedral plagioclase in a finely-crystalline and sometimes microlitic groundmass, which is generally coarser-grained and more crystalline than that of their volcanic equivalents.

Other intrusive rocks of importance include the granodiorite body truncating the Spring Well complex to the south. This body is a medium- to coarse-grained granodiorite containing tabular plagioclase interlocking with granular quartz, scattered clinopyroxene and myrmekitic quartz-plagioclase intergrowths. The minor basic intrusive bodies are usually doleritic, with subophitic textures, or gabbroic in which case they commonly contain cumulate clinopyroxene. The folded basic sill mentioned previously is clearly layered and contains a pyroxenitic lower zone merging into a doleritic upper zone.

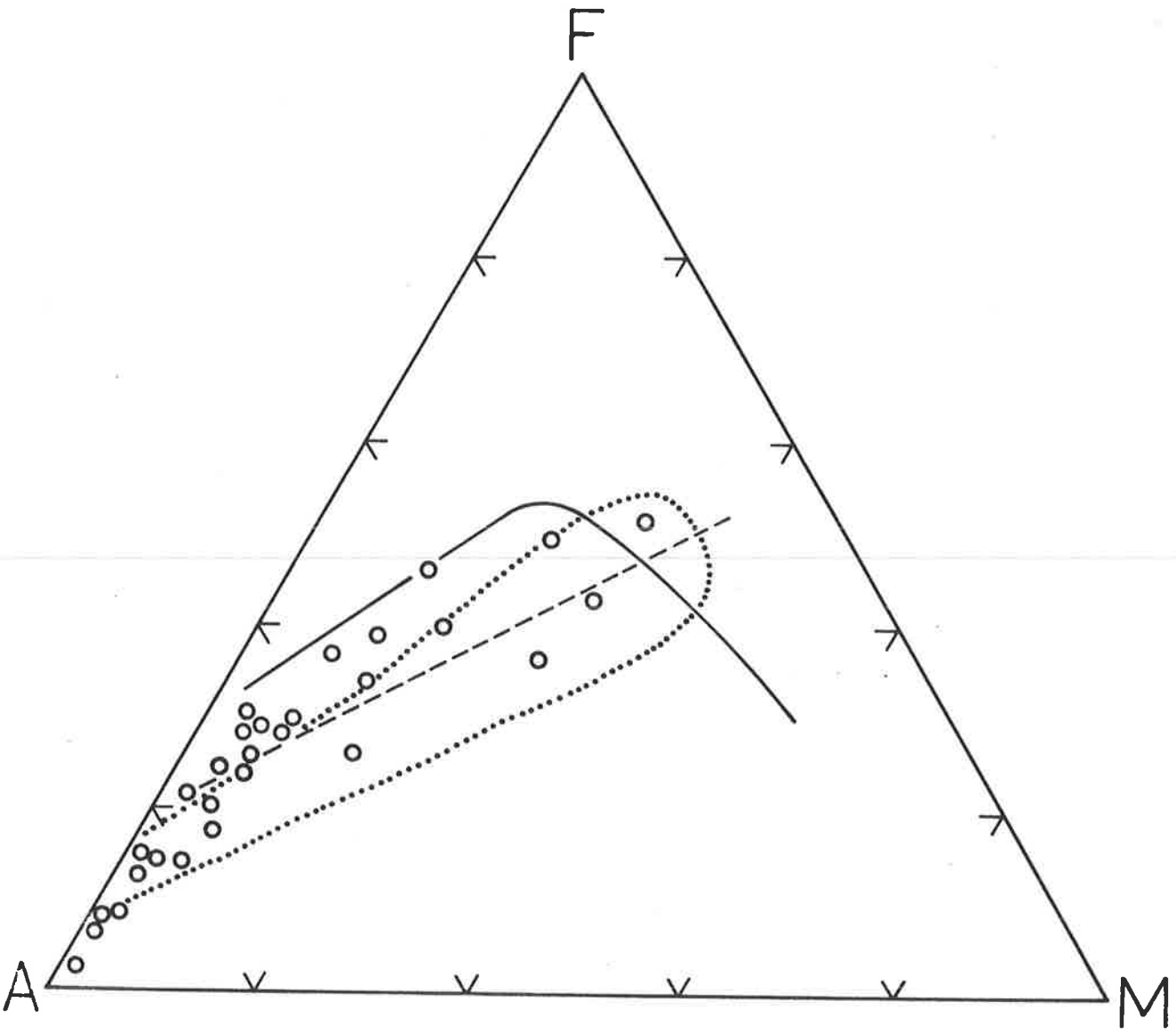

Figure 6.6 AFM plot for rocks from the Spring Well complex. The solid line separates the tholeiitic and calc-alkaline fields. The dashed line is the trend defined by the calc-alkaline Cascades lavas (after Carmichael, 1964). The dotted line encloses the field of samples from the Welcome Well complex.

Alteration of the extrusive and intrusive rocks is pervasive but seldom severe. For example, the phenocrysts of plagioclase invariably show some sericitization while clinopyroxene is often partially converted to amphibole and/or chlorite, and magnetite typically shows incipient development of leucoxene. Chlorite and epidote are ubiquitous in the matrix and have probably crystallised under the low regional grade of metamorphism. All of the alteration effects occur on the scale of individual minerals and evidence for large-scale metasomatism (e.g. silicification, sericitization, albitization and carbonation) is absent. Consequently, by careful petrographic examination, it has been possible to select a representative suite of samples which show a complete range of textures and compositions, yet minimal alteration.

6.5 GEOCHEMISTRY

Major and trace element data for a variety of rocks from the Spring Well complex is given in Table A6.2. This data reveals that there is a small compositional hiatus between the andesite-dacite and dacite-rhyolite fields, assuming the boundaries are placed at 62% SiO_2 and 70% SiO_2, respectively. A similar paucity of dacites in the 66-70% SiO_2 range has been noted in the Marda complex by Hallberg, et al. (1976) who thought "it may reflect a sampling bias due to the poor outcrop rather than an inherent geochemical discontinuity". In the present case the hiatus is not considered to be due to sampling, because careful search was made for rocks of this composition; it is therefore believed to be a real geochemical discontinuity which must be explained in any petrogenetic models.

It is also important to note that the extrusive rocks are confined to the dacite and rhyolite fields, while the intrusive rocks span all fields. Low-silica intermediate intrusive rocks are rare and are represented by only two samples (S4, S19), while basic intrusive rocks of similar geochemical affinities are absent. In the following discussion the geochemical data presented in Table A6.2 is examined with the aid of variation diagrams, and where appropriate the possible interpretations that may be placed on the data are considered.

6.5.1 Major elements

Plotting all of the samples from the Spring Well complex on an AFM diagram delineates a clear calc-alkaline trend, which overlaps that defined by samples from the Welcome Well complex (Fig. 6.6). This is consistent with the general calc-alkaline trends shown by the major elements when

Figure 6.7 Major element variation diagrams for rocks from the Spring Well complex. O extrusive rocks ● intrusive rocks. The solid lines enclose the field of Cainozoic calc-alkaline volcanics.

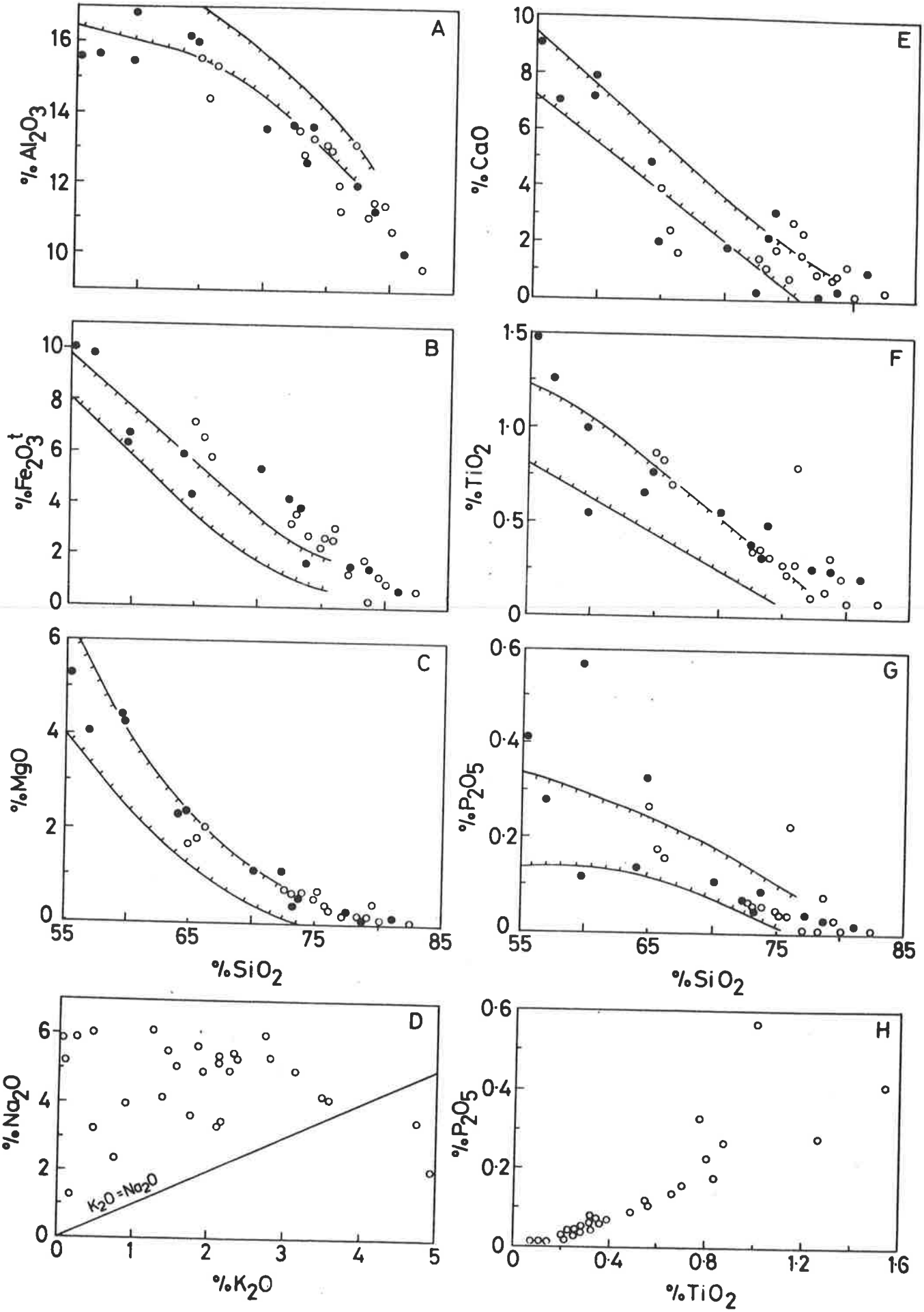

plotted against SiO_2 (Fig. 6.7). For example, the inverse correlations of Al_2O_3, $Fe_2O_3^t$, MgO, CaO, TiO_2 and P_2O_5 with SiO_2 closely parallel the trends shown by Cainozoic calc-alkaline volcanics. However, while the absolute contents of MgO, CaO and Na_2O are comparable with the Cainozoic volcanics, Al_2O_3 and K_2O are significantly lower and $Fe_2O_3^t$, TiO_2 and P_2O_5 are higher in the Spring Well rocks.

An examination of the variation diagrams for the individual major elements reveals a number of additional points:

1) The marked decrease in Al_2O_3, particularly at high SiO_2 levels, probably reflects extensive plagioclase involvement either as a residual or a fractionating mineral.
2) The inverse correlation of $Fe_2O_3^t$ and TiO_2 with SiO_2 could be due to combined control by mafic minerals (at lower SiO_2) and oxide minerals (at higher SiO_2). The moderately good correlation of $Fe_2O_3^t$ with TiO_2 (Fig. 6.8H) confirms that the same mineral(s) is probably controlling both elements.
3) The uniform decrease in P_2O_5 at high SiO_2 levels is probably a result of control by apatite as a fractionating rather than a residual mineral. The trend cannot be projected to lower SiO_2 levels, where the considerable scatter may be indicative of some primary source control. For example, the low-silica andesites (S19 and S4) have quite different P_2O_5 contents (.41% P_2O_5 in S19 and .28% P_2O_5 in S4) yet other major elements are very similar. This point is demonstrated by the P_2O_5 vs TiO_2 plot (Fig. 6.7H), where at high SiO_2 levels a typical calc-alkaline trend of decreasing P_2O_5 with TiO_2 is observed (Anderson and Gottfried, 1971), while at lower SiO_2 levels the scatter obscures any trends.
4) The considerable scatter on the K_2O and Na_2O vs SiO_2 plots is probably largely due to the effects of alteration on K_2O and Na_2O. Despite the scatter, it is significant that for the majority of samples Na_2O exceeds K_2O (Fig. 6.7D), a point which is consistent with the abnormally low K_2O contents of the Weebo rocks in comparison with typical calc-alkaline series.
5) On all of the plots the acid intrusive and extrusive rocks show considerable overlap, thus supporting a genetic relationship.
6) Despite the small compositional gaps, most of the major element trends are quite uniform, particularly at high silica levels.

6.5.2 Trace elements

A. Ni, Cr

The amount of information that can be gained from the Ni and Cr data

Figure 6.8 Selected trace elements vs. SiO_2 and Sc, TiO_2 vs. $Fe_2O_3{}^t$ for rocks from the Spring Well complex. O extrusive rocks ● intrusive rocks. The solid lines enclose the field of Cainozoic calc-alkaline volcanics.

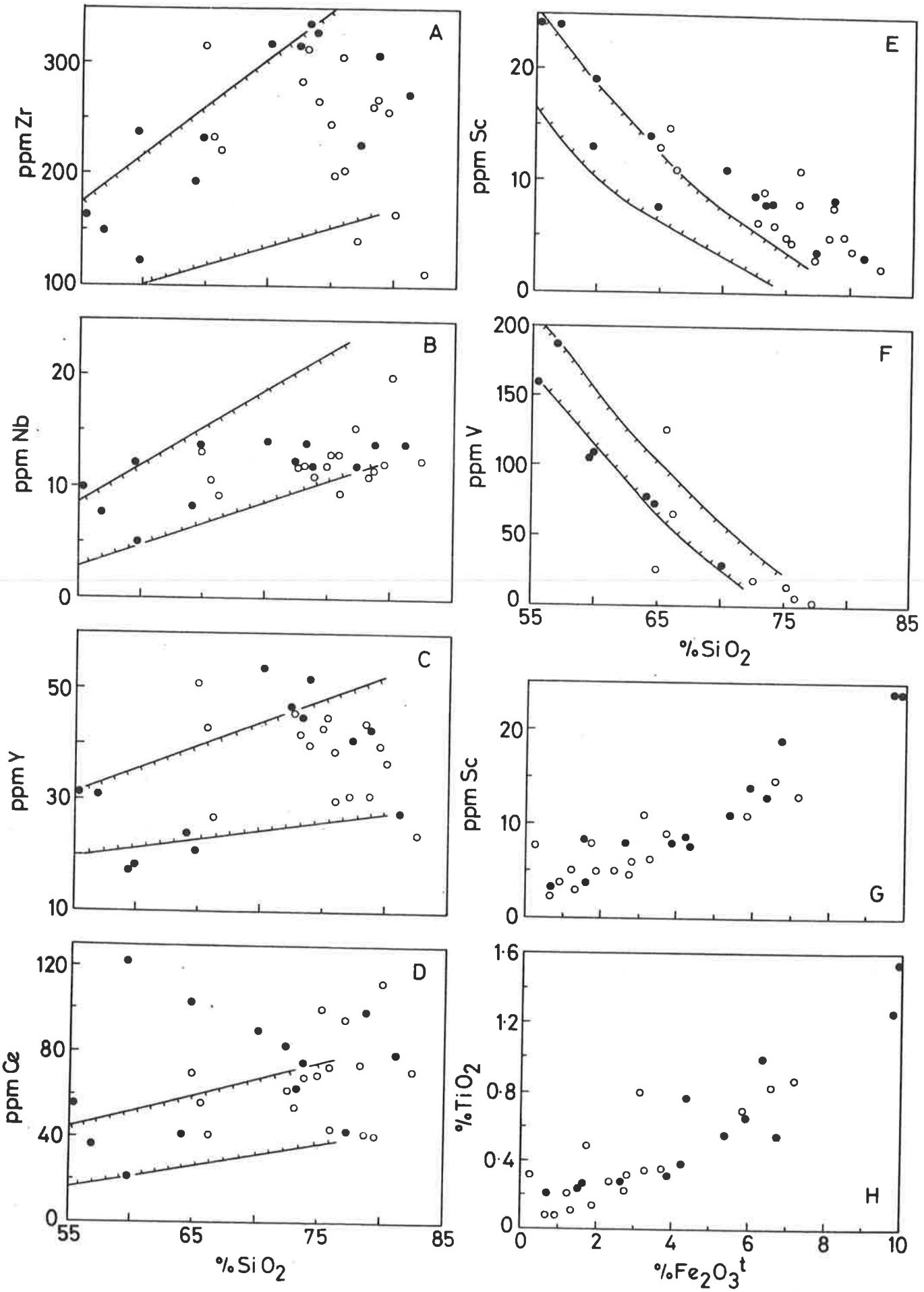

is limited to some extent by the very low Ni and Cr contents of the dacites and rhyolites (Table A6.2). The andesites have relatively high Ni and Cr contents in comparison with circumpacific andesites of similar SiO_2 content and this could reflect upon the source, or alternatively, on the crystallisation history.

B. Sc, V (and TiO_2, $Fe_2O_3^t$)

The plots of TiO_2 and Sc vs $Fe_2O_3^t$ (Figs. 6.8G and H) show a moderately good correlation of all elements and the trends are coincident with those noted for the Welcome Well complex. By analogy with the Welcome Well samples, titanium-rich magnetite probably exerted the chief control on these elements in the rhyolites and dacites, but in the andesites the controls on these elements were more complex. For example, S4 and S19 (the two low-silica andesites), have similar $Fe_2O_3^t$ and Sc contents, yet S19 contains significantly higher TiO_2 and V. Similarly S44 and S91 (high-silica andesites) have analogous MgO, SiO_2, $Fe_2O_3^t$ and V contents but differing levels of TiO_2 and Sc (Table A6.2). These differences cannot be readily explained by fractionation of magnetite or mafic minerals in a simple differentiation series.

C. Zr, Nb, Y

Zr increases progressively from andesite through dacite to rhyolite up to 73-74% SiO_2, at which point it begins to drop, although the scatter in the data introduces some ambiguity in the interpretation (Fig. 6.8A). This behaviour could be explained by the onset of zircon fractionation at approximately 73% SiO_2 which would be expected to rapidly deplete the melt in Zr, following an initial period of residual concentration. An explanation in terms of a partial melting model would be more difficult.

Nb shows a small increase with rising SiO_2 at lower silica levels, but the trend flattens out in the rhyolite field (Fig. 6.8B). This could reflect negligible control on Nb in the early stages of crystal fractionation but some control in the latter stages or alternatively it may be produced by variable control during partial melting.

Y decreases with increasing SiO_2 in the rhyolites possibly as a result of fractionation of accessory minerals such as zircon, apatite or sphene (Fig. 6.8C). The behaviour of Y in the andesites and dacites is rather more complex since the low-silica andesites (S19 and S4) have higher Y contents than the high-silica andesites (S44 and S91) and some dacites (S60 and S42). Other dacites (e.g. S1 and S141) have levels of Y comparable to those in the rhyolites (i.e. 40-50 ppm).

Figure 6.9 Chondrite-normalised REE plots for rocks from the Spring Well complex. S19 - andesite (55.06% SiO_2, 5.26% MgO). S4 - andesite (56.9% SiO_2, 4.06% MgO). S141 - dacite (65.63% SiO_2. 1.80% MgO). S48 - rhyolite (75.23% SiO_2, 0.71% MgO). S70 - rhyolite (77.24% SiO_2, 0.23% MgO).

The stipple encompasses the field of andesites from the Marda complex (after Taylor and Hallberg, 1977).

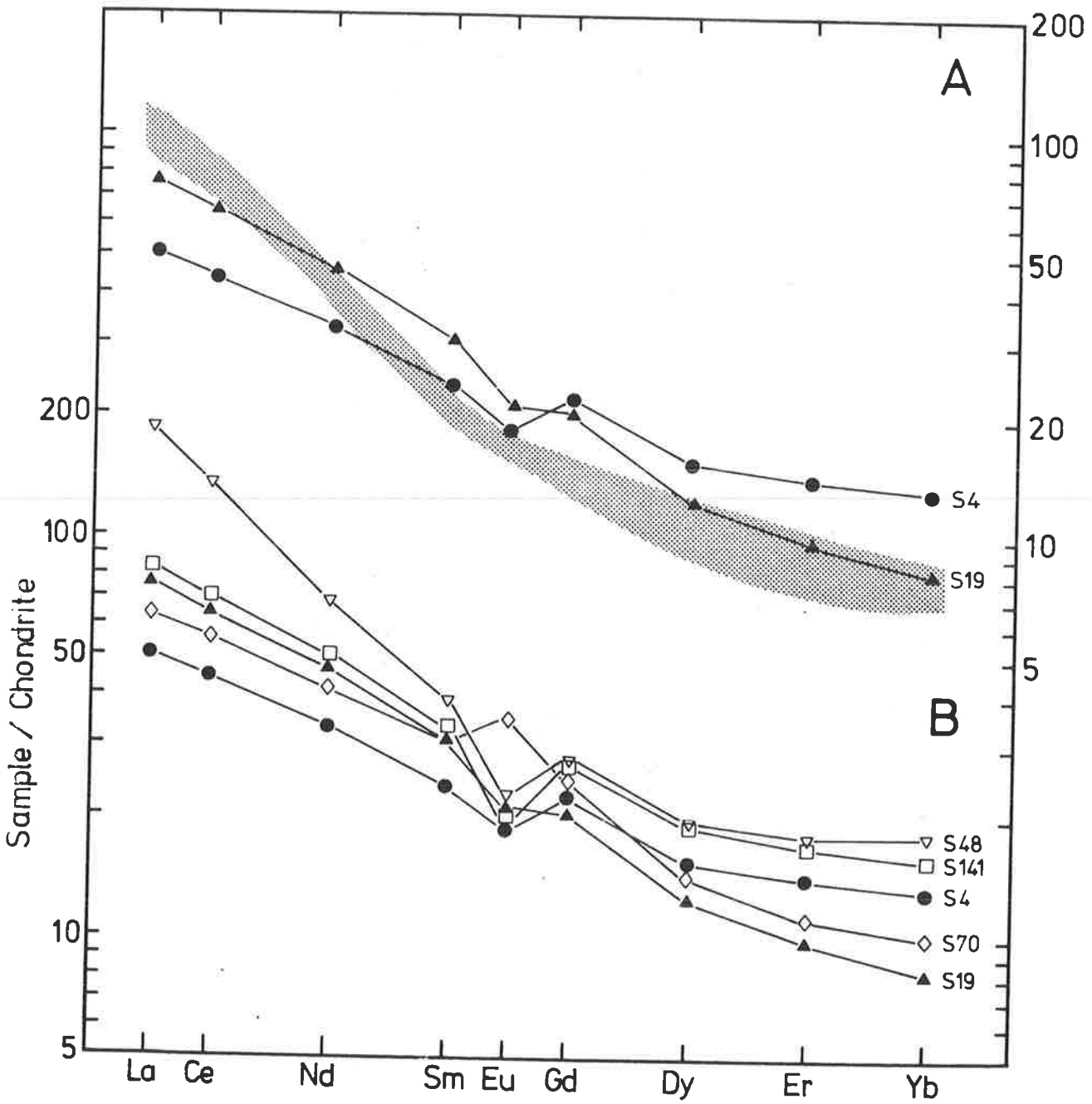

The behaviour of Y and also that of Sc, V and Ti discussed earlier, points to complexities in the origins of the intermediate rocks that may be related to differing crystallisation histories and/or variations in the parental magmas. Similar conclusions can be drawn from the Ce vs SiO_2 relationship (Fig. 6.8D), where, within the andesite, dacite and rhyolite fields respectively, significant variations occur in the observed Ce contents. To investigate this aspect further, complete REE determinations were made for five representative samples from the Spring Well complex.

D. Rare earth elements

Chondrite normalised REE plots for the two low-silica andesite dykes (S19 and S4) are given in Figure 6.9A (data in Table A6.3, Appendix 1), and although the major elements of the two rocks are very comparable their REE patterns are quite different and actually cross. S4 (57% SiO_2, 4% MgO) has a moderately fractionated REE pattern with La/Yb = 6. Various features, including the La/Yb, HREE content (13x chondrite), LREE content (50x chondrite) and the shape of the pattern are very analogous to the basalts and andesites with less-fractionated REE patterns from the Welcome Well complex (Fig. 5.11B, chapter 5). S19 (55% SiO_2, 5.3% MgO), on the other hand, has a more fractionated REE pattern with La/Yb = 14. It has a similar La/Yb, HREE content (8.3x chondrite) and LREE content (76x chondrite) to the Welcome Well complex samples with more fractionated REE patterns (Fig. 5.11A), although the shape of the pattern does differ slightly. It is notable that the differing LREE contents of the two samples are also reflected in their respective P_2O_5 contents (S19-0.41% P_2O_5, 55 ppm Ce, compared with S4-0.28% P_2O_5, 37 ppm Ce), such that the P_2O_5/Ce value remains approximately constant (P_2O_5/Ce = 745 in S19 c.f. 756 in S4).

Major element modelling, using reasonable mineral compositions, reveals that S4 could be derived from S19 by fractionation of 10% clinopyroxene, 11.5% plagioclase, 4.7% amphibole and 1.4% Ti-magnetite (Table 6.1). All of these minerals have REE mineral/melt distribution coefficients less than one when in equilibrium with an intermediate melt and therefore their removal from a parent with the composition of S19 would result in a proportional increase in all REE, which is clearly inconsistent with the cross-over relationship noted with S4 (Fig. 6.9A). Thus it is concluded that S4 and S19 cannot be related by simple fractional crystallisation. Possible reasons for the differences in the REE patterns will be considered later in the discussion on the petrogenesis of these rocks.

Chondrite normalised patterns are also presented for a dacite (S141) and two rhyolites (S48 and S70) in Figure 6.10. The dacite (S141, 65.6% SiO_2) has La/Yb = 8 which is slightly greater than that of S4 (La/Yb = 6)

TABLE 6.1. Summary of least squares modelling calculations designed to investigate possible paths of crystal fractionation in rocks from the Spring Well complex.

PARENT		MINERALS					DAUGHTER				
S19	S4	amph. W59	cpx. W22	plag. An54	mag. 76/18	apatite	S4	S141	S48	S70	ΣR^2
*		6.6	7.7	10.0	1.5	0.44	75				0.123
*		17.1	12.9	26.4	4.4	0.75		40			0.002
*		29.8	4.2	28.4	5.4	0.88			32.4		0.020
*		26.4	8.5	32.1	6.0	0.88				28	0.008
					80/14						
	*	13.4	7.2	22	4.2	0.40		54			0.0001
	*	30.4	4.5	24.5	5.6	0.57			43		0.0029
	*	25.8	1.2	29.6	6.3	0.57				37	0.0536

Notes:

1. Clinopyroxene and amphibole compositions taken from electron microprobe analyses of phenocrysts in the Archaean calc-alkaline volcanic rocks (see Table A 5.5, Appendix 1). The particular compositions chosen were considered most appropriate to the fractionation schemes tested.
2. Plagioclase and apatite compositions after Wright (1974).
3. Magnetite compositions as indicated, excepting for S19 → S141 which used 74% FeO^t and 20.5% TiO_2.
4. All weight fractions expressed as percentages.

TABLE 6.2. Calculated trace element abundances using mineral proportions and degree of crystallisation obtained from major element modelling calculations.

Rock	S19 parent	S48 obs.	S48 calc.1	S48 calc.2	S4 parent	S141 obs.	S141 calc.	S48 obs.	S48 calc.	S70 obs.	S70 calc.1	S70 calc.2
Ce	65	134.7	131	145.4	44.7	69.6	64.2	135	72.1	56.4	78.4	63.6
Nd	46.6	69.7	77.7	87.6	33.3	51	43.9	69.7	46.6	41.7	50.8	20.7
Sm	31.1	39.6	45.7	54.3	23.9	33.8	28.7	39.6	28.3	31.0	31.1	9.15
Eu	21.8	22.1	30.9	42.2	18.5	20.5	19.2	22.1	18.3	35.0	18.8	3.83
Gd	20.8	31.3	29.7	36.7	22.3	27.4	25.6	31.3	24.5	29.6	27.0	4.83
Dy	12.5	19.2	18.1	22.0	15.4	19.2	18.0	19.2	17.8	14.5	19.9	2.54
Er	9.85	18.0	16.2	19.5	14.0	17.2	16.6	18.0	16.6	11.3	18.5	2.70
Yb	8.29	18.2	15.5	18.3	13.0	15.8	15.8	18.2	16.1	10.1	18.0	4.10
Sr	378	94	228		202	129	144					
Zr i	161	199	238		149	233	207					
Nb i	9.8	13	14		7.7	10.6	10.4					
Y b	31	45	45		31	43	42					
Y i	31	45	18		31	43	28					

Distribution coefficients used				
amph.	cpx.	plag.	mag.	apatite
0.20(0.094)	0.15(0.077)	0.12(0.023)	0	18
0.33(0.16)	0.31(0.17)	0.081(0.023)	0	27.4
0.52(0.24)	0.5(0.26)	0.067(0.024)	0	29.3
0.59(0.26)	0.51(0.27)	0.34(0.055)	0	20.5
0.63(0.28)	0.61(0.32)	0.063(0.017)	0	27.2
0.64(0.31)	0.68(0.5)	0.055(0.01)	0	25.6
0.55(0.24)	0.65(0.46)	0.063(0.01)	0	20.0
0.49(0.23)	0.62(0.43)	0.067(0.006)	0	13.1
0.46	0.12	3.0	0	0
1.4	0.25	0.03	0.2	0
1.3	0.3	0.025	1	0
1.0	0.5	0.03	0.2	13.1
2.5	1.5	0.06	0.5	20

Notes:

1. All of the REE abundances quoted are chondrite normalised.
2. REE distribution coefficients used for S19 → S48 calc.1 and calc.2 are the unbracketted and bracketted values, respectively, reported in this table and correspond with the average and low values quoted by Arth (1976) for basaltic and andesitic rocks.
3. REE distribution coefficients used for S4 → S141, S48 and S70 (calc.1) are the high values quoted by Arth (1976) for basaltic and andesitic rocks and are given in Table 5.2C (in brackets).
4. REE distribution coefficients for S4 → S70 calc.2 utilize the values for dacitic rocks reported by Arth (1976), and are given in Table 5.2C (unbracketted values).
5. The Zr, Nb and Y distribution coefficients are after Pearce and Norry (1979). The subscripts i and b refer to calculations which use values reported by these authors for intermediate and basic rocks, respectively.

Figure 6.10 Observed and calculated REE distributions in rocks from the Spring Well complex.

A. Model for S141 (dashed line) calculated assuming derivation by fractional crystallisation from S4.

B. Solid triangles define the calculated REE pattern for S48, assuming derivation by fractional crystallisation from S4. Open and solid diamonds define the calculated REE patterns for S48, assuming derivation by fractional crystallisation from S19 and using different sets of Kds (see Table 6.2).

The stipple in A and B encompasses the field of dacites and rhyolites, respectively, from the Marda complex (after Taylor and Hallberg, 1977).

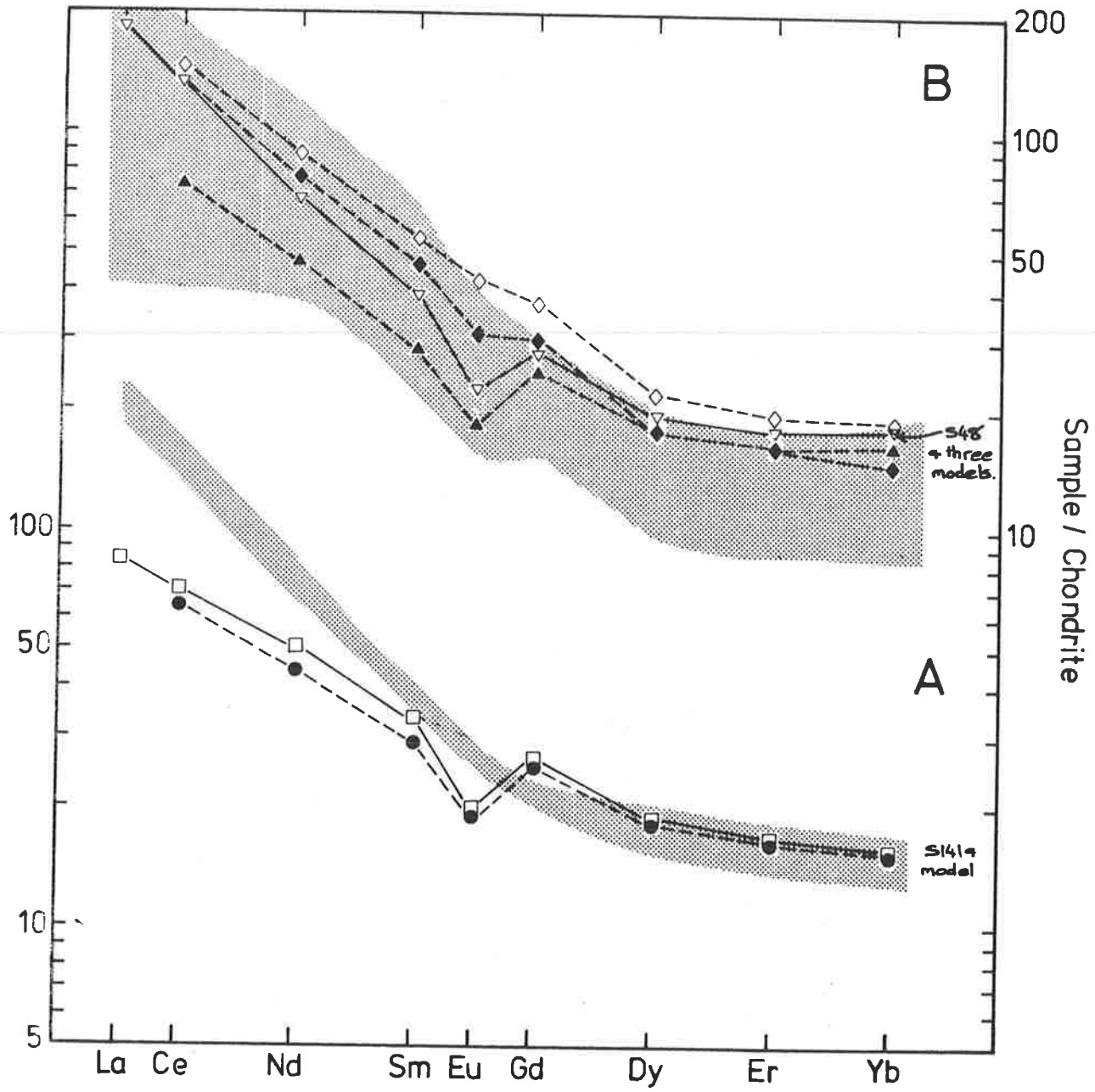

but significantly less than that of S19 (La/Yb = 14). Major element modelling shows that it would be possible to derive S141 from either an S4 or S19 type parent by fractionating the appropriate proportions of clinopyroxene, plagioclase, amphibole and Ti-magnetite (Table 6.1). Modelling of the REE using the calculated mineral proportions and appropriate distribution coefficients reveals that while S4 is a probable parent to S141, S19 is highly improbable (Fig. 6.10A, Table 6.2). The important point to note is that the geochemical data is consistent with the dacite (S141) being derived from the andesite (S4) by simple crystal fractionation. The negative Eu anomaly in the dacite may therefore be a direct result of the significant amounts of plagioclase fractionation involved. This conclusion is also supported by the Sr, Zr, Nb and Y data, which shows a close match between observed and calculated values for S141 (Table 6.2).

S48 is a rhyolitic crystal tuff (75% SiO_2) with a high LREE content and a marked negative Eu anomaly. It has La/Yb = 15 which is comparable with that of S19 (La/Yb = 14) but this tends to camouflage the differing shapes of the two REE patterns (Fig. 6.9B), which are more accurately compared via the La/Sm and Sm/Yb ratios. (e.g. S48 has La/Sm = 7.4 and Sm/Yb = 2.0 while S19 has La/Sm = 3.4 and Sm/Yb = 3.5). On the basis of major element modelling (Table 6.1), either an S19 or S4 type parent would be permissable. Modelling of the REE using the relevant mineral proportions eliminates S4 as a parent, but indicates that within the limits of the uncertainties in the distribution coefficients, S48 could be derived from a parent with the composition of S19 (Fig. 6.10B, Table 6.2).

Further information on the REE characteristics of rocks from the Spring Well complex can be gained by plotting chondrite normalized Ce, Nd, Zr, Nb, Y and Ti determined by XRF. This approach uses the fact that Y and Zr can give an indication of the HREE and MREE respectively (Sun, et al., 1979). Applying this in the case of the two high-silica andesite dykes (S44 and S91) suggests that S44 (59.7% SiO_2, 4.26% MgO) is markedly depleted in REE compared with the low-silica andesites (S19 and S4), while S91 (59.6% SiO_2, 4.43% MgO) is enriched, despite their comparable SiO_2, MgO and Ni contents (Fig. 6.11A). These differences are analogous to those noted between the two low-silica andesite dykes (Fig. 6.9A), which also have similar major element geochemistry. It is therefore likely that the marked differences in REE (and P_2O_5 and TiO_2) between S44 and S91 relate to the same ultimate causes as in the case of the two low-silica andesites (i.e., S19 and S4).

Figure 6.11 Chondrite-normalized Ce-Nd-Zr-Nb-Y-Ti plot for selected rocks from the Spring Well complex. The SiO_2 contents are given below the sample numbers. S96 is a tholeiitic basalt from beneath the Spring Well complex.

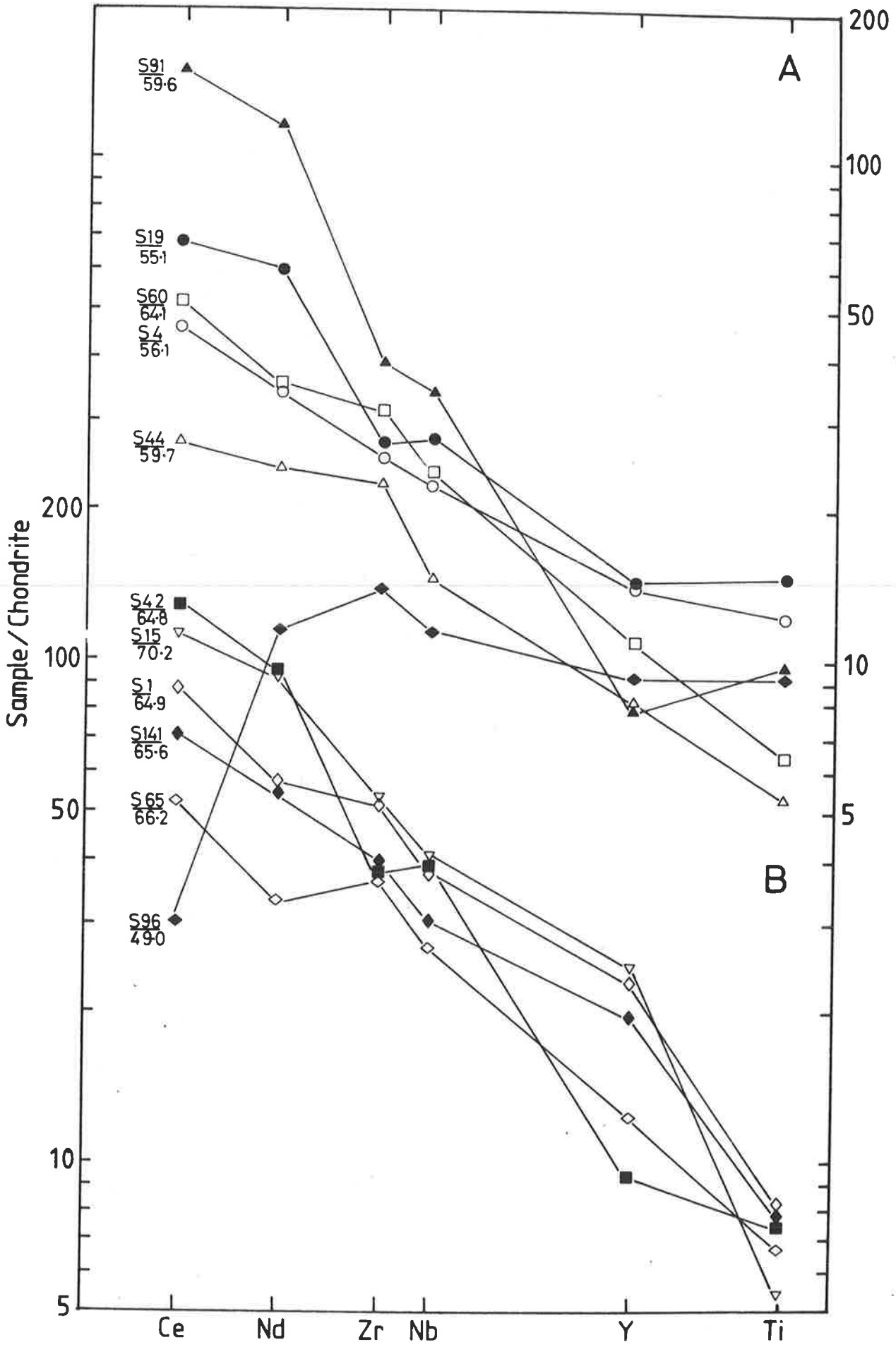

The dacites show comparable Ce-Nd-Zr-Nb-Y-Ti variations to the andesites (Fig. 6.11B). For example, S60 has significantly lower LREE than S42, despite the fact that both samples have analogous major element geochemistry, excepting for P_2O_5 which varies sympathetically with the LREE. Similar comments apply to the other two dacites (S1 and S65) and to the rhyolites which have also been plotted. This leads to the important conclusion that the andesites and dacites, and to a lesser extent, the rhyolites, cannot be readily related by crystal fractionation within their own compositional fields. However, considered as a group, the dacites and rhyolites show a similar wide range in REE (and Zr, Nb, Y, TiO_2 and P_2O_5) to the andesites. The significance of these observations will be considered in the discussion on the petrogenesis which follows.

6.6 PETROGENESIS

At this point three fundamental questions relating to the origin of the rocks comprising the Spring Well complex remain unanswered:

1) The genetic relationship (if any) between the intrusive and extrusive rocks.
2) The genetic relationship (if any) between the andesites, dacites and rhyolites.
3) The ultimate origin of the magma or magmas.

Each of these questions will be considered below in the light of the available field, petrographic and geochemical evidence.

In relation to the first question, it is believed that the close spatial association of the intrusive and extrusive rocks in the field and their petrological similarity, are of particular significance. This evidence, combined with the observation that on most of the geochemical variation diagrams the acid intrusive and extrusive rocks overlap, strongly suggests that both groups of rocks are genetically related or are comagmatic.

The relationship between the acid and intermediate rocks is not so clear, however. There appear to be two main possibilities: either the acid magmas have differentiated from intermediate parents, implying a calc-alkaline differentiation series, or the acid and intermediate magmas have separate, anatectic origins. The latter alternative has been advocated by Taylor and Hallberg (1977) to explain the origin of the acid and intermediate volcanics comprising the Marda complex, which in many ways is analogous to the Spring Well complex. Taylor and Hallberg noted that the "chemical compositions and field relationships alike suggest a continuum and hence a genetic relationship. This important observation suggests that both the ignimbrites and the andesites and dacites share a

TABLE 6.3. Results of least squares modelling calculations for S19, S4, S91, S141 and S48 in terms of likely residual minerals and a hypothetical crustal source with the composition of Hallberg and William's (1972) average Eastern Goldfields Archaean tholeiite.

Rock	S19 product	crustal source obs.	crustal source calc.	S4 product	crustal source calc.	S91 product	crustal source calc.	S141 product	crustal source calc.	S48 product	crustal source calc.
SiO_2	55.61	52.31	52.30	57.45	52.31	59.88	52.31	66.50	52.31	75.33	52.31
Al_2O_3	15.68	15.09	15.09	15.80	15.09	15.54	15.09	14.59	15.09	12.99	15.09
FeO^t	9.04	10.71	10.71	8.93	10.71	5.74	10.71	5.97	10.71	2.46	10.71
MnO	0.16			0.13		0.08		0.10		0.05	
MgO	5.31	6.83	6.80	4.10	6.84	4.45	6.83	1.83	6.83	0.71	6.83
CaO	9.07	11.01	11.05	7.10	11.00	7.21	11.01	2.48	11.01	2.75	11.01
Na_2O	2.39	2.75		4.03		3.39		6.24		3.67	
K_2O	0.78	0.18		0.91		2.14		1.27		1.76	
TiO_2	1.55	0.98	1.20	1.27	0.91	1.00	0.99	0.84	1.00	0.23	0.94
P_2O_5	0.41	0.12		0.28		0.57		0.18		0.04	
Total	100.0	100.0		100.0		100.0		100.0		100.0	

Component	Wt. fraction	Mineral proportion		Wt. fraction	Mineral proportion		Wt. fraction	Mineral proportion		Wt. fraction	Mineral proportion		Wt. fraction	Mineral proportion
S19	0.666		S4	0.524		S91	0.484		S141	0.305		S48	0.254	
amph.	0.062	0.18		0.087	0.18		0.093	0.18		0.129	0.18		0.207	0.28
cpx.	0.13	0.39		0.19	0.39		0.185	0.35		0.244	0.35		0.197	0.26
plag.	0.111	0.33		0.165	0.34		0.19	0.36		0.266	0.38		0.27	0.36
mag.	0.034	0.10		0.041	0.085		0.064	0.12		0.067	0.095		0.075	0.10
= source			= source			= source			= source			= source		
ΣR^2	0.053			0.0052			0.0001			0.0003			0.002	

Notes: 1. Na_2O, K_2O, MnO and P_2O_5 excluded from modelling calculations.

2. Mineral compositions used are those reported in Table 5.3 and similar comments apply.

common origin" (p. 1127). They considered that the "genetic relationship" involved partial melting of different levels of the crust rather than crystal fractionation. It was reasoned that the andesitic magma was derived by partial melting of a mafic source at the base of the crust while the acid magma was produced by progressively lower degrees of melting at higher levels in the crust. There is a marked analogy in the geochemistry of rocks from the Marda complex and the Spring Well complex, demonstrated for example by the REE (Figs. 6.9 and 6.10), and thus it is evident that this model needs to be tested for the case of the Spring Well complex.

The geochemistry of the rocks within each of the compositional groups (i.e., andesite, dacite, rhyolite), while very similar in terms of most major elements, show significant differences in certain trace element contents (e.g. REE, Zr, Y, Sc and V and also TiO_2 and P_2O_5). For example, the differences in the REE patterns of the two low-silica andesite dykes (S4 and S19) have been previously pointed out. It was shown by major element and REE modelling that the two rocks could not be related by simple fractional crystallisation. Implicit in this finding is the fact that they are also unlikely to have been derived by differing degrees of partial melting of the same source. The similar major element geochemistry of S4 and S19 precludes large variations in the degree of melting, necessary if the significant differences in the REE (and P_2O_5, TiO_2 and V contents) are to be explained. This objection can be negated to some extent by assuming a heterogeneous source, but the source in this case would have to show extreme (and variable) heterogeneity if it were to be able to explain similar, but more pronounced REE differences in the high-silica andesites (e.g. S44 and S91) and dacites (e.g. S60 and S42). In the case of the high-silica andesites and dacites (and rhyolites) the analogous major element contents of the rocks would place even more restrictions on the extent to which the degree of partial melting could vary. Thus, on these grounds it is questioned whether in fact variations in the degree of partial melting could alone account for the range in REE and other trace element contents within the andesite, dacite and rhyolite fields.

Another important consideration is whether the geochemistry of the low-silica andesite dykes (S4 and S19) is consistent with a mafic crustal source as proposed by Taylor and Hallberg (1977). To test this proposition a mafic crustal source, having the composition of Hallberg and William's (1972) average Archaean tholeiite with a flat 10x chondrite REE content (Condie, 1976; Sun and Nesbitt, 1978; Stolz, 1980), was assumed. It is possible to satisfactorily model the major elements of S4 and S19 from this source, assuming the residue is composed of clinopyroxene, amphibole,

TABLE 6.4 Calculated trace element abundances in S19, S4, S91, S141 and S48 assuming a basic crustal source and using mineral proportions and degree of melting obtained from major element modelling calculations reported in Table 6.3

	crustal source	S19 obs.	S19 calc.	S4 obs.	S4 calc.	S91 obs.	S91 calc.	S141 obs.	S141 calc.	S48 obs.	S48 calc.
Zr	61	161	85	149	103	237	110	233	152	199	157
Nb	3.2	9.8	4.3	7.7	5.1	12.2	5.3	10.6	7	13	6.8
Y	20	31	25	31	28	17.6	29	43	35	45	34
Ce	8	53	11.3	36	13.6	123	15	57	20	110	22
Sm	1.9	6.0	2.5	4.6	2.8			6.5	3.7	7.6	4.0
Yb	2.1	1.72	2.7	2.7	3.0			3.3	3.9	3.8	4.2
Sr	105	378	116	202	120	777	119	129	121	94	123
Sc	40	26	21	26	18	14	17.6	15	15	5	11
V	320	158	85	187	68	106	59	126	48	14	34
Cr	367	217	49	19	37	168	35	6	27	7	25
Ni	170	96	77	47	64	105	61	13	52	12	46

Notes:
1. Distribution coefficients used are those reported in Table 3.3B.
2. Zr, Ni, Cr, V and Sr values in assumed basic source are after Hallberg and Williams (1972) average Eastern Goldfields Archaean tholeiite. The remainder of the values are best estimates based on the data of Nesbitt and Sun (1976), Purvis (1979), Stolz (1980) and unpublished data of the writer.

plagioclase and magnetite (Table 6.3). However, the degree of melting in both cases is high (in excess of 50%) and if the calculated fraction of melting and mineral proportions are applied in trace-element modelling calculations, it is found that the calculated contents of Zr, Nb, LREE, MREE, Sr and V are significantly less than the observed contents in the low-silica andesites (Table 6.4). Significant discrepancies are also noted for other trace elements (e.g. Ni and Cr), but the absolute differences between calculated and actual values vary between S4 and S19 (Table 6.4). The discrepancies in the calculated and observed LREE and MREE contents could be reduced if it is assumed that the mafic source had a higher LREE and MREE content, but this would necessitate Archaean tholeiites with greater than 20x chondrite LREE, few of which are known in Archaean supracrustal successions. A more mafic source would require a lower degree of melting in order to satisfy the major elements, but in general, ultramafic rocks have lower LREE contents than mafic rocks (rarely greater than 5x chondrite, Sun and Nesbitt, 1978), so that the discrepancy in LREE and MREE would remain. Addition of a LREE and MREE enriched melt derived from a minor tonalitic component within the mafic crustal source could also be invoked, but is considered unlikely because at the temperatures of melting concerned (i.e., sufficient to cause >50% melting of basalt), most of the tonalite would have melted. Hence the LIL element-enriched melt could only be added as a dilutent and therefore its effect on the geochemical characteristics of the magma would be expected to be small. Moreover, the relatively low K_2O, Rb and Ba contents in S4 and S19 and the absence of a negative Eu anomaly (due to residual plagioclase) argues against any contribution from a tonalitic source. In any case, the discrepancies in Ni, Cr, Sr and V would probably still remain even if contribution from a tonalitic source was invoked. It is therefore concluded that a basic crustal source, with the composition of an Archaean tholeiite, cannot satisfactorily account for the trace element characteristics of the andesites.

This conclusion has some important implications. For example, if the andesites were not derived from a crustal source, then the only other realistic alternative available is a mantle source. However, experimental studies do not favour derivation of intermediate magmas by direct melting of the mantle (Green, 1976), although some workers would disagree (e.g. Mysen and Kushiro, 1973). If Green's (1976) experimental evidence is accepted, then given the fact that the andesites cannot be products of crustal melting, the inescapable conclusion is that the andesites must have fractionated from more basic parents which in turn were generated directly from the mantle. This conclusion is supported by the geochemical

TABLE 6.5. Elemental ratios for S19 and S4 compared with values for rocks from the Welcome Well complex.

Ratio	Probable chrondritic value	S19	S4	A	W3
$Zr/_{Ce}$	7.4-7.7	2.9	4.0	4.9	1.7
$Zr/_{Y}$	2.5-2.8	5.2	4.8	5.7	4.8
$Ti/_{Zr}$	100-110	57	51	49	55
$Ti/_{Y}$	250-280	298	244	278	263
$Zr/_{Nb}$	16-18	16	19	18	18
$Ti/_{V}$	8.4-10	58	40	32	31
$Ti/_{Sc}$	78-85	355	291	236	242
$TiO_2/_{P_2O_5}$	STP=10	3.8	4.5	5.5	2.7
$\%SiO_2$		55.06	56.90	56.2	50.29
%MgO		5.26	4.06	6.50	11.37

Notes:
1. A is an average compiled for five andesites from the Welcome Well complex (W4, W123, W125, W5 and W23).
2. W3 is the primitive basalt from the Welcome Well complex.
3. Source of chondritic values given in Table 2.6.

analogies between the low-silica andesites of the Spring Well and Welcome Well complexes. It will be recalled that the Welcome Well andesites were considered to be the products of fractionation of mantle-derived basic magmas (chapter 5). Apart from the analogies in the major element geochemistry, it has been pointed out that the REE pattern of S19 greatly resembles that of the relatively fractionated group from the Welcome Well complex, while the REE pattern of S4 coincides with the less-fractionated group. In addition, the elemental ratios of S4 and S19 are comparable in every respect to those for the basalts and andesites from the Welcome Well complex (Table 6.5).

The alternative interpretation that the geochemical analogies are fortuitous would require that different processes operated to yield rocks with similar geochemistry. This is considered improbable in view of the similar environments of formation of the two centres and the exclusion of a crustal source for the intermediate rocks from the Spring Well complex on geochemical grounds.

The conclusion that the andesites from the two centres have a comparable origin, based on the geochemical analogies, implies that the geochemical variations in the Spring Well andesites (e.g. between S19 and S4) can be satisfactorily explained in terms of the model outlined for the Welcome Well complex (chapter 5). In this model the primary magma was considered to have been produced by hydrous melting of a LIL element-enriched zone of the upper mantle. Thus, the variability in the absolute contents of the LIL elements in the andesites could be reflecting heterogeneities in the mantle source and/or differing pressure-temperature conditions during partial melting. Unfortunately because of the lack of basalts and basaltic-andesites in the Spring Well complex, proof for the operation of this model cannot be given, however, the marked geochemical analogy of the Spring Well andesites with those in the Welcome Well complex where the model is demonstrable, is considered to offer reliable evidence that the model is applicable to the genesis of the primary magmas for the Spring Well complex. Since the high-silica andesites (S91, S44) have comparable geochemical characteristics to the low-silica andesites (e.g. MgO, Ni, Cr, REE, Zr, Nb, Y and P_2O_5) they are inferred to have a similar origin. This conclusion is supported by modelling calculations for S91 (a high-silica andesite with 59.6% SiO_2 and 4.4% MgO), which show that the calculated levels of all trace elements modelled do not match those observed, assuming the same hypothetical mafic crustal source as before (Table 6.4).

The origin and relationships of the acid rocks still remains unresolved since they could be the products of crustal melting as Taylor and Hallberg (1977) suggest for the Marda complex, or alternatively, they may be differentiates of intermediate parents. The question of their origin can be approached in a similar manner to that adopted for the low-silica andesites, where various crustal sources are tested for closeness of "fit" with respect to the major and trace elements. As an initial test the major elements of S141 (65.6% SiO_2) were modelled from the hypothetical mafic crustal source; it was found that approximately 30% partial melting leaving a residue dominated by plagioclase and clinopyroxene yielded a satisfactory solution (Table 6.3). Applying these results in a trace element modelling calculation revealed that the calculated values of LREE, MREE, Zr and V were significantly lower than the actual contents, while Ni and Cr were higher (Table 6.4). The discrepancies are of such an order that reasonable variations in the source composition, degree of melting and mineral proportions are unlikely to produce a fit. Similar results were obtained by modelling S42 (65.4% SiO_2) from the same source (results not reported), thus supporting the conclusion that the dacites do not represent melts derived from a mafic crustal source.

In previous chapters, Proterozoic dacites have been satisfactorily modelled from a basic-intermediate granulite source (see chapters 2 and 3). However, in comparison with their Archaean counterparts these dacites are significantly higher in K_2O (e.g. 4-5% c.f. 1-3%), Rb (e.g. 150-200 ppm c.f. 20-60 ppm) Ba (e.g. 1000 ppm c.f. 600 ppm) and all REE (e.g. > 120 ppm Ce c.f. 60 ppm Ce) thus arguing against a comparable sialic crustal source for the Archaean rocks. A tonalitic source with higher Na_2O/K_2O may be more appropriate, but Archaean tonalites are relatively low in Y (and HREE), generally having contents <20 ppm (Glikson, 1979b). Thus, at the high degrees of melting necessary to produce the dacitic magma (>50% partial melting), it would be impossible to obtain the greater than two-fold enrichment in Y necessary to match the level in S141 (43 ppm) particularly as amphibole is likely to be a major residual phase. Furthermore, a tonalitic source would be unable to account for the relatively high V and Sc contents in S141. Addition of garnet to the residue would only magnify the discrepancy in Y, HREE, V and Sc.

Modelling a rhyolite (S48) in the same manner yields comparable results. For example, if a mafic crustal source is assumed, the calculated LREE, MREE, Zr and Nb contents are much less than the observed contents, while Ni, Cr and V are significantly higher (Table 6.3 and 6.4). The alternative of a tonalitic source is more complex however, since the major

TABLE 6.6. Results of major and trace element modelling calculations designed to investigate the possibility of a tonalitic crustal source for acid volcanics of the Spring Well complex typified by S48.

A. Least squares approximation of S48 in terms of a hypothetical source of tonalitic composition and a granulitic residual mineral assemblage.

Rock	tonalitic source obs.	tonalitic source est.	S48 melt	Mineral compositions used: opx.	cpx.	plag.	mag.	apatite
SiO_2	64.05	64.05	75.33	53.0	51.3	58.1		
Al_2O_3	15.91	15.91	12.99	4.7	5.2	26.4		
FeO^t	4.34	4.38	2.46	14.8	14.4	0.02	78.0	
MnO	0.07		0.05					
MgO	3.81	3.79	0.71	23.2	14.9	0.03		
CaO	5.01	5.0	2.75	3.3	12.3	7.8		56.0
Na_2O	4.25		3.67					
K_2O	1.64		1.76					
TiO_2	0.64	0.44	0.23	0.9	1.2		16.0	44.0
P_2O_5	0.26	0.27	0.04					
Total	100.0		100.0					

Mineral	Wt. fraction	Mineral proportion
opx.	0.134	0.262
cpx.	0.022	0.044
plag.	0.338	0.66
mag.	0.0114	0.022
apatite	0.0057	0.011
S48	0.480	
	= tonalitic source	
ΣR^2	= 0.0421	

Notes:
1. Na_2O, K_2O and MnO excluded from modelling calculations.
2. Orthopyroxene and clinopyroxene compositions from experimental data of Green (1969) for a starting composition comparable with the tonalitic source.
3. Plagioclase composition is after Deer, Howie and Zussman (1978) for andesine in a two-pyroxene granulite.
4. Apatite composition after Wright (1974).
5. Composition of tonalitic source is taken from an average compiled by Stolz (1980) for the Scotia tonalite, W.A., which has been shown by this author to be typical of other tonalitic plutons and gneisses in the Yilgarn Block.

B. Least squares approximation of S48 in terms of a hypothetical source of tonalitic composition and a residual mineral assemblage containing amphibole.

Rock	tonalitic source obs.	tonalitic source est.	S48 melt	Mineral compositions used: amph.	plag.	mag.	apatite
SiO_2	64.05	64.05	75.33	45.66	64.10		
Al_2O_3	15.91	15.90	12.99	11.10	22.26		
FeO^t	4.34	4.35	2.46	12.00	0.37	88.0	
MgO	3.81	3.76	0.71	15.23	0.25		
CaO	5.01	5.10	2.75	11.86	3.26		56.0
TiO_2	0.64	0.52	0.23	1.76		6.0	
P_2O_5	0.26	0.14	0.04				44.0

Mineral	Wt. fraction	Mineral proportion
amph.	0.222	0.970
plag.	0.369	0.615
mag.	0.0064	0.0107
apatite	0.0029	0.0048
S48	0.402	
	= tonalitic source	
ΣR^2	= 0.039	

Notes:
1. Amphibole composition from microprobe data for phenocrysts in an Archaean calc-alkaline dacite (I12, see Table A5.5, Appendix 1).
2. Plagioclase composition is after Deer, Howie and Zussman (1978) for oligoclase in pegmatite.
3. Notes 1, 4 and 5 from A. also apply in this case.

C. Trace element modelling results based on the major element modelling calculations reported in A. and B.

	tonalitic source	S48 obs.	S48 model A	S48 model B	Distribution coefficients used: amph.	opx.	cpx.	plag.	mag.	apatite A	apatite B
Zr a	132	199	234	99	4	0.2	0.6	0.1	0.8	0.1	0.1
Zr b	132	199		256	0.5			0.01	0.1	0	
Nb a	5	13	7.6	3.8	4	0.8	0.8	0.06	2.5	0.1	0.1
Nb b	5	13		8.6	0.8			0.01	0.4	0	
Y a	12	45	12	6.3	6	1	4	0.1	2	40	40
Yb	12	45	19	18.9	1	0.2	0.5	0.03	0.2	0	18
Ce	70	110	97	89	0.899	0.33	0.33	0.24	0	34.7	18
Sm	4.67	7.6	5.4	3.09	3.99	1.09	1.09	0.13	0	62.8	29.3
Yb	0.76	3.8	1.0	0.48	4.89	1.1	1.1	0.077	0	23.9	13.1
Rb	38	40	77	91	0.014	0.0027	0.032	0.041	0	0	0
Sr	910	94	454	449	0.022	0.0085	0.516	4.4	0	0	0
Ba	943	548	1600	1800	0.044	0.0029	0.131	0.308	0	0	0
Sc	10	5	10	3	12.5	3	3	0	2	0	0
V	82	14	82	11	32	1.1	1.1	0	30	0	0
Cr	142	7	43	20	30	13	30	0	32	0	0
Ni	74	12	41	33	8	8	6	0	8	0	0

Notes:
1. Distribution coefficients for Zr, Nb and Y after Pearce and Norry (1979); Ce, Sm, Yb, Rb, Sr and Ce after Arth (1976) and Sc, V, Cr and Ni after Gill (1978).
2. Distribution coefficients for Ce, Sm and Yb opx/liquid assumed to equal those quoted by Arth (1976) for cpx/liquid for dacitic liquids.
3. Trace element contents in tonalitic source after Stolz (1980).

elements are compatible with two models. One involves a granulitic residue containing orthopyroxene and clinopyroxene, while the other model involves a more hydrous assemblage containing residual amphibole (Table 6.6A and B). In both models there are significant discrepancies between calculated and observed Sr and Y contents which cannot be reconciled even if extreme distribution coefficients are used (Table 6.6C). Similar comments apply to MREE, HREE, Rb and Ba in both cases and also to Ce and Nb in the model involving residual amphibole. Stolz (1980) has shown that the source composition used in the modelling calculations is typical of tonalitic rocks in Archaean granite-greenstone terrains, an observation that is supported by the data given by Glikson (1979b) in his review of these rocks. A more granodioritic source, higher in Y and lower in Sr, may reduce the mismatch in these elements, but a source of this type would be expected to yield melts with higher LIL element contents (particularly K, Rb, Ba and Ce), more akin to the Proterozoic rhyolites. Thus, as in the case of the dacites, it is concluded that the rhyolites were unlikely to have been derived from either a mafic or an intermediate-acid crustal source.

The alternative origin for the acid rocks, involving fractionation from intermediate parents, does appear to be consistent with the limited major and trace element modelling carried out (e.g. between S4 and S141 and between S19 and S48, Tables 6.1 and 6.2). It is also compatible with the uniform inverse correlations of Al_2O_3, $Fe_2O_3^t$, MgO, CaO, TiO_2, P_2O_5, Sc and V observed for the acid rocks on the variation diagrams (Figs. 6.7 and 6.8). The plots of Zr, Nb, Y and Ce vs SiO_2 (Fig. 6.8), rather than showing separate, unrelated groups of samples, could be interpreted as demonstrating a transferral of the spread in trace element contents in the andesites to the dacites and rhyolites by crystal fractionation. The percentage variation in the contents of Ce, Zr and Y in the andesites and dacites is of roughly the same order, and this is a characteristic that would be expected if the variability were passed on by crystal fractionation. The variability in the rhyolites is significantly higher, however, possibly as a result of late-stage fractionation of accessory minerals such as zircon, apatite and sphene as proposed earlier. It seems unlikely that partial melting of dissimilar sources (viz. mantle for intermediate magma, crust for acid magma) could produce analogous elemental dispersions in the resultant magmas.

If the andesites, dacites and rhyolites are linked by crystal fractionation as most of the evidence would appear to suggest, then it remains to explain why there are apparent gaps in composition between

Figure 6.12 Stability fields of major crystallising phases for water-saturated and water-undersaturated conditions.

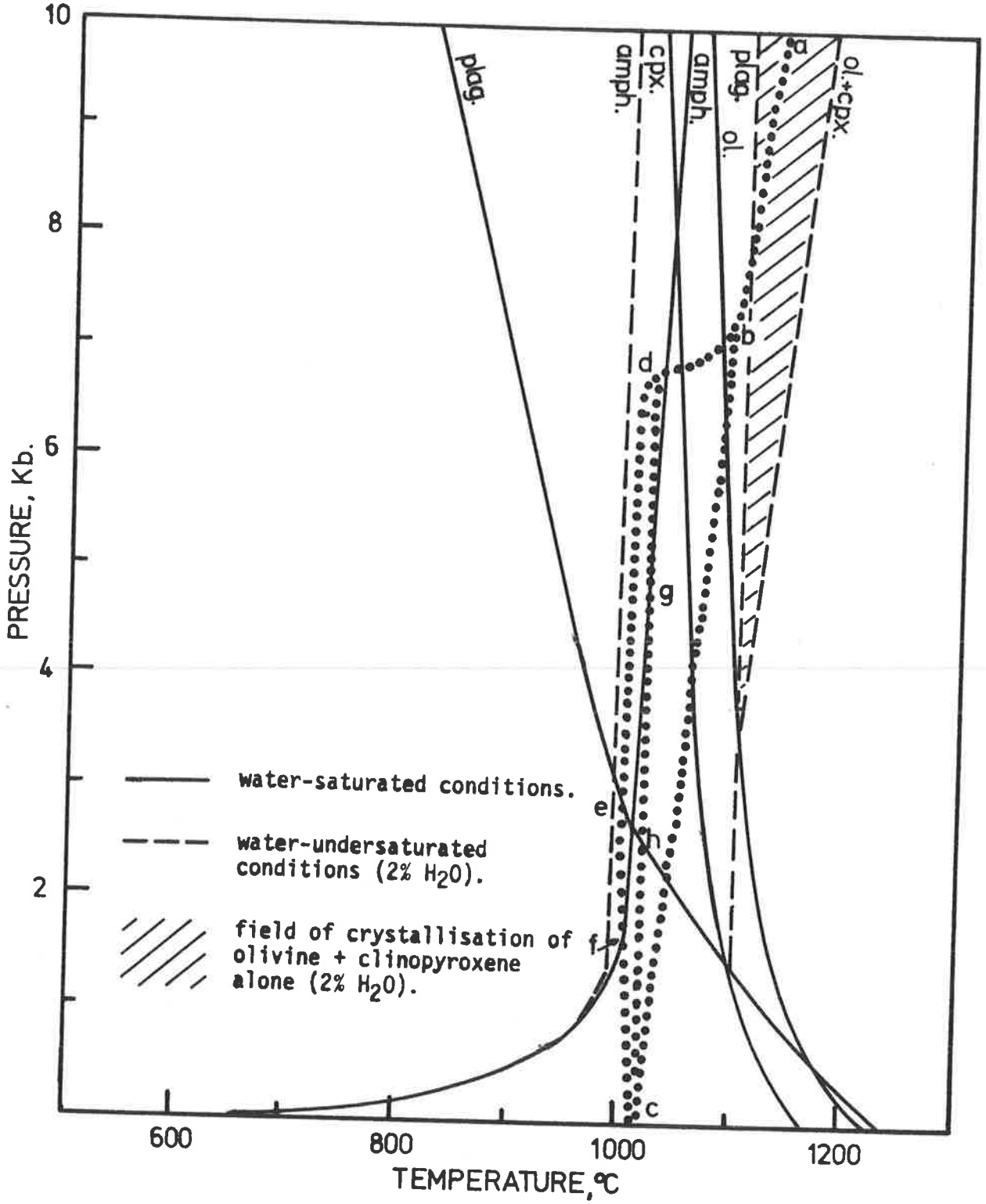

Notes:
1. Stability fields for water-saturated conditions after Yoder and Tilley's (1962) data for high-Al basalt composition.
2. Stability fields of amphibole and plagioclase for 2% H_2O after Eggler's (1971) data for Paricutin andesite and supported by Foden's (1979) data for Rindjani high-Al basalt.
3. Stability field of olivine + clinopyroxene for 2% H_2O after Foden's (1979) data for Rindjani high-Al basalt.
4. Indicated positions of stability fields will vary for the particular rock-compositions being considered.

the andesite-dacite and dacite-rhyolite fields. In answering this question an examination of the possible crystallisation paths is of relevance. A number of workers have shown that under relatively high total pressure (5-10 kb) and PH_2O, a melt of intermediate to basic composition will crystallise clinopyroxene ± amphibole ± plagioclase (e.g. Yoder and Tilley, 1962; Eggler, 1972; Eggler and Burnham, 1973). At lower confining pressures and PH_2O the stability field of plagioclase expands (relative to amphibole and, to a lesser extent, clinopyroxene) so that if PH_2O is reduced at near constant temperature, plagioclase crystallisation will eventually dominate (Fig. 6.12).

In the present case it is likely that the magma fractionated in a shallow crustal reservoir and at certain stages due to vapour build up, PH_2O could have risen to high levels. This would have promoted clinopyroxene and/or amphibole fractionation at the expense of plagioclase (Yoder and Tilley, 1962). If the confining pressure was exceeded, explosive eruption would have occurred, yielding the pyroclastics which are characteristic of the Spring Well complex. The ensuing rapid drop in PH_2O at roughly constant temperature would have caused crystallisation to swing from that dominated by clinopyroxene and/or amphibole to that dominated by plagioclase. This may explain in part, the compositional hiatus observed between the andesites and dacites because once the plagioclase field is entered, large amounts of this mineral will fractionate, thus moving the melt rapidly to more acid compositions. Some evidence for fluctuating pressures during crystallisation is seen in the abundant, zoned plagioclase phenocrysts and the frequent, partially-resorbed quartz phenocrysts. Thus, it is concluded that the apparent grouping of rocks into compositional fields, rather than argueing against crystal fractionation, could in fact be a direct result of the operation of such a process in shallow, crustal magma chambers under conditions of fluctuating vapour pressure and hence changing mineral stability fields.

6.7 SUMMARY

The Spring Well complex is an excellent example of an Archaean acid volcanic centre. It is composed of a pile of dominantly acid pyroclastic rocks that have been intruded by numerous acid and intermediate dykes and sills. The succession proximal to the vent consists of coarse tuff breccias, lapilli tuffs and thick crystal tuffs and is marked by a high density of dykes. Distal to the vent zone, the sequence is dominated by fine bedded tuffs, crystal tuffs, tuffaceous sediments and some epiclastic grits and greywackes.

As a group the acid and intermediate rocks show marked geochemical affinities with Cainozoic calc-alkaline volcanic suites. The intermediate rocks cannot be satisfactorily modelled as liquids from a basic crustal source with the composition of an average Archaean tholeiitic basalt. Their geochemical characteristics, particularly the REE and elemental ratios, are analogous with the andesites of the Welcome Well complex and thus a similar origin, involving differentiation from basic parents of ultimate mantle derivation, is inferred. By analogy with the Welcome Well andesites, it is believed that the variable LIL element contents (particularly LREE, P, Zr and Nb), could largely result from heterogeneities in the source and/or the conditions of partial melting.

Major and trace element modelling calculations demonstrate that the geochemical characteristics of the acid rocks are inconsistent with an origin in partial melting of either a basic (tholeiitic) or tonalitic composition crustal source. REE modelling shows, however, that the dacites and rhyolites could be differentiates of intermediate liquids with the compositions of the andesitic intrusive rocks that cut the volcanic pile. This interpretation is consistent with the elemental variations noted on many of the Harker diagrams, the observed continuum in petrographic features and the close association of all rock types in the field. Thus, much of the dispersion in the LIL element abundances (particularly Ce, Zr, Y and P) in the acid rocks may have been inherited from the intermediate parents through differentiation.

The distinct fields of andesite, dacite and rhyolite evident on some variation diagrams and the paucity of rocks bridging the andesite-dacite and dacite-rhyolite boundaries could possibly be explained by fluctuating PH_2O during crystallisation, with resultant migration in the stability fields of the dominant fractionating minerals. The rapid variations in PH_2O may have been dependent upon periodic venting of the magma chamber(s) to the surface in response to vapour pressure build up.

Figure 7.1 Location of the calc-alkaline volcanic centres in the Yilgarn Block referred to in the text.

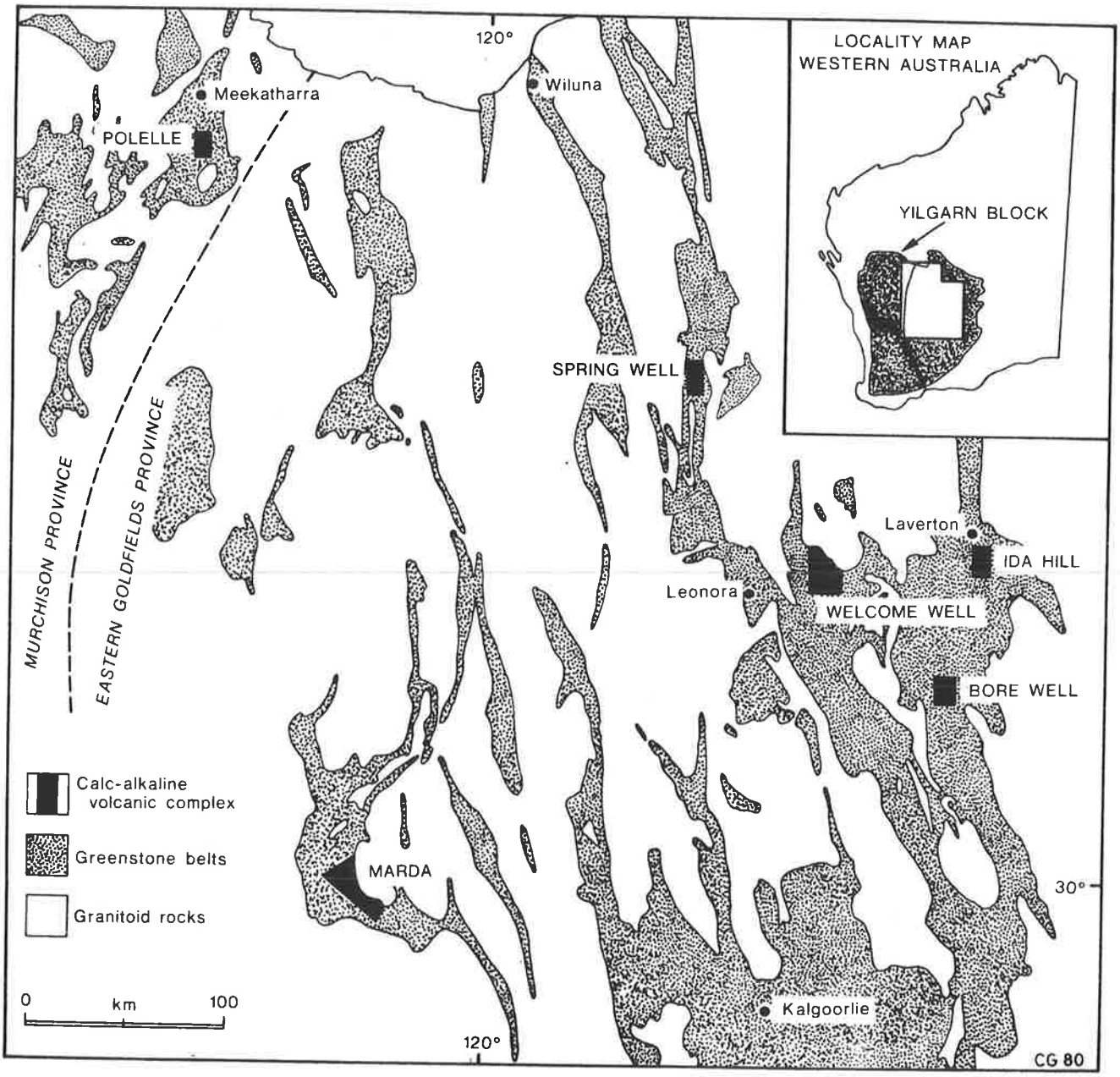

CHAPTER 7

A REVIEW OF ARCHAEAN CALC-ALKALINE VOLCANISM

7.1 INTRODUCTION

The two calc-alkaline volcanic centres examined in the previous chapters differ with respect to the modes of formation of the volcanic piles, the relative proportions of rock types and the fractionation trends. In spite of these obvious differences, it has been argued that the ultimate source of magma was the same in both cases. In view of this, it is of interest to examine other calc-alkaline volcanic centres in the Yilgarn Block to ascertain whether any general similarities exist in:

1) the processes which have operated to build the volcanic piles,
2) the origins of the primary magams, and
3) the crystallisation histories of the magmas.

Consideration will be given to each of these aspects in this chapter in an effort to determine whether any general models of origin are applicable to the calc-alkaline volcanics in the Yilgarn Block.

In pursuit of this objective the data for the Welcome Well complex and Spring Well complex is combined with the data for four other calc-alkaline volcanic centres from the Yilgarn Block. Information on two of the calc-alkaline centres (Marda complex and Polelle complex) has been obtained from the work of Hallberg, *et al.*, (1976a and 1976b), while the other two centres have been examined and sampled by the writer during a reconnaissance of felsic volcanic centres in the Yilgarn Block. To the writer's knowledge the six centres considered here contain the freshest and best-exposed calc-alkaline volcanics in the entire Yilgarn Block and thus it follows that they are likely to yield the maximum amount of reliable information concerning calc-alkaline volcanism in this region. The locations of the various centres and some general information concerning each of them is given in Figure 7.1 and Table 7.1, respectively.

In a later section of this chapter a review of the literature is made for Archaean calc-alkaline volcanics in other continents and comparisons are drawn with the volcanics from the Yilgarn Block. Other questions, such as the genetic relationship of the calc-alkaline volcanics to the tholeiitic volcanics, and the timing of the calc-alkaline volcanism with respect to the overall development of the greenstone belts, will also be considered in this chapter.

TABLE 7.1 Summary of the geology of the centres cited in the text.

CENTRE	GENERAL COMMENTS
Welcome Well	Mostly composed of andesitic flows with intercalated laharic deposits. Epiclastic sediments and tholeiitic basalts occur both at higher stratigraphic levels and contemporaneously. Genetically-related bodies of dacite porphyry flank the centre, while genetically-unrelated ultramafic and mafic sills and dykes and an adamellite pluton intrude the volcanic pile. See Chapter 5 for further details.
Ida Hill	Composed largely of andesitic flows with intercalated laharic deposits. Rare basic flows in sequence. Intruded by small, genetically-related acid-intermediate stocks. Underlain by mafic and ultramafic rocks and sediments, including shales and siltstones.
Polelle	Mostly composed of andesitic flows with minor dacitic flows. Volcanogenic sediments occur at similar stratigraphic levels. Underlain by ultramafic and mafic rocks and sediments (after Hallberg, et al., 1976b).
Spring Well	Composed largely of acid pyroclastic rocks with rare intercalated flows. Volcanic pile is intruded by numerous genetically-related acid and intermediate dykes and sills and small stocks. Minor volcanogenic sediments occur in the distal regions of the centre. Underlain by tholeiitic basalts and sediments and intruded by tholeiitic dykes and sills and an adamellite stock. See Chapter 6 for further details.
Marda	Composed of andesite, dacite and rhyolite flows, and rhyolitic pyroclastic rocks. Pile intruded by genetically-related intermediate dykes and subvolcanic rhyolite porphyry. Underlain by ultramafic and mafic rocks and magnetite-silicate rocks including true B.I.F. (after Hallberg, et al., 1976a).
Bore Well	Consists of acid and intermediate flows and some acid pyroclastic rocks. Presence of some intercalated fine sediments is suggestive of a subaqueous environment in part (after Hallberg, 1980).

7.2 ASPECTS OF THE DEVELOPMENT OF THE CALC-ALKALINE VOLCANIC PILES

An outline of the relative proportions of rock types in each of the centres and the probable modes of eruption are given in Table 7.1. The mode of eruption was determined from a combination of field observation and examination of the preserved textures in thin section. It is notable that the great majority of acid volcanics are of pyroclastic origin, while the intermediate-basic volcanics were erupted as lavas. For example, in the Marda complex ignimbrites of acid composition overlie andesitic lavas (Hallberg, et al., 1976a) and similarly in the Bore Well complex a variety of acid pyroclastics including crystal, lithic and/or vitric tuffs are intercalated with lavas of intermediate composition. This relationship is also demonstrated by comparison of the Welcome Well complex, built largely of intermediate lavas (chapter 5), and the Spring Well complex where the majority of the volcanic pile is composed of acid pyroclastics (chapter 6). A similar connection between mode of eruption and magma composition has been observed in other Archaean terrains such as the Canadian Shield (Baragar and Goodwin, 1969; Clifford and McNutt, 1971; Dimroth, et al., 1976) and southern Africa (Viljoen and Viljoen, 1969; Harrison, 1970). The relationship is commonly, though not invariably, noted for modern calc-alkaline suites (Macdonald, 1972) and it may be a result of such factors as the higher volatile contents and/or viscosity of acid magmas compared with intermediate magmas.

A characteristic feature of the calc-alkaline volcanics in the Yilgarn Block is their restriction to discrete centres. In general, the entire calc-alkaline pile in a particular part of a greenstone belt can be related to the one centre or general vent zone, suggesting a rather short and relatively simple episode of volcanism. The Archaean centres are commonly surrounded by tholeiitic basalts, which will be shown later to be unrelated to the calc-alkaline volcanics. The Welcome Well complex displays this association particularly well: it is probably underlain by an ultramafic-mafic succession (though the contact is not seen), is intruded by differentiated tholeiitic sills and is directly overlain by extensive tholeiitic basalts, which are probably related to the sills. Ultramafic sills and dykes also intrude the succession and further to the south ultramafic lavas are found at higher stratigraphic levels than the calc-alkaline volcanics (Hallberg, 1980). Distal to the centre, epiclastic sediments derived from the volcanic complex are intercalated with pillowed tholeiitic basalts thus indicating approximate contemporaneity of the tholeiitic and calc-alkaline volcanism in a lateral sense. Similar features appear to characterise many Archaean calc-alkaline volcanic piles;

for example Baragar and Goodwin (1969) have noted that within the Canadian greenstone belts "the salic rocks are commonly concentrated in clusters, probably marking ancient volcanic centres, whereas the mafic components are more broadly and evenly distributed". These observations do not support the concept of large-scale volcanic cycles grading from ultramafic through mafic to felsic igneous activity, as has been advocated for some greenstone belts in the Canadian Shield (e.g. Wilson and Morrice, 1977).

It could be argued that many modern calc-alkaline stratovolcanoes are in a sense "discrete" centres of volcanism. However, the stratovolcanoes are usually built on an existing, well-defined calc-alkaline volcanic arc which may have developed over a considerable period of time (e.g. stratovolcanoes of New Zealand - Ballance, 1976; Cascade Range - McBirney, 1978; Andes - Francis and Rundle, 1976). It is this feature, viz. the presence of a well-defined calc-alkaline volcanic arc, which more than any other characteristic, distinguishes the Cainozoic calc-alkaline provinces from their Archaean counterparts. Thus, for any petrogenetic model to be acceptable, it must explain this rather characteristic feature of the Archaean centres.

A feature of fundamental importance, yet fraught with uncertainty, is the size of the centres. The original dimensions have been greatly modified by deformation, particularly east-west compression, which has resulted in the elliptical shapes of the centres. While it is relatively easy with careful mapping to establish the approximate middle of the centres, it is considerably more difficult to determine their outer limits due to the plunges of the folds, disruption by granitoid plutons and very often, discontinuity of outcrop. Nevertheless, despite the uncertainties, it does seem clear that the Archaean centres had diameters at least 2 to 3 times smaller than modern stratovolcanoes (Macdonald, 1972).

It is of interest to speculate on the form taken by the eruptive centres. In chapter 5 evidence was presented which indicated that the Welcome Well complex represented the eroded remnant of a stratovolcano. The similarity in the rock types, and association of the various rock types, in the other dominantly intermediate centres (i.e. Ida Hill and Polelle) suggests that they too might have originated in an analogous way. The critical features which particularly indicate this are:

1) The abundance of massive and vesicular lavas intercalated with laharic deposits - suggestive of subaerial eruption onto a steep slope and subsequent mass-flow downslope (c.f. Fiske, et al., 1963 on Mt. Rainier), and
2) the thick deposits of epiclastic lithic wackes and greywackes

deposited adjacent to the main centre - suggestive of the ring-plain deposits that flank modern stratovolcanoes.

In the case of the Ida Hill complex the relative abundance of related intrusive plugs and dykes, and paucity of thick sequences of epiclastic sediments, may indicate exposure of a deeper level of the stratovolcano (Hallberg, pers. comm.).

The Spring Well complex (see chapter 6) is the only centre composed completely of acid volcanics. It is characterised by localised subaerial pyroclastics, quite unlike the vast acid ignimbrite sheets which typify the post-orogenic Proterozoic volcanic provinces (chapter 4). It is inferred that some of the pyroclastics were dispersed from small vents by nuēe ardente eruptions of limited extent while the graded deposits are thought to represent lag-fall deposits which settled out during collapse of a vertical eruptive column. An insight into the possible nature of the feeders is provided by the vent-breccia pipe cutting the Spring Well volcanic pile. This feature could be taken as evidence that eruption was from numerous, small pipe-like vents rather than from a large, central vent. This factor, combined with the total absence of intercalated laharic deposits might indicate that the acid centres had rather less relief than the intermediate centres and hence they might not have formed strato-volcanoes. This is supported by the relative paucity of thick deposits of epiclastic sediments adjacent to the acid volcanic centres, in contrast with the intermediate centres (e.g. as at Welcome Well complex and Polelle complex).

The proximal volcanic units in both the Welcome Well and Spring Well volcanic complexes appear to have been subaerially erupted, judging by the absence of hyaloclastite deposits and lack of intercalated fine sediments. However, this may not apply in all cases since fine black shales intercalated with acid and intermediate volcanics in the complex at Bore Well could indicate subaqueous volcanism, at least in part (Hallberg, 1980).

A striking feature of the volcanic deposits in these centres is their marked similarity with rock types found in modern volcanic environments. Thus it seems that the volcanic processes operative in the Archaean were little different to those observable today. Consequently, it may be inferred that the physico-chemical properties of the magmas generated in the Archaean and expressed in their movement, fractionation and subsequent eruption , were probably comparable to modern calc-alkaline magmas. However, the apparent absence of calc-alkaline volcanic arcs in the Yilgarn Block suggests that the tectonic processes which were ultimately responsible

TABLE 7.2. Geochemical data for selected rocks from the additional calc-alkaline volcanic centres.

	IDA HILL COMPLEX										BORE WELL COMPLEX		
	I50	I13	I25	I20	I56	I3	I15	I11	I12	I14	Y6	Y7	Y2
SiO_2	54.62	55.75	55.70	59.03	62.01	65.99	68.23	68.47	69.77	74.71	54.21	58.38	75.48
$Al_2O_{3_t}$	13.82	15.35	15.17	14.86	14.25	16.05	13.95	16.11	15.41	13.31	19.54	16.13	12.42
Fe_2O_3	9.42	9.84	10.85	7.59	5.72	5.18	4.51	2.80	2.28	1.48	7.62	7.95	3.06
MnO	0.16	0.15	0.14	0.13	0.08	0.06	0.07	0.04	0.03	0.02	0.13	0.12	0.06
MgO	5.37	5.95	5.31	3.96	2.82	1.93	2.88	1.42	1.21	0.57	4.05	5.19	0.37
CaO	9.99	7.06	6.69	7.34	13.75	4.07	4.98	3.31	2.92	4.31	9.38	7.50	0.71
Na_2O	4.87	3.56	3.56	4.25	0.37	4.87	3.99	5.07	5.06	3.63	3.03	2.94	4.80
K_2O	0.35	0.79	0.87	1.75	0.14	0.92	0.73	2.25	2.19	1.20	0.69	1.03	2.54
TiO_2	0.67	0.96	1.14	0.61	0.57	0.51	0.49	0.39	0.31	0.41	0.76	0.78	0.27
P_2O_5	0.15	0.23	0.21	0.16	0.16	0.14	0.10	0.14	0.10	0.13	0.16	0.15	0.03
Total	99.42	99.64	99.64	99.68	99.87	99.72	99.93	100.00	99.28	99.77	99.59	100.17	99.73
LOI	0.58	2.45	2.51	3.24	1.40	1.77	1.60	1.44	0.78	0.99	3.27	2.15	0.70
Zr	71	120	140	110	106	119	100	121	117	100	117	120	299
Nb	3.1	6.4	7.5	5.9	5.1	6.5	3.4	3.0	2.9	3.5	6.3	6.6	11
Y	19	17	21	21	13	11	8.5	6.3	4.2	8.5	21	17	34
Ce	30	32	37	36	26	31	20	45	37	23	30	30	59
Nd	19	17	17	20	12	17	12	21	16	11	17	16	30
Sc	34	24	25	22	19	8.3	12	6	6	11	24	21	7
V	190	159	186	120	107	75	78	45	38	73	140	146	-
Cr	527	330	312	193	212	33	159	32	42	143	118	158	3
Ni	213	103	90	126	74	19	70	22	23	52	59	110	-
Rb	9.6	19	18	18	4	27	24	75	75	34	19	27	52
Sr	367	257	236	238	262	208	245	503	432	328	292	255	76
Ba	292	241	237	200	110	234	139	940	647	470	210	309	421

	MARDA COMPLEX					POLELLE COMPLEX					
	M2	M3	M5	MAA	MAR	P17	P19	P22	P28	P31	P33
SiO_2	57.53	59.97	61.11	61.9	75.9	56.05	58.07	62.16	68.35	69.60	77.00
$Al_2O_{3_t}$	15.64	15.43	14.66	15.0	12.7	16.17	13.94	13.53	14.75	15.39	12.88
Fe_2O_3	9.60	8.92	8.19	7.7	2.2	8.02	7.79	6.94	2.84	2.79	0.98
MnO	0.12	0.11	0.12	0.11	0.08	0.15	0.10	0.12	0.20	0.04	0.04
MgO	3.81	3.70	4.21	3.6	0.2	7.01	6.92	6.37	1.42	1.42	0.33
CaO	7.24	7.69	6.29	5.6	0.3	6.65	7.60	5.15	6.12	4.29	2.64
Na_2O	2.70	2.94	4.58	3.7	3.9	3.55	2.82	3.55	3.92	4.47	4.89
K_2O	1.84	0.82	0.58	1.7	4.1	1.39	1.79	1.41	1.87	1.26	0.82
TiO_2	0.95	0.99	0.76	0.78	0.23	0.74	0.67	0.60	0.38	0.51	0.33
P_2O_5	0.36	0.31	0.21	0.23	0.02	0.27	0.26	0.17	0.16	0.23	0.09
Total	99.79	100.88	100.71	100.35	99.65	100.00	100.00	100.00	100.00	100.00	100.00
LOI	1.85	2.08	1.69	1.8	0.8	3.83	3.92	3.24	3.20	2.34	1.25
Zr	193*	206*	192*	200	289	140*	118*	125*	116*	140*	166*
Nb	7.9*	9.9*	7.9*	9	10	4.7*	5.7*	5.1*	4.4*	5.8*	3.2*
Y	22*	19*	22*	22	28	17*	16.5*	14*	14*	12*	7*
Ce	-	-	-	-	-	53**	68*	47**	56**	47**	23**
Nd	-	-	-	-	-	22**	32*	21**	22**	21**	9.5**
Sc	22*	22*	20*	18*	-	-	21*	-	-	-	-
V	155*	154*	128*	117	<10	154	133*	120	63	82	38
Cr	32	20	187	91	<10	181	440*	352	120	148	56
Ni	29	36	66	67	5	112	192*	160	49	58	9
Rb	44*	19*	19*	48	114	49*	39*	49*	44*	26*	22*
Sr	341*	426*	361*	319	83	391*	435*	391*	521*	571*	346*
Ba	603*	600*	421*	740	1265	447	580*	529	607	494	853

Notes:

1. All of the samples from the Ida Hill and Bore Well complexes were collected and analysed by the writer.
2. All of the samples from the Marda and Polelle complexes were collected and analysed by Hallberg, et al., (1976a and 1976b, respectively), and the data without an asterisk has been taken from these sources.

   * signifies unpublished data obtained by XRF at the University of Adelaide, using powders provided by Hallberg.

   ** signifies unpublished data obtained by mass spectrometer at the University of Adelaide, using powders provided by Hallberg, and reproduced with the kind permission of Sun.
3. MAR refers to average Marda rhyolite.
   MAA refers to average Marda andesite.
   (Averages compiled by Hallberg, et al., 1976a).

Figure 7.2 Selected major element variation diagrams for rocks from six calc-alkaline volcanic centres in the Yilgarn Block. O Spring Well complex ● Welcome Well complex △ Ida Hill complex ▲ Marda complex □ Polelle complex ■ Bore Well complex. The stipple represents the field of Archaean tholeiitic basalts.

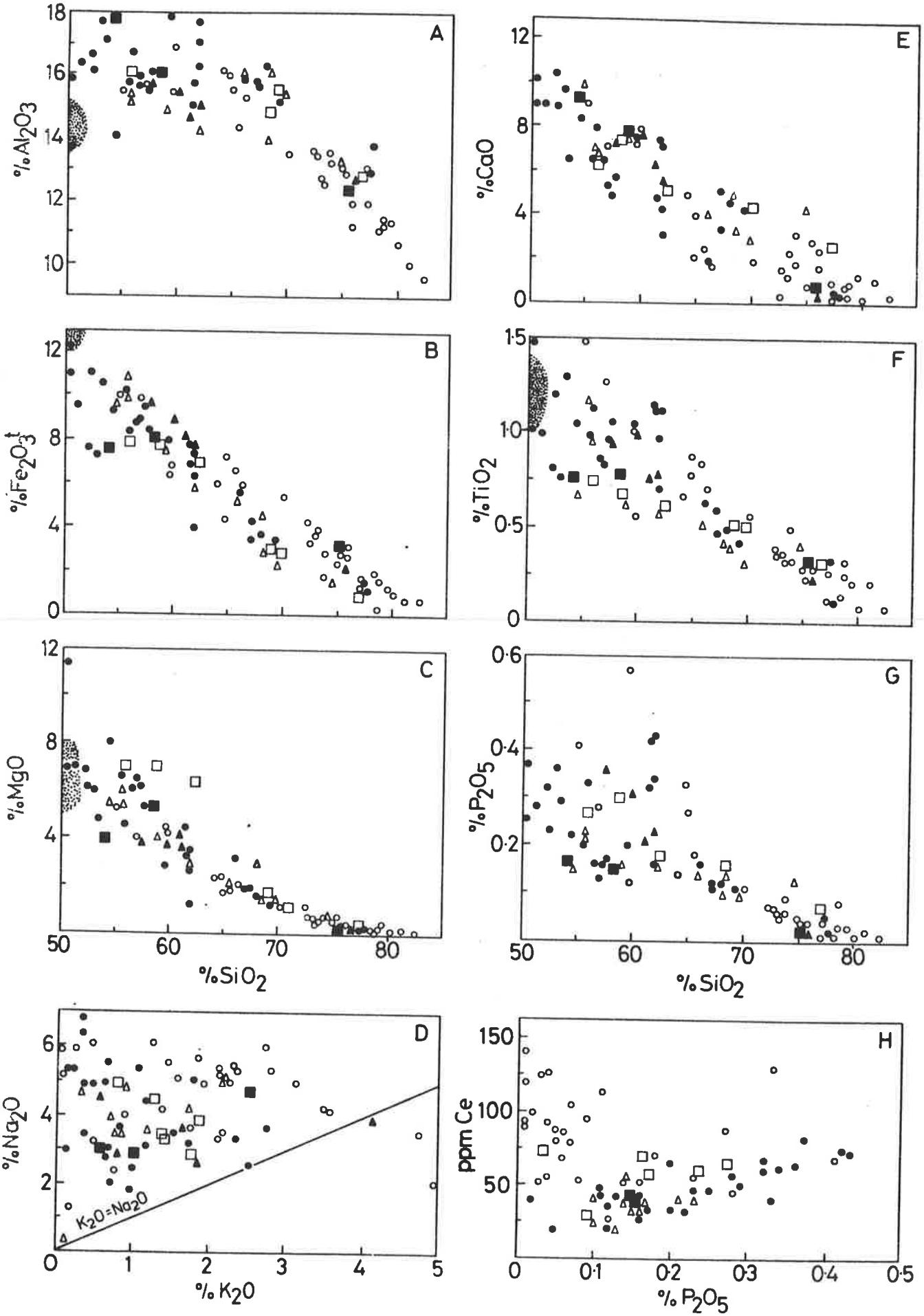

Figure 7.3 Selected trace elements vs. SiO_2 and Sc vs. V for rocks from six calc-alkaline volcanic centres in the Yilgarn Block. Symbols as for Figure 7.2. The Mt. Ararat low-Y trend is after Lambert, et al., (1974).

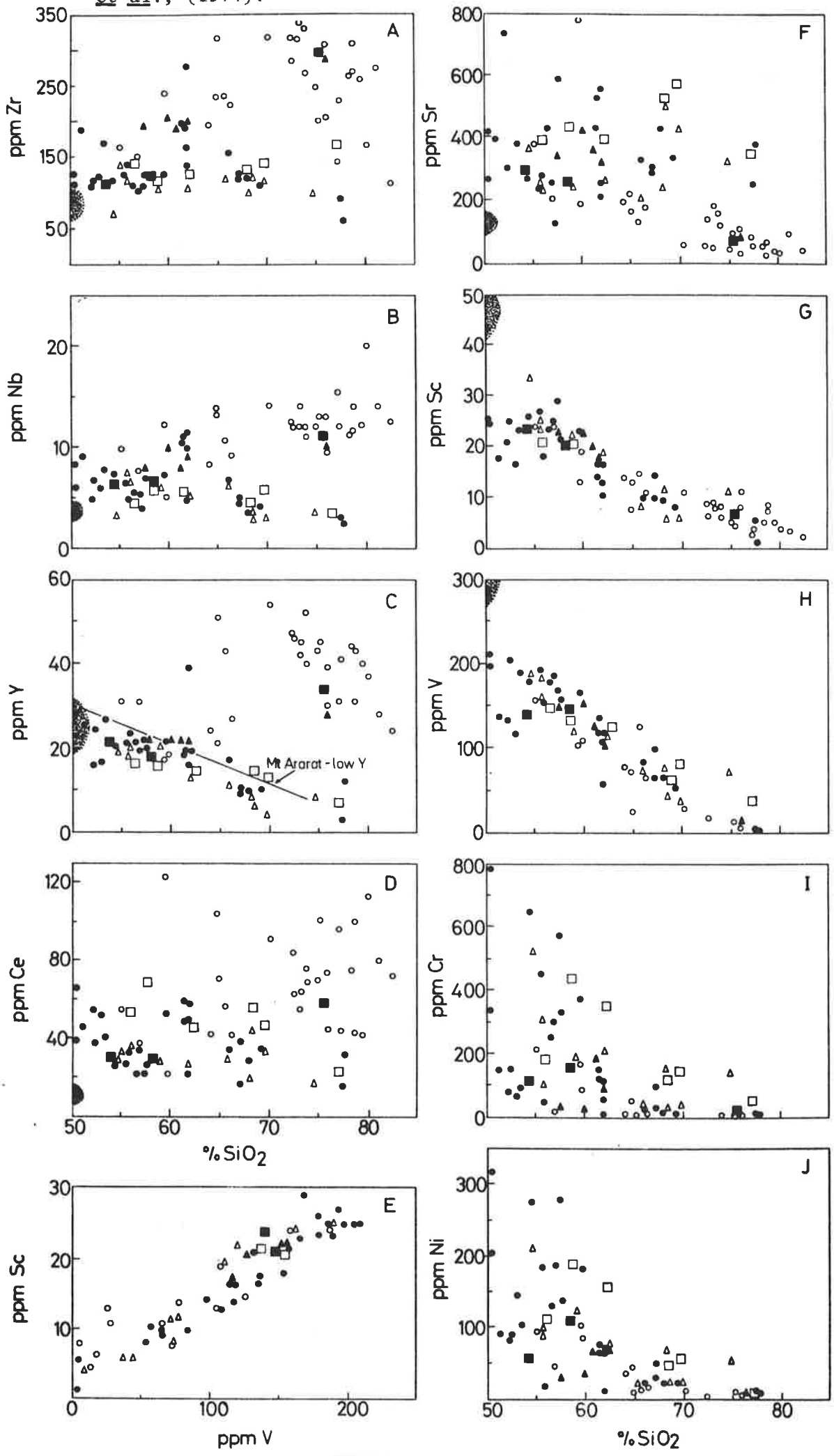

Figure 7.4 Selected variation diagrams for rocks from six calc-alkaline volcanic centres in the Yilgarn Block. Symbols as for Figure 7.2.

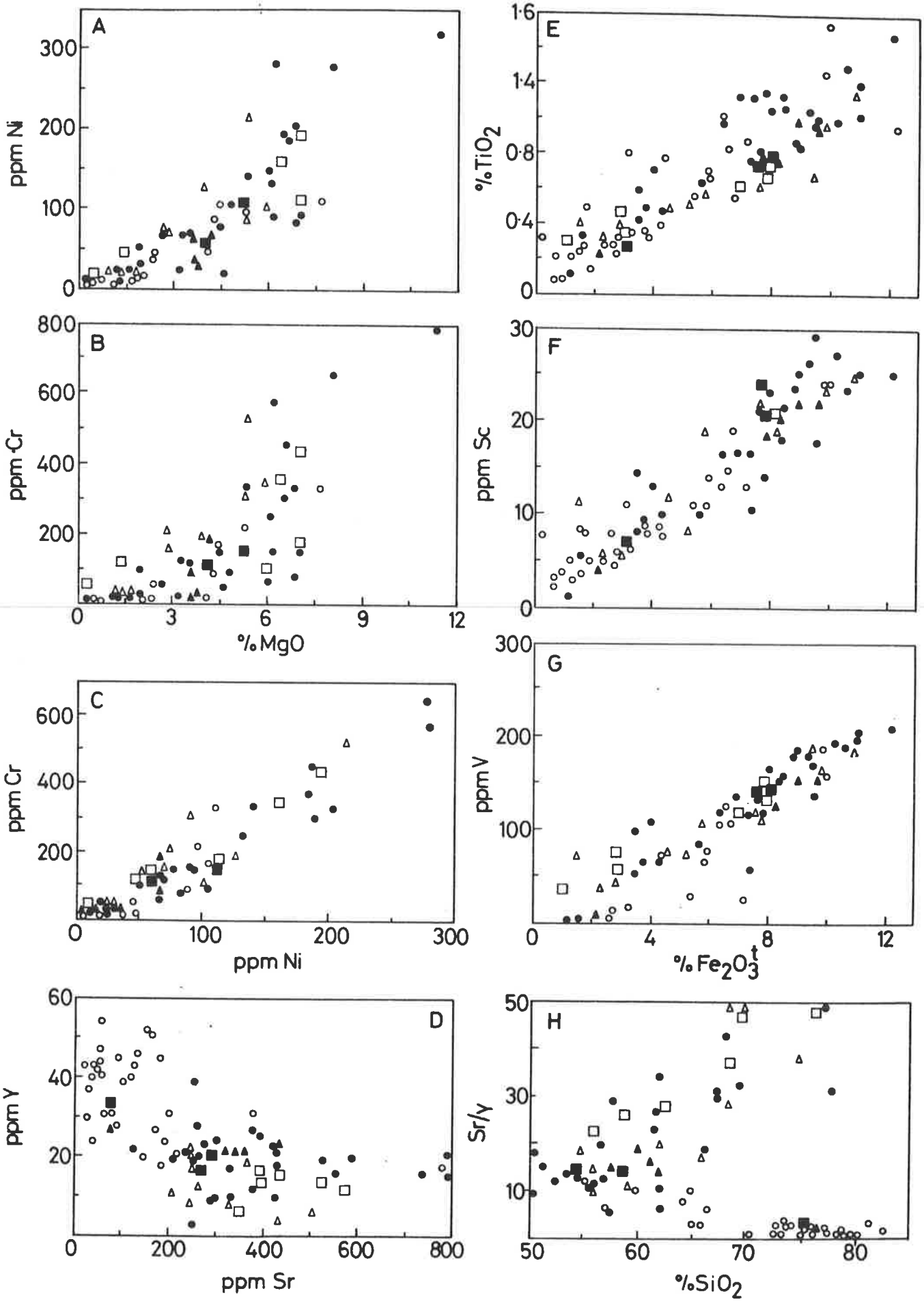

for the generation of the Archaean magmas differed from the subduction-related processes which are generally thought to have generated the primary magmas for modern calc-alkaline suites.

7.3 SOURCE OF THE PRIMARY MAGMA

7.3.1 General Discussion

The objective of this section is to determine whether the calc-alkaline volcanics from the various centres, given the continuum of field characteristics they display, have a common origin. If the volcanics have analogous geochemistry, then it can be reasonably inferred that they have similar ultimate origins. In making geochemical comparisons however, it is necessary to compare the correct rock types - in this case the most basic members from each of the centres, so that the variations produced by differentiation are minimised. Comparison of the most basic members from each of the six centres listed in Table 7.1 is made via tabulated data, variation diagrams, REE plots and elemental ratios.

A simple qualitative comparison of the geochemical data in Table 7.2 for samples from each of the centres, suggests that broad analogies do exist, but when the data for rocks with < 60% SiO_2 is examined on the SiO_2 variation diagrams, considerable scatter is evident (Figs. 7.2 and 7.3). This is particularly marked for $Fe_2O_3^t$, TiO_2, MgO, CaO, P_2O_5, Zr, Nb, Y, Ce and Sr. Some of these elements show systematic differences between centres. For example, the samples from the Marda complex are mostly slightly higher in $Fe_2O_3^t$, P_2O_5 and Y and markedly higher in Zr than samples from other centres, while the andesites from the Bore Well complex are relatively low in P_2O_5. Most of the spread is produced by non-systematic variations and in general, for individual centres the range of values is less than that for all centres combined, excepting the Welcome Well complex. Possible reasons for the apparent scatter of data in samples from the Welcome Well complex have been discussed in chapter 5, where it was concluded that variations in the conditions of partial melting and heterogeneities in the source produced a primary dispersion in the elemental contents that was subsequently magnified by varying amounts of differentiation. It is possible that a similar explanation may account for the spread in major and trace element contents in the volcanic rocks from the other calc-alkaline centres considered here.

The proposition that all of the calc-alkaline volcanics are related, can be better tested by examining plots that are less sensitive to the effects of variations in the conditions of partial melting and/or differentiation. Plots of the compatible elements (e.g. Ti, Sc, V vs

Figure 7.5 Selected variation diagrams for low-silica rocks from six calc-alkaline volcanic centres in the Yilgarn Block. Symbols as for Figure 7.2 with the addition of X for Archaean tholeiitic basalt. The chondritic lines are after Nesbitt and Sun (1976) and Nesbitt, pers. comm., (1980).

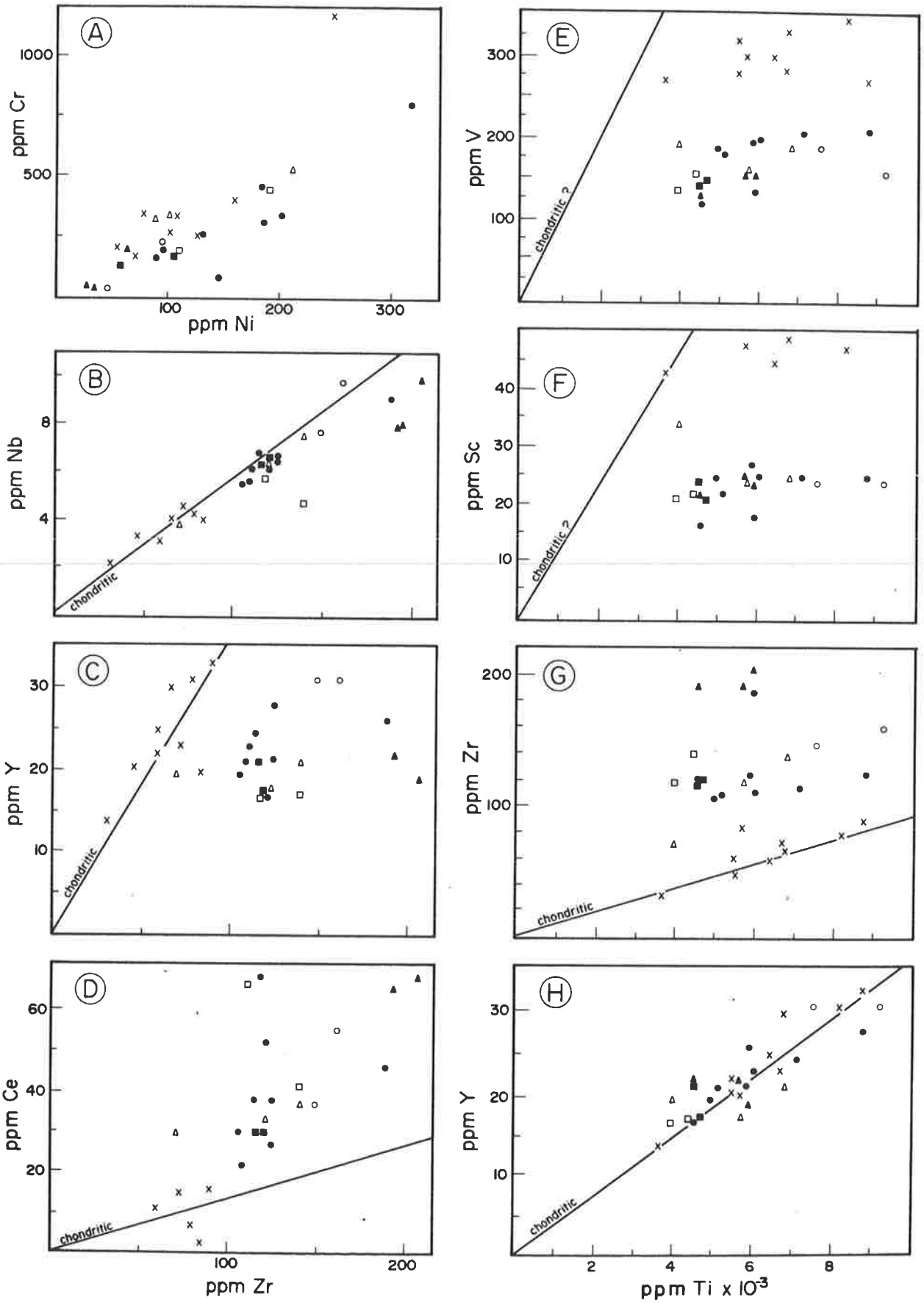

$Fe_2O_3^t$ and Sc vs V, Fig. 7.4E, F and G and Fig. 7.3E, respectively) reveal moderately good linear trends thus supporting the proposition. Positive correlations are also shown by the Zr vs Nb and Y vs Ti relationships, and significantly, the trends are almost coincident with the chondritic trends (Figs. 7.5B and H). It is therefore evident that in spite of the apparently random spread of TiO_2, Zr, Nb and Y when plotted against SiO_2, they are being controlled by the same factors in all suites, thus implying that all of the calc-alkaline volcanics have a similar ultimate origin.

The Zr vs Y and Zr vs Ti relationships are not as tight as those observed for Zr vs Nb and Y vs Ti (Fig. 7.5C and G), nevertheless all of the samples plot in a field which is quite separate from the approximately chondritic tholeiitic basalt field and as the variation diagrams show, the Zr/Ti and Zr/Y ratios are consistently greater than chondritic. The plots of V vs Ti and Sc vs Ti (Figs. 7.5E and F) show that the calc-alkaline volcanics have less than chondritic V/Ti and Sc/Ti ratios and that all samples are displaced away from the field of the similarly non-chondritic tholeiitic basalts. The observations that all of the calc-alkaline volcanics plotted show the same elemental characteristics, viz. chondritic Zr/Nb and Ti/Y, greater than chondritic Zr/Ti and Zr/Y (and by inference Nb/Ti and Nb/Y) and less than chondritic V/Ti and Sc/Ti, and in most cases plot in tight groups quite distinct from the tholeiitic basalts, provides the most powerful evidence that the ultimate origin of the calc-alkaline magmas was the same for each of the centres.

The available REE data adds further support to this conclusion. For example, it has been previously noted that the low-silica andesites from the Spring Well complex have analogous REE distributions to the andesites from the Welcome Well complex and the Marda complex (Fig. 6.9A). Unpublished REE data of Sun (1977) for andesites from the Polelle complex (using samples of Hallberg et al., 1976b) is also comparable with that for andesites from the above-mentioned centres. The levels of Ce in low-silica andesites and basalts from each of the centres (determined by XRF), although comparable, show a significant spread (Fig. 7.3D) and this may be related to the same cause as the variability noted for other LIL elements (e.g. Zr, Nb, Ti and P).

7.3.2 Petrogenetic considerations

A. Conditions of magma segregation

In chapters 5 and 6 several lines of evidence were used to show that the primary magmas for the Welcome Well complex and Spring Well complex

originated in the mantle. It follows that the calc-alkaline volcanics from the other centres considered here must also have a mantle source in view of the previous conclusion that all share a common origin.

The conditions under which the primary magmas were generated in the mantle can only be defined in the broadest terms in the absence experimental data for the particular samples being considered. In the case of the Welcome Well complex, it has been argued that the primary magmas were derived by relatively shallow, hydrous melting of a LIL element-enriched zone of the mantle. The comparable geochemical characteristics of the additional samples considered here add support to this proposal. For example, they show similar MgO, Ni and Cr behaviour to the rocks from the Welcome Well complex, viz. a range in MgO, Ni and Cr contents, such that some samples are relatively high in these elements for their particular levels of SiO_2, while others are clearly more fractionated (Figs. 7.2C and 7.3I, J). Also, within a restricted MgO range (5-8%), Ni and Cr are observed to vary greatly (Ni, 80-300 ppm and Cr 50-600 ppm; see Figs. 7.4A and B). Neither feature can be readily explained in terms of differentiation from common parental magmas. Alteration is not considered to offer a satisfactory explanation for the Ni and Cr behaviour, since both elements show an excellent positive correlation with each other (Fig. 7.4C). Thus the explanation given in the case of the Welcome Well complex, on the basis of experimental evidence (Green, 1973, 1976), is considered to have more general applicability. It was proposed that a range of primary magmas were generated, differing chiefly in their MgO and SiO_2 contents, in response to hydrous melting over a depth interval of 30-60 km. Subsequently, differentiation superimposed on the primary magmatic variation, produced the compositional range observed.

B. Nature of the mantle source

The previous discussion of the inter-element variations illustrated in Figure 7.5 has shown that the elemental ratios of the basalts and low-silica andesites can be divided into three main groups including those that are:

1) less than chondritic - Sc/Ti, V/Ti;
2) approximately chondritic - Zr/Nb, Y/Ti;
3) greater than chondritic - Zr/Ti, Zr/Y, Ce/Zr.

Nesbitt and Sun (1976) have demonstrated that Archaean ultramafic rocks have approximately chondritic values for these ratios suggesting that the mantle source for these magmas had chondritic relative elemental abundances. Thus, the non-chondritic elemental ratios for the calc-alkaline rocks indicates a non-chondritic mantle source and/or control on some

elements by residual minerals during magma segregation. The former alternative of a non-chondritic mantle source necessarily implies differential control on certain elements during the mantle enrichment processes, since if this were not the case selective elemental enrichment of the mantle source could not have occurred.

The elemental ratios indicate an order of enrichment in the primary basic magmas, compared with chondrites, of: Ce ($\sim$ P)> Zr, Nb > Ti, Y > Sc, V. It has been previously shown for the primitive basalt from the Welcome Well complex that control by residual clinopyroxene during magma segregation, can account for the levels of Sc and V. It is possible that Ti and Y behaved essentially incompatibly during the magma segregation event thus preserving the chondritic Ti/Y mantle value in the melt. The greater than chondritic Ce/Zr, Zr/Ti and Zr/Y values imply that Ce, Zr (and Nb) were probably enriched in the mantle source prior to magma segregation.

The important conclusion to be drawn is that the elemental ratios of the volcanics indicate complex enrichment processes in the mantle source prior to magma segregation. Some of the elemental ratios (e.g. Y/Ti, Sc/Ti and V/Ti) have, however, probably been inherited during the melting event.

7.4 DISCUSSION OF POSSIBLE MODELS OF ORIGIN

It is evident that any petrogenetic model proposed to explain the origin of the primary magmas for the Archaean calc-alkaline volcanics in the Yilgarn Block, must account for their rather sporadic, localised occurrence and for the relatively small volumes of magmas generated. It must also provide a means whereby hydrous melting of the upper mantle can occur over a significant vertical interval.

Subduction-related models, universally proposed to explain the origin of modern calc-alkaline magmas, satisfy the latter requirement by invoking dehydration of a descending oceanic crustal slab and flooding of the overlying mantle wedge with the released LIL element-enriched fluids or silicate melts (Best, 1975). Melting of the mantle wedge at relatively shallow levels presumably occurred in response to the depressed mantle solidus in the presence of water. It has been noted that the calc-alkaline volcanic rocks in the Yilgarn Block do not occur in arcs, but rather in discrete, isolated centres. This is difficult to reconcile with subduction, even on a small scale, and unless field evidence in support of subduction-related processes can be demonstrated in the Yilgarn Block, this hypothesis is unlikely to be directly applicable.

A variation on the subduction model which has been specifically proposed for the Archaean involves "sag-duction" (Goodwin, 1974), in which a part of the mafic-ultramafic crust sinks of its own accord and dehydrates as the amphibolite mineral assemblage is converted to eclogite. This process may have occurred on a large scale in the Archaean, particularly as many workers consider that the magmas for the voluminous sodic granitoids were derived in this manner (e.g. Arth and Hanson, 1975; Glikson and Lambert, 1976; Cooper, et al., 1978). The resultant melt was unlikely to have had the composition of a calc-alkaline andesite however (Stern, 1974), and in fact on experimental grounds it seems unlikely that liquids of intermediate composition could be produced from such a source (Arth and Barker, 1976; Wyllie, et al., 1976). In any case this model is difficult to reconcile with the small volume of the calc-alkaline volcanics compared with the granitoids and with the lack of any field association or genetic relationship between the two.

It is conceivable, as Goodwin and Smith (1980) point out, that the hydrous liquids released during "sag-duction" may have been instrumental in modifying and promoting melting of the adjacent upper mantle. If this were the case then it is puzzling why the calc-alkaline rocks are of limited volume and why they show no consistent spatial and time relation with the tholeiitic and komatiitic volcanism (i.e., calc-alkaline volcanics invariably younger than tholeiitic and komatiitic volcanics as Goodwin and Smith observe in the Abitibi Belt). This observation is not restricted to the Yilgarn Block, since Barley (1980) has documented contemporaneous calc-alkaline and tholeiitic volcanism from the significantly older (3.4-3.5 b.y.) Pilbara Block and finds no evidence to support the concept of early tholeiitic volcanism followed by later calc-alkaline volcanism. On experimental grounds it would be predicted that the "sag-ducted" crust would have lost a substantial amount of its hydrous component before reaching mantle depths regardless of the geothermal gradient (Green and Ringwood, 1967) and since this component would have risen rapidly, little opportunity would have been presented for enrichment of the mantle in LIL elements. Moreover, considerations of the densities of mafic and ultramafic rocks relative to the mantle suggest that such rocks would not have "sunk" into the mantle in the manner suggested by Goodwin and Smith (1980) unless they had undergone prior dehydration and conversion to substantially denser eclogite (Ringwood, 1974).

It is possible that crustal processes had no influence on the generation of the primary magmas for the Archaean calc-alkaline rock suites. Rather, partial melting of a pre-existing, heterogeneous, LIL

Figure 7.6 Summary of possible modes of formation of primary magmas for calc-alkaline volcanics, tonalitic plutons and tholeiitic basalts in the Archaean. As discussed in the text, generation of the primary magmas for the calc-alkaline suites above a mantle diapir or "hot-spot", is an equally plausible mechanism and cannot be distinguished from the model illustrated with the available data.

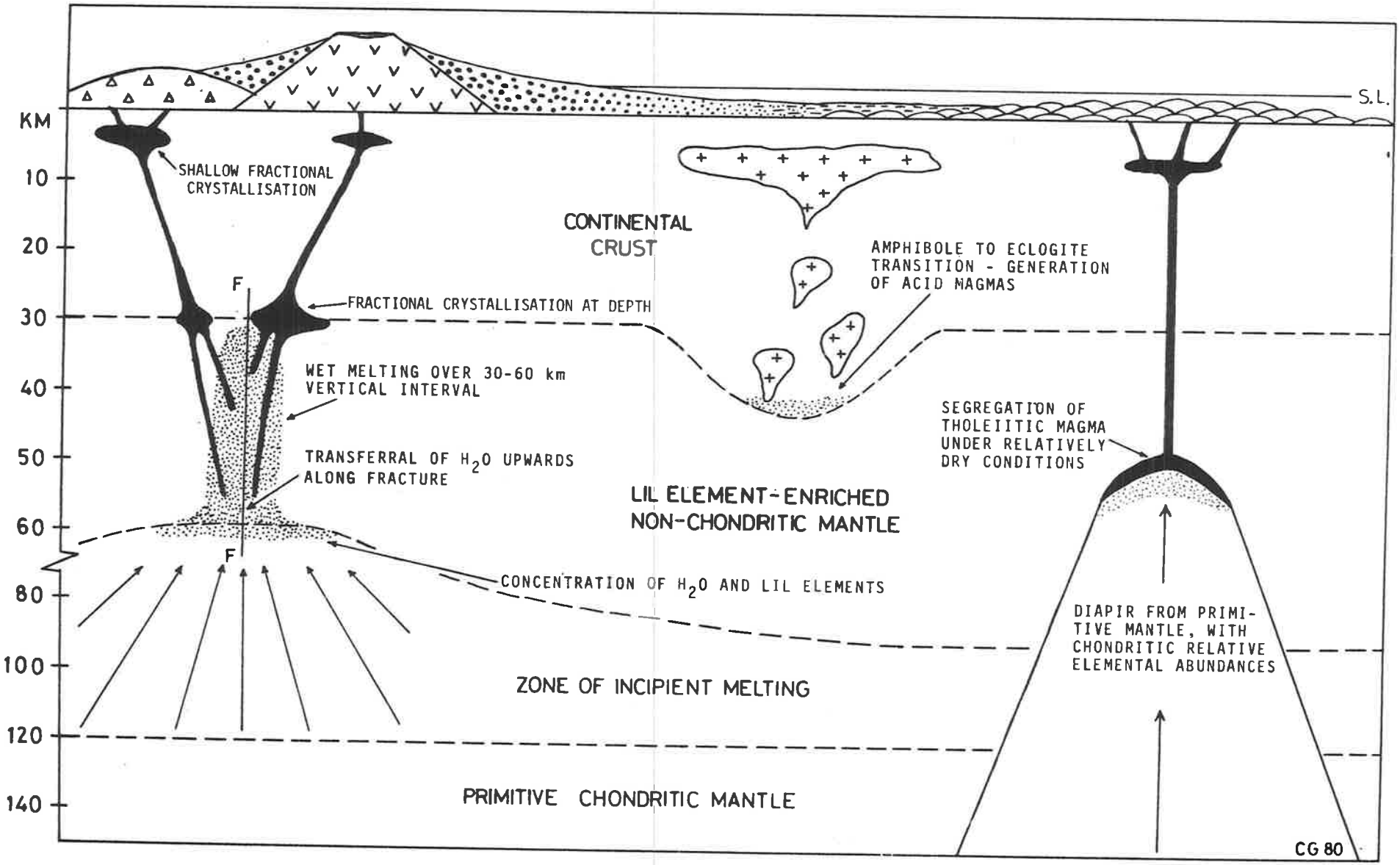

element-enriched zone of the upper mantle may have been triggered by the introduction of water, from a zone of incipient melting at greater depths (Green, 1973, see Fig. 7.6). Significant amounts of melting would have only occurred if the input of water and resultant depression of the mantle solidus was sufficient and thus the sites of melting may have been controlled to a large extent by zones of weakness such as faults which would have facilitated tapping and transport of the water-rich component from the zone of incipient melting to higher levels. This model requires the geothermal gradient to be of the correct order in the Archaean (comparable with that in modern ocean basins), to permit the development of a zone of incipient melting, possibly similar to the modern low velocity zone (Green and Liebermann, 1976).

An alternative mechanism, involving localised melting above a mantle "hot spot" (c.f. Goodwin, 1973) has been proposed by Hallberg et al., (1976a) as a possible explanation for the origin of the parental magmas in the case of the Marda calc-alkaline volcanic complex. In this case, the increased mantle heat flow, perhaps produced by diapirism or a radioactive decay process, may have been sufficient to melt the LIL element-enriched upper mantle as it moved with the lithosphere over the "hot spot". This model has the advantage of offering an explanation for the "string of beads" configuration of the calc-alkaline volcanic centres in the northern portion of the Norseman-Wiluna greenstone belt (Hallberg, 1980; Hallberg and Giles, in prep.).

Both of these models are similar in their end result in terms of the magmas generated, and distinction between them on geochemical grounds would be difficult, if not impossible. In each case it is evident that the conditions of magma generation created in the upper mantle would essentially duplicate those produced in the mantle wedge above a descending, dehydrating oceanic crustal slab in a subduction zone. This may offer an explanation for the apparent paradox evident in the Eastern Goldfields Province where the field relationships of the Archaean calc-alkaline volcanic rocks offer no direct support to subduction models, but the geochemistry indicates marked analogies with modern calc-alkaline volcanic rocks which have formed in subduction environments.

7.5 CRYSTALLISATION HISTORY OF THE MAGMAS

In view of the common, mantle origin proposed for the primary magmas of the calc-alkaline rock suites, it is pertinent at this stage to examine their subsequent crystallisation histories. Owing to the potential for significant variations in PTOTAL, PH_2O, PO_2 and T as the result of non-

systematic factors such as the depth of crystallisation, extent of vapour pressure build up prior to eruption, frequency of eruption and many others, the crystallisation history could be exceedingly complex both within and between centres.

The generally linear, inverse correlations of Al_2O_3, $Fe_2O_3^t$, MgO, P_2O_5, TiO_2, Sc and V with SiO_2 for rocks with > 58% SiO_2 is suggestive of a differentiation control on these elements (Figs. 7.2 and 7.3). Notably, the absolute contents of these elements and their variations in these rocks are similar to those observed in Cainozoic calc-alkaline suites, thus demonstrating the marked analogy that exists between the composition of Archaean and modern calc-alkaline volcanic rocks (see chapters 5 and 6).

Magnetite fractionation was probably largely responsible for the control on $Fe_2O_3^t$, TiO_2, Sc and V at high SiO_2 levels, although mafic minerals (e.g. clinopyroxene and amphibole) no doubt contributed to the control during the earlier stages of differentiation. Fractionation of differing proportions of plagioclase could be indicated by the two separate trends evident on the Sr vs SiO_2 plot (Fig. 7.3F). This appears to be supported, though less convincingly, by the Al_2O_3 vs SiO_2 relationship (Fig. 7.2A).

The acid rocks are also grouped into two fields according to their Zr, Nb, Y and Ce contents (Fig. 7.3). Notably, the samples that are relatively enriched in Zr, Nb, Y and Ce are also relatively depleted in Sr and vice versa. Included within the Zr, Nb, Y and Ce "enriched" group are samples from the Spring Well, Bore Well and Marda complexes, while the relatively depleted Zr, Nb, Y and Ce group contains all of the samples from the Welcome Well, Ida Hill and Polelle complexes. Since it has been previously shown that the samples within both the Welcome Well and Spring Well complexes can be related by differentiation, it follows that the diverse trends are the result of differing crystallisation histories.

The behaviour of Y and Sr (see also Fig. 7.4D and H) suggests that a mineral(s) capable of controlling Y is fractionating to the exclusion of plagioclase, assuming that plagioclase is exerting the dominant control on Sr. The most probable mineral is amphibole, since its crystallisation field is expanded by the same conditions that tend to contract that of plagioclase (Yoder and Tilley, 1962; Cawthorn and O'Hara, 1976). Moreover, amphibole would be expected to exert significant control on Zr, Nb and Y, since in equilibrium with intermediate and acid liquids, it has distribution coefficients greater than one for all of these elements (Pearce and Norry, 1979). The effect of minor minerals, such as apatite, in producing the two trends observed for Ce and Y is not supported by the

Figure 7.7 Stability fields of major crystallising phases for water-saturated and water-undersaturated conditions.

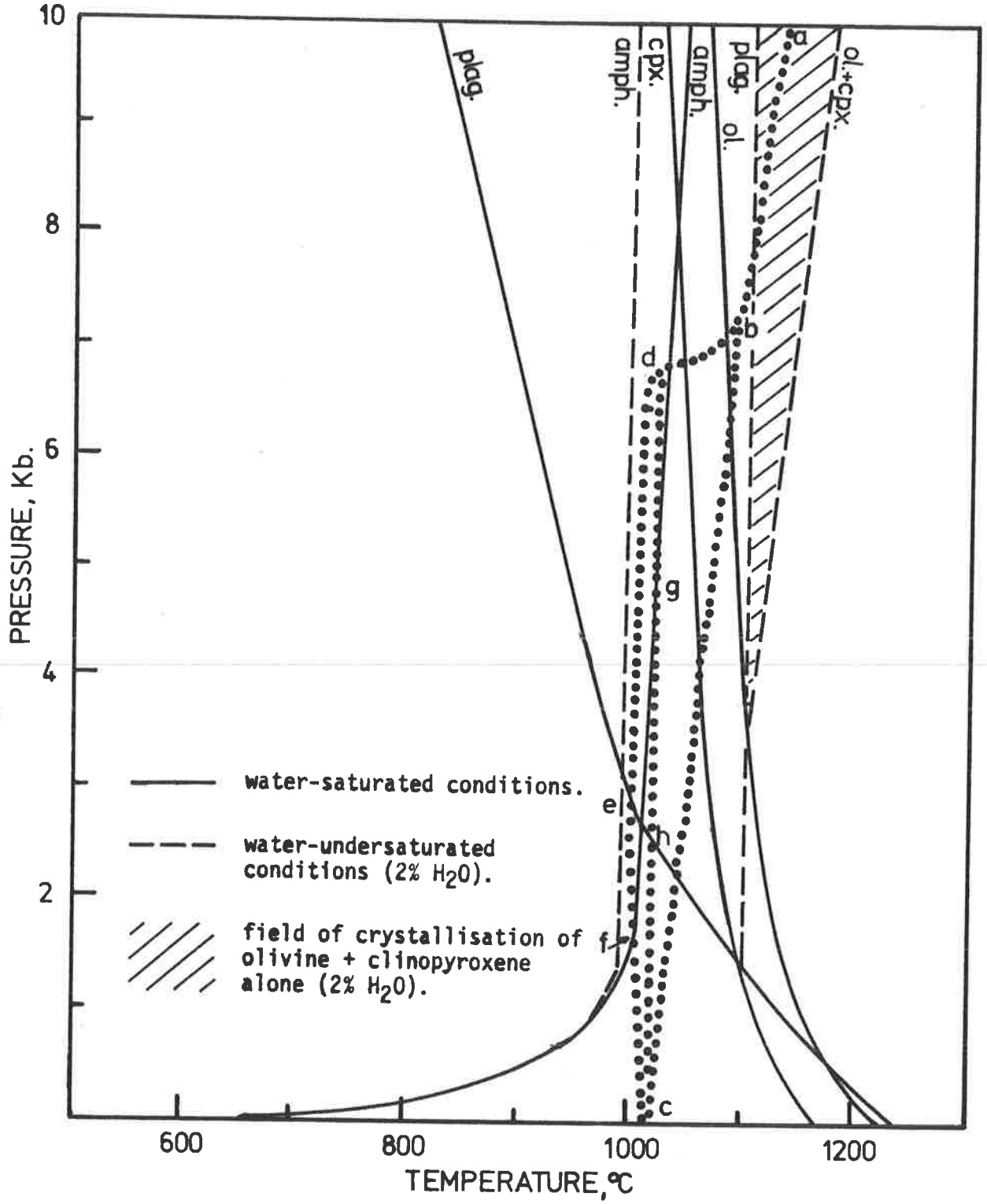

Notes: 1. Stability fields for water-saturated conditions after Yoder and Tilley's (1962) data for high-Al basalt composition.

2. Stability fields of amphibole and plagioclase for 2% H_2O after Eggler's (1971) data for Paricutin andesite and supported by Foden's (1979) data for Rindjani high-Al basalt.

3. Stability field of olivine + clinopyroxene for 2% H_2O after Foden's (1979) data for Rindjani high-Al basalt.

4. Indicated positions of stability fields will vary for the particular rock-compositions being considered.

coincidental (and linear) P_2O_5 vs SiO_2 relationship (Fig. 7.2G) which suggests a similar role for apatite in the two series, nor by the divergent Ce vs P_2O_5 relationship (Fig. 7.2H).

Lambert, et al., (1974) have recognised similar chemical trends, particularly for Y (Fig. 7.3C), in a suite of calc-alkaline rocks from Mt. Ararat. They attributed the high- and low-Y trends in their rocks to be the result of variable amounts of amphibole fractionation produced in response to fluctuating PH_2O during crystallisation. This explanation relied on the experimental observation that the crystallisation field of amphibole is expanded, while that of plagioclase is contracted, by increased PH_2O (see Fig. 7.7).

Under hydrous conditions the load pressure can also have a large influence on the relative proportions of minerals that fractionate. For example, decreasing load pressure will cause a hydrous liquid of the appropriate composition to move from the amphibole field through the amphibole + plagioclase crystallisation field and eventually, at shallow depths (probably < 10km), into the clinopyroxene + plagioclase crystallisation field (Yoder and Tilley, 1962; Fig. 7.7). The precise temperatures at which these transitions occur will be largely dependent on the composition of the liquid and its water content. It is therefore evident that the depth at which the bulk of the crystal fractionation occurred, in addition to the water vapour pressure, could have exerted a major control on the crystallisation history.

These observations can be quantified by reference to experimentally-determined stability fields of minerals in P-T space summarized in Figure 7.7, and hypothetical crystallisation paths. The curves for water-undersaturated conditions (dashed lines on Fig. 7.7) demonstrate that early olivine and clinopyroxene crystallisation will be followed by plagioclase crystallisation at lower temperatures and importantly, amphibole will not crystallise on any of the hypothetical crystallisation paths illustrated. Fractionation of these minerals probably will not yield the calc-alkaline series owing to the limited silica enrichment. The trend towards pronounced silica-oversaturation could result from early amphibole fractionation however (Cawthorn and O'Hara, 1976; Foden, 1979). This evidence, combined with the modelling calculations, all of which necessitate some amphibole fractionation, suggest that the relative positions of the stability fields were not as illustrated for the 2% H_2O conditions during crystallisation of the Archaean magmas.

For water-saturated conditions (solid curves on Fig. 7.7), path a-b-c is also improbable since it fails to intersect the amphibole stability

field. However, either of the remaining paths are acceptable since in both cases early olivine and clinopyroxene fractionation will be followed at slightly lower temperatures by amphibole fractionation. Once the amphibole stability field is entered, olivine and clinopyroxene are in reaction relationship with the liquid and will no longer crystallise (Cawthorn and O'Hara, 1976). Subsequently, the magma could rise along paths d-e-f-c or d-g-h-c or any in between, resulting in fractionation of plagioclase + clinopyroxene at shallow depths. The actual depth at which amphibole fractionation ceases (e.g. g or f) will depend upon the path taken.

The sequence of crystallisation outlined above can offer a possible explanation for the two fractionation trends noted in the Archaean calc-alkaline volcanics. For example, if the magma was hindered during its ascent, at depths, possibly corresponding to the base of the Archaean crust (e.g. 20-30 km, point d on Fig. 7.7), and if it resided at this level for some time, then prolonged amphibole-dominated fractionation would have occurred. This could have resulted in the low-Y (and Zr, Nb, Ce and HREE) and high-Sr (and Al_2O_3) differentiation series typified by the rocks comprising the greater part of the complexes at Welcome Well, Ida Hill and Polelle. If, on the other hand, the magma ascended rapidly to shallow depths, then limited early amphibole fractionation would have been followed by prolonged clinopyroxene and plagioclase fractionation to yield the high-Y and low-Sr rocks found in the complexes at Spring Well and Bore Well.

In this scheme, the abundance of clinopyroxene and plagioclase phenocrysts relative to amphibole in the andesites could be explained by the late-stage crystallisation of clinopyroxene and plagioclase at relatively low pressures and by the re-equilibration of amphibole to assemblages bearing these two minerals. Also, as pointed out for the Welcome Well complex, the compositional hiatus observed between the andesites and dacites could result in part from re-equilibration of highly plagioclase-normative liquids (produced by extended crystallisation in the amphibole field) at low pressures. The ensuing rapid transition in liquid compositions might not be preserved if the plagioclase phenocrysts were removed as cumulates.

In the above discussion it has been tacitly assumed that the acid members of the Marda complex differentiated from basic and intermediate parents, as in the case of the Spring Well complex. However it should be pointed out that Taylor and Hallberg (1977), on the basis of their detailed REE study of the Marda complex, considered that the acid volcanics (and intermediate volcanics) were the result of crustal fusion, and did not form

a simple differentiation series. Certainly, the relatively high K_2O, Zr, Nb, Y and Ce contents of the acid volcanics could be taken as evidence in support of this contention (Table 7.2).

Against this, it has been noted previously that the Marda andesites are similarly relatively enriched in these same elements over the majority of other andesites from the Yilgarn Block (see Table 7.2) and, from the analogous elemental ratios and major element characteristics, it is difficult to escape the conclusion that the Marda andesites had a similar ultimate (mantle) origin to the andesites from the other centres. If, as Taylor and Hallberg (1977) point out, "that both the (acid) ignimbrites and the andesites and dacites share a common origin", then it is equally difficult to escape the conclusion that the acid and intermediate rocks are related by differentiation. The coincidence of the average Marda rhyolite with the rhyolites from the Spring Well complex on the majority of the plots would appear to support this interpretation. However none of this evidence is entirely unequivocal as it relies heavily upon analogy. Moreover, the Sr 87/86 initial ratio of 0.7029 ± 0.0015 for the Marda suite could be interpreted as favouring derivation from either a relatively radiogenic mantle (enriched in Rb for a considerable period) or alternatively from a relatively non-radiogenic (Rb-poor) basic crustal source.

Although the writer argues in a subsequent section that the presence of andesites signifies a mantle-derived calc-alkaline rock suite, clearly it is unwise to over-generalise and in considering the origin of any Archaean calc-alkaline volcanic suite it would be imprudent to overlook the model proposed by Taylor and Hallberg (1977).

7.6 RELATIONSHIP OF THE CALC-ALKALINE VOLCANICS TO THE THOLEIITIC BASALTS

In the first section of this chapter, which considered aspects of the field geology, the close spatial association of the tholeiitic basalts and the calc-alkaline volcanics was noted. There are, however, inherent geochemical differences which set the tholeiites apart from the calc-alkaline volcanics. To facilitate comparison, analyses of tholeiites from various parts of the Yilgarn Block are given in Table 7.3 and some of this data has been plotted on the geochemical variation diagrams cited earlier.

7.6.1 Discussion of the geochemical data

An examination of the tabulated data and the data plotted on the variation diagrams reveals that the tholeiites, compared with the calc-alkaline rocks (with similar SiO_2 and MgO) are characterised by:

TABLE 7.3 Data for selected tholeiitic basalts from the Eastern Goldfields Province.

	1	2	3	4	5	6	7	8	9	10
SiO_2	47.98	49.01	49.11	51.6	49.11	51.45	51.50	50.54	50.38	50.29
Al_2O_3	14.78	15.09	14.99	14.9	14.15	14.26	14.23	14.47	11.50	13.69
Fe_2O_3 t	15.02	12.25	13.37	11.8	14.97	13.96	12.02	13.13	12.03	10.99
MnO	0.25	0.23	0.23	0.21	0.19	0.18	0.23	0.19	0.19	0.18
MgO	5.74	7.64	7.03	6.7	6.29	6.66	6.67	7.06	12.21	11.37
CaO	11.55	13.10	11.68	10.9	10.54	9.20	11.50	10.42	9.91	8.98
Na_2O	3.01	1.29	2.21	2.7	2.67	2.20	2.04	2.00	1.66	1.86
K_2O	0.02	0.19	0.30	0.18	0.20	0.48	0.18	0.18	0.08	0.97
TiO_2	1.37	0.95	1.07	0.96	1.46	1.12	0.92	1.13	0.61	1.01
P_2O_5	0.14	0.08	0.10	0.12	0.16	0.13	0.09	0.11	0.06	0.37
Total	99.88	99.83	100.09	100.0	99.74	99.64	99.38	99.23	98.63	99.71
LOI	1.92	2.14	1.38	-	-	-	-	-	-	3.70
Zr	82	84	60	61	90	73	47	67	32	111
Nb	4.3	4.0	3.1	-	-	4.6	3.3	4	2.1	6.1
Y	31	20	25	20	33	23	20.4	30	13.7	23
Ce	8	2.4	-	-	16	15	-	-	-	55
Nd	14	6.8	-	-	11	9	-	-	-	34
Sc	48	48	46	-	-	-	-	49	43	28
V	350	300	300	320	270	281	278	330	269	197
Cr	165	331	246	367	-	193	340	260	1178	799
Ni	70	110	129	170	-	57	81	103	250	317
Rb	1.5	7.7	6	9	-	-	-	-	-	24
Sr	132	147	144	105	-	-	-	102	76	421
Ba	18	43	46	-	-	-	-	-	-	270

1. Tholeiitic basalt overlying Welcome Well complex (W150).
2. Tholeiitic basalt underlying Spring Well complex (S96).
3. Average of 26 tholeiitic basalts from Scotia (after Stolz, 1980).
4. Average of 337 tholeiitic basalts from the Eastern Goldfields Province, normalised to 100% total (after Hallberg and Williams, 1972).
5. Typical Lawlers tholeiite (sample 389, after Nesbitt and Sun, 1976 and Sun and Nesbitt, 1978).
6. Typical Mt. White tholeiite (sample 405, same sources as 5).
7. Mt. White high-MgO series tholeiite (sample 410, same sources as 5).
8. Average fractionated tholeiitic basalt, Forrestania (after Purvis, 1978).
9. Average primitive tholeiitic basalt, Forrestania (same source as 8).
10. Primitive, LIL element-enriched basalt from Welcome Well complex (W3).

1) significantly lower Al_2O_3, Zr, Nb, LREE and P contents (and K_2O, Rb, Ba subject to the constraints imposed by alteration);
2) comparable Ni, Cr, Y and TiO_2 contents, and
3) significantly higher $Fe_2O_3^t$, CaO, Sc and V contents.

The magnitude of the differences in the absolute abundances for some elements (particularly LIL elements and Sc and V), implies that the calc-alkaline rocks cannot be simple differentiates of the tholeiites and vice versa. This is supported by the differing fractionation trends of the two rock groups; while the parental magmas for the calc-alkaline suites have fractionated to yield high-silica differentiates (i.e., andesites, dacites and rhyolites - see section 7.5), the primary tholeiitic magmas have yielded high-iron, low-silica differentiates (Hallberg, 1972; Nesbitt and Sun, 1976; Stolz, 1980). These differences presumably arose from differing PH_2O and/or PO_2 during crystallisation.

It could be argued that many of the geochemical differences noted arise soley from the diverse crystallisation histories of the two rock series, e.g. higher $Fe_2O_3^t$ in the tholeiites. This possibility cannot be excluded for some elements, however it still does not account for the lower LIL element contents in the tholeiites. Comparing a primitive Archaean tholeiite (Purvis, 1978) with the most primitive calc-alkaline basalt analysed (i.e. W3), shows that despite their similar MgO contents, the tholeiite is still significantly higher in $Fe_2O_3^t$ and CaO and lower in Al_2O_3 and P_2O_5 (compare analyses 9 and 10, Table 7.3). Thus the geochemical differences are fundamental and must reflect upon the differing origins of the primary magmas.

7.6.2 Petrogenetic implications

Nesbitt and Sun (1976) have suggested that the primary tholeiitic magmas were derived by 20% partial melting of the mantle leaving a residue composed of 80% olivine and 20% orthopyroxene. The absence of clinopyroxene as a residual mineral is notable as it may explain why the tholeiites are lower in Al_2O_3 but higher in CaO than the calc-alkaline volcanics. Since clinopyroxene has significantly higher distribution coefficients for V and Sc than either olivine or orthopyroxene, its absence as a residual mineral may also explain why the tholeiites are higher in both of these elements. Trace element modelling using the mantle abundances and distribution coefficients for olivine, orthopyroxene and clinopyroxene compiled by Frey, et al., (1978), demonstrates that the Sc and V contents in the tholeiites are most closely matched by the model in which only olivine and orthopyroxene are residual (Table A2.5, Appendix

Figure 7.5 Selected variation diagrams for low-silica rocks from six calc-alkaline volcanic centres in the Yilgarn Block. Symbols as for Figure 7.2 with the addition of X for Archaean tholeiitic basalt. The chondritic lines are after Nesbitt and Sun (1976) and Nesbitt, pers. comm., (1980).

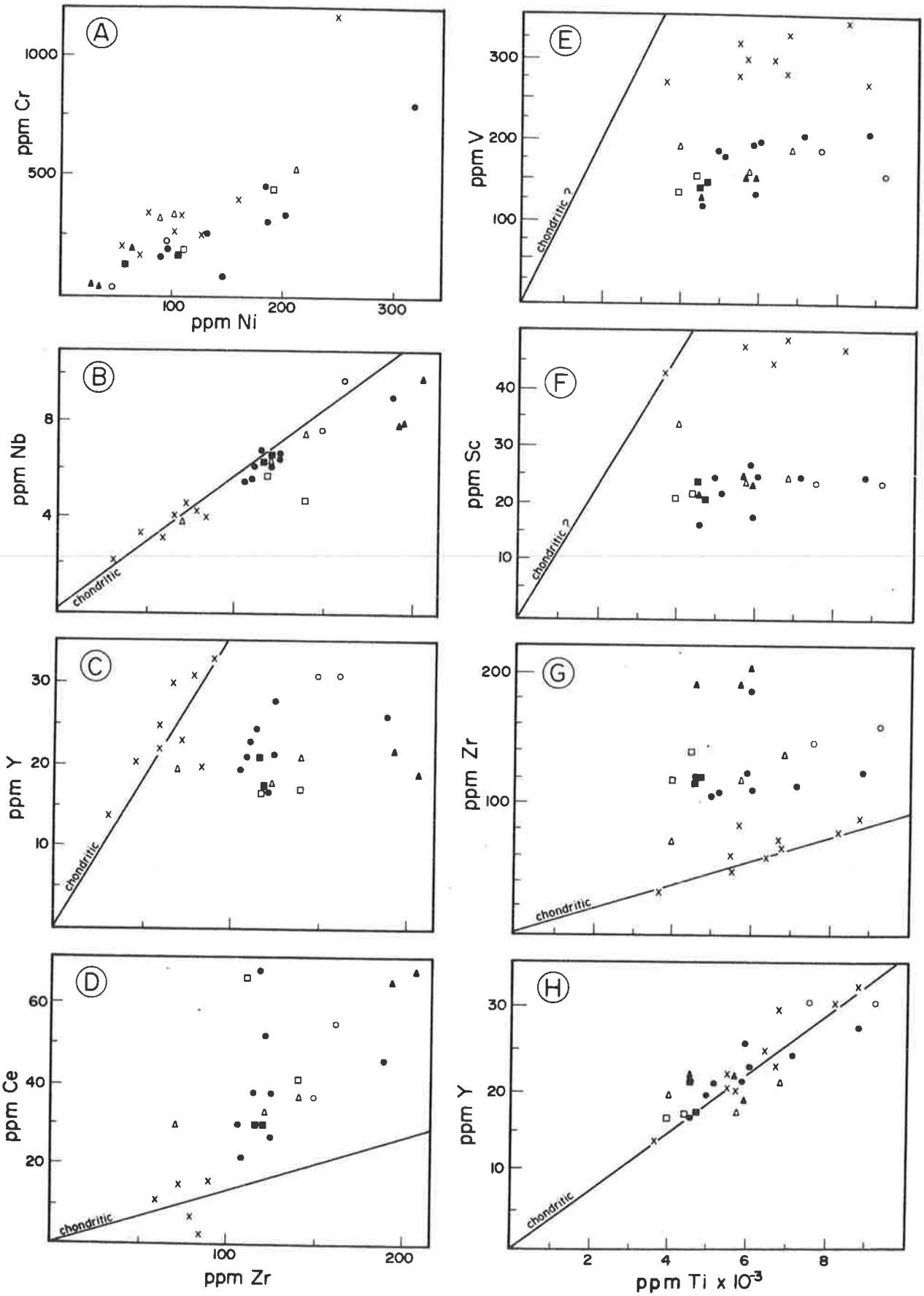

1). Therefore, it appears that the differing Al_2O_3, CaO, Sc and V contents in the tholeiites compared with the calc-alkaline rocks are a direct result of the differing residual mantle mineralogy.

The mantle mineral assemblage in equilibrium with the melt can yield information on the melting conditions (e.g. PTOTAL, PH_2O and T). Based on the experimentally-determined petrogenetic grid of Green (1971), it appears that the tholeiitic magmas could be the result of melting at higher temperatures and/or pressures than the calc-alkaline magmas. Nesbitt and Sun (1976) have implied that the primary tholeiitic magmas were derived by approximately 20% melting and for various reasons outlined previously it has been inferred that the parental calc-alkaline magmas were also the result of relatively high degrees of melting (> 20% - chapter 5). Thus variations in the degree of melting are unlikely to be the major factor leading to the compositional differences. The pressure or depth of melting could, however, have a major influence, since it is evident from Gréen's petrogenetic grid that increasing depths of melting will move the residual mineralogy out of the stability field of clinopyroxene and into that of olivine and orthopyroxene alone. Green (1976) has also shown that at low pressures (i.e., at shallow depths of melting), the stability field of clinopyroxene is greatly expanded by increasing PH_2O during melting. In the absence of detailed experimental evidence for the particular rocks being considered, the relative importance of PTOTAL and PH_2O in producing the compositional differences is uncertain, but quite clearly one or both factors have probably assumed a major role.

The differing LIL element contents of the tholeiitic and calc-alkaline rocks preclude melting of the same mantle source, owing to the similarity in the postulated degrees of melting. As outlined in a previous section of this chapter (7.3) and for the Welcome Well complex (chapter 5), a LIL element-enriched mantle source is required in order to account for the LIL element contents of the calc-alkaline volcanics. However, in the case of the tholeiitic rocks, the mantle source was unlikely to have been enriched in any LIL elements, since:

1) the tholeiitic rocks usually have flat REE patterns (Sun and Nesbitt, 1978; Stolz, 1980) and
2) the incompatible element ratios of the tholeiites are very near chondritic (including Zr/Ti, Zr/Y and Zr/Ce, see Fig. 7.5).

The important conclusion to be drawn is that the primary magmas for the tholeiitic and calc-alkaline series were derived from quite different mantle sources and therefore probably from separate regions of the mantle. Notably, the chondritic mantle source (with respect to Zr, Nb, Y, Ti and

Figure 7.6 Summary of possible modes of formation of primary magmas for calc-alkaline volcanics, tonalitic plutons and tholeiitic basalts in the Archaean. As discussed in the text. generation of the primary magmas for the calc-alkaline suites above a mantle diapir or "hot-spot", is an equally plausible mechanism and cannot be distinguished from the model illustrated with the available data.

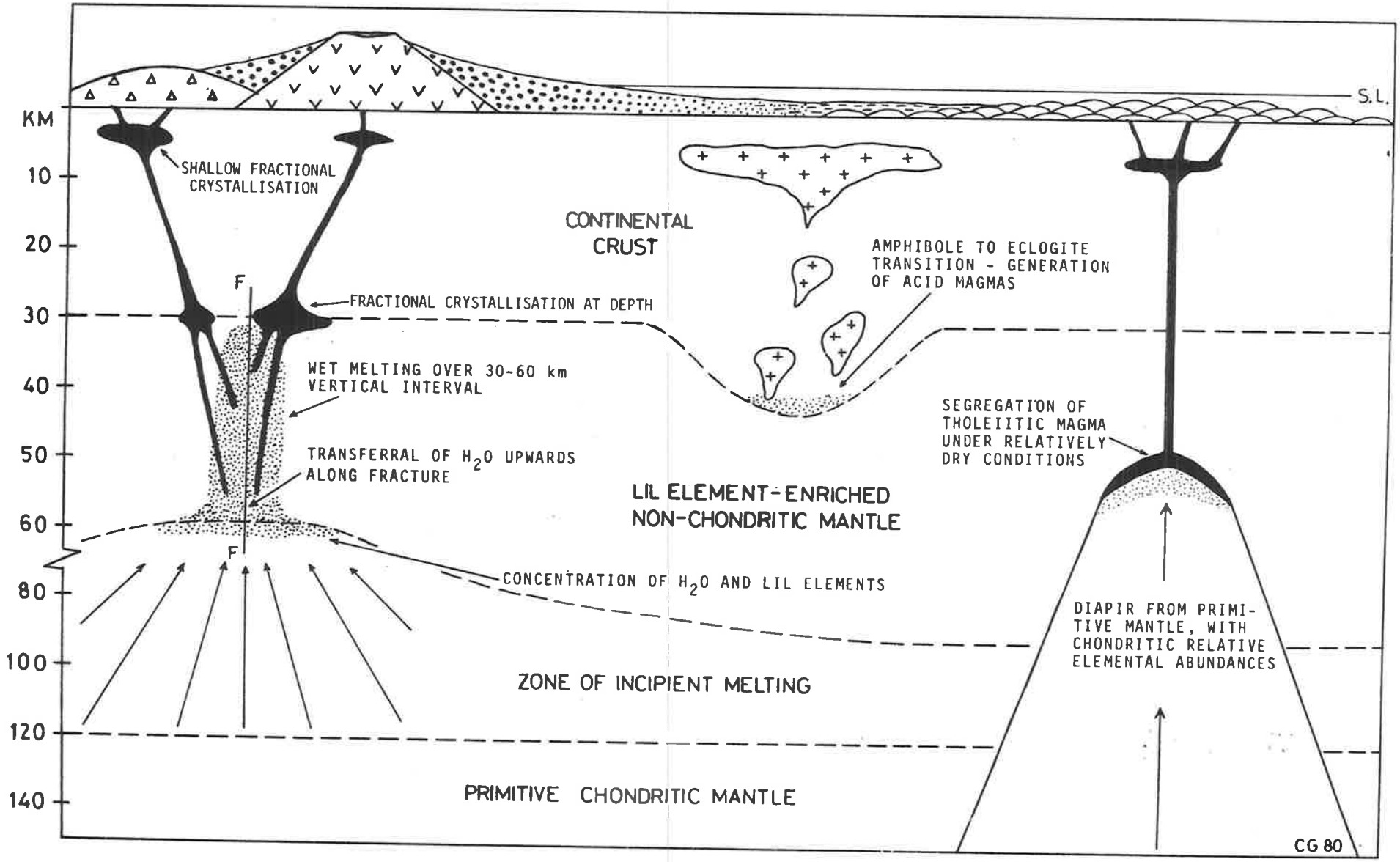

Ce) inferred for the primary magmas of the tholeiitic series is analogous to that deduced for the primary komatiitic magmas by Nesbitt and Sun (1976). This, in turn, suggests that the primary magmas which gave rise to the tholeiitic series were derived from primitive mantle at greater depths (c.f. magmas for calc-alkaline series), although magma segregation could have occurred at considerably shallower levels if the primitive mantle material rose as a diapir (Fig. 7.6). In a hypothetical model involving a low velocity zone such as that illustrated diagrammatically in Figure 7.6, it would be postulated that the primary tholeiitic magma was derived from primitive, "unenriched" mantle beneath the low velocity zone, while the primary calc-alkaline magma was derived from the enriched mantle above the low velocity zone. Following Green (1971) and Green and Liebermann (1976) the "enriched" mantle could have developed as the result of upward migration of LIL element-enriched components derived by incipient melting in the low velocity zone. Goodwin and Smith (1980) have advocated analogous sources for the calc-alkaline and tholeiitic magmas, but they considered that the upper mantle gained its LIL element-enriched character via contributions from "sag-ducted" crust, rather than from a deeper zone of incipient melting (c.f. Green and Liebermann, 1976).

7.7 A REVIEW OF CALC-ALKALINE VOLCANISM IN OTHER ARCHAEAN SHIELDS

Volcanics with calc-alkaline affinities have been documented from many Archaean greenstone belts in other continents, particularly Canada and Africa. It is the purpose of this section to briefly review a representative selection of these examples. Particular attention is directed towards the origins proposed for the calc-alkaline magmas, so that a comparison can be made with the origin suggested in this thesis for the calc-alkaline volcanics of the Yilgarn Block.

7.7.1 Examples from Africa

Hawkesworth and O'Nions (1977) have discussed the geochemistry of a suite of rocks, including calc-alkaline volcanics, from the Onverwacht Group (Kaapvaal Craton, South Africa) and from various greenstone belts in the Rhodesian Craton. They considered that the continuum of compositions from komatiites to tholeiites and calc-alkaline volcanics (particularly in LREE), indicated that the bulk of the magmas were derived by differential partial melting of essentially the same peridotitic mantle source. The relatively depleted HREE, characteristic of the calc-alkaline volcanics (c.f. tholeiites), was attributed to crystallisation and separation of iron-rich garnet.

TABLE 7.4. Compositions of selected Archaean calc-alkaline volcanic rocks from other continents.

	1	2	3	4	5	6	7	8	9	10	11	12	13	14	15	16	17	18	19
SiO_2	56.6	59.7	71.7	67.49	56.9	75.3	70.5	60.06	66.8	59.10	67.43	71.1	49.7	56.7	58.9	66.2	71.7	64.0	73.5
Al_2O_3	15.1	15.8	16.4	15.99	14.1	13.5	15.7	16.3	15.6	15.32	16.52	13.99	14.9	14.0	15.5	16.5	16.4	15.8	12.7
Fe_2O_3 t	7.81	5.76	1.60	3.57	9.39	2.28	2.20	6.7	4.6	9.72	4.0	4.64	12.38	10.08	6.5	2.0	1.7	5.8	2.23
MnO				0.05			0.03			0.17	0.06	0.06							
MgO	6.15	3.42	0.50	1.18	5.45	0.89	0.78	4.2	2.0	2.80	1.53	0.87	6.3	5.4	4.5	1.6	0.5	3.0	0.8
CaO	6.96	3.61	1.74	3.03	6.59	1.19	2.86	5.2	3.5	5.69	2.35	2.80	9.4	6.6	4.5	1.6	0.5	3.0	0.8
Na_2O	2.86	5.46	5.00	5.39	3.37	3.46	5.32	5.0	5.2	2.69	2.26	3.91	2.1	3.4	4.0	5.2	5.0	4.0	3.3
K_2O	0.85	1.62	2.05	1.56	0.79	3.53	1.88	1.4	1.9	1.42	3.74	1.17	0.32	0.67	1.9	2.0	2.0	2.7	3.0
TiO_2	0.58	0.69	0.19	0.50	0.93	0.15	0.28	0.26	0.26	1.12	0.59	0.40	1.0	0.92	0.65	0.28	0.19	0.50	0.14
P_2O_5				0.19			0.12			0.20	0.13	0.09							
Zr	75	65	30	170	177	357		101	110	147	177	301	100	150	190	50	30	260	350
Y	15	13	2	8.8	26	84	Yb 0.28	13	8	28	14	41	15	25	35	2	2	8	30
Ce	24	50	34	63	34	146	34	47	37	La 24	La 14	La 41	25	31	70	30	35	100	95
Cr	74	54	9.7	10	154					<20	~20	<20	175	125	88	30	12	45	12
Ni	50	35	7	7	73	23				<10	~20	<10	100	70	60	25	10	25	10
Rb	24	48	28	27	24	65	47	26	35	46	99	41	10	22	75	33	41	68	43
Sr	241	291	100	707	358	23	847	722	612	195	97	132	165	278	580	600	110	390	100
Ba	288	310	330	540	237	954	813	498	500	505	630	332	90	230	547	590	480	1090	750

1,2,3. Average compositions of calc-alkaline volcanic rocks from the Bulawayan Group, Midlands greenstone belt, Rhodesia (Condie and Harrison, 1976).

4. Middle Marker porphyry, lower Onverwacht Group, Barberton Mountain Land (Glikson, 1976).

5. Average composition of low-K andesite (8 samples) from the Nyanzian greenstone belts of western Kenya (Davis and Condie, 1977).

6. Single analysis of rhyolite from the same locality and source as 5.

7. Rhyodacite porphyry dyke or sill, Vermilion greenstone belt.

8, 9. Average andesite (11 samples) and average dacite (8 samples) from the Kakagi Lake metavolcanics (Wolff and Crockett, 1979).

10,11,12. Average andesite, dacite and rhyolite (70-75% SiO_2) from the Prince Albert Group, Northwest Territories, Canada (Fryer and Jenner, 1978).

13-19. Average compositions of Archaean volcanic rocks cited in Condie's (1976) review paper. 13. LIL element-enriched Archaean tholeiite; 14. Low-alkali (and LIL element) Archaean andesite; 15. High-alkali (and LIL element) Archaean andesite; 16,17. Depleted (in HREE and Y) siliceous volcanics; 18,19. Undepleted (in HREE and Y) siliceous volcanics.

Volcanics from the Rhodesian craton were also the subject of a study by Condie and Harrison (1976) who examined basic, intermediate and acid examples belonging to the Bulawayan Group in the Midlands greenstone belt. In the opinion of these authors, the sequence sampled provided some of the freshest and least-metamorphosed volcanic rocks available in any Archaean terrain in the world. They proposed a model in which:

1) the primitive tholeiites (with flat REE patterns) were derived by 30% partial melting of a lherzolite mantle source, and
2) the calc-alkaline basalts, andesites and rhyolites were generated by 50%, 20-30% and 10% partial melting respectively, of eclogite with the composition of the primitive tholeiite. The tholeiitic basalt was thought to have been converted to eclogite as it descended in an ancient subduction zone.

A model involving residual garnet (in eclogite) was believed to be necessary in order to explain the relatively low HREE contents (< 10 x chondrite) of the calc-alkaline rocks and also their relatively fractionated REE distributions (Table 7.4). It is noteworthy, however, that the Midlands rhyolites have similar, relatively high Al_2O_3 and Sr, and low Zr contents, comparable with acid rocks from the Welcome Well, Ida Hill and Polelle complexes (Table 7.2), suggesting the possibility that, by analogy with the Western Australian examples, the HREE depletion could be due to extended amphibole fractionation rather than equilibrium with garnet.

Glikson (1976) also favoured partial melting under eclogite facies conditions as an explanation for the origin of some extrusive and intrusive acid porphyries belonging to the lower Onverwacht Group of the Barberton Mountain Land region. The acid porphyries are characterised by fractionated REE patterns, with generally low HREE contents (< 10 x chondrites); some have extremely low HREE contents (~1 x chondrites) and uniformly steep REE patterns at the HREE end, supporting Glikson's interpretation that garnet has been involved in their generation. Intermediate rocks are not associated with the acid porphyries, but tonalitic intrusives which are probably genetically related, occur in close proximity.

A further example of Archaean calc-alkaline volcanism in the African continent has been documented by Davis and Condie (1977) from the Nyanzian greenstone belts of western Kenya. Geochemical modelling by these authors showed that the intermediate magmas could have been derived by equilibrium melting of an eclogite or garnet amphibolite, while the acid magmas probably had an upper crustal source in anatexis

of a siliceous granulite. The single sample of rhyolite analysed by Davis and Condie is particularly high in Zr (357 ppm) Ce (146 ppm), Y (84 pm) and K_2O (3.53%) and could be taken as support for a sialic crustal source (Table 7.4). On the other hand, some of the andesites are also relatively high in these elements and this, combined with the relatively low Al_2O_3, CaO and Sr contents in the rhyolites, could be taken as evidence that the acid magmas were derived from intermediate parents by plagioclase-dominated fractionation.

7.7.2 Examples from North America and Canada

The dacitic volcanics and tonalitic intrusives (including the Saganaga Tonalite) from the Vermilion greenstone belt of northeastern Minnesota (Arth and Hanson, 1975) have markedly similar geochemistry to the Onverwacht Group acid porphyries and associated intrusives reported by Glikson (1976). Modelling by Arth and Hanson (1972) showed that the most probable origin involved approximately 20% partial melting of a basic source leaving a residue dominated by clinopyroxene and garnet. Again, garnet was a necessary residual mineral in order to explain the depletion in HREE. It is noteworthy that, as in the Onverwacht Group, the acid rocks are not associated with intermediate intrusive and extrusive rocks.

Acid and intermediate volcanics of calc-alkaline affinities are well known in the Canadian Shield owing to their association with volcanogenic sulphide ore deposits (Goodwin, 1965; Sangster, 1972). In detail, the calc-alkaline volcanics show significant compositional variation. Hubregtse (1976) for example, has recognised a high-alkali suite in the western Superior Province (Knee Lake - Oxford Lake greenstone belt), which he considers has shoshonitic affinities. Metavolcanics from the Kakagi Lake area (Wolff and Crockett, 1979) have typical calc-alkaline features and their geochemical characteristics greatly resemble that of some of the andesites and dacites from the Yilgarn Block (Table 7.4). These authors note analogies with averages quoted by Condie (1976) and following Condie, suggest that differential partial melting of a basic source, leaving an eclogitic residue, may be the most reasonable model. The relatively low Sr 87/86 initial ratios in these rocks (0.7015 + 0.0007) certainly indicates a primitive source either in the mantle or from a mantle-derived mafic-ultramafic pile.

Volcanics from the Prince Albert Group, Northwest Territories, Canada (Fryer and Jenner, 1978) have a comparable compositional range to volcanics from the Midlands greenstone belt, Rhodesia (Condie and Harrison, 1976). Tholeiitic basalts with relatively flat REE patterns are the dominant basic

rock type, although some basalts showing LREE enrichment and with more calc-alkaline features (e.g. lower $Fe_2O_3^t$ and higher Al_2O_3) do occur. Fryer and Jenner have noted that the relatively high HREE contents of the andesites (> 15 x chondrite, Table 7.4), preclude equilibration with residual garnet, but they also found that partial melting of amphibolite was not entirely satisfactory. The dacites have a significant HREE depletion (though not as severe as that in the Saganaga Tonalite - Table 7.4) and were thought to be derived by partial melting of amphibolite with some residual orthopyroxene and garnet - i.e. basic granulite. The rhyolites, which have REE patterns very similar to the Marda rhyolites (Taylor and Hallberg, 1977 - Table 7.2), could not be explained by partial melting of a mafic source or by crystal fractionation from the HREE-depleted dacites. Fryer and Jenner considered that they were produced by melting of sialic crustal rocks (e.g. siliceous granulite or tonalite) and were subsequently modified by low-pressure fractionation dominated by plagioclase.

Condie and Baragar (1974) have presented REE data for volcanic rocks from the Yellowknife and South Pass greenstone belts in Canada. The following rock types occur in both greenstone belts:

1) tholeiitic basalt with flat 10-15 x chondrite REE distributions;
2) calc-alkaline andesite with fractionated REE distributions (100 x LREE to 5-15 x HREE) and
3) calc-alkaline dacite with fractionated REE distributions (100-300 x LREE to 10-20 x HREE).

They considered that the calc-alkaline rocks represented typical "arc type volcanism".

In a more recent review paper, Condie (1976) included this and other data to arrive at some general conclusions concerning Archaean calc-alkaline volcanism, which are summarized below.

1) Calc-alkaline volcanics are typified by fractionated REE patterns and are usually volumetrically less abundant than tholeiitic basalts (with flat REE patterns) in any given greenstone belt.
2) The calc-alkaline andesites include a relatively low LIL element group and a relatively high LIL element group. Andesites from the latter group have more fractionated REE distributions and apparently assume increasing importance at higher stratigraphic levels.
3) The "siliceous volcanics", including dacites, rhyodacites and rhyolites, also fall into two groups corresponding with those that show a relative HREE and Y depletion (c.f. modern examples) and those that do not. Condie considers that the acid volcanics from

the South Pass, Yellowknife and western Kenyan greenstone belts belong to the "normal" group (Condie and Baragar, 1974; Davis and Condie, 1977), while it is inferred that the Vermilion, Barberton and Midlands greenstone belts include examples of the "depleted" group (Arth and Hanson, 1975; Glikson, 1976; Condie and Harrison, 1976).

Trace element modelling by Condie indicated that the calc-alkaline andesites could not be derived by shallow fractional crystallisation of the tholeiites, but could possibly be generated by partial melting of an eclogitic source with the composition of the tholeiite. A similar model was favoured for the HREE-depleted siliceous volcanics, while the undepleted magmas were thought to be derived by partial melting of upper-crustal siliceous granulites.

7.7.3 Discussion

It appears from the above review that few workers favour a direct mantle origin for the calc-alkaline intermediate rocks via fractionation from basic parents as proposed in this thesis. Rather, a two-stage model is generally preferred, in which basic rocks are melted at various depths to yield the acid and intermediate magmas. Reasons for favouring the latter model appear to be both the lack of suitable basic parents (Condie, 1976 has shown that tholeiitic basalts are unsuitable), and the necessity to account for the depletion in HREE, apparently by residual garnet.

A further important point to emerge from the review is that calc-alkaline andesites, although relatively abundant in some greenstone belts (e.g. Midlands, Nyanzian, northern Norseman-Wiluna, many examples in Canada), are lacking in others (e.g. Barberton, Vermilion). The latter type of greenstone belt commonly shows a bimodal volcanic-plutonic association, consisting of tholeiitic basalts and gabbros, and sodic acid volcanics and tonalites. The distinction between the two volcanic associations in greenstone belts has been previously recognised by Condie (1976), who has been able to quantify the differences in terms of the geochemistry. He makes the important observation that the "bimodal volcanic association (is) composed dominantly of depleted Archaean tholeiite (with flat REE patterns and low LIL element contents) and related ultramafic rocks with minor depleted siliceous volcanics (severely depleted HREE) in the upper parts." Condie further notes that the other association "is characterised by an abundance of depleted Archaean tholeiite with enriched Archaean tholeiite (calc-alkaline basalt affinities), andesite and finally

TABLE 7.5. Summary of the models proposed for the origin of Archaean felsic volcanic rocks

PRODUCT 2		AUTHOR		PRODUCT 1
		Barker and Arth (1976)		
Rocks with relatively high Sr and Al_2O_3 contents and depleted HREE	← residue contains significant garnet +cpx.±plag.±amph.	BASIC SOURCE	residue of cpx. and plag.(±amph.) →	Rocks with relatively low Rb, Sr and Al_2O_3 contents, moderate LREE enrichment, negative Eu anomaly and a flat HREE distribution.
		Condie (1976)		
Condie's depleted siliceous volcanics, with relatively low HREE contents	← residue contains garnet	SIALIC GRANULITIC SOURCE BASIC SOURCE	residue contains no garnet →	Condie's undepleted siliceous volcanics, with relatively high HREE and other LIL element contents.
			residue contains ? no garnet	
		This thesis		
Rocks with relatively depleted HREE (c.f. parent), a characteristic V-shaped REE pattern and relatively high Sr contents. e.g. Welcome Well complex Chapter 5.	← fractionation of a higher proportion of amphibole relative to cpx.+plag.	LIL ELEMENT -ENRICHED BASIC LIQUID (derived from mantle)	fractionation of a lower proportion of amphibole relative to cpx.+plag. →	Rocks with relatively enriched HREE (c.f. paren significant negative Eu anomaly and relatively low Sr contents. e.g. Spring Well complex Chapter 6.

siliceous volcanics becoming more important in upper stratigraphic horizons". It may be inferred from the work of Condie and others (particularly Fryer and Jenner, 1978, and Wolff and Crockett, 1979), that while andesites and undepleted siliceous volcanics are absent from the bimodal terrains, the reverse is not true i.e., both depleted and undepleted siliceous volcanics and variably LIL element-enriched andesites can occur in the non-bimodal terrains.

Barker and Arth (1976) have considered the bimodal association in Archaean terrains in some detail. Although they were primarily concerned with explaining the origin of the tonalitic gneisses which occur in the older Archaean successions, it is clear that their conclusions can also be applied to the bimodal volcanic associations in the greenstone belts (c.f. Arth and Hanson, 1972). They observed that the trondhjemitic-tonalitic liquids were of two types:

1) a low Al_2O_3 type (< 15% Al_2O_3), with relatively low Rb and Sr contents, moderate LREE enrichment, a negative Eu anomaly and flat HREE distribution;
2) a high Al_2O_3 type (> 15% Al_2O_3) with relatively low Rb but moderate to high Sr contents, moderate LREE enrichment, a negligible Eu anomaly and depleted HREE.

In many ways this grouping is similar to the undepleted and depleted siliceous volcanics respectively, of Condie (1976). The geochemical characteristics are, moreover, analogous with the low-Sr and high-Sr acid volcanics of the Yilgarn Block (section 7.5). However, an important distinction is that the dacites and rhyolites from the volcanic centres considered in this thesis are in association with andesites and in some cases basalts, to which they can be shown to be related by crystal fractionation; no such association or differentiation series is demonstrable for the tonalites and dacites of the bimodal igneous terrains.

Barker and Arth (1976) considered that the low Al_2O_3 magmas were generated by partial melting of a basic source leaving a residue dominated by clinopyroxene and plagioclase, while the high Al_2O_3 magmas were believed to have equilibrated with a residue dominated by garnet + pyroxene or hornblende + plagioclase + clinopyroxene + garnet (Table 7.5). It is the presence or absence of residual garnet and/or hornblende to the mutual exclusion of plagioclase, which determines to a major extent the nature of the liquid. Barker and Arth (1976) explained the absence of intermediate rocks in the bimodal volcanic association by proposing that the relatively volatile-enriched acid magma separated from the residue before the degree of melting reached the level at which intermediate

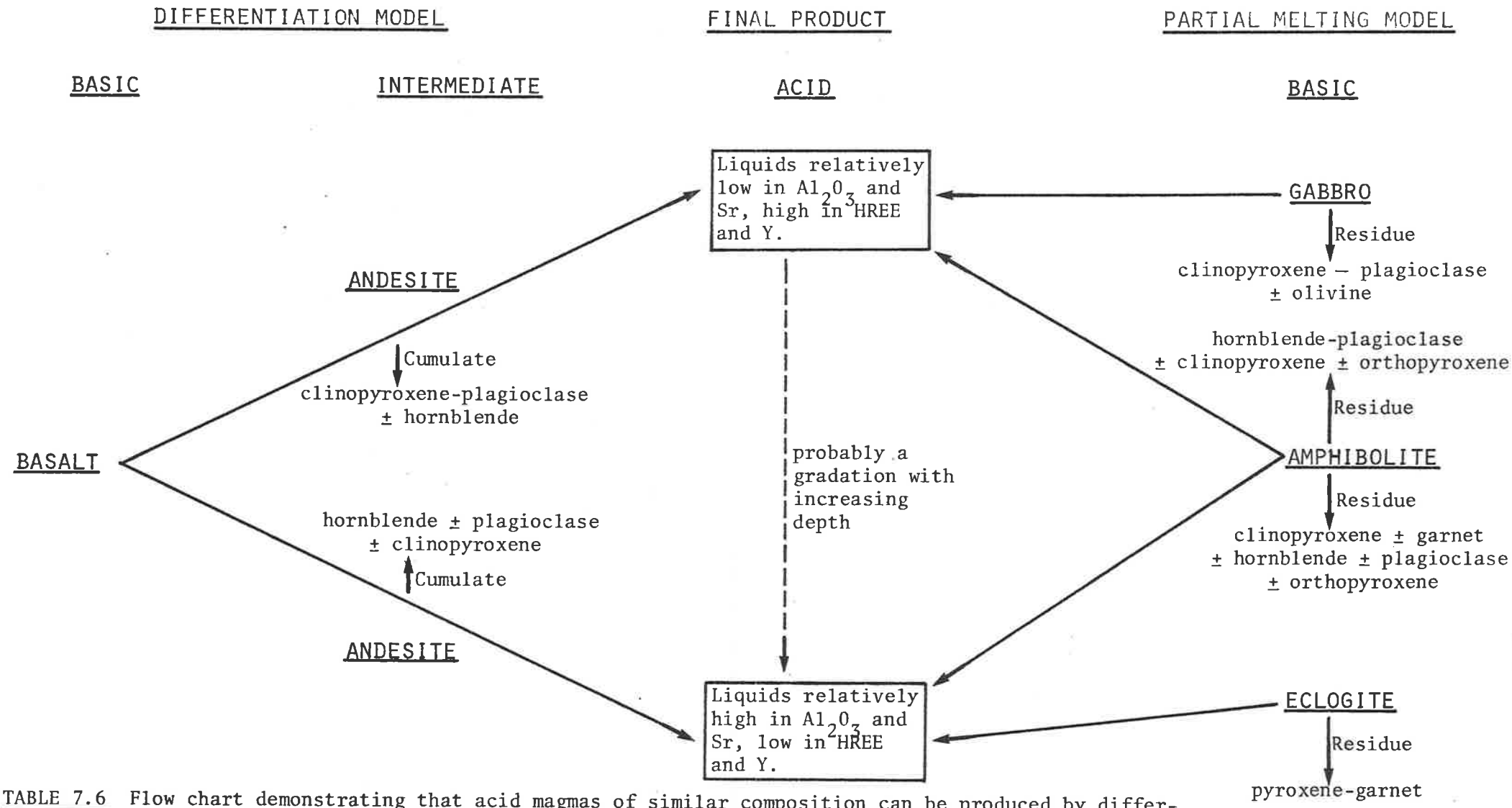

TABLE 7.6 Flow chart demonstrating that acid magmas of similar composition can be produced by differentiation from, and partial melting of, a given basic source.

Notes: 1. The differentiation model will yield intermediate liquids, while the partial melting model may not.

2. The approximate relative depths of the respective cumulate and residual mineral assemblages are indicated by their vertical position in the table.

magmas could form (F < 40%). This would have the effect of considerably raising the solidus of the residue, thus precluding further melting even if the residue sank into the mantle. This conclusion is independently supported by experimental evidence which demonstrates that excessive temperatures are required to generate intermediate liquids from a basic source (Wyllie, et al., 1976) and by calculations which show that the compositions of liquids generated by melting of basic rocks (in eclogite facies) do not resemble those of calc-alkaline andesites (Stern, 1974).

Barker and Arth (1976) recognised that acid liquids of similar composition could also be produced by fractionation of the appropriate mineral assemblages from a basic parent, viz. plagioclase + pyroxene to yield the low Al_2O_3 (and Sr) liquids, and predominantly hornblende to yield the high Al_2O_3 (and Sr) liquids. Since crystal fractionation will move the liquid through intermediate compositions, it is evident that this alternative will yield the calc-alkaline, andesite-bearing association (Table 7.6). If it is accepted that intermediate melts cannot be produced by direct partial melting of a basic source, then it follows that the presence of andesites must signify a calc-alkaline differentiation series and hence a mantle-derived rock suite. This observation applies to the rocks studied in the northern Norseman-Wiluna greenstone belt but apparently is not widely accepted for calc-alkaline suites in other Archaean shields, judging from the above review.

In summary, based on the studies reported in this thesis for Archaean calc-alkaline volcanics in the Yilgarn Block and the previous review, the following comments appear to be justified.

A. The close field association of acid and intermediate and occasionally basic volcanics, all of similar LIL element-enriched geochemical character, implies not only a genetic relationship but also a common source (e.g. same magma chamber). If the intermediate and acid rocks were only related through partial melting of the crust (quite often of different composition and at different depths), then there appears to be no reason why they should be invariably associated both in space and in time.

B. The spread in the HREE contents of the acid volcanics (associated with andesites) can be satisfactorily explained by varying amounts of amphibole fractionation relative to clinopyroxene and plagioclase. This could explain the depleted and undepleted siliceous volcanics noted by Condie (1976) in association with calc-alkaline suites.

The siliceous volcanics in the bimodal suites, because of their crustal origin, probably owe their depleted HREE character to residual garnet (Arth

and Hanson, 1972; Glikson, 1976). It is conceivable that acid volcanics of sialic crustal derivation (e.g. through partial melting of acid-intermediate granulite) could also be represented in Archaean greenstone sequences, but like the depleted siliceous volcanics of the bimodal association, they would not be expected to be in association with andesites.

C. In many of the Archaean calc-alkaline suites described in the literature, LIL element-enriched basalts are also present, even if in small amount (e.g. Condie and Harrison, 1976; Condie, 1976; Fryer and Jenner, 1978). If the LIL element-enriched basalts are not genetically related to the acid and intermediate volcanics then it is extremely coincidental that such mantle-derived rocks should only be found in close spatial association with crustal-derived acid and intermediate rocks of similar LIL element-enriched character. On the other hand this association would be expected, and indeed predicted, if the rocks formed a calc-alkaline differentiation series. The relatively small volume of LIL element-enriched basalts is not an objection to the differentiation hypothesis, since much of the basic liquid could have fractionated at depth to yield the more acid rocks of the calc-alkaline suites.

These points are made to direct attention towards the attributes of a crystal fractionation hypothesis in explaining the origin of Archaean calc-alkaline rock suites, since in the writer's opinion this alternative has not received the attention it deserves in the literature.

7.8 SUMMARY

Calc-alkaline volcanic centres, in most cases containing a high proportion of andesite , are widely developed in the Yilgarn Block. The most basic members from each of the centres, including basalts and low-silica andesites, have comparable geochemical characteristics and are therefore believed to have had a common origin. This involved shallow, hydrous melting of a LIL element-enriched zone of the mantle. Melting may have been triggered by the localised introduction of water or by a local region of high heat flow (i.e., "hot spot"). In either case, magma generation conditions approximating those created by modern subduction processes were thought to have pertained and this could explain the marked geochemical analogy noted between Archaean and Cainozoic calc-alkaline volcanic suites.

The calc-alkaline volcanics of the Yilgarn Block show two distinct differentiation trends. One, produced as the result of extensive amphibole fractionation has resulted in acid rocks with relatively high Sr and relatively low Zr, Nb, Y, HREE and MREE contents. The other, in which

clinopyroxene and plagioclase fractionation assume a greater role, has resulted in acid rocks with lower Sr and Al_2O_3 contents and higher Zr, Nb, Y and HREE contents and a significant negative Eu anomaly compared with the former group. The varying role of amphibole in relation to clinopyroxene and plagioclase, in producing the two differentiation trends, is considered to be a function of the depth at which the bulk of the crystal fractionation occurred.

Basalts belonging to the calc-alkaline and tholeiitic rock series show consistent geochemical differences. Some stem from the fact that the primary magmas for the tholeiitic series have not equilibrated with residual clinopyroxene (hence they are relatively high in Sc, V and CaO but low in Al_2O_3 compared with calc-alkaline rocks), while others from the primitive, chondritic mantle source (hence they are lower in most LIL elements compared with calc-alkaline rocks). The different mantle sources and residual mineral assemblages, imply that the calc-alkaline and tholeiitic volcanics are genetically unrelated. Moreover, the lack of any consistent time or spatial relationships between the two series indicates that the respective magma generation processes were not in any way linked.

A literature study reveals that calc-alkaline volcanics, similar in all respects to those in the Yilgarn Block, occur in Archaean greenstone terrains in other continents. The origins proposed for the acid and intermediate magmas usually involve partial melting of pre-existing crustal rocks. The literature review also showed that acid volcanics, lacking associated andesites occur in Archaean greenstone belts. In the writer's opinion, the model of Barker and Arth (1976) satisfactorily accounts for the relative proportions of rock types, geochemical characteristics and particular origins of the volcanics comprising the two associations. The critical feature of the model is that is recognises the similarity in the major element geochemistry of acid magmas produced by partial melting of, and crystal fractionation from, a given basic source, assuming the residual and fractionating minerals respectively, are the same. The partial melting case will yield the bimodal association lacking andesites, while the crystal fractionation case, because it passes through an intermediate stage, will yield the typical calc-alkaline, andesite-bearing association.

PART THREE

A DISCUSSION OF THE IMPLICATIONS FOR PRECAMBRIAN CRUSTAL AND MANTLE EVOLUTION

CHAPTER 8

8.1 INTRODUCTION

It will be apparent from the preceding chapters that the Archaean and Proterozoic volcanic terrains studied differ markedly with respect to the setting and environment of eruption, the relative volumes of material erupted and the origins of the acid magmas. For example, while Archaean felsic volcanic rocks are of limited volume and occur in small centres, the Proterozoic examples are voluminous and commonly form extensive ignimbrite sheets. Also, while the Archaean felsic volcanic rocks studied represent new additions to the crust from the mantle, the Proterozoic terrains developed largely as the result of extensive crustal reworking with very little addition at the surface of new mantle material. The latter observation, considered on its own, is consistent with the view held by many workers that the Archaean heralded a period of major crustal growth via contributions from the mantle, while the Proterozoic was a time of reworking and consolidation of this crust (Condie, 1973; Bridgwater and Fyfe, 1974; Hargraves, 1976; Fyfe, 1978; Glikson, 1977, 1979c; Tarney and Windley, 1977). Glikson (1977, 1979c) in particular, has emphasised that there is an apparent gap in the rock record in the 2.6-2.0 aeon period and that either side of this hiatus there is seemingly an abrupt change in the tectonic regimes and associated igneous activity.

It is important to note, however, that crustal reworking was not confined to the Proterozoic, since the voluminous granitoid rocks in the Archaean offer evidence for extensive crustal remobilisation during this period on a scale probably exceeding that in the Middle Proterozoic (Glikson and Lambert, 1976; Archibald, et al., 1978; Cooper, et al., 1978). It seems probable, as Hargraves (1976) has pointed out, that melting of the base of the Archaean crust was an ongoing process that would have effectively limited the thickness to which the sialic (and simatic) crust could have developed. As the geothermal gradient decreased with time, so the maximum permissable thickness of the sialic crust would have increased and possibly, the likelihood of sialic crustal reworking would have diminished.

An important distinction between Archaean and Proterozoic felsic volcanic terrains, which appears to have general validity, concerns the occurrence of calc-alkaline rock suites. To the writer's knowledge no andesite-bearing calc-alkaline volcanic associations have been convincingly demonstrated to occur within the post-orogenic Middle Proterozoic volcano-plutonic terrains. It seems likely that this feature may reflect upon

TABLE 8.1. Geochemical data for basic rocks referred to in text.

	K101	A	W3	B	W150	C	BHVO-1
SiO_2	51.91	52.04	50.29	54.56	47.98	51.73	49.79
Al_2O_3	13.65	16.62	13.69	15.88	14.78	16.35	13.75
Fe_2O_3 t	9.66	10.16	10.99	9.52	150.2	11.69	12.34
MnO	0.18	0.18	0.18	0.15	0.25	0.27	0.17
MgO	11.77	6.73	11.37	6.43	5.74	3.74	7.39
CaO	8.55	7.93	8.98	7.60	11.55	11.96	11.31
Na_2O	2.15	3.15	1.86	3.61	3.01	2.43	2.39
K_2O	1.27	1.67	0.97	1.00	0.02	0.57	0.53
TiO_2	0.64	1.02	1.01	1.02	1.37	1.15	2.76
P_2O_5	0.18	0.23	0.37	0.22	0.14	0.13	0.27
Total	99.96	99.73	99.71	99.99	99.88	100.02	
LOI	1.51	2.16	3.70	2.64	1.92		
Zr	102	141	111	117	82	61	170
Nb	5.3	7.4	6.1	6.4	4.3	3.5	20
Y	19	26	23	18.3	31	26	28
Ce	78	54	55	34	8	10	36.7
Nd	36	23	34	21	14		23.4
Sc	29	28	28	24	48	43	31.6
V	180	182	197	170	350	292	337
Cr	1050	353	799	319	165	295	349
Ni	362	150	317	170	70	150	121
Rb	45	55	24	23	1.5	19	10
Sr	510	498	421	335	132	167	404
Ba	1005	719	270	471	18	50	132

K101. Primitive basalt from the Gawler Range province (see Chapter 2).

A. Average composition of four basalts from the Gawler Range province (average of E231, E459, K110 and K33, data in Table A2.2, Appendix 1).

W3. Primitive basalt from the Welcome Well complex (see Chapter 5).

B. Average composition of eight low-silica, high-MgO rocks (basalts and andesites) from the Welcome Well complex (average of W2, W111, W131, W4, W123, W125, W5 and W23, data in Table A5.2, Appendix 1).

W150. Tholeiitic basalt, adjacent to the Welcome Well complex.

C. Average composition of thirteen evolved tholeiitic basalts from the Scotia area (data from Stolz, 1980).

BHVO-1. Kilauea Tholeiite, international standard, data from Sun, *et al.*, (1979).

fundamental changes in the processes of magma generation and/or conditions of crystal fractionation during the Precambrian.

In view of the above observation it is perhaps surprising to note that the basalts, associated in minor proportion with the Archaean and Proterozoic felsic volcanic rocks, have analogous geochemical characteristics. It will be recalled that in both cases it was postulated that the primary basic magmas originated by shallow, hydrous melting of a LIL element-enriched zone of the upper mantle. On the one hand, extended differentiation of the basic rocks yielded the calc-alkaline series of the Archaean, while on the other, differentiation was restricted and apparently did not yield calc-alkaline andesites in the Proterozoic.

These observations and the questions they pose are clearly important to an understanding of the processes of magma generation, and in turn to a knowledge of crustal and mantle evolution, in the Precambrian. To investigate the points raised in more depth, the evidence provided the basic, intermediate and acid rocks in both the Archaean and Proterozoic volcanic terrains studied, will be individually investigated in the following sections of this chapter.

8.2 EVIDENCE FROM THE BASIC ROCKS

8.2.1 General Discussion

Analyses of selected Proterozoic and Archaean basalts and their elemental ratios are listed in Tables 8.1 and 8.2 respectively. Comparison of the data for the primitive basalt from the Gawler Range province (K101) with the primitive basalt from the Welcome Well complex (W3) reveals striking similarities in the absolute contents of most major elements (e.g. Al_2O_3, $Fe_2O_3^t$, MgO, CaO and alkalis) and trace elements (particularly Zr, Nb, Y, V, Sc, Cr and Ni) and in the elemental ratios, compared with chondrites. These similarities are also seen in the more evolved rocks from the Proterozoic and Archaean terrains (compare columns A and B, Tables 8.1 and 8.2), thus adding support to the inferred compositional analogy. In addition, the chondrite-normalised Nb-Ce-Nd-Zr-Ti-Y-Yb plots (Fig. 8.1), show that the Archaean and Proterozoic rocks studied have distributions of similar shape, and notably, these differ quite markedly from other Archaean and Proterozoic basic volcanic rocks.

The elemental ratios of the Archaean and Proterozoic basalts studied can be resolved into those that are

1) less than chondritic - Sc/Ti, V/Ti;
2) approximately chondritic - Zr/Nb, Y/Ti;
3) greater than chondritic - Zr/Ti, Zr/Y and Ce/Zr (Table 8.2).

TABLE 8.2. Chondrite normalised values and elemental ratios for selected basic rocks plotted in Figure 8.1.

	Chondrite normalising factors	K101	A	W3	B	W150	C	BHVO-1	MORB	High-alumina basalt	D
Zr		102	141	111	117	82	61	170		126	62
ch.n	6.0	17	23.5	18.5	19.5	13.6	10.1	28	14	21	10.3
Nb		5.3	7.4	17.4	6.4	4.3	3.5	20		5.6	2.8
ch.n.	0.35	15.1	21	6.4	18.3	12.2	10	57	7.8	16	7.9
Y		19	26	23	21.6	31	26	28		25	25.6
ch.n.	2.2	8.6	11.8	10.5	9.8	14	11.8	12.7	15	11.4	11.6
Ti		3840	6120	6060	6120	8220	6900	16430		6600	3780
ch.n.	620	6.2	9.9	9.8	9.9	13.3	11.1	26.5	15	10.6	6.1
Ce		78	54	55	34	8	10	36.7		47	
ch.n.	0.813	96	66	68	42	9.8	12.3	45	9.2	58	
Nd		36	23	34	21	14		23			
ch.n.	0.597	60	38.5	57	36	23.5		39	10.5		
Yb			2.3	1.71	2						
ch.n.	0.208	9.5	11.06	8.2	9.6			9.1	14		
	Probable chondritic value										
$Zr/_{Ce}$	7.4-7.7	1.3	2.6	1.7	4.2	10	6.1	4.6		2.7	
$Zr/_{Y}$	2.5-2.8	5.4	5.4	4.8	5.6	2.65	2.4	6.1		5.0	2.4
$Ti/_{Zr}$	100-110	38	43	55	52	100	113	97		52	61
$Ti/_{Y}$	250-280	202	235	263	283	265	265	587		264	148
$Zr/_{Nb}$	16-18	19	19	18	18.4	19	17.4	8.5		22	22
$Ti/_{V}$	8.4-10	21	34	31	35	23	23.6	49			
$Ti/_{Sc}$	78-85	132	223	242	262	171	260	520		227	
TiO_2/P_2O_5	STP=10	3.6	4.4	2.7	5.1	9.8	8.8	10		5.2	

Notes: 1. Source of chondritic values and chondrite normalising factors given in Table 2.6.

2. Identification of samples as for Table 8.1, with the addition of:
MORB - average "typical" mid-ocean ridge basalt (data from Sun *et al.*, 1979).
High-alumina basalt - average, taken from Winchester and Floyd (1977). The data quoted is very comparable with that cited for high-alumina basalts by Taylor (1969); Jakes and White (1971), Pearce and Cann (1973) and Foden (1979).
D. - average primitive basalt from the Lower Proterozoic Halls Creek Group, Kimberley region, W.A. (data quoted with the permission of R. Allen and S. Hancock, 1980).

The non-chondritic elemental ratios of these rocks are unlikely to be fortuitous, particularly as other Precambrian basic igneous rocks that were formed roughly contemporaneously with the rocks studied, have chondritic values for many of these elemental ratios (Table 8.2). The important feature is not so much the absolute values of the ratios, but the consistently non-chondritic values shown by both the Archaean and Proterozoic rocks studied, which suggests that the primary magmas in both cases were generated from a similar source probably under analogous conditions.

8.2.2 Nature of the mantle source

The non-chondritic element ratios are considered to be significant and they should yield information concerning the nature of the mantle source. It has previously been argued that control by residual clinopyroxene can account for the levels of Sc and V in the primitive basalts (W3 and K101). It is possible that Ti and Y behaved essentially incompatibly during the magma segregation event, thus preserving the (?) chondritic Ti/Y mantle value in the melt. The greater than chondritic Zr/Ti and Zr/Y values imply that Zr was probably enriched in the mantle source prior to magma segregation. If this was the case then Zr and Nb must have been added to the mantle source in equal proportions in order to maintain the chondritic Zr/Nb value (assuming the source from which they were derived had chondritic Zr/Nb).

The alternative interpretation that Ti and Y were controlled during the magma segregation event (in addition to Sc and V), and that Zr and Nb behaved incompatibly, is not favoured, since it relies on the improbable assumption that Ti and Y were controlled in the correct proportions by the residual minerals (i.e., olivine, orthopyroxene and clinopyroxene) to yield a chondritic value for Ti/Y. This line of argument does not escape the necessity for control of Ti and Y (in proportions to yield chondritic Ti/Y) relative to Zr and Nb at some stage in the evolution of the "enriched" mantle. However, it is easier to envisage the necessary control on Ti and Y being produced by minor accessory phases (e.g. spinel, apatite, phlogopite, ilmenite, rutile and others) during an earlier stage of small-volume incipient melting rather than during the high-degree melting event associated with magma segregation.

The greater than chondritic Ce/Zr value, considered in the light of the uniformly chondritic value for Zr/Nb suggests that LREE (and probably P) were added to the mantle source in an enriching event quite independent of that for Zr and Nb. Had all of these elements been added at the same

time from an originally chondritic mantle source, it would be necessary to propose that Zr and Nb were controlled relative to Ce in the correct proportions to maintain a chondritic ratio, a situation which, as has been previously argued for the case of Ti and Y, is considered to be unlikely. The geochemical data can offer no evidence concerning the respective order in which Zr and Nb, and LREE, were enriched in the mantle source, nor the timing of the enrichment events with respect to magma segregation. However, the variability in the relative abundances of LREE in the basic volcanics (Table 8.1) and the relative variability in Zr/Ce (Table 8.2), suggests that the processes leading to LREE enrichment in the mantle source were rather more erratic than those for Zr and Nb.

The important conclusion arising from this discussion is that the elemental ratios of both the Archaean and Proterozoic basalts associated with the felsic volcanics studied, record complex processes of LIL element enrichment in their respective mantle sources prior to magma segregation. Some of the elemental ratios (e.g. Ti/Y, Ti/Sc and Ti/V) have, however, probably been inherited during the magma segregation event due to the control of Sc and V by residual clinopyroxene and the incompatible behaviour of Ti and Y.

8.2.3 Wider implications

The previous observations raise the important question of whether the Archaean and Proterozoic basic magmas were derived from the same LIL element-enriched zone of the upper mantle, that had developed at an earlier stage in earth history, and consequently had been in existence throughout the Proterozoic and possibly much of the Archaean. It is notable in this connection that Archaean calc-alkaline volcanic rocks from the Pilbara Block, with identical geochemical characteristics to those from the Yilgarn Block described in this thesis, have been recently documented by Barley (1980). This author records that the calc-alkaline volcanics occur in discrete centres that developed contemporaneously with adjacent piles of tholeiitic basalts. He further notes that while the tholeiitic basalts have flat REE patterns and approximately chondritic Zr/Ti and Zr/Y, the basalts associated with the calc-alkaline volcanics have fractionated, LREE-enriched REE patterns and greater than chondritic values for Zr/Ti and Zr/Y. The analogy in the features of the Archaean calc-alkaline volcanics assume particular significance when it is considered that the greenstone sequences in this part of the Pilbara Block are probably 800-900 m.y. older than those in the Yilgarn Block.

Figure 8.1 Chondrite-normalised Nb-Ce-Nd-Zr-Ti-Y-Yb plots for a selection of Archaean, Proterozoic and modern volcanic rocks. The sources of data for the various samples are summarized in Tables 8.1 and 8.2.

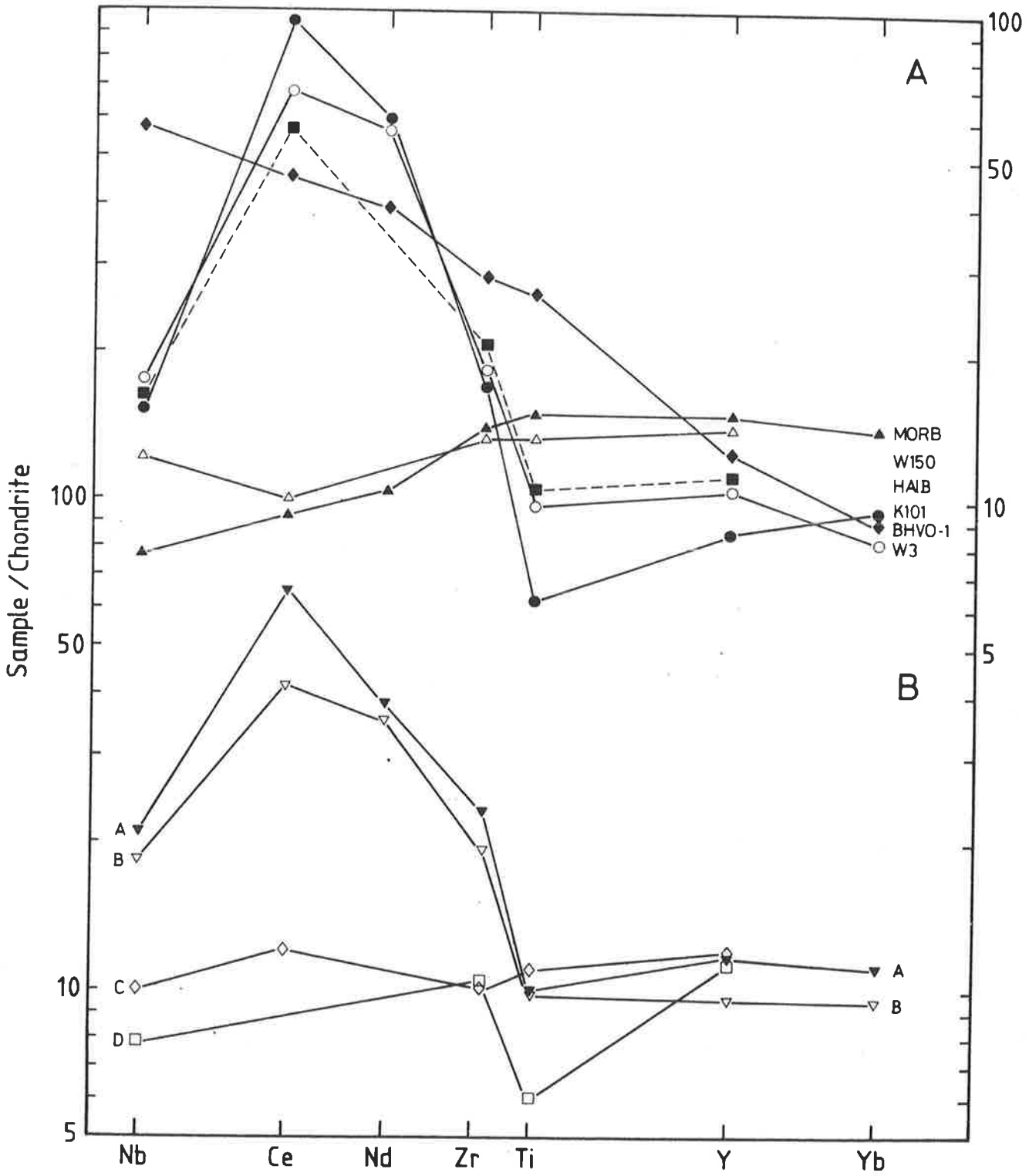

It is also notable that the Archaean and Proterozoic basalts appear to have modern analogues in island arc regions. For example, the high-alumina basalts commonly associated with the circumpacific calc-alkaline suites have comparable geochemical characteristics, demonstrated by the parallelism of the chondrite-normalised Nb-Ce-Nd-Zr-Ti-Y plots (Fig. 8.1, data after average of Winchester and Floyd, 1977 and supported by the data of Taylor, 1969; Jakes and White, 1971; Pearce and Cann, 1973; Foden, 1979). The high-alumina basalts show the near chondritic Ti/Y and Zr/Nb values and greater than chondritic Zr/Ti and Ce/Zr values characteristic of the Archaean and Proterozoic basalts studied, and also possess similar absolute abundances of these elements. This elemental distribution contrasts with that of basalts from ocean islands which are relatively enriched in Nb and have near chondritic Zr/Ti values (see BHVO-1, Kilauea tholeiite, Fig. 8.1, data after Sun, et al., 1979). It also contrasts with mid-ocean ridge basalts, in which LREE are typically relatively depleted and Nb more so.

The high-alumina basalts are unlikely to be derived from the same mantle source as either the ocean island basalts or mid-ocean ridge basalts owing to their distinct and consistent geochemical differences. Following a similar line of reasoning, it could be argued that the high-alumina basalts were derived from a comparable source to the Archaean and Proterozoic LIL element-enriched basalts, owing to their analogous geochemical characteristics. One possibility is that the LIL element-enriched mantle source developed early in the earth's history and was subsequently tapped at various stages to yield primary magmas of similar LIL element-enriched character (e.g. at 3.5 b.y. in the Pilbara Block, at 2.6 b.y. in the Yilgarn Block, at 1.5 b.y. in the Gawler Range province, at 1.1 b.y. in the Central Australian province and during the Tertiary in plate converging regions). Alternatively it could be proposed that the required LIL element-enriched mantle source was "prepared" immediately prior to, or during, each of the magma segregation events, thus excluding the necessity for a long term LIL element-enriched mantle source.

The data presented in this thesis does not permit distinction between these alternatives, however several important qualitative observations can be made. Firstly, if the magma generation occurred as a "one-off" event in each case, then it is difficult to envisage how rocks of analogous geochemical character could have developed through time, given the contrasting tectonic environments during formation. This objection can be negated however, if it is postulated that a LIL element-enriched zone of the upper mantle developed early in the earth's history and remained static in

subcontinental regions throughout time. Secondly, there is evidence that the LIL element-enriched primary basic magmas under consideration, in all cases segregated from relatively shallow levels in the uppermost zone of the mantle (this comment also applies to the parental magmas for the hypersthene and quartz-normative basalts in island arc environments, Green, 1973, 1976). The correspondence between the particular geochemical characteristics of these rocks and their shallow source would appear to be coincidental if the primary magmas were derived by a "one-off" process in each case. On the other hand the relationship would be predicted if indeed the uppermost mantle preserved the record of an early LIL element enrichment event. Finally, it is noted that many modern calc-alkaline volcanics have developed over essentially continental mantle, although sialic continental crust may not always be present. In these cases the subduction zones effectively separate the continental mantle from the presumably convecting oceanic mantle. It follows that if a long term enriched zone of the upper mantle does exist, then it might be expected to occur beneath island arcs that have developed on continental mantle. This prediction appears to be supported by recent isotopic data which suggests that the upper mantle in such regions has possessed its LREE enriched character for a considerable period of time (Hawkesworth, et al., 1979). These comments would not apply, however, to island arcs which have developed on oceanic mantle and the available isotopic data appears to reflect this distinction (e.g. De Paolo and Johnson, 1979, on the New Britain island arc).

While the qualitative arguments presented above would appear to support the proposition of a long term LIL element-enriched upper mantle, it is apparent that the available evidence is insufficiently strong to exclude other possibilities and clearly comprehensive isotopic data would be required before any particular hypothesis could be regarded as acceptable. Regardless of which model of LIL element enrichment in the mantle is favoured, it is evident that some mechanism is needed to trigger and promote melting in the upper mantle and possible causes will be briefly discussed below.

8.2.4 Possible mechanisms of origin

Two mechanisms that are commonly proposed to account for melting in the mantle are: 1) diapirism, involving the movement of hot mantle material to shallow levels with a resultant increase in the geothermal gradient (Green, 1975) and 2) movement of water with resultant lowering of the mantle solidus where significant amounts accumulate (Wyllie, 1971).

It has previously been pointed out that the latter alternative could account for the rather sporadic and localised occurrence of the Archaean calc-alkaline centres, each having developed above a localised zone of melting in the upper mantle caused by the introduction of water, perhaps along a fracture. It is more difficult to envisage this as a satisfactory explanation for the episodes of magma generation in the Proterozoic, since the Lower Proterozoic tectonothermal events and the subsequent igneous activity in the post-orogenic era appear to require a zone of high heat flow over an extended period. This would seem more consistent with some form of mantle upwelling or diapirism, which maintained a significant heat input for a long period of time. This conclusion is supported by the great volumes and the non-eutectic character of the acid magmas generated in the Middle Proterozoic, both of which necessitate an external heat input. Also, in view of the subcontinental setting it is difficult to envisage the introduction of water alone, without some heat input, as the cause of melting of the upper mantle.

While diapirism may account for the situation in the Proterozoic, it is faced with problems when applied to the Archaean. For example, if the primary magmas originated in a rising diapir, it would be necessary to propose that each of the Archaean calc-alkaline volcanic centres developed over its own diapir. It is doubtful whether the concept of numerous small diapirs rising through the mantle is realistic, particularly when the products generated in each case are geochemically analogous. Also, it seems unlikely that such diapirism on a very much larger scale in the Proterozoic would have yielded magmas of identical geochemical character.

The previous arguments against a general model involving diapirism could be negated by proposing that diapirism provided not the magmas, but rather the necessary heat for melting of the uppermost mantle and in this sense acted as a "hot spot" (c.f. Goodwin, 1973). The difference in scale of the magmatism and the differing tectonic regimes between the Archaean and Proterozoic could be explained in terms of the magnitude of the diapir and/or the longevity of heat input from it. Presumably, in the Proterozoic the diapirs would have been much larger and their period of influence much longer than in the Archaean, but because they affected the same LIL element-enriched zone of the upper mantle, the primary basic magmas generated in both cases were analogous. It is conceivable that the lithosphere (including the LIL element-enriched upper mantle) could have migrated relative to the mantle diapir or "hot spot" with melting taking place wherever a significant stand-still occurred. Such a mechanism has

been proposed by Wynne Edwards (1976) to explain his "aligned trains of plutonic complexes" in the Proterozoic of the Grenville province and by Wellman and McDougall (1974) to account for the distribution of Tertiary igneous centres in eastern Australia. This model could offer an explanation for the "string of beads" distribution of the Archaean calc-alkaline volcanic centres in the northern Norseman-Wiluna greenstone belt (Hallberg, pers. comm., 1980) and it may also explain why these rocks were generated and erupted quite independently of the often contemporaneous tholeiitic and komatiitic volcanics (see chapter 7).

8.2.5 Summary

In summary, the available geochemical evidence favours the interpretation that the primary magmas for the Archaean calc-alkaline suites, basalts of the post-orogenic, bimodal Proterozoic suites and high-alumina basalts of modern circumpacific calc-alkaline suites were derived from analogous, LIL element-enriched mantle sources at relatively shallow depths. It could be speculated that all were derived from the same zone of the uppermost mantle that gained its LIL element enriched character very early in the earth's history and has maintained its character in subcontinental regions to the present day. However, there is no compelling evidence for this view excepting the observed analogy in the trace element character of basalts erupted over a considerable period of time and testing will have to await the accumulation of detailed isotopic data. A similar line of reasoning favours the view that the Proterozoic and Archaean basic magmas were not generated from random mantle diapirs in "one-off" episodes, since it is unlikely that such processes could have duplicated their analogous geochemical characteristics. The most plausible explanation in the light of the available evidence appears to be that both the Archaean and Proterozoic basic magmas were generated from the same region of the mantle in response to the introduction of heat from mantle diapir(s) at depth. The diapirs themselves probably contributed no magmas to the Archaean and Proterozoic volcanic terrains studied.

8.3 EVIDENCE FROM THE INTERMEDIATE ROCKS

It has been previously pointed out that the paucity of calc-alkaline andesites in the post-orogenic Middle Proterozoic volcano-plutonic terrains is a real feature which appears to be characteristic of these terrains. True calc-alkaline suites containing an abundance of low-silica andesites are also rare in the Lower Proterozoic record and to the writer's knowledge are completely lacking in terrains of this age in Australia, although

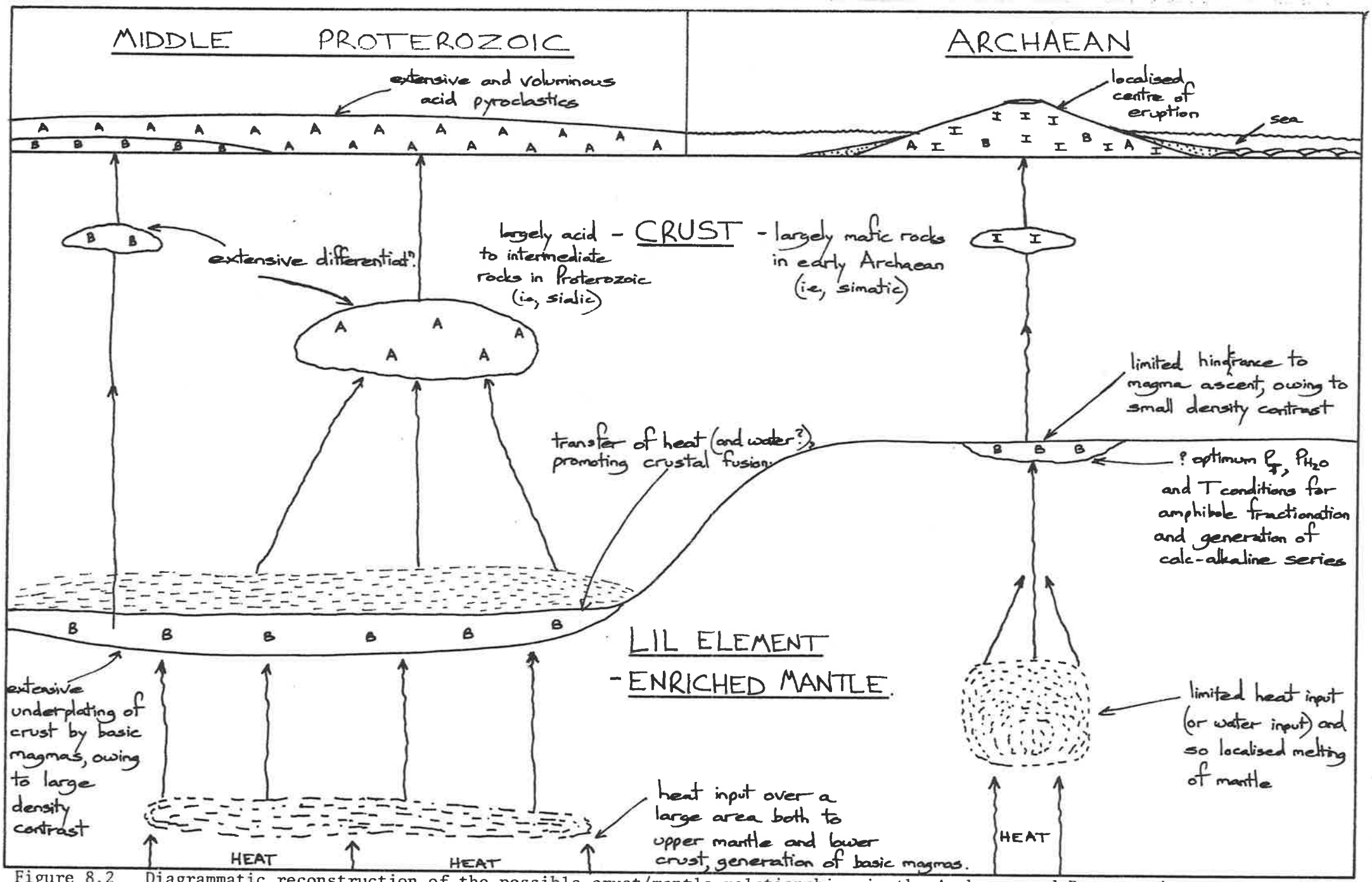

Figure 8.2 Diagrammatic reconstruction of the possible crust/mantle relationships in the Archaean and Proterozoic.

Reid (1977) has documented an example from Southern Africa. These observations appear to present a major contradiction to the previous conclusions concerning the origins of the associated LIL element-enriched basalts. For example, if the basalts were derived from the same source and under the same conditions in the Proterozoic and Archaean, why in the latter case did typical andesite-bearing, calc-alkaline differentiation suites develop whereas in the other case they apparently did not?

A major contributing factor may have been the relative thickness and composition of the crust in the Middle Proterozoic compared with that in the Archaean. Most workers consider that the geothermal gradient decreased during the Precambrian, and an inevitable consequence of this is an increase in the maximum permissable thickness of the crust, assuming that crustal thickness is limited by melting reactions at depth (Hargraves, 1976). At the same time the continuous conversion of simatic to sialic crust in the Archaean (Glikson and Lambert, 1976), culminating with the major episode of crustal reworking at the end of this era (evidenced by the abundant 2.6 b.y. granitoid plutons in the Yilgarn Block), would have greatly added to the volume of sialic rocks in the crust. The end result would have been the production of a relatively thick, bouyant crust that would have effectively "floated" on any ascending basic magmas.

The effect of this would have been to inhibit the ascent of basic magmas, so that during the Proterozoic it is possible that much of the basic magma generated was entrapped either within or at the base of the crust. Fyfe (1978) has suggested the possibility of extensive underplating of the sialic crust by basic magmas and has recognised that the entrapped magmas would have contributed heat for crustal fusion in the immediately adjacent lower crust. This situation probably differed from that in the early Archaean, where the density contrast between the basic magmas and the dominantly simatic crust would have been minimal and so little underplating would be expected (see Fig. 8.2).

Two other factors could also have contributed to the paucity of andesites by either directly or indirectly affecting the crystallisation histories of the primary basic magmas. For example, the depth at which the magmas were entrapped during the Proterozoic may not have been optimum for the stability of amphibole relative to other minerals and thus the calc-alkaline trend towards silica enrichment, normally produced by fractionation of low-silica amphibole (Cawthorn and O'Hara, 1976), did not result. The possibility also exists that the basic magma, while entrapped near the base of the crust, may have lost much of its volatile

TABLE 8.3. Compositions of high-K_2O Archaean granitoid rocks from the Eastern Goldfields Province, Yilgarn Block, compared with typical post-orogenic Proterozoic rhyolites.

	1	2	3	4	5	6	7	8
SiO_2	70.29	70.44	72.57	72.88	72.57	73.15	74.00	72.81
Al_2O_3	15.67	15.07	14.11	14.44	14.96	14.29	13.31	12.46
Fe_2O_3 t	2.12	2.65	2.17	2.03	2.01	1.89	2.49	4.13
MnO	0.04	0.05	0.02	0.04	0.04	0.03	0.05	0.09
MgO	0.82	1.13	0.46	0.40	0.0	0.44	0.75	0.20
CaO	2.41	2.85	1.01	1.27	1.28	1.65	0.28	0.84
Na_2O	5.22	4.41	3.92	4.07	3.75	4.10	2.71	3.53
K_2O	2.87	3.19	5.20	4.95	5.26	4.10	6.30	5.81
TiO_2	0.35	0.32	0.64	0.26	0.27	0.24	0.35	0.33
P_2O_5	0.15	0.11	0.08	0.12	0.11	0.08	0.03	0.06
Total	99.94	100.20	100.18	100.46	100.25		100.24	100.25
LOI	0.71	0.69	0.70	0.85			1.04	0.54
Zr	122	109	119	260	225		413	837
Nb	3.8	5					22	97
Y	4.4	7					48	156
Sc	2.6	4.7					8	5
Cr	7	14						
Ni	10	14						
Rb	72	85	220	255	210		198	230
Sr	949	521	285	250	225		38	51
Ba	843	1460	1460	900	1200		940	1270
Ce							125	297

1. Typical sample of the megacrystic adamellite body that intrudes and truncates the Welcome Well complex in the north and northeast (collected by Foden, Hallberg and Giles, 1979).
2. Typical sample of the granodiorite pluton in the vicinity of Smith Well, Edjudina 1:250,000 sheet area (collected by Foden, Hallberg and Giles, 1979).
3. Average composition of Mt. Boreas Adamellite, Duketon and Laverton 1:250,000 sheet areas (after Bunting and Chin, 1975).
4,5. Coarse- and medium-grained adamellite respectively, from the Sir Samuel 1:250,000 Sheet areas (after Bunting and Williams, 1976).
6. Average composition of 85 post-kinematic granitoids from the southern part of the Eastern Goldfields Province (after Archibald, et al., 1978).
7. Typical rhyolite from the Gawler Range Volcanics (E607, chapter 2).
8. Typical rhyolite from the Bentley Supergroup (B63, chapter 3).

content to the relatively dry granulites in close proximity. The resultant, lowered PH_2O in the basic magma might have inhibited amphibole fractionation relative to other minerals (Yoder and Tilley, 1962). If water did migrate into the granulites, then it is possible that this could have promoted anatexis, particularly in view of the heat source provided by the adjacent basic magmas.

It is further noted that the large area covered by the post-orogenic Proterozoic volcano-plutonic terrains and the great volumes of magma generated, may have been caused not only by the magnitude of the diapirs at this time, but also by underplating of extensive areas of the crust by basic magmas.

8.4 EVIDENCE FROM THE ACID ROCKS

It has been earlier noted that the Proterozoic felsic volcanics studied share few characteristics in common with the mantle-derived Archaean felsic volcanics, but that they can be compared with the voluminous, anatectic, K_2O-rich Archaean granitoids. Although the granitoids are widespread, there is a paucity of comprehensive geochemical data concerning them. What data is available suggests that they have comparable levels of K_2O, Rb, Ba and LREE to the Proterozoic acid volcanics, but generally lower contents of Zr, Nb, Y, HREE, $Fe_2O_3^t$ and TiO_2 (Table 8.3).

Condie (1980), on the basis of a detailed study of the geochemistry of a number of K_2O-rich Archaean granite batholiths, considered that they represented near minimum melts at low water pressure. He noted that they could be melts of either a high-K andesitic source or a tonalite-trondhjemite source, developed by intrusion and metamorphism of diorite and/or tonalite-trondhjemite plutons in the lower crust. This origin differs from that proposed in this thesis for the post-orogenic Proterozoic acid magmas in two important respects. Firstly, it has been argued that the primary magmas for the Proterozoic suites were not simple eutectic melts, but rather were high temperature liquids of dacite to high-silica andesite composition. Secondly, the modelling calculations reported in chapters 2 and 3 indicate a low-silica source (basic to low-silica intermediate composition), of a refractory, sialic nature. The higher levels of Zr, Nb, Y, HREE, $Fe_2O_3^t$ and TiO_2 in the Proterozoic rocks are probably a direct result of these differences.

In view of the extent of the Middle Proterozoic volcano-plutonic terrains and the great volumes of acid igneous rocks comprising them, it is evident that the source from which the magmas were generated also must

have been very extensive. This raises the important question of how such a relatively basic, refractory sialic crustal source developed in the volumes required. It is notable that Condie (1980) considers the residue left after partial melting of the high-K andesitic source to be similar in composition to the low-K pyroxene gneisses of Archaean terrains. Such a residue would fulfil the compositional requirements for the source of the post-orogenic Proterozoic magmas. Thus, it is possible that the residue remaining after generation of the low temperature acid magmas which gave rise to the high-K Archaean granitoids, provided the source for the high temperature, post-orogenic Proterozoic acid magmas.

This proposal appears to have some merit, particuarly when it is considered that the post-orogenic Proterozoic volcano-plutonic provinces developed on thick, stable continental crust and in many cases are demonstrably underlain by Archaean rocks or their reworked remnants. There seems little doubt that the huge volume of K_2O-rich Archaean granitoids generated during the Archaean would have left an equally large volume of refractory residue and since this residue would be located in the lower crust, it would be expected to melt first in response to the introduction of heat from the mantle. The possibility that higher levels of the crust melted during the Proterozoic is not excluded, however evidence for this in the two Proterozoic terrains studied is lacking. Moreover it is difficult to envisage large-scale reworking of the upper crust due to mantle heat input (i.e., excluding burial metamorphic effects), without involving the lower crust which would be closest to the heat source.

The earliest sialic crust (i.e. the high-K andesite and tonalite-trondhjemite sources of Condie, 1980) could have developed by differentiation of mantle-derived parental magmas and/or by partial melting of simatic crust. The former alternative involving differentiation has been demonstrated for the Archaean calc-alkaline volcanic suites studied in this thesis. That this process occurred in the earliest Archaean is shown by the analogous calc-alkaline volcanics in the 3.5 b.y. old greenstone sequence of the Pilbara Block (Barley, 1980). The latter process, involving partial melting of a basic crustal source, or the "sima to sial" transition as it has been referred to by Glikson and Lambert (1976) has been advocated by many workers to explain the origin of sodic acid rocks (Arth and Hanson, 1972; Cooper, et al., 1978; Glikson, 1979b; Collerson and Fryer, 1979; Stolz, 1980; Foden, et al., in prep.).

In summary, it is apparent that the Archaean and Proterozoic acid rocks are useful in providing an insight into the processes of Precambrian sialic crustal development. It seems valid to conclude that the earliest acid rocks that could form by conventional means (without resorting to unknown, hypothetical processes), were tonalitic-trondhjemitic rocks generated by partial melting of pre-existing basic (simatic) crust and calc-alkaline differentiates of mantle-derived magmas. The development of these rocks would have been limited only by the thickness of the early simatic crust and by the prevailing geothermal gradient, and once formed, they provided the basis for reworking later in the Archaean to generate the K_2O-rich granitoids and subsequent reworking at higher temperatures in the Proterozoic to yield the post-orogenic volcanics. These general trends of acid magmatism, while they may be diachronous from place to place on a restricted time scale, can be substantiated for the Precambrian as a whole.

8.5 MODERN ANALOGUES

In any study of ancient igneous rocks it is useful to look for modern analogues in the hope that if they exist, they will shed light on the environment of formation of the ancient rocks. The search for analogues relies on the empirical observation that certain types of igneous rocks are found in specific tectonic environments in the modern crust. The assumption is commonly made that ancient and modern volcanic rocks with similar geochemistry were formed in similar tectonic settings (e.g. Pearce and Cann, 1973; Pearce, 1976; Pearce, et al., 1978). This assumption may not always be valid however, since the geochemistry of a given rock suite can only yield information on the way in which the primary magmas formed and subsequently behaved; it gives no information on the large scale tectonic processes which operated to create the correct conditions of formation. It is conceivable that the same essential conditions of magma formation could have been created by more than one tectonic process. This is illustrated in modern terrains by two examples:

1) The ocean island tholeiites and continental tholeiites. Both have very similar geochemistry, yet are erupted in quite different tectonic environments.
2) The undersaturated alkaline volcanics which are found in continental rift zones (e.g. Berberi, et al., 1975 - on the East African rift system) and also in island arcs (Smith, et al., 1977).

It is also possible that a variety of magmas could be generated within the one tectonic environment. Again this appears to be demonstrated by modern terrains, where, within island arcs for example, it is not uncommon to find a spectrum of volcanics ranging from "normal" calc-alkaline through high-K calc-alkaline to undersaturated alkaline types (e.g. Taylor, 1969; Ewart, et al., 1977; Foden, 1979). Consequently it is possible to have igenous rock suites that are tectonic analogues but not strict geochemical analogues and vice versa. In order to show that ancient and modern rock suites are completely analogous it is necessary to show that they have both similar geochemistry and tectonic settings. The latter is not directly observable in ancient terrains as it is in modern terrains, and thus the field relationships and regional geological setting are of importance in evaluating this aspect. With these general comments in mind, modern analogues are sought for Archaean calc-alkaline volcanics and Proterozoic post-orogenic volcanics.

A. Possible modern analogues of the Archaean calc-alkaline volcanics

Many workers have noted the marked geochemical analogy between Archaean calc-alkaline volcanics and their modern counterparts found in destructive plate margin regions (e.g. Condie, 1976) and in this regard the Archaean calc-alkaline volcanics from the Yilgarn Block are no exception (e.g. Hallberg, et al., 1976a, b; this thesis).

The precise tectonic environment in which the Archaean calc-alkaline volcanics were erupted is a matter for considerable speculation (e.g. review by Windley, 1977). It is "orogenic" in the sense that the calc-alkaline volcanics were erupted with other rocks of the greenstone succession and were deformed together. Several features of the Archaean calc-alkaline volcanics indicate that they were unlikely to have formed above a subduction zone:

1) their confinement to discrete centres rather than arcs (see section 7.2 and 7.3);
2) association with komatiitic lavas, banded-iron formations and high-grade gneisses, none of which are found in modern calc-alkaline volcanic arcs;
3) absence of thick flysch sequences, ophiolite complexes and glaucophane-schists which, among other rock types, are commonly associated with modern calc-alkaline volcanic arcs.

The inference from this is that modern plate tectonics, in an unmodified form, was not directly responsible for the orogenesis nor the generation of the Archaean calc-alkaline magmas. It could be argued that these

features simply indicate a thinner lithosphere and higher geothermal gradient in the Archaean, and that subduction was still a viable process. If this was the case, then it is puzzling why the Archaean and modern calc-alkaline volcanics should be compositionally similar, when the other rock types contrast so markedly.

In view of the above observations, it is considered that the Archaean calc-alkaline volcanics represent a case where modern geochemical analogues can be found, but true tectonic analogues are lacking. Thus it appears that the conditions of calc-alkaline magma genesis have been duplicated in the Archaean and Cainozoic eras by quite different tectonic processes (see section 7.3, chapter 7). Consequently it is concluded that modern calc-alkaline volcanic terrains, analogous in all respects to the Archaean examples, probably do not exist.

B. Possible modern analogues of the Proterozoic post-orogenic volcanics.

The tectonic setting of the two Proterozoic volcano-plutonic provinces examined in detail in this thesis, is better known than that for the Archaean calc-alkaline volcanics: both provinces are post-orogenic, having developed after a major Lower Proterozoic tectonothermal event. Consequently the unmetamorphosed and little-deformed volcanics are observed to rest unconformably on relatively high-grade metamorphic rocks comprising the Lower Proterozoic terrains. In both cases the volcanic pile is comprised of vast, subaerial acid ignimbrite sheets and more restricted acid and basic lavas.

In the case of the Gawler Range volcano-plutonic province it is tempting to suggest that the Cainozoic ignimbrite provinces of southwestern U.S.A. or the Andean mountain chain, are modern analogues. However, when the Cainozoic provinces are examined in detail, it is evident that the analogy does not extend beyond the common, vast ignimbrite sheets. The Cainozoic acid ignimbrites of the Americas are in close association with equally voluminous calc-alkaline andesites which form large stratovolcanoes (Lipman, et al., 1972; Francis and Rundle, 1976). Such an association is not observed in the Proterozoic provinces, which are characteristically bimodal. Furthermore there is mounting geochemical and isotopic evidence in support of the contention that many of the rhyolitic ignimbrites are differentiates of the calc-alkaline andesites and that the primary magmas are mantle derived (e.g. Thorpe, et al., 1979). This origin contrasts with the crustal source proposed for the Proterozoic acid magmas. It is probable that the distinctions arise from magma generation in response

to fundamentally different tectonic processes. In the case of the Cainozoic volcanics a subduction-related mechanism is favoured by most workers (e.g. Lipman, et al., 1972).

The late-to post-orogenic acid volcanic complexes of the Tasman Province in eastern Australia offer what may be a Palaeozoic tectonic analogue. They occur from northern Queensland (e.g. Georgetown Inlier, Branch, 1966; Sheraton and Labonne, 1978) through New South Wales (e.g. New England region, Flood, et al., 1970) to Central Victoria (McLaughlin, 1976; Birch, et al., 1978). The majority of the acid volcanics are little-deformed dacitic to rhyolitic ignimbrites, often restricted to well-defined cauldron subsidence structures.

In general, for a given SiO_2 content, the Paleozoic acid volcanics are lower in K_2O, Ba, Zr, Y and REE than the Proterozoic volcanics. Sheraton and Labonne (1978) actually state that the Proterozoic acid igneous rocks from the Georgetown Inlier (i.e., Croydon Volcanics and Esmeralda Granite, see section 4.4) are higher in K_2O, Zr, Y and Ce than their Paleozoic counterparts from the same region. They also observe that the Paleozoic acid igneous rocks are lower in FeO^t and FeO^t/MgO, however this does not apply to all of the post-orogenic volcanics in the Tasman Province since the Lake Mountain Rhyodacite and Toombullup Rhyodacite from the Central Victorian region (Birch, 1975) do have comparable $Fe_2O_3^t$ and TiO_2 contents to the Proterozoic acid volcanics. In the latter case the K_2O and Zr contents of the rhyodacites are lower (Zr only marginally lower in Toombullup Rhyodacite) than the Proterozoic acid volcanics. It is generally postulated that the primary magmas were derived by partial melting of Paleozoic metasediments or basic igneous rocks, although Birch (1975) and Sheraton and Labonne (1978) do not appear to exclude the possibility of a Precambrian granulitic source. The presence of relatively minor proportions of basalt and/or andesite in some of the volcanic piles, together with the need for a high temperature heat input has prompted some workers to postulate that intermediate and/or basic magmas intruded into the lower crust, may have promoted anatexis (Birch, 1975; Sheraton and Labonne, 1978). The latter workers tentatively infer that subduction-related processes may have been responsible for the generation of the basic and intermediate magmas.

It is evident that no simple picture emerges for the Tasman Province post-orogenic volcanics in terms of their geochemistry, precise origins (whether S, I or Precambrian granulite sources) and relationship to plate tectonics. However it is clear that they are tectonic analogues of the

post-orogenic Proterozoic acid volcanics and if geochemical analogues of the latter do exist, it is believed that they will most likely be found in the Paleozoic post-orogenic volcanic complexes. The interesting possibility is raised that the geochemical characteristics of the Proterozoic rocks could be used to search for Paleozoic acid volcanics which originated from a Precambrian granulitic source (if they exist) as distinct from the previously recognised S and I type sources (c.f. Chappell and White, 1974).

In conclusion, it can be said that the Proterozoic post-orogenic provinces do have tectonic analogues in the Paleozoic, however whether they have geochemical analogues with similar origins is uncertain; if geochemical analogues do exist they are probably uncommon. To the writer's knowledge strict geochemical analogues have not been documented from any Cainozoic or modern terrains.

8.6 CONCLUDING DISCUSSION

In the previous sections several conclusions have been drawn which have important implications for hypothesis concerning the development of the Precambrian crust and mantle:

1) Basalts of similar geochemical character, derived by shallow, hydrous melting of an analogous LIL element-enriched mantle source were generated in the Archaean and the Proterozoic.
2) Andesites, forming part of a calc-alkaline magma series, are notably absent in the post-orogenic, Middle Proterozoic volcano-plutonic terrains and are scarce in the Proterozoic as a whole.
3) Crustal reworking and generation of acid magmas occurred on a large scale both in the Archaean and the Proterozoic.

While any interpretations that are placed on these observations are speculative, it is nevertheless useful to summarize the most probable sequence of events and this is attempted below.

The model most consistent with all of the data presented in this thesis appears to be one in which the subcontinental mantle developed a LIL element-enriched zone very early in the earth's history, from which basic magmas have been tapped ever since. These magmas had a distinctive geochemical signature imparted from the source and this is recognisable in the elemental ratios of the basalts they yielded. It seems most likely that mantle diapirism provided the heat for melting of the upper mantle in both the Archaean and the Proterozoic, although the scale of diapirism probably differed.

Figure 8.3 The sequence of Precambrian crustal evolution as deduced from the Archaean and Proterozoic felsic igneous rock record.

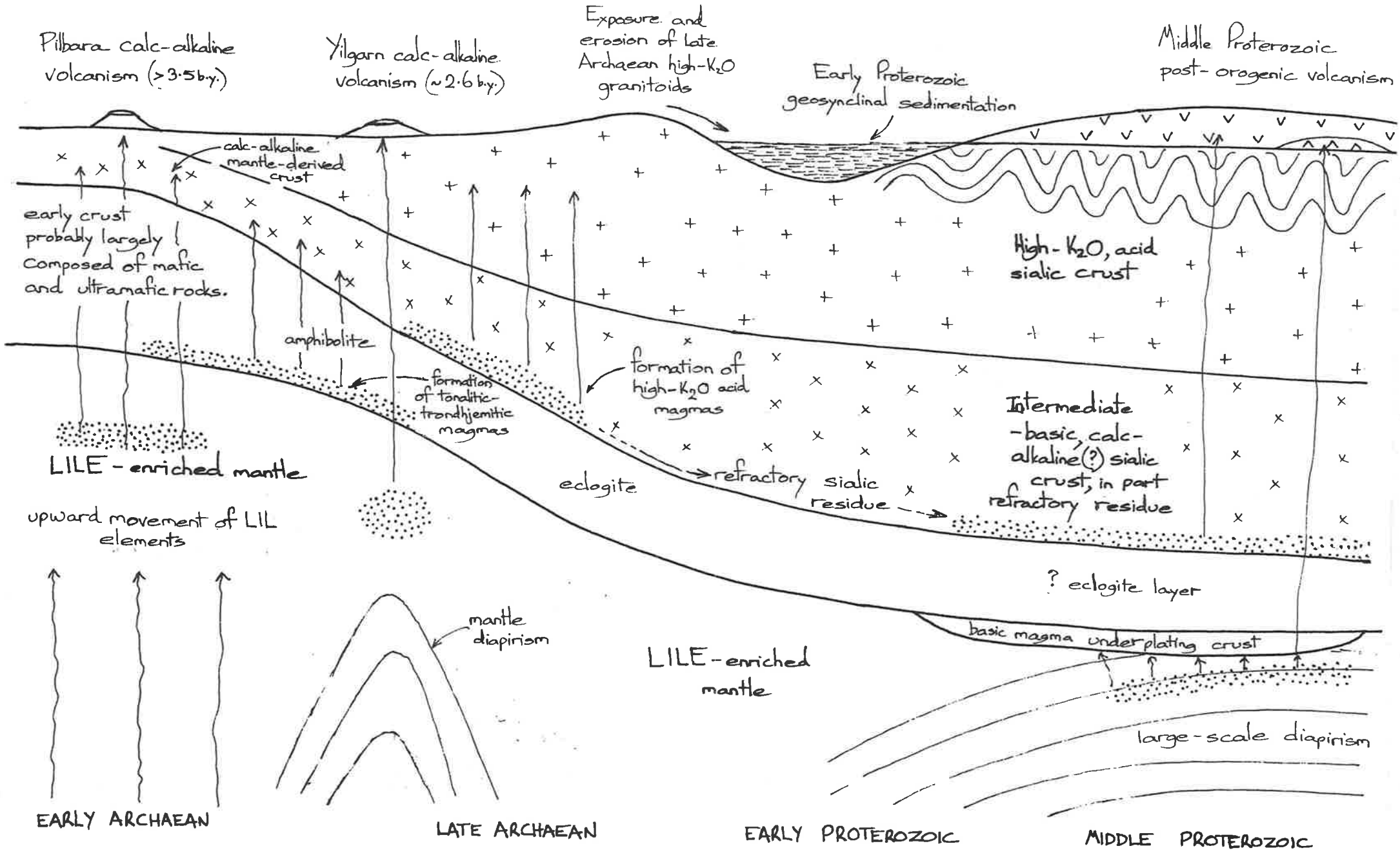

The crust, by contrast, appears to have evolved over a considerable period of time on geochemical grounds. The first development of sialic crust may have been a result of melting of a simatic precursor at a depth determined by the prevailing geothermal gradient. Alternatively, the early sialic crust may have been composed of calc-alkaline intermediate and acid rocks that differentiated from mantle-derived basic melts. The sialic crust, once formed, was reworked at various times, notably in a major episode at the close of the Archaean era (2.6 b.y.) which culminated in the development of huge volumes of relatively K_2O-rich granitoid batholiths. No doubt erosion of this relatively newly-formed terrain contributed much of the detritus for the early Proterozoic geosynclines, now represented in many cases by highly-deformed mobile belts. The apparent "sudden" increase in K_2O in early Proterozoic sediments compared with Archaean sediments (Glikson, 1977) could have been related to uplift and erosion of the recently formed K_2O-rich igneous rocks (McLennan, et al., 1979).

The post-orogenic Middle Proterozoic era heralded another major episode of crustal reworking, this time possibly involving the sialic residue left after the Archaean acid magma extraction events. Melting probably took place in the lower crust at relatively high temperatures and yielded non-eutectic magmas enriched in elements normally held in refractory minerals (e.g. Zr, Nb, Y, REE, P, Ti and Fe). The post-orogenic magma generation episodes coincided with cratonisation of the crust, and in many cases these areas have remained as stable crustal blocks to the present day. Mantle diapirism again is considered to have provided the source of heat, although in the Middle Proterozoic, owing to the greatly thickened and relatively bouyant sialic crust, much of the basic magma generated may have underplated the crust and so further promoted anatexis.

The general sequence of events outlined above is summarized diagrammatically in Figure 8.3, and if the events depicted are correct, then it is evident that the igneous rock record in the Precambrian can be explained in terms of a continually evolving earth system, without recourse to gaps in the record or cataclysmic events. The apparent absence of complete modern analogues for the Archaean calc-alkaline volcanics and the Proterozoic post-orogenic acid volcanics reinforces the view that the precise manner in which acid igneous rocks developed, has varied with time in response to an evolving crust. The latter observation indicates that direct application of concepts developed from the study of modern terrains in an unmodified form to explain the origin of ancient igneous rocks, may not be justified.

Rutland (1973) has recognised that while the same thermal driving forces may have existed within the mantle for much of the earth's history, the surface expressions may be quite different through time, owing to changes in the heat flow and crustal thickness. For example, Rutland (1973) has developed the concept of intra-continental orogeny, as opposed to inter-continental or collision orogeny, as a possible explanation for the Lower Proterozoic orogenic belts, a view shared by Kroner (1977). Such an approach seems most compatible with the sequence of igneous rock development observed in the Precambrian. It seems logical for example, to propose that the bimodal magmatism characteristic of the Proterozoic period, was the result of large scale perturbation in the mantle (in this case probably diapirism), of a similar type to that which provided the driving force for the generation of the Archaean calc-alkaline magmas. The differing proportions of rock types and their environments of eruption could relate to the scale of diapirism, which in turn may be related to convective overturn and hence heat flow, and also to the composition and thickness of the crust. In the light of this it does not seem surprising that the igneous rock record preserved in the Precambrian terrains offers few analogies in detail with more modern terrains.

To further investigate some of the points raised above, there is a need for integrated and detailed field, petrographic, geochemical and particularly isotopic studies of ancient felsic volcanic rock suites. The interpretations need to be unclouded by preconceptions arising from the study of modern volcanic terrains. It will be such studies that will permit testing and refinement of the conclusions and some of the more speculative inferences drawn in this thesis. As knowledge of Precambrian felsic volcanism grows, so too will understanding of crustal development during this large interval of earth history.

REFERENCES

ANDERSON, A.T., 1976. Magma mixing : petrological process and volcanological tool. J. Volcanol. Geotherm. Res., 1, 3-33.

ANDERSON, A.T. and GOTTFRIED, D., 1971. Contrasting behaviour of P, Ti, and Nb in a differentiated high-alumina olivine tholeiite and a calc-alkaline andesitic suite. Bull. geol. Soc. Am., 82, 1929-1942.

ANDERSON, J.L. and CULLERS, R.L., 1978. Geochemistry and evolution of the Wolf River Batholith, a late Precambrian rapakivi massif in North Wisconsin, U.S.A. Precambrian Res., 7, 287-324.

ARCHIBALD, N.J., BETTENAY, L.F., BINNS, R.A., GROVES, D.I. and GUNTHORPE, R.J., 1978. The evolution of Archaean greenstone terrains, Eastern Goldfields Province, Western Australia. Precambrian Res., 6, 103-131.

ARTH, J.G., 1976. Behaviour of trace elements during magmatic processes - a summary of theoretical models and their applications. Jour. Research, U.S. Geol. Survey, 4, 41-47.

ARTH, J.G. and BARKER, F., 1976. Rare-earth partitioning between hornblende and dacitic liquid and implications for the genesis of trondhjemitic-tonalitic magmas. Geology, 4, 534-536.

ARTH, J.G. and HANSON, G.N., 1972. Quartz diorites derived by partial melting of eclogite or amphibolite at mantle depths. Contrib. Mineral. Petrol., 37, 161-174.

ARTH, J.G. and HANSON, G.N., 1975. Geochemistry and origin of the early Precambrian crust of northeastern Minnesota. Geochim. cosmochim. Acta, 39, 325-362.

BALLANCE, P.F., 1976. Evolution of the Upper Cenozoic magmatic arc and plate boundary in northern New Zealand. Earth Planet. Sci. Lett., 28, 356-370.

BARAGAR, W.R.A. and GOODWIN, A.M., 1969. Andesites and Archean volcanism of the Canadian Shield. In, McBirney, A.R. (Ed.). Proceedings of the andesite conference. Bull. Oregon Dept. Mineral Ind., 65, 121-142.

BARKER, F. and ARTH, J.G., 1976. Generation of trondhjemitic-tonalitic liquids and Archean bimodal trondhjemite-basalt suites. Geology, 4, 596-600.

BARKER, F., WONES, D.R., SHARP, W.N. and DESBOROUGH, G.A., 1975. The Pikes Peak Batholith, Colorado Front Range, and a model for the origin of the gabbro-anorthosite-syenite-potassic granite suite. Precambrian Res., 2, 97-160.

BARLEY, M.E., 1980. Evolution of Archaean calc-alkaline volcanics. A study of the Kelly Greenstone Belt and McPhee Dome, eastern Pilbara Block, W.A. Ph.D. thesis, Univ. of W.A. (unpubl.)

BERBERI, F., FERRARA, G., SANTACROCE, R., TREUIL, M. and VARET, J., 1975. A transitional basalt-pantellerite sequence of fractional crystallisation, the Boina Centre (Afar Rift, Ethiopia). J. Petrology, 16, 22-56.

BEST, M.G., 1975. Migration of fluids in the upper mantle and K variation in calc-alkalic rocks. Geology, 3, 429-432.

BICKFORD, M.E. and MOSE, D.G., 1975. Geochronology of Precambrian rocks in the St. Francois Mountains, southeastern Missouri. Geol. Soc. Am. Spec. Pap. 165.

BIRCH, W.D., 1975. Mineralogy, geochemistry and petrogenesis of some Victorian Paleozoic rhyolites. Ph.D. thesis, Univ. of Melbourne (unpubl.)

BIRCH, W.D., CLEMENS, J.D. and PHILLIPS, G.N., 1977. Devonian acid igneous complexes in central Victoria. Excursion Guide "C", 2nd Australian Geological Convention.

BLACK, L.P., 1977. A Rb-Sr geochronological study in the Proterozoic Tennant Creek Block, central Australia. B.M.R.J. Aust. Geol. Geophys., 2, 111-122.

BLIGHT, D.F., 1969. Geology, petrology and geochemistry of an area south of Tollu, Western Australia. Hons. thesis, Univ. Adelaide (unpubl.)

BLISSETT, A.H., 1975. Rock units in the Gawler Range Volcanics, S.A. Quart. geol. Notes, geol. Surv. S. Aust., 55, 2-14.

BLISSETT, A.H. and RADKE, F., 1979. The Gawler Range Volcanics - a regional review, in, The Gawler Craton, a symposium volume compiled by A.J. Parker.

BOWDEN, P.R., 1969. Geology, petrology and geochemistry of the Tollu area, Western Australia. Hons. thesis, Univ. Adelaide (unpubl.)

BRANCH, C.D., 1966. Volcanic cauldrons, ring complexes and associated granites of the Georgetown Inlier, Queensland. B.M.R. Bull., 76.

BRANCH, C.D., 1978. Evolution of the Middle Proterozoic Chandabooka Caldera, Gawler Range acid volcano-plutonic province, S.A. J. geol. Soc. Aust., 25, 199-216.

BRIDGWATER, D. and FYFE, W.S., 1974. The pre-3 b.y. crust : fact - fiction - fantasy. Geosci. Can., 1, 7-11.

BRIDGWATER, D. and WINDLEY, B.F., 1973. Anorthosites, post-orogenic granites, acid volcanic rocks and crustal development in the North Atlantic shield during the mid-Proterozoic. Spec. Publs. Geol. Soc. S. Afr., 3, 307-317.

BROWN, G.C. and BOWDEN, P., 1973. Experimental studies concerning the genesis of the Nigerian younger granites. Contrib. Mineral. Petrol., 40, 131-139.

BROWN, G.M., HOLLAND, J.G., SIGURDSSON, H., TOMBLIN, J.F. and ARCULUS, R.J., 1977. Geochemistry of the Lesser Antilles volcanic island arc. Geochim. cosmochim. Acta, 41, 785-801.

BULTITUDE, R.J., JOHNSON, R.W. and CHAPPELL, B.W., 1978. Andesites of Bagana volcano, Papua New Guines : chemical stratigraphy, and a reference andesite composition. B.M.R. J. Aust. Geol. Geophys., 3, 281-295.

BUNTING, J.A. and CHIN, R.J., 1975. Explanatory notes on the Duketon 1:250,000 Geological Sheet, Western Australia. Geol. Surv. West. Aust., Record 1975/7.

BUNTING, J.A. and WILLIAMS, S.J., 1976. Explanatory notes on the Sir Samuel 1:250,000 Geological Sheet, Western Australia. Geol. Surv. West. Aust., Record 1976/8.

CARMICHAEL, I.S.E., 1964. The petrology of Thingmuli, a Tertiary volcano in eastern Iceland. J. Petrology, 5, 435.

CAWTHORN, R.G., CURRAN, E.B. and ARCULUS, R.J., 1973. A petrogenetic model for the origin of the calc-alkaline suite of Grenada, Lesser Antilles. J. Petrology, 14, 327-37.

CAWTHORN, R.G. and O'HARA, M.J., 1976. Amphibole fractionation in calc-alkaline magma genesis. Amer. J. Sci., 276, 309-329.

CHAPPELL, B.W. and WHITE, A.J.R., 1974. Two contrasting granite types. Pacif. Geol., 8, 173-174.

CHAYES, F., 1964. Variance-covariance relations in some published Harker diagrams of volcanic suites. J. Petrology, 5, 219-237.

CLIFFORD, P.M. and McNUTT, R.H., 1971. Evolution of Mt. St. Joseph - an Archaean volcano. Can.J.Earth Sci., 8, 150-161.

COLLERSON, K.D., 1972. High grade metamorphic and structural relationships near Amata, Musgrave Ranges, central Australia. Ph.D. thesis, Univ. Adelaide (unpubl.)

COLLERSON, K.D. and FRYER, B.J., 1978. The role of fluids in the formation and subsequent development of early continental crust. Contrib. Mineral. Petrol., 67, 151-167.

COMPSTON, W. and NESBITT, R.W., 1967. Isotopic age of the Tollu Volcanics, W.A. J. geol. Soc. Aust., 14, 235-238.

CONDIE, K.C., 1973. Archaean magmatism and crustal thickening. Bull. geol. Soc. Am., 84, 2981-2992.

CONDIE, K.C., 1976. Trace-element geochemistry of Archean greenstone belts. Earth-Sci. Rev., 12, 393-417.

CONDIE, K.C., 1978. Geochemistry of Proterozoic granitic plutons from New Mexico, U.S.A. Chem. Geol., 21, 131-149.

CONDIE, K.C., 1980. Origin of Archaean granites. Abst. Volume, Int'l Archaean Symposium, Perth 1980, 91-92.

CONDIE, K.C. and BARAGAR, W.R.A., 1974. Rare-earth element distributions in volcanic rocks from Archaean greenstone belts. Contrib. Mineral. Petrol., 45, 237-246.

CONDIE, K.C. and HARRISON, N.M., 1976. Geochemistry of the Archean Bulawayan Group, Midlands greenstone belt, Rhodesia. Precambrian Res., 3, 253-271.

CONDIE, K.C. and HUNTER, D.R., 1976. Trace element geochemistry of Archean granitic rocks from the Barberton region, South Africa. Earth Planet. Sci. Lett., 29, 389-400.

COOPER, J.A., NESBITT, R.W., PLATT, J.P. and MORTIMER, G.E., 1978. Crustal development in the Agnew region, Western Australia, as shown by Rb/Sr isotopic and geochemical studies. Precambrian Res., 7, 31-59.

DANIELS, J.L., 1974. The geology of the Blackstone Region, Western Australia. Bull. Geol. Surv. W. Aust., 123.

DAVIES, R.D., ALLSOPP, H.L., ERLANK, A.J. and MANTON, W.I., 1970. Sr-isotopic studies on various layered mafic intrusions in southern Africa. Spec. Publs. Geol. Soc. S. Afr., 1, 576-593.

DAVIES, P.A. and CONDIE, K.C., 1977. Trace element model studies of Nyanzian greenstone belts, western Kenya. Geochim. cosmochim. Acta, 41, 271-277.

DEER, W.A., HOWIE, R.A. and ZUSSMAN, J., 1962. Rock Forming Minerals, 5 volumes. Longmans.

DEER, W.A., HOWIE, R.A. and ZUSSMAN, J., 1978. An Introduction to the Rock Forming Minerals. Longmans, 1966.

DE PAOLO, D.J. and JOHNSON, R.W., 1979. Magma genesis in the New Britain island-arc: constraints from Nd and Sr isotopes and trace-element patterns. Contrib. Mineral. Petrol., 70, 367-379.

DERRICK, G.M., WILSON, I.H. and HILL, R.M., 1976. Revision of stratigraphic nomenclature in the Precambrian of north-western Queensland. 1 : Tewinga Group. Qld. Govt. Min. J., 77, 1-16.

DODGE, F.C.W. and MAYS, R.E., 1972. Rare earth element fractionation in accessory minerals, Central Sierra Nevada Batholith. Prof. Pap. U.S. geol. Surv., 800D, D165-D168.

DUKE, J.M. and NALDRETT, A.J., 1978. A numerical model of the fractionation of olivine and molten sulfide from komatiite magma. Earth Planet. Sci. Lett., 39, 255-266.

EGGLER, D.H., 1972. Water-saturated and undersaturated melting relations in a Paracutin andesite and an estimate of water content in the natural magma. Contrib. Mineral. Petrol., 34, 261-271.

EGGLER, D.H. and BURNHAM, C.W., 1973. Crystallization and fractionation trends in the system andesite-H_2O-CO_2-O_2 at pressures to 10 kb. Bull. geol. Soc. Am., 84, 2517-2532.

EICHELBERGER, J.C., 1978. Andesitic volcanism and crustal evolution. Nature, 275, 21-27.

EMSLIE, R.F., 1978. Anorthosite massifs, rapakivi granites, and late Proterozoic rifting of North America. Precambrian Res., 7, 61-98.

EWART, A., 1976. Mineralogy and chemistry of modern orogenic lavas - Some statistics and implications. Earth Planet. Sci. Lett., 31, 417-432.

EWART, A., BROTHERS, R.N. and MATEEN, A., 1977. An outline of the geology and geochemistry, and the possible petrogenetic evolution of the volcanic rocks of the Tonga-Kermadec-New Zealand island arc. J. Volcanol. Geotherm. Res., 2, 205-250.

EWART, A., MATEEN, A. and ROSS, J.A., 1976. Review of mineralogy and chemistry of Tertiary central volcanic complexes in south-east Queensland and northeast New South Wales. In, Volcanism in Australasia, R.W. Johnson (Ed.), Elsevier, 21-39.

FISHER, R.V., 1961. Proposed classification of volcaniclastic sediments and rocks. Bull. geol. Soc. Am., 72, 1409-1414.

FISHER, R.V., 1966. Rocks composed of volcanic fragments and their classification. Earth-Sci. Rev., 1, 287-298.

FISKE, R.S., HOPSON, C.A. and WATERS, A.C., 1963. Geology of Mt. Rainier National Park, Washington. Prof. Pap. U.S. geol. Surv., 444.

FLOOD, R.H., VERNON, R.H., SHAW, S.E. and CHAPPELL, B.W., 1977. Origin of pyroxene-plagioclase aggregates in a rhyodacite. Contrib. Mineral. Petrol., 60, 299-309.

FODEN, J.D., 1979. The petrology of some young volcanic rocks from Lombok and Sumbawa, Lesser Sunda Islands. Ph.D. thesis, Univ. Tasmania (unpubl.)

FORD, A.B., 1970. Development of the layered series and capping granophyre of the Dufek intrusion of Antarctica. Spec. Publs. Geol. Soc. S. Afr., 1, 492-510.

FORMAN, D.J., 1966. The geology of the south-western margin of the Amadeus Basin, Central Australia. Australia Bur. Mineral Resources, Rept. 87.

FORMAN, D.J., 1972. Petermann Ranges N.T., 1:250,000 Geological Sheet, Explan. Notes. Bur. Miner. Resour. Geol. Geophys. Aust.

FRANCIS, P.W. and RUNDLE, C.C., 1976. Rates of production of the main magma types in the Central Andes. Bull. geol. Soc. Am., 87, 474-480.

FREY, F.A., GREEN, D.H. and ROY, S.D., 1978. Integrated models of basalt petrogenesis : a study of quartz tholeiites to olivine melilitites from southeastern Australia utilizing geochemical and experimental petrological data. J. Petrology, 19, 463-513.

FRYER, B.J. and JENNER, G.A., 1978. Geochemistry and origin of the Archean Prince Albert Group volcanics, western Melville Peninsula, Northwest Territories, Canada. Geochim. cosmochim. Acta, 42, 1645-1654.

FYFE, W.S., 1978. The evolution of the earth's crust : modern plate tectonics to ancient hot spot tectonics? Ghem. Geol. 23, 89-114.

GAUDETTE, H.E., MENDOZA, V., HURLEY, P.M., FAIRBAIRN, H.W., 1978. Geology and age of the Parguaza rapakivi granite, Venezuela. Bull. geol. Soc. Am., 89, 1335-1340.

GEE, R.D., 1979. Structure and tectonic style of the Western Australian Shield. Tectonophysics, 58, 327-369.

GILES, C.W., 1977. Rock units in the Gawler Range Volcanics, Lake Everard area, South Australia. Q. geol. Notes, geol. Surv. S. Aust., 61, 7-16.

GILES, C.W. and TEALE, G.S., 1979. The geochemistry of Proterozoic acid volcanics from the Frome Basin. Q. geol. Notes, geol. Surv. S. Aust., 71, 13-18.

GILL, J.B., 1978. Role of trace element partition coefficients in models of andesite genesis. Geochim. cosmochim. Acta, 42, 709-724.

GLENN, R.A., LAING, W.P., PARKER, A.J. and RUTLAND, R.W.R., 1977. Tectonic relationships between the Proterozoic Gawler and Willyama Orogenic Domains, Australia. J. geol. Soc. Aust., 24, 125-150.

GLIKSON, A.Y., 1976. Trace element geochemistry and origin of early Precambrian acid igneous series, Barberton Mountain Land, Transvaal. Geochim. cosmochim. Acta, 40, 1261-1280.

GLIKSON, A.Y., 1977. Evidence on the radius of the Precambrian Earth. B.M.R.J. Aust. Geol. Geophys., 2, 229-232.

GLIKSON, A.Y., 1979a. Siderophile and lithophile trace-element evolution of the Archaean mantle. B.M.R.J. Aust. Geol. Geophys., 4, 253-279.

GLIKSON, A.Y., 1979b. Early Precambrian tonalite-trondhjemite sialic nuclei. Earth-Sci. Rev., 15, 1-73.

GLIKSON, A.Y., 1979c. The missing Precambrian crust. Geology, 7, 449-454.

GLIKSON, A.Y., DERRICK, G.M., WILSON, I.H. and HILL, R.M., 1976. Tectonic evolution and crustal setting of the middle Proterozoic Leichhardt River fault trough, Mt. Isa region, northwestern Queensland. B.M.R.J. Aust. Geol. Geophys., 1, 115-129.

GLIKSON, A.Y. and LAMBERT, I.B., 1976. Vertical zonation and petrogenesis of the early Precambrian crust in W.A. Tectonophysics, 30, 55-89.

GOODE, A.D.T., 1970. The petrology and structure of the Kalka and Ewarara layered basic intrusions, Giles Complex, central Australia. Ph.D. thesis, Univ. Adelaide (unpubl.)

GOODE, A.D.T. and MOORE, A.C., 1975. High pressure crystallisation of the Ewarara, Kalka and Gosse Pile intrusions, Giles Complex, Central Australia. Contrib. Mineral. Petrol., 51, 77-97.

GOODWIN, A.M., 1965. Mineralized volcanic complexes in the Porcupine-Kirkland Lake-Noranda region, Canada. Econ. Geol., 60, 955-971.

GOODWIN, A.M., 1973. Archean iron-formations and tectonic basins of the Canadian Shield. Econ. Geol., 68, 915-933.

GOODWIN, A.M., 1974. Precambrian belts, plumes and shield development. Amer. J. Sci., 274, 987-1028.

GOODWIN, A.M. and SMITH, I.E.M., 1980. Chemical discontinuities in Archean metavolcanic terrains and the development of Archean crust. Precambrian Res., 10, 301-311.

GOWER, C.F., 1974. Explanatory notes on the Laverton 1:250,000 Geological Sheet, Western Australia. Geol. Surv. West. Aust., Record 1973/28 (unpubl.)

GRAY, C.M., 1971. Strontium isotopic studies on granulites. Ph.D. thesis, A.N.U. (unpubl.)

GRAY, C.M., 1977. The geochemistry of Central Australian granulites in relation to the chemical and isotopic effects of granulite facies metamorphism. Contrib. Mineral. Petrol., 65, 79-89.

GRAY, C.M., 1978. Geochronology of granulite-facies gneisses in the western Musgrave Block, Central Australia. J. geol. Soc. Aust., 25, 403-414.

GREEN, D.H., 1971. Compositions of basaltic magmas as indicators of conditions of origin : application to oceanic volcanism. Philos. Trans. R. Soc. Lond. Ser. A., 268, 707-725.

GREEN, D.H., 1972. Magmatic activity as the major process in the chemical evolution of the crust and mantle. In, The Upper Mantle, A.R. Ritsema (Ed.). Tectonophysics, 13, 47-71.

GREEN, D.H., 1973a. Contrasted melting relations in a pyrolite upper mantle under mid-oceanic ridge, stable crust and island arc environments. Tectonophysics, 17, 284-297.

GREEN, D.H., 1973b. Experimental melting studies on a model upper mantle composition at high pressure under water-saturated and water-undersaturated conditions. Earth Planet. Sci. Lett., 19, 37-53.

GREEN, D.H., 1975. Genesis of Archaean peridotitic magmas and constraints on Archaean geothermal gradients and tectonics. Geology, 3, 15-18.

GREEN, D.H., 1976. Experimental testing of "equilibrium" partial melting of peridotite under water-saturated, high-pressure conditions. Canadian Mineralogist, 14, 255-268.

GREEN, D.H., GREEN, T.H. and RINGWOOD, A.E., 1967. The origin of high-alumina basalts and their relationships to quartz tholeiites and alkali basalts. Earth Planet. Sci. Lett., 2, 41-51.

GREEN, D.H. and LAMBERT, I.B., 1965. Experimental crystallisation of anhydrous granite at high pressures and temperatures. J. Geophys. Res., 70, 5259-5268.

GREEN, D.H. and LIEBERMANN, R.C., 1976. Phase equilibria and elastic properties of a pyrolite model for the oceanic upper mantle. Tectonophysics, 32, 61-92.

GREEN, T.H., 1969. Experimental fractional crystallisation of quartz diorite and its application to the problem of anorthosite origin. Y. Isachsen (Ed.), Mem. New York State Mus. Sci. Serv., 18, 23-30.

GREEN, T.H., BRUNFELT, A.O. and HEIER, K.S., 1972. Rare-earth element distribution and K/Rb ratios in granulites, mangerites and anorthosites, Lofoten-Vesteraalen, Norway. Geochim. cosmochim. Acta, 36, 241-257.

GREEN, T.H. and RINGWOOD, A.E., 1968. Genesis of the calc-alkaline igneous rock suite. Contrib. Mineral. Petrol., 18, 105-162.

GREENLAND, L.P., 1970. An equation for trace element distribution during magmatic crystallisation. Amer. Miner., 55, 455-465.

GSA (Geological Society of Australia), 1971. Tectonic Map of Australia and New Guinea 1:5,000,000. Sydney.

HALLBERG, J.A., 1972. Geochemistry of Archaean volcanic belts in the Eastern Goldfields region of Western Australia. J. Petrology, 13, 45-56.

HALLBERG, J.A., 1980. Archaean geology of the Leonora-Laverton area. International Archaean Symposium, Perth 1980. Northeast Yilgarn Block Excursion Guide.

HALLBERG, J.A. and WILLIAMS, D.A.C., 1972. Archaean mafic and ultramafic rock associations in the Eastern Goldfields region, Western Australia. Earth Planet. Sci. Lett., 15, 191-200.

HALLBERG, J.A., JOHNSTON, C. and BYE, S.M., 1976a. The Archaean Marda igneous complex, Western Australia. Precambrian Res., 3, 111-136.

HALLBERG, J.A., CARTER, D.N. and WEST, K.N., 1976b. Archaean volcanism and sedimentation near Meekatharra, Western Australia. Precambrian Res., 3, 577-595.

HAMILTON, W., 1960. Silicic differentiates of lopoliths. Internat. Geol. Cong., Pt. 13, 59-67.

HARGRAVES, R.B., 1976. Precambrian geological history. Science, 193, 363-371.

HARRISON, N.M., 1970. The geology of the country around Que Que. Bull. geol. Surv. Rhodesia, 67.

HAWKESWORTH, C.J., NORRY, M.J., RODDICK, J.C., BAKER, P.E., FRANCIS, P.W. and THORPE, R.S., 1979. $^{143}Nd/^{144}Nd$, $^{87}Sr/^{86}Sr$, and incompatible element variations in calc-alkaline andesites and plateau lavas from South America. Earth Planet. Sci. Lett., 42, 45-57.

HAWKESWORTH, C.J. and O'NIONS, R.K., 1977. The petrogenesis of some Archaean volcanic rocks from southern Africa. J. Petrology, 18, 487-520.

HAYNES, D.W., 1972. Geochemistry of altered basalts and associated copper deposits. Ph.D. thesis, A.N.U. (unpubl.)

HEIER, K.S., 1973. A model for the composition of the deep continental crust. Fortschritte der Mineralogie, 50, 174-187.

HELZ, R.T., 1976. Phase relations of basalts in their melting ranges at PH_2O = 5 kb. Part II. Melt compositions. J. Petrology, 17, 139-193.

HJELMQVIST, S., 1956. On the occurrence of ignimbrite in the Precambrian. Sver. geol. Unders., Ser C., 542, 3-12.

HOLLOWAY, J.R., 1973. The system pargasite-H_2O-CO_2 : a model for melting of a hydrous mineral with a mixed-volatile fluid. Experimental results to 8 kbar. Geochim. cosmochim. Acta, 37, 651-666.

HOLLOWAY, J.R. and BURNHAM, C.W., 1972. Melting relations of basalt with equilibrium water pressure less than total pressure. J. Petrology, 13, 1-29.

HORWITZ, R.C. and DANIELS, J.L., 1967. A late Precambrian belt of volcanicity in central Australia. West. Australia Geol. Survey Ann. Rept. 1966, 50-53.

HUBREGTSE, J.J.M.W., 1976. Volcanism in the western Superior Province in Manitoba. In, The Early History of the Earth, B.F. Windley (Ed.), 279-287.

JAKES, P. and SMITH, I.E., 1970. High potassium calc-alkaline rocks from Cape Nelson, Eastern Papua. Contrib. Mineral. Petrol., 28, 259-271.

JAKES, P. and WHITE, A.J.R., 1971. Composition of island arcs and continental growth. Earth Planet. Sci. Lett., 12, 224-230.

JOPLIN, G.A., 1971. A Petrography of Australian Igneous Rocks. Angus and Robertson, Sydney.

KAY, R.W., 1978. Aleutian magnesian andesites : melts from subducted pacific ocean crust. J. Volcanol. Geotherm. Res., 4, 117-132.

KISVARSANYI, E.B., 1972. Petrochemistry of a Precambrian igneous province, St. Francois Mountains, Missouri. Missouri Geol. Survey and Water Resources, Report of Investigations No. 51.

KOVACH, A., FAIRBAIRN, H.W., HURLEY, P.M., BASEI, M.A.S. and CORDANI, U.G., 1976. Reconnaissance geochronology of basement rocks from the Amazonas and Maranhao Basins in Brazil. Precambrian Res., 3, 471-480.

KRANCK, E.H., 1969. Anorthosites and rapakavi, magmas from the lower crust. In, Origin of anorthosites and related rocks. Y. Isachsen (Ed.), Mem. New York State Mus. Sci. Serv., 18, 93-97.

KRONER, A., 1977. The Precambrian geotectonic evolution of Africa : plate accretion versus plate destruction. Precambrian Res., 4, 163-213.

KUNO, H., 1969. Andesite in time and space. In, McBirney, A.R., (Ed.) Proceedings of the andesite conference. Bull. Oregon Dept. Mineral Ind., 65, 13-20.

LAMBERT, I.B. and HEIER, K.S., 1968. Geochemical investigations of deep seated rocks in the Australian shield. Lithos, 1, 30-53.

LAMBERT, R.S. and HOLLAND, J.G., 1974. Yttrium geochemistry applied to petrogenesis, utilising calcium-yttrium relationships in minerals and rocks. Geochim. cosmochim. Acta, 38, 1393-1414.

LAMBERT, R.S., HOLLAND, J.G. and OWEN, P.F., 1974. Chemical petrology of a suite of calc-alkaline lavas from Mt. Ararat, Turkey. J. Geol., 82, 419-438.

LEEMAN, W.P., MA, M.-S., MURALI, A.V. and SCHMITT, R.A., 1978. Empirical estimation of Magnetite/Liquid distribution coefficients for some transition elements. Contrib. Mineral. Petrol., 65, 269-272.

LENTHALL, D.H. and HUNTER, D.R., 1977. The geochemistry of the Bushveld granites in the Potgietersrus tin-field. Precambrian Res., 5, 359-400.

LIPMAN, P.W., 1975. Evolution of the Platoro Caldera complex and related volcanic rocks, southeastern San Juan Mountains, Colorado. Prof. Pap. U.S. geol. Surv., 852.

LIPMAN, P.W., PROSTKA, H.J. and CHRISTIANSEN, R.L., 1972. Cenozoic volcanism and plate-tectonic evolution of the Western United States. 1. Early and Middle Cenozoic. Royal Soc. London Philos. Trans., 271, 217-248.

LOPEZ-ESCOBAR, L., FREY, F.A. and VERGARA, M., 1977. Andesites and high-alumina basalts from the central-south Chile High Andes : geochemical evidence bearing on their petrogenesis. Contrib. Mineral. Petrol., 63, 199-228.

LUNDQVIST, T., 1968. Precambrian geology of the Los-Hamra region, Central Sweden. Sver. geol. Unders., Ser. Ba, 23.

MACDONALD, G.A., 1972. Volcanoes. Prentice Hall, New Jersey.

MACKENZIE, D.E. and CHAPPELL, B.W., 1972. Shoshonitic and calc-alkaline lavas from the highlands of Papua New Guinea. Contrib. Mineral. Petrol., 35, 50-62.

McBIRNEY, A.R., 1978. Volcanic evolution of the Cascade Range. Ann. Rev. Earth Planet. Sci., 6, 437-456.

McDOUGALL, I., 1962. Differentiation of Tasmanian dolerites : Red Hill dolerite - granophyre association. Bull. geol. Soc. Am., 73, 279-316.

McLAUGHLIN, R.J.W., 1976. Central Victorian cauldron volcanic province. In, Geology of Victoria, J.G. Douglas and J.A. Ferguson (Eds.). Geol. Soc. Aust. Spec. Pubs., 5, 81.

McLENNAN, S.M., FRYER, B.J. and YOUNG, G.M., 1979. Rare earth elements in Huronian (Lower Proterozoic) sedimentary rocks : composition and evolution of the post-Kenoran upper crust. Geochim. cosmochim. Acta, 43, 375-388.

MERTZMAN, S.A., 1977. The petrology and geochemistry of the Medicine Lake Volcano, California. Contrib. Mineral. Petrol., 62, 221-247.

MITCHELL, J., 1976. Precambrian geology of the Westmoreland region, Northern Territory Part III : Cliffdale Volcanics. B.M.R., Australia, Record, 1976/34 (unpubl.)

MUEHLBERGER, W.R., DENISON, R.E. and LIDIAK, E.G., 1967. Basement rocks in continental interior of United States. Bull. Amer. Ass. Petrol. Geol., 51, 2351-2380.

MYSEN, B.O. and BOETTCHER, A.L., 1975. Melting of a hydrous mantle : II Geochemistry of crystals and liquids formed by anatexis of mantle peridotite at high pressures and high temperatures as a function of controlled activities of water, hydrogen and carbon dioxide. J. Petrology, 16, 549-593.

MYSEN, B.O., KUSHIRO, I., NICHOLLS, I.A. and RINGWOOD, A.E., 1973. A possible mantle origin for andesitic magmas : discussion of a paper by Nicholls and Ringwood. Earth Planet. Sci. Lett., 21, 221-229.

NANCE, W.B. and TAYLOR, S.R., 1977. Rare earth patterns and crustal evolution II : Archaean sedimentary rocks from Kalgoorlie, Australia. Geochim. cosmochim. Acta, 41, 225-31.

NESBITT, R.W., 1966. The Giles igneous province, Central Australia. An example of an eroded volcanic zone. Bull. volcan., 29, 271-282.

NESBITT, R.W., GOODE, A.D.T., MOORE, A.C., HOPWOOD, T.P., 1970. The Giles Complex, Central Australia : a stratified sequence of mafic and ultramafic intrusions. Spec. Publs. Geol. Soc. S. Afr., 1, 547-564.

NESBITT, R.W. and HAMILTON, D.L., 1970. Crystallisation of an alkali-olivine basalt under controlled PO_2, PH_2O conditions. Phys. Earth Planet. Interiors, 3, 309-315.

NESBITT, R.W., MASTINS, H., STOLZ, G.W. and BRUCE, D.R., 1976. Matrix corrections in trace element analysis by X-ray fluorescence : An extension of the Compton Scattering technique to long wave-lengths. Chem. Geol., 18, 203-213.

NESBITT, R.W. and SUN, S.S., 1976. Geochemistry of Archaean spinifex-textured peridotites and magnesian and low magnesian tholeiites. Earth Planet. Sci. Lett., 31, 433-453.

NESBITT, R.W. and TALBOT, J.L., 1966. The layered basic and ultrabasic intrusions of the Giles Complex, Central Australia. Contrib. Mineral. Petrol., 13, 1-11.

NOBLE, D.C., KORRINGA, M.K., CHURCH, S.E., BOWMAN, H.R., SILBERMAN, M.L. and HEROPOULOS, C.E., 1976. Elemental and isotopic geochemistry of non-hydrated quartz latite glasses from the Eureka Valley Tuff, east-central California. Bull. geol. Soc. Am., 87, 754-762.

NORRISH, K. and HUTTON, J.T., 1969. An accurate X-ray spectrographic method for the analysis of a wide range of geological samples. Geochim. cosmochim. Acta, 33, 431-453.

OSBORN, E.F., 1969. Experimental aspects of calc-alkaline differentiation. In, McBirney, A.R. (Ed.) Proceedings of the andesite conference. Bull. Oregon Dept. Mineral Ind., 65, 33-42.

PADOVANI, E.R. and CARTER, J.L., 1977. Aspects of deep crustal evolution beneath south central New Mexico. Am. Geophys. Union. Geophys. Mon., 20.

PAGE, R.W., 1978. Response of U-Pb zircon and Rb-Sr total-rock and mineral systems to low-grade regional metamorphism in Proterozoic igneous rocks, Mt. Isa, Australia. J. geol. Soc. Aust., 25, 141-164.

PAGE, R.W., BLAKE, D.H. and MAHON, M.W., 1976. Geochronology and related aspects of acid volcanics, associated granites, and other Proterozoic rocks in the Granites-Tanami region, northwestern Australia. B.M.R. J. Aust. Geol. Geophys., 1, 1-13.

PARSONS, W.H., 1969. Criteria for the recognition of volcanic breccias : review. Geol. Soc. Am., Memoir 115.

PEACOCK, M.A., 1931. Classification of igneous rock series. J. Geol., 39, 54-67.

PEARCE, J.A., 1976. Statistical analysis of major element patterns in basalts. J. Petrology, 17, 15-43.

PEARCE, J.A. and CANN, J.R., 1973. Tectonic setting of basic volcanic rocks determined using trace element analyses. Earth Planet. Sci. Lett., 19, 290-300.

PEARCE, T.H., GORMAN, B.E. and BIRKETT, T.C., 1978. The relationship between major element chemistry and tectonic environment of basic and intermediate volcanic rocks. Earth Planet. Sci. Lett., 36, 121-132.

PEARCE, J.A. and NORRY, M.J., 1979. Petrogenetic implications of Ti, Zr, Y and Nb variations in volcanic rocks. Contrib. Mineral. Petrol., 69, 33-47.

PLUMB, K.A., 1979. Structure and tectonic style of the Precambrian shields and platforms of northern Australia. Tectonophysics, 58, 291-325.

PLUMB, K.A. and DERRICK, G.M., 1975. Geology of the Proterozoic rocks of the Kimberley to Mt. Isa region. In, Economic Geology of Australia and Papua New Guinea. Vol. 1, C.L. Knight, (Ed.), Aust. Inst. Min. Met., 217-252.

PRICE, R.C. and TAYLOR, S.R., 1977. The rare earth element geochemistry of granite, gneiss, and migmatite from the western metamorphic belt of south-eastern Australia. Contrib. Mineral. Petrol., 62, 249-263.

PURVIS, A.C., 1978. The geochemistry and metamorphic petrology of the Southern Cross-Forrestania greenstone belt at Diggers Rock, Western Australia. Ph.D. thesis, Univ.Adelaide (unpubl.)

REID, D.L., 1977. Geochemistry of Precambrian igneous rocks in the Lower Orange River region. Bull. Dept. Geology, University of Capetown, Precambrian Research Unit, 22.

RINGWOOD, A.E., 1966. The chemical composition and origin of the Earth, In Hurley, P.M. (Ed.), Advances in Earth science, Cambridge, Massachusetts Inst. Technology Press, 287-356.

RINGWOOD, A.E., 1974. Petrological evolution of island arc systems. J. Geol. Soc. London, 130, 183-204.

ROEDER, P.L. and OSBORN, E.F., 1966. Experimental data for the system MgO-FeO-Fe_2O_3-$CaAl_2Si_2O_8$-SiO_2 and their petrological implications. Am. J. Sci., 264, 428-430.

ROEDER, P.L. and EMSLIE, R.F., 1970. Olivine-liquid equilibrium. Contrib. Mineral. Petrol., 29, 275-289.

ROGERS, N.W., 1977. Granulite xenoliths from Lesotho kimberlites and the lower continental crust. Nature, London, 270, 681-684.

ROSS, C.S. and SMITH, R.L., 1961. Ash-flow tuffs : their origin, geologic relations and identification. Prof. Pap. U.S. geol. Surv., 366.

RUTLAND, R.W.R., 1973. On the interpretation of Cordilleran orogenic belts. Amer. J. Sci., 273, 811-849.

SANGSTER, D.F., 1972. Precambrian volcanogenic massive sulphide deposits in Canada - a review. Paper Canada Geol. Surv., 72-22.

SATO, H., 1977. Nickel content of basaltic magmas : identification of primary magmas and a measure of the degree of olivine fractionation. Lithos, 10, 113-121.

SCHILLING, J.G. and WINCHESTER, J.W., 1967. Rare earth fractionation and magmatic processes, in Mantles of the Earth and Terrestrial Planets, S.K. Runcorn, ed. Interscience Publishers London and New York, 267-283.

SCHMINCKE, H. and SWANSON, D.A., 1967. Laminar viscous flowage structures in ash-flow tuffs from Gran Canaria, Canary Islands. J. Geol., 75, 641-664.

SHAW, D.M., 1978. Trace element behaviour during anatexis in the presence of a fluid phase. Geochim. cosmochim. Acta, 42, 933-943.

SHERATON, J.W. and LABONNE, B., 1978. Petrology and geochemistry of acid igneous rocks of northeast Queensland. B.M.R. Bull., 169.

SIGHINOLFI, G.P., 1971. Investigations into deep crustal levels : fractionating effects and geochemical trends related to high grade metamorphism. Geochim. cosmochim. Acta, 35, 1005-1021.

SMITH, E.I., 1978. Precambrian rhyolites and granites in south-central Wisconsin : Field relations and geochemistry. Bull. geol. Soc., Am., 89, 875-890.

SMITH, I.E.M., CHAPPELL, B.W., WARD, G.K. and FREEMAN, R.S., 1977. Peralkaline rhyolites associated with andesitic arcs of the southwest Pacific. Earth Planet. Sci. Lett., 37, 230-236.

SMITH, K.G., STEWART, J.R. and SMITH, J.W., 1961. The regional geology of the Davenport and Murchison Ranges, Northern Territory. B.M.R. Aust. Report, 58.

SMITH, R.E. and SMITH, S.E., 1976. Comments on the use of Ti, Zr, Y, Sr, K, P and Nb in classification of basaltic magmas. Earth Planet. Sci. Lett., 32, 114-120.

SMITH, R.L., 1960. Ash flows. Bull. geol. Soc. Am., 71, 795-842.

STANLEY, J., 1979. Summary of trace element data for local and international standards. The University of Adelaide, analytical geochemistry report, 6/79. In, Compilation of Analytical Geochemistry Reports 1973-1979, R.W. Nesbitt and J. Stanley (Eds.), Research Report, 3, 188-190.

STERN, C.R., 1974. Melting products of olivine tholeiite basalt in subduction zones. Geology, 2, 227-230.

STEVEN, T.A. and LIPMAN, P.W., 1976. Calderas of the San Juan volcanic field, southwestern Colorado. Prof. Pap. U.S. geol. Surv., 958.

STEWART, J.R., 1965. Middle Proterozoic volcanic rocks in the Katherine-Darwin area, Northern Territory. B.M.R. Aust. Report 90.

STOLZ, G.W., 1980. A textural and geochemical interpretation of the volcanic pile in the vicinity of the Scotia orebody, W.A. Ph.D. thesis, Univ. Adelaide (unpubl.).

SUN, S.S. and NESBITT, R.W., 1977. Chemical heterogeneity of the Archaean mantle, composition of the earth and mantle evolution. Earth Planet. Sci. Lett., 35, 429-448.

SUN, S.S. and NESBITT, R.W., 1978. Petrogenesis of Archaean ultrabasic and basic volcanics : evidence from rare earth elements. Contrib. Mineral. Petrol., 65, 301-325.

SUN, S.S., NESBITT, R.W. and SHARASKIN, A.Y., 1979. Geochemical characteristics of mid-ocean ridge basalts. Earth Planet. Sci. Lett., 44, 119-138.

TARNEY, J. and WINDLEY, B.F., 1977. Chemistry, thermal gradients and evolution of the lower continental crust. J. geol. Soc. London, 134, 153-72.

TAYLOR, S.R., 1965. The application of trace element data to problems of petrology. In, Ahrens, L.H., Press, F., Runcorn, S.K. and Urey, H.C. (Eds.). Phys.Chem.Earth, 6, 133-213.

TAYLOR, S.R., 1969. Trace element chemistry of andesites and associated calc-alkaline rocks. In, McBirney, A.R. (Ed.) Proceedings of the andesite conference. Bull. Oregon Dept. Mineral Ind., 65, 43-63.

TAYLOR, S.R. and HALLBERG, J.A., 1977. Rare earth elements in the Marda calc-alkaline suite : an Archaean geochemical analogue of Andean-type volcanism. Geochim. cosmochim. Acta, 41, 1125-1129.

TAYLOR, S.R. and McLENNAN, S.M., 1979. Discussion on 'Chemistry, thermal gradients and evolution of the lower continental crust' by J. Tarney and B.F. Windley. J. geol. Soc. London, 136, 497-500.

THOMSON, B.P., 1975. Musgrave Block - regional geology. In, Economic Geology of Australia and Papua New Guinea. Vol. 1, C.L. Knight, (Ed.), Aust. Inst. Min. Met., 451-454.

THOMSON, B.P., 1975. Regional geology of the Gawler Craton, In, Economic Geology of Australia and Papua New Guinea. Vol. 1, C.L. Knight, (Ed.), Aust. Inst. Min. Met., 461-466.

THORPE, R.S., POTTS, P.J. and FRANCIS, P.W., 1976. Rare earth data and petrogenesis of andesite from the North Chilean Andes. Contrib. Mineral. Petrol., 54, 65-78.

THORPE, R.S., FRANCIS, P.W. and MOORBATH. S., 1979. Stontium isotope evidence for petrogenesis of Central American andesites. Nature, 277, 44-45.

TUREKIAN, K.K. and WEDEPOHL, K.H., 1961. Distribution of the elements in some major units of the earth's crust. Bull. geol. Soc. Am., 72, 175-192.

TURNER, A.R., 1975. Petrology of the eastern Gawler Ranges Volcanic Complex. Bull. geol. Surv. S. Aust., 45.

VANCE, J.A., 1969. On synneusis. Contrib. Mineral. Petrol., 24, 7-29.

VILJOEN, M.J. and VILJOEN, R.P., 1969. An introduction to the geology of the Barberton granite-greenstone terrane. Spec. Publs. Geol. Soc. S. Afr., 2, 9-28.

VORMA, A., 1975. On two roof pendants in the Wiborg rapakivi massif, southeastern Finland. Geol. Surv. Finland. Bull. 272.

VORMA, A., 1976. On the petrochemistry of rapakivi granites with special reference to the Laitila Massif, southwestern Finland. Geol. Surv. Finland. Bull. 285.

WAHL, W., 1947. A composite lava flow from Lounatkorkia, Hogland. Bull. Com. geol. Finlande, 140, 287-302.

WALPOLE, B.P., CROHN, P.W., DUNN, P.R. and RANDAL, M.A., 1968. Geology of the Katherine-Darwin region, Northern Territory. B.M.R. Bull. 82.

WALRAVEN, F., 1976. Notes on the late-stage history of the western Bushveld Complex. Trans. geol. Soc. S. Afr., 79, 13-21.

WEBB, A.W., 1973. The geochronology of the younger granites of the Musgrave Block, Prog. Rep. No. 11 Amdel AN1/1/123 (unpubl.)

WEBB, A.W., 1978. Geochronology of the younger granites of the Gawler Craton and its northwest margin - report No. 1215. Rept. Austral. Mineral. Devel. Lab. 1/1/122 (unpubl.)

WEBB, A.W. and THOMSON, B.P., 1977. Archaean basement rocks in the Gawler Craton, South Australia. Search, 8, 34-36.

WELLMAN, P. and McDOUGALL, I., 1974. Cainozoic igneous activity in eastern Australia. Tectonophysics, 23, 49-65.

WHITE, A.J.R. and CHAPPELL, B.W., 1977. Ultrametamorphism and granitoid genesis. Tectonophysics, 43, 7-22.

WILSON, H.D.B. and MORRICE, M.G., 1977. The volcanic sequence in Archaean Shields. Geol. Assoc. Canada, Spec. Paper, 16, 355-376.

WILSON, I.H., 1978. Volcanism on a Proterozoic continental margin in northwestern Queensland. Precambrian Res., 1, 205-235.

WINCHESTER, J.A. and FLOYD, P.A., 1977. Geochemical discrimination of different magma series and their differentiation products using immobile elements. Chem. Geol., 20, 325-343.

WINDLEY, B.F., 1977. The Evolving Continents. Wiley, London.

WOLFF, J.M. and CROCKET, 1979. Geochronology and geochemistry of felsic rocks in an Archean volcanic-plutonic suite in the Wabigoon Belt, northwestern Ontario. Can. J. Earth Sci., 16, 1978-1897.

WRIGHT, J.V. and WALKER, G.P.L., 1977. The ignimbrite source problem : Significance of a co-ignimbrite lag-fall deposit. Geology, 5, 729-732.

WRIGHT, T.L., 1974. Presentation and interpretation of chemical data for igneous rocks. Contrib. Mineral. Petrol., 48, 233-248.

WYLLIE, P.J., 1971. Role of water in magma generation and initiation of diapiric uprise in the mantle. J. geophys. Res., 76, 1328-1338.

WYLLIE, P.J., 1977. Crustal anatexis : an experimental review. Tectonophysics, 43, 41-71.

WYLLIE, P.J., HUANG, W.L., STERN, C.R. and MAALOE, S., 1976. Granitic magmas : possible and impossible sources, water contents, and crystallisation sequences. Can. J. Earth Sci., 13, 1007-1019.

WYNNE-EDWARDS, H.R., 1976. Proterozoic ensialic orogenesis : the millipede model of ductile plate tectonics. Amer. J. Sci., 276, 927-953.

WYNNE-EDWARDS, H.R. and HASAN, Z., 1970. Intersecting orogenic belts across the North Atlantic. Amer. J. Sci., 268, 189-308.

YODER, H.S. and TILLEY, C.E., 1962. Origin of basalt magmas : An experimental study of natural and synthetic rock systems. J. Petrol., 3, 342-532.

APPENDIX 1

Tabulated data relevant to chapters 1, 2, 3

5 and 6.

TABLE A1.1 References used to compile the field of Cainozoic calc-alkaline volcanics, plotted on many of the variation diagrams.

BAKER, R.E., 1969. Comparative volcanology and petrology of the Atlantic island arcs. Bull. volcanol., 32, 189-206.

BARBERI, F., INNOCENTI, F., FERRARA, G., KELLER, J. and VILLARI, L., 1974. Evolution of Eolian arc volcanism (southern Tyrrhenian Sea). Earth Planet. Sci. Lett., 21, 269-276.

BROWN, G.M., HOLLAND, J.G., SIGURDSSON, H., TOMBLIN, J.F. and ARCULUS, R.J., 1977. Geochemistry of the Lesser Antilles volcanic island arc. Geochim. cosmochim. Acta, 41, 785-801.

BULTITUDE, R.J., JOHNSON, R.W. and CHAPPELL, B.W., 1978. Andesites of Bagana volcano, Papua New Guinea : chemical stratigraphy, and a reference andesite composition. B.M.R. J. Aust. Geol. Geophys., 3, 281-295.

CARMICHAEL, I.S.E., 1964. The petrology of Thingmuli, a Tertiary volcano in eastern Iceland. J. Petrology, 5, 435

CONDIE, K.C., 1976. Trace-element geochemistry of Archean greenstone belts. Earth-Sci. Rev., 12, 393-417. (Used averages compiled by this author for modern volcanics.)

DERUELLE, B., 1978. Calc-alkaline and shoshonitic lavas from five Andean volcanoes (between latitudes $21^{o}45'$ and $24^{o}30'S$) and the distribution of the Plio-Quaternary volcanism of the south-central and southern Andes. J. Volcanol. Geotherm. Res., 3, 281-298.

DOSTAL, J., ZENTILLI, M., CAELLES, J.C. and CLARK, A.H., 1977. Geochemistry and origin of volcanic rocks of the Andes (26^{o} - $28^{o}S$). Contrib. Mineral, Petrol., 63, 113-128.

DOSTAL, J. and ZERBI, M., 1978. Geochemistry of the Savalan Volcano (northwestern Iran). Chem. Geol., 22, 31-42.

EL-HINNAWI, E.E., PICHLER, H. and ZEIL, W., 1969. T.E. distribution in Chilean Ignimbrites. Contrib. Min. & Pet., 24, 50-62.

EWART, A., 1976. Mineralogy and chemistry of modern orogenic lavas - Some statistics and implications. Earth Planet. Sci. Lett., 31, 417-432.

EWART, A., BROTHERS, R.N. and MATEEN, A., 1977. An outline of the geology and geochemistry, and the possible petrogenetic evolution of the volcanic rocks of the Tonga-Kermadec-New Zealand island arc. J. Volcanol. Geotherm. Res., 2, 205-250.

EWART, A. and STIPP, J.J., 1968. Petrogenesis of the volcanic rocks of the central North Island, New Zealand, as indicated by a study of $^{87}Sr/^{86}Sr$ ratios, and Sr, Rb, K. U, and Th abundances. Geochim. cosmochim. Acta, 32, 699-736.

EWART, A., TAYLOR, S.R. and CAPP, A.C., 1968. Trace and minor element geochemistry of the rhyolitic volcanic rocks of the Taupo Volcanic Zone, New Zealand. Total rock and residual liquid data. Contrib. Mineral. Petrol., 18, 76-104.

FODEN, J.D., 1979. The petrology of some young volcanic rocks from Lombok and Sumbawa, Lesser Sunda Islands. Ph.D. thesis, Univ. Tasmania (unpubl.).

TABLE A1.1 Cont'd.

GILL, J.B., 1970. Geochemistry of Viti Levu, Fiji, and its evolution as an island arc. Contrib. Mineral. Petrol., 27, 179-203.

HAYNES, D.W., 1972. Geochemistry of altered basalts and associated copper deposits. Ph.D. thesis, A.N.U. (unpubl.). (Used averages compiled by this author for modern volcanics).

JAKES, P. and WHITE, A.J.R., 1971. Composition of island arcs and continental growth. Earth Planet. Sci. Lett., 12, 224-230.

JOHNSON, R.W., MACKENZIE, D.E. and SMITH, I.E.M., 1978. Volcanic rock associations at convergent plate boundaries : reappraisal of the concept using case histories from Papua, New Guinea. Bull. geol. Soc. Am., 89, 96-106.

KLERKX, J., DEUTSCH, S., PICHLER, H. and ZEIL, W., 1977. Strontium isotopic composition and trace element data bearing on the origin of Cenozoic volcanic rocks of the central and southern Andes. J. Volcanol. Geotherm. Res., 2, 49-71.

KUSSMAUL, S., HORMANN, P.K., PLASKONKA, E. and SUBIETA, T., 1977. Volcanism and structure of southwestern Bolivia. J. Volcanol. Geotherm. Res., 2, 73-111.

LAMBERT, R.S., HOLLAND, J.G. and OWEN, P.F., 1974. Chemical petrology of a suite of calc-alkaline lavas from Mt. Ararat, Turkey. J. Geol., 82, 419-438.

LOPEZ-ESCOBAR, L., FREY, F.A. and VERGARA, M., 1977. Andesites and high-alumina basalts from the central-south Chile High Andes : geochemical evidence bearing on their petrogenesis. Contrib. Mineral. Petrol., 63, 199-228.

MACKENZIE, D.E. and CHAPPELL, B.W., 1972. Shoshonitic and calc-alkaline lavas from the highlands of Papua New Guinea. Contrib. Mineral. Petrol., 35, 50-62.

MIYASHIRO, A., 1974. Volcanic rock series in island arcs and active continental margins. Amer. J. Sci., 274, 321-355.

NICHOLLS, I.A., 1971. Petrology of Santorini Volcano, Cyclades, Greece. J. Petrology, 12, 67-119.

PEARCE, J.A., 1976. Statistical analysis of major element patterns in basalts. J. Petrology, 17, 15-43.

PEARCE, J.A. and CANN, J.R., 1973. Tectonic setting of basic volcanic rocks determined using trace element analyses. Earth Planet. Sci. Lett., 19, 290-300.

PECCERILLO, A. and TAYLOR, S.R., 1976. Rare earth elements in east Carpathian volcanic rocks. Earth Planet. Sci. Lett., 32, 121-126.

PECCERILLO, A. and TAYLOR, S.R., 1976. Geochemistry of Eocene calc-alkaline volcanic rocks from Kastamonu Area, Northern Turkey. Contrib. Mineral. Petrol. 68, 63-81.

TAYLOR, S.R., 1969. Trace element chemistry of andesites and associated calc-alkaline rocks. In, McBirney, A.R. (Ed.) Proceedings of the andesite conference. Bull. Oregon Dept. Mineral Ind., 65, 43-63.

THORPE, R.S., POTTS, P.J., FRANCIS, P.W., 1976. Rare earth data and petrogenesis of andesites from the North Chilean Andes. Contrib. Mineral. Petrol., 54, 65-78.

WINCHESTER, J.A. and FLOYD, P.A., 1977. Geochemical discrimination of different magma series and their differentiation products using immobile elements. Chem. Geol., 20, 325-343.

TABLE 2.1. Brief thin section descriptions of a representative selection of rocks from the Gawler Range province.

SAMPLE	ROCK	DESCRIPTION	% MINERALS	ALTERATION		COMMENTS
E33	Porphyritic andesite	Med.-fine grained phenos. euhedral plag. & cpx. in a pilotaxitic matrix of suboriented plagioclase microlites + quartz (rare) + hematite-stained K-feldspar + chl. + opaques	Phenos. 20% of which Plag. 80% Cpx. 20%	plag.-sericitized (twinning destroyed) cpx. fresh & altered to chlorite	✓	Mangaroongah Dacite-andesitic varient. Near upper contact. May be of lava-flow origin
E36	Amygdaloidal porphyritic andesite	Fine-med. gr. phenos. plag. (euhedral) + amygdales→chlorite-filled & quartz-rimmed in a pilotaxitic matrix of oriented plag. laths	Phenos. 10% Amygdales 35%	Qtz.-chlorite in amygdales. Plag.-sericitized		From contact Mangaroongah Dacite & Arburee Rhyolite. Could be of lava-flow origin.
E46	Flow-banded rhyolite	Fine-med. gr. angular chips, embayed quartz & K-feldspar in a fluidal banded devitrified matrix. Flow bands curved around rotated crystals	Phenos. ~ 8%	Matrix completely devitrified		Dyke from field relations. Flow-banding is vertical.
E48	Porphyritic dacite	Med. gr. phenos. plag. + chloritized, fine gr. phenos. cpx in matrix of reddened K-feldspar and quartz, which form a microgranular intergrowth. Scattered fine opaques	Phenos. 15% of which Plag. 85% Cpx. 15%	plag.-sericitized cpx.-chloritized K-feldsp. in matrix is hematite stained	✓	Mangaroongah Dacite-typical example. Ash-flow from field relationships.
E50	Porphyritic dacite	Sparse, fine gr. phenos. plag. + cpx. in a micro-crystalline matrix of reddened K-feldspar + quartz + opaques + chl. + plag. Few basic rock fragments	Phenos. 8% of which Plag. 60% Cpx. 40%	plag.-sericitized cpx.-fresh & chloritized opqs.→ leucoxene & some fresh	✓	Childera Dacite-typical example
E51	Sparsely-porphyritic andesite	Fine-med. gr. phenos. plag. + fine gr. "granules" of cpx, (occasionally med. gr. cpx in plag.). Chlorite + opaques + plag. in matrix	Crystals 12% of which Plag. 50% Cpx 50%	Cpx. mainly fresh, some chloritized Plag.-sericitized		Childera Dacite - andesitic variant in south.
E62	Fine-grained dacite	Sparse, med. gr., euhedral phenocrysts plagioclase in a patchy polarised matrix, consisting of plates of plag. microlites + qtz. + reddened K-feldsp. + chlorite mosaics	Phenos. 2% Matrix contains: Chl. 15% Plag. ~ 40% Qtz.+ K-feldsp.45%	mafic mineral(?) → chlorite K-feldsp.→ hematite stained	✓	Bunburn Dacite-typical. Probably originally a vitric tuff.
E69	Autobrecciated rhyolite	Monolithologic rhyolite rock frags. (phenos K-feldspar & quartz in siliceous, devit. matrix) in matrix of curved, angular rock frags. + crystals. Frags. highly angular.		Have crystals K-feldspar projecting from fragments. Fragments highly angular on all scales. Numerous crystals in matrix vaguely resembling epiclastic. Brecciation due to flowage		
E78	Porphyritic rhyolite	Med.-coarse gr. phenos. anhedral, embayed quartz, euhedral K-feldspar, multiply-twinned plag. in granular matrix of quartz aggregates + K-feldspar + plag. + chlorite	Phenos. 7% of which K-felds.80% Quartz 10% Plag. 10%	K-felsp. phenos → sericitized matrix is hematised	✓	Arburee Rhyolite - typical example. 2 types of feldspars as phenocrysts.
E84	Porphyritic dacite	Med. gr. euhedral phenos. plag., some with square X.S. and multiple twinning at 90°. Fine gr. clots chlorite & opaques in a microgranular qtz. + K-feldspar matrix	Phenos. 35% of which Plag. 80% Chlorite (after cpx.) 20%	Plag.-fresh to partially sericitized Cpx. → chlorite K-feldsp. → hematised	✓	Dacite dyke. Complex pericline-albite twinning in plagioclase.

E96	Porphyritic rhyolite	Med. gr. phenos. quartz + K-feldspar + plag. in a spherulitic devit. quartz-feldspar matrix. Spherulites 1 mm across, composed of radiating qtz. + feldsp. needles	Phenos. 20% of which Qutz. 40% K-feld. 30% plag. 30%	Feldspars sericitized. Chlorite + hematite scattered throughout		Intrusive dyke Spherulitic devitrification textures are notable
E113	Spherulitic rhyolite	Completely devitrified quartz-feldspar-hematite rock. Devit. has produced coarse gr. (> 4 mm diam.) spherulites, consisting of radiating fern-like qtz.-feldsp. intergrowths		Much hematite causing reddening & outlining spherulites		Spherulites apparently produced during devitrification
E121	Porphyritic dacite	Fine gr. phenos. plag. & cpx. (& rare quartz) in a patchy devit. matrix of qtz. + K-feldsp. Contains numerous basic rock frags. consisting of chlorite + plag. microlites + plag. phenos.	Phenos. ~ 6% Rock frags. 10%	Plag.-sericit.		
E126	Porphyritic dacite	Similar description to E48			✓	Mangaroongah Dacite - typical example
E130	Vitric tuff	Fine grained rock - superficially like a chert. Composed almost entirely of very fine glass shards, chips & wisps which are largely undeformed. Rare, angular chips qutz. & feldspar	Nearly all devitrified glass shards			Waurea Pyroclastics - probably on air-fall rather than ash-flow tuff
E132	Vitric-lithic tuff	Rare, euhedral plag. phenos. and ash-size fragments (< 2 mm) in a quartz-sericite matrix. Some frags. show spherulitic & axiolitic devit. Ghosted outlines of possible vitric fragments in matrix	Phenos. 3% Frags. 10% Matrix 87%	Much sericite (after feldspar) in matrix	✓	Waurea Pyroclastics
E133	Lithic tuff	Variety of highly angular acid volc. rock frags. + crystals of plag., K-feldspar, quartz, biotite + pumice in a devit. glassy matrix in which is the hint of vitroclastic textures	All angular rock frags. + crystals. Fine devit. matrix indicates is of pyroclastic origin			Waurea Pyroclastics - probably an air-fall tuff
E136	Porphyritic rhyodacite	Medium gr. phenocrysts of plagioclase and fine-grained chlorite clots (after cpx.) in a microgranular matrix of quartz + reddened K-feldspar + plagioclase	Phenos. 10% of which Plag. 85% Cpx. 15%	Plag. → sericitized Matrix K-feldspar → hematised	✓	Yantea Rhyodacite
E147	Lithic tuff	Variety acid volc. rock frags., particularly perlitic cracked rhyolites + flow-banded rhyolites + plag. + K-feldspar phenos. + collapsed pumice in vitroclastic matrix				Waurea Pyroclastics - probably a poorly-welded ash-flow tuff
E154	Porphyritic rhyodacite	Medium gr. phenocrysts of plagioclase (rimmed with K-feldsp.) + K-feldspar, both in glomeroporphyritic aggregates and isolated, in granophyric groundmass of qtz. + K-feldspar	Phenos. 12% of which Plag. 75% K-feldsp. 25%	Plag. & K-feldspar sericitized. Matrix K-feldspar → hematised	✓	Yantea Rhyodacite (top of hill from which E155 collected)
E155	Porphyritic rhyodacite	Med. gr. phenos. plagioclase + K-feldspar in a granophyric groundmass of qtz. + reddened K-feldspar. Single crystals & glomeroporph. aggregates.	Phenos. 15% of which Plag. 60% K-feldsp. 40%	Plag. & K-feldspar sericitised Matrix K-feldspar → hematised	✓	Yantea Rhyodacite (base of hill). Slightly coarser ground mass than 154 and more K-feldspar, otherwise similar
E166 (also E222)	Autobrecciated dacite	Typical fine gr. devit. texture of Bunburn Dacite with numerous minute plag. laths. An "in situ" fragmentation, probably caused by gas-streaming				Bunburn Dacite - possibly steam explosion breccia

E168	Fine-grained dacite	Fine gr. euhedral phenos. plag. in matrix of oriented plag. microlites + opaques + reddened K-feldspar + quartz	Phenos. 2% of rock	Phenos. → sericitized Matrix K feldspar hematised	✓	Bunburn Dacite - typical example. Originally probably a vitric-tuff
E172	Lithic-vitric tuff	Fine gr. devit. rock fragments in a glassy devit. groundmass showing excellent vitroclastic textures of contorted, partially-compressed shards. Few phenos. of qtz. & plag.	(In hand specimen, rock extremely hard & "quartzitic")			Waurea Pyroclastics Moderately welded ash-flow tuff. Good textures.
E197	Crystal-lithic tuff	Fine to med. gr. phenos. quartz & K-feldspar + flattened rock & pumice fragments (showing axiolitic devit.) within vitroclastic, shard- & pumice-rich matrix	Phenos. 8% Rock frags. 10% Ashy matrix remainder	Much sericitization of matrix		Waurea Pyroclastics. Moderately-welded ash-flow tuff.
E203	Crystal-vitric tuff	Fine-med. gr. phenos. plag. + K-feldspar + qtz. within an originally glassy, completely devit. matrix. Some vitric rock frags. Extremely flattened shards visible	Phenos. 15% of which Qtz. 33% Plag. 33% K-feldsp. 33%	Plag.& K-feldspar sericitized. Some sericite in matrix	✓	Waurea Pyroclastics. Welded tuff of ash-flow origin.
E205	Lithic tuff	Unusual rock, composed of a variety of highly angular rock frags. (produced by gas streaming?) in a glassy shard-rich matrix. All rock frags. show axiolitic devit. textures - possibly some were pumice, although no cellular textures.				Waurea Pyroclastics. - an ash-flow tuff showing the effects of brecciation due to gas-streaming-possibly caused by late-stage fumarolic activity.
E211	Crystal-lithic-vitric tuff	Variety of rhyolitic rock frags. (mainly flow-banded) + collapsed pumice frags. with ragged ends (fiamme) + crystal chips of quartz, K-feldspar & plagioclase in a devitrified, glassy, contorted, moderately compressed matrix - showing excellent vitroclastic textures.				Waurea Pyroclastics - moderately-welded ash-flow tuff. Excellent example. Abundant pumice
E221	Fine-grained rhyolitic vitric tuff	Microgranular mosaic of granular quartz aggregates + aphanitic quartzo-feldspathic intergrowths + scattered opaques. Rare plag. phenocrysts	Phenos. < 1% of rock	None obvious on account of fine grainsize	✓	Block from Waurea Pyroclastics
E224	Air-fall tuff	Ash-size crystal chips, glassy material and rock fragments in bedded, graded layers. Excellent example of diapirism in original soft ash bed	Generally aphanitic		✓	Waurea Pyroclastics
E227	Amygdaloidal dacite	Elongated, cuspate, quartz-filled amygdales in a pilotaxitic matrix of plag. microlites + opaques + reddened K-feldspar. Rare fine gr. plag. phenos.	Plag. phenos. < 2% Amygdales 15% Plag. comprises 70% of matrix	Plag. → sericitized K-feldsp. → hematised	✓	Amygdaloidal varient of Bunburn Dacite. High Al_2O_3 due to abundant plag. in matrix
E230	Porphyritic rhyolite	Med.-coarse gr. euhedral phenos. plag. + K-feldspar + anhedral quartz in granular matrix quartz + K feldspar + biotite + plag.	Phenos. 45% of which Quartz 25% Plag. 45% K-feldsp. 30%	Feldspars extensively sericitized & hematised	✓	Moonamby dyke-suite. Rhyolite dyke
E231	Basalt	Tabular, fine-grained plagioclase microlites define a pilotaxitic texture through which is scattered granules of cpx. and opaques & aphanitic material	Plag. 60% Cpx. 15% Opqs. 10% Aphantic 15%	Plagioclase & aphanitic matrix extensively sericitized	✓	Nuckulla Basalt. Cpx. & opqus. fresh, some possibility of K_2O introd^n. during sericitization of plag.

E242	Fine-grained dacite	Very rare plag. phenos. in a fine gr. matrix of wispy plag. microlites + reddened K-feldspar + quartz + chlorite	Phenos. < 1% Matrix is 70% plagioclase	Plag. sericite dusted. K-feldspar hematised	✓	Bunburn Dacite
E255	Porphyritic rhyolite	Med.-coarse grained phenos. anhedral, embayed quartz + complexly-twinned plag. (euhedral) + perthite + clots chlorite in a granophyric qtz.-K-feldsp. matrix	Phenos. 45% of which Quartz 20% Plag. 70% Perthite 30%	Both feldspars sericit, K-feldsp. more so. Cpx. → chlorite	✓	Moonamby dyke-suite. Rhyolite dyke. Extremely coarse, complex and composite plagioclase phenos.
E258	Porphyritic rhyodacite-dacite	Med. gr. phenos. plag. + clots cpx. + chlorite-rich rock fragments within matrix of plag. microlites (< .2 mm long) + quartz + red K-feldspar + finely-divided chlorite	Phenos. 15% of which Plag. 85% Cpx. 15%	Plag. → sericitized Cpx. → chlorite K-feldsp. → finely divided hematite throughout.	✓	Mangaroongah Dacite from Nuckulla Hill
E270	Porphyritic rhyodacite	Med.-coarse gr. phenos. complexly-twinned plag. + K-feldspar + med. gr. clots chlorite in a spherulitic matrix of quartz + reddened K-feldspar. No quartz phenos.	Phenos. 45% of which Plag. 55% K-feldsp. 25% Chlorite 20%	Cpx. → chlorite Feldspars → sericitized	✓	Moonamby dyke-suite. Rhyodacite dyke
E278	Fine-grained andesite	Fine-grained mosaic plagioclase microlites + scattered opaques + chlorite. Rare euhedral sericitized plag. phenocrysts.	Phenos. < 1% of rock	Plag.-sericite dusted Cpx. → chlorite Opqs. → leucoxene	✓	Childera Dacite - andesitic variant
E282	Porphyritic rhyolite	Med. gr. phenos. plag. + biotite in glomeroporphyritic aggregates within a finely devit. felsic matrix. Scattered clots quartz.	Phenos. 10% of which Plag. 80% Biotite 20%			Karkulta Rhyolite - most significant feature is glomeroporphyritic aggs. biotite + plag.
E290	Porphyritic dacite	Similar description to E747			✓	Mangaroongah Dacite
E294	Porphyritic rhyodacite	Med.-coarse phenos. plag., often in glomero-porph. aggregates with chlorite (after cpx.), in a microgranophyric matrix of qtz. + K-feldspar + minor chlorite	Phenos. 12% of which Plag. 95% Cpx. 5%	Plag. phenos. completely sericitized. Orthoclase reddened with hematite	✓	Yantea Rhyodacite - typical example
E298	Lithic wacke	Variety of closely-packed, subrounded volcanic rock fragments in a matrix of finer fragments + crystals + ash. Little matrix, mainly close-packed rock fragments.				Epiclastic, separating Bunburn Dacite & Yantea Rhyodacite
E312	Porphyritic andesite	Fine gr. phenos. plag. and granular cpx. + opaques in a felsic matrix of unoriented plag. microlites + reddened K-feldspar + chlorite	Phenos. 15% of which Plag. 50% Cpx. 35% Opq. 15%	Plag.-sericitized Cpx.-fresh. Chlorite in matrix	✓	Whyeela Dacite - andesitic variant. Plag. unzoned., cpx - extremely fine gr. & granular
E322	Rhyolitic vitric-tuff	Flattened, oriented glass shards & pumice fragments now entirely devitrified (often axiolitic textures in shards) defining a eutaxitic texture. Some good evidence for post-depositional flowage - continuous & contorted flow bands.	Rare crystals, originally entirely glassy		✓	Baldry Rhyolite - a welded-tuff of ash-flow origin, excellent textural preservation

E326	Rhyolitic vitric tuff	Flattened & stretched, glassy fragments. Lenticular nature of frags. imparts a psuedo flow-banding- due to post-depositional movement	Rare crystals, originally entirely glassy		✓	Baldry Rhyolite. Example of welded tuff that has flowed - i.e. rheoignimbrite
E340	Lithic-vitric-crystal tuff	Strongly orientated & slightly flattened, devitrified rhyolitic rock fragments + crystal chips of quartz, plag. & K-feldspar + pumice fiamme (ragged ends) in a glassy matrix composed of abundant flattened glass shards. Are curved & squashed around crystals & rock fragments				Baldry Rhyolite. Welded ash-flow tuff. Excellent textures
E376	Fine-grained dacite	Rare-fine-grained phenos. plag. in microcrystalline felsic matrix consisting of plag. microlites + aphanitic quartz-K feldspar intergrowths	Phenos. < 1% of rock	K-feldspar contains much hematite	✓	Bunburn Dacite
E394	Porphyritic rhyodacite	Similar description to E294			✓	Yantea Rhyodacite- from lower part of unit
E395	Porphyritic rhyodacite	Medium gr. phenos. & glomerophorph. aggregates of plagioclase + vesicles partially infilled with quartz in a microgranular felsic matrix rich in plagioclase	Phenos. 18% of rock. Are all plag.	Extensive sericitization of plag.	✓	Yantea Rhyodacite - upper, purplish ash-flow sheet, separated from E394 by an ash layer
E402	Porphyritic rhyodacite	Similar description to E294			✓	Yantea Rhyodacite
E411	Porphyritic rhyodacite	Fine-med. gr. phenos. plagioclase, often in glomero-porphyritic aggregates in a microlitic matrix consisting of quartz needles which interlock with reddened K-feldspar	Phenos. 10% of which Plag. 90% Cpx. 10%	Cpx. → chlorite Plag. → sericitized	✓	Mordinyabee Rhyodacite
E417	Porphyritic rhyodacite	Med. gr. phenos. plagioclase, perthite, quartz, chlorite clots (after cpx.) in a fine gr. matrix (crypto-crystalline and devit.) with fine gr. crystal chips. Shard outlines preserved	Phenos. 30% of which Plag. 45% Perthite 45% Cpx. 10%	Cpx. → chlorite Feldspars → sericitized	✓	Unnamed rhyodacitic-dacitic ash-flow sheet. Contains a few rock frags.
E434	Porphyritic rhyolite	Med. gr. phenos. quartz + med.-coarse gr. phenos. plag. & K-feldspar in a micro-granophyric quartz-K-feldspar matrix. Minor chlorite & opaque clots	Phenos. 18% of which Plag. 50% Qtz. 20% K-feldsp. 30%	Feldspars sericitized. Chlorite + opaques in matrix	✓	Wheepool Rhyolite
E438	Lithic-vitric tuff	Chloritized, highly angular acid volcanic rock fragments - mostly devitrified and some showing excellent vitroclastic textures + highly angular crystal chips of quartz + plag. + K-feldsp. + glassy frags. in a devit. glassy matrix. Of ash-flow origin.				Wheepool Rhyolite. Fragmental zone at upper contact
E445	Porphyritic rhyolite	Med. gr. phenocrysts plagioclase, K-feldspar and quartz in a finely-granophyric matrix of quartz and reddened K-feldspar	Phenos. 35% of which Plag. 40% K-feldsp. 40% Quartz 20%	Feldspars sericitized (particularly K-feldspar)	✓	Wheepool Rhyolite
E457	Lithic tuff	Variety of angular, acid volc. rock fragments, e.g. flow-banded rhyolites + vitric tuffs + pumice fragments, in a fine, devitrified glassy matrix showing abundant fine shards. Clearly of pyroclastic origin, possibly air-fall deposit.				Waurea Pyroclastic - from lapilli-tuff above Nuckulla Basalt

E459	Basalt	Similar description to E231			✓	Nuckulla Basalt
E468	Fine-grained dacite	Sparse fine gr. phenos. plag. + chloritized cpx. + opaques in micro-granophyric qtz. + K-feldspar + chlorite matrix. Hematised K-feldspar	Phenos. < 4% Mainly plagio-clase	Cpx. → chlorit. Plag. → sericit. Much hematite in matrix	✓	Childera Dacite
E488	Granite	Holocrystalline rock composed of interlocking quartz + microcline + plagioclase + biotite + sphene. Some of microcline is perthitic	Qtz.40% Mic. 45% Plag. 10% Biot. + sph. 5%	Slight		Granite outcrop associated with Moonamby Dyke-suite in west.
E494	Fine-grained dacite	Sparse, fine-med. gr. phenos. plag. + flattened chlorite-epidote-quartz-filled amygdales (vapour phase minerals) within microcrystalline quartz-reddened feldspar-chlorite matrix	Phenos. < 2% are entirely plagioclase. Amygdales ~ 4%	Plag. → sauss-uritized. Much chlorite in matrix.	✓	Childera Dacite
E500	Fine-grained andesite	Sparse fine gr. phenos. euhedral plag. in a micro-crystalline matrix of chlorite + opaques + plag. microlites + reddened K-feldspar + quartz	Phenos. < 2% of which Opaques 20% Plag. 40% Chlorite 30%	Cpx. → chlorite Plag.(phenos.)→ sericitized opaques → leucoxene	✓	Childera Dacite - andesitic variant
E509	Porphyritic rhyolite	Coarse gr. phenos. perthite in mosaic of quartz aggregates + K-feldspar. Outlines of contorted shards under P.P. light	Phenos. 15% of which Perthite 90% Quartz 10%	Perthite → sericitized (except for albite exsolution)	✓	Arburee Rhyolite - visible shard outlines
E512	Fine-grained dacite	Similar description to E62			✓	Bunburn Dacite
E515	Porphyritic rhyolite	Med. gr. phenos. anhedral quartz + plagioclase + K-feldspar + sphene + chlorite (after biotite) + biotite in a microgranular qtz.-rich matrix. Many crystal "chips" (especially of quartz)	Phenos. 60% of which K-fels. 35% plag. 20% quartz 35% others 5%	Plag. → sauss. biotite → chlorite some secondary hematite	✓	Yandoolka Rhyolite. Abundance and variety of pheno-crysts is striking
E516	Granophyre	Granophyric intergrowth of quartz & K-feldspar i.e., blebs of quartz in regular orientation in K-feldspar. A few complete crystals of qtz. & K-feldsp. & rarer plag.	Quartz 40% K-felds 45% plag. 15%	Feldspars extensively sericitized	✓	Palthrubie Granophyre
E519	Porphyritic dacite	Similar description to E48			✓	Mangaroongah Dacite
E524	Porphyritic andesite	Fine gr. phenos. plagioclase and cpx. in an intersertal matrix consisting of plag. microlites surrounded by aphanitic minerals (after glass) & opaques	Phenos. 20% of which Plag. 50% Cpx. 50%	Cpx. fresh & → chloritized Plag.→ sericitized Opaq. → leucoxene	✓	Mangaroongah Dacite - andesitic variant
E530	Porphyritic rhyodacite	Med. gr. euhedral phenos. plag. in a finely-granophyric matrix of redcened K-feldspar + quartz + minor chlorite	Phenos. 18% of which Plag. 95% Cpx. 5%	Cpx. → chlorite Plag. → sericit.	✓	Yantea Rhyodacite

E532	Porphyritic andesite	Fine-med. gr. phenos. plag. + fine gr. cpx., sometimes in glomeroporphyritic aggregates, in a matrix of unoriented plag. microlites + chlorite + leucox. + aphanitic material.	Phenos. 15% of which Plag. 60% Cpx. 40%	Cpx.-fresh Plag. partially sericitized	✓	Mangaroongah Dacite - andesitic variant
E540	Porphyritic dacite	Fine to med. gr. phenos. plag. and green biotite in microcrystalline felsic matrix of qtz. + plag. microlites + reddened K-feldspar. Vitroclastic textures preserved	Phenos. 10% of which Plag. 60% Biotite 40%	Plag. → sericitized Biotite partially altered to chlorite K-feldsp.→ hematised	✓	Bunburn Dacite slightly more phenocryst -rich & biotite-rich variant
E554	Porphyritic rhyolite	Med.-coarse gr. phenos. orthoclase + perthite + plagioclase + quartz in patchy matrix composed of quartz plates interlocking with acicular qtz. + K-feldspar	Phenos. 15% of which K-feldsp.65% Plag. 30% Quartz 15%	Feldsp. phenos. sericitized Matrix reddened by hematite	✓	Aburee Rhyolite
E558	Porphyritic rhyodacite	Similar description to E294			✓	Yantea Rhyodacite
E561	Porphyritic dacite	Sparse, med.-fine gr. phenos. plag. in a microlitic matrix composed of plag. microlites + leucoxenised opaques + qtz. + reddened K-feldspar + chlorite	Phenos. 10% of which Plag. 95% Cpx. 5%	Feldspars are sericite dusted K-felds.→ hematite stained. Cpx → chlorite Opaq.→ leucox.	✓	Whyeela Dacite - typical example
E574	Porphyritic dacite	Fine-coarse gr. phenos. plag. (one markedly zoned) + cpx. in matrix of oriented plag. microlites + chlorite + opaques + quartz + reddened K-feldspar	Phenos. 8% of which Plag. 70% Cpx. 30%	Plag.-sericite dusted Cpx.- fresh	✓	Mangaroongah Dacite - green spots correspond to chlorite-rich patches. Zoned plag. of note
E579	Porphyritic rhyodacite	Medium gr. subhedral phenos. plag., often in glomero-porph. aggregates with clots chlorite (after cpx.) in matrix quartz + reddened K-feldspar which is patchy in part	Phenos. 15% of which Plag. 85% Cpx. 15%	Cpx. → chlorite Plag. → sericite dusted	✓	Mordinyabee Rhyodacite
E590	Porphyritic rhyodacite	Similar description to E579, except less abundant plag. phenos. & more chlorite in matrix	Phenos. 10% of which Plag. 80% Cpx. 20%	Cpx. → chlorite Plag.→ sericitized K-fels.→ hematised	✓	Mordinyabee Rhyodacite
E599	Porphyritic dacite	Fine-med. gr. phenos. plag. + chlorite psuedomorphs (after cpx.) + skeletal opaques (altering to leucoxene) in snow-flake textured g/mass consisting of plates of quartz & reddened K-feldspar	Phenos. 18% of which Plag. 75% Cpx. 20% Opaques 5%	Plag.→ sericitized Cpx. →chloritized Matrix K-felds → hematised Opaques →leucoxene	✓	Mordinyabee Rhyodacite - skeletal, altered opaques & snowflake texture are distinctive
E607	Porphyritic rhyolite	Med.-coarse phenos. anhedral, embayed quartz + plagioclase + perthite in a snowflake-textured matrix with optically coherent plates quartz + reddened K-feldspar	Phenos. 20% of which Plag. 40% Perthite 40%	Feldspar phenos. sericitized-especially K-feldspar. Matrix hematised	✓	Wheepool Rhyolite
E615	Porphyritic rhyolite	Similar description to E607			✓	Wheepool Rhyolite

E618	Lithic tuff	Subrounded fragments of devitrified rhyolite (mainly Wheepool Rhyolite) + vitric tuff + crystals of quartz + K-feldspar in vitric matrix - composed entirely of contorted & flattened shards. Excellent textural preservation				Ash-flow tuff unit separating Wheepool Rhyolite & Yantea Rhyodacite
E627	Porphyritic rhyolite	Medium gr. subhedral phenos. plag. + plates of altered biotite (see E282) in microgranular matrix of K-feldsp. microphenocrysts + devitrified quartzo-feldspathic mosaic	Phenos. 8% Microphenos. 10% Matrix 77% Biotite 5%	Plag.&K-feldsp. sericitized. Biotite → opaques + leucox.+sphene	✓	Karkulta Rhyolite - presence of biotite + K-feldspar micro-phenocrysts is distinctive
E630	Air-fall tuff	Graded, bedded & unwelded. Crystal chips + fine ashy material + delicately-shaped shards - are completely undeformed. Excellent textural preservation				Air-fall tuff separating Karkulta Rhyolite & Yantea Rhyodacite
E633	Porphyritic rhyolite	Medium gr. phenos. plag. + K-feldspar + anhedral quartz + biotite in a devitrified quartz + K-feldspar + opaque-rich matrix, showing excellent vitroclastic textures - mainly compressed shards	Phenos. 10% of which Plag. 60% Quartz 15% K-felds. 25%	Feldspars → sericitized. Biotite → opaques + sphene	✓	Karkulta Rhyolite-superficially resembles E627. Vitroclastic textures clear evidence of ash-flow origin
E664	Porphyritic rhyolite	Med.-coarse gr. phenos. plag. + albitized K-feldspar in a microgranular qtz. + plag. + K-feldsp. matrix	Phenos. 15% of which Plag. 85% K-feldsp. 15%	Extreme sericitization of plag. Albiti-zation of K-feldsp.	✓	Arburee Rhyolite, a plagioclase-rich variant
E665	Porphyritic rhyolite	Medium gr. phenos. plag. & perthite + aggregates of granular quartz in a microcrystalline devitrified matrix of quartzo-feldspathic material showing vitroclastic textures	Phenos. 15% of which Plag. 50% Perthite 50%	Feldspars - sericitized. Matrix reddened by hematite	✓	Unnamed unit of small areal extent
E670 & E671	Welded tuffs	Crystals of quartz, K-feldsp. & plag. + rock fragments + collapsed pumice in a contorted, glassy matrix of extremely flattened shards				Baldry Rhyolite. Both welded, ash-flow tuffs with well pre-served textures
E674	Fine-grained rhyolite	Sparse med. gr. phenos. plag. in a microcryst., devitrified matrix of quartz + plag. + K-feldspar + opaques + clots of sericite	Phenos. < 2% of rock	Plag.-sericitized	✓	Bunburn Dacite - originally a vitric tuff
E689	Fine-grained andesite	Sparse, fine gr. phenos. plag. within a microcryst. felsic matrix with abundant chlorite. Little visible qtz. in matrix, some chlorite-filled amygdales	Phenos. < 1% Amyg. ~ 3%	Plag.sericitized Abundant chlorite in matrix	✓	Bunburn Dacite - andesitic variant
E696	Lithic wacke	Variety of fine gr. devitrified acid volcanic rock fragments + crystals quartz, K-feldspar & plag. all closely packed, with little fine matrix.	Rock frags. 60% Crystals 40%	Some secondary hematite		Epiclastic - at base of Yantea Rhyodacite
E704	Porphyritic rhyodacite	Fine to med. gr. phenos. plag. + K-feldspar + quartz + rock fragments in a spherulitic devit. matrix showing excellent vitroclastic textures (e.g. compressed shards)	Phenos. 15% of which Plag. 60% K-feldsp.25% Quartz 15%	Plag.-sericite dusted. Matrix K-feldspar is hematite stained	✓	Unnamed rhyodacite unit, overlying Yantea Rhyodacite - of small areal extent
E705	Porphyritic rhyodacite	Coarse gr. anhedral phenos. K-feldspar + med. coarse gr. plag. + fine-med. gr. cpx. + granular cpx. - plag. aggregates (rock frags.?) in a granophyric qtz.-K-feldspar-chlorite matrix	Phenos. 40% of which K-feldsp.60% Plag. 20% Cpx. 20%	Cpx.→ chlorite & biotite Plag. →sericitized K-feldsp.-fresh Hematite in matrix	✓	Rhyodacite plug, probably an eroded feeder. Granular aggregates & phenos. probably accessory

E713	Porphyritic rhyodacite	Med. gr. phenos. plag. + clots chlorite (often in glomeroporphyritic aggregates with plag.) in microgranular matrix qtz. + plag. + reddened K-feldspar + minor chlorite	Phenos. 15% of which Plag. 80% Cpx. 20%	Plag.→ sauss. Cpx.→ chlorite Matrix K-feldsp is hematite stained	✓	Yantea Rhyodacite
E714	Porphyritic rhyolite	Med. gr. phenos. anhedral, embayed quartz + anhedral K-feldspar in a patchy, devitrified matrix consisting of qtz.-feldspar intergrowths. Hematite & chlorite are scattered throughout	Phenos. 20% of which Quartz 50% K-feldspar 50%	K-feldsp.→sericitized. Much hematite & chlorite in rock	✓	Wheepool Rhyolite. Primary devitrification textures preserved in matrix
E718	Porphyritic dacite	Fine-med. gr. phenos. plag. + cpx. + opaques (plag. & cpx. commonly in glomeroporph. aggs.) in microgranular qtz.-K-feldspar matrix. Although devitrified, vitroclastic textures still evident	Phenos. 35% of which Plag.65% Cpx. 30% Opaque 5%	Plag.→ sauss. Cpx.mainly fresh but partially altered to chlorite	✓	Yardea Dacite - at base of ash-flow sheet
E725	Porphyritic dacite	Med. gr. euhedral-subhedral phenos. plag. & cpx. & anhedral opaques (ilmenite?) in micro-granophyric matrix of quartz + reddened K-feldspar + chlorite	Phenos. 35% of which Plag. 60% Cpx. 30% Opqs. 10%	Plag.→ sericitized Cpx.→ fresh & chloritized Opaques→ leucoxene Matrix K-feldsp.→ hematised	✓	Yardea Dacite - typical example
E742	Porphyritic dacite	Med. gr. plag. phenos. of two types: (1) coarser, highly corroded & sericitized (2) finer, euhedral, well twinned, $comp^{n}$-Ab_{56}. Fine-med. gr. phenos. opx (hypersthene) + rarer cpx. + opaques. Some rock frags. + crystal chips. In matrix, finely microlitic texture produced by devitrification. Rare grains of altered biotite	Phenos. 20% of which Plag. 70% Opx. 25% Cpx. 2% Opq. 3%	Plag.-larger (earlier?)phenos. sericitized. Cpx & Opx-fresh but cracks & margins chloritized Matrix not reddened by hematite	✓	Whyeela Dacite - Presence of opx. as dominant pyroxene unusual, as is presence of biotite. Texture clearly indicative of ash-flow origin
E747	Porphyritic dacite	Fine-med. gr. euhedral phenos. plag. + rare cpx. + opaques + large rock fragment in a matrix composed of unaltered plag. microlites + aphanitic material (after glass)	Phenos. 15% of which Plag. 85% Cpx. 11% Opq. 4%	Plag.→ sericitized Cpx.→ chloritized Matrix reddened by hematite	✓	Mangaroongah Dacite.
	The following samples, prefixed "Y" are from the Hiltaba area.					
Y9	Gneiss	Metamorphically-recrystallised aggregate of quartz, porphyroblasts K-feldspar & plag. layered with chlorite-epidote-opaque rich bands & streaks	Variable, due to patchy development of mafic mineral streaks	Mafic minerals→ chlorite & epidote Plag.→ sericitized	✓	From basement gneiss outcrop
Y16	Adamellite	Holocrystalline rock consisting of coarse grains qtz. + perthitic K-feldspar + plagioclase + biotite + opaques	Perthite 45% Quartz 35% Plag. 17% Biot.+ opq. 3%	Some albitization of K-feldspar	✓	Hiltaba Granite, near Hiltaba homestead

Y28	Porphyritic dacite	Medium-grained phenos. plag. + rare K-feldspar + fine gr. cpx. + opaques (often in glomeroporph. aggregates) in a granophyric qtz.-K-feldspar matrix	Phenos 45% of which Plag. 70% Cpx. 25% K-feldsp. 3%	Plag.-completely sericitized Cpx.fresh & chloritized	✓	Yardea Dacite near Lake Acraman
Y743	Granite	Holocrystalline rock consisting of coarse gr. K-feldspar (mainly microcline) + pericline twinned plag. + intergranular qtz. & biotite	K-feldsp.50% Qtz. 35% Plag. 14% Biotite 1-2%	Plag. & K-feldspar show some sericitization	✓	Hiltaba Granite, near Hiltaba homestead. A "true" granite
Y752	Amphibolite	Recrystallised texture of green amphibole interlocking with plag. + abundant scattered, fine gr. opaques, within quartz-K-feldspar matrix typical of Yardea Dacite	Amphib. 50% Plag. 46% Opaques 4%	Plag.-sericitized Amph.-some haematite added	✓	Basic inclusion within Yardea Dacite. No primary textures preserved
Y771	Plagioclase-rich amphibolite	Laths plagioclase interlocking with granular amphibole, amphibole needles (up to 4 mm long) and scattered opaques. Quartz is intergranular and in veins.	Plag. 70% Amphib. 20% Opaque 5% Quartz 5%	Plag.-sericitized Other minerals fresh	✓	Basic inclusion in Yardea Dacite. No diagnostic primary textures
Y774	Aphanitic chlorite-rich rock	Recrystallised to a microcrystalline mosaic of chlorite + feldspar + opaques. Mosaic forms plates, exhibiting patchy polarisation	Chlorite & plag. in approx. equal proportions	Extensive alteration and recrystallisation	✓	Basic inclusion in Yardea Dacite
	The following samples, prefixed "K" are from Kokatha area					
K101	Basalt	Subophitic texture consisting of tabular plag. laths interlocking with granular cpx. + opaques + chlorite. Fine-med. gr. phenos. olivine - typical shape, now completely uralitized	Olivine 15% Plag. 30% Cpx. 40% Rest 15%	Olivine→uralite. Plag. is fresh. Cpx. mostly fresh	✓	Basalt from lowest exposed stratigraphic level of GRV in Kokatha area
K33	Basalt	Subophitic texture consisting of tabular plag. laths interlocking with uralitized cpx. Occasional fresh cpx. grains & scattered opaques. Some original glassy mesostasis	Plag. 45% Cpx. 45% Opaques 5% Mesostasis 5%	Plag. → sericite - dusted. Cpx.→ fresh grains but largely uralitized Opaques fresh	✓	Basalt from lowest part of sequence, Kokatha
K110	Basalt	Similar description to K33 Plag. laths average 1.5 mm long	As for K33	Plag. extremely sericitized Cpx - uralitized	✓	Basalt low in sequence, same locality as K33
K122	Basaltic-andesite	Mass of felted plagioclase microlites, ave length .1 mm, oriented & defining pilotaxitic texture, interlocking with chlorite + opaques. Rare altered plag. phenos.			✓	Differentiated basalt, upper part of western basalt sequence
K153	Basaltic-andesite	Oriented plag. microlites defining pilotaxitic texture in which are scattered grains of cpx. + opaques + much intergranular chlorite	Plag. ~ 45% Cpx. 20% Chl. 30% Opaque 5%	Plag.→sericite-dusted. Chlorite after glass &/or cpx.	✓	Typical differentiated basalt from unit in east. Pilotaxitic texture of note.
K132	Granite	Holocrystalline rock consisting of coarse gr. crystals of perthitic microcline + quartz + biotite + rare plagioclase	Microc.60% Quartz 35% Plag. 3% Biotite 2%	Plag.-sericitized Biotite partially chloritized	✓	Hiltaba Granite equivalent in Kokatha area

TABLE A2.2. Geochemical data for selected rocks from the Gawler Range province, listed in order of increasing SiO_2.

	E231	E459	E532	E524	E312	E689	E33	E278	E227	E376	E747	E500	E290
SiO_2	52.14	52.05	58.16	59.64	59.70	60.11	60.37	61.65	62.30	62.58	62.88	63.33	63.34
Al_2O_3	17.13	17.45	16.15	15.58	15.35	17.21	15.37	14.11	17.65	17.41	15.32	14.10	15.44
$Fe_2O_3^t$	10.48	10.15	8.30	8.74	8.14	7.26	8.39	8.09	5.59	5.46	7.61	6.74	7.06
MnO	0.16	0.16	0.16	0.16	0.15	0.21	0.17	0.23	0.16	0.15	0.17	0.18	0.15
MgO	5.59	5.15	2.79	2.88	2.69	2.22	3.10	2.12	2.63	2.63	2.33	1.83	2.20
CaO	6.56	7.64	6.99	3.82	4.37	1.18	2.46	4.23	1.20	0.82	2.04	3.38	2.57
Na_2O	3.79	3.68	3.84	3.39	3.80	5.69	2.88	4.88	5.48	4.42	3.11	4.73	3.79
K_2O	2.39	1.97	1.97	3.90	3.84	3.73	5.05	1.90	3.68	5.06	5.06	3.25	4.42
TiO_2	1.18	1.21	1.15	1.22	1.23	1.16	1.21	1.39	0.95	0.99	1.13	1.19	1.10
P_2O_5	0.21	0.21	0.43	0.49	0.50	0.71	0.47	0.74	0.55	0.45	0.41	0.61	0.41
Total	99.63	99.67	99.94	99.82	99.77	99.48	99.47	99.34	100.09	99.97	100.06	99.34	100.48
LOI	2.52	2.54	2.63	1.80	2.06	2.12	2.18	1.71	1.78	2.08	1.57	2.48	1.87
Zr	159	158	294	310	309	311	315	281	273		371	251	408
Nb	8.6	9.3	13	12.5	12	15	14	17	13		13	19	14
Y	28	28	42	43	42	47	41	50	37		47	48	46
Ce	52	-	104	106	113	144	112	104	136		122	84	-
Nd	25	-	-	-	54	59	-	-	62		55		-
Sc	24	23	21	-	20	14	20	22	14.4		20	19	20
V	188	183	160	138	131	80	133	119	61		109	98	-
Cr	106	86	-	-	-	-	24	-	-		-	-	-
Ni	112	98	21	23	24	11	28	17	9		25	15	-
Rb	85	58	77	117	104	113	193	63	127		155	117	126
Sr	529	446	308	454	486	395	540	340	493		453	286	298
Ba	695	619	1000	1460	1450	1765	1780	975	1340		2830	1240	2170

	E50	E574	E512	E126	E519	E48	E742	E494	E561	E468	E705	E62	E718	Y28
SiO_2	63.97	64.33	64.42	64.44	64.84	65.02	65.14	65.19	65.42	65.95	66.12	66.15	66.90	66.97
$Al_2O_{3_t}$	14.83	14.86	17.65	15.65	14.98	15.04	15.16	14.35	14.83	14.12	16.39	16.27	14.36	14.24
Fe_2O_3	6.40	6.35	5.03	6.15	6.65	5.27	5.93	7.15	6.37	4.86	3.86	3.92	6.13	6.10
MnO	0.13	0.14	0.14	0.14	0.12	0.15	0.16	0.14	0.15	0.14	0.14	0.11	0.10	0.11
MgO	2.24	1.96	1.50	2.65	2.04	2.35	1.77	1.13	2.23	1.69	1.23	1.63	1.20	0.96
CaO	3.11	2.86	0.80	1.07	1.44	1.26	3.36	1.73	1.07	2.38	2.39	1.80	2.71	2.23
Na_2O	3.43	3.81	5.00	4.22	3.87	4.04	2.90	3.90	3.34	3.51	3.30	4.14	4.06	3.25
K_2O	4.58	4.26	4.69	4.50	4.68	5.50	4.21	4.82	4.82	5.37	5.30	4.95	4.07	4.70
TiO_2	1.03	0.96	0.79	0.97	1.10	0.97	1.00	1.23	1.01	0.76	0.59	0.72	0.79	0.82
P_2O_5	0.41	0.42	0.33	0.33	0.38	0.26	0.34	0.72	0.38	0.32	0.22	0.20	0.24	0.24
Total	100.13	99.05	100.35	100.12	100.10	99.86	99.97	100.36	99.62	99.10	99.54	99.89	100.56	99.62
LOI	0.63	1.69	2.23	2.27	2.01	1.54	0.55	1.33	2.59	2.77	1.35	1.65	1.29	1.11
Zr	282		365			542	476		402	243	324	334		402
Nb	16		16			16	16		14	16	17	16		22
Y	43		40			48	52		44	44	41	35		54
Ce	106		-			115	136		118	115	165	125		-
Nd	48		-			-	-		52	-	68	52		-
Sc	16		8			15	17		17	12	8	11		13
V	97		-			68	65		93	-	53	24		35
Cr	-		-			-	14		-	-	-	-		-
Ni	19		-			15	-		-	-	-	-		13
Rb	149		176			142	139		139	170	174	159		195
Sr	404		476			220	336		339	250	405	500		189
Ba	1670		2945			2940	2390		4110	1160	1610	1870		1290

	E168	E725	E713	E242	E84	E590	E599	E417	E258	E154	E704	E540	E530	E558
SiO_2	67.00	67.03	67.27	67.48	67.83	68.38	68.54	68.54	69.15	71.08	70.19	70.27	70.79	71.24
Al_2O_{3t}	15.86	14.03	14.77	15.83	14.02	14.34	13.88	14.41	14.26	14.45	14.07	15.40	14.28	13.85
Fe_2O_3	4.70	5.85	5.56	3.67	5.89	5.46	5.16	5.17	4.42	4.02	4.25	2.72	3.59	3.58
MnO	0.11	0.13	0.11	0.12	0.09	0.11	0.11	0.09	0.09	0.06	0.10	0.06	0.07	0.09
MgO	1.55	0.63	0.96	1.10	2.33	1.32	1.03	0.76	0.73	0.81	1.65	0.04	0.42	1.19
CaO	0.57	2.71	1.21	1.03	0.40	0.40	1.49	1.37	0.80	0.13	0.48	0.28	0.65	0.69
Na_2O	4.38	3.48	4.14	4.74	3.11	2.46	2.98	3.74	3.77	2.67	3.08	4.87	4.25	3.44
K_2O	5.01	4.68	5.26	4.71	5.33	6.19	5.55	5.21	5.96	6.31	5.14	5.39	6.00	6.36
TiO_2	0.67	0.83	0.65	0.68	0.75	0.81	0.65	0.63	0.84	0.44	0.58	0.37	0.40	0.43
P_2O_5	0.26	0.21	0.17	0.20	0.18	0.17	0.19	0.16	0.20	0.07	0.21	0.02	0.08	0.04
Total	100.11	99.58	100.10	99.55	99.03	99.64	99.58	100.08	100.22	100.04	99.75	99.42	100.53	99.91
LOI	1.40	1.43	1.87	1.73	1.90	2.47	1.94	1.12	1.03	1.50	.076	1.88	1.12	1.15
Zr	341	401	457		406	324	432	418	600		156	426	653	
Nb	14	20	15		21	15	22	24	16		21	19	21	
Y	36	54	49		60	47	66	65	50		45	45	53	
Ce	-	143	139		160	-	180	174	149		-	-	-	
Nd	-	59	58		-	-	69	-	53		-	-	-	
Sc	11.5	13	2.4		13	18	14	14	14		4.4	6	10	
V	-	43	12		47	-	-	-	-		-	-	-	
Cr	-	-	-		-	-	-	-	-		-	-	-	
Ni	-	12	-		10	-	-	-	-		-	-	-	
Rb	156	184	135		167	154	219	196	163		178	155	186	
Sr	430	181	104		79	148	168	188	137		44	296	65	
Ba	1730	1215	2760		1270	5200	1710	1520	3270		515	1940	1240	

	E294	E411	E579	E402	E136	E155	E515	E394	E255	E434	E395	E270	E674
SiO_2	71.37	71.41	71.48	71.51	71.56	71.66	72.03	72.17	72.34	72.86	73.33	73.56	73.61
$Al_2O_{3_t}$	13.93	13.97	13.69	13.46	14.22	13.93	14.03	13.71	13.58	13.04	14.14	12.71	13.68
Fe_2O_3	3.43	4.40	4.12	3.49	3.80	3.85	2.22	3.52	2.97	3.58	2.48	1.95	1.97
MnO	0.06	0.06	0.08	0.05	0.08	0.07	0.06	0.05	0.07	0.06	0.04	0.05	0.06
MgO	0.50	0.33	1.00	0.44	1.53	0.67	0.35	0.51	0.99	0.76	0.28	0.50	0.41
CaO	0.37	0.21	0.65	0.17	0.27	0.31	1.33	0.18	0.29	0.20	0.29	0.17	0.18
Na_2O	3.67	3.32	3.17	3.30	2.19	3.67	3.60	2.40	3.57	2.54	5.88	3.39	4.23
K_2O	6.13	5.85	4.59	6.41	6.25	5.59	5.48	6.48	5.36	6.54	2.48	7.31	5.22
TiO_2	0.44	0.32	0.66	0.41	0.45	0.40	0.37	0.45	0.42	0.35	0.36	0.31	0.14
P_2O_5	0.05	0.06	0.17	0.04	0.06	0.08	0.10	0.05	0.10	0.03	0.04	0.06	0.05
Total	99.95	99.93	99.61	99.28	100.41	100.23	99.57	99.52	99.69	99.96	99.32	100.01	99.55
LOI	0.92	1.25	1.49	1.00	1.33	1.21	1.07	2.06	1.07	1.11	1.02	1.47	0.75
Zr	654			643			239		347	412	569		
Nb	20			20			19		20	20	17		
Y	49			47			33		51	48	41		
Ce	144			-			139		-	-	-		
Nd	61			-			-		-	-	-		
Sc	11			8			5		7.5	8	9		
V	8			-			-		-	-	-		
Cr	-			-			-		-	-	-		
Ni	-			-			-		-	-	-		
Rb	174			174			209		220	205	70		
Sr	49			58			240		84	45	76		
Ba	1170			1160			930		997	1005	550		

	E627	E607	E554	E636	E615	K132	E455	E78	Y16	E197	E145	E326	Y734	E230
SiO_2	73.90	74.00	74.57	74.67	74.67	74.97	75.39	75.68	75.81	76.37	76.43	76.63	76.64	76.71
$Al_2O_{3_t}$	13.75	13.31	13.06	13.53	12.94	13.00	12.56	12.40	11.69	12.85	11.42	13.29	11.92	12.54
Fe_2O_3	1.85	2.49	2.40	1.41	3.37	1.88	2.26	1.45	1.53	1.06	2.51	1.48	1.71	1.95
MnO	0.04	0.05	0.04	0.05	0.03	0.04	0.08	0.04	0.03	0.03	0.04	0.02	0.03	0.00
MgO	0.38	0.75	0.36	0.59	0.20	0.21	0.09	0.32	0.26	0.62	0.70	0.24	0.16	0.45
CaO	0.34	0.28	0.09	0.35	0.12	0.89	0.50	0.18	0.69	0.21	0.13	0.29	0.44	0.15
Na_2O	3.91	2.71	2.28	3.37	2.64	3.12	2.65	2.11	5.17	2.96	2.06	3.00	2.98	2.63
K_2O	4.91	6.30	7.14	5.06	5.89	5.47	6.01	7.27	4.74	5.88	5.84	5.51	5.45	5.60
TiO_2	0.14	0.35	0.32	0.14	0.28	0.22	0.29	0.31	0.21	0.16	0.36	0.17	0.17	0.18
P_2O_5	0.02	0.03	0.06	0.06	0.06	0.02	0.02	0.04	0.05	0.01	0.17	0.03	0.01	0.12
Total	99.24	100.24	100.26	99.23	100.20	99.82	99.85	99.80	100.18	100.14	99.66	100.66	99.51	100.33
LOI	1.62	1.04	0.69	0.94	0.86	0.59	1.38	0.95	0.43	1.31	1.10	0.81	0.69	0.85
Zr	132	413	312		328	213		298	184	168			218	191
Nb	14	22	24		20	18		23	24	24			23	21
Y	23	48	53		49	48		60	19	42			64	47
Ce	-	125	143		-	151		117		-			147	-
Nd	-	46	50		-	-		45		-			55	-
Sc	2.4	8	6		6	4		5	6	3			3	3
V	-	9.6	-		-	-		-		-			-	-
Cr	-	-	-		-	-		-		-			-	-
Ni	-	-	-		-	-		-		-			-	-
Rb	133	198	210		214	253		211	375	241			318	321
Sr	131	38	50		44	86		85	61	19			30	45
Ba	2120	940	676		888	681		2010	284	87			206	443

	E664	E665	E132	E516	E224	E714	E221	E633	E322	E203	E509
SiO_2	76.72	76.85	77.26	77.37	77.38	77.82	78.93	79.48	79.64	82.77	85.12
$Al_2O_{3_t}$	12.01	12.52	12.67	11.86	12.61	11.65	11.12	10.69	10.11	8.70	7.49
Fe_2O_3	2.24	2.72	1.50	1.48	0.66	1.83	0.94	0.82	0.39	0.56	1.23
MnO	0.02	0.04	0.05	0.01	0.03	0.02	0.02	0.03	0.00	0.00	0.01
MgO	0.21	0.30	0.56	0.00	0.34	0.33	0.13	0.11	0.00	0.02	0.16
CaO	0.24	0.11	0.22	0.12	0.24	0.13	0.07	0.12	0.15	0.14	0.23
Na_2O	5.62	2.07	2.43	2.55	2.65	2.19	1.65	0.59	0.35	1.00	0.55
K_2O	2.08	4.81	4.48	6.09	5.57	5.95	6.92	8.17	8.81	6.52	5.10
TiO_2	0.29	0.12	0.16	0.19	0.13	0.20	0.12	0.12	0.07	0.10	0.18
P_2O_5	0.02	0.04	0.01	0.01	0.03	0.07	0.01	0.02	0.01	0.00	0.03
Total	99.45	99.58	99.24	99.68	99.64	100.17	99.91	100.15	99.53	99.81	100.12
LOI	0.87	0.99	1.39	0.78	0.71	0.60	1.99	0.93	0.82	0.67	1.04
Zr	270			239		289			92	121	
Nb	21			20		20			28	21	
Y	44			50		54			19	30	
Ce	-			136		-			-	-	
Nd	-			-		-			-	-	
Sc	4			4		4			2	1	
V	-			-		-			-	-	
Cr	-			-		-			-	-	
Ni	-			-		-			-	-	
Rb	52			283		215			353	270	
Sr	135			58		26			29	21	
Ba	724			595		480			257	403	

TABLE A2.3. Geochemical data for selected rocks from the Gawler Range province, grouped according to formation.

	CHILDERA DACITE					MANGAROONGAH DACITE								
	E278	E500	E50	E468	E494	E532	E524	E33	E747	E290	E126	E574	E519	E48
SiO_2	61.65	63.33	63.97	65.95	65.19	58.16	59.64	60.37	62.88	63.34	64.44	64.33	64.84	65.02
Al_2O_3	14.11	14.10	14.83	14.12	14.35	16.15	15.58	15.37	15.32	15.44	15.65	14.86	14.98	15.04
Fe_2O_3 t	8.09	6.74	6.40	4.86	7.15	8.30	8.74	8.39	7.61	7.06	6.15	6.35	6.65	5.27
MnO	0.23	0.18	0.13	0.14	0.14	0.16	0.16	0.17	0.17	0.15	0.14	0.14	0.12	0.15
MgO	2.12	1.83	2.24	1.69	1.13	2.79	2.88	3.10	2.33	2.20	2.65	1.96	2.04	2.35
CaO	4.23	3.38	3.11	2.38	1.73	6.99	3.82	2.46	2.04	2.57	1.07	2.86	1.44	1.26
Na_2O	4.88	4.73	3.43	3.51	3.90	3.84	3.39	2.88	3.11	3.79	4.22	3.81	3.87	4.04
K_2O	1.90	3.25	4.58	5.37	4.82	1.97	3.90	5.05	5.06	4.42	4.50	4.26	4.68	5.50
TiO_2	1.39	1.19	1.03	0.76	1.23	1.15	1.22	1.21	1.13	1.10	0.97	0.06	1.10	0.97
P_2O_5	0.74	0.61	0.41	0.32	0.72	0.43	0.49	0.47	0.41	0.41	0.33	0.42	0.38	0.26
Total	99.34	99.34	100.13	99.10	100.36	99.94	99.82	99.47	100.06	100.48	100.12	99.95	100.10	99.86
LOI	1.71	2.48	0.63	2.77	1.33	2.63	1.80	2.18	1.57	1.87	2.27	1.69	2.01	1.54
Zr	281	251	282	243		294	310	315	371	408				542
Nb	17	19	16	16		13	12.5	14	13	14				16
Y	50	48	43	44		42	43	41	47	46				48
Ce	104	84	106	115		104	106	112	122	-				115
Nd	-	-	48	-		-	-	-	55	-				-
Sc	22	19	16	12		21	-	20	20	20				15
V	119	98	97	-		160	138	133	109	-				68
Cr	-	-	-	-		-	-	24	-	-				-
Ni	17	15	19	-		21	23	28	25	-				15
Rb	63	117	149	170		77	117	193	155	126				142
Sr	340	286	404	250		308	454	540	453	298				220
Ba	975	1240	1670	1160		1000	1460	1780	2830	2170				2940

	ARBUREE RHYOLITE				KARKULTA RHYOLITE			BUNBURN DACITE					
	E554	E78	E664	E509	E627	E636	E633	E689	E227	E376	E512	E62	E168
SiO_2	74.57	75.68	76.72	85.12	73.90	74.67	79.48	60.11	62.20	62.58	64.42	66.15	67.00
$Al_2O_{3_t}$	13.06	12.40	12.01	7.49	13.75	13.53	10.69	17.21	17.65	17.41	17.65	16.27	15.86
Fe_2O_3	2.40	1.45	2.24	1.23	1.85	1.41	0.82	7.26	5.59	5.46	5.03	3.92	4.70
MnO	0.04	0.04	0.02	0.01	0.04	0.05	0.03	0.21	0.16	0.15	0.14	0.11	0.11
MgO	0.36	0.32	0.21	0.16	0.38	0.59	0.11	2.22	2.63	2.63	1.50	1.63	1.55
CaO	0.09	0.18	0.24	0.23	0.34	0.35	0.12	1.18	1.20	0.82	0.80	1.80	0.57
Na_2O	2.28	2.11	5.62	0.55	3.91	3.37	0.59	5.69	5.48	4.42	5.00	4.14	4.38
K_2O	7.14	7.27	2.08	5.10	4.91	5.06	8.17	3.73	3.68	5.06	4.69	4.95	5.01
TiO_2	0.32	0.31	0.29	0.18	0.14	0.14	0.12	1.16	0.95	0.99	0.79	0.72	0.67
P_2O_5	0.06	0.04	0.02	0.03	0.02	0.06	0.02	0.71	0.55	0.45	0.33	0.20	0.26
Total	100.26	99.80	99.45	100.12	99.24	99.23	100.15	99.48	100.09	99.97	100.35	99.89	100.11
LOI	0.69	0.95	0.87	1.04	1.62	0.94	0.93	2.12	1.78	2.08	2.23	1.65	1.40
Zr	312	298	270		132			311	273		365	334	314
Nb	24	23	21		14			15	13		16	16	14
Y	53	60	44		23			47	37		40	35	36
Ce	143	117	-		-			144	136		-	125	-
Nd	50	45	-		-			59	62		-	52	-
Sc	6	5	4		2.4			14	14.4		8	11	11.5
V	-	-	-		-			80	61		-	24	-
Cr	-	-	-		-			-	-		-	-	-
Ni	-	-	-		-			11	9		-	-	-
Rb	210	211	52		133			113	127		176	159	156
Sr	50	85	135		131			395	493		476	500	430
Ba	676	2010	724		2120			1765	1340		2945	1870	1730

	BUNBURN DACITE cont.			BALDRY RHYOLITE		WAUREA PYROCLASTICS					NUCKULLA BASALT	
	E242	E540	E674	E326	E322	E197	E145	E132	E224	E203	E231	E459
SiO_2	67.48	70.27	73.61	76.63	79.64	76.37	76.43	77.26	77.38	82.77	52.14	52.05
Al_2O_{3t}	15.83	15.40	13.68	13.29	10.11	12.84	11.42	12.67	12.61	8.70	17.13	17.45
Fe_2O_3	3.67	2.72	1.97	1.48	0.39	1.06	2.51	1.50	0.66	0.56	10.48	10.15
MnO	0.12	0.06	0.06	0.02	0.00	0.03	0.04	0.05	0.03	0.00	0.16	0.16
MgO	1.10	0.04	0.41	0.24	0.00	0.62	0.70	0.56	0.34	0.02	5.59	5.15
CaO	1.03	0.28	0.18	0.29	0.15	0.21	0.13	0.22	0.24	0.14	6.56	7.64
Na_2O	4.74	4.87	4.23	3.00	0.35	2.96	2.06	2.43	2.65	1.00	3.79	3.68
K_2O	4.71	5.39	5.22	5.51	8.81	5.88	5.84	4.48	5.57	6.52	2.39	1.97
TiO_2	0.68	0.37	0.14	0.17	0.07	0.16	0.36	0.16	0.13	0.10	1.18	1.21
P_2O_5	0.20	0.02	0.05	0.03	0.01	0.01	0.17	0.01	0.03	0.00	0.21	0.21
Total	99.55	99.42	99.55	100.66	99.53	100.14	99.66	99.24	99.64	99.81	99.63	99.67
LOI	1.73	1.88	0.75	0.81	0.82	1.31	1.10	1.39	0.71	0.67	2.52	2.54
Zr		426			92	168				121	159	158
Nb		19			28	24				21	8.6	9.3
Y		45			19	42				30	28	28
Ce		-			-	-				-	52	-
Nd		-			-	-				-	25	-
Sc		6			2	3				1	24	23
V		-			-	-				-	188	183
Cr		-			-	-				-	106	86
Ni		-			-	-				-	112	98
Rb		155			353	241				270	85	58
Sr		296			29	19				21	529	446
Ba		1940			257	87				403	695	619

	WHEEPOOL RHYOLITE					MORDINYABEE RHYODACITE				YANTEA RHYODACITE			
	E434	E607	E615	E445	E714	E590	E599	E411	E579	E258	E530	E154	E558
SiO_2	72.86	74.00	74.67	75.39	77.82	68.38	68.54	71.41	71.48	69.15	70.79	71.08	71.24
$Al_2O_{3_t}$	13.04	13.31	12.94	12.56	11.65	14.34	13.88	13.97	13.69	14.26	14.28	14.45	13.85
Fe_2O_3	3.58	2.49	3.37	2.26	1.83	5.46	5.16	4.40	4.12	4.42	3.59	4.02	3.58
MnO	0.06	0.05	0.03	0.08	0.02	0.11	0.11	0.06	0.08	0.09	0.07	0.06	0.09
MgO	0.76	0.75	0.20	0.09	0.33	1.32	1.03	0.33	1.00	0.73	0.42	0.81	0.19
CaO	0.20	0.28	0.12	0.50	0.13	0.40	1.49	0.21	0.65	0.70	0.65	0.13	0.69
Na_2O	2.54	2.71	2.64	2.65	2.19	2.46	2.98	3.32	3.17	4.77	4.25	2.67	3.44
K_2O	6.54	6.30	5.89	6.01	5.95	6.19	5.55	5.85	4.59	5.96	6.00	6.31	6.36
TiO_2	0.35	0.35	0.28	0.29	0.20	0.81	0.65	0.32	0.66	0.84	0.40	0.44	0.43
P_2O_5	0.03	0.03	0.06	0.02	0.07	0.17	0.19	0.06	0.17	0.20	0.08	0.07	0.04
Total	99.96	100.24	100.20	99.85	100.17	99.64	99.58	99.93	99.61	100.22	100.53	100.04	99.91
LOI	1.11	1.04	0.86	1.38	0.60	2.47	1.94	1.25	1.49	1.03	1.12	1.50	1.15
Zr	412	413	348		289	324	432			600	653		
Nb	20	22	20		20	15	22			16	21		
Y	48	48	49		54	47	66			50	53		
Ce	-	125	-		-	-	180			149	-		
Nd	-	46	-		-	-	69			53	-		
Sc	8	8	6		4	18	14			14	10		
V	-	9.6	-		-	-	-			-	-		
Cr	-	-	-		-	-	-			-	-		
Ni	-	-	-		-	-	-			-	-		
Rb	205	198	214		215	154	219			163	186		
Sr	45	38	44		26	148	168			137	65		
Ba	1005	940	888		480	5200	1710			3270	1240		

	YANTEA RHYODACITE cont.						WHYEELA DACITE			YARDEA DACITE		
	E294	E402	E136	E155	E394	E395	E312	E742	E561	E718	Y28	E725
SiO_2	71.37	71.51	71.56	71.66	72.17	73.33	59.70	65.14	65.42	66.90	66.97	67.03
Al_2O_{3t}	13.93	13.46	14.22	13.93	13.71	14.14	15.35	15.16	14.83	14.36	14.24	140.3
Fe_2O_3	3.43	3.49	3.80	3.85	3.52	2.48	8.14	5.93	6.37	6.13	6.10	5.85
MnO	0.06	0.05	0.08	0.07	0.05	0.04	0.15	0.16	0.15	0.10	0.11	0.13
MgO	0.50	0.44	1.53	0.67	0.51	0.28	2.69	1.77	2.23	1.20	0.96	0.63
CaO	0.37	0.17	0.27	0.31	0.18	0.29	4.37	3.36	1.07	2.71	2.23	2.71
Na_2O	3.67	3.30	2.19	3.67	2.40	5.88	3.70	2.90	3.34	4.06	3.25	3.48
K_2O	6.13	6.41	6.25	5.59	6.48	2.48	3.84	4.21	4.82	4.07	4.70	4.68
TiO_2	0.44	0.41	0.45	0.40	0.45	0.36	1.23	1.00	1.01	0.79	0.82	0.83
P_2O_5	0.05	0.04	0.06	0.08	0.05	0.04	0.50	0.34	0.38	0.24	0.24	0.21
Total	99.95	99.28	100.41	100.23	99.52	99.32	99.77	99.97	99.62	100.56	99.62	99.58
LOI	0.92	1.00	1.33	1.21	2.06	1.02	2.06	0.55	2.59	1.29	1.11	1.43
Zr	654	643				569	309	476	402		402	401
Nb	20	20				17	12	16	14		22	20
Y	49	47				41	42	52	44		54	54
Ce	144	-				-	113	136	118		-	143
Nd	61	-				-	54	-	52		-	59
Sc	11	8				9	20	17	17		13	13
V	8	-				-	131	65	93		35	43
Cr	-	-				-	-	14	-		-	-
Ni	-	-				-	24	-	-		13	12
Rb	174	174				70	104	139	139		195	184
Sr	49	58				76	486	336	339		189	181
Ba	1170	116-				550	1450	2390	4110		1290	1215

	YANDOOLKA RHYOLITE	PALTHRUBIE GRANOPHYRE	HILTABA GRANITE			MOONAMBY DYKE - SUITE					
	E515	E516	K132	Y16	Y734	E705	I84	E417	E255	E270	E230
SiO_2	72.03	77.37	74.97	75.81	76.64	66.12	67.83	68.54	72.34	73.56	76.71
$Al_2O_{3_t}$	14.03	11.86	13.00	11.69	11.92	16.39	14.02	14.41	13.58	12.71	12.54
Fe_2O_3	2.22	1.48	1.88	1.52	1.71	3.86	5.89	5.17	2.97	1.95	1.95
MnO	0.06	0.01	0.04	0.03	0.03	0.14	0.09	0.09	0.07	0.05	0.00
MgO	0.35	0.00	0.21	0.26	0.16	1.24	2.33	0.76	0.99	0.50	0.45
CaO	1.33	0.12	0.89	0.69	0.44	2.39	0.40	1.37	0.29	0.17	0.15
Na_2O	3.60	2.55	3.12	5.17	2.98	3.30	3.11	3.74	3.57	3.39	2.63
K_2O	5.48	6.09	5.47	4.74	5.45	5.30	5.33	5.21	5.36	7.31	5.60
TiO_2	0.37	0.19	0.22	0.21	0.17	0.59	0.75	0.63	0.42	0.31	0.18
P_2O_5	0.10	0.01	0.02	0.05	0.01	0.22	0.18	0.16	0.10	0.06	0.12
Total	99.57	99.68	99.82	100.18	99.51	99.54	99.93	100.08	99.69	100.01	100.33
LOI	1.07	0.78	0.59	0.43	0.69	1.35	1.90	1.12	1.07	1.47	0.85
Zr	239	239	314	184	218	324	406	418	347		191
Nb	19	20	18	24	23	17	21	24	20		21
Y	33	50	48	19	64	41	60	65	51		47
Ce	139	136	151	-	147	165	160	174	-		-
Nd	-	-	-	-	55	68	-	-	-		-
Sc	5	4	4	6	3	8	13	14	7.5		3
V	-	-	-	-	-	53	47	-	-		-
Cr	-	-	-	-	-	-	-	-	-		-
Ni	-	-	-	-	-	-	10	-	-		-
Rb	209	283	253	375	318	174	167	196	220		321
Sr	240	58	86	61	30	405	79	188	84		45
Ba	930	595	681	284	206	1610	1270	1520	997		443

	VOLCANICS FROM LOCALISED, UNNAMED UNITS IN THE LAKE EVERARD AREA				BASALTS FROM THE KOKATHA AREA					BASIC XENOLITHS WITHIN YARDEA DACITE, HILTABA			BASEMENT GNEISS
	E713	E704	E665	E221	K101	K33	K110	K122	K153	Y752	Y774	Y771	Y9
SiO_2	67.27	70.19	76.85	78.93	51.91	52.01	51.94	54.28	53.69	48.62	54.69	57.65	70.57
Al_2O_{3t}	14.77	14.07	12.52	11.12	13.65	16.02	15.87	14.64	14.81	13.92	14.08	14.53	14.69
Fe_2O_3	5.56	4.25	2.72	0.94	9.66	0.79	10.18	12.02	13.57	15.04	13.29	11.05	3.82
MnO	0.11	0.10	0.04	0.02	0.18	0.19	0.18	0.23	0.21	0.39	0.31	0.25	0.07
MgO	0.96	1.65	0.30	0.13	11.77	8.44	7.72	3.27	3.53	2.91	2.87	2.31	0.64
CaO	1.21	0.48	0.11	0.07	8.55	8.62	8.88	6.57	6.54	7.09	5.67	4.94	1.82
Na_2O	4.14	3.08	2.07	1.65	2.15	2.51	2.59	3.01	3.23	3.30	2.85	3.22	3.00
K_2O	5.26	5.14	4.81	6.92	1.27	1.06	1.23	2.75	2.20	3.62	3.31	2.80	5.28
TiO_2	0.65	0.58	0.12	0.12	0.64	0.82	0.85	2.32	1.74	3.03	2.43	1.96	0.48
P_2O_5	0.17	0.21	0.04	0.01	0.18	0.25	0.24	1.07	0.40	1.57	0.88	0.78	0.16
Total	100.10	99.75	99.58	99.91	99.96	99.71	99.68	100.16	99.92	99.49	100.38	99.49	100.53
LOI	1.87	0.76	0.99	1.99	1.51	1.46	2.12	0.80	0.70	0.57	1.44	0.94	0.73
Zr	457	156			102	124	119	234	229	292	261	358	227
Nb	15	21			5.3	5.9	5.6	11	9.5	16	13	15	16
Y	49	45			19	23	24	52	40	98	58	68	29
Ce	139	-			78	58	54	120	86	172	129	135	-
Nd	58	-			36	-	21	63	45	-	-	-	-
Sc	2.4	4.4			29	30	32	32	28	36	33	23	-
V	12	-			180	176	179	167	280	178	205	140	32
Cr	-	-			1050	600	619	14	8.1	63	93	150	-
Ni	-	-			362	192	197	8.4	8.4	10	13	11	-
Rb	135	178			45	36	42	82	67	217	222	111	216
Sr	104	44			510	480	547	519	433	189	269	338	163
Ba	2760	515			1005	718	842	1700	976	1280	1220	1160	-

TABLE A 2.4. Rare earth element contents in selected samples from the Gawler Range province.

Sample Unit	K101 Kokatha Basalt	E231 Nuckulla Basalt	E312 Whyeela Dacite	E227 Bunburn Dacite	E747 Mangaroon-gah Dacite	E725 Yardea Dacite	E294 Yantea Rhyodacite	E607 Wheepool Rhyolite	E554 Arburee Rhyolite	E78 Arburee Rhyolite	Y734 Hiltaba Granite	Chondrite normalising factors
La	35	22	51.5	64	53.3	68	68	53.5	58	47	72	0.315
Ce	78	52	113	136	122	143	144	125	143	117	147	0.813
Nd	36	24.6	54.2	62	55.4	59	61	46	50	45	54.6	0.597
Sm	6.4	5.2	10.4	10.6	10.7	11	11.2	8.2	8.6	8.1	10.2	0.192
Eu	1.6	1.37	2.7	2.5	2.8	2.25	1.82	1.00	1.07	1.1	0.46	0.0722
Gd	5.0	5.1	9.3	8.4	11.4	10.6	9.4	6.7	7.4	7.9	9.6	0.259
Dy	3.8	4.4	7.5	6.3	7.33	8.9	8.3	6.1	8.0	9.3	9.2	0.325
Er	2.1	2.5	4.2	3.4	4.5	5.2	4.7	3.5	4.9	5.5	6.1	0.213
Yb	1.14	2.3	3.7	3.03	3.9	5.0	4.5	3.5	4.8	4.8	5.95	0.208
$\%SiO_2$	51.91	52.14	59.70	62.20	62.88	67.03	71.37	74.00	74.57	75.68	76.64	
%MgO	11.77	5.59	2.69	2.63	2.33	0.63	0.50	0.75	0.36	0.32	0.16	

Notes:
1. All values determined by mass spectrometer using an isotope dilution technique.
2. The chondrite normalising factors used to obtain the chondrite - normalised values plotted in Fig. 2.10 are listed in the last column.

TABLE A2.5. Calculated Sc, V and Y contents in mantle derived basic melts, assuming varying degrees of melting and a range of residual mineral assemblages.

Residue			% p.m.	Sc	V	Y	Residue			% p.m.	Sc	V	Y
Ol	Opx	Cpx					Ol	Opx	Cpx				
65	15	20	0.05	21.0	173	58	70	22.5	7.5	0.05	29.8	267	77.8
			0.10	21.0	162	37.9				0.10	29.0	235	45.0
			0.15	20.9	152	28.2				0.15	28.3	210	31.7
			0.20	20.9	143	22.4				0.20	27.6	190	24.4
			0.25	20.8	136	18.6				0.25	27.0	174	19.9
			0.30	20.7	129	15.9				0.30	26.4	160	16.8
			0.40	20.6	117	12.3				0.40	25.2	137	12.8
65	25	10	0.05	26.3	235	73	75	25	5	0.05	32.9	304	84.0
			0.10	25.9	211	43.3				0.10	31.8	262	47.0
			0.15	25.5	192	30.9				0.15	30.8	230	32.6
			0.20	25.1	176	24.0				0.20	29.8	205	24.9
			0.25	24.7	162	19.6				0.25	28.9	185	20.2
			0.30	24.3	150	16.6				0.30	28.1	169	17.0
			0.40	23.6	132	12.7				0.40	26.6	143	12.9
70	20	10	0.05	27.8	242	73	80	20	0	0.05	44.5	428	98.6
			0.10	27.2	217	43.4				0.10	41.8	343	50.9
			0.15	26.7	196	30.9				0.15	39.5	286	34.3
			0.20	26.2	179	24.0				0.20	37.3	245	25.9
			0.25	25.7	165	19.6				0.25	35.4	215	20.8
			0.30	25.2	153	16.6				0.30	33.7	191	17.4
			0.40	24.3	133	12.7				0.40	30.7	157	13.1
			K101	29	180	19							
			W3	28	197	23							
Primitive Archaean tholeiite				43	269	14							

Notes:

1. Assumed mantle contents are Sc = 20 ppm, V = 75 ppm and Y = 5.25 ppm (after Frey et al., 1977).
2. Distribution coefficients used are:

	Ol	Opx	Cpx
Sc	0.25	1.1	3.1
V	0.09	0.3	1.5
Y	0.002	0.009	0.20

(after compilation of Frey et al., 1977).
3. The calculations assume equilibrium or batch melting and use the form of the equation cited by Schilling and Winchester (1967), which requires a knowledge of the residual mineral assemblage at the time of magma segregation.

TABLE 3.1. Brief thin section descriptions of a representative selection of rocks from the Central Australian province.

SAMPLE NUMBER	ROCK NAME	DESCRIPTION	% MINERALS	ALTERATION	ANAL.	COMMENTS
B1	Lithic tuff (of dacitic comp^{n})	Variety of angular, accessory dacite fragments in a devitrified quartz-feldspar-chlorite matrix. Matrix originally glassy and shows excellent vitroclastic textures.	Rock frag. in glassy matrix. Some glomporph. plag.	Plag. → fresh Some chlorite and epidote in matrix		Glassy (shard-rich) matrix indicates of ash flow origin and is moderately welded
B2	Glassy rhyolite	Scattered phenos. plag. & K-feldspar within a devitrified matrix. Matrix contains numerous perlitic cracks, the cores of which are filled with granular, recryst. qtz. + epidote.	Phenos. comprise approx. 10% of rock		✓	Originally glassy. Perlitic cracking & quartz cores notable
B3	Leuco-gabbro	Tabular laths plagioclase up to 4mm long interlocking with amphibole and chlorite (after cpx.) forming subophitic texture. Scattered fine opaques.	Plag. 70% Amph.+ chlor.28% Opaque ~ 2%	Plag. fresh, minor epidote. Cpx→amph. + chl. Opaque → leucox. + sph.		Plagioclase-rich gabbro. Undoubtedly related to other gabbros
B4	Non-porphyritic rhyodacite	Fine gr. tabular laths plag. (randomly oriented) + acicular amphibole (partially altered to chlorite) in a "patchy" devit. felsic matrix. Scattered opaques.	Plag.laths ~ 18% Amph.~ 15% Matrix the remainder	Opaques → leucox. Amph. → chlorite Plag. → epidote in part.	✓	A volcanic, but unusual texture and high Na_2O due to abundant plag..
B6	Porphyritic rhyolite	Medium to fine gr. subhedral phenos. plag. and K-feldspar in a "snowflake" devit. felsic matrix. Some granular aggregates quartz.	Phenos. ~ 12% of which K-felds.~ 60% Plag. ~ 40%	K-feldsp. → albitized. Scattered hem. in matrix.		Typical acid volcanic, very comparable with Gawler Range rhyolite
B7	Porphyritic dacite	Fine-med. gr. phenos. plag. and cpx. in an unusual devit. matrix composed of interlocking, acicular glass microlites now dusted (& defined by) opaques. Scattered grains of opaques.	Crystals make up ~ 15% rock of which Plag. 60% Cpx 40%	Completely fresh. Finely-divided opaques give impress^{n} of isotropic glass.	✓	Originally a highly glassy rock. Acicular needles indicate rapid chilling
B8	Gabbro	Laths plag. up to 4cm long interlocking with cpx, chlorite and opaques forming a subophitic texture. Holocrystalline and no interstitial matrix.	Plag. 60% Cpx. 35% Opaques 5%	Plag. epidotized & sericited, some fresh Cpx. fresh, partially chloritized.	✓	Intrusive dyke, approx. 5m wide, offshoot from larger gabbro mass to south
B9 (1)	Recryst-allised acid volcanic	Non-porphyritic rock composed of spherulites of quartz-feldspar in radiating needles. Long thin needles of green amphibole. Trains of fine opaques follow outlines of radiating spherulites.	Quartz & feldspar, mainly. Amph. + Opaques ~ 5%	Opaques →leucox. Otherwise fresh		Fine granular qtz. indicates recryst. Minor granophyric texture. Contact metamorphosed acid volcanic?
B9 (2)	Recryst-allised acid volcanic	Non-porphyritic rock composed of an interlocking mosaic of quartz-K-feldspar & plagioclase in microgranophyric intergrowth. Scattered opaques & epidote.	Mainly qtz. & feldspars. Epid. ~ 5% Opaques ~5%	Much epidote & a little chlorite after plagioclase phenos?		Similar comments to B9(1). Possibly recryst. acid volcanic
B10	Contam-inated-gabbro	Non-porphyritic, holocrystalline rock composed of med. gr. plag. laths + altered cpx. + opaques in a microgranophyric + granular qtz. matrix	Plag. 60% Cpx 15% Opaques 4% Matrix 21%	Plag. fresh to epidotized & sericitized Cpx-fresh & chloritized	✓	Similarities in texture to B9, but opaques + plag. laths indicate related to gabbro

B11	Contaminated-gabbro	Similar texture & description to above, plag. more altered & more recrystallisation of matrix - margins of plag. been extensively corroded	Similar to above	Plag. → sericitized & epidotized (some fresh). Cpx → chlorite. Opaques → leucox. + sphene	✓	Clearly related to typical gabbros.
B12	Porphyritic rhyodacite	Fine to med. gr. phenos. plag. (euhedral & lath-like) + tabular & acicular amph. form "trails" on all scales in a felsic, recrystallised matrix	Phenos. ~ 10%	Opaq. → sphene + leucox. Cpx → amph. + chlorite. Plag. - sericitized	✓	Probably a volcanic, but could be a contaminated gabbro
B13	Recrystallised acid volcanic	Almost identical to B9(1), i.e., much recryst., acicular, spherulitic felsic intergrowths, linear and curved trains of opaques. Some possible plag. phenos.	Qtz.-feldspar ~ 90%. Rest opaques & amphibole	Much recrystallisation. Opaques → leucoxene + sphene. Plag. phenos. epidotized	✓	Has some volcanic features - porphyritic, spherulitic, but also some gabbroic texts
B14	Coarse dolerite	Holocrystalline rock composed of interlocking plag. laths (fresh & twinned) + cpx + opaques forming a true ophitic texture	Plag. 40% Cpx. 50% Opaques 10%	Plag. → sericitized & fresh. Cpx fresh & altered to amphibole (in part)	✓	Fresh example of basic intrusive related to gabbro
B15	Porphyritic rhyolite	Med.-coarse gr., embayed, plag. phenos. often in glomporph. aggregates (none zoned) in a micro-cryst. devit. matrix with "ghosty" compressed shards	Phenos. are all plag. & comprise 12% of rock	Plag. phenos. fresh but embayed. Much epidote & seric. in matrix	✓	Typical acid volcanic from region. Welded ash-flow tuff
B16	Porphyritic dacite	Euhedral, fine gr. phenos. plag. in a plag.-rich matrix composed of euhedral plag. laths + granular, recrystallised qtz. "Phenos." grade smaller in grainsize into matrix plagioclase	Mainly plagioclase + quartz. Minor opaques + amphibole ~ 10%	Opaque → leucoxene + sphene. Epidote + green amphibole present	✓	Plagioclase-rich volcanic. Volcanic from field observation. May be unrecrystallised equivalent of B13
B17	Porphyritic dacite	Scattered fine gr. phenos. plag. + amphibole - epidote rich clots in a matrix of plag. laths + quartz + acicular green amphibole	Plag. + qtz. ~ 85% Amphibole 15%	Epidotization sericitization of plag. Opaques → sphene.	✓	Volcanic from field relationships. Unrecryst. equivalent of B13 or B9? Plag.-rich
B18	Porphyritic rhyolite	Medium gr., altered & corroded plag. phenos. in a recrystallised quartz-rich matrix. No primary textures preserved		Much recrystallisation Clots of quartz. Plag.-epidotized		Recrystallisation due to proximity to gabbro
B19	Granophyre	Holocrystalline rock composed of tabular plag. laths + quartz-K feldspar granophyric intergrowths + trains of linear opaques + acicular green amphib.	Plag. ~ 25% Granoph. qtz.-K-feldsp. ~ 70% Op.+ amph. 5%	Epidotization & sericit. of plag.	✓	True granophyre. Gradational into B13 & B9. Possible recryst. volcanic?
B23	Basalt (uralitized)	Interlocking plag. laths (up to .5mm long) & green amphibole in an ophitic intergrowth. Scattered opaques + clots of granular quartz	Plag. 35% Amph. 60% Opaques, Qtz. } 5%	Plag. partially sericitized. Cpx. uralitized		Basalt from a sequence of basalts & rhyolites. Basalt is fractionated (high TiO_2)
B25	Recryst. dacite	Scattered med. gr. phenos. of plag. in a microcryst. quartz-feldspar-epidote matrix. Oriented acicular needles of green amphibole	Phenos. < 2% Amphibole 15% Qtz.-feldsp. comprise remainder	Much epidote. Extreme metamorphic recrystallisation		Dacite from same basalt-acid volcanic sequence that B23 taken from

B26	Porphyritic rhyolite	Med.-coarse gr. phenos. of microcline, often in glomeroporph. aggregates within microcryst. felsic matrix + opaques + sphene + amph.	Phenos. 25% all microcline	Fresh, some minor hematite scattered thro'		From same basalt-rhyolite sequence that B23 & 25 collected
B27	Porphyritic rhyolite	Med.-coarse gr. phenos. of plag. & K-feldspar & embayed quartz in a microcryst. devit. matrix which contains finely-divided opaques - imparting grey colour	Phenos 20% Plag. 75% K-feldsp. 20% Qtz. 5%	Plag. sericite-dusted, minor epidote		Typical acid volcanic. No diagnostic textures but probably ash-flow tuff
B28	Recrystallised acid volcanic	Identical description to B25 - i.e., rare plag. phenos. in a granular (recryst.) qtz-feldsp.-amphibole-opaque matrix	Felsic mins. 85% Rest 15%	Completely recryst. due to metamorphism		Metamorphosed & recrystallised acid volcanic. Due to proximity of Blackstone Range Gabbro
B29	Recrystallised acid volcanic	Similar to B28 - i.e., recryst. granoblastic aggregate of quartz-feldspar-green hornblende. Micro-phenocrysts of microline. Amph. defines foliat^{n}.	Felsic component ~ 85% Amph. 15%	Complete metamorphic recrystallisation	✓	As for B28 - from same area near Blackstone Range Gabbro
B30	Recrystallised acid volcanic	Similar to B28 & 29 - i.e. mosaic of quartz, feldspar, amphibole & minor opaques. Epidote common. Weak foliation. Rare plag. phenos.	As above	"		"
B31	Microgabbro	Holocrystalline, equigranular aggregate of cpx. + brown hornblende + plagioclase + opaques. Even grainsize ~ ave. 0.3mm diam.	Plag. 60% Cpx 25% Amph. 13% Opaque 2%	Quite fresh	✓	Marginal phase of Blackstone Range gabbro
B32	Troctolite or olivine gabbro	Holocrystalline rock composed of med.-coarse gr. plag. with olivine & cpx at grain boundaries	Plag. 80% Olivine 15% Cpx 5%	Cpx & olivine rimmed by brown amphibole. Completely fresh	✓	Typical Blackstone Range gabbro - very rich in basic plag.
B33	Gabbro	Coarse-grained, holocrystalline rock composed of interlocking plagioclase + cpx + olivine. Very similar to B32, but higher % cpx & lower % olivine	Plag. 80% Cpx 15% Olivine 5%	Minor sericitization of plag. & conversion of cpx to amph.	✓	Typical gabbro from Cavenagh Range - rich in basic plag.
B35	Adamellite	Coarse gr. holocrystalline rock consisting of interlocking plag. + perthite + albitized microcline + quartz + biotite + minor opaques.	Qtz. 35% K-felds. 40% Plag. 20% Biotite 5%	Albitization of K-feldspar. Minor sericitization of plagioclase	✓	Granite at Winburn Rocks, assoc. with Palgrave Cauldron
B36	Porphyritic rhyodacite	Fine gr. euhedral phenos. plag. (nearly all zoned), commonly in glomeroporph. aggregates + blue/green amphibole + opaques in a devit. felsic matrix	Phenos. 18% Plag. 90% Amph. 10%	Plag. sericitized Amphibole may be after cpx	✓	Probably an ash-flow tuff although no diagnostic textures, interlayered with ignimbrites
B37	Porphyritic rhyodacite	Fine-med. gr. phenos. plag. & K-feldspar + scattered green amphibole & opaques in a recrystallised felsic matrix showing microgranophyric textures	Phenos. 15% Plag. 70% K-feldsp. 30%	Secondary epidote & amphibole. Plag. partially sericitized		As for B36. Typical acid volc. from Palgrave Cauldron. Similar to B13 in matrix

B38	Lithic tuff	Subangular, devitrified acid volcanic rock frags. of lapilli size in close-packed matrix of ash size rock frags. & crystal chips + devit. glass	Mostly rock frags. + qtz. & feldspar crystal chips	Matix rich in epidote, sericite & fine opaques & green amph.		Of ash-flow origin. Some "fragment in fragment" lithic fragments.
B39	Lithic tuff	As above, variety of frags. - some glassy with perlitic cracking, some pilotaxitic lavas and others devitrified, all in a matrix rich in crystal-chips & ash-size fragments	"	"		Field relationship indicate of ash-flow origin. Same locality as B38
B42	Porphyritic rhyolite	Med. gr. phenos. of embayed quartz & K-feldspar in a devitrified & partially recrystallised matrix. Some "patch" & microgranophyric devit. Fine opaques throughout	Phenos. 20% Qtz. 50% K-feldsp. 50%	Secondary opaques → leucoxene & sphene & green amphibole	✓	Ghosted, glassy outlines indicating is a welded ash-flow tuff
B44	Granophyre	Holocrystalline rock composed of plag. laths + quartz + qtz.-K-feldspar granophyric intergrowths + green biotite-opaque-epidote intergranular clusters	Quartz 40% K-feldsp. 40% Plag. 15% Biotite etc. 5%	Biotite → green chlorite Plag. - sericite dusted	✓	Intrusive dyke. Appears aplitic in hand specimen
B45	Porphyritic rhyodacite	Fine-med. gr. phenos and crystal chips of quartz, plagioclase and K-feldspar in a matrix of angular chips & devitrified glass. Well oriented crystal frags.	Crystals approx. 25% of rock Quartz 40% K-feldsp. 40%	Scattered opaques & green amphibole & minor carbonate	✓	Typical "chippy" crystal-tuff with glassy matrix. Of ash-flow origin
B46	Recrystallised acid volcanic	Mosaic of granular quartz and feldspar (recrystallised) + needles and equant prisms of green hornblende. Scattered opaques + leucox. + sph.	Amphibole ~ 3% Rest is qtz. + feldspar	Minor sphene & leucox. after opaques		Metamorphically recryst. acid volcanic. Contorted flow bands in hand specimen
B47	Recrystallised acid volcanic	Mosaic of microcrystalline qtz. & feldspar with a foliation defined by oriented brown hornblende. No phenos, clots of quartz. Spherulitic vein with flerite	As above but finer grained	None, but metamorphic recrystallisation pervasive	✓	Kathleen Ignimbrite, Scamp Cauldron. Flow-banded in field
B49	Uralitized basalt	Interlocking green amphibole and plagioclase. Scattered opaques (relatively coarse) + epidote. Minor qtz.	Amphibole 70% Plag. 25% Opaque 5% + others	Cpx → utalitized Plag. → epidoitized in part	✓	Basalt at margin of Scamp Cauldron
B50	Recrystallised acid volcanic	Microcrystalline felsic, granular, mosaic. Occasional fine gr. albitized K-feldspar phenos. Scattered opaques and epidote	Nearly all qtz. & feldspar		✓	Typical acid volcanic from Scamp Volcanic Assoc^{n}. Flow-banded in field.
B53	Altered basalt	Interlocking feldspar (mainly plag.) & biotite & lesser qtz. + carbonate + opaques (typical of basalt). Some med. gr. phenos. of primary amph.	Biotite 40% Plag. 50% Amph.phenos. 5%	Cpx → biotite much carbonate, epidote, sph. leucox.		Altered basalt from within basalt-rhyolite sequence in Scamp Assoc^{n}
B54	Altered basalt	Mosaic of quartz + plagioclase + green amphibole. Scattered leucoxenised opaques. No primary textures, completely recrystallised	Plag. & qtz. ~ 60%. Amph. 40%	Cpx → amphibole Recrystallised throughout		As above

B55	Intermediate tuff	Subangular acid volcanic rock frag. (devit. & qtz. rich), plag. phenos. & qtz. aggregates + clots green amphibole in an amphibole + qtz. + feldspar matrix	Plagioclase + qtz. + green amphibole	Cpx → amphibole Completely recrystallised	✓	Pyroclastic, containing basic & acid rock frags. in a basic matrix. Clearly fragmental
B56	Microgranite dyke	Holocrystalline, partially-recrystallised rock consisting of granular quartz + plagioclase + K-feldspar (some albitized) + biotite + amphibole	Quartz 40% K-feldsp. 41% Plag. 15% Rest 4%	K-feldp→sometimes albitized. Minor epidote & sericite		Field relationships establish is a dyke intrusive into B53 & B54 basalts & B57 tuff
B57	Lithic tuff	Subangular acid volc. frags. (devit. & qtz. rich) + basic rock frags. (Plag. - amphibole aggregates) + amph. phenos. + quartz aggregates + plag. phenos in a similar matrix	Mixture of basic & acid components	Much secondary green amphibole i.e., uralitized		In bedded deposits, interlayered with basic lavas. Pyroclastic - an air-fall tuff
B58	Lithic tuff	As above, but fragments are mainly uralitized basalt in a siliceous matrix. Few devit. acid volc. frags.; glassy matrix shows perlitic cracking	As above	"		"
B59	Altered basalt	"Amphibolite", composed of interlocking needles of green amphibole + quartz + plagioclase. Very rare opaques	Amph. ~ 35% Plag. + quartz comprise remainder	Cpx → uralitized Much epidote after plag.	✓	Non-porphyritic, probably a silicified basaltic-andesite differentiate
B60	Uralitized basalt	Feathery green amphibole interlocking with plagioclase. Lesser epidote & leucoxene + sphene (after opaques)	Amph. 50% Plag. 35% Epidote 10% Opaques 5%	Cpx → uralitized Plag. - fresh. Secondary epidote + sph. + leucoxene	✓	Typical basalt from margin of Scamp "Cauldron"
B61	Porphyritic rhyolite	Anhedral med. to coarse gr. phenos. of quartz + plagioclase + K-feldspar (perthite, which is sometimes albitized) in a devit. oriented, glassy matrix	Phenos. 30% K-feldsp. 60% Quartz 15% Plag. 25%	Opaques → leucoxene in part Secondary green amphibole	✓	Regional map indicates is intrusive. But glassy matrix + crystal chips suggests is crystal tuff
B62	Amygdaloidal basalt	Coarse gr. amygdales infilled with epidote in an altered basic matrix consisting of plagioclase + green amphibole + epidote + leucoxenised opaques		Highly altered - uralitized & epidotized		Gurgadi Basalt - example amygolaloidal
B63	Porphyritic rhyolite	Med. gr. phenos. plag. often zoned & in glomero porphyritic aggregates in a devit. felsic matrix with scattered opaques	Phenos. approx. 10%. Are all plagioclase	Plag. sericitized Some secondary amphibole in matrix	✓	Thomas Rhyolite - typical acid volcanic from west
B65	Amygdaloidal basalt	Coarse gr. epidote-filled amygdales in a subophitic uralitized basalt matrix. Plag. fresh & lath-like interlocking with uralite + epidote + opaques	Not significant on account of vesicle infillings	Plag. - fresh Cpx → uralitized Opaques → leucoxene Secondary epidote		Warubuyu Basalt amygdaloidal type. Very similar to B62
B66	Basalt	Interlocking plag. + uralite + epidote + leucoxenized opaques in a subophitic intergrowth	Plag. ~ 55% Uralite ~ 17% Epidote ~ 20% Opaques ~ 8%	Plag. - fresh Cpx → uralitized Opaques → leucoxene	✓	Warubuyu Basalt - non vesicular and fresher example
B67	Porphyritic rhyolite	Med.-coarse gr. subhedral phenos. microcline, (with cross hatching), perthitic in part, minor plag. in a microcryst. qtz.-feldspar-minor opaque matrix	Phenos. ~ 10% Mainly K-feld - Approx. 85%	K-feldsp. → albitized in part. Secondary amphibole in matrix	✓	Hilda Rhyolite to the east of Warburton

B69	Porphyritic rhyolite	Similar description to B67. Matrix is microcryst. & has been recrystallised, obliterating primary textures. Scattered secondary amphibole & opaques in matrix	As above	As above. Feldspars all clouded by sericite		Hilda Rhyolite to north of Warburton. Probably of ash flow origin
B70	Amygdaloidal basalt	Coarse-gr., ovoid quartz-epidote filled amygdales within a hyalopilitic matrix composed of randomly-oriented plag. microlites & finely divided opaques (after glassy matrix)		Much epidote. Some chlorite. Finely-divided (secondary) opaques		Warubuyu Basalt - highly amygdaloidal example
B71	Air-fall (crystal) tuff	Closely-packed angular crystal chips of quartz, plagioclase + fine-grained (recryst.) angular rock fragments. Some bedding. Much fine gr. quartz indicating recrystallisation	Crystal chips of plag. & qtz. comprise 35% rock	Secondary epidote & amphibole scattered throughout		Within Warubuyu Basalt unit, local air-fall tuff horizon
B72	Intermediate tuff	Subangular basic rock frags. (plag + uralite) + crystal chips quartz & plag. within a "basic" matrix of epidote + plagioclase + carbonate + uralite		Altered to epidote + uralite + carbonate	✓	Within Warubuyu Basalt unit, probably air-fall tuff, large basic component
B73	Porphyritic rhyolite	Fine-med. gr. phenos. embayed K-feldspar + plagioclase, sometimes in glomeroporph. aggregates, within microcryst., devit. felsic matrix (with some secondary amphibole)	Phenos ~ 15% Sericite alt^{n}. makes feldspar separat^{n}. difficult	Feldspars (especially) plag.)→sericitized Opaques →sphene + leucoxene	✓	Thomas Rhyolite to north of Warburton. No primary textures but probably ash-flow tuff
B74	Porphyritic rhyolite	Corroded & sericitized K-feldspar phenos. + granular (recrystallised) aggregates of quartz in a recryst. felsic matrix with scattered fine opaques	Highly felsic. Fine opaques make up ~ 4%	K-feldspar sericitized. Some epidote		As for B73. K-feldspar phenos. corroded during recrystallisation
B76	Basalt	Laths plag. (ave. length 1mm) interlocking with green amphibole & chlorite (after cpx) in a true ophitic texture. No opaques, but much granular sphene & leucox. after opaques	Plag. 42% Cpx 55% Opaques 3%	Cpx → uralitized & chloritized Plag. - fresh Opq.→ leucox.+ sph.	✓	Gurgadi Basalt to north of Warburton. Texturally well preserved. No olivine originally present
B77	Altered basalt	Tabular laths of plag. up to 3cm long (now epidote + sericite + relic plag.) interlocking with chloritized & epidotized cpx & leucoxenised opaques	Mainly alteration minerals	Extreme. Mixture of epidote & chlorite + leucox. + sphene	✓	Miller Basalt - relatively enriched in opaques - approx. 5% of rock
		Clasts from The Olgas.				
O1.1	Uralitized basalt	Fine gr. interlocking plag. laths and uralite + chlorite (after cpx). Scattered and abundant epidote + partially altered opaques	Plag.& uralite + chlorite of approx. equal %	Plag.→sericitized & epidotized Cpx → chloritized & uralitized		Altered basalt. Identical to some from Warburton area
O1.2	Uralitized basalt	Interlocking plag. laths and green amphibole, preserving original subophitic texture. Scattered leucoxenised opaques and epidote	Plag. ~ 45% Cpx ~ 45% Epidote ~ 3% Opaques ~ 2%	Cpx → uralitized Plag.→sericite dusted. Opaques → leucoxene	✓	Typical of uralitized basalts seen to the west e.g. B49 or B23

01.3	Uralitized basalt	Tabular, randomly-oriented plag. laths interlocking with amphibole + chlorite + epidote + scattered opaques. Excellent ophitic texture. Qtz.-filled amygdales	Plag. ~ 40% Cpx (orig.) 56% Opaques 4%	Plag.→sericited dusted. Cpx → uralitized		Coarser-grained example than 01.2. Very similar to B76
01.4	Uralitized basalt	Interlocking tabular plag. laths up to 3mm long & green amphibole defining excellent ophitic texture. Finely-divided opaques scattered thro'	Plag. 60% Amph. 36% Opaques 4%	Plag.→sericitized Cpx → uralitized		As above
01.5	Porphritic dacite	Oriented fine-med. gr. euhedral phenos. plag. within microcryst. felsic (plag.rich) matrix + green amphibole. No primary textures	Phenos. ~ 10% Are all plag. Much secondary amphibole in matrix	Plag.-sericitized Much amphib. in matrix.	✓	Typical porphyritic dacite
01.6	Uralitized basaltic-andesite	Tabular, randomly-oriented plag. laths + finer microlites interlocking with green amphibole forming a subophitic texture. Possible interstitial glass-now epidote.	Plag. 45% Amph. 45% Matrix + opaques rest	Plag. → sericitized Cpx → uralitized Secondary qtz. + epidote	✓	Similar to above basalts, but possibly some glass. originally
01.7	Porphyritic andesite	Med. gr. phenos. plag. and green amphibole (often in clusters) in a matrix of green amph. + plag. laths + qtz.-feldspar microcrystalline intergrowths (after glass?)	Phenos. ~ 12% equal % amph. & plag. as phenos. and in matrix	Plag.→ sericitized Cpx → uralitized glass (?) now felsic intergrowths	✓	Matrix similar to 01.6, but more felsic patches. Phenos. present
01.8	Porphy ritic rhyodacite	Med. gr. phenos. plag & albitized K-feldspar & altered cpx (?) within a microgranophyric (in part) matrix, containing abundant plates of K-feldspar + needles amphibole + opaques arranged in lines	Phenos ~ 15% of which Plag. 85% Cpx. 15%	Feldspars sericitized Opaques fresh & Leucoxenised Cpx → hematite + chlorite		What appears to be cpx. now altered; it occurs in glomporph. aggs. with plag. Matrix felsic
01.9	Porphyritic rhyolite	Med. gr. phenos. subhedral plag., albitized K-feldspar + embayed quartz in a snowflake devitrified matrix with scattered hematite & epidote	Phenos. ~ 10% Clouding makes it difficult to distinguish feldspars	Feldspars sericitized. Minor hematite & epidote in matrix	✓	Good example, similar to rhyolites from Gawler Ranges
01.11	Granophyre	Holocrystalline, med. gr. rock composed of interlocking pericline-twinned plag. + granophyric quartz-K-feldspar intergrowths. Scattered green amph. + opaques	85% qtz - K-feldspar intergrowths	Minor epidote Plag. sericitized extensively		Typical subvolcanic granophyre (probably shallow intrusive)
01.12	Granophyre	Very similar to 01.11, except less plag. Few anhedral, embayed qtz. phenos. Recryst. qtz. aggregates. Mostly granophyric qtz.-K-feldspar intergrowths		Plag. sericitized Minor secondary hematite, epidote & amphibole		As above
01.13	Amygdaloidal porphyritic dacite	Med. gr. sericitized phenos. plag. + fine gr. green amphibole (after cpx?) + qtz—amphibole filled amygdales within a recryst. qtz. + amphibole + epidote + hematite + plag. matrix	Vesicles ~ 10% of rock Phenos ~ 8% rest matrix	Matrix recrystallised & Amph. + epidote + hem. are secondary		Dacitic volcanic, possible vapour phase zone of ash flow
01.14	Porphyritic rhyodacite	Fine to med. gr. euhedral phenos plag. - often in glomeroporph. aggregates, + finer phenos. altered cpx. in matrix of devitrified qtz. + feldspar + hematite	Phenos.~ 12% 95% plag. 5% cpx.	Cpx → epidote + green amph. Plag.→ sericitized Much secondary hematite		Similar to rhyodacites from Gawler Ranges

01.16	Microgran-ite	Holocrystalline, granular aggregate of equigranular quartz, K-feldspar, plagioclase, opaques and green amphibole. Some med. gr. phenos. plag.	Qtz. ~ 40% K-felds.~ 40% Plag. ~ 12% Amph.+ op. ~ 8%	Plag. & to lesser extent K-feldsp. sericitized		Probable shallow intrusive - i.e., subvolcanic
01.17	Epiclas-tic or arkose	Fine, closely-packed subangular to angular grains of quartz, K-feldspar (including microcline), plagioclase & altered, epidotized rock frags. & plagioclase	Epidote ~ 35% Qtz. ~ 30% K-felds. ~ 20% Plag. ~ 15%	Much epidote & hematite in matrix. K-felds.- fresh		Typical of matrix of lithic wacke which composes the "Olgas". Good sorting
AY-1	Arkose (epiclas-tic of volcanic provenance)	Closely-packed, subangular coarse sand size fragments of quartz, plagioclase & K-feldspar (including microcline). Well sorted, but poorly rounded. No fine cementing matrix of mud size	Approx. equal % of qtz., plag. & K-feldspar	Sericitization of all feldspars especially plag. Sec. hematite. No epidote		Typical of rock which composes "Ayres Rock". Very similar to 01.17 but lacks epidote

TABLE A3.2. Geochemical data for selected rocks from the Central Australian province, listed in order of increasing SiO_2.

	B32	B33	B31	B60	B49	B76	B14	B8	B77	B23	B66	B55	B59	B11
SiO_2	47.68	48.32	48.33	47.41	48.88	50.57	50.13	48.83	48.57	51.64	52.77	59.53	61.77	63.17
Al_2O_3	22.69	22.91	14.80	15.48	15.39	16.42	13.58	13.78	14.25	12.85	13.66	11.80	13.18	13.68
$Fe_2O^t_3$	8.27	7.43	13.71	14.26	14.85	12.66	15.41	15.73	16.04	16.55	13.90	8.52	8.10	8.22
MnO	0.10	0.11	0.21	0.19	0.21	0.20	0.21	0.22	0.18	0.25	0.16	0.15	0.10	0.13
MgO	7.73	6.78	8.18	7.67	6.68	6.01	5.83	5.05	4.23	3.61	3.16	4.28	3.22	1.15
CaO	10.45	11.59	11.77	9.27	9.23	7.31	9.20	8.62	8.63	8.58	7.82	7.67	7.28	3.90
Na_2O	2.79	2.43	2.06	3.36	2.87	4.75	2.41	2.75	1.56	2.58	4.35	2.91	3.95	3.70
K_2O	0.22	0.30	0.16	0.20	0.27	0.29	0.37	0.54	2.26	0.81	2.29	4.15	0.78	3.44
TiO_2	0.20	0.30	0.92	1.89	1.86	1.61	2.46	3.01	3.20	2.77	1.95	0.98	1.06	1.20
P_2O_5	0.04	0.04	0.16	0.43	0.34	0.21	0.29	0.35	0.95	0.70	0.19	0.21	0.15	0.35
Total	100.16	100.21	100.31	100.15	100.50	100.02	99.88	98.89	100.24	100.33	100.24	100.19	99.58	98.93
LOI	0.15	0.19	0.10	2.38	1.55	2.65	0.89	0.90	2.42	0.55	1.44	0.46	1.56	0.20
Zr	10.4	26	83	148	134	158	246	295	495	385	339	251	280	628
Nb	<1	1.2	6.2	9	9	7.8	20	20	40	29	21	16	16	39
Y	2	7	29	37	36	39	47	55	72	75	66	42	41	96
Ce	-	5.3	33	69	46	32	69	85	130	96	88	75	-	185
Nd	-	6.3	22	29	28	22	-	44	63	-	40	-	-	-
Sc	8.8	15	48	33	36	32	29	28	30	34	39	24	21	15
V	-	-	297	290	305	234	337	391	316	170	346	167	225	34
Cr	24	29	102	414	307	36	147	134	177	18	56	104	88	8.5
Ni	-	157	109	185	170	88	110	115	96	23	40	78	57	5
Co	-	-	66	54	65	58	59	-	53	42	50	35	32	-
Rb	2	7.6	1	7	6	7	19	21	87	28	32	129	35	155
Sr	376	267	222	270	340	144	290	277	447	265	272	120	390	189
Ba	79	131	203	217	307	152	162	736	1810	329	2820	709	677	808

	B72	B10	B29	B7	B45	B44	B25	B36	B12	B13	B75	B15	B73
SiO_2	64.54	64.44	65.87	66.84	66.88	67.11	68.97	68.97	69.97	71.10	71.10	71.16	71.33
Al_2O_3	10.24	13.64	13.07	12.90	12.63	12.80	12.44	12.41	12.81	12.86	13.12	13.29	12.47
$Fe_2O_3^t$	7.23	7.51	8.13	7.39	7.06	6.78	6.75	7.71	5.43	4.73	4.44	4.48	4.43
MnO	0.11	0.13	0.11	0.14	0.09	0.12	0.14	0.12	0.10	0.09	0.07	0.10	0.14
MgO	2.94	0.98	0.49	0.55	1.01	0.95	0.28	0.30	0.28	0.19	0.12	0.15	0.36
CaO	8.44	3.71	2.74	2.91	2.32	2.62	2.27	1.67	1.92	1.36	0.79	1.00	1.81
Na_2O	2.49	3.72	3.94	4.06	3.57	3.72	3.81	3.60	3.81	3.83	3.98	2.83	2.77
K_2O	2.95	3.77	4.28	4.23	4.55	4.50	4.25	4.46	4.65	4.85	5.33	7.02	5.54
TiO_2	1.03	1.02	0.80	0.75	1.02	1.00	0.42	0.52	0.51	0.40	0.33	0.36	0.44
P_2O_5	0.15	0.27	0.16	0.15	0.24	0.30	0.08	0.10	0.10	0.07	0.03	0.05	0.08
Total	100.42	99.19	90.59	99.91	99.37	99.09	99.41	99.86	99.58	99.45	99.32	100.44	99.35
LOI	2.06	0.15	0.34	0.10	0.35	0.80	0.34	0.20	0.10	0.28	0.35	0.32	0.91
Zr	277	646	1320	915	691	519	1020	1030	885	935	880	738	836
Nb	14.5	41	80	53	75	72	64	69	55	60	102	32	97
Y	39	93	144	114	143	153	137	164	111	124	190	112	165
Ce	73	178	228	213	229	245	229	235	207	226	291	-	269
Nd	32	86	135	105	116	115	120	-	100	-	138	-	133
Sc	22	11	6.4	12	12	13	7.4	10.4	7.4	6	4.5	6	7
V	165	33	-	24	54	-	4	-	-	-	-	-	-
Cr	77	4.3	<1	4	-	6	-	6	11	-	-	-	-
Ni	41	11	11	13	12	-	-	-	-	-	-	-	-
Co	32	-	-	26	-	-	-	-	-	-	-	-	-
Rb	38	159	137	174	199	224	147	156	184	204	173	258	254
Sr	236	180	164	149	91	97	129	113	119	98	135	84	187
Ba	634	732	2120	850	1010	878	992	1130	1005	1080	1660	1840	1470

	B17	B19	B67	B4	B35	B2	B63	B16	B42	B61	B47	B50	012
SiO_2	71.58	71.76	72.04	72.04	72.38	72.68	72.81	72.73	73.81	73.54	75.93	77.20	52.69
Al_2O_3	12.98	12.53	12.76	13.05	13.44	13.50	12.46	12.15	12.09	12.75	12.15	11.15	14.27
$Fe_2O_3^t$	4.44	4.75	4.27	5.00	2.55	3.29	4.13	3.84	2.72	2.97	2.09	2.47	11.81
MnO	0.07	0.09	0.11	0.05	0.04	0.06	0.09	0.06	0.08	0.05	0.04	0.02	0.18
MgO	0.30	0.13	0.22	0.63	0.44	0.17	0.20	0.33	0.42	0.34	0.22	0.08	7.44
CaO	1.36	1.55	0.92	2.29	1.10	0.96	0.84	1.68	0.70	1.10	0.78	0.28	9.51
Na_2O	3.03	3.77	3.70	5.43	3.35	3.62	3.53	3.86	2.06	3.89	3.43	2.66	2.06
K_2O	5.52	4.73	5.33	0.83	5.66	5.67	5.81	4.48	7.46	4.89	5.33	6.25	0.88
TiO_2	0.49	0.36	0.32	0.59	0.49	0.31	0.33	0.43	0.32	0.33	0.13	0.18	0.92
P_2O_5	0.07	0.05	0.03	0.12	0.11	0.02	0.06	0.07	0.04	0.05	0.01	0.01	0.14
Total	99.77	99.72	99.71	100.01	99.55	100.27	100.25	99.64	99.70	99.90	100.10	100.30	99.89
LOI	0.49	0.48	0.59	0.94	0.57	0.45	0.54	0.40	0.26	0.45	0.64	0.24	2.05
Zr	616	1160	595	741	358	588	837	581	415	386	270	385	109
Nb	28	61	83	43	44	30	97	34	77	68	117	86	5.6
Y	93	135	178	104	41	105	156	77	123	117	184	135	26
Ce	-	222	328	217	125	210	297	162	291	-	280	-	20
Nd	-	115	149	-	-	-	135	69	117	-	107	-	14
Sc	8.4	6.3	3	8.5	4.3	4.4	5	7	3	3	1	1	35
V	-	-	-	-	-	-	-	-	-	-	-	-	256
Cr	13	2	4	2	5.4	-	-	-	-	-	-	-	248
Ni	-	-	-	-	-	-	-	-	-	-	-	-	172
Co	-	-	-	-	-	-	-	-	-	-	-	-	59
Rb	169	200	200	18	226	204	230	135	319	208	351	307	64
Sr	103	110	56	186	156	71	51	106	58	66	32	37	178
Ba	1550	1350	928	221	980	1380	1270	1190	1000	745	61	637	292

	016	017	015	019	H.B.	M.D.	H.R.
SiO_2	53.56	56.56	61.52	75.73	47.49	50.00	71.36
Al_2O_3	14.95	13.95	13.66	11.96	15.02	15.95	12.31
$Fe_2O_3^t$	12.75	10.45	8.76	2.66	14.75	10.80	4.17
Mno	0.20	0.17	0.15	0.05	0.19	0.02	0.09
MgO	5.66	5.23	2.00	0.17	5.42	8.90	0.34
CaO	7.65	7.26	4.12	0.66	8.59	10.95	1.12
Na_2O	2.89	2.42	2.83	2.93	3.87	2.28	3.45
K_2O	1.09	2.57	5.19	5.35	1.14	0.54	5.22
TiO_2	1.31	1.19	1.29	0.26	2.63	0.54	0.43
P_2O_5	0.22	0.22	0.38	0.16	0.53	-	0.07
Total	100.26	100.02	99.89	99.78	99.63	99.98	98.56
LOI	1.83	1.77	0.52	0.36	-	-	-
Zr	245	232	537	574	230		762
Nb	11	12.4	20	41	14		76
Y	44	37	71	120	34		146
Ce	58	58	144	249	-		-
Nd	33	30	68	123	-		-
Sc	35	33	21	1	-		-
V	274	233	145	4	244		11
Cr	64	198	141	29	89		2
Ni	97	113	19	10	98		-
Co	49	24	24	-			-
Rb	102	106	165	198	29		199
Sr	144	147	257	32	261		60
Ba	289	633	1450	599	510		907

H.B. - average basalt from the Warburton area (after Haynes, 1972).

H.R. - average rhyolite from the Warburton area after Haynes, 1972).

M.D. - marginal, chilled phase of the Mt. Davies layered basic intrusive (part of the Giles Complex, data from Nesbitt, et al., 1970).

TABLE A5.1. Brief thin section descriptions of a representative selection of rocks from the Welcome Well complex.

SAMPLE NUMBER	ROCK NAME	DESCRIPTION	% MINERALS	ALTERATION	ANAL.	COMMENTS
W1	Altered andesite	Finely crystalline mosaic feldspar + quartz + chlorite throughout, except for patches coarse chlorite after cpx. Ghosted outlines plag. & cpx phenos.	Too altered to tell original plag. & cpx prop^{n}.	Extreme, but also much recrystallisation & secondary quartz		Extreme alteration and recryst. has obliterated primary textures
W2	Porphyritic basalt	Med.-fine grained euhedral, tabular plagioclase phenos. Chlorite after cpx. Matrix unaltered plag. microlites interlocking with feathery brown uralite	Phenos 30% of which plag. 85% cpx 15%	Plag. completely sauss. cpx - chlorite matrix cpx - feathery uralite	✓	Atypical basalt because of abundant plag. phenos. Matrix too mafic for typical andesite
W3	Porphyritic basalt	Abundant, fine gr. phenos. cpx. No plag. phenos. Chlorite after olivine phenos? Matrix mainly plag. with qtz. + carbonate + chlorite + sphene	Cpx phenos. 35% Olivine 20% Rest matrix	Cpx fresh. Olivine - chlorite plag. sauss. a little carbonate chlorite, sphene in matrix	✓	Basalt, probably originally containing olivine
W4	Porphyritic andesite	Med.-grained phenos. plag. (tabular & euhedral) & zoned cpx. Matrix flow-oriented plag. microlites + aphanitic brownish/green chlorite	Phenos. 40% of which Plag. 50% cpx. 50%	Plag. - sauss. cpx - chlorite complete alt^{n}. of phenos.	✓	Excellent example of porphyritic andesite. Lava flow origin
W5	Porphyritic andesite agglomerate	Fragments of porphyritic andesite, all of similar texture, with diffuse margins, giving appearance of homogeneous porphyritic andesite	Phenos. 40% of which Plag. 70% Cpx. 30%	plag. - fresh & twinned. cpx - chl. + uralite. matrix - chl.	✓	Probably flow-top of lava because frags. homogeneous & closely-packed
W6	Porphyritic andesite	Med. gr. euhedral plag. & cpx. phenos. Very fine-grained matrix of plag. microlites + alterat^{n}. products. A few chlorite-filled amygdules	Phenos. 40% of which Plag. 85% Cpx 15%	plag. - sauss. cpx - chlorite matrix all altered to chl.+ ep.+ sph.		Badly altered
W7	Porphyritic ultramafic rock	Fresh subhedral olivine phenocrysts and skeletal cpx. in dark, feathery, originally glassy matrix	Phenos. 50% of which olivine 60% clinopyroxene 40%	olivine - fresh cpx. - fresh matrix is glassy - dark & aphanitic	✓	Ultramafic dyke intruding volcanic pile
W8	Dacitic agglomerate	Variety dacitic rock fragments (mainly fresh plag. & rare cpx. phenos.), variable textures. Set in matrix of similar texture - abundant plagioclase	Phenos. 45% of which Cpx. 15% Plag. 85%	Plag. fresh & twinned. Much chlorite in g/mass.		Probable flow-top breccia. Could be a pyroclastic - but no glassy textures preserved
W9	Andesitic agglomerate	Fragments of typical porphyritic andesite in a texturally identical matrix. Matrix between phenos. is chlorite + finely-divided opaques	Phenos. 40% of which Plag. 70% Cpx. 30%	Plag. - sauss. dusted. cpx - chlorite matrix - chl.+ opq. + qtz.		Under X polars rock appears homogeneous. Flow-top breccia on lava.
W10	Andesitic agglomerate	Fragments of altered andesite with cuspate margins "suspended" in a quartz-chlorite matrix. Frags. contain phenos. plag. & cpx. and have angular shapes	Frags. 65% Matrix 35%	matrix - qtz., chl. frags. - entirely chl. + carbonate cpx. phenos. fresh		Fragments homogeneous, cuspate margins & glassy matrix indicate flow-top breccia on lava

W11	Altered andesite	Evenly fine-grained mosaic chlorite, carbonate, quartz & sericite after fine-gr. porphyritic, vesicular andesite		Extreme, composed of chl.+ carbonate + qtz.+ sericite		Example of extreme alteration. Original porphyritic & vesicular texture still visible
W12	Porphyritic andesite	Phenocrysts sauss. plag. & cpx. of med. to fine grainsize. Matrix oriented plag. laths & chlorite. Scattered chlorite-filled, qtz.-rimmed amygdales	Phenos. 30% of which Plag. 60% and Cpx 40% Amyg. 15%	Moderate. plag.→ sauss. cpx.→ fresh matrix- chl.+ seric.		Typical porph. andesite, but altered considerably. Lava-origin
W13	Altered porphyritic andesite	Phenocrysts euhedral, saus. plag. and chloritized cpx. both medium gr. size. Groundmass of chlorite and feldspar	Phenos. 30% of which Plag. 70% Cpx. 30%	Extreme plag. → saus.+ epidote cpx.→ chlorite matrix → chl.+ ser.		Extremely altered andesite, yet textures well-preserved in hand specimen. Lava origin
W14	Porphyritic andesite	Medium-grained phenocrysts plagioclase and cpx. Fine-grained matrix of plag. microlites + chlorite + sphene + opaques + epidote	Phenos. 35% of which Plag. 70% Cpx. 30%	plag. → sauss. cpx.→ fresh & chloritized matrix → chl.+ ep. + sph.	✓	Textures well preserved. Not so altered as W13
W15	Andesitic agglomerate	Rounded fragments of amygdalar, finely-porphyritic andesite in an identical matrix. Abundant chlorite &/or carbonate &/or sericite-filled cuspate amygdales	Amyg. 30%	fresh cpx. & plag. much carbonate, chlorite, sericite, epidote in anygdules		Fragments similar to each other & matrix. Frothy flow top of lava flow
W16	Vesicular andesite	Abundant cuspate amygdules filled with quartz &/or chlorite &/or carbonate and fine phenos. plag. in a plagioclase-chlorite matrix	Amyg. 30% Plag. 50% Matrix 20%	plag.→ partially sauss. cpx → pumpellyite matrix → qtz.+ chl. + ep.+ carbonate		Non brecciated. Abundant amygdules indicate vesicular lava
W17	Fine-grained dacite	Consists of oriented plagioclase microlites, rare fine-grained cpx. phenos. in matrix of plag. + chlorite + epidote + sphene + carbonate clots	Plag. 65% Cpx. ~ 5% Matrix ~ 30%	plag. → partially saussuritized carbonate, chl. epidote in matrix	✓	A dacite since almost entirely fine gr. plagioclase
W18	Dolerite	Medium-grained, partially-altered cpx. sitting in a saussuritized matrix (after plagioclase). Scattered opaques	Cpx. - 45% Opqs. - 4% Rest saus. plag.	cpx. → fresh Plag. → sauss. opaques → sphene + leucoxene		Spotted appearance caused by fresh cpx. surrounded by sauss. plag.
W19	Altered andesite	Scattered medium-grained phenocrysts of chloritized cpx. in fine gr. matrix of chlorite + plagioclase + sphene + epidote	Cpx. - 4% Rest matrix	Extreme cpx. → chlorite matrix → sauss. plag.+ chl.+ sph.+ ep.		
W20	Porphyritic andesite	Med. to coarse-grained phenos. plag. Rare cpx. Matrix altered mosaic of bladed opaques + chlorite + quartz + epidote + sphene	Plag. - 45% Cpx. - 5% Rest matrix	Extreme plag. → saus. matrix → sec descrpt^{n}.		Altered, but textures in hand specimen well preserved
W21	Andesitic agglomerate	Rounded, porphyritic & vesicular andesite fragments in identical matrix. Abundant chlorite & carbonate-filled vesicles. Numerous small frags.		Extreme cpx.→ fresh. Much pumpell. + chlorite + carbonate + qtz. in matrix & vesicles		Numerous small frags. suggesting epiclastic, but cuspate amygdules show is brecciated flow-top

W22	Porphyritic andesite	Abundant fine to med.-grained plagioclase & twinned cpx. phenos., in fine-grained matrix quartz + plag. + chlorite + carbonate + epidote + sphene	Phenos. 30% of which Plag. 50% Cpx. 50%	plag.→ saus. + carbonate + epidote cpx.→ fresh matrix → see descrp^{n}.	✓	Typical porphyritic andesite, extreme alteration of plag., but fresh cpx.
W23	Porphyritic andesite	Fine-grained phenos. plag. & cpx. in an aphanitic matrix. Numerous granular aggregates epidote after cpx. Matrix sphene + chl. + plag.	Phenos. 40% Plag. 60% Cpx. 40%	plag. → sauss. & fresh. cpx. → chl.+ epidote matrix → see descrp^{n}.	✓	Atypical porphyritic andesite due to fine gr. phenos. Epidote alt^{n}. of cpx.
W24	Peridotite	Cumulus anhedral olivine in intercumulus cpx. Cracks & rims of olivine filled with serp. & opaques. Cracks in cpx. filled with opaques. A few scattered grains of chromite (?)	Ol. 50% Cpx. 50%	Completely fresh, except for serp. rims on olivine	✓	Excellent, fresh example. Intrusive sill
W25	Andesitic agglomerate	Scattered rounded fragments of vasicular andesite in highly vesicular & "glassy" matrix. Entirely quartz + chlorite + plag. (seric.) + carbonate		Extreme largely qtz. + chl. + sauss. plag.		Example of extreme alteration in a frothy flow-top lava
W26	Andesitic agglomerate	Rounded fragments porphyritic andesite containing med. gr. phenos. saus. plag. and amphibole-chlorite after cpx. (?) in highly altered plag. rich matrix	Phenos. 35% of which Plag. - 65% Cpx. - 35%	Extreme plag.→ sauss. cpx. → chl.+ amphibole matrix → seric.+ ep. + chl.+ qtz.		Autobrecciated lava (possibly flow top but not vesicular or glassy)
W27	Vesicular glassy andesite	Abundant fine-grained euhedral phenos. plag. + chlorite filled amygdules in a contorted glassy matrix, now all chlorite	Phenos. 35% of rock	Extreme plag. → sauss. matrix entirely chl.+ qtz.+ seric.		Excellent textures. Convincing glassy flow top
W28	Altered porphyritic andesite	Plagioclase phenos. of fine grainsize set in a matrix of granular pale green amphibole (often in clusters after cpx.) + plag. + qtz.	Too jumbled to estimate	plag. → sauss. dusted cpx. → granular amphibole		Near contact with major dolerite dyke, possibly contact metamorphic recryst.
W29	Porphyritic dacite	Fine to medium-grained phenocrysts of eu edral plagioclase and cpx. in aphanitic plagioclase - chlorite -sphene matrix. One even-grained rock fragment with section.	Phenos. 35% of which Plag. 70% Cpx. 30%	plag. partially saus. cpx.→ chlorite + epidote	✓	Typical porphyritic lava texture but more dacitic than usual.
W30	Fine-grained dacite	Sparse fine-grained phenocrysts of plagioclase and quartz in a felted plagioclase-rich matrix. Veined by quartz	Largely plagioclase Phenos. 2%	None		Dyke adjacent to ultrabasic
W31	Horneblende -clinopyroxene porphyry	Euhedral phenocrysts brown hornblende and rarer cpx. in a crystalline matrix of plagioclase & brown hornblende + sphene + epidote. No plagioclase phenocrysts	Phenos. 30% of which h/b. 80% Cpx. 20%	Cpx. & h/b fresh. some sphene & epidote in fresh g/mass.	✓	In sequence, atypical of andesites
W32	Porphyritic andesite	Fine-grained phenocrysts of plagioclase, well oriented. Quartz-filled amygdules & chloritized cpx. phenos. in fine gr. matrix chlorite + epidote + sphene	Plag. phenos. approx. 35% of rock	Cpx. → chlorite plag. → fresh. Much chl.+ sericite + epidote + qtz. in matrix		Marked orientation of phenos. & squashing but probably glassy flow top of lava rather than pyroclastic

W33	Uralitized porphyritic andesite	Phenocrysts well twinned & fresh plagioclase (fine to med. gr. size) in matrix of uralite + plag. + epidote. Few rock fragments	Phenos. 20% of rock	Plag. fresh. Abundant uralite & epidote in matrix		Contact metamorphosed andesite (near granite)
W34	Uralitized porphyritic andesite	Phenocrysts plagioclase and cpx. (now completely altered to fibrous pale green amphibole), med.-coarse gr. in matrix quartz + pale green amph. + plag.	Phenos. 30% of which Plag. 60% Cpx. 40%	Extreme. plag. → sauss. cpx. → pale amph. matrix → pale amph. + qtz.		As above, textures well preserved in hand specimen
W35	Uralitized porphyritic andesite	Abundant fine-grained phenocrysts plagioclase and coarse-grained cpx. in matrix green amphibole + plagioclase + granular quartz aggregates	Phenos. ~ 30% In matrix plag. ~ 60% amphibole ~ 40%	Plag. fresh cpx. → entirely green amphibole secondary qtz.		Contact metamorphosed andesite (near granite)
W36	Uralitized porphyritic andesite	Phenocrysts fine-to medium-grained plagioclase & cpx. (now green amphibole) in matrix of green amphibole & plagioclase	Phenos. ~ 45% of which Plag. ~ 75% Cpx. ~ 25%	Plag. fresh to sauss. Cpx.→ all green amphibole. Matrix roughly equal amph. & plag.		As above
W37	Amphibolite (after andesite)	Fine-to medium-grained plagioclase phenocrysts & green amphibole (after cpx?) in crystalline matrix of green amphibole + plagioclase + sphene	Phenos. ~ 15% originally	Extensive metamorphic recrystallisation		Extensive recrystallisation, almost obliterating original textures
W38	Amphibolite	Granular green amphibole interlocking with carbonate + quartz + plagioclase. Recrystallised texture	Green amphibole 70% rock	As above		Recrystallisation has obliterated original textures
W39	Recrystallised andesitic agglomerate	Rounded fragments of porphyritic andesite and fine-to med.-grained phenocrysts of plagioclase in a matrix of green amph. + plag. + quartz		Extensive recryst. of matrix, but some fragments escaped. Plag. is sauss.		Extensive recrystallisation but selective, so that fragmental textures preserved
W40	Recrystallised porphyritic andesite	Fine to med.-grained phenocrysts of cpx. (altered), & rare plagioclase. Very coarse elongate vesicles filled with quartz. Matrix foliated, abundant colourless amphibole	Rare plagioclase phenocrysts, mainly Cpx.	Cpx. → amphibole Matrix recryst.		Extensive recryst. & introduction of quartz
W41	Porphyritic dacite	Euhedral fine-grained phenos. plagioclase in a finely-crystalline quartz-rich matrix containing needles of tremolite which impart a foliation	Phenos. 35% of rock & entirely plagioclase	plag.→ sauss. dusted		Excellent porphyritic texture. Dyke adjacent to granite
W42	Porphyritic dacite	Ragged-edged, fine - med. gr. phenos. plagioclase in matrix of granular recryst. quartz + plagioclase + green amphibole	Phenos. 35% of rock & entirely plag.	plag. → fresh. Matrix recrystallised, also introduced quartz		Either dyke or volcanic with introduced quartz. Adjacent to granite
W43	Megacrystic adamellite	Megacrysts of microcline in a fine to medium-grained holocrystalline matrix of quartz, orthoclase and zoned plagioclase. Minor biot. & h/b.	Amphibole/biotite ~ 3% Plag., K-feldsp. & quartz equal %	plag. → sauss. dusted amphibole → biotite		Typical of granitoid body intruding volcanics in north

W44	Amphib-olite after andesite	Ragged med. → fine gr. phenocrysts plagioclase in a recrystallised amphibolite matrix of plagioclase, quartz and green amphibole	Difficult to estimate	Extensive recry-stallisation of green amph. & introd^{n}. quartz		Andesite, recryst. near granite
W45	Porphy-ritic dacite	Euhedral med. → fine gr. phenocrysts of plag. in glomeroporphyritic aggregates in matrix quartz + plagioclase + green amphibole + epidote	As above	plag. fresh, much epidote & minor carb., introd. quartz		Porphyritic texture preserved despite introduction of much quartz
W46	Amphib-olite after andesite	Ragged med. → fine gr. phenocrysts plag. and cpx. (now green amphibole) in granular matrix of green amphibole + plag. + quartz	granular amph. ~ 50% rock. Plag. + qtz. ~ 50%	plag. → sauss. (almost unrecog.) cpx. → green amph. introduced qtz.		Contact metamorphism almost obliterated primary textures
W47	Recryst-allised porphy-ritic andesite	Abundant fine gr. phenocrysts of plag. & rarer cpx. (now chl. or green amph.) in matrix of matted amphibole needles & plag.	Phenos. 55% of which Plag. 85% cpx. 15%	plag. fresh, recrystallised matrix		Extensive recryst. of matrix to needle-like amphibole by contact metamorphism
W48	Porphy-ritic andesite	Medium, grained glomeroporph. phenocrysts of cpx. + fine gr. plagioclase laths in matrix of green amphibole + plag. + sph. + epidote	Phenos. 45% of which cpx. 60% Plag. 40%	cpx. fresh & partially uralitized ~ plag. partially sauss. matrix recryst.		Great similarities to h/b-cpx. porphyry(W31) but do have plag. phenos. in this case
W49	Non-por-phyritic andesite	Randomly-oriented fine gr. plagioclase laths interlocking with green amphibole and sphene and epidote & qtz. (rare opaques)	Plag. 45% Amph. 40% Sph.+ ep. 5%	Plag. fresh epidote, sph.^{n} & amphibole alt^{n}. products	✓	Atypical, fine-grained non-porphyritic andesite. Not dolerite since plag. too abundant
W50	Cumulus gabbro	Med. - coarse gr. phenocrysts cpx. mostly uralitized. Intercumulus plagioclase and rare quartz	Plag.~ 55% Cpx. ~ 45%	Plag. → sauss. Cpx. → uralitized		Typical gabbroic dyke
W51	Finely porphy-ritic andesite	Fine-grained suboriented phenos. plagioclase & cpx. (uralitized) in a matrix of plag. + chlorite + epidote + green amphibole. Cpx. often in glomporph. aggregates	phenos. ~ 40% of which cpx. 55% plag. 45%	plag. → sauss. cpx. → uralitized matrix altered- see descript^{n}.		Altered considerably but originally a cpx-rich fine gr. porph. andesite
W52	Crystal-lithic tuff	Superficially a homogeneous porphyritic andesite, but have rock frags. (diffuse outlines) of varying texture, surrounded by plag. phenos & rare cpx. + chlorite + colourless amphibole-epidote-plat. matrix	rock frags. ~ 35% plag. phenos. ~ 40% matrix ~ 25%	plag. → fresh cpx. → uralitized matrix uralitized & much epidote		Abundant phenos. + crystal chips & variable rock frags. indicates pyroclastic origin
W53	Altered porphy-ritic andesite	Med. → fine gr. phenocrysts plag. & cpx. in altered matrix containing clots granular quartz + carbonate + ep. + sph. + pale amph. + chlorite	phenos. 35% of which Plag. 50% Cpx. 50%	Extreme plag. → sauss. cpx. → chlorite secondary qtz + carbonate + ep.		Excellent porphyritic texture in hand specimen but severely altered
W54	Altered Porphy-ritic andesite	Closely-packed medium - fine-grained phenocrysts of plag. & cpx. in altered matrix of carbonate + plag. + epidote + sphene + colourless amphibole	Phenos. 55% of which Plag. 60% Cpx. 40%	Extreme plag. → sauss. Cpx. → uralitized matrix -see descript^{n}.		Closely-packed porphyritic texture. Badly altered

W55	Altered porphyritic dacite	Sparse phenocrysts epidotised plagioclase in matrix of oriented plag. laths + epidote + colourless amphibole		Plag. → fresh to epidotized, uralitized. Rock is veined with qtz.		Dacite with a few phenocrysts, mainly plag. matrix
W56	Amphib-olite after andesite(?)	Entirely interlocking pale green amphibole, granular quartz, plagioclase & epidote. No coarse opaques	amphibole 50% plag. 40% qtz.+ ep. 10%	complete re-crystallisation due to contact met?		Recrystallisation has obliter-ated original textures. Near granite
W57	Amphib-olite	Medium-grained green amphibole interlocking with altered + recrystallised plagioclase & rare qtz. & epidote	amphibole 55% plag. & other mins. 45%	Completely recrystallised		Originally a dolerite or basalt. Adjacent to granite
W58	Weathered gabbro(?)	Quartz-plagioclase-limonite rock. Qtz. & plagioclase in clusters (+ sericite) surrounded by limonite		Weathered		Original rock type hard to determine. Texture suggests gabbro
W59A	Altered porphy-ritic dacite	Med. gr. phenos. epidotized plagioclase in matrix of plag. + quartz + ep. + green amphibole	phenos. 25% (all plag.) matrix 75%	plag. → fresh & epidotized matrix recryst. & epidotized		Recrystallised & altered near granite
W59B	Porphy-ritic horn-blende andesite	Medium gr. phenos. horn blende and fine-grained phenos. plag. in matrix plag. + h/b. + qtz. Horn blende probably primary, no cpx. in cores	phenos. 45% of which h/b. 60% plag. 40%	plag. → fresh h/b fresh matrix recryst.	✓	Variation on normal plag. + cpx. andesite & h/b porphyry (see W31)
W60	Altered recryst. andesite	Possibly originally a vesicular, plag. + cpx. andesite. Now a mosaic of amphibole + sericite + epidote + qtz., in granular aggregates. Amph. after cpx. phenos.		cpx. → uralitized plag. → sauss. sec. quartz + seric. + ep.+ amph.+ chl.		Almost complete obliteration of original textures by recrystallisation
W61	Weathered granite	Quartz-sericite rock. Quartz in angular aggregates surrounded by sericite (after feldspar?)		Weathered		Almost certainly a granite, hand specimen more convincing
W62	Porphy-ritic andesite	Fine (rare med.) gr. phenos. plag. + cpx. + amygdales (qtz.-chlorite filled) in microcryst. matrix of unoriented plag. microlites + qtz. + chl. + epidote	Phenos. 45% of which Plag. 60% Cpx. 40%	plag. → sauss. completely cpx. - fresh epidote + chl. in matrix		Typical andesitic lava, but finer-grained phenos. than usual
W63	Weathered rock-granite?	Globular quartz-sericite microcrystalline mosaics surrounded by hematite. No textures preserved in T.S. Hand spec. indicates might be granite		Completely weathered		Probable granite (on basis of hand specimen)
W64	Weathered porphy-ritic andesite	Rock is a quartz-kaolinite mixture due to weathering. Can make out outlines of plag. phenos in a matrix	Phenos. - approx. 45% rock	Weathered - kaolinitic zone of laterite profile		Hand specimens exhibit typical andesite lava textures & appearance

W65	Andesitic agglom-erate	Rounded fragments porphyritic and/or vesicular andesite in an andesitic matrix with abundant cpx. & plag. phenos. + epidote + chlorite + carbonate + sphene + leucoxene	Fragments make up 70% of rock	Cpx fresh Plag. sauss.	✓	Fragments rounded & uniformity suggests flow-brecciated lava
W66	Altered andesite	Mixture of epidote + chlorite + quartz (possibly in vesicles) + carbonate + sauss. plag. Abundant plag. in matrix & phenos. + some cpx. - all altered.		Severe		Highly altered, but probably originally a typical andesite
W67	Vesicular, altered andesite	Carbonate &/or quartz &/or chlorite-filled amygdales + fine-med. gr. sauss. plag. phenos. & cpx. in a f. gr. chlorite, epidote, qtz, matrix	Amygs. 10% Phenos. 8% of rock	"		Highly altered, but originally probably a typical andesite lava
W68	Lithic tuff	Variety of lapilli-size rock frags. e.g. vesic. andesite, fine gr. & med. gr. porph. andesite in a highly contorted, "squashed" glassy matrix with some crystals and squashed pumice frags.	Rock frags. 85% rock. Fresh cpx., altered plag.	Plag. - sauss. Abundant epid. + chlorite + pumpell. + qtz.		The variety of frags. + vitro-clastic matrix indicates pyroclastic origin
W69	Lithic tuff	Variety of lapilli-size rock frags. - vesic. andesite + fine gr. pheno.-rich andesite in fine gr. contorted matrix, no good vitroclastic textures preserved	Rock frags. 80%	Plag. sauss. dusted Cpx. - altered Much ep.+ chl. + qtz.		Probably a pyroclastic (as for W68), but textures not well preserved
W70	Lithic wacke	Variety of subangular to subrounded andesitic rock frags. in close-packed texture with quartz-chlorite cement. Some cpx. phenos. in matrix		Abundant epidote, carbonate, qtz. chlorite & pumpellyite		Close packing, matrix, rounding of frags. all indicates epiclastic
W71	Lithic wacke	Same comments as for W70. However extreme alteration - especially carbonate has tended to obscure matrix & grain boundaries		Cpx. in rock frags. fresh. Matrix extremely altered		Clearly an epiclastic
W72	Lithic wacke	Variety subangular volcanic rock fragments closely packed & often quartz rimmed in qtz.-chl. matrix. Isolated plag. & cpx. phenos. also		Cpx. → fresh to uralitized Plag.-sauss. Ep.+ chl.+ carb. between grains		Excellent example of epiclastic
W73	Lithic wacke	Large fragment (> 4cm) of porphyritic, vesicular andesite within typical epiclastic matrix composed of close packed fragments (2mm ave. grain size) in qtz.-chl. matrix		Abundant sericite + chl. + epidote between clastic grains		"
W74	Porphy-ritic dacite	Med.-fine gr. phenos. plag. in matrix suboriented plag. microlites + chlorite + hematite + qtz. + hematite/chlorite clots (after opaques?) Plagioclase zoned.		Plag. → sauss. dusted. Opaques → hem. + chl.		Good example of dacite, probably of lava-flow origin
W75	Lithic wacke	Large porphyritic amygdaloidal andesite fragment (5cm across) in typical epiclastic matrix - as for W73. Quartz rimming of fragments very obvious		Cpx. fresh. Plag. → sauss. qtz. + chl. in amygdales		Typical epiclastic
W76	Andesitic agglom-erate	Rounded fragments of porphyritic &/or amygdaloidal andesite in "frothy" vesicular matrix of identical texture & mineralogy. Stretching of matrix indicates flowage	Abundant cpx. & plag. Phenos. in rock frags.	Plag. → sauss. Cpx. mainly fresh. Much chl.+ ep. + pump.+ carb.		Rounded frags., & compositional uniformity suggests flow-breccia horizon within lava

W77	Greywacke	Moderately sorted, immature epiclastic, composed entirely of volcanic detritus, including plag. crystals + fine gr. pilotaxitic andesite frags. + porph. andesite. Minor qtz.-chl. cement	Rock frags. & plag. make up 95% rock. Matrix only 5%	Plag. - sauss. dusted. Chlorite & epidote alt^{n} of andesite frags.		Good example of epiclastic. Better sorting indicates more transport, but frags. still subangular
W78	Bedded greywacke	Moderately sorted, sub-angular to sub-rounded andesitic frags. + plag. grains in altered matrix of carbonate + qtz. + chl. + epidote		Extreme - much chlorite & carbonate		Textures preserved well — enough to be certain rock is epiclastic
W79	Carbonat-ized greywacke	Extreme alterat^{n}. has largely obscurred original textures. Mainly fine gr. chips of plag. + rare rock frags. + opaques in felsic matrix	Plag. chips approx. 30% Carbonate 35%	Extreme - carbonate makes up 35% also chl. + ep.+ sph.+ leucox.		Rarity of rock frags. + abundant chips plag. suggests might be reworked tuff
W80	Dolerite	Holocrystalline, interlocking uralitized cpx. + altered plag. + leucoxenised opaques + interstitial pools quartz	Opaques 5% Qtz. 5% Altered Cpx.+ plag comprise remainder	Cpx. - fresh & uralitized Plag. → sauss. Opaq. → leucox.		Relatively coarse opaques (skeletal in part) indicate is dolerite rather than basalt
W81	Carbonat-ized dolerite	Granular mosaic of carbonate & chlorite. Have relic intergranular pools quartz & skeletal opaques indicating originally a dolerite	Opaques 5% Quartz 5% Chlorite 50% Carbonate 40%	Extreme. Complete alt^{n}. to carbonate & chlorite		As above
W82	Lithic wacke	Subrounded dacitic & andesitic rock frags. extremely closely packed in chlorite-carbonate matrix. Frags. are devitrified to microgranular felsic mosaics		Plag. → sauss. Cpx. → chlorit. Chl.+ carbonate in matrix		Could be locally reworked lava or tuff
W83	Uralitized dolerite	Mosaic of uralite + quartz + carbonate + opaques. Can see outlines of long (up to 2mm), plag. laths under PP. light	Mainly qtz. + carbonate + uralite	Cpx. → ural. Plag. → sauss. Abundant carbonate		Highly altered, but probably dolerite from coarse opaques & plag. laths
W84	Dolerite	Interlocking uralitized cpx. + sauss. plag. + intergranular (skeletal) quartz + skeletal ilmenite with exsolved magnetite	Opaq. 5% Qtz. 15% Plag. 45% Cpx. 35%	Cpx. fresh & uralitized Plag.- sauss. & epidotized Opaque - leucox.		Typical dolerite. Exsolution textures in opaques, notable
W86	Brecciated basalt (weathered	Quartz-hematite-sericite rock. Brecciated texture defined by microgranular qtz.-sericite surrounded by hematite rich zones		Completely altered by weathering		From pillowed basalt sequence - brecciated zone in basalt
W87	Altered dolerite	Identical description to W83				
W88	Greywacke	Close-packed aggregate angular plag. + subrounded pilotaxitic andesite & dacite frags. in matrix chl. + epidote + carbonate + qtz. No cpx. chips. Angular plag. suggests <u>may</u> be reworked tuff	Plag. 50% Frags. 20% Matrix comprises rest	Plag. → fresh to sauss. dusted Much chl. + ep. + carb. in matrix		Similar to W82 in abundance plag. + dacitic rock frags. and lack of cpx. Different provenance or due to sorting

W90	Weathered rock	Quartz-sericite-hematite rock. No distinctive textures preserved in T.S. No clues as to original rock type		Extreme weathering caused much alteration		Field relationships indicate could be epiclastic, collected near W89
W89	Weathered epiclastic	Quartz-sericite-hematite rock. Under P.P. Light can see ghosted outlines of subrounded rock frags. + plag. phenos. in close packed texture		"		Textures indicate is an epiclastic
W91	Weathered epiclastic	Quartz-kaolin rock. Abundant volcanic rock frags. + quartz + plag. visible in T.S. & H.S.		"		"
W93	Lithic wacke	Variety andesitic rock frags. - vesicular &/or porph. of all sizes + plag. + cpx. crystals in qtz.-chl.-carbonate matrix. Frags. in matrix are subangular	Abundant plag. & cpx. grains	Cpx. → chlorite Plag. → sauss. Chl.+ carb. + qtz.-rich matrix		Typical epiclastic. Mostly fragments are closely-packed porph. andesite
W94	Porphyritic andesite-dacite	Closely-packed euhedral phenos. plag. + chloritized cpx. in devit. matrix consisting of plag. microlites + opaques - primary devit. texture	Phenos. 55% of which Plag. 70% Cpx. 30%	Cpx. - chlorite + carbonate Plag.- sauss. dusted	✓	Lithic fragment from within W93 type lithic-wacke
W95	Porphyritic dacite-andesite	Subrounded, anhedral phenos. plag. + euhedral cpx. (twinned) - often in glomeroporph. aggregates in a dense matrix of chlorite + epidote + qtz. + sauss. plag.	Phenos. 15% of which Plag. 70% Cpx. 30%	Cpx. fresh Plag. sauss.	✓	Lithic fragment from lithic wacke. Typical of med. gr. sparsely porphyritic intermediate volcanic
W96	Porphyritic dacite-andesite	Med. gr. subhedral phenos. plag. + chlorite (after cpx.) + opaques in matrix of randomly-oriented plag. microlites + qtz. + opaques + chlorite	Phenos. 25% of which Plag. 90% Cpx. 10%	Cpx. → chlorite Plag. → sauss. dusted. Matrix of chl.+ carb.+ ep.	✓	Variant on normal - matrix is unusually plag. rich
W97	Andesitic agglomerate	Fragments of vesicular, porphyritic andesite - with abundant fine gr. phenos. plag. oriented in a trachytic texture. Frags. are uniform & boundaries of them only defined by divergent alignment of plag. laths	Plag.laths 50% Amyg. 15% Chl.+ ep.+ qtz. matrix rest	Plag. sauss. dusted Cpx. → chlorite + chl.+ ep. in matrix		Textural & mineralogical uniformity of fragments indicates probably a flow breccia
W98	Lithic wacke	Large porphyritic-vesicular andesite fragment (> 2cm across) surrounded by subangular fine gr. volcanic rock frags. (qtz. rimmed) & in chl.-carbonate cement	No plag. fragments	Extreme, to carbonate + chlorite + ep.		Excellent textures preserved - clearly an epiclastic
W99	Lithic tuff	Variety of andesitic rock fragments, all highly angular in an altered matrix in which textures not preserved. No vesic.frags.		Extreme, to carbonate + sericite + qtz. + chlorite		Lack vesic. frags., variety frags. & angularity suggests pyroclastic origin
W100	Lithic wacke	Rounded fragments porphyritic andesite, ave. diam. 6cm, in very fine-grained matrix of subangular andesitic rock frags. - closely packed, in chlorite-carbonate cement	Larger rock frags. make up 60% rock	Extreme - mainly qtz.+ chl. + carbonate + epidote		Most unusual rock. Bimodal size - large well rounded rock frags. in typical f.g. epiclastic matrix
W101	Porphyritic amygdaloidal andesite	Randomly oriented, euhedral laths of plagioclase (ave. length .5mm) + qtz.-chlorite or carbonate-filled amygdales within matrix chlorite + plag. microlites	Plag. laths 15% Amyg. 30%	Matrix mainly chlorite. Much carbonate & chl.& qtz. in amygdales		Field relationships show rock from flow-brecciated top of andesite lava flow

W102	Highly altered dolerite	Mixture of carbonate + chlorite + epidote + qtz. Vague outlines plag. laths can be seen + coarse opaques		Extreme		Coarse opaques indicate rock originally a dolerite
W103	Bedded sediment	Quartz-sericite-hematite rock. No distinctive textures, except vague grain outlines & occasional relic(?) plag. fragments		Completely weathered		In close proximity to W102 (dolerite)
W104	Altered andesite	Scattered, altered phenos. plag. in an altered plag.-rich matrix. Completely altered to chlorite + epidote + quartz + carbonate		Extreme		Andesitic lava (or dyke?) within epiclastics
W105	Andesitic agglom-erate	Rounded fragments porphyritic (non-vesicular) andesite - all uniform texture & mineralogy & similar to matrix. All frags. of lava origin	Phenos. 45% of which Plag. 60% Cpx. 40%	Extreme. Plag. → sauss. Cpx.→ uralit. Matrix, chl. + ep.		Probably flow breccia near top of andesitic lava flow
W106	Lithic wacke	Variety larger andesitic rock frags. with trachytic, pilotaxitic, vesicular textures all > 1cm across within fine gr. matrix plag. frags. + andesite frags.		Chlorite-qtz.-carbonate matrix. Plag. sauss. dusted		Typical textures of epi-clastic. Variety frags. from variety sources
W107	Weathered lithic wacke	Quartz-sericite-hematite rock. Fragments now sericite + quartz & surrounded by hematite after cement(?)		Weathering has caused extreme alt^{n}.		Textures in T.S. & field relationships consistent with epiclastic origin
W108	Andesitic agglom-erate	Fragments vesicular, porphyritic andesite, texturally & mineralogically uniform, in a similar matrix. Frags. angular to subrounded		Mainly alt^{n}. minerals -carbonate in amygdules + chlorite + epidote + pumpellyite + qtz. + sphene. Plag. entirely saussuritized		Probably a flow breccia within lava flow
W109	Andesitic agglom-erate	Identical description to W108. Fragment boundaries slightly clearer		Some fresh cps. As above		"
W110	Bedded tuff	Altered, crystal & pumice(?) rich layers alternating with fine ash-size layers. Some layers truncated, but no obvious reworking. Coarser crystal-rich bands well oriented		Extreme- to carbonate, epidote, chlorite, sphene, qtz.		Within epiclastic sequence. Probably a bedded air-fall tuff, no reworking evident in section
W111	Porphy-ritic pyroxene basalt	Fine gr. phenos. cpx. often in glomeroporphyritic aggregates + opaques within pilotaxitic matrix of plag. microlites + cpx. + chlorite + epidote	Cpx. phenos. make up 18% rock. No plag. phenos.	Cpx. fresh. Plag. fresh to saussuritized. Chl.+ ep. in matrix	✓	Relatively mafic rock
W112	Lithic tuff(?)	Variety of angular andesitic rock frags. including trachytic, pilotaxitic, non porphyritic types within altered andesitic matrix. Vesicular frags. not abundant		Extreme, to carbonate & chlorite + epidote + qtz.+ sphene		Variety of non vesicular frags. & spacing apart suggests pyroclastic. No diagnostic textures.
W113	Andesitic agglom-erate	Rounded, porphyritic amygdaloidal andesite fragments cemented by carbonate + chlorite + qtz. + small rock frags. formed by brecciation - in places resembling an epiclastic		Extreme - abundant carbonate + chlorite + epidote + qtz.+ pumpellyite		Field relationships clearly establish this as a flow-top breccia on andesitic lava flow

W114	Altered, porphyritic andesite	Quartz-chlorite-carbonate-epidote rock. Euhedral phenos. plag. completely replaced by carbonate. Ghosted cpx.(?) replaced by chlorite		Complete alt^{n}. to carbonate + chlorite + epidote + quartz		Field relationships suggest almost certainly was a typical porph. andesite
W115	Porphyritic pyroxene andesite	Sparse glomeroporphyritic phenos. cpx. within pilotaxitic matrix composed of well oriented plag. laths + granular cpx. + epidote + qtz. + chlorite + opaques. Similar to W111	Phenos. ~ 3% of rock. Are all cpx.	Cpx. mainly fresh Plag. → sauss. Much chlorite + ep. in matrix		Almost certainly lava flow within sequence
W116	Andesitic lithic wacke	Subrounded porphyritic andesite frags. (some amygdaloidal) + grains cpx. & plag. in matrix chlorite + qtz. + carbonate + epidote	All rock frags. + crystals	Plag. → sauss. Much chl. + carbonate + epidote		Epiclastic - within sequence of dominantly lava flows comparable with W115
W117	Reworked tuff	In hand spec.- bedded & graded. Composed of angular, chloritized (vitric?) frags., closely packed within chlorite-qtz.-carbonate-epidote matrix	All rock frags. Rare crystal chips	Extreme. Rock frags. → chloritized. Much carb. + chl. + ep.		Grading & subangular frags. indicates a tuff. Lack of matrix suggests reworked(?)
W118	Porphyritic andesite	Abundant, close packed, fine-med. gr. tabular laths plag. in matrix opaques + chlorite + uralite + minute plag. laths. Some uralit. cpx. phenos.	Phenos. 65% of which 95% plag & 5% altered cpx.	Cpx. → chlorite & uralite. Plag. partially sauss.	✓	Plag. only partially oriented. Originally a lava flow. Abundant phenos.
W119	Porphyritic pyroxene andesite	Fine-med. gr. phenos. euhedral cpx., often in glomeroporph. aggregates in holocrystalline, interlocking matrix plag. + epidote + amphibole (after cpx.)	Phenos. 12% Are all cpx.	Cpx. mainly fresh, some uralite. Plag. fresh. epid. + amph. in matrix		Originally lava flow. Fresh, twinned cpx. phenos. & absence of plag. are significant
W120	Porphyritic andesite	Med. to coarse gr. phenos. plag. + cpx. - euhedral to subhedral, in matrix of plag. + qtz. + epidote + chlorite + opaques. Fresh, cpx. often twinned	Phenos. 35% of which Plag. 65% Cpx. 35%	Plag. completely sauss. Cpx. fresh & chloritized. Matrix altered		Lava flow. Notable features are coarse plag. phenos. - up to 1cm & twinned cpx.
W121	Porphyritic basalt-andesite	Fine gr. (rare med. gr.) phenos. plag. + cpx. - oriented, in a matrix plag. + chlorite + opaques + epidote. Close packing of phenos. similar to 118	Phenos. 60% of which Plag. 60% Cpx. 40%	Plag. sauss. & Cpx. chlorit. Epidote in matrix	✓	Lava flow. Excellent preservation textures
W122	Porphyritic andesite	Identical description to W121 - taken from same unit		More severe than W121. No primary minerals.		As for W121
W123	Porphyritic andesite	Med.-coarse gr. euhedral phenos. plag. + cpx. + amygdules (qtz.-chl.-carb. filled) all strongly oriented in hyalopilitic matrix plag. microlites + altered glass	Phenos. 45% of which Plag. 80% Cpx. 20%	Cpx. → chlorite Plag. → sauss. Altered plag. + aphanitic g/mass	✓	Lava flow. Excellent texture preservation although altered. Rock frag. from lithic tuff
W124	Porphyritic andesite	Identical description to W123. In particular, cpx. commonly zoned. Pilotaxitic matrix of strongly oriented plag. microlites. Phenos. also oriented	Phenos. 30% of which Plag. 60% Cpx. 40%	As above		Lava flow. Rock frag. - typical example from lithic tuff in north

W125	Porphyritic andesite	Fine-med. gr. phenos. plag. + cpx. Cpx. fresh & often in glomporph. aggregates. Matrix of epidote + chlorite + carbonate + sphene + leucoxene	Phenos. 50% of which Plag. 60% Cpx. 40%	As above	✓	Lava flow. Rock frag. from lithic-tuff in north. Twinned Cpx.
W126	Lithic tuff(?)	Variety of andesitic rock frags. - some porphyritic & resembling W125, others amygdaloidal. One frag. is largely altered to pumpellyite, whereas other show no pumpellyite alt^{n}. Matrix is largely quartz + carbonate - obscures textures. Contortion and flattening indicates was glassy.	All rock frags. + carbonate + quartz	Extreme: much carbonate + qtz. + pumpellyite. Carbonate & qtz. after glassy matrix?		Matrix rock within which W123, 4, 5 occur. Probably a pyroclastic but could be an autobrecc. lava-field relationships indicate less likely. Pumpellyite development synvolcanic
W127	Vitric-crystal tuff	Qtz.-chlorite-carbonate rock + altered cpx. & plag. phenos. Pumpellyite has replaced glass shards(?)- highly cuspate & angular. Surrounded by carbonate & qtz.		Extreme - abundant pumpellyite, chlorite, epidote, qtz, carbonate		Unwelded tuff. Probably of ash flow origin. Abundant glass shards
W128	Lithic tuff	Similar to W126 - i.e., variety of andesitic rock fragments - some completely altered to pumpellyite, others not. Glassy matrix - psuedo shard shapes & collapsed pumice		Abundant pumpellyite + chlorite + carbonate + quartz + epidote + sericite		Probable pyroclastic. Clear evidence of synvolcanic alt^{n}. to pumpellyite
W129	Possible granite?	Quartz-hematite-sericite rock. Some anhedral, composite grains qtz.		Completely altered by weathering		In hand specimen looks like a granite, despite weathering
W130	Lithic tuff	Porphyritic andesite rock fragments of varying grainsize & textures in an originally glassy matrix with crystal chips of plag. Microcryst. felsic (devit.) matrix	Abundant plag. phenos.	plag. fresh & twinned Abundant carbonate, chlorite		Superficially a porphyritic andesite, but devit. matrix + chips + rock frags. indicate is pyroclastic
W131	Porphyritic hornblende -cpx.andesite	Fine-med. grained phenos. hornblende & cpx. in holocrystalline matrix of interlocking plag. + amphibole. Some h/b is primary & zoned, some is after cpx.	Phenos. 20% of which H/b 70% Cpx. 30%	Cpx. → amphibole in part. Abundant uralite in matrix	✓	Along strike from W31 & W119. Identical in thin section
W132	Weathered porph. andesite	Quartz-hematite-sericite rock. No obvious textures in thin section, but hand specimen shows typical porphyritic andesite textures		Completely weathered		Porphyritic andesite - probably lava
W133	Porphyritic amygdaloidal andesite	Sparse phenos. med-fine gr. plag. + qtz.-filled amygdales + one anhedral qtz. pheno. in a pilotaxitic matrix of oriented plag. microlites	Phenos. 10% Amyg. 15%	Plag. entirely saussuritized. Much epidote + chlorite in matrix		Altered, sparsely porphyritic lava
W134	Altered porphyritic andesite	Fine gr. phenos. plag. in a recrystallised (devit.?) matrix rich in quartz + carbonate + sericite	Phenos. 25% Nearly all plag.	Extreme. Alt^{n}. phenos. & matrix to carbonate & sericite		Lava-flow origin

W135	Weathered porphyritic andesite	Sericitized fine-med. gr. phenos. plag. + ferruginised cpx. in quartz-sericite matrix	Phenos. 20% of which Plag. 60% Cpx. 40%	Weathered, hence qtz.-hematite-sericite assemblage		Lava-flow origin
W136	Weathered porphyritic andesite	Identical description to W135. Can distinguish ghosted outlines of med. gr. euhedral plagioclase		Weathering has caused conversion to clay		Lava-flow origin
W137	Lithic wacke	Variety of closely-packed, subangular andesitic rock fragments (mostly porphyritic) in a qtz.-chlorite-carbonate matrix		Severe to chlorite + qtz. + carbonate ± epidote		Typical altered lithic wacke.
W138	Lithic wacke	Identical description to W137. One large (~ 1½ cm) amygdaloidal andesite frag. Typical close packing with quartz-chlorite cement. Much carbonate		Alt^{n}. to chlorite + qtz. + carbonate + epidote		"
W139	Altered porphyritic andesite	Fine gr. phenos. plag. + cpx. - both completely altered, in a microcrystalline qtz. + sericite + chlorite + epidote + carbonate matrix	Too altered to determine	Extreme, to components mentioned in description		Originally an andesitic lava
W140	Andesitic agglomerate	Porphyritic, amygdaloidal andesite fragments (subrounded & with pilotaxitic matrix) in an identical matrix. Some evidence for shearing		Plag. - sauss. Much chlorite + epidote + qtz. in matrix		Possibly a flow-brecciated lava
W141	Lithic tuff	Variety of subangular andesitic rock fragments - mostly porphyritic in a carbonate-quartz matrix. No diagnostic textures except shape of rock frags.	Mostly rock frags. Much carbonate in matrix	Extreme - matrix now entirely carbonate & qtz.		Fragment texture - not typical of epiclastic. Therefore probably a pyroclastic
W142	Lithic tuff	Variety of subangular to subrounded rock fragments (andesitic) + crystals plag. + glassy frags. in a glassy matrix showing ghosted shard outlines	Mostly rock frags. - some glassy. Much carbonate	Extreme - to epidote + chlorite + carbonate + qtz. + sericite		Texture not that of epiclastic. Vitroclastic textures indicate is pyroclastic-probably ash-flow tuff
W143	Porphyritic andesite	Med. gr. phenos. plag. + cpx., usually as euhedral crystals but sometimes in glomeroporphyritic aggs. in aphanitic matrix of chlorite +epidote + sph.+ leucox.	Phenos. 40% of which Plag. 55% Cpx. 45%	Cpx.- fresh & chloritized Plag. sauss. Matrix altered		Typical andesitic lava
W144	Porphyritic dacite	Med.-fine-grained phenos. plag. rare amphibole & anhedral quartz in a fine gr. matrix of oriented plag. laths & microlites + quartz + clots epidote & chlorite + sphene. & carbonate	Phenos. 60% of which Plag. 95% Plag. has Ab65 composition	Plag. - sauss. & epidotised. Epidote + chlorite + sphene + carbonate in matrix	✓	Field relationships indicate is intrusive-forming part of extensive uniform outcrop
W145	Porphyritic dacite	Med.-coarse grained euhedral, zoned, phenos. plagioclase & fine-med. gr. euhedral, twinned, brown hornblende in a fine gr. devit. matrix. Phenos. oriented	Phenos. 50% of which Plag. 85% Hornblende 15%	Plag. - sauss. Clots epidote & chlorite after h/b. H/b mostly fresh.	✓	Field relationships indicate is intrusive (JAH pers.comm.) Uniform throughout

W146	Porphyritic rhyolite	Fine-med. gr. phenos. subhedral plag. (unzoned) + rare K-feldspar in a siliceous microcrystalline matrix of quartz + feldspar + hematite + sericite	Phenos. 40% of which Plag. 95%	Plag. sericite dusted. Hematite & seric. in matrix	✓	Oriented phenos, good crystal preservat^{n}. suggests <u>not</u> pyroclastic. Possibly intrusive or lava
W147	Porphyritic rhyolite	Sparse fine-med. gr. phenos. plag. in a devitrified(?) matrix quartz + sericite. Some psuedo-shard outlines	Phenos. ~ 4% All Plag.	Plag. sericitized & much sericite in matrix	✓	Possibly a pyroclastic i.e. rhyolitic tuff of probable ash-flow origin
W148	Porphyritic rhyodacite	Med. gr. euhedral, zoned phenos. plagioclase & fine gr. embayed quartz + brown amphibole (some altered to epidote + chlorite+ in microcryst. devit. matrix	Phenos. 30% of which Plag. 50% H/b. 15% Quartz 35%	Plag. sericite dusted H/b - epidote & chlorite	✓	Great affinities with W145, but slightly more acid - indicated by qtz. phenos. Probably intrusive

TABLE A5.2. Geochemical data for selected rocks from the Welcome Well complex, listed in order of increasing SiO_2.

	W24	W7	W150	W3	W2	W121	W111	W31	W131	W118	W4	W123	W14	W125	W5
SiO_2	40.78	50.25	47.98	50.29	50.03	51.22	52.39	52.19	53.01	53.43	54.42	55.55	55.87	56.51	56.90
Al_2O_3	3.48	10.49	14.78	13.69	15.78	16.35	16.12	16.63	17.70	17.11	14.03	15.73	16.70	15.93	15.65
$Fe_2O_3^t$	16.17	11.60	15.02	10.99	12.14	9.53	11.01	7.60	7.28	10.57	9.29	10.22	8.37	8.80	8.95
MnO	0.22	0.18	0.2	0.18	0.17	0.15	0.16	0.11	0.10	0.15	0.16	0.16	0.15	0.15	0.15
MgO	34.95	17.26	5.74	11.37	6.82	7.00	6.13	6.84	5.99	4.78	8.02	6.58	4.60	6.07	6.51
CaO	3.35	8.12	11.55	8.98	10.03	9.01	8.89	10.37	9.64	6.51	8.32	6.50	7.90	6.44	5.30
Na_2O	0.24	1.00	3.01	1.86	2.50	2.61	2.78	4.93	4.92	5.34	3.15	3.50	3.71	3.25	5.34
K_2O	0.02	0.49	0.02	0.97	1.00	2.53	0.65	0.36	0.49	0.17	1.18	0.38	0.85	1.74	0.19
TiO_2	0.31	0.51	1.37	1.01	1.47	0.99	1.19	0.81	0.76	1.29	1.04	0.98	1.12	0.86	0.83
P_2O_5	0.03	0.06	0.14	0.37	0.25	0.28	0.23	0.32	0.36	0.29	0.22	0.20	0.33	0.16	0.13
Total	99.55	99.95	99.88	99.71	100.20	99.67	99.55	100.15	100.22	99.64	99.83	99.80	99.60	99.91	99.94
LOI	6.06	0.19	1.92	3.70	3.02	2.79	1.96	1.55	2.12	2.03	2.22	3.80	1.81	3.12	2.14
Zr	13.4	54	82	111	125	188	115	108	115	169	116	125	138	109	106
Nb	1.8	3.4	4.3	6.1	7.0	9.1	6.8	4.9	5.9	7.8	7.4	6.5	5.3	5.6	5.0
Y	3.2	13	31	23	28	26	25	16	17	27	21	21	24	21	20
Ce	7.0	8.7	8	55	35	46	38	55	63	41	27	27	29	22	34
Nd	2.0	6.4	14	34	24	32	25	39	33	32	24	21	17	14	19
Sc	13	29	48	28	26	18	26	21	16.5	23	26	27	18	23	25
V	92	168	350	197	209	136	205	133	117	189	179	193	154	179	186
Cr	4990	2536	165	799	331	150	152	81	67	94	650	455	51	253	304
Ni	1860	687	70	317	203	93	91	84	147	105	276	186	20	132	188
Rb	1.5	16	1.5	24	22	20	15	5.3	7	4.7	25	13	18	46	2.5
Sr	18	114	132	421	262	394	302	734	1350	377	266	235	278	428	253
Ba	12	155	18	270	299	346	195	554	449	113	256	80	251	1066	145

	W49	W23	W22	W65	W59B	W94	W95	W96	W29	W17	W145	W144	W148	W146	W147
SiO_2	57.30	57.63	59.52	61.40	61.55	61.86	61.90	61.92	66.05	67.12	67.16	67.96	69.23	77.38	77.66
$Al_2O_{3_t}$	15.46	16.07	17.94	15.01	15.73	17.70	16.25	17.04	15.82	15.78	15.71	16.28	15.16	12.95	13.78
Fe_2O_3	9.47	8.45	7.98	7.79	6.89	3.98	6.34	7.35	5.60	3.46	4.29	3.71	3.46	1.55	1.13
MnO	0.15	0.13	0.11	0.10	0.08	0.07	0.10	0.06	0.07	0.06	0.07	0.06	0.06	0.03	0.01
MgO	6.19	5.31	2.84	4.47	3.28	2.66	3.53	1.24	3.18	1.92	1.95	1.63	1.21	0.22	0.22
CaO	4.84	5.69	7.49	4.75	7.38	4.24	7.07	3.06	1.92	5.08	3.37	4.55	4.24	0.50	0.34
Na_2O	4.44	3.41	2.03	3.53	3.02	8.02	3.07	7.54	6.40	5.57	5.09	5.00	3.70	6.84	5.41
K_2O	1.17	2.37	0.73	1.55	0.14	0.18	0.69	0.24	0.34	0.68	1.80	0.64	2.76	0.33	1.08
TiO_2	0.96	1.05	1.04	1.14	1.12	0.70	0.97	1.11	0.63	0.59	0.47	0.49	0.42	0.33	0.11
P_2O_5	0.16	0.17	0.20	0.32	0.42	0.16	0.34	0.43	0.16	0.12	0.11	0.12	0.11	0.05	0.02
Total	100.14	100.27	99.88	100.04	99.62	99.47	100.63	100.01	100.17	100.37	100.02	100.43	100.35	100.16	99.74
LOI	4.27	2.77	3.39	2.79	2.82	4.11	2.26	1.94	2.20	2.00	1.35	1.69	1.33	1.32	1.99
Zr	108	125	125	197	193	137	160	277	155	121	123	119	110	91	61
Nb	4	7	7.3	10.5	11	4.8	9	11.5	6.8	4.5	5.1	3.6	4.2	3.1	2.5
Y	22	20	22	18	20	20	16	39	17	9.4	10	9.9	10.2	2.9	12
Ce	22	27	53	49	60	22	49	58	35	18	39	25	35	14.3	32
Nd	21	11	28	32	37	20	27	40	18	9	14	17	11	3.6	11
Sc	29	21	23	14	16	13	16	10.5	10	14	10	9.5	8.2	5.6	1.3
V	169	158	166	118	136	109	119	58	85	99	66	66	54	49	3.5
Cr	575	336	376	151	126	60	119	14	28	101	31	19	16	16	4.6
Ni	279	140	184	78	68	66	70	12	24	51	31	24	24	12	8.6
Rb	22	54	65	49	3	3.5	18	7	7	12	36	16	84	26	22
Sr	128	586	1029	428	526	211	552	255	329	294	300	426	333	251	379
Ba	271	1275	1551	436	48	358	129	128	292	271	411	320	844	362	2021

TABLE A5.3. Geochemical data for selected rocks from the Welcome Well complex, grouped according to their geochemical affinities.

	Basalts relatively enriched in P_2O_5 and LREE			Transitional basalt	Basalts and andesites less enriched in P_2O_5 and LREE							
	W3	W31	W131	W121	W2	W111	W4	W123	W125	W5	W49	W23
SiO_2	50.29	52.19	53.01	51.22	50.03	52.39	54.42	55.55	56.51	56.90	57.30	57.63
Al_2O_3	13.69	16.63	17.70	16.35	15.78	16.12	14.03	15.73	15.93	15.65	15.46	16.07
Fe_2O_3 t	10.99	7.60	7.28	9.53	12.14	11.01	9.29	10.22	8.80	8.95	9.47	8.45
MnO	0.18	0.11	0.10	0.15	0.17	0.16	0.16	0.16	0.15	0.15	0.15	0.13
MgO	11.37	6.84	5.99	7.00	6.82	6.13	8.02	6.58	6.07	6.51	6.19	5.31
CaO	8.98	10.37	9.64	9.01	10.03	8.89	8.32	6.50	6.44	5.30	4.84	5.69
Na_2O	1.86	4.93	4.92	2.61	2.50	2.78	3.15	3.50	3.25	5.34	4.44	3.41
K_2O	0.97	0.36	0.49	2.53	1.00	0.65	1.18	0.38	1.74	0.19	1.17	2.37
TiO_2	1.01	0.81	0.76	0.99	1.47	1.19	1.04	0.98	0.86	0.83	0.96	1.05
P_2O_5	0.37	0.32	0.36	0.28	0.25	0.23	0.22	0.20	0.16	0.13	0.16	0.17
Total	99.71	100.15	100.22	99.67	100.20	99.55	99.83	99.80	99.91	99.94	100.14	100.27
LOI	3.70	1.55	2.12	2.79	3.02	1.96	2.22	3.80	3.12	2.14	4.27	2.77
Zr	111	108	115	188	125	115	116	125	109	106	108	125
Nb	6.1	4.9	5.9	9.1	7.0	6.8	7.4	6.5	5.6	5.0	4	7
Y	23	16	17	26	28	25	21	21	21	20	22	20
Ce	55	55	63	46	35	38	27	27	22	34	22	27
Nd	34	39	33	32	24	25	24	21	14	19	21	11
Sc	28	21	16.5	18	26	26	26	27	23	25	29	21
V	197	133	117	136	209	205	179	193	179	186	169	158
Cr	799	81	67	150	331	152	650	455	253	304	575	336
Ni	317	84	147	93	203	91	276	186	132	188	279	140
Rb	24	5.3	7	20	22	15	25	13	46	2.5	22	54
Sr	421	734	1350	394	262	302	266	235	428	253	128	586
Ba	270	554	449	346	299	195	256	80	1066	145	271	1275

	Andesitic differentiates relatively enriched in P_2O_5, LREE, Zr and Nb				Andesitic differentiates less enriched in P_2O_5, LREE, Zr and Nb				Acid differentiates				
	W65	W59B	W95	W96	W118	W14	W22	W94	W29	W17	W145	W144	W148
SiO_2	61.40	61.55	61.90	61.92	53.43	55.87	59.52	61.86	66.05	67.12	67.16	67.96	69.23
Al_2O_{3t}	15.01	15.73	16.25	17.04	17.11	16.70	17.94	17.70	15.82	15.78	15.71	16.28	15.16
Fe_2O_3	7.79	6.89	6.34	7.35	10.57	8.37	7.98	3.98	5.60	3.46	4.29	3.71	3.46
MnO	0.10	0.08	0.10	0.06	0.15	0.15	0.11	0.07	0.07	0.06	0.07	0.06	0.06
MgO	4.47	3.28	3.53	1.24	4.78	4.60	2.84	2.66	3.18	1.92	1.95	1.63	1.21
CaO	4.75	7.38	7.07	3.06	6.51	7.90	7.49	4.24	1.92	5.08	3.37	4.55	4.24
Na_2O	3.53	3.02	3.07	7.54	5.34	3.71	2.03	8.02	6.40	5.57	5.09	5.00	3.70
K_2O	1.55	0.14	0.69	0.24	0.17	0.85	0.73	0.18	0.34	0.68	1.80	0.64	2.76
TiO_2	1.14	1.12	0.97	1.11	1.29	1.12	1.04	0.70	0.63	0.59	0.47	0.49	0.42
P_2O_5	0.32	0.42	0.34	0.43	0.29	0.33	0.20	0.16	0.16	0.12	0.11	0.12	0.11
Total	100.04	99.62	100.63	100.01	99.64	99.60	99.88	99.47	100.17	100.37	100.02	100.43	100.35
LOI	2.79	2.82	2.26	1.94	2.03	1.81	3.39	4.11	2.20	2.00	1.35	1.69	1.33
Zr	197	193	160	277	169	138	125	137	155	121	123	119	110
Nb	10.5	11	9	11.5	7.8	5.3	7.3	4.8	6.8	4.5	5.1	3.6	4.2
Y	18	20	16	39	27	24	22	20	17	9.4	10	9.9	10.2
Ce	49	60	49	58	41	29	53	22	35	18	39	25	35
Nd	32	37	27	40	32	17	28	20	18	9	14	17	11
Sc	14	16	16	10.5	23	18	23	13	10	14	10	9.5	8.2
V	118	136	119	58	189	154	166	109	85	99	66	66	54
Cr	151	126	119	14	94	51	376	60	28	101	31	19	16
Ni	78	68	70	12	105	20	184	66	24	51	31	24	24
Rb	49	3	18	7	4.7	18	65	3.5	7	12	36	16	84
Sr	428	526	552	255	377	278	1029	211	329	294	300	426	333
Ba	436	48	129	128	113	251	1551	358	292	271	411	320	844

	Acid differentiates cont.		Genetically unrelated ultramafic intrusives		Tholeiitic basalt
	W146	W147	W24	W7	W150
SiO_2	77.38	77.66	40.78	50.25	47.98
$Al_2O_{3_t}$	12.95	13.78	3.48	10.49	14.78
Fe_2O_3	1.55	1.13	16.17	11.60	15.02
MnO	0.03	0.01	0.22	0.18	0.2
MgO	0.22	0.22	34.95	17.26	5.74
CaO	0.50	0.34	3.35	8.12	11.55
Na_2O	6.84	5.41	0.24	1.00	3.01
K_2O	0.33	1.08	0.02	0.49	0.02
TiO_2	0.33	0.11	0.31	0.51	1.37
P_2O_5	0.05	0.02	0.03	0.06	0.14
Total	100.16	99.74	99.55	99.95	99.88
LOI	1.32	1.99	6.06	0.19	1.92
Zr	91	61	13.4	54	82
Nb	3.1	2.5	1.8	3.4	4.3
Y	2.9	12	3.2	13	31
Ce	14.3	32	7.0	8.7	8
Nd	3.6	11	2.0	6.4	14
Sc	5.6	1.3	13	29	48
V	49	3.5	92	168	350
Cr	16	4.6	4990	2536	165
Ni	12	8.6	1860	687	70
Rb	26	22	1.5	16	1.5
Sr	251	379	18	114	132
Ba	362	2021	12	155	18

TABLE A 5.4. Rare earth element contents in selected samples from the Welcome Well complex.

Sample Rock	W3 basalt	W2 basalt	W131 basalt	W5 andesite	W14 andesite	W95 andesite	W17 dacite	W146 rhyolite	Chondrite normalising factors
La	22.3	14.85	28.12	15.95	12.6	23.0	8.43	8.66	0.315
Ce	54.5	34.8	63.1	34.39	29	48.5	18.0	14.33	0.813
Nd	34.1	23.85	33.2	19.0	16.8	27.2	8.96	3.55	0.597
Sm	6.47	5.60	6.64	4.50	3.80	5.11	1.98	0.553	0.192
Eu	1.73	1.73	1.88	1.39	1.13	1.53	0.64	0.183	0.0722
Gd	5.34	5.95	5.42	4.85	3.92	4.24	1.86	0.466	0.259
Dy	3.79	5.35	3.32	4.60	3.59	2.81	1.52	0.412	0.325
Er	1.92	3.01	1.49	2.86	2.17	1.64	0.805	0.311	0.213
Yb	1.71	2.73	1.27	2.60	2.02	1.35	0.803	0.347	0.208
$\%SiO_2$	50.29	50.03	53.01	56.90	55.87	61.90	67.12	77.38	
%MgO	11.37	6.82	5.99	6.51	4.60	3.53	1.92	0.22	

Notes:
1. All values determined by mass spectrometer using an isotope dilution technique.
2. The chondrite normalising factors used to obtain the chondrite-normalised values plotted in Fig. 5.11 are listed in the last column.

TABLE A 5.5. Electron microprobe analyses of phenocrysts in Archaean calc-alkaline volcanic rocks from the northern Norseman-Wiluna greenstone belt.

A. Clinopyroxene

Sample	W3				W22				W95				W119			
Number of determ.	6	1	4		5	5	5		4	5	4		4	4	4	
Location	centre	int.	edge	average	centre	int.	edge	average	centre	int.	edge	average	centre	int.	edge	average
SiO_2	51.50	53.43	52.19	51.92	51.14	51.45	52.32	51.64	51.63	50.78	51.67	51.31	50.49	50.58	50.30	50.45
Al_2O_3	2.55	1.53	2.53	2.45	3.00	3.05	2.68	2.91	1.79	1.88	2.25	1.97	3.89	3.61	3.76	3.75
FeO^t	6.19	6.59	7.83	6.82	9.92	10.33	8.09	9.45	10.11	9.51	9.14	9.58	5.32	6.04	6.02	6.45
MgO	17.88	18.75	17.07	17.67	15.58	15.43	16.54	15.85	14.92	15.47	15.49	15.31	16.27	15.89	12.96	15.04
CaO	21.88	19.69	20.38	21.14	20.36	19.73	20.38	20.16	21.55	22.35	21.46	21.83	24.02	23.89	25.02	24.31

B. Amphibole

Sample	W31			W59			I12		
Number of determ.	4	4		6	5		4	4	
Location	centre	edge	average	centre	edge	average	centre	edge	average
SiO_2	42.12	42.03	42.80	45.47	45.76	45.62	45.92	45.39	45.66
Al_2O_3	14.54	1.50	1.49	10.50	9.76	10.13	11.03	11.18	11.10
FeO^t	10.17	10.41	10.29	12.49	15.08	13.79	11.75	12.24	12.00
MnO				0.22	0.22	0.22			
MgO	15.39	15.14	15.27	14.80	13.08	13.58	15.40	15.06	15.23
CaO	12.57	12.50	12.53	12.33	12.64	12.49	11.77	11.95	11.86
Na_2O	2.02	2.07	2.05	1.59	1.26	1.43	1.98	1.96	1.97
K_2O	1.38	1.24	1.31	0.24	0.25	0.25	0.38	0.42	0.40
TiO_2	1.47	1.50	1.49	1.43	1.10	1.27	1.74	1.78	1.76

Note: 1. Analyses obtained using the energy dispersive method.

TABLE 6.1. Brief thin section descriptions of a representative selection of rocks from the Spring Well complex.

SAMPLE NUMBER	ROCK NAME	DESCRIPTION	% MINERALS	ALTERATION	ANAL.	COMMENTS
S1	Lithic-vitric-crystal tuff	Lithic fragments of fine-grained lava(with oriented plag. microlites) & vitric-crystal tuff + crystals plag. & quartz within glassy, vitroclastic matrix complsed of flattened shards & pumice - i.e. welded tuff		Plag. fresh, but abundant epidote. Extensive devitrification. Textures preserved	✓	Typical of tuff-breccia to lapilli-tuff units. Clearly of ash flow origin
S2	Devitrified rhyolite	Microcrystalline granular mosaic of quartz + plagioclase + K-feldspar. Scattered opaques + coarser grained patches quartz + carbonate	Difficult to estimate	Opaques → leucoxene. Secondary carbonate	✓	Block within tuff-breccia from which S1 was taken
S4	Micro-diorite	Holocrystalline medium-grained rock consisting of interlocking plag. laths, clinopyroxene, leucoxene. Intergranular pools qtz. & microcrystalline felsic material & chlorite. Minor sphene	Plag. 60% Cpx. 20% Opaques 4% Intergran. 16%	Cpx. - fresh & chloritized. Opaque → leucoxene Plag.→saussuritized	✓	Typical of ubiquitous intrusives into volcanic pile. NB. zoned opaques
S7	Rhyolitic vitric-crystal tuff	Scattered fine-med. gr. phenos. plag. + anhedral quartz, often in glomeroporph. aggregates within matrix of finely crystalline qtz. + feldsp. + sphene + leucox.	Phenos. 5% Plag. 60% Qtz. 40%	Abundant epidote. Completely devitrified matrix	✓	Block within tuff-breccia from which S1 was taken
S8	Rhyolitic vitric-crystal tuff	Fine-med. gr. size amygdales infilled with quartz or carbonate + plag. & quartz phenos. in microlitic devitrified matrix with minute, flattened shards - i.e., welded tuff	Amyg. 20% Phenos. 5% Matrix 75%	Opaques → leucoxene Carbonate + secondary qtz. in amygdales	✓	Block within tuff-breccia from which S1 was taken
S9	Micro-diorite	Med. gr. tabular laths plagioclase interlocking with opaques, cpx. & interstitial pools of microcrystalline felsic material, cut by acicular needles amphibole	Plag. 60% Cpx. 20% Opaques 4% Intergran. 16%	Plag. - sauss. dusted. Opaques → leucoxene Cpx. → chloritized, uralitized,epidotized		Similar comments to S4. Narrow dyke within tuff-breccia pile
S15	Porphyritic rhyodacite	Fine-med. grained phenos. plag. + circular, granular aggregates quartz (after qtz. phenos?) within matrix plag. microlites (unoriented) + qtz. + sph. + leuxoc. + chlorite	Phenos. 15% rock (including quartz aggregates)	Plag.-fresh Opaques → leucox. + sph.	✓	Field relations suggest is a crystal tuff. No diagnostic textures in section
S16	Porphyritic rhyolite	Fine-med. grained phenos. embayed & corroded plag. & quartz + patches granular quartz (after phenos?) + chlorite (after cpx.) in microgranular devitrified matrix + leucox. & sph.	Phenos. 20% Plag. 80% Qtz. 20%	Plag. - fresh, but extensively embayed. Cpx.→ chlorite Opaque → leucox.+sph.	✓	Typical of crystal tuff units in area
S17	Lithic tuff	Flattened rock fragments (mostly vitric-crystal tuffs) within vitric matrix, showing vitroclastic textures with flattened shards & pumice frags. + epidote, chlorite, qtz., carbonate		Abundant grains epidote + clots quartz & carbonate. Chlorite throughout matrix. Plag. phenos. saussuritized.		Typical lapilli-tuff. Clearly welded tuff of ash flow origin

S19	Micro-diorite	Laths plag. (ave. length 1mm) interlocking with altered cpx. & altered opaques plus microcrystalline matrix. Intergranular pools quartz & epidote	Plag. 60% Cpx. & opaques 35% Intergran. 5%	Plag. → sauss. Cpx. → uralitized + epidotized Opaques → leucox.	✓	Typical of dykes intruding volcanic pile
S21	Porphyritic rhyolite	Oriented, fine-med. gr. phenos. plag. & quartz within microcrystalline matrix quartz, feldspar & epidote. Some perlitic cracking & coarser aggregates quartz	Phenos. 8% of which 90% are plag.	Abundant epidote in matrix		Within pyroclastic. Could be lava flow or dyke. No pyroclastic textures
S27	Lithic tuff	Lapilli-size rock fragments (mainly vitric tuffs) within a vitroclastic matrix consisting of deformed shards curved around frags. Completely devitrified	Rock frags. make up 80% rock	Extreme. Much epidote, sericite, sphene, leucoxene, chlorite		Typical example of lapilli-tuff, clearly a welded tuff
S29	Autobrecciated rhyolite	Completely devitrified. Various fragments defined by varying orientations of plag. microlites & conc^{n}. of epidote & hematite. Separated by microcryst. felsic mosaic	Difficult to estimate	Abundant epidote, hematite & chlorite		Uniform mineralogy throughout fragmentation possibly by flowage. Intrusive plag.
S30	Micro-diorite	Similar description to S4, except intergranular felsic material occupies 25% of rock				Typical example of one of intermediate intrusives into pile
S33	Porphyritic rhyolite	Medium gr. phenos. anhedral quartz + plagioclase (completely twinned) within granular, devitrified matrix (some spherulitic devit^{n}.) composed of qtz. + feldsp. + epidote	Phenos. 45% Plag. 50% Qtz. 50%	Plag. sauss.-dusted. Some in matrix	✓	Either a crystal tuff or lava. Field relationships not definitive
S38	Lithic tuff	Variety of lithic fragments ranging from vitric tuffs to amygdaloidal lavas within vitroclastic-textured matrix composed of flattened shards & pumice frags.		Abundant epidote, carbonate, chlorite, sph. & leucox.		Typical lapilli-tuff-welded, of ash flow origin
S39	Porphyritic rhyolite	Fine-med. gr. granular aggregates quartz (probably after phenos.) + plag. phenos. within microcryst. matrix quartz & feldspar + rare epidote & sphene.	Phenos. make up 10% rock. Plag. 30% phenos. Quartz 70%	Very rare carbonate Opaque → sphene	✓	Intrusive plug from field relationships
S40	Fine-grained rhyolite	Sparse med. gr. phenos. plag. + fine gr. qtz. aggregates within microlitic quartz - plag. matrix. Matrix highly siliceous, scattered epidote	Plag. phenos. ~ 2%. Abundant plag. microlites in matrix	Minor chlorite & epidote in matrix. Plag. → sauss. Opaque → leucox.	✓	Rhyolite dyke from field relationships
S41	Altered rhyolite	Fine-grained phenos. plag. within granular mosaic quartz + epidote + sericite. Unusual type of alteration, not seen elsewhere in complex	Phenos. make up 5% rock - are all plag.	Plag. sericitized & epidotized, particularly that in matrix		Rock from near vent breccia, alteration attributed to fluid emanations from vent zone
S42	Porphyritic dacite	Medium gr. phenos. plag. + pale green hornblende in matrix of unoriented plag. laths & microlites + amphibole + quartz + opaques. Rare cpx. phenos.	Phenos. 50% Plag. 85% H/b. 15%	Plag. sericite-dusted. H/b fresh, minor epidote & chl. alt^{n}.	✓	Intrusive dyke near vent. Matrix texture appears ch. of intrusives

S43	Porphyritic rhyolite	Fine-med. gr. phenos. plag. within microcrystalline granular matrix quartz-feldspar-chlorite. Fine-grained plates K-feldspar. Possible shard outlines	Phenos. 35% - all plagioclase	Plag.→ sericite-dusted. Abundant uralite & chlorite in matrix	✓	Isolated outcrop. Probable crystal tuff of ash flow origin
S44	Microdiorite	Interlocking laths plag. (ave. length .8mm), cpx., interstitial quartz + opaques. Holocrystalline, non porphyritic. Abundant epidote, leucox. - sphene.	Opaques 3% Plag. 50% Cpx. 30% Qtz. 17%	Plag. → extensively sericit. & epidot. Cpx. → fresh & uralitized	✓	Typical of dioritic intrusives into volcanic pile
S45	Porphyritic microdiorite	Med. gr. phenos. plag. + cpx. + brown hornblende (after cpx.) within interlocking matrix plag. + epidote + quartz + leucoxene (after opaques)	Phenos. 45% of which Plag. 60% Cpx. 35% H/b. 5%	Cpx.→ hornblende + chlorite + uralite Plag.→ sericitized extensively		Porphyritic variant on diorite intrusives into volcanic pile
S47	Rhyolitic tuff	Fine-grained phenos. plag. + rock fragments (ash size) within a devitrified quartzo-feldspathic mosaic + chlorite + epidote + carbonate + leucox. - sphene (after ilmenite). Distinctly layered in hand specimen.	Phenos. 15% of rock	Plag. → saussuritized. Matrix badly altered		Fine tuff band, within pyroclastic. Devitⁿ. & alteration has obscured primary textures
S48	Porphyritic rhyolite	Med. gr. phenos. embayed, anhedral quartz + altered plagioclase + fine-grained crystal chips within microcryst. devit. matrix - qtz. + feldspar. + ep. + uralite	Phenos. 40% of which Quartz 55% Plag. 45%	Plag. → sauss & epidotized. Matrix → partially sericitized	✓	Typical crystal tuff from field relationships. Crystal chips & nature of matrix support ash flow origin
S51	Crystal-lithic tuff	Med.-fine gr. phenos. plag. & quartz + devitrified rhyolitic rock fragments (& dacite) within highly-contorted matrix of squashed pumice & flattened shards. Matrix completely devitrified	Phenos. 25% Rock frags. 40% Matrix 35%	Plag. → sauss. Much epidote in matrix & leucox. after opaques		Textures show rock is of ash flow origin. From basal zones of S48 crystal tuff unit
S53	Lithic-crystal tuff	Med.-fine gr. phenos. embayed quartz + plag. + granular devitrified rock fragments in a devitrified matrix - has obliterated all primary textures	Section not representative	Plag. slightly sericitized. Much chlorite & sericite in matrix		Part of tuff-breccia unit. No diagnostic textures on account of devitrification
S54	Porphyritic rhyolite	Medium gr. phenos. plag. & quartz. Local quartz aggregates from fine → med. gr. size (secondary) within microgranular, devitrified felsic matrix + fine opaques + chl.	Phenos. 12% of which Plag. 80% Quartz 20%	Plag. extensively sericitized. brownish colour due to minor hematite		Block from a tuff-breccia unit
S57	Porphyritic dacite	Fine-med. gr. phenos. plag. (in glomeroporph. aggregates) in microgranular matrix plag. microlites + quartz granules + epidote + chlorite. No cpx.	Phenos. 10% (all plag.)	Plag.- saussuritized & epidotized, both in phenos. & matrix	✓	Textures not diagnostic of intrusive or extrusive origin
S60	Porphyritic dacite	Med. gr. phenos. plag. + rare cpx. (often in glomporph. aggregates) within a holocrystalline matrix of interlocking plag. + quartz + epidote (no obvious mafics).	Phenos. 15% (95% plag.) Plag.-rich matrix	Plag.- saussuritized & epidotized in phenos. & matrix	✓	Porphyritic, slightly more plag. rich varient of intrusives into pile
S63	Porphyritic rhyolite	Fine gr. phenos. plag., usually in glomeroporphyritic aggregates with opaques & chlorite (after cpx.) in a devitrified, patchy polarising matrix of qtz. + feldspar	Phenos. 15% of which 95% plag. 5% chlorite + opaques	Plag.-sericite dusted. Cpx.→ chlorite. Some carbonate	✓	No primary textures preserved, but probably an ash-flow tuff from devitrified matrix

S65	Porphyritic dacite	Randomly oriented, med. gr. phenos. plag. + chlots chlorite (after cpx.) within devitrified matrix composed of plag. microlites + chlorite + epidote + opaques + quartz. Some zoned plagioclase	Phenos. 18% of which Plag. 90% Cpx. 10%	Cpx. → chlorite Plag. → sauss. Much chlorite & epidote in matrix	✓	Field relationships not definitive as to origin. Thin section also not conclusive
S70	Porphyritic rhyolite	Fine-med. gr. phenos. anhedral, embayed quartz + embayed plagioclase + clots chlorite (after cpx.) within microcryst. matrix quartz aggregates + plag. microlites + chlorite + K feldspar	Phenos. 15% Plag. 80% Qtz. 15% Cpx. 5%	Plag. → sauss. Cpx. → chlorite Otherwise fresh	✓	Probable rhyolite dyke intrudin, tuff-breccia unit. Field & T.S. inconclusive
S71	Porphyritic rhyolite	Fine-med. gr. phenos. anhedral, embayed quartz + plagioclase within microgranular, felsic matrix (devitrif.). Scattered epidote + opaques (altered to leucox. + sphene) + carbonate	Phenos. 25% of which Plag. 70% Qtz. 30%	Plag.- sericitized Some secondary epidote & carbonate	✓	Typical sample from crystal tuff unit. Primary textures obliterated by devitrification
S81	Porphyritic rhyolite	Fine-med. gr. phenos. plag. + quartz in matrix plag. microlites + quartz. Clots carbonate & chlorite. Chlorite + opaques + red hematite scattered through matrix	Phenos. 12% of which Plag. 80% Qtz. 20%	Plag. sericite dusted Significant amount secondary chlorite	✓	From a unit that could be intrusive or crystal tuff. T.S. non diagnostic
S83	Porphyritic rhyodacite	Med. gr. phenos. plag. + patches chlorite within matrix of randomly-oriented plag. microlites + quartz + chlorite + scattered opaques. Matrix holocrystalline & relatively coarse	Phenos. 8% all plag. Plag. & qtz. approx.equal % in matrix	Plag. sericite dusted. Much chlorite scattered through rock		Field relationships suggest is intrusive, supported by relatively coarse matrix
S86	Lithic tuff	Devitrified rhyolite & dacite rock fragments within a devitrified matrix showing ghosty shard and pumice outlines - contorted & squashed around frags.	Not representative. Some plag. phenos. & numerous microlites	Abundant epidote, sphene, leucox., chlorite, sericite i.e., altered		Typical of tuff-breccia unit. Welded tuff of ash flow origin
S86(2)	Porphyritic rhyolite	Med. gr. phenos. plag., often in glomeroporphyritic aggregates + anhedral quartz + clots chlorite within microgranular matrix of quartz + plag. + K-feldsp. + chl. + epidote	Phenos. 25% of which Plag. 90% Quartz 6% Chlorite 4%	Plag. → minor sericite & epidote alt^{n}. Chl. epidote, sphene leucox. thro' matrix	✓	Matrix completely recrystallised. No hint of primary textures. Most likely a crystal tuff
S91	Porphyritic andesite	Med. gr. phenos. zoned plagioclase + med.-fine euhedral, zoned cpx. within microcrystalline matrix plag. microlites + opaques + uralite needles + minor qtz. Plagioclase composition An54	Phenos. 45% of which Plag. 60% Cpx. 40%	Plag. → sauss. & epidotized. Cpx. fresh, but uralit. in matrix	✓	Intrusive dyke. Greatly resembles andesitic flows from Welcome Well complex.
S95	Greywacke (sediment)	Devitrified volcanic rock fragments + crystals quartz & plagioclase within highly-altered chlorite-uralite matrix		Abundant chlorite, uralite, sericite scattered throughout		Epiclastic sediment. Detritus shed from volcanic pile.
S96	Basalt or Dolerite	Ophitic texture consisting of plag. laths (ave. length .5mm) within cpx. Scattered intergranular quartz & fine opaques	Plag. 40% Cpx. 55% Qtz.+ opq.5%	Plag. → sauss. Cpx. fresh & uralitized	✓	Probably a basalt, but field relationships & T.S. not conclusive
S97	Porphyritic andesite	Medium gr. phenos. plag. + cpx. within a finely-devitrified matrix plus uralite needles. Typical lava flow or intrusive rock texture	Phenos. 40% of which Plag. 60% Cpx. 40%	Plag. → sauss. Cpx. fresh		Field relationships suggest is a dyke probably related to S91

S98	Micro-grano-diorite	Tabular laths plagioclase interlocking with granular quartz and myrmekitic quartz-plagioclase intergrowths & cpx. Medium grainsize, holocrystalline	Plag. laths 35% Myrmekite 35% Quartz. 25% Cpx. 5%	Plag. → sericitized Cpx. → amphibole & chlorite	✓	Granitoid intrusive into volcanic pile in south of area
S100	Rhyolitic-crystal tuff	Fine gr. crystals and crystal "chips" (with highly angular shapes) of quartz & plagioclase within microgranular devitrified matrix showing ghosty shard outlines	Crystals 40% of which Plag. 50% Quartz 50%	Plag. → sericit. Minor sericite & chlorite scattered thro' matrix		At contact of massive crystal tuff unit & tuff-breccia. Clearly a welded tuff of ash flow origin
S102	Rhyolitic crystal tuff	Fine-med. gr. phenos. plag. & quartz in a microgranular devitrified, felsic matrix. Ghosted outlines of squashed pumice & flattened shards	Phenos. 12% of which Plag. 40% Quartz 60%	Plag. → sericiti zed Matrix devitrified mosaic	✓	Typical rhyolite from YANDAL area - clearly welded tuff of ash flow origin
S103	Rhyolitic crystal tuff	Identical description to S102, except slightly high % crystals. Numerous crystal chips - all oriented & matrix too, is markedly foliated	Phenos. 19%	As above		" (matrix entirely glassy-shards originally)
S105	Uralitized basalt	Interlocking fine gr. laths plag. & feathery uralite with scattered very fine-grained leucoxenised opaques. Odd carbonate clots	Uralite 50% Plag. 36% Opaques 4%	Cpx. → uralite Plag. → saussuritized Opaques → leucox.		Basalt on basis of grainsize, texture & alteration. Within acid volc. sequence, YANDAL
S106	Rhyoltic vitric tuff	Devitrified microgranular mosaic in which are scattered quartz & plag. crystal chips (confined to bands). Marked orientation evident in matrix & crystals	Too fine-grained to determine			No clear textures, but almost certainly a vitric tuff of ash flow origin. Not reworked.
S108	Epiclastic	Well sorted rock, consisting of fine-grained subangular quartz, K-feldspar, plagioclase (including albite) + opaques + rare rock frags., all close packed	Feldspar 45% Quartz 30% Matrix 20% Rock frags.5%	Feldspars sericitized Some sericite in in matrix		Epiclastic occurs inter-calated with vitric tuffs (S106) & crystal tuffs (S102,3)
S111	Rhyolitic crystal tuff	Fine-med. gr. crystals & crystal chips of quartz, plagioclase (including "chequered" albite) within microgranular devit. matrix showing ghosty shard outlines	Phenos. 12% Plag. 45% Quartz 55%	Feldspars sericite dusted		Typical crystal tuff - i.e. welded tuff of ash flow origin
S112	Crystal-lithic-vitric tuff	Fine-med. gr. crystals & crystal chips quartz + plagioclase + devitrified microcryst. crystal-vitric tuff rock fragments within devit. vitroclastic matrix	Phenos. 30% Rock frags. 30% Matrix 40%	Plag. phenos. sericitized. Seric.+ epid. + sph.+ leucox. in matrix	✓	Good example of ash-flow welded-tuff from Yandal area
S114	Epiclastic	Moderately sorted, immature sediment consisting of closely packed subangular quartz, plagioclase, albite + rock frags. in matrix of finer material + recrystallised qtz. aggregates	Qtz. 30% Plag. 30% Frags. 20% Matrix 20%	Plag. phenos. sericitized. Biotite, sericite, epidote, sphène in matrix		Superficially resembles aplite in close-packed med. gr. qtz.+ plag., but sedimentary textures

S117	Crystal-vitric tuff	Scattered medium-fine gr. crystals & crystal chips quartz + plag. + K-feldspar - all strongly oriented in an oriented, devit. microcryst. felsic matrix. Ghosted outlines of flattened shards	Crystals 12% of which Quartz 60% Feldsp. 40%	Feldspars sericite dusted. Minor chlorite in matrix	✓	Vitroclastic textures show rock is of ash flow origin
S119	Crystal-lithic-vitric tuff	Variety lapilli-size frags. - mainly rhyolitic vitric & crystal-vitric tuffs within vitroclastic textured matrix thro' which scattered crystals qtz. & plag.	Not representative Crystals qtz. & plag.	Feldspar sericitized Chlorite & epid. thro' matrix		Ash-flow, welded tuff upon basis of flattened shards in matrix
S124	Recrystallised fine sediment(?)	Fine grained quartzo-feldspathic mosaic-recrystallised & no relic primary textures. Patches coarser quartz, superficially resembling crystals	Impossible to determine from T.S.	Extensive sericitization		Possible fine sediment along strike from seds. at Ockerbury Hill
S128	Vesicular non porph. dacite	Amygdales, infilled with chlorite & epidote & rimmed with quartz, + sparse phenos. oriented plag. within matrix of oriented plag. microlites & opaques	Amyg. 10% rock Phenos. < 4%	Leucox. + sphene after opaques. Plag. → sericitized		Field relationships suggest this unit is a dyke. Consistent with textures
S136	Micro-diorite	Identical description to S19 i.e. holocrystalline, non-porphyritic plag. - cpx. rock				Typical of intermed. composition dykes intruding volcanic pile
S137	Porphyritic rhyolite	Med.-fine gr. phenos. plag. & quartz + granular aggregates quartz within devitrified matrix plag. microlites + plates granular quartz + ep. + carb. + leucox.	Phenos. 10% of which Plag. 85% Quartz 15%	Plag. - sericite dusted. Carbonate + epid. + leucox. in matrix		No diagnostic textures, but orientation phenos. & in matrix + flattening suggests ash flow origin
S142	Non porphyritic dacite	Holocrystalline rock consisting of interlocking plag. laths + chlorite + opaques + interstitial quartzo-feldspathic matrix. Rare euhedral plag. phenos. in glomeroporphyritic aggregate	Plag. 70% of rock	Plag. fresh Cpx.→ chloritized & uralitized		Holocrystalline texture suggests is an intrusive. Not inconsistent with field evidence
S148	Fine tuff	Consists entirely of a microgranular felsic mosaic - completely devitrified & no primary textures preserved. In hand specimen the banding, indicates is a tuff	Difficult to estimate	Abundant epidote & sericite		Is a tuff from the top of a graded sequence. No tuffaceous textures preserved in T.S.
S163	Porphyritic rhyolite	Fine-med. grained phenos. embayed plag. & quartz + crystal chips within microgranular devitrified matrix - no primary textures. Also contains devitrified rhyolitic rock fragments similar to S2	Phenos. 25% rock of which 95% are plag. Rock frags. 40%	Plag.→ sericitized & epidotized as is matrix		Transitional crystal-rich unit between typical tuff breccia-(S1) & fine tuff (S148)

TABLE A6.2. Geochemical data for selected rocks from the Spring Well complex, listed in order of increasing SiO_2.

	S96	S19	S4	S44	S91	S60	S42	S1	S141	S65	S15	S43	S71	S81	S57
SiO_2	49.01	55.06	56.90	59.74	59.58	64.10	64.76	64.91	65.63	66.24	70.15	72.41	72.60	73.15	73.28
Al_2O_3	15.09	15.52	15.65	16.92	15.46	16.18	16.00	15.54	14.40	15.32	13.56	13.62	13.58	12.84	12.63
Fe_2O_3 t	12.25	9.96	9.82	6.72	6.34	5.91	4.35	7.16	6.55	5.82	5.36	4.23	3.27	3.71	3.85
MnO	0.23	0.15	0.13	0.10	0.08	0.08	0.07	0.10	0.10	0.08	0.08	0.09	0.05	0.05	0.07
MgO	7.64	5.26	4.06	4.26	4.43	2.32	2.38	1.68	1.80	2.04	1.13	1.13	0.73	0.66	0.39
CaO	13.10	8.99	7.03	7.88	7.17	4.85	2.04	3.92	2.44	1.64	1.85	0.29	1.48	1.14	2.22
Na_2O	1.29	2.37	4.00	3.26	3.37	4.19	6.03	3.49	6.15	5.37	5.54	5.50	4.15	5.70	5.39
K_2O	0.19	0.77	0.90	0.49	2.13	1.39	2.74	2.17	1.26	2.81	1.46	2.33	3.57	1.86	2.14
TiO_2	0.95	1.54	1.26	0.55	1.00	0.66	0.77	0.87	0.83	0.70	0.56	0.39	0.35	0.36	0.32
P_2O_5	0.08	0.41	0.28	0.12	0.57	0.14	0.33	0.27	0.18	0.16	0.11	0.07	0.07	0.06	0.05
Total	99.83	100.03	100.02	100.04	100.13	99.81	99.47	100.11	99.34	100.17	99.81	100.05	99.85	99.52	100.33
LOI	2.14	2.40	2.39	2.32	1.74	1.70	1.86	2.01	1.36	1.92	1.34	1.25	1.49	1.36	1.14
Zr	84	161	149	122	237	193	232	316	233	221	317	315	283	313	336
Nb	4.0	9.8	7.7	5	12	8.3	14	13	10.6	9	14	12.4	12	12	14
Y	20	31	31	18	17.6	24	21	51	43	27	54	47	46	42	45
Ce	2.4	53	36	22	123	42	104	71	57	42	91	84	63	55	64
Nd	6.8	28	20	14	70	21	56	34	30	20	56	43	30	31	33
Sc	48	25	25	19	14	14	8	14	15	11	11	9	6.3	9	8
V	300	158	187	108	106	78	73	26	126	66	29	-	18	-	-
Cr	331	217	19	88	168	13	54	9	6	7	2	3	8	5	4
Ni	110	96	47	87	105	37	45	10	13	18	11	3	-	-	-
Rb	7.7	22	24	17	56	36	55	52	23	62	28	47	79	26	53
Sr	147	378	202	186	777	193	218	164	129	173	57	54	136	48	182
Ba	43	261	260	142	551	335	653	673	613	773	232	887	596	325	439

	S98	S86(2)	S16	S48	S63	S8	S70	S112	S2	S7	S39	S33	S117	S40	S102
SiO_2	73.80	73.90	74.92	75.23	75.88	75.97	77.24	77.10	78.64	78.31	78.69	79.45	80.05	81.07	82.42
$Al_2O_{3_t}$	13.63	13.30	13.13	12.98	11.99	11.27	12.00	13.15	11.52	11.17	11.27	11.43	10.72	10.09	9.65
Fe_2O_3	1.73	2.80	2.34	2.73	2.62	3.11	1.59	1.31	0.24	1.87	1.54	1.21	0.91	0.68	0.65
MnO	0.02	0.04	0.04	0.05	0.06	0.09	0.01	0.04	0.02	0.02	0.04	0.02	0.01	0.02	0.02
MgO	0.60	0.64	0.54	0.71	0.38	0.36	0.23	0.19	0.09	0.18	0.12	0.45	0.11	0.15	0.07
CaO	3.10	1.78	0.76	2.75	1.59	2.36	0.13	0.93	0.87	0.73	0.31	1.20	0.15	1.00	0.30
Na_2O	6.07	4.97	5.33	3.67	4.95	5.23	3.51	5.27	4.98	5.88	4.24	5.93	0.35	5.10	2.06
K_2O	0.46	2.28	2.37	1.76	1.93	0.10	4.73	2.14	3.13	0.06	3.49	0.25	8.41	1.58	4.92
TiO_2	0.49	0.32	0.28	0.23	0.28	0.80	0.26	0.11	0.32	0.14	0.25	0.21	0.08	0.21	0.08
P_2O_5	0.09	0.06	0.05	0.04	0.04	0.23	0.04	0.01	0.08	0.01	0.03	0.03	0.01	0.02	0.01
Total	99.99	100.09	99.74	100.15	99.73	99.52	99.73	100.23	99.89	98.37	99.99	100.17	100.75	99.93	100.17
LOI	0.63	1.17	0.92	1.05	2.10	1.57	0.57	0.57	0.73	0.76	0.70	0.84	0.35	0.58	0.61
Zr	328	265	245	199	306	203	227	141	267	261	307	256	165	272	112
Nb	12	11	12	13	13	9.5	12	15	11.6	11	14	12	20	14	12.5
Y	52	40	43	45	39	30	41	31	31	44	43	40	37	28	24
Ce	76	69	70	110	74	45	46	96	43	75	100	42	113	80	72
Nd	36	34	35	42	40	25	25	42	27	40	47	28	54	39	30
Sc	8	6	5	5	8	11	4	3	8	5	8	5	4	3	2
V	-	-	-	-	14	6	-	-	-	-	-	-	-	-	-
Cr	6	8	7	7	9	-	4	-	-	-	-	-	-	-	-
Ni	-	-	-	12	7	-	-	-	-	-	-	-			11
Rb	6	52	49	40	37	3	84	100	72	2	57	5	232	30	128
Sr	155	120	42	94	105	29	54	81	65	55	24	39	32	93	40
Ba	243	520	314	548	457	45	804	449	750	53	584	195	905	427	810

TABLE A 6.3. Rare earth element contents in selected samples from the Spring Well complex.

Sample Rock	S19 andesite	S4 andesite	S141 dacite	S48 rhyolite	S70 rhyolite	Chondrite normalising factors
La	24	16.1	26.5	56.5	19.96	0.315
Ce	52.8	36.3	56.6	109.5	45.83	0.813
Nd	27.8	19.9	30.4	41.6	24.9	0.597
Sm	5.96	4.60	6.50	7.61	5.95	0.192
Eu	1.58	1.33	1.48	1.59	2.52	0.0722
Gd	5.38	5.76	7.09	8.11	7.67	0.259
Dy	4.07	5.00	6.23	6.25	4.72	0.325
Er	2.10	2.98	3.67	3.84	2.40	0.213
Yb	1.72	2.71	3.29	3.78	2.09	0.208
$\%SiO_2$	55.06	56.90	65.63	75.23	77.24	
%MgO	5.26	4.06	1.80	0.71	0.23	

Notes:
1. All values determined by mass spectrometer using an isotope dilution technique.
2. The chondrite normalising factors used to obtain the chondrite-normalised values plotted in Fig. 6.9 are listed in the last column.

APPENDIX 2

Locations of all samples for which data is tabulated in Appendix 1.

FIGURE A2.1

Sample locations in the Lake Everard area.

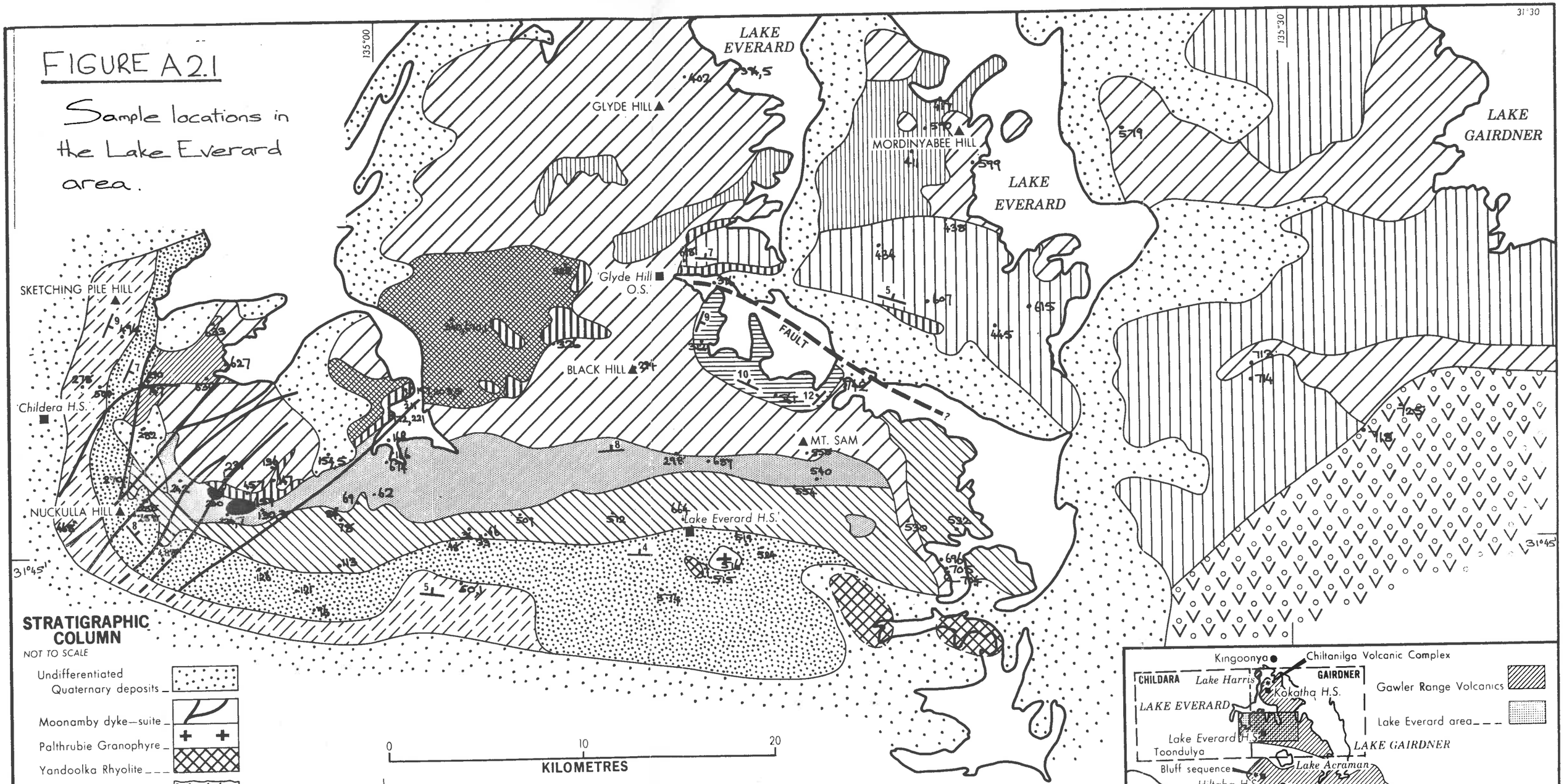

STRATIGRAPHIC COLUMN

NOT TO SCALE

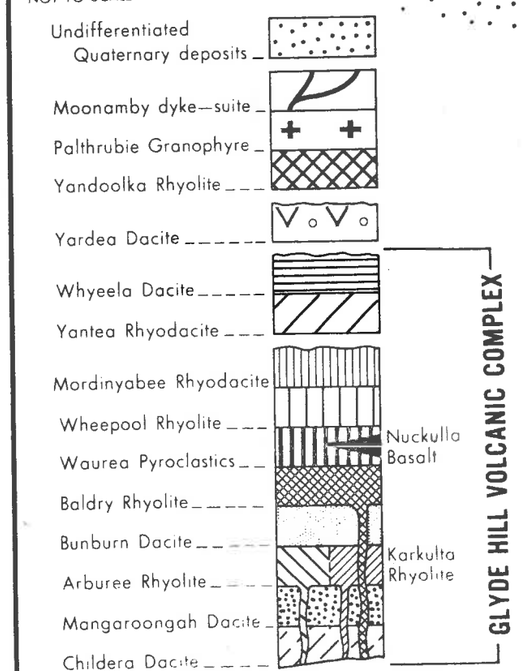

ROCK RELATIONSHIP DIAGRAM

NOT TO SCALE

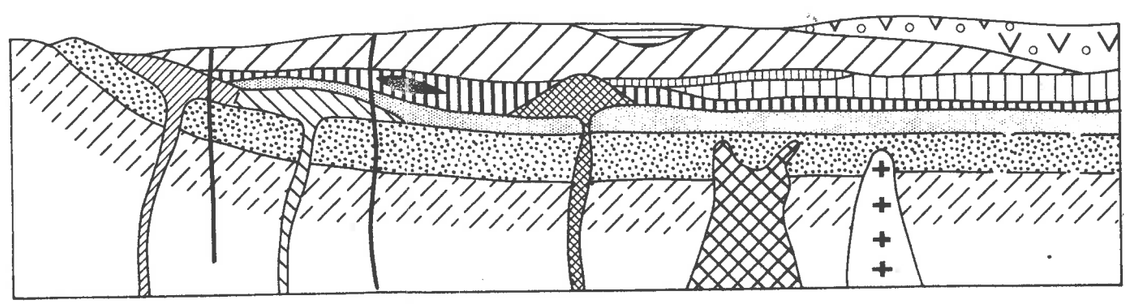

(A Department of Mines 76-929)

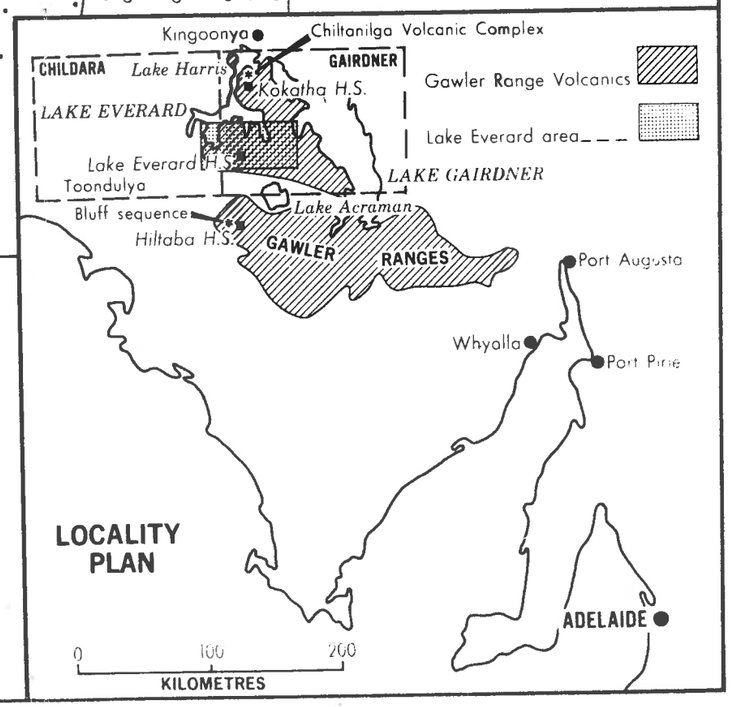

FIGURE A3.1

Sample locations in the Central Australian province

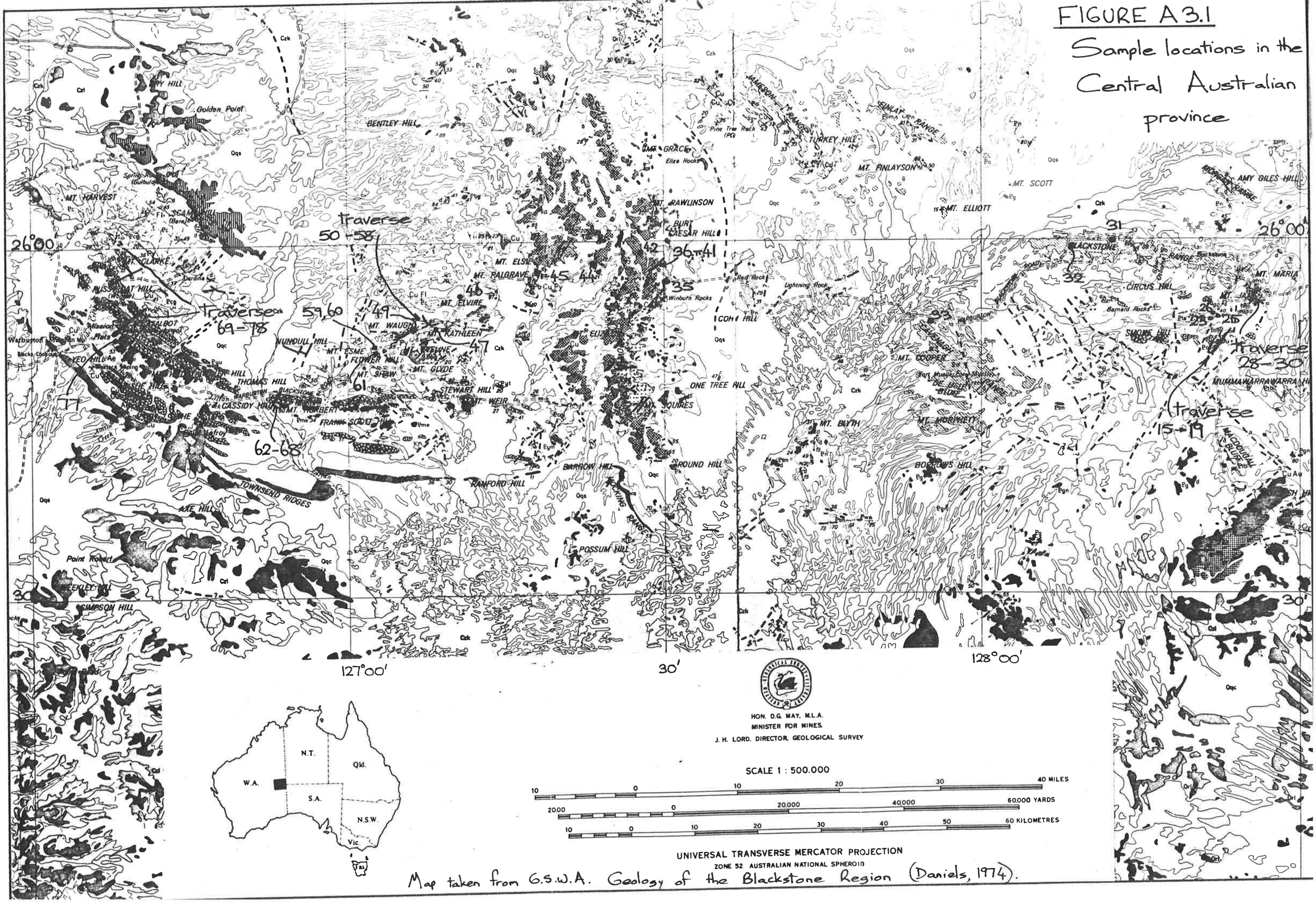

HON. D.G. MAY, M.L.A.
MINISTER FOR MINES.
J. H. LORD, DIRECTOR, GEOLOGICAL SURVEY

SCALE 1 : 500.000

10 0 10 20 30 40 MILES
20,00 0 20,000 40,000 60,000 YARDS
10 0 10 20 30 40 50 60 KILOMETRES

UNIVERSAL TRANSVERSE MERCATOR PROJECTION
ZONE 52 AUSTRALIAN NATIONAL SPHEROID

Map taken from G.S.W.A. Geology of the Blackstone Region (Daniels, 1974).

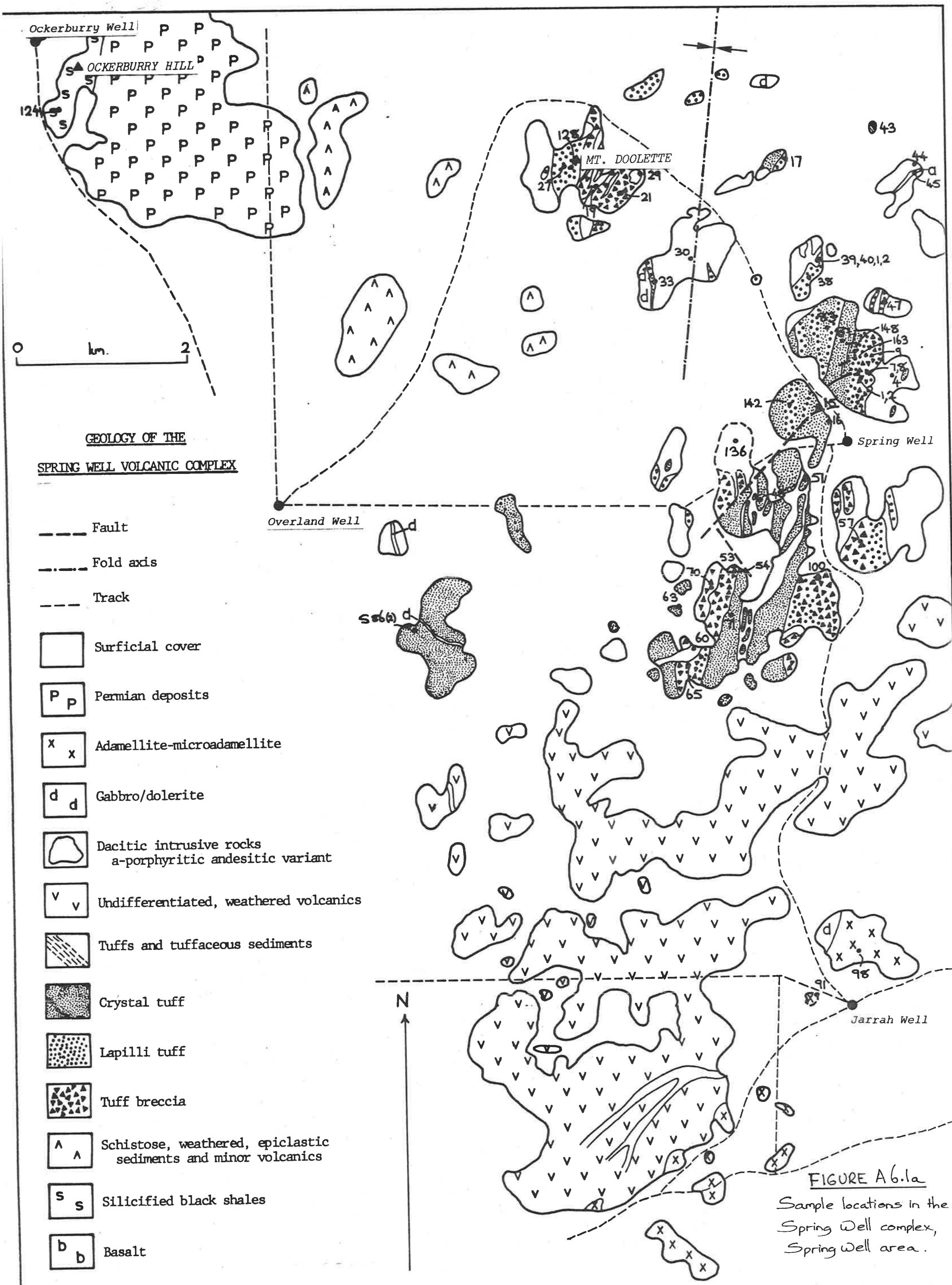

FIGURE A6.1a
Sample locations in the Spring Well complex, Spring Well area.

FIGURE A6.1b

Sample locations in the Spring Well complex, Yandal area.

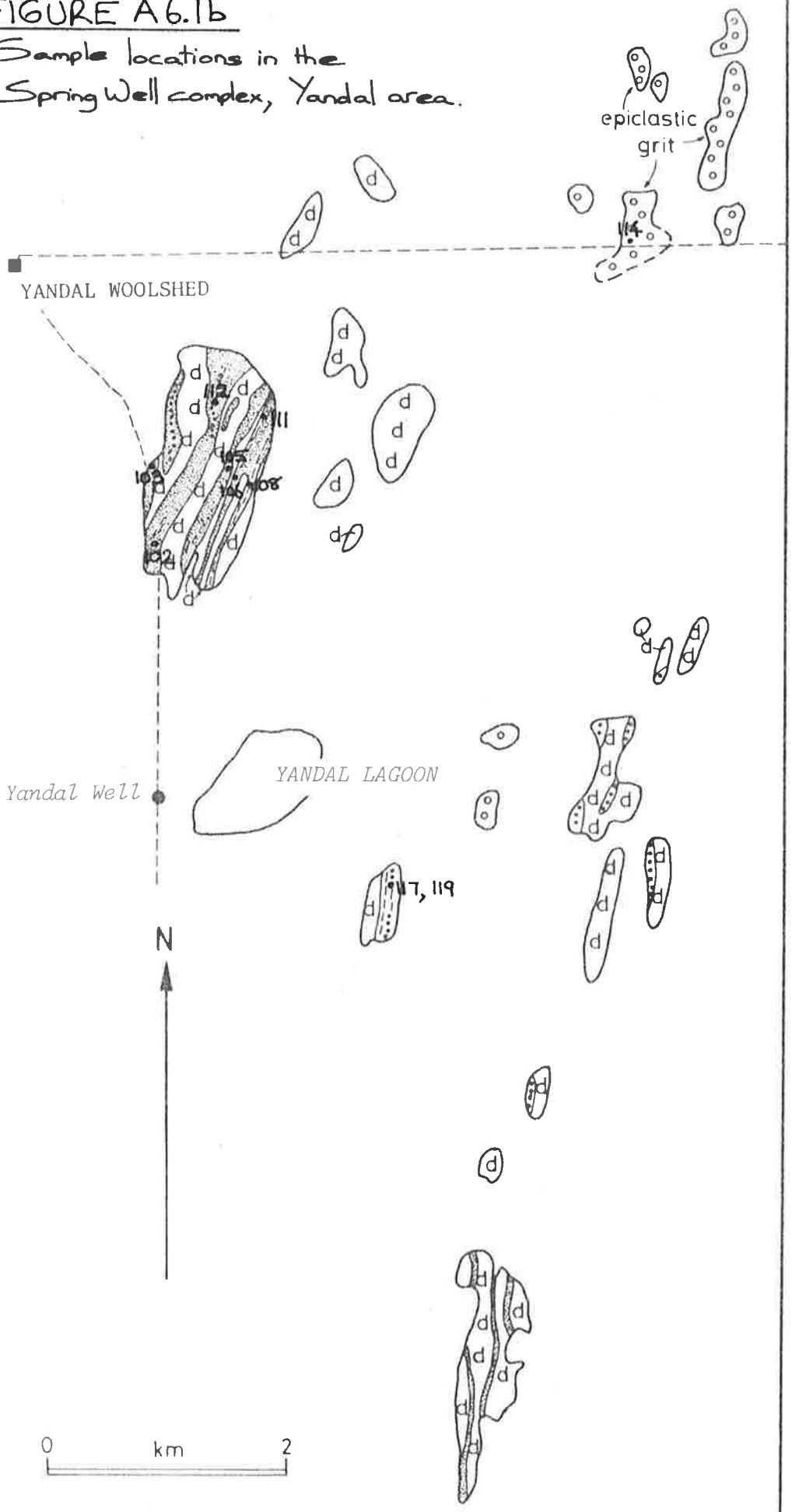

symbols as for 1A, with the addition of $\overset{\circ}{\circ}$ for epiclastic grit

REFERENCE for Figure A3.1

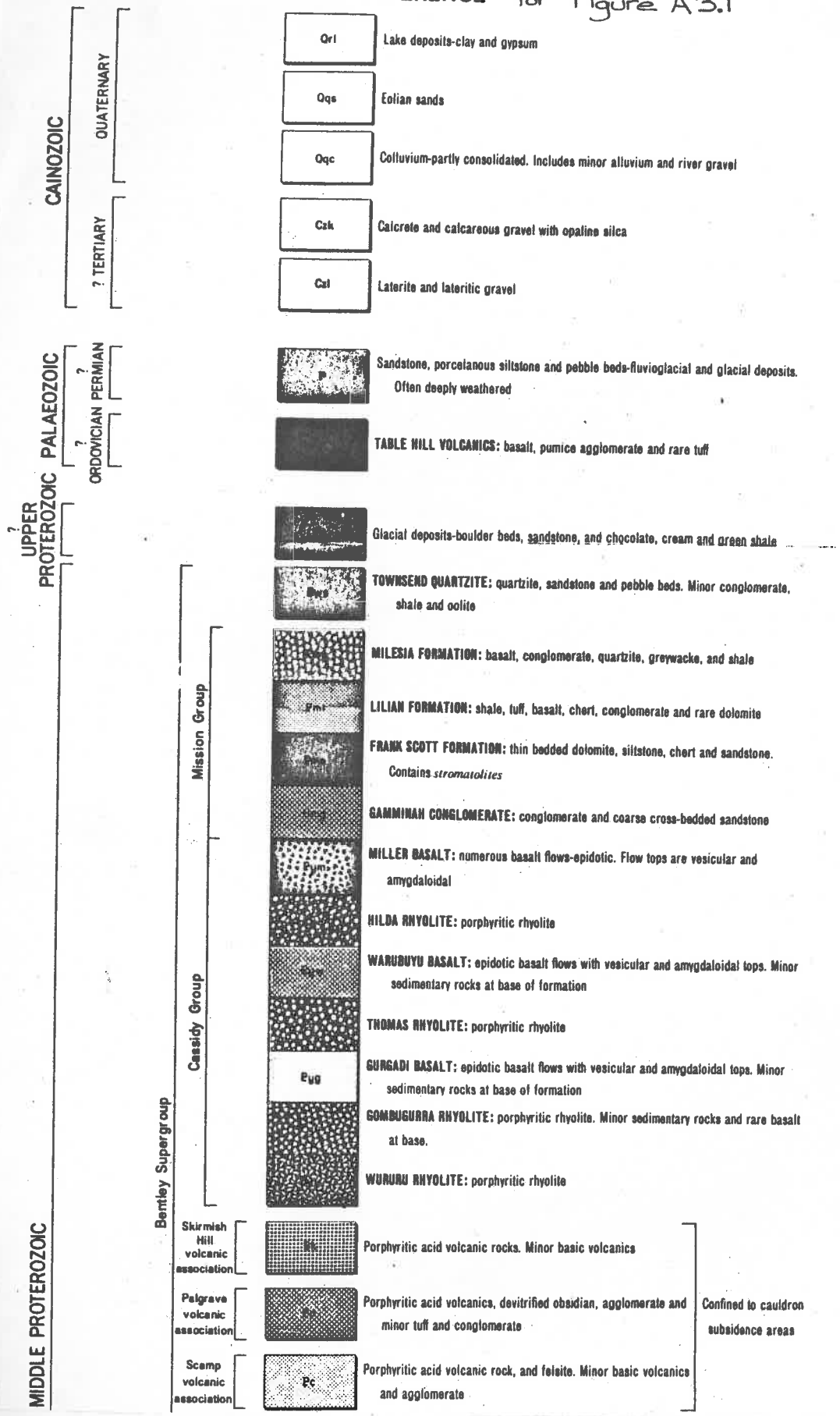

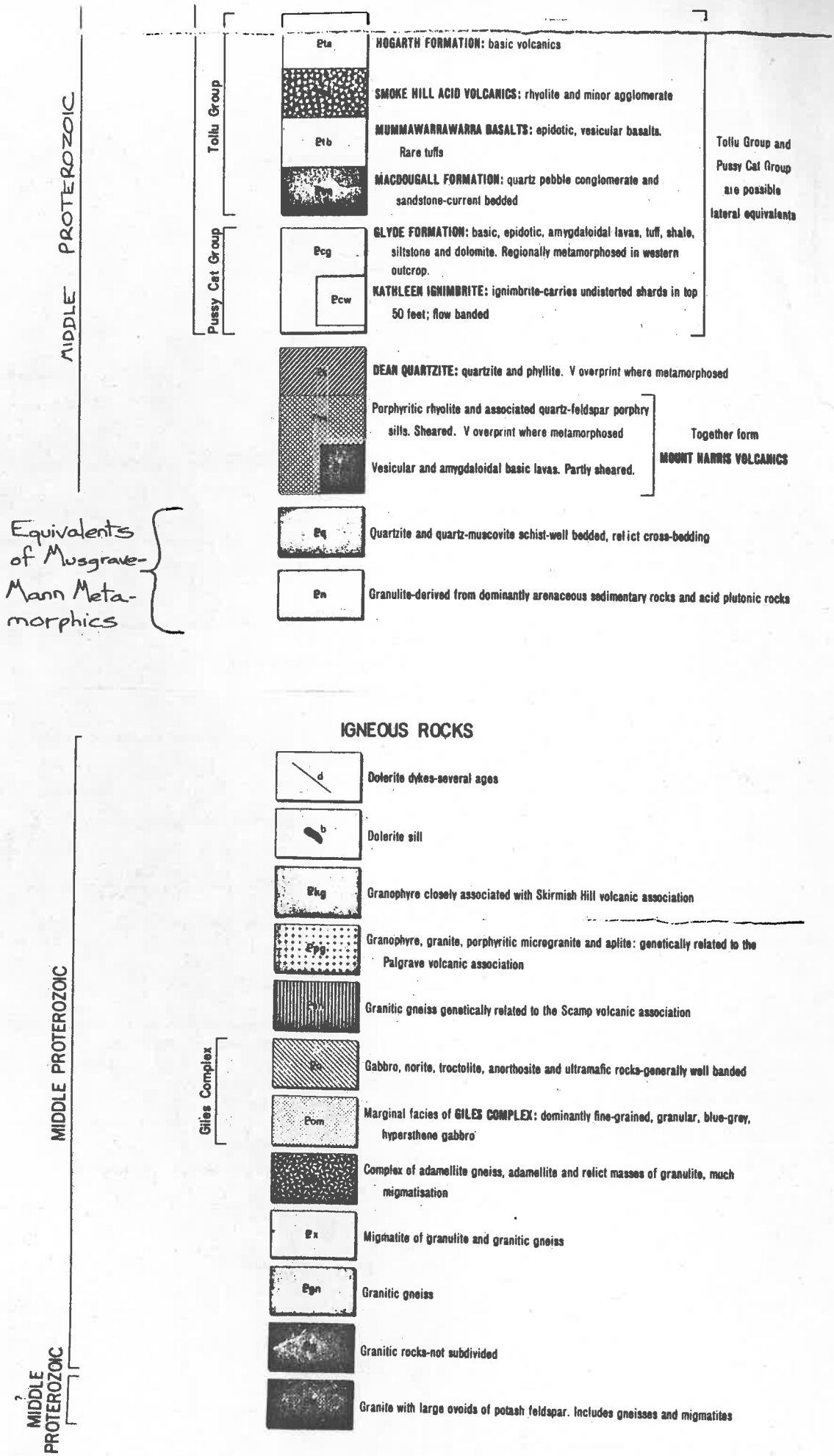

from G.S.W.A, Geobgical Map of the Blackstone Region.

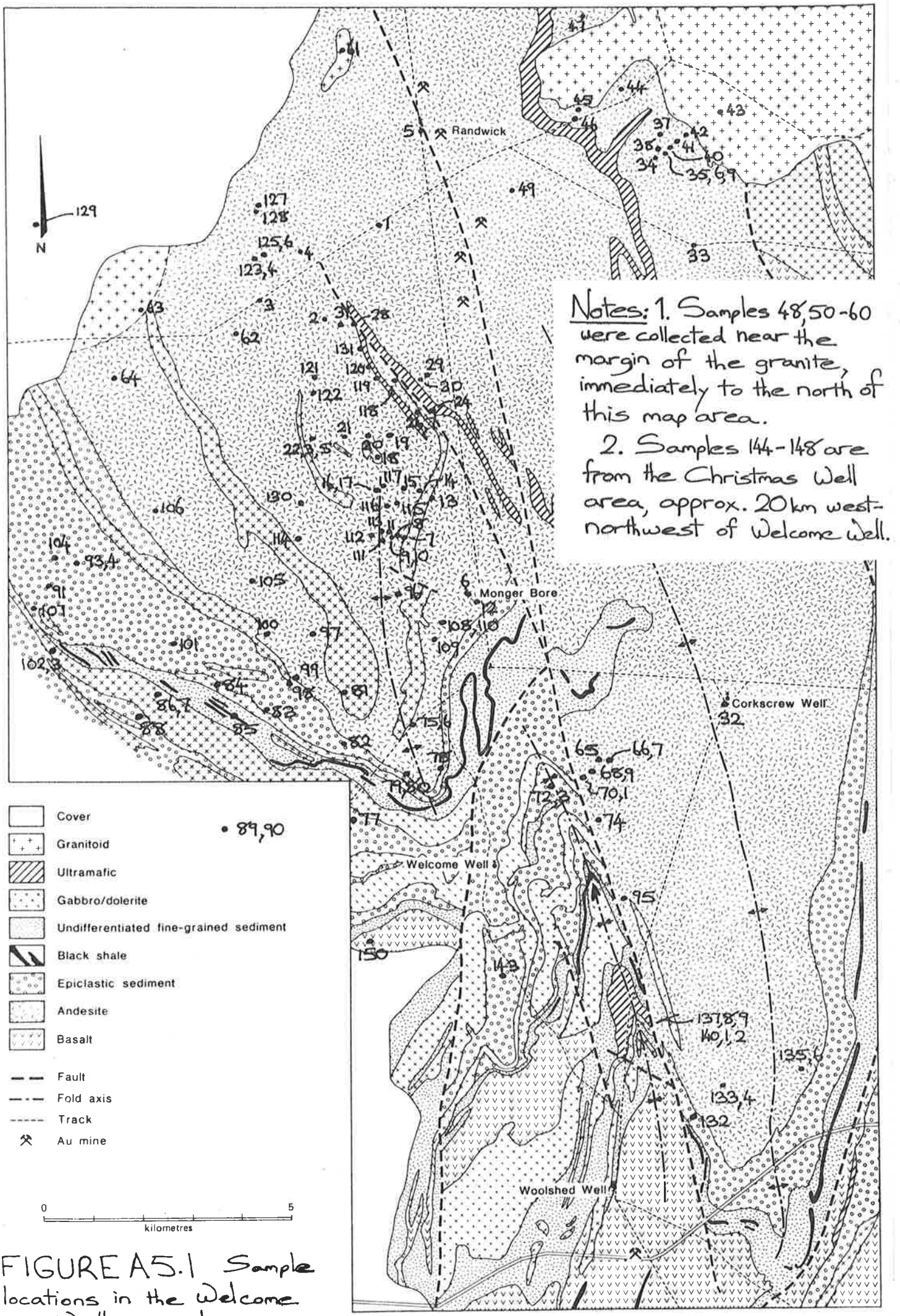

FIGURE A5.1 Sample locations in the Welcome Well complex.

Giles, C.W., 1977, Rock units in the Gawler Range Volcanics, Lake Everard area, South Australia., *Geological Survey of South Australia, Quarterly Geological Notes*, 61, p7-16

Giles, C.W. , Teale, G.S. 1979 The geochemistry of Proterozoic acid volcanics from The Frome Basin. *Geological Survey of South Australia, Quarterly Geological Notes* 71 p13-18

CHILDARA (portion of)

GEOLOGICAL SURVEY OF SOUTH AUSTRALIA

DEPARTMENT OF MINES ADELAIDE

S.A. GEOLOGICAL ATLAS SERIES SHEET SH 53-14 ZONE 5

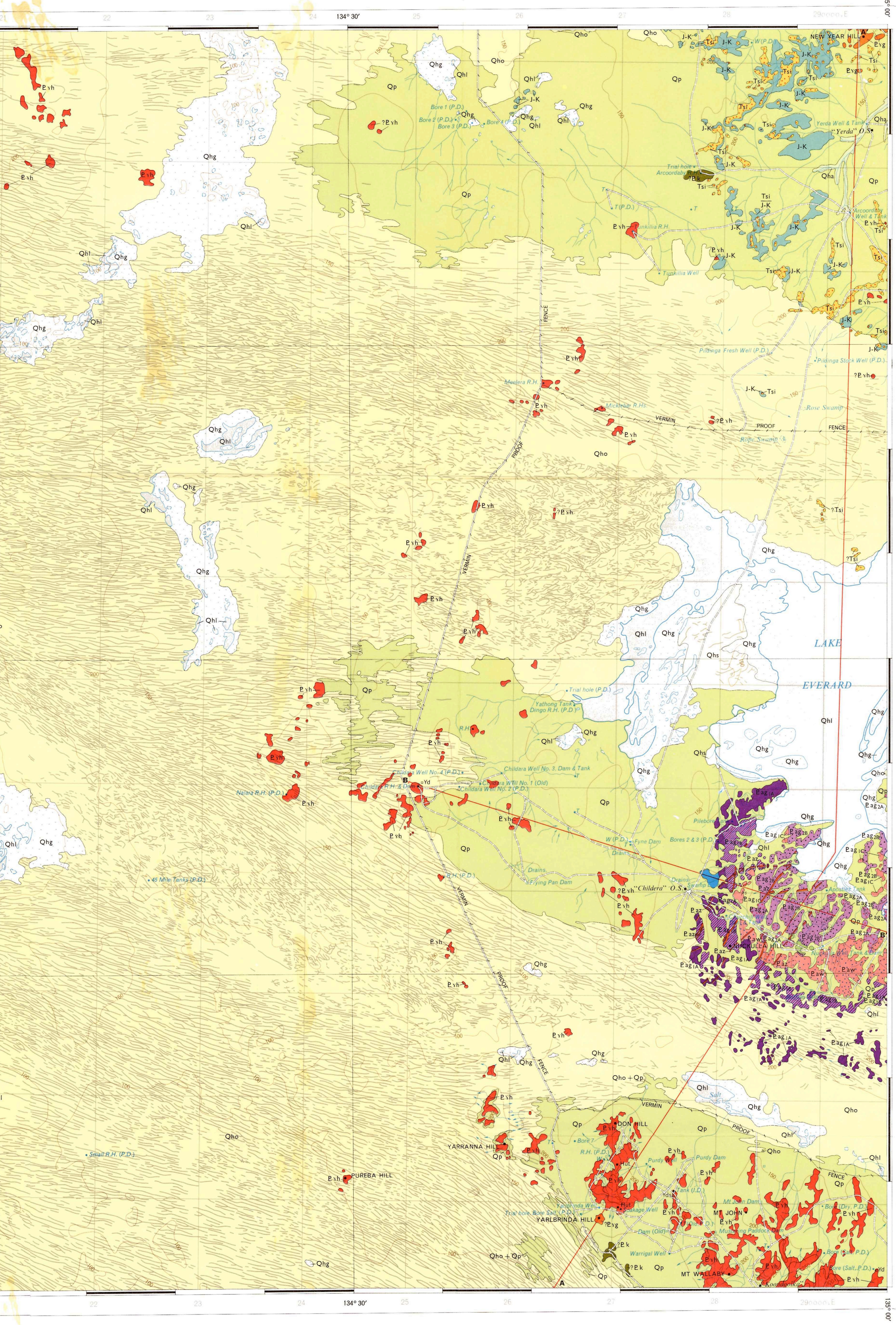

SCALE

5 10 15 20 25 KILOMETRES

6 8 10 12 14 16 18 20 MILES

PRINTED IN AUSTRALIA
D. J. WOOLMAN, GOVERNMENT PRINTER
SOUTH AUSTRALIA

TECTONIC SKETCH

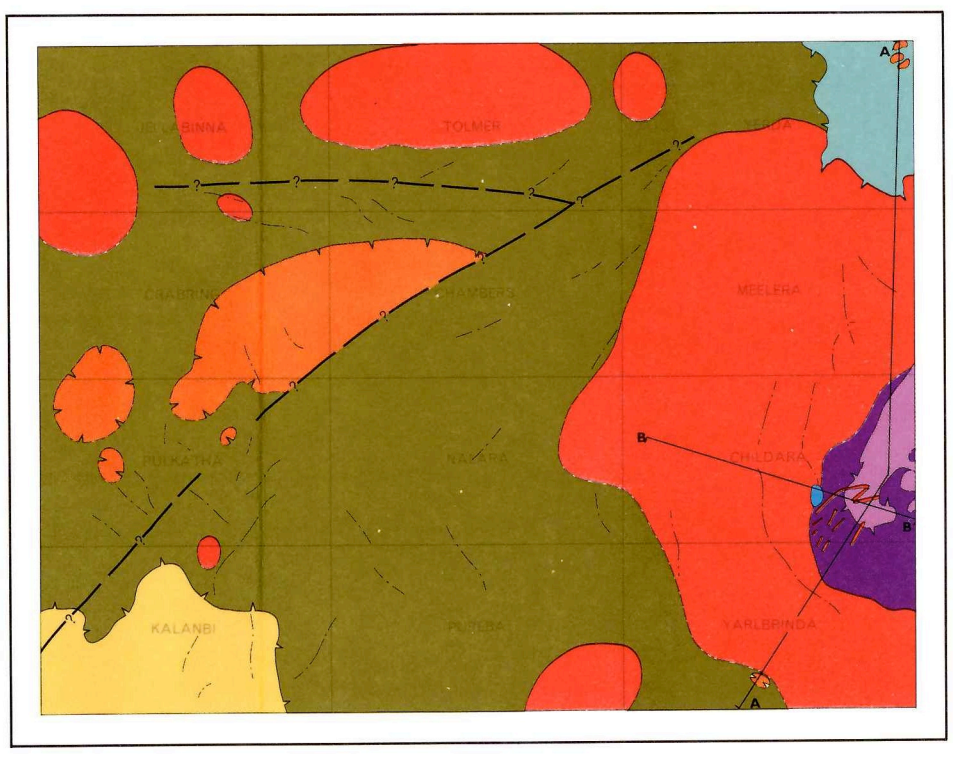

GRAM

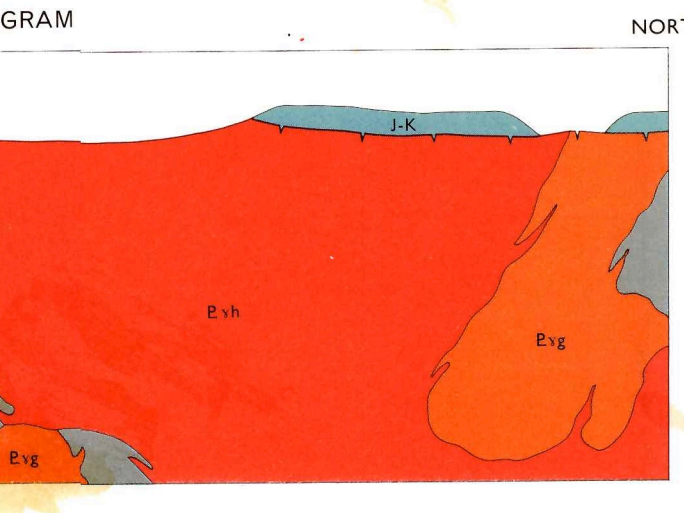

Tertiary

?Pidinga Formation

Late Jurassic or Early Cretaceous

Carpentarian

Hiltaba Granite

?Gawler Range Volcanics

Rhyolite and rhyodacite dykes

Gawler Range Volcanics

"Younger" assemblage ($E ag_{2B}$)

"Older" assemblage ($E ag_1$, $E ag_{2A}$ $E aw$)

Basal basaltic andesite (Childera)

Gneiss and gneissic granite

Glenloth Granite

Unconformity or Disconformity

Possible fault—from aeromagnetic survey

Magnetic lineation—from aeromagnetic survey

Geological section A A'

AUSTRALIA 1:250 000

S.A. GEOLOGICAL ATLAS SERIES SHEET SH 53-15 ZONE 5

FIRST EDITION 1977

GAIRDNER
SHEET SH53-15

REFERENCE

CAINOZOIC — QUATERNARY — HOLOCENE

- Qha — Alluvial gravels, sands, silts and clays of modern drainage channels. Fan deposits of lake margins.
- Qht — Talus and downwash on slopes. Lower part forms mantle on the equivalent of the POORAKA FORMATION.
- Qhs — Aeolian dunes and sand spreads. Pale yellowish-brown and pale orange-brown quartz sands, with some gypsum.
- Qhg — Aeolian gypsiferous dunes and flats, bordering playa lakes: White to pale grey sands and silts with soft crusts of gypsum.
- Qhl — Lake deposits: Gypsiferous muds, clays and silts, with gypsum crystals and halite crusts. Some aeolian quartz sand.
- Qho — MOORNABA SAND: Vegetated self dunes and sand spreads. Pale yellowish-brown, orange-brown and brownish aeolian quartz sands, with calcrete in places.

CAINOZOIC — QUATERNARY — PLEISTOCENE

- Qp2 — High-level reddish-brown lag gravels and gravelly clay, with blocks and fragments of quartzose grit and silcrete. Includes the equivalent of the CALLABONNA CLAY. Rests on nodular and tabular calcrete.
- Qp1 — ?Equivalent of the POORAKA FORMATION: Reddish-brown and dark yellowish-brown gravelly and gritty clays, silts and sands with soft earthy carbonates. Thin reddish-brown sandy clay in the upper part may be the equivalent of the CALLABONNA CLAY. Unit overlies nodular and tabular calcrete.

CAINOZOIC — TERTIARY — PLIOCENE

- Tsi — Silcrete: Hard, dense, nodular-weathering duricrust capping up to about 3 m thick on Adelaidean sandstones, and also on kaolinised Mesozoic, granite and Gawler Range Volcanics. Angular to sub-rounded grains of quartz (with fragments of volcanics near Lake Gairdner) in pale grey or brownish-grey cryptocrystaline siliceous matrix. (Silcrete outcrops in Lake Gairdner may be remnants of a younger duricrust profile).

MESOZOIC — JURASSIC — CRETACEOUS

- J-K — White kaolinitic quartzose sandstone, pebbly grit, and granule to cobble conglomerate, with capping of silcrete.

ADELAIDEAN — TORRENSIAN — BURRA GROUP

- Ebp — PANDURRA FORMATION: Cross-bedded, medium to coarse grained, reddish-brown, purplish-red and pale greenish-grey gritty sandstone and arkosic grit, with pale grey mottling. Interbedded micaceous silty shale with pale greenish spots and bands.

ADELAIDEAN — HARNIDIAN — WILPENA GROUP

- Ewt — SIMMENS QUARTZITE MEMBER: (Upper member of the TENT HILL FORMATION—Ewt). Silicified, hard, massive to flaggy, cross-bedded, pale grey fine to medium grained sandstone. On north side of Lake Hart, overlies yellowish-brown shaly sandstone and shale of the CORRABERRA SANDSTONE MEMBER which rests upon the TREGOLANA SHALE MEMBER.

CARPENTARIAN

- Eth — HILTABA GRANITE: Pink leucocratic graphic biotite—granite and adamellite, often porphyritic. Intrudes GAWLER RANGE VOLCANICS. Radiometric age 1478 ± 38 Ma (Rb/Sr).

?GAWLER RANGE VOLCANICS

- Esp — Porphyritic rhyolite and rhyodacite dykes. Intrude main mass of Gawler Range Volcanics including YARDEA DACITE. Radiometric age 1457 ± 92 Ma (Rb/Sr).

GAWLER RANGE VOLCANICS

- Esk — YANDOOLKA RHYOLITE: Pale reddish-brown, highly porphyritic rhyolite with phenocrysts of quartz and K-feldspar up to over 5 mm across. Some phenocrysts of plagioclase. Finely granular to graphic groundmass. (?Possible vent).

LAKE EVERARD AREA

- Esy — YARDEA DACITE: Predominantly coarsely-porphyritic dacite, grading locally to rhyodacite and andesite. Cream and pale-grey phenocrysts of plagioclase up to 10 mm long, partly replaced by dark green chlorite and epidote, in dark reddish-brown or purplish-brown matrix.
- Esx — Dykes of porphyritic andesite, and dacite grading to rhyodacite. Intrude WHEPOOL RHYOLITE.
- Esc — WHYEELA DACITE: Dark reddish-brown and purplish-red dacite with small scattered feldspar phenocrysts partly replaced by chlorite and epidote. Some vesicular and pumiceous bands.
- Esa — Andesite S. of Glyde Hill outstation.
- Esw — YANTEA RHYOLITE: Reddish-brown porphyritic rhyodacite grading to dacite locally. Phenocrysts of pink K-feldspar and some of cream-coloured plagioclase up to about 5 mm across.
- Disconformity
- Esb — BUNBURN DACITE: Brick-red and purplish-grey dacite with small scattered feldspar phenocrysts, grading to rhyodacite.
- Esg — WHEPOOL RHYOLITE (Esw): Red-dish-brown porphyritic rhyolite with phenocrysts of pink K-feldspar and rounded quartz.
- Esc — Rhyolite (Esgc): Fine grained flow-banded rhyolite, rhyolitic welded tuff and ash. Rounded phenocrysts of quartz in places.
- Esa — Breccia E. of Glyde Hill outstation.
- Esa — Andesite S. of Yandoolka Well.
- Esm — MANGAROONGAH DACITE: Pur-plish-brown and purplish-grey por-phyritic dacite, grading to rhyodacite. Many phenocrysts of cream-coloured plagioclase partly replaced by chlorite and epidote. Upper part vesicular near Yandoolka Well.
- Esk — CHILDERA DACITE: Reddish-brown, purplish-grey and greenish-grey dacite. Small scattered feldspar phenocrysts up to about 2 mm long with ferromagnesian alteration.

Base not exposed

KOKATHA AREA

- Esn — CHANDABOOKA DACITE (?Equiv-alent of YARDEA DACITE): Por-phyritic dacite and subordinate rhyo-dacite. Many phenocrysts of feldspar, partly replaced by chlorite and epi-dote. (Banded greenish-grey welded tuff at base).

Disconformity

- Esn, Esl — Predominantly rhyodacite grading to rhyolite. Brick-red or black in colour with small scattered K-feldspar pheno-crysts. Complex flow or compaction-banding.
- Esa — Andesite (Esac)
- Esl — Basalt (Esag)
- Esl — ?Equivalent of LAKE GAIRDNER RHYOLITE: Grey to black welded tuff with rounded phenocrysts of quartz. Banded pale grey fine rhyolitic tuff at base. Red and black rhyolite and rhyodacite lava flows, welded tuffs and breccias in upper part.
- Disconformity
- Esc, Esl — Basalt
- Esa — Predominantly reddish-brown and black rhyodacite with complex flow or compaction-banding. Fine-grained with scattered K-feldspar pheno-crysts.
- Esa — Andesite
- Esl — Basalt: Dark bluish-grey to greenish-grey. Probably succession of lava flows with amygdaloidal upper sur-faces. Several bands of rhyodacite, andesite and air-fall tuff.
- Esa — Breccia E. of Glyde Hill outstation.
- Esr — Rhyodacite
- Esr — Rhyodacite

Unconformity

N.W. LAKE GAIRDNER

- Esn — CHANDABOOKA DACITE: Radio-metric age 1511 ± 36 Ma (Rb/Sr).

Disconformity

- Esl — LAKE GAIRDNER RHYOLITE: Vari-able assemblage of yellowish-brown weathered, cream, pale purplish, red and green rhyolites (usually con-taining rounded phenocrysts of quartz), grading to rhyodacite with rare quartz phenocrysts. Sequence includes rhyolite lava flows, welded tuffs with breccias in places. Flow-banding common. Base not visible near Lake Gairdner, but the formation is prob-ably unconformable on the GLEN-LOTH GRANITE north of Kokatha; and on the GLENLOTH GRANITE or "older" metamorphics north of Glenloth.

ARCHAEAN — PROTEROZOIC — CARPENTARIAN — GLENLOTH RHYOLITE COMPLEX

- Esg — GLENLOTH GRANITE: Pale yellowish-brown weathered, grey and cream gneissic granite, adamellite and grano-diorite with sinuous biotite-rich and amphibolitic bands. Medium to coarse-grained. (Intruded by dykes of andesite, dacite, rhyodacite and rhyolite, tentatively assigned to the GAWLER RANGE VOLCANICS, and also dolerite dykes of unknown age) Radiometric age 2900 ± 83 Ma (Rb/Sr). Dolerite dykes.
- "OLDER" METAMORPHICS: Calc-silicate hornfels and metavolcanics with possible pillow structures (Kokatha). *Tremolitic and actinolitic schists, amphibolite, serpentine* (Glenloth).

*Ma = 1 megayear = 10^6 years. ($\lambda Rb^{87} = 1.42 \times 10^{-11}\ yr^{-1}$). Radiometric ages determined by A. W. Webb, Australian Mineral Development Laboratories.

GEOLOGICAL BOUNDARY
- OBSERVED
- INFERRED

FAULT
- INFERRED

TUFF
BEDDING IN TUFF
- INCLINED
- VERTICAL

FLOW BANDING
- INCLINED
- VERTICAL

JOINTING
- INCLINED
- VERTICAL
- TREND OBSERVED ON AERIAL PHOTOGRAPH

SHEAR ZONE
GEOLOGICAL SECTION — A — A'
MAIN ROAD
SECONDARY ROAD
TRACK

NATIONAL ROUTE NUMBER
RAILWAY
VERMIN PROOF FENCE
BOUNDARY FENCE
ASTRONOMICAL STATION
TRIANGULATION STATION
IDENTIFIED POINT
SPOT HEIGHT (APPROXIMATE, IN METRES)
CONTOUR (50 METRE INTERVAL)
EPHEMERAL STREAM
PLAYA LAKE
CLAYPAN, SALTPAN
SWAMP
STRATIGRAPHIC BORE
WELL
DAM
TANK
WATERHOLE
ROCKHOLE
MINE
- GOLD — Au
- TIN — Sn

SECTION A-A'

SECTION B-B'

SECTION C-C'

SECTION D-D'

SCALE: V = H = 15

INDEX TO ADJOINING SHEETS

Magnetic Declination 1970

Annual variation +1 minute

SCALE

KILOMETRES 5 0 5 10 15 20 25 KILOMETRES

MILES 2 1 0 2 4 6 8 10 12 14 16 18 20 MILES

PRINTED IN AUSTRALIA
D. J. WOOLLARD, GOVERNMENT PRINTER
SOUTH AUSTRALIA

Geology by A. H. Blissett, M.Sc.,

Acknowledgement to C. W. Giles, B.Sc (Hons.), University of Adelaide (Lake Everard Area).

B. P. Thomson, M.Sc., Supervising Geologist, Regional Geology Division.

Map preparation by Cartographic Division, Department of Mines, S.A.

Base map supplied by Division of National Mapping.

Compiled under the direction of B. P. Webb, M.Sc., Government Geologist, Director of Mines.

Issued under the authority of the Honourable H. R. Hudson, B.Ec., M.P., Minister of Mines and Energy.

Published 1977

ROCK RELATION DIAGRAM

TECTONIC SKETCH

- Late Jurassic or Early Cretaceous
- Adelaidean
- Wilpena Group
- Burra Group
- Carpentarian
- Hiltaba Granite
- Rhyolite and rhyodacite dykes
- Yandoolka Rhyolite(?vent)
- Gawler Range Volcanics
- "Younger" assemblage (Esy, Esn, Esg(Eth, gc))
- "Older" assemblage (Esg), Esw, Esc, Esl, Esg(sa))
- Basal unit (Basalt near Kokatha)
- Glenloth Granite
- "Older" Metamorphics
- Geological Section B — B'
- Magnetic lineation—from aeromagnetic surveys
- Possible fault—from gravity and aeromagnetic surveys
- Unconformity or Disconformity

GAIRDNER
SHEET SH53-15

FIRST EDITION 1977

REFERENCE

CAINOZOIC

QUATERNARY

HOLOCENE

Qha — Alluvial gravels, sands, silts and clays of modern drainage channels.

Qhs — Aeolian dunes and sand spreads. Pale yellowish-brown and pale orange-brown quartz sands, with some gypsum.

Qhg — Aeolian gypsiferous dunes and flats, bordering playa lakes. White to pale grey sands and silts with soft crusts of gypsum.

Qhl — Lake deposits. Gypsiferous muds, clays and silts with gypsum crystals and halite crusts. Some aeolian quartz sand.

Qho — MOORNABA SAND: Vegetated seif dunes and sand spreads. Pale yellowish-brown, orange-brown and brownish quartz sands, with soft carbonates in places.

PLEISTOCENE

Qpo — WIABUNA FORMATION: Pale brownish calcareous silty sand, with soft earthy, rubbly and nodular carbonates of the LOVEDAY SOIL developed locally.

Qp — ?Equivalent of the POORAKA FORMATION: Reddish-brown and dark yellowish-brown gravelly and gritty clays, silts and sands with soft, earthy carbonates in the upper part. Rests on nodular and tabular calcrete.

TERTIARY

Tsi — Silcrete: Hard, dense, nodular-weathering duricrust up to about 3 m thick, capping kaolinised granite and Mesozoic. "Terrazzo" type, with angular to sub-rounded fragments of quartz in pale grey and brownish-grey cryptocrystalline siliceous matrix.

MESOZOIC

JURASSIC-CRETACEOUS

J-K — Quartzose conglomerate and grit with kaolinitic matrix, capped by Tertiary silcrete.

PROTEROZOIC

CARPENTARIAN

Pγh — HILTABA GRANITE: Pink leucocratic graphic biotite granite and adamellite, locally porphyritic. Scattered aplite and microgranite veins.

?GAWLER RANGE VOLCANICS

Pαz — Reddish-brown porphyritic rhyolite dykes.
Reddish-brown porphyritic rhyodacite dykes.
Up to about 100 m wide. Intrude layered volcanics.

GAWLER RANGE VOLCANICS

GLYDE HILL VOLCANIC COMPLEX

Pag2B — YANTEA RHYODACITE: Reddish-brown porphyritic rhyodacite grading to dacite locally. Phenocrysts of pink K-feldspar and some of cream-coloured plagioclase up to about 10 mm long.

Disconformity

NUCKULLA BASALT

Pag2A — BUNBURN DACITE: At base, dark purplish-grey, pale grey and purplish lapilli tuff and flowbanded porphyritic rhyodacitic welded tuff. Overlain by dark greenish-grey dacite passing up into reddish-brown rhyodacite. Below the NUCKULLA BASALT west of Nuckulla Dam, upper part of the rhyodacite is tuffaceous and pumiceous.

Pag1C, Paw — WHEEPOOL RHYOLITE (Paw): Yellowish-brown weathered reddish-brown porphyritic rhyolite, grading to rhyodacite locally. Phenocrysts of pink K-feldspar and rounded quartz. Rhyolite (Pag1C): Yellowish-brown weathered rhyolitic breccia, and cream and pale brownish flowbanded welded tuff. (North of road from Lake Everard homestead to Childera outstation.)

Pag1B — MANGAROONGAH DACITE: Purplish-brown and purplish-grey porphyritic dacite, grading to rhyodacite. Many phenocrysts of cream-coloured plagioclase, partly replaced by chlorite and epidote. Upper part more rhyodacitic, and vesicular in places.

Pag1A — CHILDERA DACITE: Reddish-brown, purplish-grey and greenish-grey dacite. Scattered feldspar phenocrysts up to about 2 mm long in granular felsic or aphanitic matrix. Grades to rhyodacite upwards. Northeast of Childera outstation, dacite overlies dark greenish-grey basaltic andesite.

Unconformity

Pk — Foliated granitic gneiss SSE of Yarlbrinda Hill and gneissic granite at Arcoordaby Rockhole.

Unconformity

Pγg — GLENLOTH GRANITE: Pink and cream foliated granite with pods and irregular bands of calc-silicate hornfels.

GEOLOGICAL BOUNDARY
OBSERVED
TUFF
FLOW BANDING
INCLINED
FOLIATION
INCLINED
JOINTING
TREND OBSERVED ON AERIAL PHOTOGRAPHY
GEOLOGICAL SECTION — A — A'
MAIN ROAD
SECONDARY ROAD
TRACK
NATIONAL ROUTE NUMBER
RAILWAY (ABANDONED)
VERMIN PROOF FENCE
BOUNDARY FENCE
TRIANGULATION STATION
IDENTIFIED POINT
SPOT HEIGHT (APPROXIMATE) — 65·5
CONTOUR (50 m INTERVAL) — 150
EPHEMERAL STREAM
PLAYA LAKE
CLAYPAN, SALTPAN
BORE
WELL — W
DAM
TANK — T
ROCKHOLE — R.H.

Geology by A. H. Blissett, M.Sc.,

Acknowledgements to C. W. Giles, B.Sc.(Hons.), University of Adelaide (Lake Everard Area); and to V. Vitols, B.Sc.

B. P. Thomson, M.Sc., Supervising Geologist, Regional Geology Division.

Map preparation by Cartographic Division, Department of Mines, S.A.

Base map supplied by Division of National Mapping.

Compiled under the direction of B. P. Webb, M.Sc., Government Geologist, Director of Mines.

Issued under the authority of the Honourable H. R. Hudson, B.Ec., M.P., Minister of Mines and Energy.

Published 1977